

ADVANCES IN CHEMICAL PHYSICS

VOLUME XVIII

EDITORIAL BOARD

- THOR A. BAK, Universitetets Fysik Kemiske Institut, Copenhagen, Denmark
- J. DUCHESNE, University of Liège, Liège, Belgium
- H. C. LONGUET-HIGGINS, The University Chemical Laboratory, Cambridge, England
- M. MANDEL, University of Leiden, Leiden, Holland
- V. MATHOT, Université Libre de Bruxelles, Brussels, Belgium
- P. MAZUR, Institut Lorentz, Leiden, Holland
- A. MÜNSTER, Institut für theoretische physikalische Chemie, Frankfurt-am-Main, Germany
- S. ONO, Institute of Physics, College of General Education, Tokyo, Japan
- B. PULLMAN, Institute de Biologie Physico-Chimique, Université de Paris, Paris, France
- J. W. STOUT, Institute for the Study of Metals, University of Chicago, Chicago, Illinois, U.S.A.
- G. SZASZ, General Electrical Company, Zurich, Switzerland
- M. V. VOLKENSTEIN, Institute of Macromolecular Chemistry, Leningrad, U.S.S.R.
- B. H. ZIMM, School of Science and Engineering, University of California at San Diego, La Jolla, California, U.S.A.

Advances in CHEMICAL PHYSICS

EDITED BY

I. PRIGOGINE

University of Brussels, Brussels, Belgium

AND

STUART A. RICE

Department of Chemistry
and

The James Franck Institute
The University of Chicago
Chicago, Illinois

VOLUME XVIII

INTERSCIENCE PUBLISHERS

A DIVISION OF JOHN WILEY AND SONS
NEW YORK • LONDON • SYDNEY • TORONTO

Copyright © 1970, by John Wiley & Sons, Inc.

All rights reserved. No part of this book may be reproduced by any means, nor transmitted, nor translated into a machine language without the written permission of the publisher.

10 9 8 7 6 5 4 3 2 1

Library of Congress Catalogue Card Number: 58-9935

SBN 471 69923 3

Printed in the United States of America

INTRODUCTION

In the last decades, chemical physics has attracted an ever-increasing amount of interest. The variety of problems, such as those of chemical kinetics, molecular physics, molecular spectroscopy, transport processes, thermodynamics, the study of the state of matter, and the variety of experimental methods used, makes the great development of this field understandable. But the consequence of this breadth of subject matter has been the scattering of the relevant literature in a great number of publications.

Despite this variety and the implicit difficulty of exactly defining the topic of chemical physics, there are a certain number of basic problems that concern the properties of individual molecules and atoms as well as the behavior of statistical ensembles of molecules and atoms. This new series is devoted to this group of problems which are characteristic of modern chemical physics.

As a consequence of the enormous growth in the amount of information to be transmitted, the original papers, as published in the leading scientific journals, have of necessity been made as short as is compatible with a minimum of scientific clarity. They have, therefore, become increasingly difficult to follow for anyone who is not an expert in this specific field. In order to alleviate this situation, numerous publications have recently appeared which are devoted to review articles and which contain a more or less critical survey of the literature in a specific field.

An alternative way to improve the situation, however, is to ask an expert to write a comprehensive article in which he explains his view on a subject freely and without limitation of space. The emphasis in this case would be on the personal ideas of the author. This is the approach that has been attempted in this new series. We hope that as a consequence of this approach, the series may become especially stimulating for new research.

Finally, we hope that the style of this series will develop into something more personal and less academic than what has become the standard scientific style. Such a hope, however, is not likely to be completely realized until a certain degree of maturity has been attained—a process which normally requires a few years.

At present, we intend to publish one volume a year, and occasionally several volumes, but this schedule may be revised in the future.

In order to proceed to a more effective coverage of the different aspects of chemical physics, it has seemed appropriate to form an editorial board. I want to express to them my thanks for their cooperation.

I. PRIGOGINE

CONTRIBUTORS TO VOLUME XVIII

ALAN CARRINGTON, Department of Chemistry, University of Southampton,
Southampton, England

ARON KUPPERMANN, California Institute of Technology, Pasadena,
California

DONALD H. LEVY, Department of Chemistry and the James Franck
Institute, University of Chicago, Chicago, Illinois

TERRY A. MILLER, Bell Telephone Laboratories, Inc., Murray Hill, New
Jersey

B. J. NICHOLSON, Trinity College, Cambridge, England

MURRAY PESHKIN, The Weizmann Institute of Science, Rehovot, Israel, and
Argonne National Laboratory, Argonne, Illinois

JAMES K. RICE, California Institute of Technology, Pasadena, California

HOWARD S. TAYLOR, Department of Chemistry, University of Southern
California, Los Angeles, California

SANDOR TRAJMAR, California Institute of Technology, Pasadena, California

CONTENTS

| | |
|--|-----|
| ANGULAR DISTRIBUTIONS OF PHOTOELECTRONS: CONSEQUENCES OF SYMMETRY | |
| <i>By Murray Peshkin</i> | 1 |
| ELECTRON-IMPACT SPECTROMETRY | |
| <i>By Sandor Trajmar, James K. Rice, and Aron Kuppermann</i> | 15 |
| MODELS, INTERPRETATIONS, AND CALCULATIONS CONCERNING RESONANT ELECTRON SCATTERING PROCESSES IN ATOMS AND MOLECULES | |
| <i>By Howard S. Taylor</i> | 91 |
| ELECTRON RESONANCE OF GASEOUS DIATOMIC MOLECULES | |
| <i>By Alan Carrington, Donald H. Levy, and Terry A. Miller</i> | 149 |
| APPROXIMATE MOLECULAR ORBITAL THEORIES | |
| <i>By B. J. Nicholson</i> | 249 |
| AUTHOR INDEX | 313 |
| SUBJECT INDEX | 319 |

ADVANCES IN CHEMICAL PHYSICS

VOLUME XVIII

ANGULAR DISTRIBUTIONS OF PHOTOELECTRONS: CONSEQUENCES OF SYMMETRY

MURRAY PESHKIN*

*The Weizmann Institute of Science, Rehovot, Israel, and
Argonne National Laboratory, Argonne, Illinois*

CONTENTS

| | |
|--|----|
| I. Introduction and Conclusions | 1 |
| II. Polarization States of a Photon | 2 |
| III. Multipole Decomposition | 5 |
| IV. The Photon Density Matrix | 6 |
| V. Expansion in Standard Tensors | 8 |
| VI. Angular Distribution of One Electron | 10 |
| VII. Two-Electron Angular Distributions | 13 |
| References | 14 |

I. INTRODUCTION AND CONCLUSIONS

This article addresses itself to two questions which arise in the design of experimental facilities for measuring the angular distributions of electrons ejected from atoms or molecules by light: What angular distributions are possible? What is gained by using plane or circularly polarized light? These questions have partially been answered previously in the context of calculations involving specific models for the target atoms or molecules.¹ Here they are answered by giving a simple systematic treatment based on symmetry. The only dynamical assumption is the rapid convergence of the multipole expansion of the absorbed light.

This sort of analysis has been common for many years in nuclear reaction theory, where it yields maximum-complexity theorems for angular distributions and polarizations. The results for electrons ejected from atoms or molecules by light are stronger for two reasons: the multipole absorp-

* Weizmann Fellow, 1968/69. Work performed partly under the auspices of the U.S. Atomic Energy Commission.

tion amplitudes decrease rapidly, and the transverse nature of light gives useful restrictions which are absent in the case of particle-induced reactions.

Sections II-V develop the mathematical machinery for describing the symmetry of the absorbed light: The photon is regarded as a particle of unit spin. Its polarization state is described by a density matrix in the multipole representation. That density matrix is expressed as a sum of standard matrices which have definite symmetry under rotation and which refer to particular terms in the multipole expansion.

Section VI gives the consequences of symmetry for any one group of electrons, selected by energy or any other scalar criterion, independently of other groups that may accompany it. It is shown that when the normalized angular distribution is written in the form

$$I(\theta, \phi) = \sum_{L,M} b_{LM} Y_{LM}(\theta, \phi),$$

the b_{LM} for positive L correspond to particular products of multipole absorption amplitudes. Specifically, the b_{2M} depend only upon pure $E1$ and pure $M1$ absorption, the b_{1M} only upon $E1 \cdot M1$ and $E1 \cdot E2$ interference, and the b_{3M} only upon $E1 \cdot E2$ interference. Circular polarization has no influence upon $I(\theta, \phi)$. Plane polarization modifies the angular distribution in a predictable way, independently of the target atom or molecule. It increases the magnitude of the asymmetry and changes its shape, but plane polarization introduces no dynamical quantity which is not measured with unpolarized light. All these results depend only upon symmetry and the assumed decreasing amplitudes in the usual multipole expansion of the absorbed light.

Section VII presents a similar classification of the joint angular distribution of two ejected electrons. Here the results are less satisfactory, because they are much more complicated and to make sense of them would require additional restrictions from specific dynamical models. However, it is apparent from the general analysis that the dependence of two-electron angular distributions upon polarization is not determined by symmetry alone. In particular, circular polarization can reveal dynamical information which is unavailable with unpolarized or plane-polarized light, even in the pure electric-dipole approximation. Certain interference terms can be seen only with plane polarization, and others only with circular polarization.

It is assumed throughout this article that the target atoms or molecules are oriented at random. The same methods can be extended to see what information is gained by the use of polarized targets, but that is not done here.

II. POLARIZATION STATES OF A PHOTON

The consequences of symmetry for the angular distributions of photoelectrons depend only upon considerations of angular momentum and parity, and not at all upon a detailed description of the interaction of light with matter. It is therefore convenient to adopt the simple-minded view that a photon is a unit-spin particle, whose spin wave function χ may be written in the usual way:

$$\left. \begin{aligned} \chi &= \sum_{\mu} \alpha_{\mu} \chi_{1\mu} \\ S^2 \chi_{1\mu} &= 2\chi_{1\mu} \\ S_z \chi_{1\mu} &= \mu \chi_{1\mu} \end{aligned} \right\} \mu = 0, \pm 1. \quad (2.1)$$

Here, \mathbf{S} is the spin angular momentum operator and $\hbar = 1$. The interaction of light with matter happens to be such that photons are emitted into, or absorbed from, states wherein the component of \mathbf{S} in the direction of the momentum \mathbf{k} is necessarily ± 1 , never 0. For such states,

$$(\mathbf{k} \cdot \mathbf{S})^2 \chi = k^2 \chi. \quad (2.2)$$

As the photon momentum direction will consistently be used to define the positive z -axis, that means

$$\alpha_0 = 0. \quad (2.3)$$

The usual polarization vector \mathbf{e} , which represents the electromagnetic vector potential, has components e_x, e_y, e_z given by

$$\begin{aligned} e_x &= (1/\sqrt{2})(\alpha_{-1} - \alpha_1) \\ e_y &= (i/\sqrt{2})(\alpha_{-1} + \alpha_1) \\ e_z &= \alpha_0 = 0. \end{aligned} \quad (2.4)$$

As \mathbf{e} is a polar vector, the spin wave function χ must be endowed with odd intrinsic parity. Under space inversion P , it transforms according to

$$P\chi_{1\mu} = -\chi_{1\mu} \quad (2.5)$$

The photon wave functions for the pure circular- and pure plane-polarization states are given respectively by

$$\begin{aligned} \text{left circular:} \quad \Phi_1 &= \chi_{11} e^{ikz} \\ \text{right circular:} \quad \Phi_{-1} &= \chi_{1,-1} e^{ikz} \end{aligned} \quad (2.6)$$

$$\begin{aligned}
 \text{xz plane:} \quad \Phi_x &= -\frac{1}{\sqrt{2}}(\Phi_1 - \Phi_{-1}) \\
 \text{yz plane:} \quad \Phi_y &= -\frac{i}{\sqrt{2}}(\Phi_1 + \Phi_{-1}).
 \end{aligned} \tag{2.7}$$

All other pure polarization states of a plane wave are represented by linear combinations of any two of these four pure states. Impure polarization states are represented by statistical mixtures of pure states.

III. MULTIPOLE DECOMPOSITION

For studying angular distributions, it is useful to introduce basis states which have definite parity and definite total angular momentum j . To that end, the spatial part of the photon wave function is expressed as a sum of partial waves having definite orbital angular momentum l .

$$e^{ikz} = \sum_{l=0}^{\infty} i^l [4\pi(2l+1)]^{1/2} j_l(kr) Y_{l0}(\theta, \phi). \tag{3.1}$$

Here, Y_{l0} is the usual spherical harmonic, j_l is the spherical Bessel function, and (r, θ, ϕ) are the usual polar variables. The angular-momentum analysis of the photon wave functions (2.6) is accomplished by introducing the vector coupling scheme

$$\psi_{j\mu}^{(l)} \equiv \sum_m C(l, 1, j; m, \mu - m) Y_{lm}(\theta, \phi) \chi_{1, \mu-m} \tag{3.2}$$

where $C(l, S, j; m_L, m_S, \mu)$ is the vector-coupling coefficient² for

$$\mathbf{J} = \mathbf{L} + \mathbf{S}, \quad \mu = m_L + m_S. \tag{3.3}$$

Inversion of (3.2) gives

$$Y_{l0}(\theta, \phi) \chi_{1\mu} = \sum_{j=|l-1|}^{l+1} C(l, 1, j; \mu, 0, \mu) \psi_{j\mu}^{(l)}. \tag{3.4}$$

The only cases of physical interest are $\mu = \pm 1$. For those, there is no term with $j=0$. Substitution of (3.4) into (2.6) and grouping the terms according

to total angular momentum j and parity $(-)^{l+1}$ gives, for $\mu = \pm 1$,

$$\Phi_\mu = \chi_{1\mu} e^{ikz} = \sum_{j=1}^{\infty} \{\mu |Mj, \mu\rangle + |Ej, \mu\rangle\}. \quad (3.5)$$

The basis states, which are called the magnetic and electric 2^j -pole states, are defined by

$$|Mj, \mu\rangle \equiv -i^j [2\pi(2j+1)]^{1/2} j_j(kr) \psi_{j\mu}^{(j)} \quad (3.6M)$$

$$|Ej, \mu\rangle \equiv i^{j-1} (2\pi)^{1/2} \{(j+1)^{1/2} j_{j-1}(kr) \psi_{j\mu}^{(j-1)} - (j)^{1/2} j_{j+1}(kr) \psi_{j\mu}^{(j+1)}\}. \quad (3.6E)$$

Because of the odd intrinsic parity of the photon, they transform under space inversion according to

$$\begin{aligned} P|Mj, \mu\rangle &= (-)^{j+1} |Mj, \mu\rangle \\ P|Ej, \mu\rangle &= (-)^j |Ej, \mu\rangle, \end{aligned} \quad (3.7)$$

and they obey*

$$\begin{aligned} \mathbf{J}^2 |Kj, \mu\rangle &= j(j+1) |Kj, \mu\rangle \\ J_z |Kj, \mu\rangle &= \mu |Kj, \mu\rangle, \end{aligned} \quad (3.8)$$

where K stands for M or E .

The plane-polarized photon wave functions may be expressed in the multipole basis by combining (3.5) with (2.7) to obtain

$$\begin{aligned} \Phi_x &= \frac{-1}{\sqrt{2}} \sum_{j=1}^{\infty} \{|Mj, 1\rangle + |Mj, -1\rangle + |Ej, 1\rangle - |Ej, -1\rangle\} \\ \Phi_y &= \frac{-i}{\sqrt{2}} \sum_{j=1}^{\infty} \{|Mj, 1\rangle - |Mj, -1\rangle + |Ej, 1\rangle + |Ej, -1\rangle\}. \end{aligned} \quad (3.9)$$

All the kinematical information needed to see how angular distributions depend upon polarization is contained in (3.5) and (3.9). The specific dynamical assumptions involve only the invariant amplitudes for the absorption of the multipole states by particular atoms or molecules. Here, it is simply assumed that electric-dipole absorption dominates, and that

* The phase conventions used here are the standard ones; the multipole basis states transform under rotation as angular-momentum eigenstates, and under time reversal according to

$$T|Kj, \mu\rangle = (-)^{j+\mu} |Kj, -\mu\rangle.$$

the orders of magnitude of the amplitudes (Kj) for absorption of other multipoles obey*

$$\begin{aligned} (Ej)/(E1) &\sim (kR)^{j-1} \\ (Mj)/(Ej) &\sim k/mc \end{aligned} \quad (3.10)$$

where R is the radius of the target atom or molecule, and m is the mass of the electron. Then in practical situations it is usually sufficient to neglect all contributions to the angular distributions except those proportional to $(E1)^2$, $(E1) \cdot (M1)$, or $(E1) \cdot (E2)$.

IV. THE PHOTON DENSITY MATRIX

Even for a pure polarization state, the density matrix⁴ provides a more transparent approach to angular distributions than does the wave function. In particular, the density matrix for a randomly oriented target atom or molecule is spherically symmetric. Then the symmetry properties of the density matrix for the combined system, photon plus target, are just those of the density matrix for the photon alone.

The density matrix elements $\langle K'j', \mu' | \rho | Kj, \mu \rangle$ for a photon in a pure polarization state Φ are given by

$$\langle K'j', \mu' | \rho | Kj, \mu \rangle = \langle K'j', \mu' | \Phi \rangle \cdot \langle \Phi | Kj, \mu \rangle, \quad (4.1)$$

where K stands for M or E . For a statistical mixture of pure states, the density matrices of the individual pure states are added with weights equal to their statistical weights in the mixture. The matrix (4.1) has infinitely many rows and columns, labeled by (Kj, μ) with $-j \leq \mu \leq j$. However, only terms with $\mu = \pm 1$ appear in the plane wave functions (3.5) and (3.9), or in fact in any plane wave function for the photon. Therefore, all rows and columns of ρ vanish identically, except those with $\mu = \pm 1$ and $\mu' = \pm 1$. Inspection of (3.5) and (3.9) shows that the coefficients $\langle \Phi | Kj, \mu \rangle$ depend upon K and μ , but not upon j . Consequently, the infinite-dimensional matrix ρ is really a repetition of four two-dimensional submatrices $\rho(K', K)$, defined for $\mu' = \pm 1, \mu = \pm 1$ by

$$\langle \mu' | \rho(K', K) | \mu \rangle \equiv \langle K'j', \mu' | \rho | Kj, \mu \rangle. \quad (4.2)$$

In the multipole representation, with nonvanishing columns labeled by (Kj, μ) and nonvanishing rows by $(K'j', \mu')$, the density matrix appears as

* The estimates (3.10) are not quite correct because they are based on non relativistic theory. For instance, $(E2)$ has a relativistic term³ whose order of magnitude is given by $(k/mc) \cdot (E1)$.

| $Kj \backslash K'j' \mu \mu'$ | | $E1$ | | $M1$ | | $E2$ | | $M2$ | | |
|-------------------------------|------|------|----|------|----|------|----|------|----|-------|
| | | 1 | -1 | 1 | -1 | 1 | -1 | 1 | -1 | |
| $\rho =$ | $E1$ | 1 | | | | | | | | (4.3) |
| | -1 | | | | | | | | | |
| | $M1$ | | | 1 | | | | | | |
| | -1 | | | | | | | | | |
| | $E2$ | | | | | 1 | | | | |
| | -1 | | | | | | | | | |
| | $M2$ | | | | | | | 1 | | |
| | -1 | | | | | | | | | |
| | | | | | | | | | | |
| | | | | | | | | | | |
| | | | | | | | | | | |

For the states of pure circular polarization discussed above, the submatrices may be read off from (3.5) and (4.1).

$$\rho_1(E, E) = \rho_1(M, M) = \rho_1(E, M) = \rho_1(M, E) = \begin{pmatrix} 1 & 0 \\ 0 & 0 \end{pmatrix} = \frac{1}{2}(\mathbf{1} + \sigma_z)$$

$$\rho_{-1}(E, E) = \rho_{-1}(M, M) = -\rho_{-1}(E, M) = -\rho_{-1}(M, E) = \begin{pmatrix} 0 & 0 \\ 0 & 1 \end{pmatrix} \quad (4.4)$$

$$= \frac{1}{2}(\mathbf{1} - \sigma_z)$$

Here, $\rho_{\pm 1}$ is the density matrix for the circular polarization state $\Phi_{\pm 1}$ of (3.5), and the notation

$$\mathbf{1} = \begin{array}{c|cc} & \mu & \\ \hline \mu' & 1 & -1 \\ \hline 1 & \begin{pmatrix} 1 & 0 \\ 0 & 1 \end{pmatrix} & \end{array} \quad \sigma_z = \begin{pmatrix} 1 & 0 \\ 0 & -1 \end{pmatrix}$$

$$\sigma_+ = \begin{pmatrix} 0 & 1 \\ 0 & 0 \end{pmatrix} \quad \sigma_- = \begin{pmatrix} 0 & 0 \\ 1 & 0 \end{pmatrix} \quad (4.5)$$

is introduced for later convenience. In the same way, the density matrices for the plane polarized states are determined by (3.9) to be

$$\begin{aligned}
 \rho_x(E, E) &= \rho_y(M, M) = \frac{1}{2}(1 - \sigma_+ - \sigma_-) \\
 \rho_x(M, M) &= \rho_y(E, E) = \frac{1}{2}(1 + \sigma_+ + \sigma_-) \\
 \rho_x(E, M) &= \rho_y(M, E) = \frac{1}{2}(\sigma_z + \sigma_+ - \sigma_-) \\
 \rho_x(M, E) &= \rho_y(E, M) = \frac{1}{2}(\sigma_z - \sigma_+ + \sigma_-).
 \end{aligned} \tag{4.6}$$

For unpolarized light, the density matrix ρ_u is given by

$$\rho_u = \frac{1}{2}(\rho_1 + \rho_{-1}) = \frac{1}{2}(\rho_x + \rho_y) \tag{4.7}$$

$$\begin{aligned}
 \rho_u(E, E) &= \rho_u(M, M) = \frac{1}{2}1 \\
 \rho_u(E, M) &= \rho_u(M, E) = \frac{1}{2}\sigma_z.
 \end{aligned} \tag{4.8}$$

The five special density matrices written out here are manifestly not independent, and in fact do not form a complete set. The reduction to a repetition of four two-dimensional matrices does go through in the same way for the general polarization state of a plane wave, and so does the tensor analysis which will follow.

V. EXPANSION IN STANDARD TENSORS

The symmetry of the photon density matrix is exposed by expressing it as a sum of irreducible tensor operators, that is of matrices T_{LM} which transform under rotation in the same way as the spherical harmonic functions Y_{LM} . The standard tensors used here are defined by their matrix elements,

$$\begin{aligned}
 \langle K'j', \mu' | T_{LM}(\kappa'\lambda', \kappa\lambda) | Kj, \mu \rangle \\
 \equiv \left[\frac{2L+1}{2j'+1} \right]^{1/2} \delta_{K'j', \kappa'\lambda'} \delta_{Kj, \kappa\lambda} C(j, L, j'; \mu, M, \mu'), \tag{5.1}
 \end{aligned}$$

which vanish except for $|j' - j| \leq L \leq j' + j$. The vector-coupling coefficient $C(j, L, j'; \mu, M, \mu')$ is required for an irreducible tensor by the Wigner-Eckart theorem.² The remaining (scalar) factors are arbitrary. They have been chosen so that $T_{LM}(K'j', Kj)$ has nonvanishing matrix elements between the multipole states Kj and $K'j'$, and no others. The

Hermitian conjugates of the standard tensors can be found from the properties of the vector-coupling coefficients.

$$T_{LM}(K'j', Kj)^\dagger = (-)^{j'-j+M} T_{L, -M}(Kj, K'j') \quad (5.2)$$

The standard tensors form an orthonormal set in the sense that their traces obey

$$\begin{aligned} & \text{Tr}\{T_{L'M'}(K'j', \kappa'\lambda')^\dagger T_{LM}(Kj, \kappa\lambda)\} \\ & \equiv \sum_{K''j'', \mu''} \langle K''j'', \mu'' | T_{L'M'}(K'j', \kappa'\lambda')^\dagger T_{LM}(Kj, \kappa\lambda) | K''j'', \mu'' \rangle \\ & = \delta_{L, L'} \delta_{M, M'} \delta_{Kj, K'j'} \delta_{\kappa\lambda, \kappa'\lambda'}. \end{aligned} \quad (5.3)$$

They form a complete basis for the expansion of any photon density matrix in the form

$$\rho = \sum_{L, M} \sum_{K'j', Kj} a_{LM}(K'j', Kj) T_{LM}(K'j', Kj), \quad (5.4)$$

where the tensor moments a_{LM} may be obtained by applying (5.3) to (5.4) to obtain

$$a_{LM}(K'j', Kj) = \text{Tr} \{ \rho T_{LM}(K'j', Kj)^\dagger \}. \quad (5.5)$$

In terms of the two-dimensional submatrices of ρ , (5.5) becomes

$$\begin{aligned} a_{LM}(K'j', Kj) &= \text{Tr} \{ \rho (K'j', Kj) T_{LM}(K'j', Kj)^\dagger \} \\ &= (-)^{j'-j+M} \text{Tr} \{ \rho (K'j', Kj) T_{L, -M}(Kj, K'j') \} \end{aligned} \quad (5.6)$$

$$\begin{aligned} &= (-)^{j'-j+M} \sum_{\mu', \mu} \langle \mu' | \rho (K'j', Kj) | \mu \rangle \\ &\quad \times \langle Kj, \mu | T_{L, -M}(Kj, K'j') | K'j', \mu' \rangle. \end{aligned} \quad (5.7)$$

As the density matrix is necessarily Hermitian, it follows from (5.2) and (5.4) that the complex conjugates of the tensor moments are given by

$$a_{LM}(K'j', Kj)^* = (-)^{j'-j+M} a_{L, -M}(Kj, K'j'). \quad (5.8)$$

In the sum (5.7), the matrix elements of ρ vanish outside the two-dimensional submatrix with $\mu' = \pm 1$, $\mu = \pm 1$. Therefore, only the same submatrices of the standard tensors $T_{LM}(K'j', Kj)$ are needed for evaluation of the sum. Those submatrices have been evaluated, using (5.1), for small values of j and j' . They are listed in Table I, with the notation (4.5). The values of L and M are restricted by (5.1) to $|j' - j| \leq L \leq j' + j$ and $M = \mu' - \mu = 0, \pm 2$. The numerical values of the nonvanishing matrix elements are shown by (5.1) to be independent of K and K' .

TABLE I.

Values of All the Nonvanishing Standard Tensors $\langle K'j', \mu' | T_{LM}(K'j, Kj) | Kj, \mu \rangle$ in the Subspace $\mu' = \pm 1, \mu = \pm 1$, for $j + j' \leq 3$. The Notations $1, \sigma_z, \sigma_+, \sigma_-$ are defined in Eq. (4.5).

| L | M | $j' = 1, j = 1$ | $j' = 2, j = 1$ | $j' = 1, j = 2$ |
|-----|-----|------------------------|-------------------------|-------------------------|
| 0 | 0 | $(1/3)^{1/2} 1$ | 0 | 0 |
| 1 | 0 | $(1/2)^{1/2} \sigma_z$ | $(3/10)^{1/2} 1$ | $-(3/10)^{1/2} 1$ |
| 2 | 0 | $(1/6)^{1/2} 1$ | $(1/2)^{1/2} \sigma_z$ | $-(1/2)^{1/2} \sigma_z$ |
| 2 | 2 | σ_+ | $-(1/3)^{1/2} \sigma_+$ | $-(1/3)^{1/2} \sigma_+$ |
| 2 | -2 | σ_- | $(1/3)^{1/2} \sigma_-$ | $(1/3)^{1/2} \sigma_-$ |
| 3 | 0 | 0 | $(1/5)^{1/2} 1$ | $-(1/5)^{1/2} 1$ |
| 3 | 2 | 0 | $(2/3)^{1/2} \sigma_+$ | $-(2/3)^{1/2} \sigma_+$ |
| 3 | -2 | 0 | $(2/3)^{1/2} \sigma_-$ | $-(2/3)^{1/2} \sigma_-$ |

TABLE II.

Nonvanishing Tensor Moments of the Density Matrices for Unpolarized, Circular-Polarized, and Plane-Polarized Photons of $E1, M1$, and $E2$ Multipolarities. All Nonvanishing Tensor Moments for $j + j' \leq 3$ are Given. An Asterisk in the Last Column Indicates that the Tensor Moment Has Natural Parity i.e., Parity Equal to $(-)^L$.

| Tensor moments | Polarization states | | | | | Natural parity ? |
|------------------------------------|-------------------------|----------------|----------------|----------------|-----------------|------------------|
| | Unpolarized ρ_u | Circular | | Plane | | |
| | | ρ_1 | ρ_{-1} | ρ_x | ρ_y | |
| $a_{00}(E1,E1) = a_{00}(M1,M1)$ | $(1/3)^{1/2}$ | $(1/3)^{1/2}$ | $(1/3)^{1/2}$ | $(1/3)^{1/2}$ | $(1/3)^{1/2}$ | * |
| $a_{00}(E1,M1) = a_{00}(M1,E1)$ | 0 | $(1/3)^{1/2}$ | $-(1/3)^{1/2}$ | 0 | 0 | |
| $a_{10}(E1,E1) = a_{10}(M1,M1)$ | 0 | $(1/2)^{1/2}$ | $-(1/2)^{1/2}$ | 0 | 0 | |
| $a_{10}(E1,M1) = a_{10}(M1,E1)$ | $(1/2)^{1/2}$ | $(1/2)^{1/2}$ | $(1/2)^{1/2}$ | $(1/2)^{1/2}$ | $(1/2)^{1/2}$ | * |
| $a_{10}(E2,E1) = -a_{10}(E1,E2)$ | $(3/10)^{1/2}$ | $(3/10)^{1/2}$ | $(3/10)^{1/2}$ | $(3/10)^{1/2}$ | $(3/10)^{1/2}$ | * |
| $a_{20}(E1,E1) = a_{20}(M1,M1)$ | $(1/6)^{1/2}$ | $(1/6)^{1/2}$ | $(1/6)^{1/2}$ | $(1/6)^{1/2}$ | $(1/6)^{1/2}$ | * |
| $a_{20}(E1,M1) = a_{20}(M1,E1)$ | 0 | $(1/6)^{1/2}$ | $-(1/6)^{1/2}$ | 0 | 0 | |
| $a_{20}(E2,E1) = -a_{20}(E1,E2)$ | 0 | $(1/2)^{1/2}$ | $-(1/2)^{1/2}$ | 0 | 0 | |
| $a_{22}(E1,E1) = a_{2,-2}(E1,E1)$ | 0 | 0 | 0 | $-1/2$ | $1/2$ | * |
| $a_{22}(M1,M1) = a_{2,-2}(M1,M1)$ | 0 | 0 | 0 | $1/2$ | $-1/2$ | * |
| $a_{22}(E1,M1) = a_{2,-2}(M1,E1)$ | 0 | 0 | 0 | $1/2$ | $-1/2$ | |
| $a_{22}(M1,E1) = a_{2,-2}(E1,M1)$ | 0 | 0 | 0 | $-1/2$ | $1/2$ | |
| $a_{22}(E2,E1) = a_{2,-2}(E1,E2)$ | 0 | 0 | 0 | $(1/12)^{1/2}$ | $-(1/12)^{1/2}$ | |
| $a_{22}(E1,E2) = -a_{2,-2}(E2,E1)$ | 0 | 0 | 0 | $(1/12)^{1/2}$ | $-(1/12)^{1/2}$ | |
| $a_{30}(E2,E1) = -a_{30}(E1,E2)$ | $(1/5)^{1/2}$ | $(1/5)^{1/2}$ | $(1/5)^{1/2}$ | $(1/5)^{1/2}$ | $(1/5)^{1/2}$ | * |
| $a_{32}(E2,E1) = -a_{3,-2}(E1,E2)$ | 0 | 0 | 0 | $-(1/6)^{1/2}$ | $(1/6)^{1/2}$ | * |
| $a_{32}(E1,E2) = -a_{3,-2}(E2,E1)$ | 0 | 0 | 0 | $(1/6)^{1/2}$ | $-(1/6)^{1/2}$ | * |

The tensor moments $a_{LM}(K'j', Kj)$ can now be evaluated by using Eq. (5.5) and Table I. That has been done for the five polarization states whose density matrices are given in Section IV. The results for $j + j' \leq 3$ are listed in Table II.

From (3.7) and (4.1) it can be seen that the density matrix elements $\langle Ej', \mu' | \rho | Ej, \mu \rangle$ and $\langle Mj, \mu | \rho | Mj', \mu' \rangle$ have parity $(-)^{j+j'}$, while $\langle Ej', \mu' | \rho | Mj, \mu \rangle$ and $\langle Mj', \mu' | \rho | Ej, \mu \rangle$ have parity $(-)^{j+j'+1}$. The tensor moments $a_{LM}(K'j', Kj)$, which are linear combinations of density matrix elements with the same $(K'j', Kj)$, follow the same rule. The last column of Table II has an asterisk in cases of "natural parity," i.e., parity equal to $(-)^L$. The natural parity coefficients are the only ones which contribute to one-electron angular distribution, because for one electron, the parity of Y_{LM} is the angular distribution is equal to $(-)^L$.

VI. ANGULAR DISTRIBUTION OF ONE ELECTRON

The normalized angular distribution of an electron ejected from an atom or a molecule is denoted by $I(\theta, \phi)$.

$$I(\theta, \phi) = \sum_{L, M} b_{LM} Y_{LM}(\theta, \phi) \quad (6.1)$$

$$b_{00} = \frac{1}{(4\pi)^{1/2}} \quad (6.2)$$

$$b_{L, -M} = (-)^M b_{LM}^* \quad (6.3)$$

The angular distribution is a scalar linear function of the photon density matrix ρ ; linear because a statistical mixture of photon states must give the same statistical mixture of the resulting angular distributions, and scalar because rotation (or space inversion) of the initial state must result in the same rotation (or space inversion) of the angular distribution. The most general scalar linear function is expressed by

$$b_{LM} = \sum_{Kj, K'j'} G_L(K'j', Kj) a_{LM}(K'j', Kj), \quad (6.4)$$

where the scalar coefficients $G_L(K'j', Kj)$ depend upon the dynamics of the system, but not upon the photon density matrix ρ .

Assumption (6.4) relies upon all of the following conditions:

I. The target atoms or molecules are oriented at random, so that the density matrix for the target is invariant under rotation.

II. External fields, as in a crystal, may be neglected.

III. In the detection of the electron, all selection criteria other than the angles (θ, ϕ) are invariant under rotation. Thus if several electrons are ejected, selection according to energy or time is permitted, but requiring a second electron to be ejected in a particular direction is not permitted.

The assumed invariance under space inversion implies that $G_L(K'j', Kj)$ must vanish for cases of unnatural parity, because b_{LM} in (6.1) has parity $(-)^L$.

The dynamical coefficients $G_L(K'j', Kj)$ are subject to certain general restrictions. For instance, the Hermitian condition (5.8), combined with (6.3) gives

$$G_L(K'j', Kj) = (-)^{j'-j} G_L(Kj, K'j')^*. \quad (6.5)$$

Obviously, the $G_L(K'j', Kj)$ must also be restricted to give $I(\theta, \phi) \geq 0$ for every photon density matrix ρ .

If it is assumed that electric-dipole absorption is the dominant process and that all multipole contributions may be neglected except pure $E1$, pure $M1$, and the interference terms $E1 \cdot M1^*$ and $E1 \cdot E2$, then the tensor moments listed in Table II determine all the nonvanishing angular-distribution coefficients b_{LM} , through (6.4). Those coefficients are displayed in Table III, for each of the five polarization states, using the notation

$$\begin{aligned} B_1 &= B_1^* \equiv \text{Re} \{ \sqrt{2} G_1(M1, E1) + (6/5)^{1/2} G_1(E2, E1) \} \\ B_{2E} &= B_{2E}^* \equiv (1/6)^{1/2} G_2(E1, E1) \\ B_{2M} &= B_{2M}^* \equiv (1/6)^{1/2} G_2(M1, M1) \\ B_3 &= B_3^* \equiv (4/5)^{1/2} \text{Re} \{ G_3(E2, E1) \}. \end{aligned} \quad (6.6)$$

Table III summarizes what can be said about the angular distribution of one electron, under the assumption that only the lowest multipole states contribute to the absorption of the light and with no additional dynamical assumptions. Pure electric-dipole radiation gives rise to a one-parameter angular distribution involving only Y_0 and Y_2 . Polarization of the light gains no qualitatively new information, but plane polarization doubles the relative strength of the Y_2 contribution and rotates it. Specifically, for pure electric-dipole absorption,

$$I_u(\theta, \phi) = I_{\pm 1}(\theta, \phi) = \frac{1}{4\pi} + B_{2E}(5/16\pi)^{1/2} [3 \cos^2 \theta - 1] \quad (6.7)$$

$$I_x(\theta, \phi) = \frac{1}{4\pi} - 2B_{2E}(5/16\pi)^{1/2} [3 \cos^2 \theta_x - 1], \quad (6.8)$$

TABLE III.

Angular Distribution Coefficients, Defined by $I(\theta, \phi) = \sum b_{l,M} Y_{l,M}(\theta, \phi)$, for one electron. The Dynamical Coefficients B Are Defined through Eqs. (6.4) and (6.6).

| Coefficient | Polarization state | | | | |
|---------------------|-------------------------|-------------------|-------------------|--------------------------------|--------------------------------|
| | Unpolarized ρ_u | Circular | | Plane | |
| | | ρ_1 | ρ_{-1} | ρ_x | ρ_y |
| b_{00} | $(1/4\pi)^{1/2}$ | $(1/4\pi)^{1/2}$ | $(1/4\pi)^{1/2}$ | $(1/4\pi)^{1/2}$ | $(1/4\pi)^{1/2}$ |
| b_{10} | B_1 | B_1 | B_1 | B_1 | B_1 |
| b_{20} | $B_{2E} - B_{2M}$ | $B_{2E} + B_{2M}$ | $B_{2E} + B_{2M}$ | $B_{2E} + B_{2M}$ | $B_{2E} + B_{2M}$ |
| $b_{22} - b_{2,-2}$ | 0 | 0 | 0 | $(3/2)^{1/2}(B_{2M} - B_{2E})$ | $(3/2)^{1/2}(B_{2E} - B_{2M})$ |
| b_{30} | B_3 | B_3 | B_3 | B_3 | B_3 |
| $b_{32} - b_{3,-2}$ | 0 | 0 | 0 | $-(5/6)^{1/2} B_3$ | $+(5/6)^{1/2} B_3$ |

where θ_x is the polar angle with respect to the x -axis. The nonnegativity condition for pure electric-dipole absorption follows from* (6.8).

$$-1 \leq (20\pi)^{1/2} B_{2E} \leq \frac{1}{2}. \quad (6.9)$$

It can be seen in the examples of Table II, and it is true in general, that circular polarization has no effect upon the natural-parity coefficients, which are the only ones relevant to the angular distribution of one electron.

If all contributions are neglected other than those appearing in (6.6), then Table III shows that the coefficient of Y_1 measures a mixture of $E1 \cdot M1$ and $E1 \cdot E2$ interference, and the coefficient of Y_3 measures only the $E1 \cdot E2$ interference. These terms have no first-order effect on the coefficient of Y_2 , which measures the pure electric- or pure magnetic-dipole absorption. Polarization has no effect upon the $E1 \cdot M1$ term. Plane polarization enhances the $E1 \cdot E2$ term by a factor $[1 + 2 \times (5/6)]^{1/2} \approx 1.6$, and changes its shape. Specifically, the Y_3 term for unpolarized light is proportional to $\cos \theta [\cos^2 \theta - \frac{1}{3}]$, while for xz plane polarization that factor becomes $2 \cos \theta_x [\frac{1}{3} - \cos^2 \theta_x]$.

VII. TWO-ELECTRON ANGULAR DISTRIBUTIONS

The results of Section VI apply to the angular distribution $I(\theta, \phi)$ of any polar vector in the final state. That vector could, for instance, be the momentum of one electron selected for its energy, the total momentum of all electrons, or the difference between two momenta. Only the values of the dynamical G coefficients depend upon which polar vector is chosen. (For

* It has not been proved here that (6.9) is the tightest possible restriction. In fact, it is,

an axial vector, such as $\mathbf{p}_1 \times \mathbf{p}_2$ for two electrons, the parity selection rules are changed.)

One way to express a two-electron angular distribution is

$$I(\theta_1, \phi_1, \theta_2, \phi_2) = \sum_{L, M, l_1, l_2} C_{LM}(l_1, l_2) V_{LM}(l_1, l_2). \quad (7.1)$$

$$V_{LM}(l_1, l_2) \equiv \sum_{m_1} C(l_1, l_2, L; m, M - m_1, M) \times Y_{l_1 m_1}(\theta_1, \phi_1) Y_{l_2, M - m_1}(\theta_2, \phi_2) \quad (7.2)$$

The moments C_{LM} are then related to the tensor moments $a_{LM}(K'j', Kj)$ of the photon density matrix through

$$C_{LM}(l_1, l_2) = \sum_{K'j', Kj} G_L(K'j', Kj, l_1, l_2) a_{LM}(K'j', Kj). \quad (7.3)$$

Assumption (7.3) relies upon all the conditions of Section VI, except that $(\theta_1, \phi_1, \theta_2, \phi_2)$ replaces (θ, ϕ) in condition III. The dynamical G coefficients may depend upon the scalars (energy or time of emission) of the two electrons considered separately, but not upon the angle between the momenta of the two electrons.

The coefficient $C_{LM}(l_1, l_2)$ has parity $(-)^{l_1+l_2}$. Therefore, the tensor moments of unnatural parity $(-)^{L+1}$ can influence the two-particle angular distribution, and polarization can provide information which would otherwise be unavailable. In particular, it is apparent from (7.3) and Table II that $G_1(E1, E1, l_1, l_2)$ can be measured only with circular polarization, $G_3(E1, E2, l_1, l_2)$ only with plane polarization, and $G_2(E1, M1, l_1, l_2)$ and $G_2(E1, E2, l_1, l_2)$ only with plane or circular polarization. Whether these G coefficients provide qualitatively new dynamical information depends, of course, upon the dynamical model.

Acknowledgment

This article was written during my stay at the Weizmann Institute of Science, for whose hospitality I am most grateful.

References

1. H. A. Bethe, *Handbuch der Physik*, Vol. 24, Springer, Berlin, 1933, pp. 483-484. J. Cooper and R. N. Zare, *J. Chem. Phys.*, **48**, 942 (1968). J. C. Tully, R. S. Berry, and B. J. Dalton, *Phys. Rev.*, **176**, 95 (1968). J. W. Cooper and S. T. Manson, *Phys. Rev.*, **177**, 157 (1969).
2. The notation in angular-momentum matters is that of M. E. Rose, *Elementary Theory of Angular Momentum*, Wiley, New York, 1957.
3. H. A. Bethe and E. E. Salpeter, *Quantum Mechanics of One- and Two-Electron Atoms*, Springer, Berlin, 1957, pp. 310-311.
4. The notation in density-matrix matters is that of U. Fano, *Rev. Mod. Phys.*, **29**, 74 (1957).

ELECTRON-IMPACT SPECTROMETRY

SANDOR TRAJMAR,*† JAMES K. RICE,† AND
 ARON KUPPERMANN†

*California Institute of Technology
 Pasadena, California*

CONTENTS

| | |
|---|----|
| I. Introduction | 15 |
| II. Historical Development | 19 |
| III. Experimental | 21 |
| A. Pressure Dependence | 24 |
| B. Effective Path Length Correction | 26 |
| C. Energy Independent Electron Optics | 26 |
| VI. Electronic Excitation | 27 |
| A. Helium | 30 |
| B. Molecules | 41 |
| 1. Nitrogen | 42 |
| 2. Carbon Monoxide | 48 |
| 3. Hydrogen | 51 |
| 4. Acetylene | 56 |
| 5. Ethylene | 61 |
| C. Summary | 67 |
| V. Vibrational-Rotational Excitation | 70 |
| VI. Superelastic Scattering | 83 |
| VII. Positron Scattering | 86 |
| References | 86 |

I. INTRODUCTION

The collision of an electron with an isolated atom or molecule can have a number of outcomes. Among them are the transfer of translational energy, electron exchange, excitation or deexcitation of internal states of the target, ionization, negative ion formation, molecular fragmentation, or a combination of several of these. For any case, the quantity which charac-

* Jet Propulsion Laboratory. Work supported in part by the National Aeronautics and Space Administration under Contract No. NAS 7-100.

† A. A. Noyes Laboratory of Chemical Physics, Contribution No. 3814. Work supported in part by the U.S. Atomic Energy Commission, Report Code CALT 767P4-50.

terizes the scattering process is known as the cross section. Phenomenologically, the cross section for the occurrence of a certain type of event during a collision is equal to the number of these events per unit time per target particle divided by the current density (particles per unit time per unit area) of incident electrons relative to the target.¹ As a consequence of this definition, the cross section has the units of area per target particle.

For the particular process in which an electron collides with a stationary target and then scatters into a given direction (defined by spherical polar angles θ , ϕ), the cross section per unit solid angle is called the "differential scattering cross section" (hereafter abbreviated as DCS) and has the units of area per unit solid angle per target particle. The corresponding "total cross section" is the integral of the DCS over all scattering directions θ , ϕ . If we define a spherical polar coordinate system whose z axis lies along the incident beam direction, then the scattering angle θ is the colatitude of this coordinate system and ϕ is the azimuth (or longitude) measured with respect to an arbitrary reference plane containing the z axis. If the target particles are randomly oriented with respect to the incident beam direction, then the DCS will not depend on ϕ .

Electron-impact spectrometry is concerned with the excitation of atoms and molecules and therefore with the measurement of the energy lost by the electron during the scattering process. In essence, the experimental method most often used involves the production of a monochromatic beam of electrons (incident beam), the passage of this beam through a gaseous sample of the target particles, and the measurement of the scattered electron intensity as a function of the incident electron energy, scattering angle, and energy loss (the kinetic energy lost by the incident electron through an inelastic collision). In elastic or inelastic scattering of electrons, a small part δE of an electrons' kinetic energy E in the laboratory system is transformed into laboratory kinetic energy of the target. Namely, for elastic scattering,

$$\frac{\delta E}{E} \cong \frac{4m}{M} \sin^2 \frac{\theta}{2} \quad (1)$$

and for inelastic scattering

$$\frac{\delta E}{E} \cong \frac{2m}{M} \left[1 - \frac{W}{2E} - \left(1 - \frac{W}{E} \right)^{1/2} \cos \theta \right]. \quad (2)$$

M and m are the mass of the target and electron, respectively; θ is the scattering angle, and W is the energy lost by the incident electron into the internal states of the target. These equations can be derived from the

conservation of total energy and momentum during the collision.⁵³ (For electronic excitation in the energy ranges discussed here, $\delta E \sim 10^{-3}$ eV and for vibrational excitation, $\delta E \sim 10^{-2}$ eV).

This paper deals with the limited area of low-energy electron-impact spectrometry in the 5 to 100 eV incident electron energy range. These energies are comparable to the binding energies of valence electrons in molecules and represent a most important region as far as chemistry is concerned. We have not attempted a complete review of even this limited area, but will consider several illustrative examples which are of special interest to the authors. The phenomena of resonances and some other aspects of low-energy electron scattering will not be discussed. We will consider scattering theory only insofar as it is directly related to the evaluation of experimental data except for a more detailed summary of some new calculations¹¹⁹ for the excitation of nuclear motion (Section V). Detailed descriptions of the omitted subjects are available in the literature.²⁻¹⁰ A short historical background is given in Section II and the description of our electron-impact spectrometer and experimental procedures in Section III. Electronic excitation of He, H₂, N₂, CO, C₂H₂, and C₂H₄ will be discussed in Section IV, while Section V deals with the vibrational excitation of the ground electronic state of H₂ and N₂.

It is of some interest to first summarize the important differences between optical and electron-impact spectroscopy.

(1) The probabilities of observing different excitations by means of optical spectroscopy are governed by fairly stringent selection rules. In electron-impact spectrometry at high energies (over 100 eV), the selection rules²⁵ closely resemble the optical ones and the cross sections are related to optical absorption coefficients. Many of the normal optical selection rules,¹¹ however, can be broken by the judicious choice of incident electron energy and scattering angle. In particular, low-energy electrons (within a few tens of electron volts of the excitation threshold) can be quite effective in causing transitions between states of different spin multiplicity through the mechanism of electron-exchange excitation. This exchange process involves the interchange of the incident electron and one of the bound ones. These transitions are highly forbidden under photon impact in the absence of appreciable spin-orbit coupling. In addition, the probability of producing transitions which are optically symmetry forbidden can often be dramatically increased by the use of low-energy electrons.

To illustrate these marked differences, Table I presents a comparison of relative optical transition probabilities with the ones obtained by electron impact for three transitions in helium. The relative probability of exciting the 2¹P level (optically-allowed transition) is taken as unity. The last two

TABLE I

A Comparison of Some Relative Electron-Impact Excitation Probabilities in Helium with Typical Optical Transition Probabilities. P_{opt} is the Relative Optical Excitation Probability; P_{elec}^T is the Relative Electron-Impact Excitation Probability for an Incident Energy of 35 eV; and $P_{\text{elec}}(\theta)$ is the Relative Probability for Electrons to Scatter at an Angle θ after Causing the Excitation for an Incident Energy of 35 eV

| Transition | Type according to optical selection rules | P_{opt} | P_{elec}^T | $P_{\text{elec}}(\theta)^f$ | |
|-------------------------|--|------------------------|---------------------|-----------------------------|---------------------|
| | | | | $\theta = 0^\circ$ | $\theta = 70^\circ$ |
| $1^1S \rightarrow 2^1P$ | Electric dipole allowed | 1 ^a | 1 ^a | 1 ^a | 1 ^a |
| $1^1S \rightarrow 2^1S$ | Electric dipole forbidden, electric quadrupole allowed | 10^{-5} – 10^{-8b} | 0.18 ^d | 0.40 | 0.21 |
| $1^1S \rightarrow 2^3P$ | Spin-forbidden, electric dipole allowed | $\sim 10^{-10c}$ | 0.12 ^e | 0.023 | 1.3 |

^a The relative probability of this transition is taken as unity.

^b Ref. 11a.

^c M. S. Yurev, *Opt. Spectry.*, **25**, 157 (1968).

^d D. R. Bates, A. Fundaminsky, J. W. Leech, and H. S. W. Massey, *Trans. Roy. Soc.*, **A243**, 93 (1950).

^e Ref. 69.

^f Ref. 71.

columns in the table give the relative probabilities for electrons which have caused a particular excitation to be scattered by a given angle θ .

(2) In conventional optical spectroscopy the process of excitation by photons is a resonance phenomena; that is, all of the energy of the photon is absorbed by the system and the photon is annihilated. In electron-impact excitation the electron loses only part of its kinetic energy (in analogy to Raman spectroscopy). This makes possible the observation of the scattered electron and the study of the energy and angular dependence of the DCS—two powerful sources of information that have no analogy in the optical case.

(3) In optical spectroscopy, it is much more difficult to measure atomic and molecular excitation corresponding to the extreme vacuum uv (wavelengths shorter than 500 Å) than to measure those corresponding to the visible region. In electron-impact spectroscopy, such a difference does not exist. In fact, the entire energy loss or excitation spectrum from ir to the uv can be covered by a single scan on the same instrument. To be sure, optical techniques offer some important advantages such as better resolution (about two or three orders of magnitude better in the visible region,

but comparable in the vacuum uv), the ability to work with solid and liquid samples, and a well-developed practical theory with which to interpret experimental results.

II. HISTORICAL DEVELOPMENT

In 1914 Franck and Hertz¹² initiated the field of electron-impact spectrometry with their classic experiments on the measurement of energy losses of electron swarms in atomic gases. However, it was not until 1927 that Dymond¹³ carried out the first measurements of the angular distribution of inelastically scattered electrons. At about this same time, Oppenheimer¹⁴ pointed out the possibility of an electron-exchange mechanism whereby optically spin-forbidden transitions could be produced. During the next few years, until the middle 1930's, the study of electron-impact phenomena reached a peak only to be followed by two decades of relative inactivity. A comprehensive review of this early work has been presented by Massey and Burhop.⁴

Since the late 1950's there has been a renewed and increasing interest in this field, due possibly to the development of more sophisticated experimental techniques and a heightened awareness of the importance of electron-molecule (atom) interactions in radiation chemistry, upper-atmosphere phenomena, and plasma physics. A recent review of electron impact phenomena is given by Massey and Burhop.⁵ Up-to-date bibliographies and reference surveys are available from two information centers.^{15,16}

At present there are essentially two methods used to study molecular excited states through electron-impact excitation and the detection of the scattered electrons. One method, introduced by Schulz¹⁷ and usually denoted the "trapped-electron" method, involves the use of an incident electron beam of variable kinetic energy E and the detection of only those electrons which have lost nearly all of their kinetic energy through single collisions with the target particles. If W is a particular molecular excitation threshold, then a scattered signal is obtained for $E \approx W$. This signal, which contains contributions from electrons scattered at all angles, is proportional to the total excitation cross section in the vicinity of the excitation threshold. Since total cross sections for optically-forbidden transitions are usually larger near threshold than those for allowed ones,¹⁷ the "threshold excitation spectra" obtained by this method are often dominated by spin- and symmetry-forbidden transitions.

This method has been applied to several systems by Schulz¹⁸ and Bowman and Miller.¹⁹ Recently, relatively high resolution data have been ob-

tained by Brongersma and Oosterhoff,²⁰ and Dowell and Sharp.²¹ However, the possibility of negative ion formation and the uncertainties in energy scale calibration and threshold behavior complicate the identification of the excited state.

An interesting variation of the threshold excitation method utilizes the fact that certain electron attachment or dissociative attachment reactions have sharply peaked cross sections at zero incident electron energy. Each electron that has lost almost all of its energy to excitation of a molecule produces a negative ion which can be detected by means of mass spectrometry²² or ion cyclotron resonance techniques.²³

The other electron scattering method involves the use of an incident electron beam of fixed (or variable) energy and the detection of electrons which have been scattered by single collisions with the target in a particular θ , ϕ direction (or range of angles) after undergoing a particular energy loss (W). Although it has been recognized for some time that the angular dependence of the scattered electron intensity for a particular energy loss is sensitive to the nature of the transition giving rise to it,^{4,24} very little data have yet been obtained about these distributions. Most of the experiments have been performed at fixed angles (or a fixed range of angles), usually near 0 or 90°.

Lassette and co-workers²⁵ were among the pioneers in the field of electron-impact spectrometry. The bulk of their work has been on relatively small molecules with incident electron energies above 200 eV and scattering angles below about 20°. The results of their early work generally agreed with optical absorption measurements and indicated the validity of the Born approximation at low scattering angles and high incident energies. Later, they extended their studies to lower impact energies and observed many optically-allowed and several symmetry-forbidden (quadrupole allowed) transitions.²⁶⁻³¹ At lower incident energies (30 to 60 eV) Skerbele, Dillon, and Lassette^{29,30} have resolved several singlet \rightarrow triplet transitions in both N₂ and CO. However, they pointed out that in a survey of 16 additional polyatomic molecules at incident energies as low as 35 eV, they failed to observe any singlet \rightarrow triplet transitions.^{29,30} The results of high angle experiments^{32-34,56} indicate that the restriction of their observations to small scattering angles was probably responsible for this failure. More recently, Lassette and co-workers published high-resolution electronic³⁵ and pure vibrational³⁶ excitation spectra of many molecules at impact energies between 33 and 100 eV and scattering angles up to 16°.

Several years ago, Simpson³⁷ constructed a high resolution, $\theta = 0^\circ$, electron-impact spectrometer. This instrument and a later version³⁸ (with variable angle) provided the basis for the design of our spectrometer. The

work of Simpson and co-workers with the 0° instrument has been confined to impact energies below 100 eV. Although their early investigations of He,³⁹ H₂,⁴⁰ and C₂H₄³⁹ did not reveal any singlet \rightarrow triplet transitions at impact energies as low as 30 eV, improvements in the apparatus led to the detection of several such transitions in He,⁴¹ N₂,⁴² and H₂.⁴³

Recently their variable angle instrument was used to measure the scattered electron distribution: ($\vartheta' < \theta < 20^\circ$) for three excitations in He at impact energies of 100 to 400 eV.⁴⁴ A large part of their work is presently directed toward the study of resonance phenomena and instrument design.

Kuppermann and Raff³² obtained energy-loss spectra for He, Ar, H₂, and C₂H₄ with impact energies on the order of 50 eV and an instrument geometry which collected electrons scattered in the range $22^\circ < \theta < 112^\circ$ (with 90° favored). Under these conditions, singlet \rightarrow triplet transitions were prominent features in the reported spectra. They were the first to detect triplet states by energy analysis of the scattered electrons. Recently Wei and Kuppermann^{32d} have improved this machine and extended the list of molecules studied with it.

Doering and Williams³³ have investigated the 90° scattering of low-energy electrons by He, N₂, C₂H₄, and C₆H₆ and observed several spin-forbidden transitions.

Recently Ehrhardt and co-workers⁴⁵ have put into operation an elegant electron-impact spectrometer in which the target is a molecular beam. This instrument has been used primarily for the study of resonances although the angular distribution (7 to 110°) of electrons causing the $1^1S \rightarrow 2^3S$ transition in helium and the vibrational excitation of H₂⁴⁶ have been measured in nonresonant regions. In the field of electron impact ionization, their experiments on simultaneous detection of both electrons and their energy and angular correlations represent a unique effort.⁴⁷

Finally, the $\theta=0^\circ$ energy-loss spectra of H₂,⁸⁵ N₂,⁴⁸ and C₂H₄⁵⁰ have been obtained at very high incident energies (~ 33 keV) with very good resolution (~ 0.03 eV) by Geiger and co-workers. Under these conditions (high energy, low angle), the Born approximation seems quite reliable and, as expected, these spectra are nearly identical with uv absorption spectra.

III. EXPERIMENTAL

A short description of the electron-impact spectrometer used by us will serve as an example to illustrate the requisite experimental apparatus and procedures. More details are available elsewhere.^{51,52} Figure 1 shows a

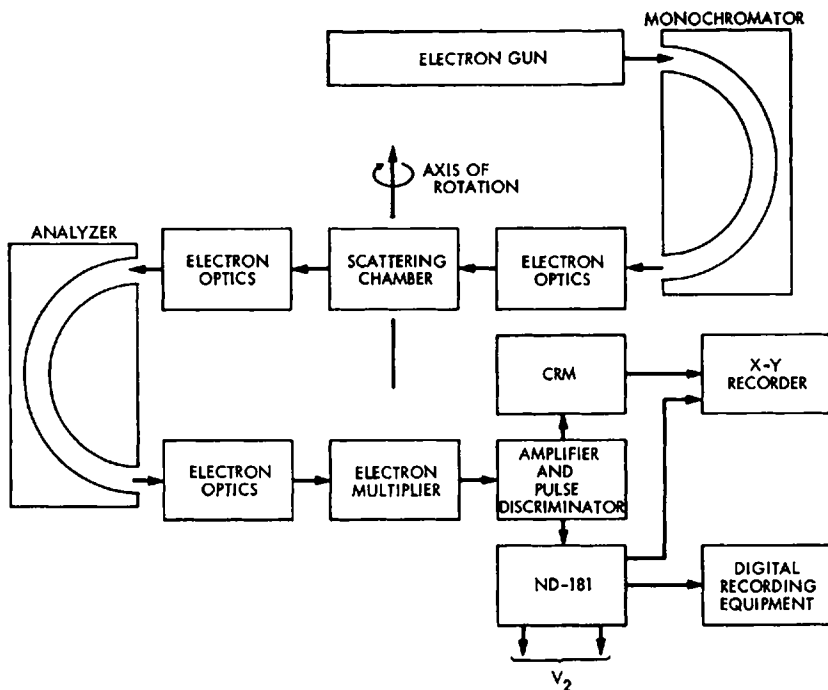


Fig. 1. Schematic diagram of the electron-impact spectrometer.

schematic diagram of the apparatus which is basically the same type as the one discussed by Simpson³⁷ and Kuyatt and Simpson.³⁸ It consists of an electron gun, a scattering chamber, two hemispherical electrostatic analyzers (for generating a monochromatic electron beam and analyzing the energy of the scattered electrons), and a detector. The resolution of each of the two electrostatic analyzers is variable from 0.030 to 0.300 eV by appropriately adjusting the sphere potentials. The scattering chamber is a welded-bellows cylinder which allows a variation in scattering angle from -30 to $+90^\circ$. The convolutions of the bellows have an "S" shape and form an electron trap that reduces the effect of wall scattering which could seriously interfere with measurements at high angles. The scattering chamber sample pressure is normally in the 10^{-5} to 10^{-2} Torr region. The detector is a 20-stage electron multiplier coupled to a count ratemeter or to a 1024-channel scalar system (Nuclear Data 181). An energy-selected electron beam with the required impact energy is introduced into the scattering chamber. Electrons that have lost a specific amount of energy and have undergone scattering by a specific angle are passed by the analyzer and

are detected. (The solid angle of collection is about 10^{-3} sr.) An analog signal V_2 (see Figure 1) generated by the scalar and synchronized with the memory advance is utilized to determine the energy loss of the electrons that will pass through the analyzer to the detector. A plot of the scattered signal intensity as a function of the sweep voltage (at a fixed scattering angle and electron-impact energy) represents an energy-loss spectrum. V_2 can also be used for sweeping the electron-impact energy (at a fixed scattering angle and energy loss) for the purpose of studying the energy dependence of a particular differential cross section. The sweeps can be repeated automatically until an acceptable signal-to-noise ratio is achieved.

This apparatus was designed for relative cross section measurements and is particularly suited for studying the variation of DCS with scattering angle and impact energy.

A schematic diagram of the scattering geometry is shown in Figure 2.

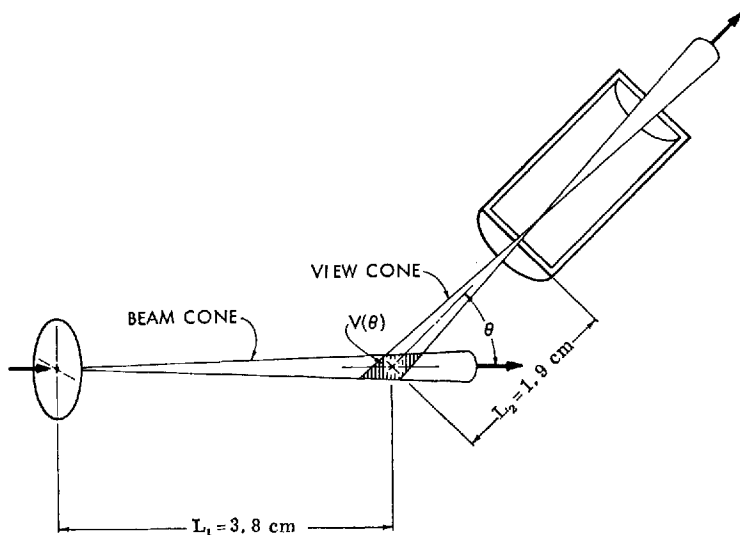


Fig. 2. Schematic diagram of the incident and scattered beam configuration at a scattering angle of $\theta \sim 45^\circ$. $V(\theta)$ is the volume in which single scattering events must occur if they are to be detected.

The scattered electron signal I_D that is measured in the laboratory can be related to the DCS by the following equation:⁵²

$$I_D(E_2, \theta) \simeq \frac{I_0 L(\theta)}{kT} \Delta\Omega P \exp(-P/P_0) \epsilon(E_2) \bar{S}(E, E_2, \theta) \quad (3)$$

with

$$\Delta\Omega \equiv \int_{\Omega} d\Omega \text{ (the acceptance solid angle),}$$

$$\bar{S}(E, E_2, \theta) \equiv \frac{1}{(\pi\Delta)^{1/2}} \int_W \sigma(E, W, \theta) \exp [-(E_2 - W)^2/\Delta^2] dW,$$

and

$$P_0 \equiv kT/[\bar{Q}(E)L_1 + \bar{Q}(E - E_2)L_2].$$

Here I_0 is the total beam intensity entering the scattering chamber, $L(\theta)$ is the "effective scattering path length" (see below), k is the Boltzmann constant, T is the absolute temperature of the target gas, P is its pressure, $\epsilon(E_2)$ is the overall efficiency of the apparatus for detecting electrons which after a collision have energy $E - W$, E is the electron-impact energy; $E_2 = |e|V_2$, Δ is related to the analyzer resolution, $\bar{Q}(E)$ is the average total scattering cross section, and $\sigma(E, W, \theta)$ is the DCS. Phenomenologically, P_0 is the pressure (for a given apparatus, incident energy, and scattering angle) for which the mean free path of an electron in the scattering chamber is equal to the length of that chamber.

There are several requirements one has to satisfy in order to be able to relate the signals measured at different angles, impact energies, and energy losses to the appropriate differential cross sections. Kuyatt⁵³ has reviewed several quantitative aspects of the measurement of electron scattering from a static gas target. Three especially pertinent considerations are discussed below.

A. Pressure Dependence

It has been pointed out⁵⁴ that double scattering events may cause serious errors in the measurement of DCS. This problem seems most severe for inelastic processes measured at large scattering angles and high incident energies. However, the demonstration that the pressure dependence indicated by Eq. (3) holds at every angle, for all incident energies, and for every process investigated is sufficient to insure that only single scattering events are contributing to the measured signal. Although such a complete study is indeed sufficient, it may not be necessary. It seems more "economical" to determine the particular experimental conditions for which double scattering would have the highest probability and then demonstrate that Eq. (3) holds in this case.

The principal contribution to double scattering usually comes from large-angle elastic scattering in or near the scattering volume $V(\theta)$ pre-

ceded, or followed, by small-angle inelastic scattering along the view cone. In particular, the current (I_2) due to electrons which have scattered twice compared to that (I_1) due to electrons which have scattered once varies approximately as⁵²

$$\frac{I_2(\theta)}{I_1(\theta)} \approx \frac{\rho l_{\text{eff}} \langle \sigma(E, 0, \theta') \sigma(E, W, \theta - \theta') \rangle_{\theta'}}{\sigma(E, W, \theta)} \quad (4)$$

where ρ is the density of the target molecules, $\sigma(E, W, \theta)$ is the differential cross section for the particular inelastic process being considered, $\sigma(E, 0, \theta)$ is that for the elastic one, and l_{eff} is an "average" scattering path length on the order of 5.7 cm (see Figure 2). $\langle \sigma(E, 0, \theta') \sigma(E, W, \theta - \theta') \rangle_{\theta'}$ is the product of DCS averaged over all possible combinations of scattering angles for the two events which would be detected as if from a single scattering event occurring within $V(\theta)$ at an angle θ .

At incident energies high enough for the Born approximation to be valid $\sigma(E, W, \theta)$ is much more sharply peaked forward than is $\sigma(E, 0, \theta)$.⁵⁵ The principal contribution to the average in (4) will come from terms in which $\theta - \theta' \approx 0$. Then

$$\frac{I_2(\theta)}{I_1(\theta)} \approx \rho l_{\text{eff}} \frac{\sigma(E, 0, \theta) \sigma(E, W, 0)}{\sigma(E, W, \theta)} \quad (5)$$

and double scattering becomes increasingly more important at higher scattering angles.⁵⁴

The situation is not so clear for impact energies below about 50 eV. Inelastic processes, though certainly less intense, do not seem to decrease much more rapidly with angle than the elastic one. For example, the ratio of elastic to inelastic ($\tilde{X}^1\Sigma_g^+ \rightarrow \tilde{C}^1\Pi_u$) scattering in acetylene was found to be constant from 40 to 80° at an impact energy of 35 eV.⁵⁶ In addition, spin-exchange inelastic processes are often nearly isotropic, and hence the ratio of elastic to inelastic scattering is actually largest at small angles.

For cases in which the elastic/inelastic ratio is nearly constant with angle, the value of the cross section product in (4) will be the same at both high and low θ' . If it is assumed that the principal contribution to the product is for $\theta' \approx 0$,

$$I_2(\theta)/I_1(\theta) \sim \rho l_{\text{eff}} \sigma(E, 0, 0). \quad (6)$$

Equation (6) implies, as expected, that double scattering will be least important in those instances for which the forward elastic DCS is lowest, regardless of the magnitude of the inelastic DCS. It also indicates that the effect is independent of angle.

Finally, there is the case of spin-exchange excitations in which $\sigma(E, W, \theta)$ can be assumed to be independent of angle but $\sigma(E, 0, \theta)$ is still forward peaked. The result (6) is also obtained under these conditions.

In conclusion, it seems that the relative effect of double scattering will not be highly angular dependent for low (< 50 eV) incident energies. Thus, checking relation (3) as a function of pressure at one high and one low angle for the most sharply forward peaked cross section should be sufficient. Parenthetically, Doering³³ did not observe double scattering effects at 90° scattering angles and 0.05 Torr sample pressures for low incident energies (of the order of 10–30 eV) while Chamberlain and co-workers⁵⁴ found such effects to be quite prominent at higher energies.

B. Effective Path Length Correction

It is apparent from Figure 2 that the scattering volume is a function of the scattering angle, and further that the solid angle of acceptance $\Delta\Omega$ is not constant over the length of the collision volume (it is a maximum at the volume center and vanishes at the ends). Therefore intensity measurements carried out at different scattering angles cannot be directly compared to each other. The matter is further complicated by the fact that the electron density of the incoming beam is not uniform.

The effective path length correction can be made by multiplying the signal at each angle by $\sin \theta$, provided that θ is much larger than the beam divergence angle. Otherwise a more accurate correction procedure has to be applied. Trajmar and co-workers⁵⁷ considered the incoming electron beam to be a cone with a Gaussian electron density distribution having its maximum along the cone axis. Two apertures at the exit of the scattering chamber define the view cone (Figure 2). Scattered electrons can reach the detector from the volume defined by the intersection of the two cones. The volume elements were weighed for electron density, and the solid angle subtended at the exit apertures and integrated within the limits defined by the intersecting cone surfaces. The measured intensities at each angle were then divided by the value of this integral to obtain a differential cross section on an arbitrary scale.

C. Energy Independent Electron Optics

Spectral features of the spectrum corresponding to different energy losses (and therefore to different molecular excitations) and spectra obtained at different impact energies can be related to each other only if the efficiency of the spectrometer is a known function of energy. Due to the extreme difficulty in actually measuring such a dependence, it is a practical necessity that the efficiency be independent of energy-loss (for a fixed

impact energy) or impact energy (for a fixed energy loss). By the proper design of electron optics, such a situation can obtain over a fairly wide energy range.

The cross sections in most experiments are obtained in arbitrary units. Only very few absolute measurements are available and they are almost exclusively total cross sections. There are several routes one can follow to obtain absolute DCS. The straightforward way of accurately measuring all the quantities required to normalize the cross section (beam current, scattered current, pressure, scattering geometry, and instrument efficiency) is very difficult. Another approach is to calculate or measure a particular absolute DCS for some gas and then utilize this to calibrate cross sections in other samples by mixing the two. This method requires knowledge of the partial pressures of the constituents under flow conditions. If absolute total cross sections are available (e.g., from excitation functions), a third way to calibrate the DCS measured in arbitrary units is to integrate it over θ and ϕ and normalize the integral to the known total cross section. To do this one needs DCS up to 180° or a reliable extrapolation beyond the angular range actually covered.⁴⁴ Several attempts are under way to measure absolute DCS directly.^{58,59} In our laboratory, a simple scattering apparatus is being assembled which will allow the measurement of the total scattered signal at 40 and 80° (without energy resolution) as well as the pressure, temperature, scattering geometry, and efficiency. The incoming electron beam will be energy selected. The information obtained by these measurements combined with spectra obtained by the high-resolution spectrometer will make it possible to normalize all cross sections to an absolute scale.

IV. ELECTRONIC EXCITATION

The excitation of atomic and molecular electronic states by electron impact and the concomitant measurement of the energy loss and direction of the scattered electron can provide information about optically-forbidden states that may not be available from any other method. In particular, a measurement of the energy loss determines the energy of the excited state and, in principle, the corresponding differential excitation cross section contains the information needed to characterize the electronic state of the target. For impact energies within a few electron volts of an excitation threshold, the DCS are often dominated by resonance scattering.^{9,10} Potential scattering by both direct and electron exchange mechanisms becomes increasingly more important at higher energies and predominates in the region (5 – 50 eV above threshold) to be discussed below. At still higher impact energies ($\gtrsim 100$ eV), exchange excitation becomes negligible.

The effective use of the DCS measurements in this intermediate energy range is hampered by the lack of adequate theoretical calculations. There are as yet no precise *ab initio* calculations for even the simplest system of an electron + H atom, and the first-order, high-energy Born and Born-Oppenheimer approximations and their many modifications⁶⁰ do not yield reliable results when applied at these intermediate energies.

Nevertheless, the primary difference between the angular distribution of electrons scattered after causing an optically spin-allowed transition and that due to electrons which cause a spin-forbidden one can be explained by applying the method of partial waves. This method involves the expansion of the total wave function in radial functions times spherical harmonics. If the possibility of exchange excitation is included, the desired radial functions are solutions of an infinite set of coupled integrodifferential equations.⁶¹

A more fruitful qualitative approach (though certainly less rigorous) is to treat the electron plus target scattering as if it were due to an effective central field potential. The differences between the direct excitation mechanism, leading to optically allowed transitions, and the exchange one, leading to spin-forbidden transitions, are then included through the use of effective potentials of different ranges. To see that these interactions are indeed quite different, consider the following example. In a three-electron system, the "potential"^{3a} leading to direct excitation is in some sense proportional to the electronic matrix element

$$V_D(\mathbf{r}_1) \propto \int \phi_n^*(\mathbf{r}_2, \mathbf{r}_3) \frac{1}{r_{12}} \phi_0(\mathbf{r}_2, \mathbf{r}_3) d\mathbf{r}_2 d\mathbf{r}_3 \quad (7)$$

while that for exchange is

$$V_{EX}(\mathbf{r}_1) \propto \int \phi_n^*(\mathbf{r}_1, \mathbf{r}_2) \frac{1}{r_{12}} \phi_0(\mathbf{r}_2, \mathbf{r}_3) d\mathbf{r}_2 d\mathbf{r}_3. \quad (8)$$

\mathbf{r}_3 , \mathbf{r}_2 , and \mathbf{r}_1 are the respective coordinates of the two initially bound electrons and the incoming one. ϕ_n and ϕ_0 are the final and initial bound state spatial wavefunctions, respectively, of the target, $r_{12} \equiv |\mathbf{r}_1 - \mathbf{r}_2|$. $1/r_{12}$ can be expanded as

$$\frac{1}{r_{12}} = \sum_{l=0}^{\infty} \frac{r_2^l}{r_1^{l+1}} P_l(\cos \theta_{12}) \quad \text{for } r_1 > r_2. \quad (9)$$

The $P_l(\cos \theta_{12})$ are Legendre polynomials and $\cos \theta_{12} = \mathbf{r}_1 \cdot \mathbf{r}_2 / r_1 r_2$. Substitution of (9) into (7) and (8) yields the asymptotic behaviors

$$V_D(\mathbf{r}_1) \underset{[r_1 \gg r_2, r_3]}{\sim} \frac{r_1}{r_1^2} \cdot \int \phi_n^*(\mathbf{r}_2, \mathbf{r}_3) r_2 \phi_0(\mathbf{r}_2, \mathbf{r}_3) d\mathbf{r}_2 d\mathbf{r}_3 + O\left[\frac{1}{r_1^3}\right] \quad (10)$$

and

$$V_{EX}(\mathbf{r}_1) \widetilde{[r_1 \gg r_2, r_3]} \frac{1}{r_1} \int \phi_n^*(\mathbf{r}_1, \mathbf{r}_2) \phi_0(\mathbf{r}_2, \mathbf{r}_3) d\mathbf{r}_2 d\mathbf{r}_3 \\ + \frac{\hat{r}_1}{r_1^2} \cdot \int \phi_n^*(\mathbf{r}_1, \mathbf{r}_2) \mathbf{r}_2 \phi_0(\mathbf{r}_2, \mathbf{r}_3) d\mathbf{r}_2 d\mathbf{r}_3 + O\left[\frac{1}{r_1^3}\right] \quad (11)$$

respectively, where \hat{r}_1 is a unit vector in the \mathbf{r}_1 direction. However,

$$\phi_n^*(\mathbf{r}_1, \mathbf{r}_2) \widetilde{[r_1 \gg r_2]} r_1^m \exp(-\alpha_n r_1) \chi^*(\mathbf{r}_2; \theta_1, \varphi_1) \quad (12)$$

since \mathbf{r}_1 is the coordinate of a bound electron in the excited state. Substitution of (12) into (11) yields

$$V_{EX}(\mathbf{r}_1) \widetilde{[r_1 \gg r_2, r_3]} r_1^{m-1} \exp(-\alpha_n r_1) \int \chi^*(\mathbf{r}_2; \theta_1, \varphi_1) \phi_0(\mathbf{r}_2, \mathbf{r}_3) d\mathbf{r}_2 d\mathbf{r}_3 \\ + O[r_1^{m-2} \exp(-\alpha_n r_1)]. \quad (13)$$

As a result $V_{EX}(\mathbf{r}_1)$ is of much shorter range than $V_D(\mathbf{r}_1)$ since the former decays exponentially while the latter decreases only as $1/r_1^2$. Thus if we apply the partial wave method rigorously to the problem of elastic scattering from a central potential, the angular dependence of the direct and exchange differential cross sections can be qualitatively explained in terms of the different effective ranges of the direct and exchange "potentials."

The well-known result for the differential cross section in the partial wave expansion representation is³

$$\sigma(k, \theta) = \frac{1}{4k^2} \left| \sum_{l=0}^{\infty} (2l+1) [\exp(2i\eta_l) - 1] P_l(\cos \theta) \right|^2. \quad (14)$$

k is the wave number of the incoming electron and η_l is the phase shift for the l th partial wave. If η_l is small, then it can be shown^{3b} that

$$\eta_l \cong -\frac{\pi}{2} \int_0^{\infty} U(r) [J_{l+1/2}(kr)]^2 r dr \quad (15)$$

where $U(r)$ is the electron-molecule interaction potential and $J_{l+1/2}$ is a Bessel function.

Suppose that $r^2 U(r)$ has an effective range r_{\max} and that within that range it never exceeds some finite value, i.e.,

$$\begin{aligned} r^2 |U(r)| &\leq a & 0 < r \leq r_{\max} \\ &= 0 & r_{\max} < r \end{aligned} \quad (16)$$

If the impact energy is low enough so that $kr_{\max}/2 \ll 1$, then the small argument form ⁶² of $J_{l+1/2}$ can be used in (15), the result being

$$\begin{aligned} |\eta_l| &\approx \frac{\pi}{2} \frac{a}{[\Gamma(l + \frac{1}{2})]^2} \int_0^{r_{\max}} \left(\frac{kr}{2}\right)^{2l+1} \frac{dr}{r} \\ &= \frac{2\pi a}{(2l+1)^3} \left(\frac{kr_{\max}}{2}\right)^{2l+1} \frac{1}{[\Gamma(l + \frac{1}{2})]^2} \end{aligned} \quad (17)$$

If η_l is small then (14) implies that

$$\sigma(k, \theta) \approx \frac{1}{k^2} \left| \sum_{l=0}^{\infty} (2l+1) \eta_l P_l(\cos \theta) \right|^2. \quad (18)$$

Each term in the expansion is called a "partial wave" and is often designated as an s , p , d , etc., wave depending on whether $l = 0, 1, 2$, etc.

Since the range of the interaction leading to excitation via a direct mechanism is much larger than that leading to excitation via exchange, many more η_l 's contribute to the DCS (18) in the former case, due to the r_{\max} term in (17). From the nature of Legendre polynomials, the more of them which are included in (18), the more sharply peaked toward $\theta = 0^\circ$ can be the differential cross section. Thus, we expect the angular distribution of electrons scattered after causing direct excitations to be relatively more forward peaked than that of electrons causing excitations via an exchange mechanism. Indeed, this has been found to be the case as shown below. Notice also that if k is lowered (lower impact energy), fewer η_l 's are required and both direct and exchange cross sections should become more isotropic. This also is observed experimentally.

A. Helium

The electron-impact excitation of helium has been the subject of a great many experimental and theoretical investigations.^{63,64} However, relatively few of these dealt specifically with the angular dependencies of inelastic DCS. Measurements at fixed scattering angles near $0^{25j,39,41}$ and 90° ^{32,33} over a wide range of incident electron energies disclosed significant differences in the relative DCS for optically-allowed and -forbidden transitions. It was generally found that the ratios of DCS for forbidden transitions to those for allowed ones were greater for lower impact energies at a fixed scattering angle and for larger scattering angles at a fixed incident energy. Although the basis for this behavior is qualitatively well understood, no theoretical calculations have yet proved completely reliable in predicting the shape of the various inelastic DCS below about 100 eV (nor above this

for exchange excitation⁴⁴). Silverman and Lassette⁶⁵ have shown that the Born approximation prediction of the total cross section for the $1^1S \rightarrow 3^1P$ transition is significantly in error below about 100 eV. Vriens, Simpson, and Mielczarek⁴⁴ have concluded that the Born approximation is not valid for predicting the DCS at $\theta \gtrsim 15^\circ$ below about 200 eV for the $1^1S \rightarrow 2^1P$ transition nor below 400 eV for the $1^1S \rightarrow 2^1S$ one. They also point out that the DCS for the $1^1S \rightarrow 2^3S$ transition decreases rapidly for angles greater than 5° at incident electron energies between 100 and 225 eV. According to Miller and Krauss,⁶⁶ this is in direct contradiction to the Born-Oppenheimer or Ochkur-Rudge exchange approximations. It is interesting to note, however, that the Ochkur-Rudge approximation apparently predicts nearly the correct shape (peak near $\theta = 90^\circ$) of the DCS for this transition at impact energies quite close to threshold.⁶⁷ This agreement is perhaps fortuitous since the Ochkur-Rudge approximation should work better at higher impact energies.

Truhlar and co-workers⁶⁸ have made a detailed comparison of the helium 2^1P DCS ($0-70^\circ$) with the predictions of several first-order theories (including exchange) at incident energies between 26.5 and 81.6 eV. The Born calculations generally agree in shape with the experimental DCS to about 40° for energies of 34 eV or greater. However, the calculated total 2^1P cross section is about twice as large as that measured by Jobe and St. John⁶⁹ in this intermediate energy range. A similar study of the 2^1S transition is presently underway.⁷⁰

Rice, Kuppermann, and Trajmar⁷¹ have noted marked differences in the angular and energy dependencies of the DCS ($0-70^\circ$) for excitation of the 2^3S , 2^1S , and 2^3P states of helium relative to that of the 2^1P one. Since such differences can provide a basis for determining the nature of transitions detected by electron-impact spectroscopy, they will be discussed below in some detail.

Figure 3 shows an energy-loss spectrum of helium at an impact energy of 34 eV and a scattering angle of 25° . The positions of the centers of the observed peaks are given in eV by the numbers labelled "obs." Those labelled "opt" were obtained from Moore's table⁷² of atomic energy levels (optical data).

Figure 4 shows three impact spectra of helium under identical conditions except for different scattering angles of 0 , 30 , and 60° .⁷¹ The four peaks in these spectra correspond to transitions from the 1^1S ground state to the 2^3S (spin- and symmetry-forbidden), 2^1S (symmetry-forbidden), 2^3P (spin-forbidden), and 2^1P (optically-allowed) states.

The sweep voltage in these experiments is equal to the energy loss and is unaffected by contact potentials. The electron-impact energy, however, is

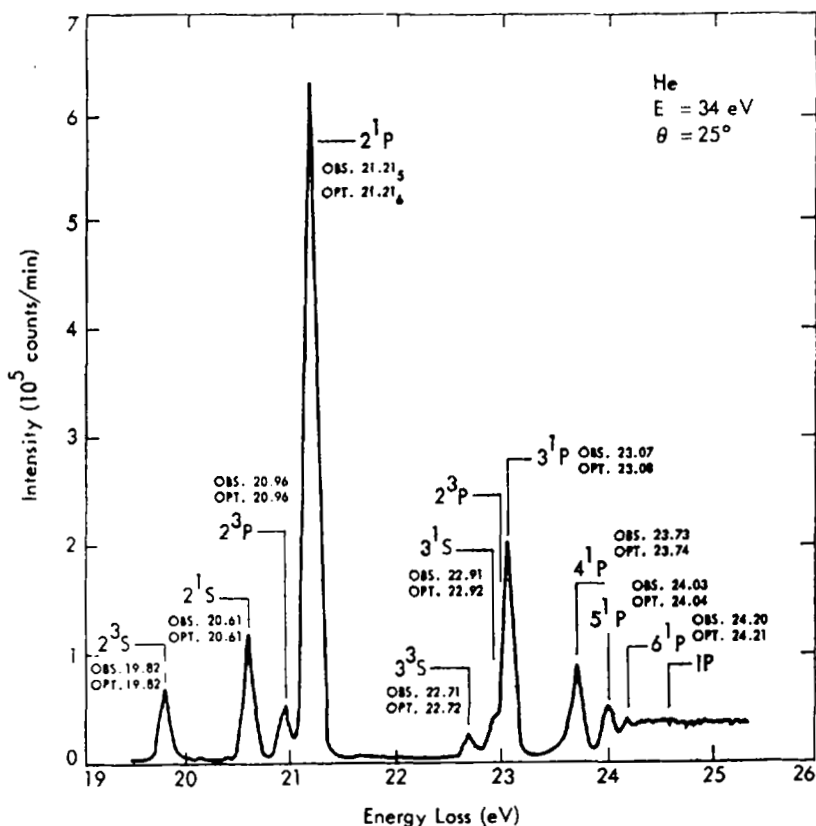


Fig. 3. Energy-loss spectrum of helium.

effected by a contact potential which is associated with the beam. This potential was determined experimentally for He by observing the 57.1 and 58.2 eV resonances,⁷³ and a correction to all quoted impact energies for helium has been applied.

Figures 5-8 contain plots of the $2^3S/2^1P$ and $2^3P/2^1P$ peak intensity ratios (and hence the DCS ratios) as a function of scattering angle for incident electron energies of 55.5, 44, 34, and 26.5 eV.⁵² In addition, Figure 7 includes the $3^3S/2^1P$ and $2^1S/2^1P$ intensity ratios. The $2^1S/2^1P$ ratios at the other energies are discussed fully elsewhere.⁷⁰ Table II compares the triplet/singlet ratios at $\theta = 0^\circ$ with those of Chamberlain and co-workers,⁴⁰ and indicates agreement with them.

Figures 9-12 show some of the measured DCS (in arbitrary units) at 55.5, 44, 34, and 26.5 eV, respectively. These data were obtained from the

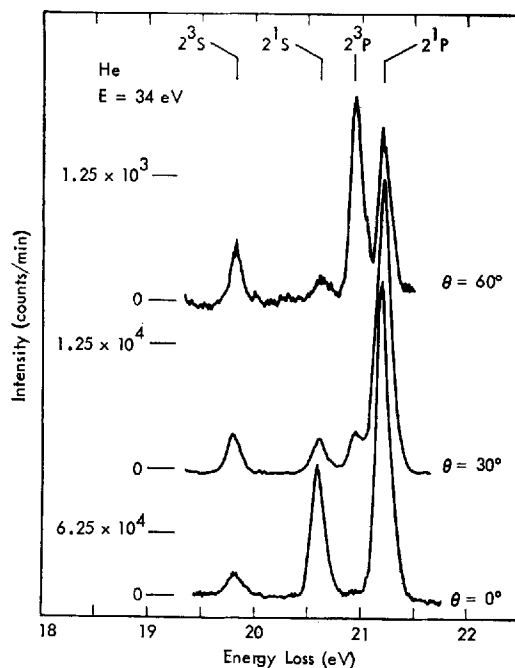


Fig. 4. Energy-loss spectra of helium at different scattering angles.

same energy-loss scans which were used to derive the ratio data of Table II and Figures 5–8.

The data in Figures 9–12 can be placed on an absolute scale (but only in an approximate way) by integrating the experimental distributions⁶⁸ and comparing them with total cross-section measurements.⁶⁹ The appropriate conversion factors are given in the figure captions.

Cartwright⁶⁷ has calculated the DCS for the $1^1S \rightarrow 2^3S$ and 2^3P transitions in helium using the Ochkur-Rudge (OR) method. Figures 13 and 14 show the experimental results of Rice, Kuppermann, and Trajmar⁵² and these calculations for two different impact energies. The agreement between the general magnitudes of the cross sections is remarkable but the lack of similarity in the shapes represents a definite failure of the OR approximation. At higher impact energies (100 to 225 eV) the deviations between the experimental shapes⁴⁴ and those predicted by the OR and Born-Oppenheimer approximations⁶⁶ become even more pronounced. Finally, Figure 15 shows the ratio of the DCS for excitation of the 2^3S state with respect to that of the 2^3P one according to the OR approximation⁶⁷ and from the experimental results of Rice.⁵² Again, the calculated

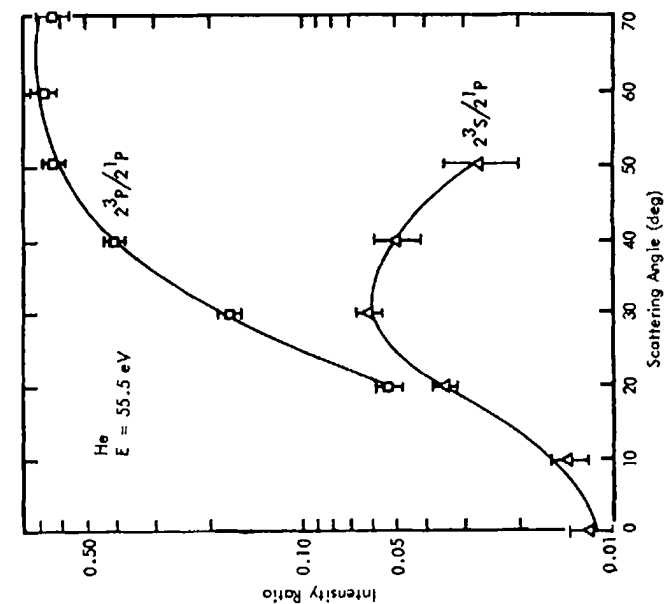


Fig. 5. Ratios of intensities of the $1^1S \rightarrow 2^3S$, and 2^3P transitions in helium to that of the $1^1S \rightarrow 2^1P$ transition as a function of scattering angle at $E = 55.5$ eV.

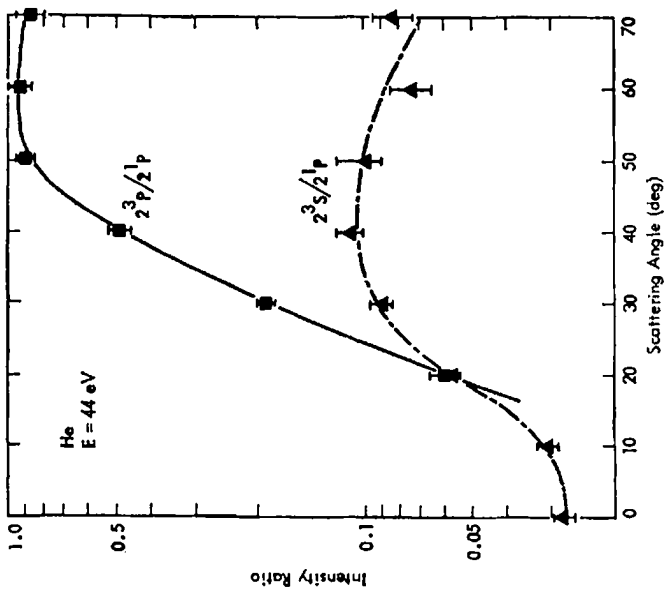


Fig. 6. Same as Fig. 5 except that $E = 44$ eV.

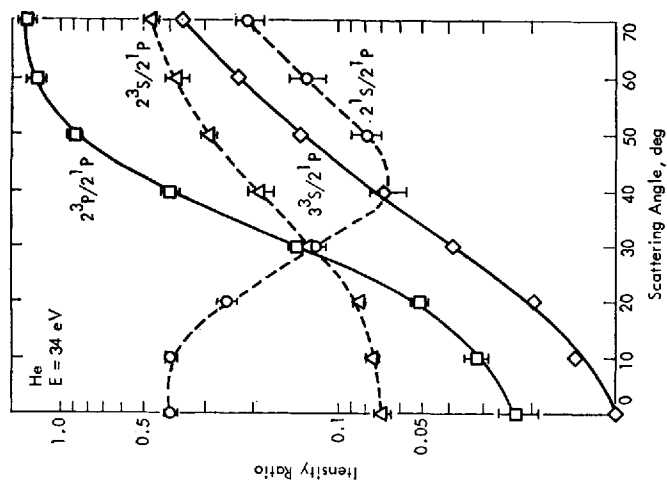


Fig. 7. Same as Fig. 5 except that the $1^1S \rightarrow 2^1S$ and 3^3S transition ratios are included and $E = 34$ eV.

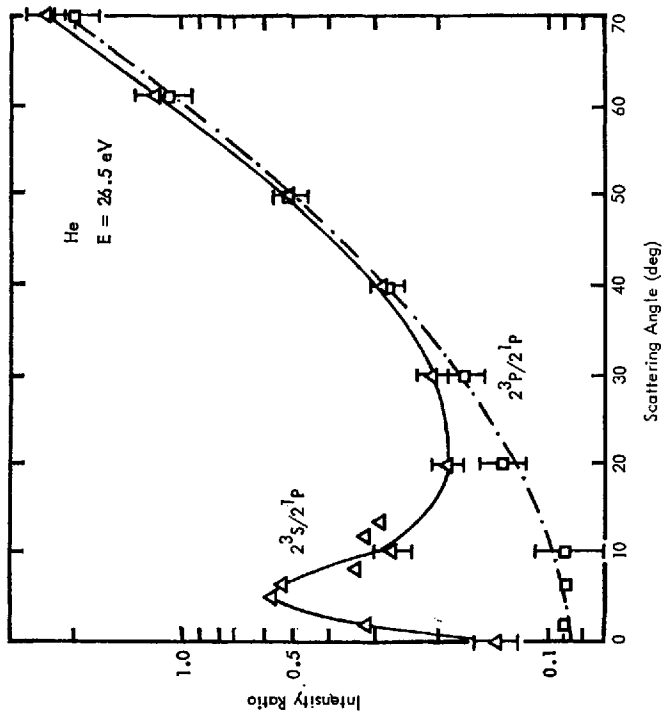


Fig. 8. Same as Fig. 5 except that $E = 26.5$ eV.

TABLE II.

Peak Intensity Ratios at $\theta = 0^\circ$ for Several Transitions in Helium. Column *a* Contains the Results of Rice, Kuppermann, and Trajmar⁵² and *b* the results of Chamberlain and Co-workers.⁴⁰ The Values in Column *b* Were Obtained by Plotting the Ratio Data of Ref. 40 as $\log_{10}(\text{ratio})$ versus Incident Energy and Fitting the points to a Smooth Curve. Reference 40 Gives No Error Estimates

| Incident energy (eV) | $(2^3S/2^1P) \times 100$ | | $(2^3P/2^1P) \times 100$ | |
|----------------------|--------------------------|----------|--------------------------|----------|
| | <i>a</i> | <i>b</i> | <i>a</i> | <i>b</i> |
| 55.5 | 1.2 ± 0.2 | 1 | — | 0 |
| 44 | 2.9 ± 0.2 | 3 | — | 0 |
| 34 | 7.0 ± 0.5 | 7 | 2.3 ± 0.4 | 2 |
| 26.5 | 14 ± 2 | 13 | 9 ± 2 | 7 |

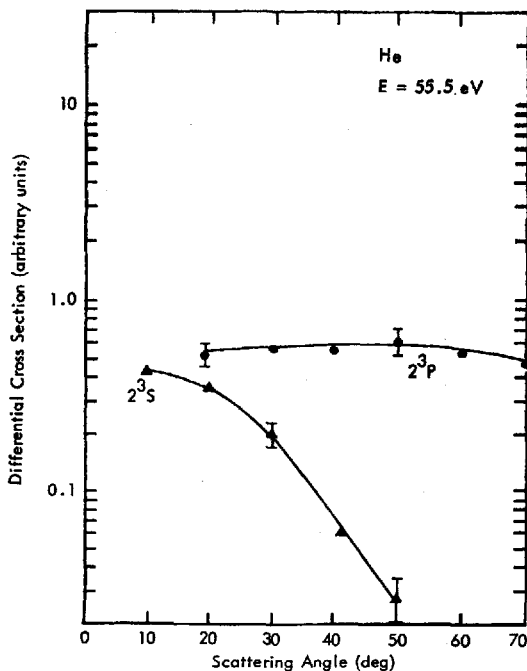


Fig. 9. DCS (arbitrary units) for excitation of the 2^3S and 2^3P states of helium from its 1^1S state. The data may be placed on an absolute scale (see text) by multiplying the DCS of this figure by $4.7 \times 10^{-3} \pi a_0^2/\text{ster}$.

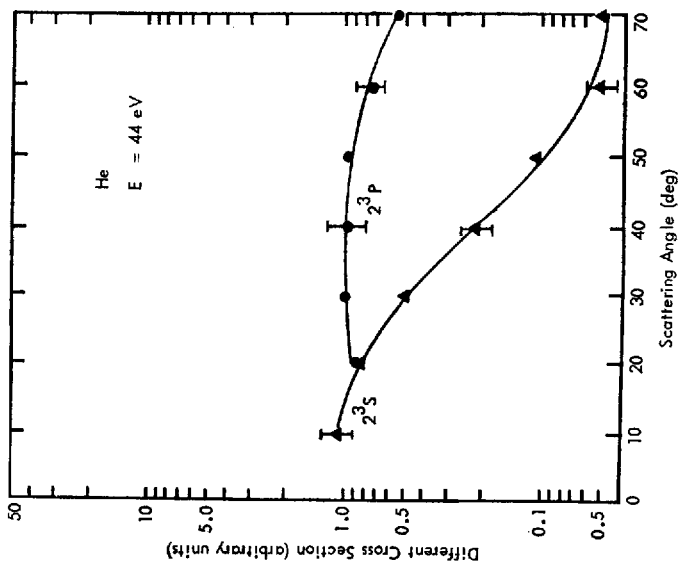


Fig. 10. Same as Fig. 9 except that $E = 44$ eV and the conversion factor $= 3.3 \times 10^{-3} \pi a_0^2/\text{ster.}$

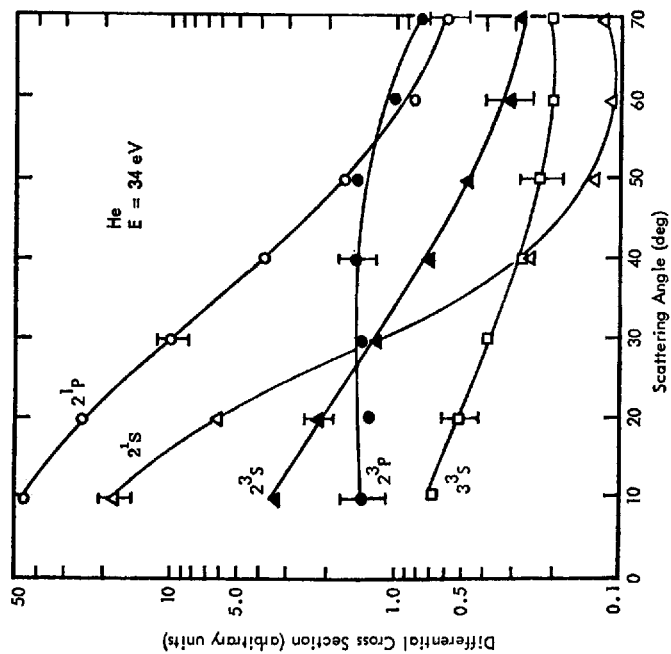


Fig. 11. Same as Fig. 9 except that $E = 34$ eV; the 2^3S , 2^1P , and 2^1S DCS are included, and the conversion factor $= 1.4 \times 10^{-3} \pi a_0^2/\text{ster.}$

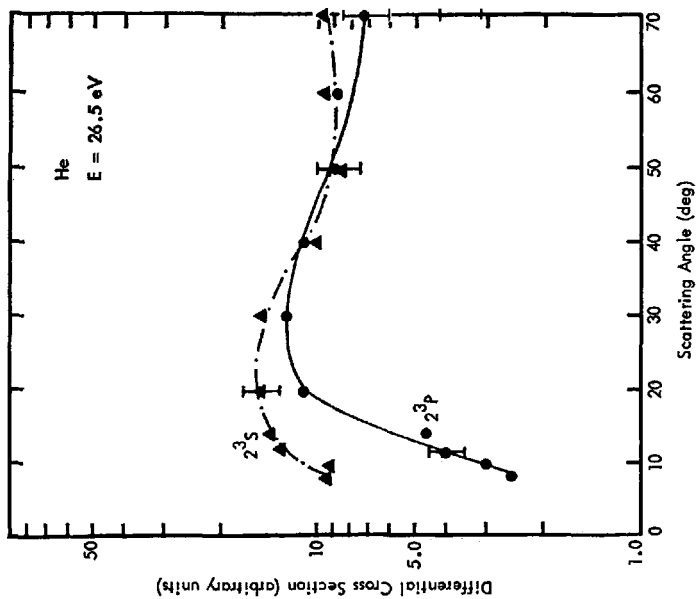


Fig. 12. Same as Fig. 9 except that $E = 26.5$ eV and the conversion factor $\approx 1.4 \times 10^{-4} \pi a_0^2/\text{ster}$.

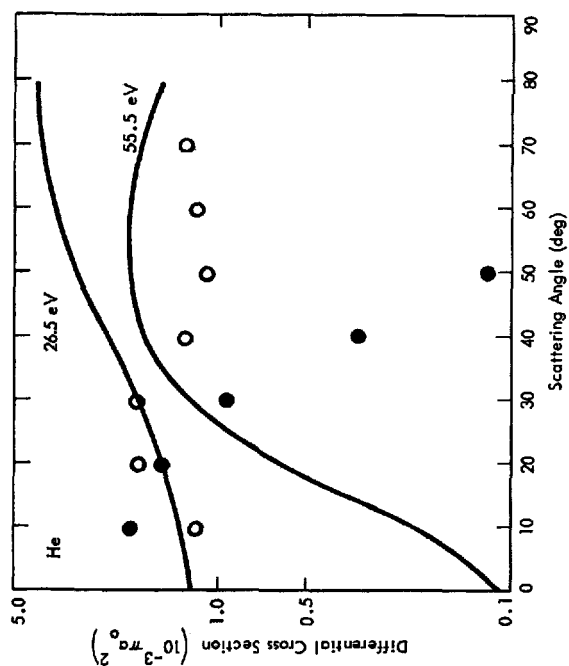


Fig. 13. The $1^1S \rightarrow 2^3S$ DCS for helium. The solid lines are theoretical and the points are experimental results for $E = 26.5$ eV (open circles) and at $E = 55.5$ eV (filled circles.)

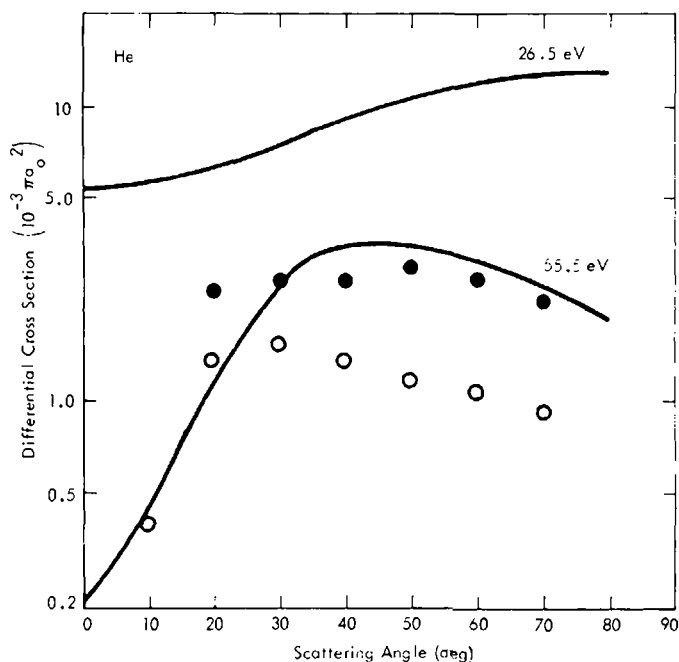


Fig. 14. $1^1S \rightarrow 2^3P$ DCS for helium. The solid lines are theoretical and the points are experimental results for $E = 26.5$ eV (open circles) and 55.5 eV (filled circles).

ratios are of the correct order of magnitude, but their variations with θ bear little resemblance to the experimental ones.

As mentioned earlier, a primary concern in electron-impact spectroscopy is to use electron-scattering data to determine the nature of a given transition (i.e., to determine whether it is spin- and/or symmetry-forbidden) for cases in which this information may not be available from optical studies. The inherent differences between the DCS for these transitions can be enhanced by studying the DCS ratios (rather than the DCS themselves as a function of angle. (Further, such a study eliminates one source of experimental error, the angle-dependent effective path length correction.) The most invariant ratio behavior with respect to changes of impact energy is that of the $2^3P/2^1P$ DCS ratio (spin-forbidden/optically-allowed), which increases by about two orders of magnitude from $\theta = 0$ to 70° at all energies studied. The variation of the $2^3S/2^1P$ DCS ratio (spin- and symmetry-forbidden/allowed) is less uniform with changes in the incident energy. Generally, this ratio increases with increasing angles, reaching a maximum which shifts to higher angles at lower incident energies. Its maximum increase over the 0 to 70° angular range is usually significantly

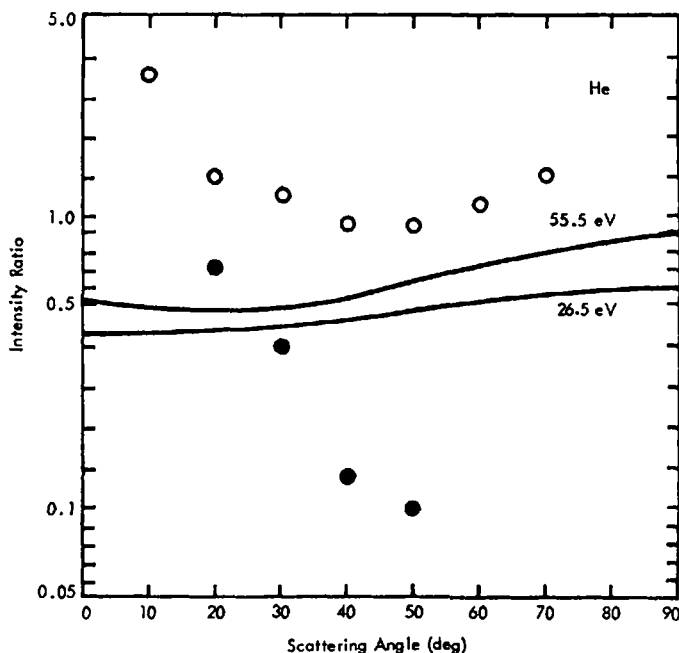


Fig. 15. Ratio of intensity of the $1^1S \rightarrow 2^3S$ transition to that of the $1^1S \rightarrow 2^3P$ one for helium. The solid lines are theoretical and the points are experimental results for $E = 26.5$ eV (open circles) and 55.5 eV (filled circles).

less than that of the $2^3P/2^1P$ ratio. Finally, the $2^1S/2^1P$ DCS ratio (symmetry-forbidden/allowed) generally decreases with increasing angle, reaching a broad minimum at about 40° , and thereafter increases.⁷⁰ Silverman and Lassette^{25j} have reported that the $2^1S/2^1P$ DCS ratio increases by a factor of about 10 from $\theta = 3.8^\circ$ to $\theta = 15.3^\circ$ at an incident energy of 500 eV. It is interesting to note that at intermediate energies (34 to 56 eV), this ratio decreases over the same angular range.⁷⁰

In addition to the characteristic variation of these triplet/singlet ratios with angle, they exhibit a dependence on incident energy which (in some cases) is to be expected from previous considerations. As the incident energy is lowered toward threshold, spin-forbidden total cross sections are usually enhanced relative to spin-allowed ones. We might expect the respective differential cross sections to vary in a similar way. Then, the triplet/singlet ratios should increase with decreasing energy more rapidly than the singlet/singlet one. This behavior is obtained for $\theta = 0^\circ$.⁴⁰

However, the magnitude of this effect is sensitive to the particular θ considered. Table III presents the ratios at $\theta \approx 40^\circ$ for which the $2^3P/2^1P$

TABLE III
Peak Intensity Ratios in Helium
at $\theta = 40^\circ$

| E (eV) | $2^3S/2^1P$ | $2^3P/2^1P$ |
|-------------|-------------|------------------|
| 55.5 | .050 | .40 |
| 44 | .11 | .49 |
| 34 | .19 | .40 |
| 26.5 | .28 | .29 ^a |

^a This decrease can be understood from the data of Ref. 69 which show that the total cross section for excitation of the 2^3P state is lower at 26 eV than at 34 eV.

ratio is nearly constant. The enhancement with decreasing energy of the triplet/singlet ratios compared to the $2^1S/2^1P$ one is most evident in the region of low ($\theta \approx 0^\circ$) and high ($\theta \approx 70^\circ$) scattering angles.

The DCS themselves for the various transitions also show a number of interesting features. First, the 2^1S or 2^1P DCS are more sharply peaked forward than the 2^3S or 2^3P DCS (as expected). Second, as the incident energy is decreased the 2^1P and 2^3S DCS become more isotropic. The 2^3P DCS is relatively flat over a wide range of angles at all of these energies. Third, the behavior of the 2^1S DCS presents an interesting variation. At 55.5 eV it reaches a distinct minimum at about 40° while at 44 and 34 eV the minimum moves out to 50 and 60° , respectively, and apparently lies beyond 70° at 26.5 eV.⁷⁰ This behavior is similar to the diffraction effects observed in both elastic and inelastic scattering from atoms.^{3c}

Finally, the behavior of the 2^1P , 2^1S , and 2^3P DCS at 26.5 eV for $\theta < 20^\circ$ is unique in that these DCS appear to decrease markedly toward smaller angles. This effect is not predicted by first-order theories^{68,70} and is probably not due to a resonance, since none have been observed in this impact-energy region.^{73,74}

B. Molecules

The excitation of molecular electronic states occurs with concomitant vibrational and rotational transitions. In many cases the vibrational structure of these molecular states can be resolved, but as yet no rotational features have been observed.

Let the DCS for the excitation of the n' 'th electronic, v' 'th vibrational, and $J'M'$ rotational state of molecules that are initially in their ground electronic and vibrational states with a thermal (300°K) distribution of rotational

ones (JM) be $\sigma_{n'v',J'M'}^{JM}$. Since rotational excitations are not resolved and since each molecule scatters independently of all the others, the observed DCS is

$$\sigma_{n'v'} = \left\langle \sum_{J'=0}^{J'_{\max}} \sum_{M'=-J'}^{J'} \sigma_{n'v',J'M'}^{JM} \right\rangle_{JM} \quad (19)$$

where $\langle \rangle_{JM}$ indicates a statistical-mechanical average over the initial rotational states JM and J'_{\max} is the maximum J' value allowed by the conservation of energy during the collision.⁷⁵ It is observed experimentally that $\sigma_{n'v'}(E, \theta)/\sigma_{n'v'}(E, \theta)$ is a constant, independent of angle and incident energy, i.e., that the relative vibrational intensities within a given electronic band are constant.³⁵ It is further noted that these relative intensities equal the respective relative Franck-Condon factors. This seems to imply that $\sigma_{n'v'}$ can be expressed in the form

$$\sigma_{n'v'}(E, \theta) \cong G_{n'v'} f_n(E, \theta) \quad (20)$$

where $G_{n'v'}$ is the Franck-Condon factor associated with the $(00) \rightarrow (n'v')$ electronic-vibrational transition and $f_n(E, \theta)$ is a function of energy, angle, and the electronic state. First-order approximations do not predict this form but the deviations they do imply are usually 5% or less. Experimental uncertainties ($\lesssim 5\%$) and the failure of these approximations to predict reliable DCS in this intermediate energy range for the electronic states themselves preclude a quantitative comparison.

1. Nitrogen

The transition from the $X^1\Sigma_g^+$ ground state of N_2 to the $b^1\Pi_u$ state is the first optically allowed one in our spectra.⁴⁹ Transitions to the lower lying states are forbidden by symmetry ($g \leftrightarrow g$, e.g., $a^1\Pi_g$, $^1\Sigma_g^+$), electron spin multiplicity (e.g., $A^3\Sigma_u^+$, $C^3\Pi_u$) or both (e.g., $B^3\Pi_g$, $E^3\Sigma_g^+$). Transitions to the symmetry-forbidden states are electric-quadrupole allowed. Gilmore⁷⁶ has summarized the potential energy curves for most of these states.

The electron-impact excitation of N_2 has been studied at both low and high angles at a number of incident energies. Many electronic states have been observed although the assignment of the $E^3\Sigma_g^+$ one has been in question.

Lassettre and Krasnow^{25a} investigated the behavior of the unresolved $X^1\Sigma_g^+ \rightarrow a^1\Pi_g$ (Lyman-Birge-Hopfield) transition with scattering angle (0 to 15°) at 500 eV. They found that the ratio of the DCS for excitation of the $a^1\Pi_g$ state to that of the $b^1\Pi_u$ one varied from about 0.05 at $\theta = 4^\circ$ to 0.3 at $\theta = 10^\circ$. Later these studies were extended²⁸ to lower energies (60 eV)

and higher resolution but at low angles ($\theta < 2.5^\circ$). Recently, Skerbele, Dillon, and Lassette²⁹ reported high resolution spectra of N_2 at 50 and 36 eV ($\theta = 0$ to 12°). In this case, transitions to many electronic states were observed although singlet-triplet transitions were a minor part of the overall spectrum.

Heideman, Kuyatt, and Chamberlain⁴² obtained energy-loss spectra for $\theta = 0^\circ$ at incident energies of 15.7 and 35 eV. Neither the A nor B states were observed at either energy while the C state was evident at the lower one.

Doering and Williams^{33c} have presented lower resolution energy-loss spectra at impact energies down to 16.1 eV for $\theta = 90^\circ$. As expected, the singlet-triplet transitions comprise a major part of the N_2 spectrum under these conditions. No vibrational structure was resolved, but transitions to the $B^3\Pi_g$, $a^1\Pi_g$, $C^3\Pi_u$, and $b^1\Pi_u$ states were evident.

The N_2 excitation spectrum has also been studied by Brongersma and Oosterhoff²⁰ and Compton and co-workers²² using a trapped-electron technique. Although the reported spectra of these authors are similar in appearance, their state assignments are quite different. This is probably the result of an energy calibration error in the results of Compton and co-workers.²² Brongersma and Oosterhoff²⁰ were able to verify the identity of the B state by resolving its vibrational structure. It is interesting to note that these threshold studies do not reveal excitations to the A or C states but are dominated by transitions to the B and E ones (all four of these states are triplets).

Figures 16 and 17 show energy-loss spectra of N_2 taken at an impact energy of 40 eV (uncalibrated) and scattering angles of 20 and 80° , respectively.³⁴ The low angle spectrum agrees with that of Ref. 29, while the high angle one is similar to the one of Ref. 33c. As in He, at high angles the intensity of triplet transitions with respect to singlet ones is greatly enhanced. Figure 18 shows a separate scan at $\theta = 80^\circ$ of the energy-loss region from about 6 to 11.5 eV.⁵² In this figure, transitions to several of the $A^3\Sigma_u^+$ vibrational levels can be weakly observed.

It is of interest to examine the validity of the previously discussed Franck-Condon factor considerations over a wider angular range. If they are valid, we expect the relative vibrational peak intensities to be (1) independent of incident energy, (2) independent of scattering angle, and (3) in accord with the results from optical measurements and reliable calculations. The $C^3\Pi_u$ state is a good "test" case since its vibrational levels are well resolved and the electronic band itself is relatively isolated. Table IV summarizes the relative intensity data obtained by Rice, Kuppermann, and Trajmar⁵² at 25 eV as well as the calculations of Benesch and

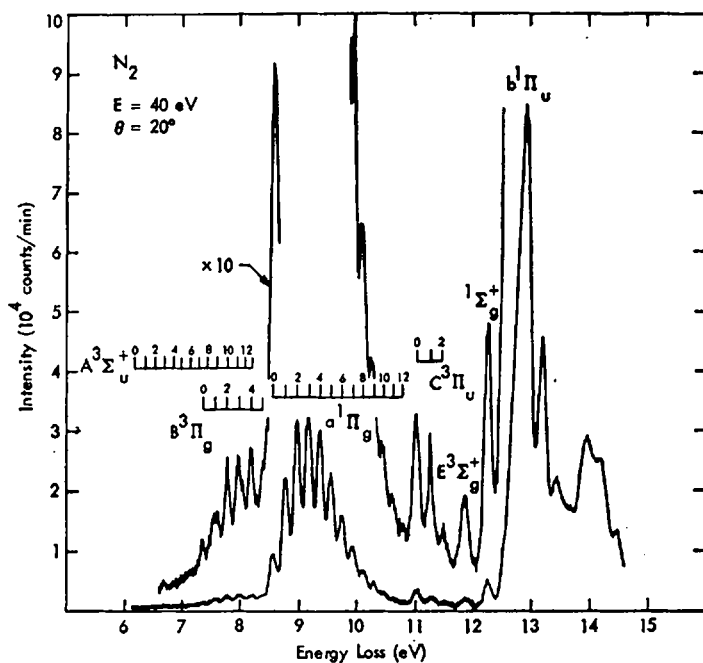


Fig. 16. Energy-loss spectrum of N_2 . $E = 40 \text{ eV}$, $\theta = 20^\circ$.

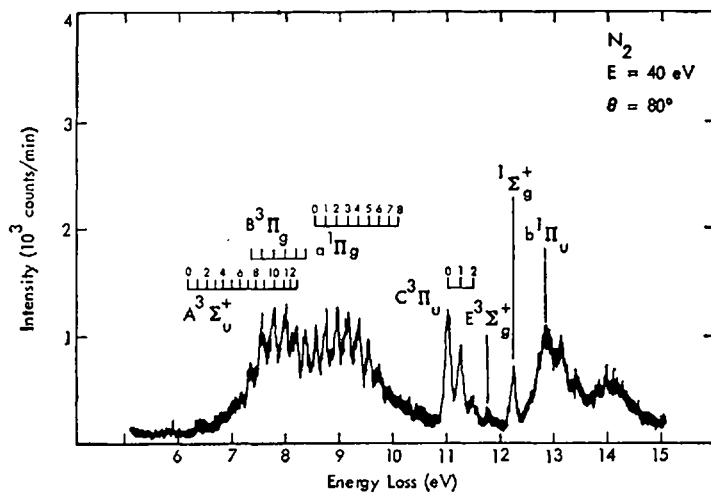


Fig. 17. Energy-loss spectrum of N_2 . $E = 40 \text{ eV}$, $\theta = 80^\circ$.

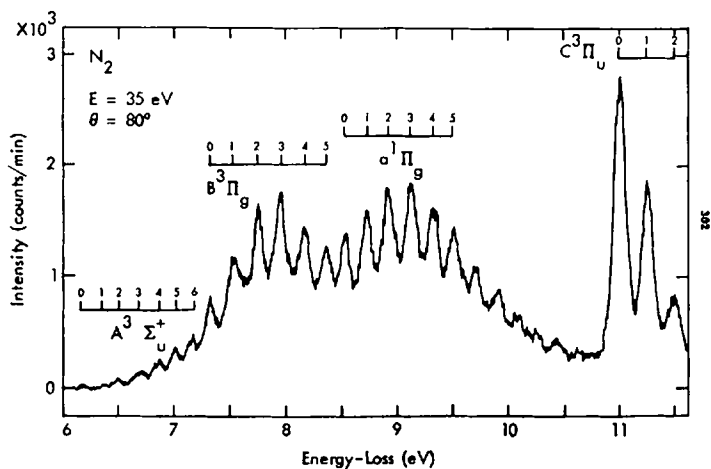


Fig. 18. Energy loss spectrum of N_2 . $E = 35$ eV, $\theta = 80^\circ$.

TABLE IV

Relative Intensity Distribution of the $X^1\Sigma_g^+ (v=0) \rightarrow C^3\Pi_u (v'=0, 1, 2)$ Transitions of N_2 . The Incident Energy is 25 eV. The $v'=0$ Peak Intensity is Normalized to 1.00. Columns 2 and 3 Contain the Relative Peak Intensities

| Scattering angle (degrees) | v' | |
|-------------------------------|---------------|---------------|
| | 1 | 2 |
| 10 | .61 \pm .05 | .21 \pm .04 |
| 20 | .62 \pm .04 | .21 \pm .04 |
| 30 | .60 \pm .04 | .20 \pm .02 |
| 40 | .59 \pm .04 | .22 \pm .03 |
| 50 | .66 \pm .07 | .22 \pm .03 |
| 60 | .68 \pm .03 | .24 \pm .03 |
| 70 | .64 \pm .03 | .27 \pm .03 |
| 80 | .68 \pm .04 | .27 \pm .02 |
| Average over all angles | .63 \pm .03 | .23 \pm .02 |
| Calculated values* | .588 | .193 |

* Ref. 77.

co-workers.⁷⁷ Within the errors of this determination there is no change with scattering angle, and the overall average is in reasonable agreement with the calculations.

A similar determination was performed for the $C^3\Pi_u$ state at an impact energy of 35 eV.⁵² An average of 28 scans at angles from 10 to 80° yielded a $v' = 1$ relative intensity of 0.60 ± 0.03 and a $v' = 2$ relative intensity of 0.21 ± 0.03 . Notice that the relative intensities are also independent of incident energy (at least in this 25 to 35 eV energy range). The relative vibrational intensities within the $a^1\Pi_g$ band have been measured for $\theta \gtrsim 15^\circ$ by Rice, Kuppermann, and Trajmar⁵² and the conclusions were the same as for the $C^3\Pi_u$ excitation.

Lassette and co-workers³⁵ studied the relative intensities of the vibrational progressions in the $a^1\Pi$ and $b^1\Pi$ excitations of N_2 . They found that the averaged relative intensities agreed well with the Franck-Condon factors of Benesch⁷⁷ and that the relative intensities were independent of angle up to 16° over a wide energy range except for a small deviation for the $v' = 0$ and 1 bands in the $a^1\Pi$ excitation.

The only doubtful state assignment below the $b^1\Pi_u$ one is that of the $E^3\Pi_g^+$ at 11.87 eV. The state at 12.26 eV seems clearly to be a $^1\Sigma_g^+$ one⁷⁸ while the one at 11.87 eV may be either $^1\Sigma_g^+$ (Refs. 26, 28, 79) or $^3\Sigma_g^+$ (Ref. 42). Meyer and Lassette²⁶ and Lassette, Skerbele, and Meyer²⁸ argue for the former (singlet) assignment primarily because they observe it at an impact energy of 400 eV. Heideman, Kuyatt, and Chamberlain⁴² prefer the latter assignment since the $\theta = 0^\circ$ excitation function of this state is sharply peaked near threshold—a behavior indicative of a singlet-triplet transition. This disagreement can be resolved by comparing the relative angular dependencies of the DCS for excitation of the 11.87 and 12.26 eV states. Figure 19 shows the peak intensity ratios of the $E^3\Sigma_g^+$ (11.87 eV), $^1\Sigma_g^+$ (12.26 eV), and $C^3\Pi_u$ (11.03 eV) excitations with respect to the $b^1\Pi_u$ (12.92 eV) one as a function of scattering angle from $\theta = -30$ to $+80^\circ$ for $E = 35$ eV (uncalibrated).⁵² The $b^1\Pi_u$ peak intensity probably contains a significant contribution from the $p'^1\Sigma_u^+$ transition.⁴⁹ The $C^3\Pi_u$ intensity is the sum of the $v' = 0, 1$, and 2 vibrational level peak intensities while the intensity of the others are measured at their respective peaks. (Figure 19 clearly shows the expected symmetry of these ratios about $\theta = 0^\circ$.) Since the relative intensities of the vibrational levels within a given electronic band seem to be independent of angle (or incident energy), these ratios are equal to the absolute DCS ratios times a constant (independent of angle but dependent on resolution). Of prime importance is the fact that the variation with θ of these plotted ratios is the same as that of the absolute DCS ratios. It is clear that the triplet/singlet ratios behave with θ as we

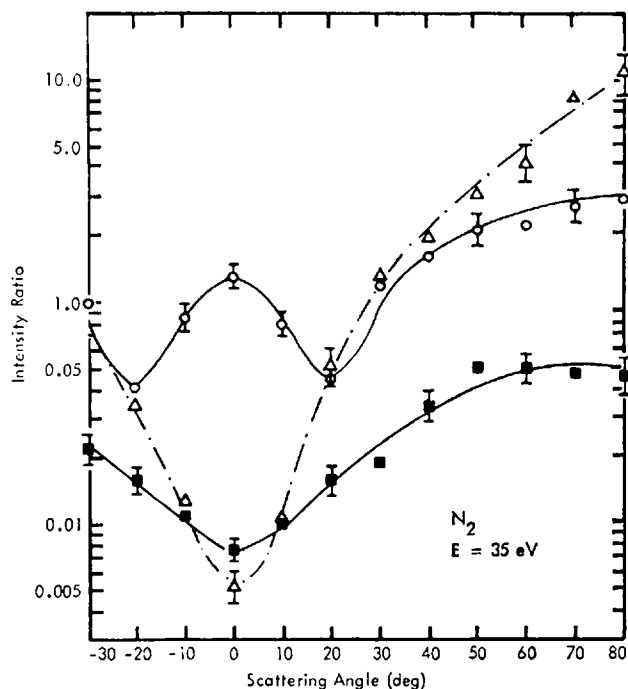


Fig. 19. Intensity ratios in N_2 . The common lower (ground) state is $X^1\Sigma_g^+$. The common reference state is the 12.92 eV feature. ■, $E^3\Sigma_g^+$ (11.87 eV); ○, $^1\Sigma_g^+$ (12.26 eV); △, $C^3\Pi_u$ (11.03 eV). Peak intensities were used for the $E^3\Sigma_g^+$ and 12.92 eV features while the sum of $v' = 0, 1, 2$ vibrational level peak intensities was used for the C state.

expect (qualitatively) from theory and agree with observations in helium.

The $X-b$ transition in N_2 and the 1^1S-2^1P transition in helium are similar in that the change in orbital angular momentum quantum number ($\Delta\Lambda$) is 1 while the change in spin angular momentum quantum number (ΔS) is 0. Likewise the $X \rightarrow C(N_2)$ and $1^1S \rightarrow 2^3P(He)$ transitions have $\Delta\Lambda = 1$ and $\Delta S = 1$. Thus, we might expect the $C/b(N_2)$ and $2^3P/2^1P(He)$ ratios to behave in a similar manner with angle for impact energies which are higher than their corresponding threshold energies by about the same amount. A comparison of Figure 19 (the incident energy is ~ 24 eV above threshold) and Figure 6 shows this to be the case. In an analogous way, we expect the $^1\Sigma_g^+$ (12.26 eV)/ b and $2^1S/2^1P$ ratios to exhibit similar behavior with θ . This also is observed.⁷⁰ Finally, the assignment of the 11.87 eV transition as $E^3\Sigma_g^+$ is completely consistent with the similarity in the behavior of the $2^3P/2^1P$ and $E^3\Sigma_g^+$ (11.87)/ b ratios ($\Delta\Lambda = 0$, $\Delta S = 1$ for both upper states). Even if these somewhat qualitative comparisons are not

convincing, it is clear from Figure 19 that the 11.87 and 12.26 eV transitions are fundamentally different. Further, the assignment of the 11.87 eV transition as a singlet would be entirely inconsistent with our understanding of the way in which singlet/singlet and triplet/singlet ratios differ with θ . The results obtained for the iso-electronic molecule CO (see next section) provide an additional justification for assigning the 11.87 eV state as a triplet. Intensity ratios and DCS measured at other energies⁵² show the same characteristic behavior with scattering angle.

The N_2 DCS cannot be placed on an absolute scale primarily because there is no absolute determination of either the total cross section or any DCS with which the relative measurement could be normalized for E less than 100 eV.*

2. Carbon Monoxide

CO is isoelectronic with N_2 and as expected exhibits a somewhat similar energy-loss spectrum under electron impact. Potential energy curves for these states and a summary of available optical data on CO can be found in the review of Krupenie.⁸⁰

The electron-impact excitation spectrum of CO was first obtained by Schulz^{18a} using the trapped-electron technique. Transitions to the $a^3\Pi$ state (Cameron bands) were the most intense feature in his spectrum. Brongersma and Oosterhoff,²⁰ with an improvement of this same technique, were able to resolve some vibrational structure in the $a^3\Pi$ state. Transitions to the $A^1\Pi$ state were not observed while those to the $B^1\Sigma^+$ and $b^3\Sigma^+$ ones were relatively intense.

Lassette and his co-workers have measured the relative vibrational intensities within the $X^1\Sigma^+ \rightarrow A^1\Pi$ transition at several incident energies over a small range of angles. Their earlier measurements, at 400⁸¹ and 200 eV,⁸² disagreed with the Franck-Condon factor calculations of Nichols⁸³ for the higher vibrational levels. However, their more recent measurements³⁵ at 98 and 48 eV showed no variation with angle (0–16°) and agreed quite well with calculations,⁸³ except for the $v' = 0$ and 1 levels. Rice, Kuppermann, and Trajmar⁵² have also measured these relative intensities over a wider range of angles (0–75°) at 35 and 25 eV. No dependence on either energy or angle was noted. The results of these various observations are summarized in Table V.

* Note added in proof: Since the writing of this article, Burns Simpson and McConkey published absolute electron impact excitation functions for the $C^3\Pi$ state (*J. Phys. B.* 2, 52, 1969) and Stanton and St. John (*J.O.S.A.*, 59, 252, 1969) and McConkey and Simpson (*J. Phys. B.* 2, 923, 1969) for the $B^3\Pi_g$ state.

TABLE V

Relative Vibrational Intensity Distribution in the $A^1\Pi$ band of CO. The $X^1\Sigma^+ (v=0) \rightarrow A^1\Pi (v'=2)$ Transition Intensity is Normalized to 1

| v' | Incident energy (eV) | | | | | | | Calculations ^f |
|------|----------------------|------------------|-----------------|-----------------|-----------------|-----------------|-----------------|---------------------------|
| | 400 ^a | 200 ^b | 98 ^c | 50 ^d | 48 ^c | 35 ^e | 25 ^e | |
| 0 | .44 ± .02 | .45 ± .02 | 0.48 | 0.55 | 0.50 | .48 ± .02 | .51 ± .02 | 0.492 |
| 1 | .87 ± .02 | .89 ± .02 | 0.91 | 0.94 | 0.92 | .95 ± .03 | .94 ± .02 | 0.940 |
| 2 | 1.00 | 1.00 | 1.00 | 1.00 | 1.00 | 1.00 | 1.00 | 1.000 |
| 3 | .83 ± .03 | .88 ± .02 | 0.80 | 0.80 | 0.81 | .81 ± .04 | .78 ± .03 | 0.788 |
| 4 | .56 ± .03 | .62 ± .02 | 0.54 | 0.52 | 0.55 | .54 ± .03 | .52 ± .03 | 0.517 |
| 5 | .34 ± .01 | .39 ± .02 | 0.32 | 0.32 | 0.33 | .34 ± .04 | .31 ± .02 | 0.299 |
| 6 | .20 ± .01 | .24 ± .02 | 0.16 | 0.17 | 0.17 | — | .16 ± .02 | 0.159 |

^a Ref. 81.

^b Ref. 82.

^c Ref. 35.

^d Derived from the spectrum of Ref. 30.

^e Ref. 52.

^f Ref. 83.

Skerbele, Dillon, and Lassette³⁰ reported a high resolution study of CO at 50 eV impact energy in which excitations of the $a^3\Pi$ and $b^3\Sigma^+$ states were observed in addition to those of the $A^1\Pi$, $B^1\Sigma^+$, $C^1\Sigma^+$, $E^1\Pi$, and $F^1\Pi$ ones. The relative vibrational intensities within the $a^3\Pi$ band agreed well with the calculations of Nichols.⁸³ A similar agreement was found by Rice, Kuppermann, and Trajmar⁵² at 25 and 35 eV for $0^\circ < \theta < 75^\circ$.

Figures 20 and 21 show electron energy-loss spectra of CO at an impact energy of 25 eV (uncalibrated) and $\theta = 10$ and 75° , respectively. Figure 22 shows the relative angular dependence of the DCS for excitation of the $a^3\Pi$ ($v' = 0 + 1 + 2$), $b^3\Sigma^+$ ($v' = 0$), $B^1\Sigma^+$ ($v' = 0$), and $C^1\Sigma^+$ ($v' = 0$) states with respect to that of the $A^1\Pi$ ($v' = 0 + 1 + 2$) one at incident energies of 35 eV.⁵² The a/A intensity ratio is quite characteristic of a (singlet-triplet)/(singlet-singlet) ratio as evidenced by the $2^3P/2^1P$ ratio of helium and the $B^3\Pi_g/b^1\Pi_u$ and $C^3\Pi_u/b^1\Pi_u$ ratios of N_2 . Also, the b/A intensity ratio is quite similar to the $E^3\Sigma_g^+/b^1\Pi_u$ one of N_2 and the $2^3S/2^1P$ ratio of helium. This striking similarity with the E/b ratio of N_2 provides an additional confirmation of the triplet designation of that E state. The B/A and C/A intensity ratios exhibit a more complex behavior. At 35 eV they closely resemble the $^1\Sigma_g^+/b^1\Pi_u$ ratio of N_2 while at 25 eV they are more like the $a^1\Pi_g/b^1\Pi_u$ and $p^1\Sigma_u^+/b^1\Pi_u$ ratios. In any case, they

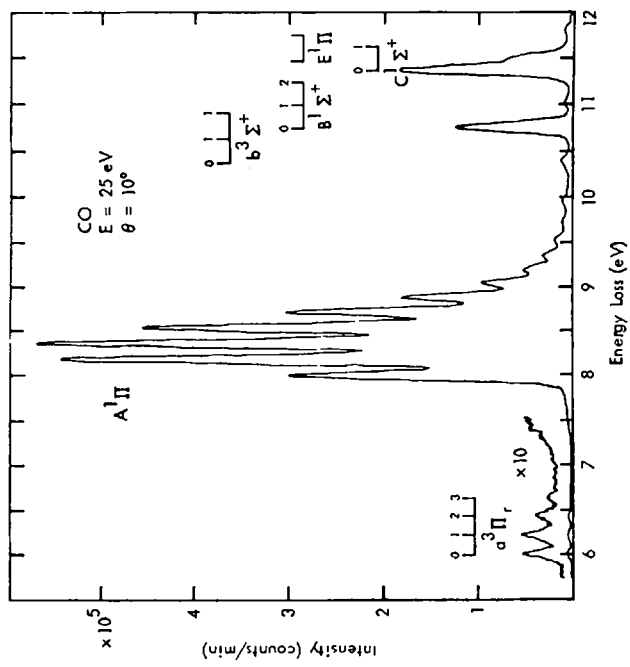


Fig. 20. Energy-loss spectrum of CO. $E = 25$ eV, $\theta = 10^\circ$.

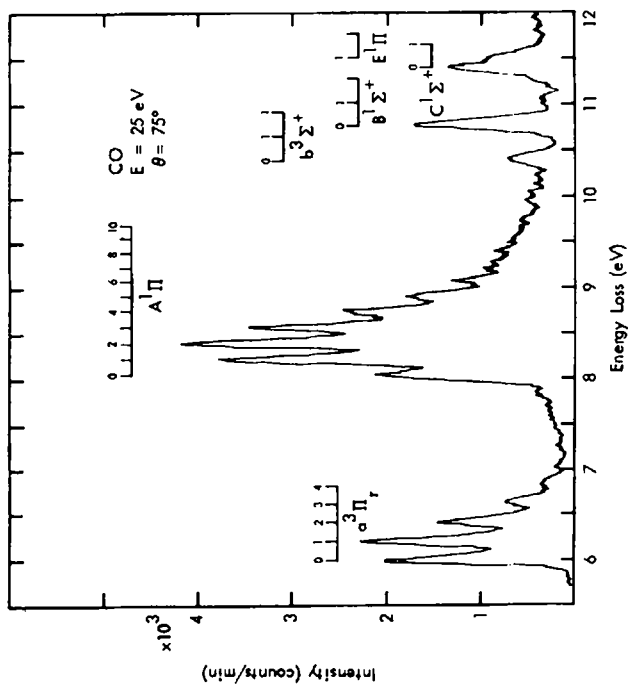


Fig. 21. Energy-loss spectrum of CO. $E = 25$ eV, $\theta = 75^\circ$.

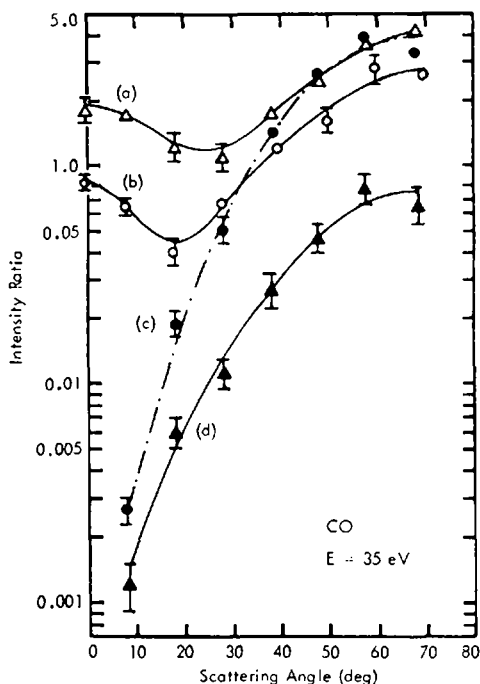


Fig. 22. Intensity ratios in CO. Common lower (ground) state is $X^1\Sigma^+$ ($v = 0$). Upper reference state is $A^1\Pi$ ($v' = 0, 1, 2$). Curve (a), $C^1\Sigma^+$ ($v' = 0$); Curve (b), $B^1\Sigma^+$ ($v' = 0$); Curve (c), $a^1\Pi$ ($v' = 0, 1, 2$); and Curve (d), $b^3\Sigma^+$ ($v' = 0$). $E = 35$ eV.

exhibit the oscillatory behavior which seems characteristic of ($\Delta S = 0$, $\Delta \Lambda = 0$, symmetry-forbidden)/($\Delta S = 0$, $\Delta \Lambda = 1$, allowed) intensity ratios.

3. Hydrogen

H_2 has been exhaustively studied by optical methods (Ref. 11b, pp. 530–532). Relatively few electron-impact studies of H_2 have been reported, although excitations from the $X^1\Sigma_g^+$ ground state to the $b^3\Sigma_u^+$, $B^1\Sigma_g^+$, $C^1\Pi_u$, $c^3\Pi_u$, and $D^1\Pi_u$ states have been observed.

Schulz¹⁷ used a trapped-electron technique to observe excitations to the $b^3\Sigma_u^+$ (repulsive) state and a second band, peaked at about 12 eV, which he assigned as $X \rightarrow B, C, D$ (singlets). In view of the recent high-resolution trapped-electron work of Dowell and Sharp,²¹ this 12 eV peak probably contained substantial contributions from the $c^3\Pi_u$ state.

Kuppermann and Raff^{32a} observed transitions to the $b^3\Sigma_u^+$ states as well as several of the unresolved singlets using a retarding field method of

energy analysis and the collection of electrons scattered between $22^\circ \leq \theta \leq 112^\circ$. Lassettre and co-workers^{25b,25d} have reported unresolved energy-loss spectra at impact energies from 300 to 500 eV and $0^\circ < \theta < 5^\circ$. No forbidden excitations were observed, nor was any vibrational structure in the B , C , D , etc. states resolved.

Kuyatt, Mielczarek, and Simpson⁸⁴ and Heideman, Kuyatt, and Chamberlain⁴³ were able to resolve many vibrational levels in the B , C , and D states at incident energies from 90 to 13.7 eV at $\theta \cong 0^\circ$. They did not observe excitation of the $b^3\Sigma_u^+$ state. However, below about 30 eV, transitions to the $c^3\Pi_u$ and/or $a^3\Sigma_g^+$ state (unresolved) were noted.

At an incident energy of 25 keV ($\theta \approx 0^\circ$), Geiger⁸⁵ reported a well-resolved energy-loss spectrum of H_2 . Transitions to the singlet states (B , C , and D) are clearly evident, but no forbidden excitations were observed (nor are they expected to be at this high energy).

Trajmar and co-workers⁵⁷ have previously reported measurements of the DCS (10 – 80°) for excitation of the $b^3\Sigma_u^+$ (repulsive-triplet) state at intermediate impact energies and have compared them with first-order theoretical calculations. In contrast to the situation for the exchange excitations of helium, the Ochkur-Rudge theory and experiment were found to agree reasonably well from 40 to 60 eV. Below 40 eV the experimental DCS were more isotropic than were the calculated ones. No data is yet available above 60 eV.

There are a number of additional unreported aspects of this study which will be discussed below.

Since several vibrational members of the $B^1\Sigma_u^+$ and $C^1\Pi_u$ states were resolved at 40 eV, it is of interest to compare the relative vibrational peak heights within each band to the corresponding Franck-Condon factor ratios. However, H_2 presents an extremely unfavorable case in which to obtain a meaningful comparison. As is evident from the figures of Ref. 57, transitions from the $X^1\Sigma_g^+$ ground state to the $b^3\Sigma_u^+$ state overlap those to the $B^1\Sigma_u^+$ state, which in turn overlap those to the $C^1\Pi_u$ state. In addition, transitions to the $a^3\Sigma_g^+$ and $c^3\Pi_u$ states overlap part of the $B^1\Sigma_u^+$ band and all of the $C^1\Pi_u$ one. Consequently, each particular peak height is proportional to the sum of a number of DCS, each one contributing an amount which depends on the resolution and scattering angle. It would require a resolution which is well beyond the present "state of the art" to separate all of these excitations.

The results discussed below were obtained at an impact-energy of 40 eV (uncalibrated). This value is chosen because (1) the highest resolution (FWHM = 0.04 eV) data were obtained at this energy and (2) excitations to the a , b , and c triplet states, although observable, cause relatively little

distortion of the strong $X \rightarrow B, C$ transitions. This latter condition is required if we are to make any meaningful Franck-Condon factor comparisons.

First, let us examine the relative vibrational peak intensities within the $C^1\Pi_u$ band which were measured for scattering angles from $\theta = 0^\circ$ to $\theta = 80^\circ$. No change in relative intensity was noted (within the accuracy of these measurements). If the transitions to the triplet states (a, c) were contributing significantly to the $C^1\Pi_u$ band intensity, we would expect some distortion of the relative intensity distribution in this band. Such effects would presumably become more noticeable at higher angles since the ratio of triplet to singlet DCS generally increases markedly with angle. The distortion of the $C^1\Pi_u$ relative vibrational intensities due to the incompletely resolved $B^1\Sigma_u^+$ vibrational peaks should be less dependent on angle since the $B^1\Sigma_u^+/C^1\Pi_u$ DCS ratio does not change much with this variable (see below).

Table VI summarizes the average (over all θ 's) relative intensities and

TABLE VI

Relative Vibrational Peak Intensity Distribution for the $X^1\Sigma_g^+ (v=0) \rightarrow C^1\Pi_u (v'=0$ to 5) Transitions in H_2 . The Intensity of the $X(v=0) \rightarrow C(v'=1)$ Transition is Normalized to 1.00. The Data from All Angles Have been Averaged.

| Investigator | v' | | | | | |
|---|---------------|------|---------------|---------------|---------------|---------------|
| | 0 | 1 | 2 | 3 | 4 | 5 |
| Rice, Kuppermann, and Trajmar ^a | | | | | | |
| (40 eV) | .72 \pm .02 | 1.00 | .91 \pm .03 | .67 \pm .03 | .43 \pm .02 | .26 \pm .02 |
| Geiger ^b | | | | | | |
| (25 KeV) | .62 | 1.00 | .96 | .62 | .40 | .23 |
| Hutchisson ^c | | | | | | |
| (calculation) | .635 | 1.00 | .961 | .697 | .411 | .236 |

^a Ref. 52.

^b Ref. 85.

^c Ref. 86.

presents as a comparison the high-energy data of Geiger⁸⁵ and the calculations of Hutchisson.⁸⁶ The agreement is quite good, with the exception of the $v' = 0$ relative intensity. This is to be expected since the $B^1\Sigma_u^+ (v' = 7)$ level is practically coincident with the $C^1\Pi_u (v' = 0)$ one.

The measurement and interpretation of the relative vibrational intensity distribution within the $B^1\Sigma_u^+$ band is somewhat more complicated. From Ref. 57 it is quite clear that at $\theta = 80^\circ$ the intensities of both the $v' = 4$ and 6 levels are strongly enhanced by the $a^3\Sigma_g^+$ ($v' = 0, 1$) and/or $c^3\Pi_u$ ($v' = 0, 1$) levels, respectively. Further, the intensity of v' members of the $B^1\Sigma_u^+$ state may be significantly increased at higher angles by the $b^3\Sigma_u^+$ state. Apparently the least affected level (which we can observe) will be the $B^1\Sigma_u^+$ ($v' = 5$) one. Thus, Table VII presents the relative vibrational in-

TABLE VII

Relative Vibrational Peak Intensity Distribution for the $X^1\Sigma_g^+(v=0) \rightarrow B^1\Sigma_u^+(v'=0$ to 6) Transitions in H_2 . The Intensity of the $X(v=0) \rightarrow B(v'=5)$ Transition is Normalized to 1.00. The scans for $\theta = 0$ to 10° and 15 to 20° Have Been Averaged as Indicated

| θ | v' | | | | | | |
|---|---------------|---------------|---------------|---------------|------------------|------|------------------|
| | 0 | 1 | 2 | 3 | 4 | 5 | 6 |
| $\langle 0-10^\circ \rangle$ | .08 \pm .01 | .24 \pm .02 | .47 \pm .03 | .72 \pm .03 | .91 \pm .04 | 1.00 | 1.06 \pm 0.05 |
| $\langle 15-20^\circ \rangle$ | .08 \pm .01 | .22 \pm .03 | .51 \pm .03 | .72 \pm .04 | .92 \pm .04 | 1.00 | 1.09 \pm 0.05 |
| 30° | .08 | .25 | .47 | .73 | .95 | 1.00 | 1.2 ₀ |
| 40° | .12 \pm .02 | .25 \pm .04 | .52 \pm .04 | .74 \pm .03 | .95 \pm .04 | 1.00 | 1.19 \pm 0.04 |
| 50° | .16 | .32 | .57 | .78 | .90 | 1.00 | 1.2 |
| 60° | .21 | .33 | .63 | .79 | 1.2 _s | 1.00 | 1.4 _s |
| 80° | .22 | .36 | .56 | .73 | 1.2 | 1.00 | 1.3 _s |
| Geiger ^a (25 KeV, $\theta = 0^\circ$) | .10 | .19 | .38 | .59 | .84 | 1.00 | 1.06 |
| Hutchisson ^b (calculation) | .082 | .345 | .860 | 1.246 | 1.316 | 1.00 | 0.556 |

^a Ref. 85.

^b Ref. 86.

tensities within the $B^1\Sigma_u^+$ state (with respect to that of the $v' = 5$ level) obtained at 40 eV together with the results of Geiger⁸⁵ and calculations.⁸⁶ (Since Geiger used 25 keV incident electrons, only singlet \rightarrow singlet transitions were observed.)

It is clear that neither the results of Geiger at 25 keV nor the 40 eV data agree with the calculations (except fortuitously perhaps at $v' = 0$). We would expect the agreement of the 40 eV data with that of Geiger to be best at the lowest angles, since the ratio of triplets to singlets is smallest there. However, the former seems consistently high by about 10% (except for $v' = 0$ and 6) for $\theta \lesssim 20^\circ$. This is probably not due to the overlapping

$b^3\Sigma_u^+$ state since the b/B DCS ratio changes by more than a factor of 10 in the same angular range (see below). (Further, below $\theta \approx 30^\circ$ excitation of the $b^3\Sigma_u^+$ state was not observed in these high resolution scans.) In any case, for angles greater than $\sim 40^\circ$, the enhancements of the $v' = 0$ and 1 peak intensities (due to excitation of the $b^3\Sigma_u^+$ state), the $v' = 4$ peak intensity [due to the transitions to the $a^3\Sigma_g^+$ ($v' = 0$) and/or $c^3\Pi_u$ ($v' = 0$) levels], and the $v' = 6$ peak intensity [due to excitation of the $a^3\Sigma_g^+$ ($v' = 1$) and/or $c^3\Pi_u$ ($v' = 1$) states] are clearly evident. This distortion with angle of the relative vibrational intensity distribution within an electronic band can presumably be used to detect forbidden transitions which are strongly masked by overlapping allowed ones.

Let us next consider the variation with scattering angle of the relative DCS for excitation of the $b^3\Sigma_u^+$, $B^1\Sigma_u^+$, and $C^1\Pi_u$ states. Figure 23 shows the peak intensity ratios of the $X^1\Sigma_g^+$ ($v = 0$) \rightarrow $b^3\Sigma_u^+$ and $B^1\Sigma_u^+$ ($v' = 5$) transitions with respect to that of the $X^1\Sigma_g^+$ ($v = 0$) \rightarrow $C^1\Pi_u$ ($v' = 1$) one. The $B^1\Sigma_u^+$ ($v' = 5$)/ $C^1\Pi_u$ ($v' = 1$) intensity ratio was determined from the

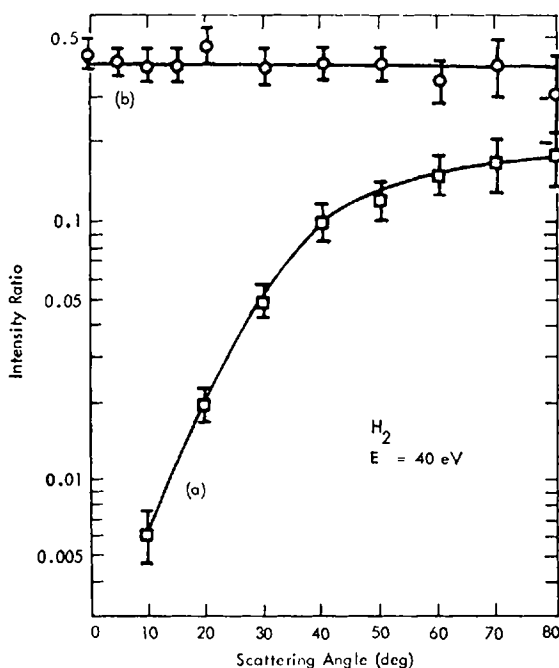


Fig. 23. Intensity ratios in H_2 . Common lower (ground) state is $X^1\Sigma_g^+$. Upper reference state is $C^1\Pi_u$ ($v' = 1$). Curve (a), $b^3\Sigma_u^+$ (peak); Curve (b), $B^1\Sigma_u^+$ ($v' = 5$) $E = 40$ eV.

same high-resolution data used to obtain the results presented in Tables VI and VII. The $b^3\Sigma_u^+/C^1\Pi_u (v'=1)$ intensity ratio was obtained from lower resolution (FWHM ≈ 0.10 eV) scans at the same 40 eV impact energy). Both the $b/C (v'=1)$ and $B (v'=5)/C (v'=1)$ peak intensity ratios are directly proportional to the corresponding DCS ratios. Since the proportionality constant depends somewhat on the resolution but not on the angle, the magnitude of the ratios are not directly comparable although their relative angular dependencies are. As expected, the b/C intensity ratio increases rapidly with angle while the B/C one is practically constant. The angular variation of the b/C ratio is quite similar to the $^3\Sigma^+/^1\Pi$ ratios already noted (N_2 , CO). This tends to reinforce the tentative hypothesis that for $\Delta S = 1$, the value of $\Delta\Lambda$ (0 or 1) is more important in determining the relative angular distribution than is the $g \rightarrow g$ or u nature of the transition. The $B^1\Sigma_u^+/C^1\Pi_u$ intensity ratio does not exhibit the oscillations noted in the previous $^1\Sigma/^1\Pi$ ratios. Although the $X^1\Sigma_g^+ \rightarrow B^1\Sigma_u^+$ transition in H_2 is the only case yet observed of a $\Delta\Lambda = 0, g \rightarrow u, \Delta S = 0$ transition, the fact that its intensity, relative to that of the $^1\Pi$ one, does not oscillate as do those of the $\Delta\Lambda = 0$ or 1, $g \rightarrow g, \Delta S = 0$ transitions (N_2) is consistent with the conjecture that for $\Delta S = 0$, the $g \rightarrow g$ or u nature of the transition is more important in determining the relative angular distribution than is the $\Delta\Lambda$ value.

Finally, Figure 24 shows the DCS (in arbitrary units) for excitation of the $C^1\Pi (v'=1)$ and $b^3\Sigma_u^+$ states at 40 eV for $\theta = 10$ to 80° . As expected, the singlet \rightarrow singlet DCS is sharply forward peaked, while the singlet \rightarrow triplet one is more isotropic.

4. Acetylene

Since acetylene (C_2H_2) is isoelectronic with N_2 and CO, we might expect that it would exhibit a similar energy-loss spectrum. An electron-impact study of C_2H_2 has been reported by Bowman and Miller¹⁹ using the trapped-electron method. A comparison of their results with those of Schulz^{18a} for CO and N_2 does indeed show this similarity which is not reflected in the tentative state assignments of Ref. 19, particularly with regard to the feature peaking at 6.2 eV.⁸⁷ In both N_2 and CO a low-lying triplet state ($B^3\Pi_g$ in N_2 and $a^3\Pi$ in CO) was responsible for the peak which appears to correspond to the 6.2 eV transition observed by Bowman and Miller. Ingold and King⁸⁸ had observed a weak singlet \rightarrow singlet transition ($X^1\Sigma_g^+ \rightarrow \tilde{A}^1A_u$) in absorption peaking at about 6 eV. Since the observation of a trapped-electron excitation spectrum is not sufficient to identify a transition as singlet \rightarrow singlet or triplet,⁸⁹ Bowman and Miller apparently assumed that they had observed the $\tilde{X} \rightarrow \tilde{A}$ excitation.

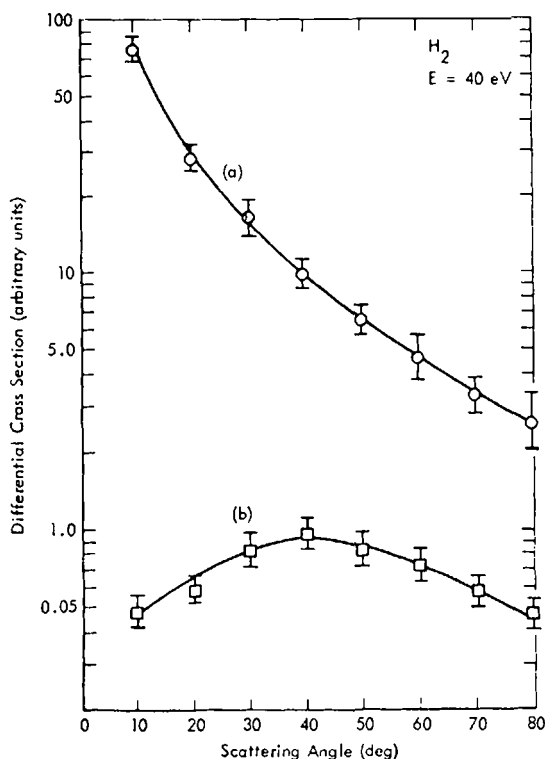


Fig. 24. DCS (arbitrary units) for excitation of the $C^1\Pi_u$ ($v' = 1$) Curve (a) and $b^3\Sigma_g^+$ Curve (b) states in H_2 .

Lassettre and co-workers³⁵ observed the electron-impact spectrum of C_2H_2 at 0 and 10° scattering angles with a 50 eV impact energy. They found two peaks at 6.35 and 6.49 eV energy loss which are very weak in the uv spectrum, although these peaks seem to be the result of optically-allowed singlet-singlet transitions. Their spectrum shows no singlet-triplet transitions.

Trajmar and co-workers⁵⁶ have reported an electron-impact investigation of acetylene. This study disclosed two previously unknown low-lying triplet states at 5.2 and 6.1 eV which were identified by the characteristic angular dependencies of their DCS. Some further results of this study will be discussed below.

Figure 25 shows an energy-loss spectrum of acetylene from about 5 to 12 eV for an impact energy of 45 eV and a scattering angle $\theta = 10^\circ$. It is similar in appearance to the optical absorption spectrum obtained by Nakayama and Watanabe⁹⁰ and to the electron-impact spectrum of

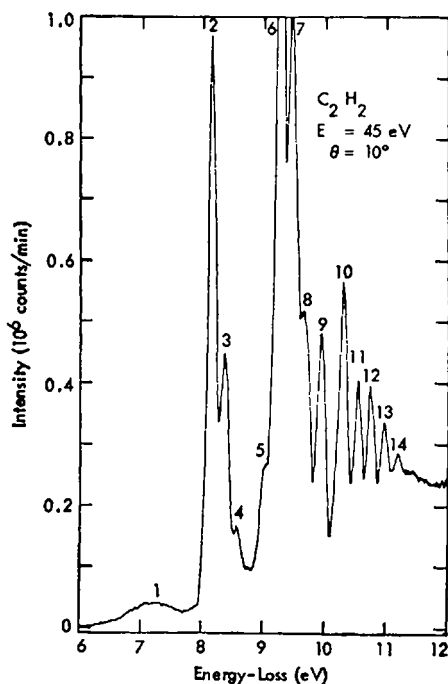


Fig. 25. Energy-loss spectrum of acetylene. $E = 45$ eV, $\theta = 10^\circ$. The excitation energies for the numbered features are listed in Table VIII.

Lassette.³⁵ The energy losses of the main features of Figure 25 are listed in Table VIII along with possible state assignments. Beyond 9 eV the uv absorption spectrum is too complex for these correspondences to be more than tentative. Figure 26 shows the triplet transitions.⁵⁶ The two weak features found by Lassette at 6.35 and 6.49 eV show up only as shoulders in our lower resolution spectrum.

From the results of Ref. 56 it is clear that (singlet \rightarrow triplet)/(singlet \rightarrow singlet) DCS ratios are sharply increasing functions of angle while the (singlet \rightarrow singlet)/(singlet \rightarrow singlet) ones vary much more slowly. It is also apparent that the $C^1\Pi_u$ ($v_2' = 1$)/ $C^1\Pi_u$ ($v_1' = 0$) intensity ratio gradually increases with increasing θ . This is not expected, since these peaks arise from transitions to two vibrational members of the same electronic state. The 70% change at impact energies of 35 and 25 eV for $\theta = 0$ to 70° (see Figure 2 of Ref. 56) is well outside the reasonable error limits of the data. This leaves two possible explanations: (1) the previous Franck-Condon factor considerations are not valid in this case, or (2) there is an underlying excitation (probably forbidden) which produces an apparent enhancement

TABLE VIII

Excitation Energies Observed in the Electron-Impact Spectrum of Acetylene. The First Column is the Peak Identification Number from Fig. 25. The Second Column is the Energy Loss at Which the Peak is Observed by Electron Impact, the Third Column is the Most Likely Corresponding Optical-Excitation Energy, and the Fourth Column is the Assignment of the Upper State (the Ground State is $X^1\Sigma_g^+$, Point Group $D_{\infty h}$).

| Peak number | Energy loss (eV) | Optical excitation energy ^a | Assignment ^b | | |
|-------------|------------------|--|-------------------------|---|-------------------|
| | | | Point group | State | Vibrational level |
| 1 | 5.2 ± 0.1^c | (7.3)(broad) | | \tilde{a} (triplet) | unresolved |
| | 6.1 ± 0.1^c | | | \tilde{b} (triplet) | unresolved |
| | 7.2 ± 0.1 | | | \tilde{B} (diffuse, unassigned bands) | |
| 2 | 8.16 ± 0.01 | 8.16 | $D_{\infty h}$ | $\tilde{C}(^1\Pi_u), [3R]$ | $v_2' = 0$ |
| 3 | 8.37 ± 0.01 | 8.38 | $D_{\infty h}$ | $\tilde{C}(^1\Pi_u), [3R]$ | $v_2' = 1$ |
| 4 | 8.61 ± 0.01 | 8.62 | $D_{\infty h}$ | $\tilde{C}(^1\Pi_u), [3R]$ | $v_2' = 2$ |
| 5 | 9.02 ± 0.02 | 9.24 | $D_{\infty h}$ | $\tilde{D}, [3R']$ | $v_2' = 0$ |
| 6 | 9.26 ± 0.01 | | | | |
| | | 9.25 | C_{2h} | $\tilde{E}, \{B\}$ | $v_2' = 0$ |
| | | 9.27 | C_2 | $\tilde{F}, \{C\}$ | $v_2' = 0$ |
| 7 | 9.47 ± 0.01 | 9.46 | $D_{\infty h}$ | $\tilde{D}_{\infty h}, [3R']$ | $v_2' = 1$ |
| | | 9.48 | C_{2h} | $\tilde{F}, [C]$ | $v_2' = 1$ |
| 8 | 9.66 ± 0.02 | 9.68 | $D_{\infty h}$ | $\tilde{D}, [3R']$ | $v_2' = 2$ |
| | | (9.68) | C_{2h} | $\tilde{F}, [C]$ | $v_2' = 2$ |
| 9 | 9.94 ± 0.01 | (9.93) | $D_{\infty h}$ | $[4R]$ | $v_2' = 0$ |
| 10 | 10.29 ± 0.01 | (10.28) | $D_{\infty h}$ | $[4R']$ | $v_2' = 0$ |
| 11 | 10.54 ± 0.02 | (10.52) | $D_{\infty h}$ | $[4R']$ | $v_2' = 1$ |
| 12 | 10.74 ± 0.02 | Probably Rydberg states [nR], [nR'] | | | |
| 13 | 10.96 ± 0.02 | | | | |
| 14 | 11.19 ± 0.03 | | | | |

^a Optical excitation energies in parentheses were determined from Figure 1 of Ref. 90.

^b States in square brackets [] are from Price [*Phys. Rev.*, **47**, 44 (1934)], those in { } are from Wilkinson [*J. Mol. Spectry.*, **2**, 387 (1953)], the other designations are from Herzberg.^{11c}

^c Refer to Figure 1 of Ref. 56.

of the $v_2' = 1$ peak relative to the $v_2' = 0$ one. As to the first possibility, we can only point out that in all reported cases (only six transitions) no significant ($\geq 5\%$) deviations in relative vibrational intensities have been noted as a function of angle. On the other hand, the second possibility has been clearly demonstrated for one case in H_2 . Based on this, the second explanation seems to be the most likely one. In Ref. 19, we note that the

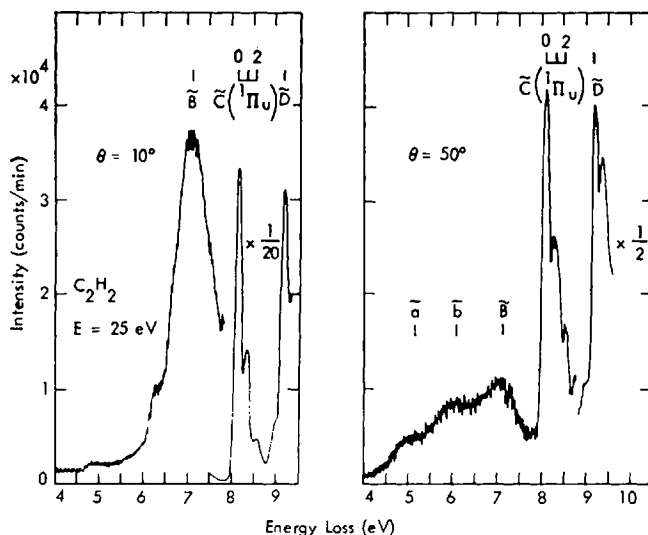


Fig. 26. Energy-loss spectrum of acetylene. $E = 25$ eV, $\theta = 10$ and 50° .

most intense excitation occurs at ~ 8.2 eV. From the results of Schulz^{18a} and Brongersma,²⁰ we observed that the most intense features (excluding negative ion formation) in the trapped-electron spectra of both CO and N₂ are due to singlet \rightarrow triplet transitions. In particular, the $X \rightarrow B^3\Pi_g$ and $X \rightarrow E^3\Sigma_g^+$ transitions are the most intense in N₂ while the $X \rightarrow a^3\Pi$ and $X \rightarrow b^3\Sigma^+$ are the most intense in CO. In view of these comparisons, it is not unlikely that the excitation observed at 8.2 eV in Ref. 19 is due to a singlet \rightarrow triplet transition, analogous to the $^1\Sigma \rightarrow ^3\Sigma$ transitions of N₂ and CO. In order to explain the intensity ratio variation observed in the $\tilde{C}^1\Pi_u$ band of C₂H₂, the maximum transition intensity for this hypothetical forbidden excitation should lie somewhat higher than 8.16 eV, in agreement with Ref. 19.

The steeply rising (with increasing θ) \tilde{a}/\tilde{C} and \tilde{b}/\tilde{C} intensity ratios⁵⁶ are quite similar in appearance to the $^3\Pi/\text{singlet}$ and $^3P/\text{singlet}$ ratios already discussed. In particular, all of these ratios are much steeper than are $^3\Sigma/\text{singlet}$ ones. Thus, we tentatively suggest that \tilde{a} and \tilde{b} are $^3\Pi$ states. In analogy with N₂, they might correspond to the $B^3\Pi_g$ and $C^3\Pi_u$ states. These would be states of a linear C₂H₂ configuration. It is also possible that the excited state is "bent" (a possibility which does not exist for N₂).

In this case a ${}^3\Pi_{g(u)}$ state of the linear molecule (point group $D_{\infty h}$) would correlate with ${}^3A_{g(u)} + {}^3B_{g(u)}$ states of the "trans-bent" (point group C_{2h}) molecule.⁹¹ (We have not considered the "cis-bent" configuration or the possibility of spin-orbit coupling mixing singlets with triplets.) Essentially, the potential function for the degenerate Π electronic state of the linear molecule splits into two when the molecule is bent. The magnitude of this splitting depends on the magnitude of the vibronic interaction (Renner-Teller effect).⁹²

From the presently available data, we cannot decide between the possibilities of (1) excitation of two ${}^3\Pi$ states of the linear molecule, or (2) excitation of a single ${}^3\Pi$ state of the linear molecule which splits into two states of the "bent" system.

In any case, this assignment apparently eliminates the possibility that $\tilde{X} \rightarrow \tilde{a}$, \tilde{b} are $\pi \rightarrow \pi^*$ transitions, since the resulting electron configuration ($\pi^3\pi$) leads only to Σ and Δ states.⁹³ Π states can be obtained by either promoting an electron from a σ orbital into a π orbital or vice versa. Since MO calculations⁹⁴⁻⁹⁸ predict that a ${}^3\Sigma$ is the lowest triplet state (as in N_2), apparently the \tilde{a} state is not the lowest triplet in C_2H_2 .

Figures 27 and 28 present the DCS (in arbitrary units) for several excitations in acetylene. The \tilde{a} and \tilde{b} DCS are quite similar to the 2^3P (He), $a^3\Pi$ (CO), and $C^3\Pi_u$ (N_2) ones. The singlet cross sections are sharply peaked forward, more so at 35 eV than at 25 eV incident energy.

5. Ethylene

Ethylene is a molecule of considerable interest to both theoretical and experimental chemists. Since C_2H_4 is an example of the simplest pi-electron system, it has been used extensively as a model for testing theoretical calculations. Unfortunately, the overlapping nature of its electronic bands has complicated experimental investigations⁹⁹ while *ab initio* calculations have as yet been somewhat limited by the computational effort involved.¹⁰⁰

The optical absorption spectrum of ethylene has been studied by a number of investigators in the solid,¹⁰¹ liquid,¹⁰² and gaseous state.¹⁰³ The optically observed transitions (from the \tilde{X}^1A_g planar ground state, N state of Mulliken¹⁰⁴) can be briefly summarized as follows:

(1) At long wavelengths (low energy), a progression of extremely weak diffuse bands, beginning at about 3.6 eV and peaking at ~ 4.6 eV, is observed.¹⁰⁵ The upper state for this system is the lowest triplet \tilde{a}^3B_{1u} .¹⁰⁶ (Mulliken's T state¹⁰⁴).

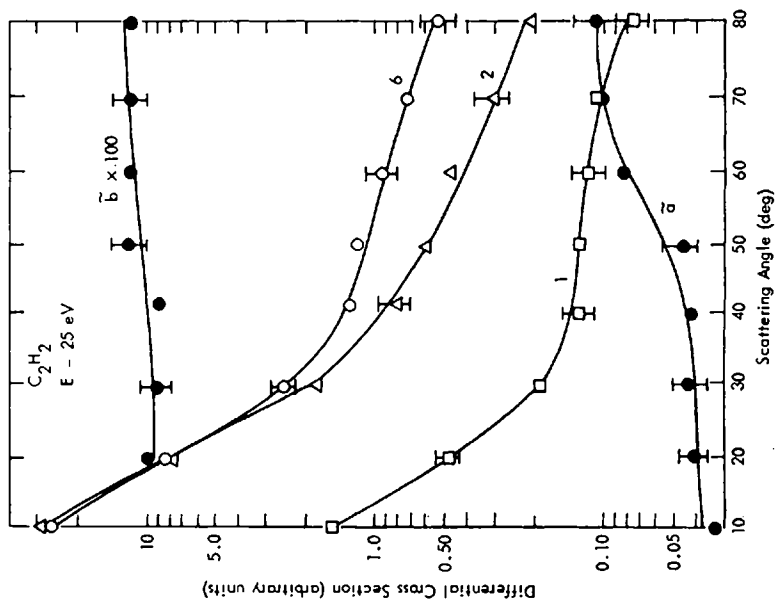


Fig. 27. DCS (arbitrary units) for excitation of the \bar{a} ; \bar{b} ; \bar{B} , (1); \bar{C} ($v_2' = 0$), (2); and \bar{D} ($v_2' = 0$), (6) states of acetylene. $E = 25$ eV.

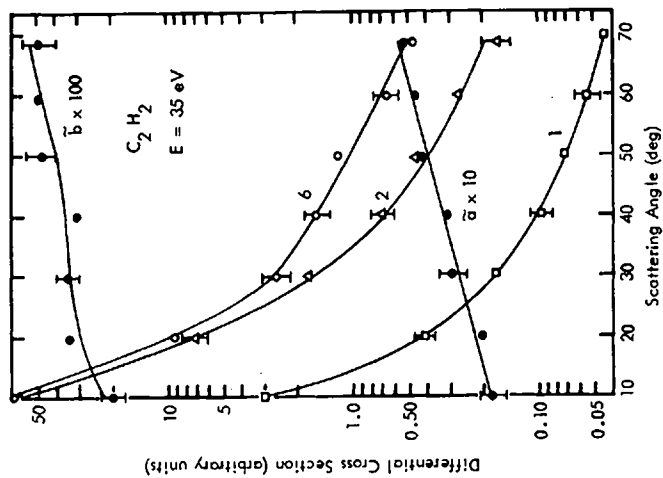


Fig. 28. Same as Fig. 27 except that $E = 35$ eV.

(2) A stronger absorption consisting of a progression of diffuse bands beginning at about 5 eV, merging into a continuum at about 7 eV, and reaching a flat maximum at ~ 7.6 eV occurs next. It is generally agreed¹⁰⁶ that the upper state is the first excited singlet, $^1B_{1u}$ (V state of Mulliken¹⁰⁴).

(2) At 7.11 eV, the first Rydberg transition is observed¹⁰⁷ (R state of Mulliken). Nearly all features observed at higher energies can be attributed to additional Rydberg transitions.⁹⁹

(4) The first ionization potential is found to be 10.50₇ eV.¹⁰⁷ The relative intensities and order of these transitions from 6.2 to 11.64 eV are conveniently shown in the figures of Zelikoff and Watanabe.¹⁰⁸

Kuppermann and Raff³² were the first to observe electronic excitation of ethylene via electron impact. The peaks they observed at 4.6 and 7.7 eV correlate well with the $N \rightarrow T$ and $N \rightarrow V$ (or R) transitions observed optically. Trapped-electron spectra reported by Brongersma¹⁰⁹ and Bowman and Miller¹⁹ show peaks at nearly these same locations as well as one at ~ 9.2 eV (and negative ion formation at lower energies). Doering's^{33c} investigations at large scattering angles ($\theta = 90^\circ$) and low energies (down to 10.9 eV) revealed approximately these same features (4.4, 7.7, and 9.3 eV). At somewhat higher energies (50 eV) and $\theta = 0^\circ$, Simpson and Mielczarek³⁹ observed energy-loss peaks which coincided with several Rydberg transitions. The 4.4 (4.6) eV transition was not observed and the broad peak near 7.7 (actually peaking at 7.5 eV) was clearly due to the lowest $N \rightarrow R$ transition. The energy loss spectrum of Lassettre and Francis,^{25b} obtained at an incident energy of ~ 400 eV and $\theta \approx 0^\circ$, was quite similar to that of Ref. 39 (except that the resolution of the former was about 0.6 eV while that of the latter was 0.1 eV).

Significantly higher resolution studies have been reported by Geiger and Wittmaack⁵⁰ (FWHM ≈ 0.025 eV, $E \approx 33$ KeV, $\theta \approx 0^\circ$) and Ross and Lassettre³¹ (FWHM ≈ 0.03 , $E \approx 150$ eV, $\theta \approx 0^\circ$). Neither the $N \rightarrow T$ nor $N \rightarrow V$ transitions are observed, but the $N \rightarrow R$ and higher Rydberg transitions are clearly evident. The highest energy results⁵⁰ agreed in detail with optical absorption data.¹⁰⁸ (Except, of course, for the $N \rightarrow T$ transition, which is spin-forbidden, and the $N \rightarrow V$ one which is masked by the much stronger $N \rightarrow R$ transition.) However, the data of Refs. 29 and 25b indicate a maximum in the $N \rightarrow R$ (plus underlying $N \rightarrow V$) transition intensity at 7.5 eV whereas the optical absorption reaches a maximum at 7.28 eV. Ross and Lassettre³¹ have attributed this anomaly to an underlying quadrupole-allowed (but dipole-forbidden) electronic transition. There has been great interest, recently, in the electronic states of mono-olefins lying in the 5–7 eV region.^{101,110} and in particular in a "mystery band" around 6.5 eV. A transition in that region was seen by electron impact by

Kuppermann and Raff,^{32a,b} but was not reproduced in an improved version^{32d} of their original apparatus. It was also not seen by Doering and Williams.^{33c} For these reasons we made a special search for such a transition. At $E = 40$ eV and $\theta = 40^\circ$, the energy-loss region between 5.5 and 6.6 eV exhibits no discernible features above the background noise. With a large number of repeated scans using the multichannel scalar, this noise was made as low as 0.5% of the $N \rightarrow T$ triplet state (4.4 eV) peak height. Above 6.6 eV the onset of the optically-allowed Rydberg transitions masks any weak transitions. We conclude that the early electron-impact observations^{32a,b} were spurious, and that the "mystery band" in question is either very much weaker than the $N \rightarrow T$ transition under the conditions just mentioned or, more likely, does not lie in this region of the spectrum.

Figure 29 shows an energy-loss spectrum of ethylene under low resolu-

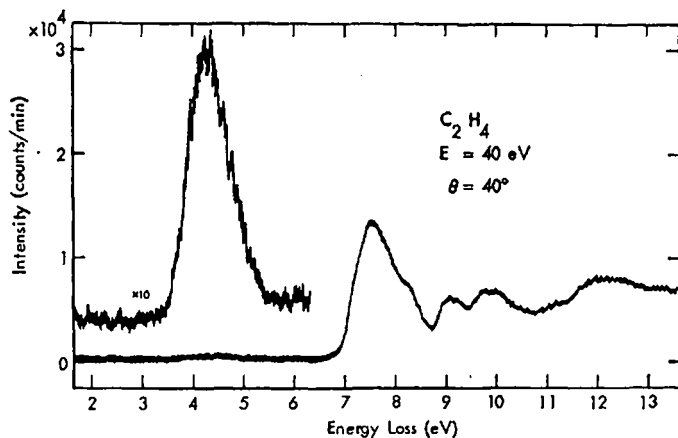


Fig. 29. Energy-loss spectrum of ethylene. $\theta = 40^\circ$. $E = 40$ eV. FWHM of the elastic peak = 0.15 eV.

tion (FWHM of elastic peak = 0.15 eV) at $\theta = 40^\circ$ and $E = 40$ eV.⁵² The $N \rightarrow T$ and $N \rightarrow R$ (or V) transitions are clearly evident as well as higher Rydberg transitions. Figure 30 shows the energy-loss region from about 7 to 10 eV under relatively high resolution (FWHM ≈ 0.05 eV) at $E = 40$ eV and $\theta = 10^\circ$.⁵² The peaks observed in these figures along with their probable assignment are listed in Table IX. These spectra agree quite well with the previous results. We⁵² found that the relative intensity of the bands above 7.5 eV belonging to the $N \rightarrow R$ transition were enhanced with respect to that of the optical and very high energy electron-impact spectra and that the enhancement is more pronounced at higher angle. This discrepancy

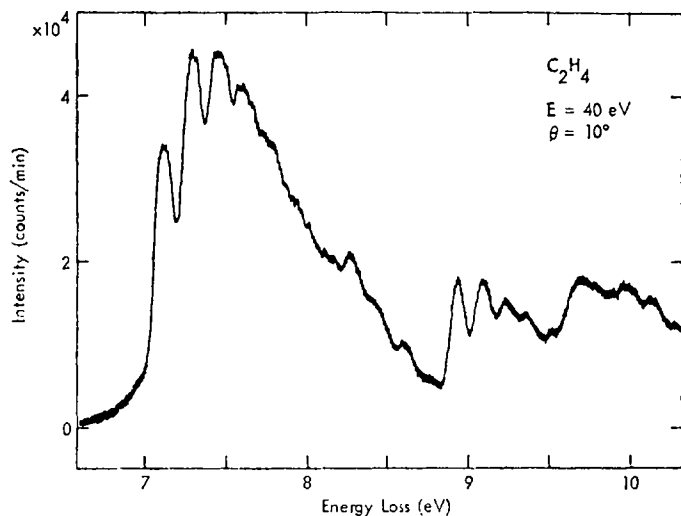


Fig. 30. Same as Fig. 29 except that $\theta = 10^\circ$ and FWHM of the elastic peak is 0.05 eV.

between optical and electron-impact measurements can be explained by an optically-forbidden transition underlying the $N \rightarrow R$ one. Recent measurements of the relative intensities of the N - R bands by Lassette and co-workers³⁵ (at 0 and 7° with $E = 50$ eV) agree very well with those of Ref. 52 ($E = 40$ eV) at low angles. However, these relative intensities are the same as the ones measured by Ross and Lassette³¹ at 150 eV. Furthermore, the intensity ratio of the 7.5 eV $N \rightarrow R$ feature to dipole-allowed transitions was found to be the same at 150 and at 50 eV impact energies.^{31,35} The assumption of an underlying electric quadrupole transition is therefore inconsistent with the theoretical predictions of the Born approximation³⁵ that the intensity ratio of electric dipole to electric quadrupole transition should increase with energy.

Figure 31 shows the intensity ratios for the peaks of the $N \rightarrow T$, $N \rightarrow R$, and $N \rightarrow 3R'$ ($v_2' = 0$) transitions to that of the $N \rightarrow 3R$ ($v' = 0$) one.⁵² These data were obtained from scans of intermediate resolution (FWHM = 0.10 eV). The $N \rightarrow 3R$ ($v_2' = 0$) peak intensity was used as a reference because: (1) the resolution was not sufficient to use the $N \rightarrow R$ ($v_2' = 0$) peak intensity as a reference (the most "logical" choice), (2) the peak of the $N \rightarrow R$ transition could not be used since an underlying-forbidden transition might enhance it at higher angles, (3) the $N \rightarrow 3R'$ ($v_2' = 0$)/ $N \rightarrow 3R$ ($v_2' = 0$) intensity ratio is nearly constant with angle, indicating that both transitions are most likely "isolated" from underlying-forbidden

TABLE IX

Energy-Loss Peak Locations in the Electron-Impact Spectrum of C_2H_4 . The First Column Lists the Excitation Energies (below Ionization) of the Peaks in Figs. 29 and 30; the Second Column Lists the Corresponding Optical Values; and the Third Column Presents the Upper State Assignment Corresponding to the Optical Values. The Ground Electronic State of Ethylene is X^1A_g (Point Group D_{2h})

| Excitation energy from this research (eV) | Optical excitation energy ^a | Assignment of upper state | |
|---|--|------------------------------|------------------------|
| | | Electronic ^b | Vibration ^c |
| 4.4 ± 0.1 (onset: 3.4 ± 0.1) | <3.6) | $\bar{a}^3 B_{1u}$ | |
| | | | v_2' v_4' |
| 7.12 ± 0.01 | 7.11 | $\bar{B}_1(2R)$ | 0 0 |
| | 7.17 | | 0 2 |
| 7.30 ± 0.01 | 7.28 | | 1 0 |
| | 7.34 | | 1 2 |
| 7.46 ± 0.01 | 7.45 | | 2 0 |
| | 7.50 | | 2 2 |
| 7.59 ± 0.02 | 7.61 | | 3 0 |
| | 7.67 | | 3 2 |
| (7.79) ^d | 7.77 | | 4 0 |
| 8.27 ± 0.01 | 8.26 | $\bar{C}_1(3R')$ | 0 0 |
| | 8.32 | | 0 2 |
| (8.41) ^d | 8.42 | | 1 0 |
| 8.60 ± 0.02 | 8.62 | $\bar{D}_1(3R'')$ | 0 0 |
| 8.93 ± 0.01 | 8.90 | $\bar{E}_1(3R)$ | 0 0 |
| | 8.95 | | 0 2 |
| 9.08 ± 0.02 | 9.08 | | 1 0 |
| | 9.13 | | 1 2 |
| 9.24 ± 0.02 | 9.25 | | 2 0 |
| 9.36 ± 0.02 | 9.36 | (4R') | 0 0 |
| 9.70 ± 0.02 | | | |

^a Optical excitation energies for the \bar{a} state are from Refs. 19, 32a, 33c; those for the \bar{B} from Ref. 103, and all others from Ref. 99.

^b Electronic states in parentheses are from Refs. 103 and 99; the others are from Ref. 11c, p. 629.

^c The vibrational assignments are from Refs. 103 and 99.

^d Shoulder.

transitions, and (4) the $N \rightarrow 3R$ ($v_2' = 0$) transition is not strongly overlapped as is the $N \rightarrow 3R'$ one.

The singlet/singlet ratios are relatively flat while the triplet/singlet one

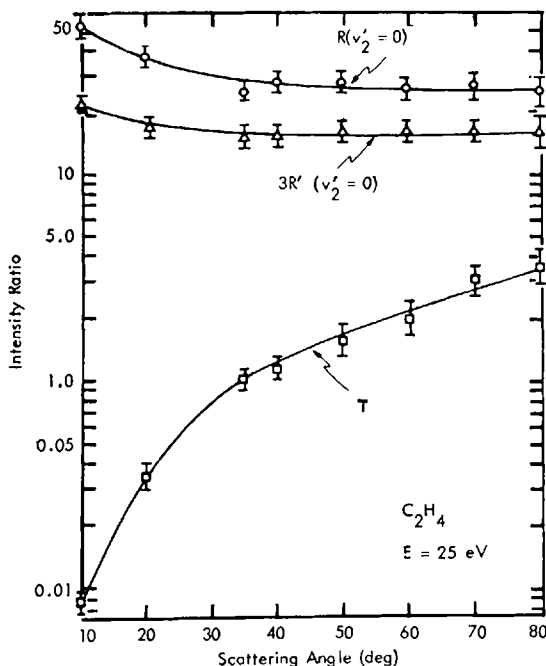


Fig. 31. Peak intensity ratios in ethylene. The upper reference state is $3R(v_2' = 0)$. The peak labels can be correlated with energy losses from Table IX. Each data point is an average of three scans. The FWHM of the elastic peak was 0.10 eV for these data.

increases markedly with angle. The latter ratio is quite characteristic of those for which transitions to the upper state have $\Delta S = 1$, $\Delta \Lambda = 0$. Since this transition is a $\pi \rightarrow \pi^*$ type, our conclusion concerning the acetylene triplets (i.e., they are not $\pi \rightarrow \pi^*$) is consistent with these results. The \tilde{a} (or \tilde{b})/ \tilde{C} ratio in acetylene increased by a factor $> 10^2$ from $\theta = 10$ to 80° while the $\tilde{a}/3R$ ratio in ethylene only increases by a factor of about 30 over the same angular range and at nearly the same incident energy above threshold.

Figure 32 gives the DCS (in arbitrary units) for the $N \rightarrow R$ (peak), $N \rightarrow 3R(v_2' = 0)$, and $N \rightarrow 3R'(v_2' = 0)$ transitions at 25 eV. These singlet \rightarrow singlet Rydberg transitions are strongly peaked in the forward direction with very similar shapes.

C. Summary

The work described in this section demonstrates the use of the measurement of electron-impact differential cross sections as a function of scattering angle to characterize and identify singlet \rightarrow triplet (spin-forbidden)

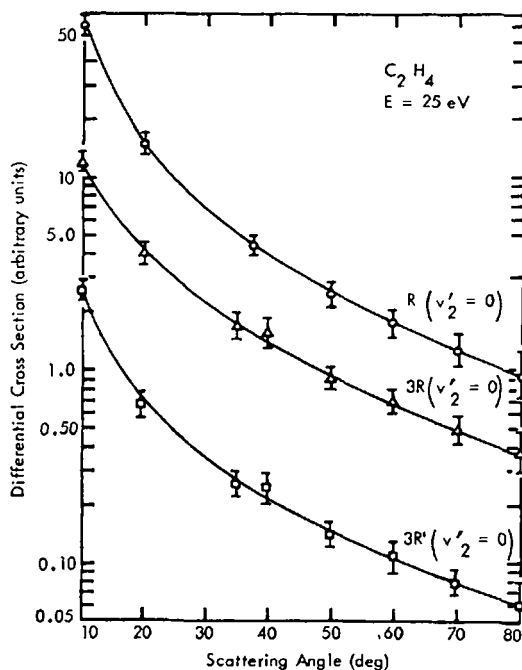


Fig. 32. DCS (arbitrary units) for several transitions in ethylene.

transitions. We are hampered in our endeavor to draw general "spectroscopic rules" for the identification of such transitions from these DCS measurements by two things:

(1) The theory of electron-molecule scattering, though formally well developed, has not been applied with much success to DCS in the low-energy region (a few tens of eV above threshold) in which exchange excitations are important.

(2) Very few experimental measurements of DCS angular dependencies (in this low-energy region) have been made.

These handicaps mean that our "rules," which will be given below, are a self-consistent set of generalizations based primarily on a limited set of empirical results. Nevertheless, it is worth reiterating the consistent trends we have noted.

The character of an excited state (of the target molecule) is reflected in the corresponding DCS. Differences in the behavior with scattering angle of the DCS for the excitation of states of different character can be enhanced by comparing cross-section ratios. The DCS for an optically-allowed transition in each molecule can be used as a "standard" for ratio

comparisons. Let DCSA be the DCS for excitation of the optically-allowed "standard" state (*A*) of some molecule and DCSB be the DCS for excitation of some other state (*B*) of the same molecule. Then, we will designate the quantity "DCSB/DCSA" (DCS ratio as used before) as simply "the *B* ratio."

Table X presents a summary of some of the ratio data already discussed for singlet \rightarrow triplet ($\Delta S = 1$) transitions. An examination of this table and the actual behavior with θ of various triplet state ratios leads us to the following conclusions:

(1) Triplet state ratios increase markedly with increasing θ ($0^\circ \leq \theta \leq 80^\circ$) for impact energies that are 20 to 30 eV above threshold. This behavior clearly distinguishes them from singlet state ratios.

(2) The magnitude of the triplet state ratio increase is sensitive to the

TABLE X

Summary of Some Pertinent Data on All of the Singlet-Triplet Transition Ratios We Have Investigated. The First Column Lists the Molecule (Atom) and the Transition whose DCS Is Used as a Reference for the Ratio Determination (State *A*). The Second Column Gives the *B* State Associated with the Factor Increase (*B* Ratio at High Angle Limit Divided by *B* Ratio at Low Angle Limit) Listed in the Third Column. The Fourth, Fifth, and Sixth Columns Give the Value of $\Delta\Lambda$, the Impact Energy above Threshold, and the Limits of the Angular Range Used to Determine the Factor Increase, Respectively

| Molecule (atom) | <i>B</i> state | Factor increase | $\Delta\Lambda$ | Impact energy above threshold (eV) | Angular range (degrees) |
|---|-------------------|--------------------|------------------|--|-------------------------------|
| He | 2^3S | 6 | 0 | 24 | 0-70 |
| $1^1S \rightarrow 2^1P$ | 2^3P | 60 | 1 | 23 | 0-70 |
| N ₂ | $E^3\Sigma_g^+$ | 6 | 0 | 23 | 10-80 |
| $X^1\Sigma_g^+ \rightarrow b^1\Pi_u$ | $C^3\Pi_u$ | 100 | 1 | 24 | 10-80 |
| | $B^3\Pi_g$ | 100 | 1 | 32 | 10-80 |
| CO | $b^3\Sigma^+$ | 30 | 0 | 25 | 10-80 |
| $X^1\Sigma^+ \rightarrow A^1\Pi$ | $a^3\Pi$ | 100 | 1 | 29 | 10-80 |
| C ₂ H ₂ | \bar{a} | 1000 | (1) ^a | 30 | 10-80 |
| $X^1\Pi_g^+ \rightarrow \tilde{C}^1\Pi_u$ | \bar{b} | 1000 | (1) ^a | 29 | 10-80 |
| C ₂ H ₄ | <i>T</i> | 35 | 0 | 21 | 10-80 |
| (<i>N</i> \rightarrow 3 <i>R</i>) | | | | | |
| H ₂ | $b^3\Sigma_g^+$ | 30 | 0 | 30 | 10-80 |
| $X^1\Sigma_g^+ \rightarrow C^1\Pi_u$ | | | | | |

^a Presumably, $\Delta\Lambda = 1$ for these two transitions.

value of $\Delta\Lambda$ associated with the singlet \rightarrow triplet transition. Notice that the ratios for which $\Delta\Lambda = 1$ increase sharply by about two orders of magnitude over the angular range in a manner that is independent of the $g \rightarrow g$ (or u) nature of the transition. On the other hand, triplet state ratios for which $\Delta\Lambda = 0$ increase by about one order of magnitude. From the examples of this latter type, those which are symmetry-allowed (SA) increase by about a factor of five more than those which are symmetry-forbidden (SF). Further, these $\Delta S = 1$, $\Delta\Lambda = 0$ ratios tend to reach a plateau at intermediate angles, contrary to the $\Delta S = 1$, $\Delta\Lambda = 1$ ratios.

In summary, triplet state excitations as a whole can be clearly identified by their ratio behavior (11 examples). The determination of $\Delta\Lambda$ from the ratio behavior also seems reasonably reliable (5 examples of $\Delta\Lambda = 0$ and presumably 6 examples of $\Delta\Lambda = 1$). There is no apparent difference in the ratio dependencies of SA and SF ratios for $\Delta\Lambda = 1$ (at least 1 SF example and 2 SA examples), while for $\Delta\Lambda = 0$ the SF ratios seem to increase less than do the SA ones (1 SF example and 3 SA examples). The reliability of these generalizations can be judged by the number of examples.

For singlet state ratios ($\Delta S = 0$), the situation seems more complex. In particular, these ratios do not exhibit any general trend with angle as do the triplet ones (this in itself, however, points up the $\Delta S = 0$ character of the former). Some singlet ratios are practically constant while others increase or decrease with θ at small scattering angles. In the case of CO, the signs of the initial slopes of the $^1\Sigma^+$ ratios change from negative to positive as the impact energy is lowered from 35 to 25 eV while a similar singlet state ratio ($p'^1\Sigma_u^+$) in N_2 has the same behavior at 25 eV that it has at 40 eV.

The applicability of these semiempirical rules to atomic, diatomic, and polyatomic molecular targets indicates that to a first approximation the angular distribution of the scattering process is determined by the outer (valence) shell electrons of the target. In other words, the incoming electron at these low energies do not interact directly with the nuclei or the lower shell electrons.

V. VIBRATIONAL-ROTATIONAL EXCITATION*

Pure rotational excitation of H_2 has been studied under multiple-scattering conditions,¹¹¹ observed in a single-scattering beam experiment,¹¹² and treated theoretically.^{113,114} It is doubtful, however, that the experimental study of rotational excitation of other molecules is possible with present-day techniques. The vibrational excitation of molecules is also accompanied

* This part has been written in cooperation with D.G. Truhlar, Department of Chemistry, California Institute of Technology, Pasadena, California.

by rotational transitions. These have been resolved only in the case of H_2 (by Ehrhardt and Linder¹¹²).

Diffusion and swarm experiments carried out in the early 1930's^{115,116} indicated the importance of vibrational excitation of molecules by low-energy electrons. It was found that the energy losses suffered by the electrons were larger than purely momentum transfer considerations of elastic scattering would allow. The actual observation of discrete vibrational excitation and the detailed study of this phenomenon became possible, however, only recently with the advances of electron beam techniques.

Vibrational excitation of molecules by very low-energy electrons (below about 10 eV) has been studied extensively both experimentally and theoretically. At these energies the scattering process is often dominated by a resonance. In such cases, the magnitude of the cross section and its energy and angular dependence are well described by resonance theories.^{6,7,117} Vibrational excitation of N_2 at low impact energies is an example of a resonance-dominated scattering process. The vibrational excitation cross section is small from threshold to about 2 eV impact energy. It increases by about two orders of magnitude (to about 18 a_0^2) in the 2 to 4 eV energy range, and the cross section versus energy curve shows very pronounced resonance structure.^{18c} Above these energies the cross section becomes small again. In general, potential scattering dominates outside of the resonance regions, and in some cases (e.g., CO, H_2) the effect of potential scattering is clearly apparent even in the resonance regions.⁴⁶

Schulz and Dowell,¹¹⁸ using the trapped-electron method, observed excitations in O_2 to the 8 lowest vibrationally excited states. They could not assess from their data the relative extent of direct vibrational excitation and that due to temporary negative ion formation. Skerbele, Dillon, and Lassette³⁶ observed vibrational excitation of N_2 , O_2 , CO, and NO at 45 eV and H_2O and CO_2 at 30–60 eV impact energies at scattering angles below 15° . They found that for the homonuclear diatomic molecules, the ratio of the vibrational excitation cross section to the elastic scattering cross section was independent of angle between 3 and 14° , while this was not the case for the optically-allowed vibrational excitations of H_2O and CO_2 . It is interesting to note that this ratio for the electric dipole-allowed excitation of the first excited vibrational state in CO was only five times larger than for the electric dipole-forbidden excitation of the same state for N_2 and O_2 at 4° . For the polyatomic molecules they found that the fundamental vibrational excitations appear much more strongly than overtone and combination bands. Trajmar and co-workers studied the vibrational excitation of H_2 ($E = 7$ to 81.6 eV)¹¹⁹ and N_2 ($E = 20 \text{ eV}$)¹²⁰ from 10 to 80° . Some of their results will be discussed and compared to other investigations below.

At very high energies (~ 35 keV) and at zero scattering angle, Geiger and Wittmaack¹²¹ studied vibrational excitation in CO_2 , H_2O , and C_2H_4 and were able to observe only electric dipole-allowed transitions, in agreement with the predictions of the Born approximation.

The straightforward and most complete way of treating the electron-molecule scattering problem quantum mechanically—by considering all molecular states explicitly and solving the full set of coupled equations—is also the most impractical one at present. One is therefore forced to approximations of varying degrees. The only close coupling calculation on pure vibrational excitation was reported by Fajen and Lin.¹²² They found that for vibrational excitations within the ground electronic state the inclusion of higher electronic states into the wavefunction was necessary. This is an indication of the importance of the polarization of the electronic charge cloud of the molecule by the incident electron. Takayanagi¹²³ calculated vibrational excitation cross sections for H_2 by a distorted wave method using as the electron-molecule interaction a simplified polarization potential. The calculation was in order of magnitude agreement with experimental data; however, a greater accuracy cannot be expected because of the very simplified form of the potential. Most of the calculations have been made in the Born approximation. Massey,¹²⁴ Wu,¹²⁵ Morse,¹²⁶ and Carson¹²⁷ assumed short-range electrostatic interactions to be responsible for the transition. In a more realistic treatment, Breig and Lin¹²⁸ and Takayanagi¹²³ calculated the scattering including all important long range forces. All these calculations were concerned with total cross sections.

We will now consider our measurements of the elastic and vibrational DCS of H_2 ¹¹⁹ and N_2 .¹²⁰ Typical vibrational spectra of H_2 at $E = 10$ eV and $\theta = 25^\circ$, and of N_2 at $E = 20$ eV and $\theta = 83.5^\circ$ are shown on Figures 33 and 34, respectively. The intensities of the inelastic features were determined by a curve-fitting procedure that unfolded the contribution of the tail of the elastic peak. (The smooth solid line on top of the noisy experimental curve is the calculated spectrum.) From spectra obtained at different angles the ratios of the inelastic to elastic intensities were obtained. Due to the long time required to build up adequate signal-to-noise ratios, measurements taken at different angles do not correspond to exactly identical experimental conditions and therefore cannot be directly related to each other. The only meaningful quantity is the ratio of the inelastic to elastic intensity. Since all proportionality factors relating scattered signal intensities to DCS cancel out, the above ratios are equal to the ratios of the corresponding DCS's. Figure 35 shows these ratios for H_2 at 13.6 and 81.6 eV impact energies (uncalibrated). The angular distribution of the elastic scattering was separately determined under experimental conditions

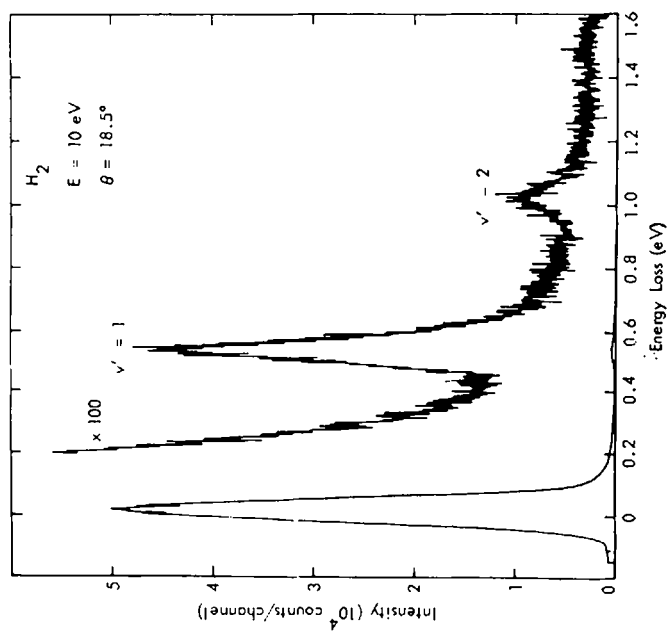


Fig. 33. Vibrational excitation spectrum of H_2 , $p \approx 10^{-3}$ Torr. Superposition of 15 scans with 1 sec dwell time and 1.75 mV/channel.

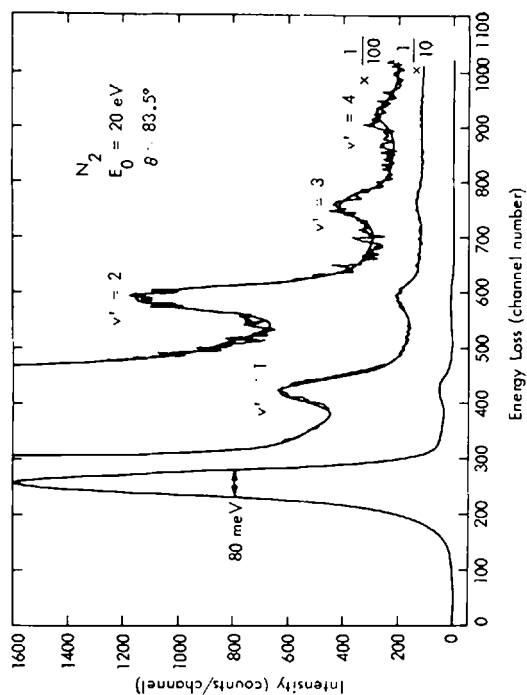


Fig. 34. Vibrational excitation spectrum of N_2 , $p \approx 10^{-3}$ Torr. Superposition of 54 scans with 1 sec dwell time and 1.75 mV/channel.

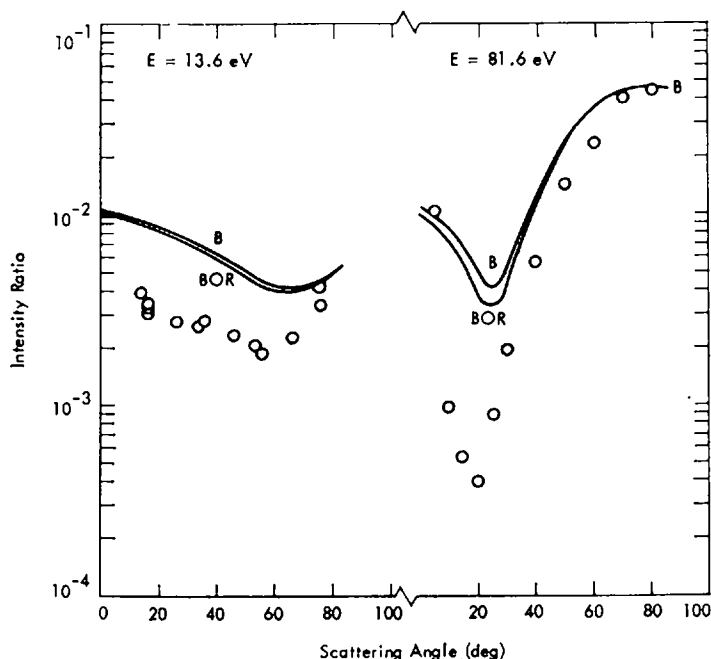


Fig. 35. The ratio of the fundamental vibrational excitation cross section to the elastic scattering cross section for H_2 at 13.6 and 81.6 eV as a function of scattering angle. Individual points are experimental values, the solid curves marked by BOR and B correspond to values calculated with and without electron exchange respectively.¹¹⁹

that were constant for each angle. After correction for the change of effective path length with scattering angle, the elastic DCS were obtained on an arbitrary scale and the product of the ratios and the elastic DCS yielded the vibrational excitation cross sections on the same arbitrary scale. They were then put on an absolute scale by normalization to theory as described subsequently in this section. The results are shown in Figures 36–38 for 13.6 and 81.6 eV. The 10 eV cross sections have been normalized to an absolute scale by utilizing the total $e-H_2$ scattering cross sections measured by Golden, Bandel, and Salerno¹²⁹ and by extrapolation of our experimental elastic and inelastic DCS curves to 0 and 180°. The results are shown in Figures 39 and 40.

The differential cross sections were calculated at these energies in the Born approximation with a potential that included polarization, the interaction of the incident electron with the molecular electric quadrupole moment, and short-range interaction terms.¹¹⁹ The scattering problem was

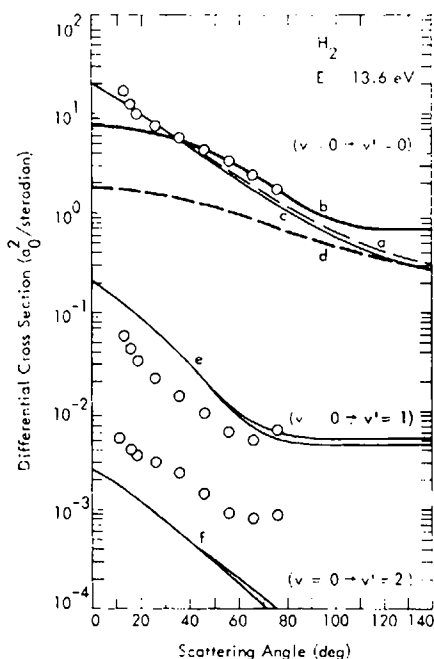


Fig. 36. DCS for H_2 at 13.6 eV. The points are experimental and the solid curves are theoretical results. Elastic cross sections: Curves (a) and (c)¹¹⁹ with and without exchange, respectively; Curve (b) calculated from the published phase shifts¹³⁶; Curve (d) Born approximation.¹³⁸ Inelastic cross sections: Curves (e) vibrational fundamental excitation, Curves (f) excitation of the first overtone vibration, Curves (e) and (f) are from Ref. 119—upper curves with exchange, lower curves without exchange.

treated as the collision of a particle and rotating vibrator with an approximate local potential that depends parametrically on the nuclear positions. The polarized Born treatment used is outlined here for homonuclear diatomic molecules. [For heteronuclear molecules the inclusion of the dipole term into the multipole expansion of the interaction potential is necessary (see Eq. 25 below) and the summation over the final rotational states has to be slightly modified.]

A calculation of this type can be justified because the calculations of Breig and Lin in the polarized Born approximation¹²⁸ and Takayanagi in the polarized Born and polarized distorted wave approximations¹²³ agree qualitatively for total cross sections and even the quantitative agreement is within about a factor of two. Furthermore, Gerjuoy and Stein¹³⁰ have argued that the plane wave approximation is valid at low energies for rotational excitation collisions because most of the contribution to the transition integral comes from large electron-molecule separations at low energy

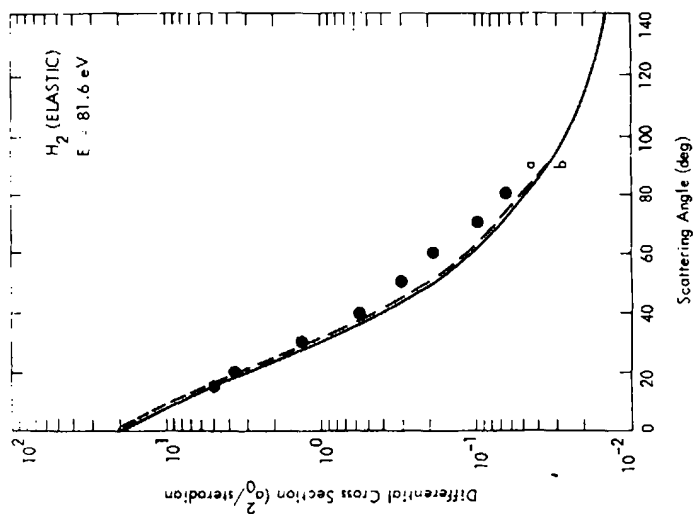


Fig. 37. Elastic DCS for H_2 at 81.6 eV.¹¹⁹ Points are experimental values, Curves (a) and (b) are calculated with and without exchange, respectively.

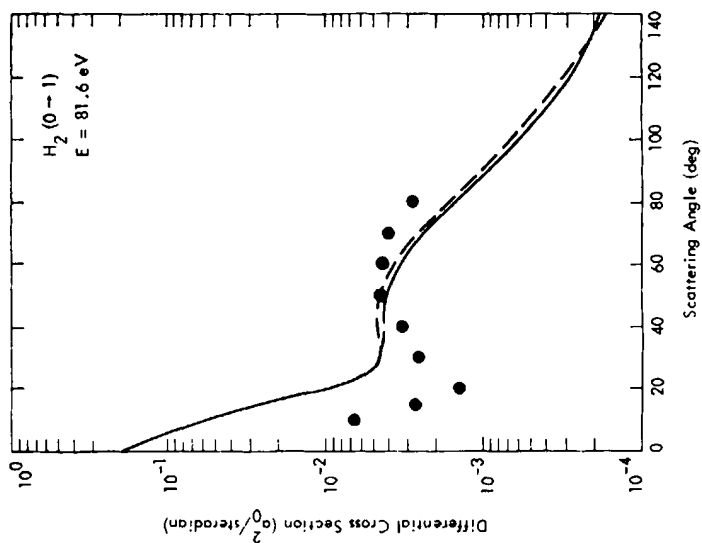


Fig. 38. Vibrational excitation DCS for H_2 at 81.6 eV.¹¹⁹ Points are experimental values, the solid and dashed curves are calculated in the polarized Born and polarized BOR approximations, respectively.

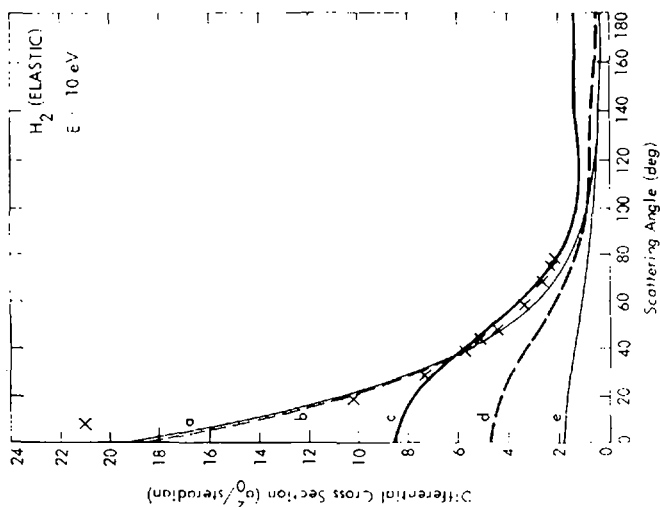


Fig. 39. Elastic DCS for H_2 at 10 eV. Crosses are experimental values. Solid curves are the results of calculations. Curves (a) and (b)¹¹⁹ without and with exchange, respectively. Curves (c) and (d) calculated from published shifts¹³⁶ with and without exchange, respectively; Curve (e) Born approximation without polarization or exchange.¹³⁸

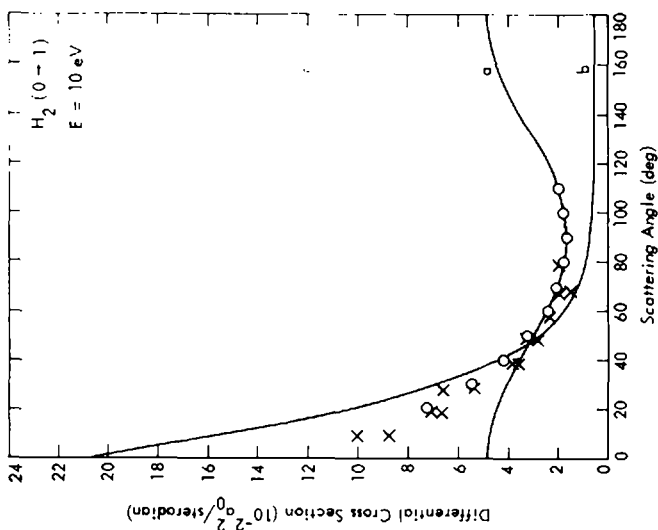


Fig. 40. Vibrational excitation DCS for H_2 at 10 eV. Crosses and circles are experimental values (Refs. 119 and 46, respectively). Curve (a) $\sim (1 + 2 \cos^2 \theta)$; Curve (b) was calculated in the polarized Born approximation. (The polarized BOR curve can not be distinguished from curve (b) on the scale of this figure.)

(due to the long-range potentials). This argument should be equally valid for vibrational excitations. (However, Takayanagi and Geltman¹¹³ reconsidered this problem and concluded that distortion of the s and p waves may be important.)

For the transition from state p with vibrational quantum number v and rotational quantum numbers J and M to state $p'(v', J', M')$ the integral ($Q_{p'p}$) and differential ($\sigma_{p'p}$) cross sections are given by

$$Q_{p'p}(E) = \int \sigma_{p'p}(\theta, E) \sin \theta \, d\theta \, d\phi \quad (21)$$

$$\sigma_{p'p}(\theta, E) = \frac{k'}{k} |f_{p'p}(\theta)|^2 \quad (22)$$

in terms of the initial and final wavenumber k and k' and the direct scattering amplitude $f_{p'p}$. In the plane wave approximation

$$f_{p'p}(\theta) = -\frac{1}{2\pi} \int \exp[i(\mathbf{k} - \mathbf{k}') \cdot \mathbf{r}] V_{p'p}(\mathbf{r}) \, d\mathbf{r} \quad (23)$$

where, assuming separability of vibrational and rotational motions,

$$V_{p'p}(\mathbf{r}) = \int \psi_v^*(R) Y_{J'M'}^*(\hat{\mathbf{R}}) V(\mathbf{r}, \mathbf{R}) \psi_v(R) Y_{JM}(\hat{\mathbf{R}}) \, d\mathbf{R} \quad (24)$$

and $\psi_v(R) Y_{JM}(\hat{\mathbf{R}})$ is the molecular nuclear coordinate wavefunction for state p . Here the coordinates of the scattering electron and internuclear motion are denoted \mathbf{r} and \mathbf{R} , respectively.

Only the first two terms in the multipole expansion of the potential were considered, i.e.,

$$V(\mathbf{r}, \mathbf{R}) \cong V_0(r, R) P_0(\hat{\mathbf{r}} \cdot \hat{\mathbf{R}}) + V_2(r, R) P_2(\hat{\mathbf{r}} \cdot \hat{\mathbf{R}}) \quad (25)$$

The explicit forms of $V_0(r, R)$ and $V_2(r, R)$ in Eq. (30) were approximated by

$$V_0(r, R) = V_0^C(r, R) - \frac{\alpha(R)}{2r^4} g(r) \quad (26)$$

$$V_2(r, R) = V_2^C(r, R) - \frac{Q(R)}{2r^3} f(r) - \frac{\alpha'(R)}{2r^4} g'(r) \quad (27)$$

where $V_0^C(r, R)$ and $V_2^C(r, R)$ are the first two terms of the multipole expansion of the approximate potential obtained by considering two spherically symmetric atomic electron distributions centered at the two hydrogen nuclei (see Refs. 127 and 119 for details). Since such a charge distribution does not have a quadrupole moment [$Q(R)$], the second term in $V_2(r, R)$ was added to account for the electron molecular quadrupole interaction. The polarization is represented by the last terms in each of

$V_0(r, R)$ and $V_2(r, R)$. They were taken in a form that corresponds to the adiabatic approximation as $r \rightarrow \infty$. $f(r)$, $g(r)$, and $g'(r)$ are "cut-off functions" negating the singularities at small r . They are determined to make the potential agree with less semiempirical calculations.^{4,131,132} $\alpha(R)$ and $\alpha'(R)$ are given in terms of static dipole polarizability of the molecule parallel and perpendicular to the internuclear axis by

$$\alpha = \frac{1}{3}(\alpha_{\parallel} + 2\alpha_{\perp})$$

$$\alpha' = \frac{1}{3}(\alpha_{\parallel} - \alpha_{\perp})$$

Substituting (25), (26), and (27) into (24) gives

$$V_{p'p}(\mathbf{r}) = V_{0,v'v}(r) \delta_{J'J} \delta_{M'M} + (-1)^M \left[\frac{4\pi(2J'+1)(2J+1)}{5} \right]^{1/2} \\ \times V_{2,v'v}(r) \begin{pmatrix} J' & 0 & J \\ 0 & 0 & 0 \end{pmatrix} \begin{pmatrix} J' & 2 & J \\ -M & M'-M & M \end{pmatrix} Y_{2,M-M'}(\hat{r}) \quad (28)$$

where the z-axis in the \mathbf{r} coordinate system was chosen to be along \mathbf{R} . In (28) the standard notation¹⁴⁸ is used for the 3- j symbol and

$$V_{L,v'v}(r) = \int \psi_{v'}^*(R) V_L(r, R) \psi_v(R) R^2 dR \quad (29)$$

where $L = 0$ or 2 . The integral (29) was computed numerically using potential curves given by Kolos and Wolniewicz¹³³ for Ref. 119 and Sahni and Sahney¹³⁴ for Ref. 120. Scattering off the potential (25) strictly implies the selection rule $\Delta J = 0, \pm 2$.

Substituting (29) into (23) and (22), summing over J' and M' and averaging over M one obtains

$$\sigma_{v',vJ} = S_0 + S_2 \quad (30)$$

where

$$S_0 = \frac{k'}{k} N_{v'v}^2 q^2 \quad (31)$$

$$N_{v'v} = -\frac{2}{q^2} \int \sin qr V_{0,v'v}(r) r dr \quad (32)$$

$$S_2 = \frac{k'}{5k} M_{v'v}^2 \quad (33)$$

$$M_{v'v} = 2 \int r^2 V_{2,v'v}(r) j_2(qr) dr \quad (34)$$

$$q = |\mathbf{k}_{p'} - \mathbf{k}_p| \quad (35)$$

j_2 represents the spherical Bessel function of order 2. This DCS, to our approximation, is independent of the initial rotational state J . It can therefore be compared directly with experimental cross sections (which are for an average over a thermal distribution of initial rotational states).

The effect of exchange was included in some calculations¹¹⁹ through the polarized Born-Ochkur-Rudge approximation (BOR).¹³⁵

The measured and calculated ratios of the vibrational to elastic scattering signal intensities are shown in Figure 35 for 13.6 and 81.6 eV electrons (energy scale uncalibrated). Individual points are experimental values and the solid curves denoted by BOR and B correspond to the calculated ratios by the polarized Born-Ochkur Rudge and polarized Born approximations, respectively, as outlined above. Although the agreement is quantitatively poor, the calculated ratios are of the right order of magnitude and the shape of the experimental curves is qualitatively reproduced by the calculation. At impact energies of 7 to 60 eV, the ratio curves (both experimental and calculated) show that the dip shifts gradually to lower angles and becomes more pronounced as the electron energy increases.

The experimental and calculated elastic DCS for H_2 at 10 eV are given in Figure 39. The individual points represent the experimental values normalized to the total $e-H_2$ scattering cross section measured by Golden, Bandel, and Salerno.¹²⁹ To carry out the normalization, the elastic and vibrational DCS curves were extrapolated to 0 and 180°. The vibrational contribution is about 1% of the total cross section; contribution from the $b^3\Sigma_u^+$ electronic excitation should be very small and was neglected. An error of about $\pm 30\%$ is estimated for each experimental point. Curves (a) and (b) are the results of the polarized Born and polarized BOR calculations, respectively. Both calculations give good agreement with experiment both for the magnitude and for the angular dependence of the cross section. The inclusion of the exchange contributions calculated by the polarized BOR approximation lowers the DCS at small angles. Curve (c) was calculated¹¹⁹ from the interpolated phase shifts of Wilkins and Taylor¹³⁶ by a method described by Temkin (see Tully and Berry¹³⁷). The phase shifts were obtained by solving numerically the static exchange equations for an electron moving in the potential field of the neutral homonuclear diatomic hydrogen molecule. This treatment takes full account of electron exchange. The agreement with experiment is excellent from about 30 to 80° scattering angles. At lower scattering angles, however, the agreement is poor and the reason for this discrepancy seems to be the neglect of the polarization. Curve (d) was obtained the same way as Curve (c) except from phase shifts where the exchange was intentionally neglected. Curve (e) is calculated by Rozsnyai¹³⁸ in the first Born approximation (no exchange or polarization

was taken into account). From a comparison with Curve (a) we can conclude again that polarization plays a very important role in determining the low-angle elastic DCS while its effect at high angles is negligible.¹¹⁹

The vibrational excitation DCS for H_2 at 10 eV are summarized in Figure 40. The crosses are the experimental values¹¹⁹ (normalized by the same factor as the 10 eV elastic DCS). The open circles were obtained from the relative measurements of Ehrhardt and co-workers⁴⁶ by normalizing them to our DCS at 60° . The angular shape of the two sets of data is in excellent agreement. Curve (a) corresponds to $(1 + 2 \cos^2 \theta)$ normalized to the experimental data at high angles. This is the predicted angular distribution for vibrational excitation of H_2 if the scattering process is dominated by the single resonant state $^2\Sigma_u^+$ of H_2^- ^{117,139,140} and is in agreement with the experimental data from 40° to 110° . However, there are several reasons why the single resonance state model (SRS) cannot be accepted as completely proved in this case. (1) The SRS curve was normalized to experiment at high angles and it is uncertain whether it can account quantitatively for the magnitude of the cross section. (2) Below 40° the agreement of the SRS and experiment is poor. (3) The H_2^- resonance state under consideration is at about 3 eV with a width estimated to be about 2 to 4 eV^{46,137} while the electron impact energy is 10 eV. (4) The $^2\Sigma_g^+$ negative ion state (which is responsible for dissociative attachment) is energetically accessible at 10 eV¹⁴¹ and may cause deviation from the SRS. (5) The shape of the angular distribution can also be explained in terms of direct scattering as indicated by the calculation discussed next.

Curve (b) is calculated for direct scattering¹¹⁹ by Trajmar and co-workers. The polarized Born and polarized BOR curves are not distinguishable on the scale of this figure. They differ by no more than 20% anywhere in the whole angular range, indicating that the sum of the exchange and the interference between direct and exchange terms are not important in the BOR in this case. Although the calculated DCS rises too fast at low angles as the scattering angle is decreased and fails to reproduce the dip at around 90° ,¹⁴² it gives the correct value at 30° to 70° and without renormalization gives as good an overall agreement for the angular distribution as the empirically normalized SRS.

The individual DCS for H_2 at 13.6 eV are summarized in Figure 36. The experimental points were normalized to the absolute DCS at 60° calculated from the phase shifts of Wilkins and Taylor.¹³⁶ The solid lines correspond to calculated cross sections. The conclusions one can draw are similar to those discussed above for the 10 eV case.

Figures 37 and 38 show the elastic scattering and vibrational excitation DCS for 81.6 eV electrons. The experimental points were normalized to

the polarized BOR calculation for the elastic scattering at 30° as summarized above. The calculated and experimental angular behaviors are in good agreement for the elastic scattering and the effect of exchange is quite small. For the vibrational DCS, the agreement between the shape of the experimental and calculated curves is not good. They differ by about one full order of magnitude in the 10 to 20° region, although they agree in the 50 to 80° region.

The experimental vibrational to elastic scattering intensity ratios are shown in Figure 41 from 10° to 85° for N_2 at 20 eV. It is found in agreement

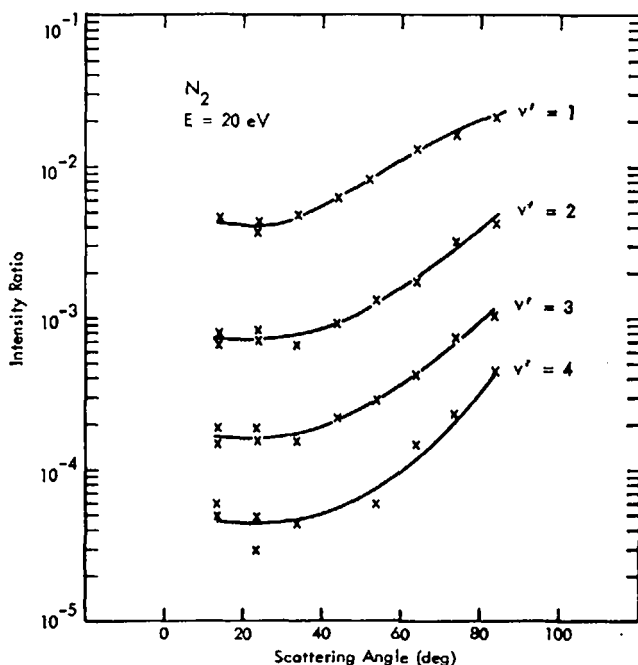


Fig. 41. Ratios of the vibrational over elastic scattering intensities for N_2 at 20 eV.

with previous low-angle studies (which were at 45 eV impact energy),³⁶ that the ratio is independent of angle at low angles up to about 20° . At higher angles, however, this ratio increases and at 80° its value is about five times larger than at low angles. In contrast to H_2 , these curves do not show a minimum but they smoothly increase with increasing angle. The differential cross sections are given in the same arbitrary units on Figures 42 and 43. No sharp minimum is present in the vibrational DCS, again in contrast to the H_2 curves. These DCS decrease monotonically by about a factor of

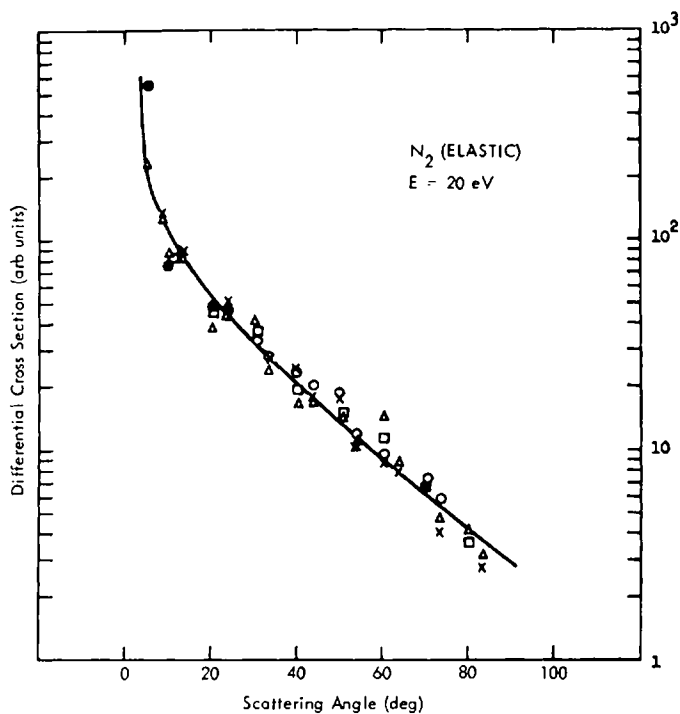
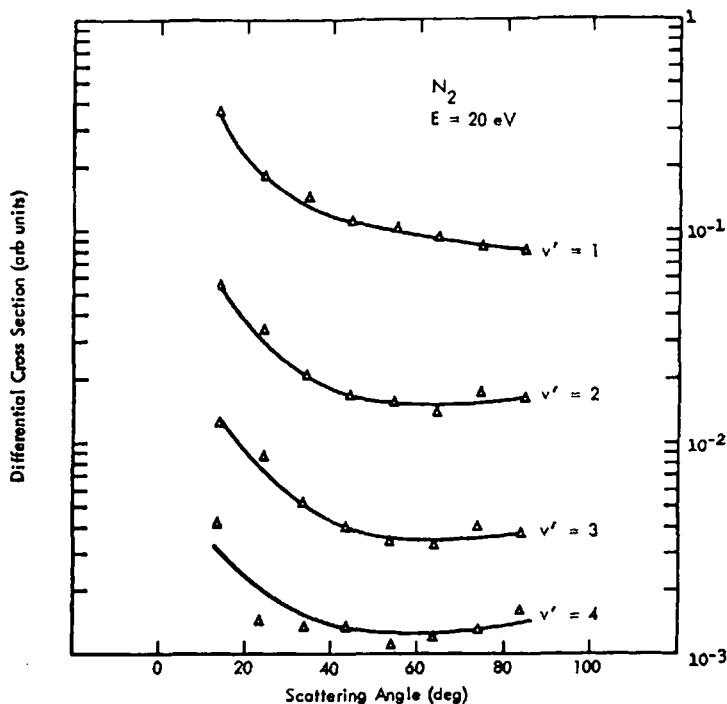


Fig. 42. Elastic DCS for N_2 at 20 eV.

five from 10 to 80°. Within experimental accuracy the DCS curves corresponding to the different vibrational excitations are parallel to each other. Preliminary plane wave calculations (the potentials were not yet as well calibrated as for the H_2 calculation described above) indicate that a possible explanation for the differing behavior of H_2 and N_2 is that the terms associated with P_2 in the multipole expansion of the potential contribute less to the cross section in the case of N_2 than they do for H_2 .¹²⁰ The part of the cross section coming from this term increases with increasing scattering angle, while the P_0 contributions behave in the opposite manner. This explanation is shown pictorially in Figure 44.

VI. SUPERELASTIC SCATTERING

The process of electron deexcitation of atoms and molecules is called superelastic scattering. During this process, the electron gains energy by colliding with excited molecules. Under normal (room temperature) conditions for small molecules, the population of excited electronic and vibrational states is negligible and that of the "higher" rotational states is small. In

Fig. 43. Vibrational DCS for N_2 at 20 eV.

high temperature atmospheres, in glow discharges, and in plasmas, however, superelastic collisions could become important.

Simultaneous measurement of the vibrational excitation and deexcitation scattering intensities (I_v and I_s , respectively) yields the ratio of the ground state to vibrationally excited state population density,

$$I_s/I_v \cong \rho^*/\rho \quad (36)$$

where ρ and ρ^* are the densities of molecules in their ground and vibrationally excited states, respectively. I_s and I_v are the signals (either at a particular scattering angle or integrated over all angles) corresponding to superelastic scattering and vibrational excitation between the same states. The only assumption here is that the cross sections for the two processes are the same. This would follow from detailed balancing^{143,144} if the vibrational excitation energies ΔE were zero. For $\Delta E \neq 0$, this is still a good assumption at impact energies which are large compared to ΔE and where there is

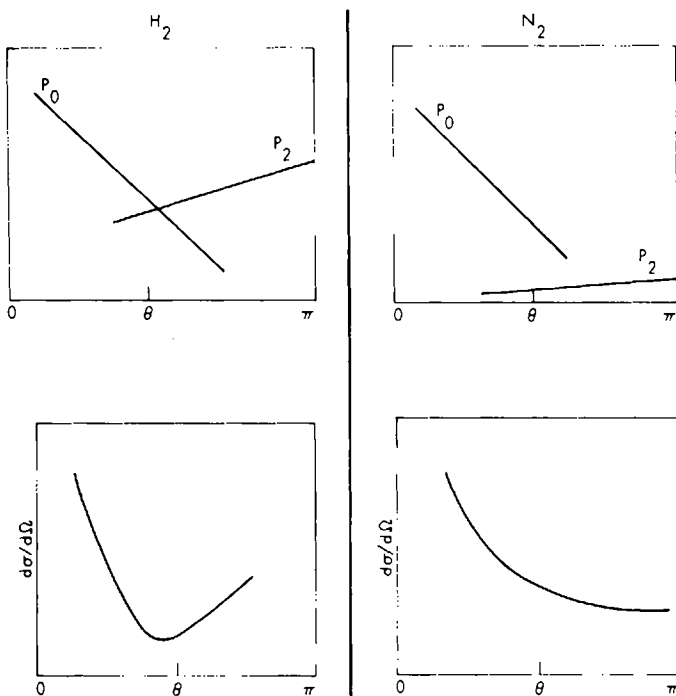


Fig. 44. Explanation for the different angular behavior of the vibrational DCS for H_2 and N_2 .¹²⁰ In the upper figures, the individual contributions from the (non-interfering) scattering off the symmetric and asymmetric parts of the potential are indicated schematically. The lower figures give the sum of these contributions.

no strong resonance present (that is, where the cross section does not change very rapidly with impact energy).

Experimental data on superelastic electron scattering are very scarce. The process has been studied recently with excited mercury¹⁴⁵ and rubidium.¹⁴⁶ Burrow and Davidovits¹⁴⁷ observed superelastic electrons scattered from nitrogen molecules vibrationally excited by quenching collisions with optically excited rubidium atoms. By measuring superelastic scattering, it is possible to study collisional processes involving vibrationally excited molecules. This technique is particularly important for homonuclear molecules where its observation is not possible. They have also observed experimentally that the equation^{144,147}

$$\sigma_{21}(E) = \frac{g_1}{g_2} \frac{E + \Delta E}{E} \sigma_{12}(E + \Delta E) \quad (37)$$

relating the superelastic cross section to the vibrational excitation cross section was qualitatively verified. A more rigorous examination of this problem with higher energy and angular resolution is desirable.

VII. POSITRON SCATTERING

The use of positrons instead of electrons opens up a new and interesting field and makes possible the observation of direct scattering without exchange scattering. A high-resolution positron source has been developed and reported by Groce and co-workers^{14,9} and interesting results should be forthcoming.

Acknowledgments

The authors wish to thank Donald G. Truhlar for his collaboration on Vibrational Rotational -1 Excitation (Section V) and for reading and correcting the rest of the manuscript.

References

1. A. Messiah, *Quantum Mechanics*, Vol. 2, Wiley, New York, 1961, p. 833.
2. M. L. Goldberger and K. M. Watson, *Collision Theory*, Wiley, New York, 1964.
3. N. F. Mott and H. S. W. Massey, *The Theory of Atomic Collisions*, 3rd ed., Clarendon Press, Oxford, 1965; (a) p. 420, (b) p. 28, (c) p. 593.
4. H. S. W. Massey and E. H. S. Burhop, *Electronic and Ionic Impact Phenomena*, Clarendon Press, Oxford, 1952.
5. H. S. W. Massey and E. H. S. Burhop, *Electronic Impact Phenomena*, Vols. 1 and 2, Clarendon Press, Oxford, 1969.
6. J. N. Bardley and F. Mandl, *Rep. Prog. Phys.*, **31**, 471 (1968).
7. H. S. Taylor, *Advan. Chem. Phys.*, **18**, 91 (1970).
8. P. G. Burke, *Advan. At. Mol. Phys.*, **4**, 173 (1968).
9. K. Smith, *Rep. Prog. Phys.*, **29**, Part II, 373, (1966).
10. P. G. Burke, *Advan. Phys.*, **14**, 521 (1965).
11. G. Herzberg, (a) *Atomic Spectra and Atomic Structure*, Dover Publications, New York, 1944 (b) *Spectra of Diatomic Molecules*, 2nd ed., Van Nostrand, New York, 1950; (c) *Electronic Spectra of Polyatomic Molecules*, Van Nostrand, Princeton, N.J., 1966.
12. J. Franck and G. Hertz, *Verh. Deut. Phys. Ges.*, **16**, 457 (1914).
13. E. G. Dymond, *Phys. Rev.*, **29**, 433 (1927).
14. J. R. Oppenheimer, *Phys. Rev.*, **32**, 361 (1928).
15. Information Center Joint Institute for Laboratory Astrophysics, University of Colorado, Boulder, Colorado.
16. Atomic and Molecular Processes Information Center, Oak Ridge National Laboratory, Oak Ridge, Tennessee.
17. G. J. Schulz, *Phys. Rev.*, **112**, 150 (1958).
18. G. J. Schulz, (a) *Phys. Rev.*, **116**, 1141 (1958); (b) **125**, 229 (1962); (c) **135**, A988 (1960); (d) **136**, A650 (1964); (e) *J. Chem. Phys.*, **33**, 1661 (1960); (f) **34**, 1778 (1961); (g) *Phys. Rev. Lett.* **10**, 104 (1963); (h) **13**, 583 (1964).
19. C. R. Bowman and W. D. Miller, *J. Chem. Phys.*, **42**, 681 (1965).
20. H. H. Brongersma and L. J. Oosterhoff, *Chem. Phys. Lett.*, **1**, 169 (1967).

21. J. T. Dowell and T. E. Sharp, *J. Chem. Phys.*, **47**, 5068 (1967).
22. L. G. Christophorou, D. N. Compton, G. S. Hurst, and P. W. Reinhardt, *J. Chem. Phys.*, **43**, 4273 (1965); **45**, 536 (1966); D. N. Compton, R. H. Heubner, P. W. Reinhardt, and L. G. Christophorou, *J. Chem. Phys.*, **48**, 901 (1968).
23. D. P. Ridge, and J. L. Beauchamp, *J. Chem. Phys.*, **51**, 470 (1969).
24. F. H. Read and G. L. Whiterod, (a) *Proc. Phys. Soc.*, **82**, 434 (1963); (b) **83**, 619 (1964); (c) **85**, 71 (1965).
25. Their early work (prior to 1959) has been reviewed by: (a) E. N. Lassettre, *Radiat. Res., Suppl.*, **1**, 530 (1959). The first full report of this work appeared in 1964: E. N. Lassettre and co-workers, *J. Chem. Phys.*, **40**, (b) 1208, (c) 1218, (d) 1222, (e) 1232, (f) 1242, (g) 1248, (h) 1256, (i) 1261, (j) 1265, and (k) 1271 (1964).
26. V. D. Meyer and E. N. Lassettre, *J. Chem. Phys.*, **44**, 2535 (1966).
27. A. Skerbele and E. N. Lassettre, *J. Chem. Phys.*, **42**, 395 (1963).
28. E. N. Lassettre, A. Skerbele, and V. D. Meyer, *J. Chem. Phys.*, **45**, 3214 (1966).
29. A. Skerbele, M. A. Dillon, and E. N. Lassettre, *J. Chem. Phys.*, **46**, 4161 (1967).
30. A. Skerbele, M. A. Dillon, and E. N. Lassettre, *J. Chem. Phys.*, **46**, 4162 (1967).
31. K. J. Ross and E. N. Lassettre, *J. Chem. Phys.*, **44**, 4633 (1966).
32. A. Kuppermann and L. Raff, (a) *J. Chem. Phys.*, **37**, 2497 (1962); (b) *Discussions Faraday Soc.*, **35**, 30 (1963); (c) *J. Chem. Phys.*, **39**, 1067 (1963); (d) P. S. P. Wei, Ph.D. Thesis, California Institute of Technology 1967.
33. J. P. Doering, (a) *J. Chem. Phys.*, **45**, 1065 (1966); (b) **46**, 1194 (1967); (c) J. P. Doering and A. J. Williams, IV, *J. Chem. Phys.*, **47**, 4180 (1967).
34. A. Kuppermann, J. K. Rice, and S. Trajmar, *J. Phys. Chem.*, **72**, 3894 (1968).
35. E. N. Lassettre, A. Skerbele, M. A. Dillon, and K. J. Ross, *J. Chem. Phys.*, **48**, 5066 (1968).
36. A. Skerbele, M. A. Dillon, and E. N. Lassettre, (a) *J. Chem. Phys.*, **49**, 3543 (1968); (b) 5042 (1968).
37. J. A. Simpson, *Rev. Sci. Instr.*, **35**, 1968 (1964).
38. C. E. Kuyatt and J. A. Simpson, *Rev. Sci. Instr.*, **38**, 103 (1967).
39. J. A. Simpson and S. R. Mielczarek, *J. Chem. Phys.*, **39**, 1606 (1963).
40. G. E. Chamberlain, H. G. M. Heideman, J. A. Simpson, and C. E. Kuyatt, *Fourth International Conference on the Physics of Electronic and Atomic Collisions, Abstracts*, Science Book Crafters, Hastings-on-Hudson, N.Y., 1965, pp. 378-381.
41. C. E. Kuyatt, J. A. Simpson, and S. R. Mielczarek, *Bull. Am. Phys. Soc.*, **9**, 266 (1964).
42. H. G. M. Heideman, C. E. Kuyatt, and G. E. Chamberlain, *J. Chem. Phys.*, **44**, 355 (1966).
43. H. G. M. Heideman, C. E. Kuyatt, and G. E. Chamberlain, *J. Chem. Phys.*, **44**, 440 (1966).
44. L. Vriens, J. A. Simpson, and S. R. Mielczarek, *Phys. Rev.*, **165**, 7 (1968).
45. (a) D. Andrick and H. Ehrhardt, *Z. Phys.*, **192**, 99 (1966); (b) H. Ehrhardt and K. Willman, *Z. Phys.*, **203**, 1 (1967); (c) **204**, 462 (1967).
46. H. Ehrhardt, L. Langhans, F. Linder, and H. S. Taylor, *Phys. Rev.*, **173**, 222 (1968).
47. H. Ehrhardt, N. Schultz, T. Tekaas, and K. Willman, *Phys. Rev. Lett.*, **22**, 89 (1969).
48. J. Geiger, and W. Stickel, *J. Chem. Phys.*, **43**, 4535 (1964).
49. R. S. Mulliken (*The Threshold of Space*, Ed. M. Zelickoff, London, Pergamon Press, 1957) lists three states below the $b^1\Pi_u$ one to which excitations from the ground state are optically allowed (another $^1\Pi_u$, an $i^1\Sigma_u$, and a $j^1\Sigma_u^+$). The first two of these have not been observed in electron impact spectra.

- Note added in proof: The 12.92 eV feature in our spectra (Figs. 16 and 17) has been resolved by J. Geiger and W. Stickel (*J. Chem. Phys.*, **43**, 4535 (1965)), E. N. Lassette (*Can. J. Chem.*, **44**, 1733 (1969)), and A. J. Williams and J. P. Doering (to be published) into the $j^1\Sigma_u^+(v' = 0)$ and $b^1\Pi_u(v' = 0, 1, 2, 3)$ levels and into a composite peak (at 12.93 eV) which is an overlap of the $b^1\Pi_u(v' = 4, 5)$ and the $l^1\Pi_u$ and $p^1\Sigma_u^+$ transitions. K. Dressler (*Can. J. Phys.*, **47**, 547 (1969)) gave new assignments for these states and other low-lying valence and Rydberg states in the electric dipole-allowed absorption spectrum of N_2 .
50. J. Geiger and K. Wittmaack, *Z. Naturforsch.*, **20A**, 628 (1965).
 51. S. Trajmar, J. K. Rice, and A. Kuppermann, Jet Propulsion Laboratory Internal Document, March 1968.
 52. J. K. Rice, Ph.D. Thesis, California Institute of Technology, 1968.
 53. C. A. Kuyatt, *Methods of Experimental Physics*. Vol. 7, Part A, Academic Press, New York, 1968, Chapter 1.
 54. G. E. Chamberlain, J. A. Simpson, S. R. Mielczarek, and C. E. Kuyatt, *J. Chem. Phys.*, **47**, 4266 (1967).
 55. K. Gottfried, *Quantum Mechanics*, Benjamin, New York, 1966, pp. 449-450.
 56. S. Trajmar, J. K. Rice, P. S. P. Wei, and A. Kuppermann, *Chem. Phys. Lett.*, **1**, 703 (1968).
 57. S. Trajmar, D. C. Cartwright, J. K. Rice, R. T. Brinkmann, and A. Kuppermann, *J. Chem. Phys.*, **49**, 5464 (1968).
 58. C. A. Kuyatt, National Bureau of Standards, private communication.
 59. J. P. Bromberg, *J. Chem. Phys.*, **50**, 3906 (1969).
 60. D. G. Truhlar, D. C. Cartwright, and A. Kuppermann, *Phys. Rev.*, **175**, 113 (1968).
 61. I. C. Percival and M. J. Seaton, *Proc. Cambridge Phil. Soc.*, **53**, 654 (1957).
 62. H. Wayland, *Differential Equations Applied in Science and Engineering*, Van Nostrand, Princeton, N.J., 1957, p. 199.
 63. L. J. Keiffer, *Bibliography of Low Energy Electron Collision Cross Section Data*, National Bureau of Standards Miscellaneous Publication 298, March, 10, 1967.
 64. B. L. Moiseiwitsch and S. J. Smith, *Rev. Mod. Phys.*, **40**, 238 (1968).
 65. S. M. Silverman and E. N. Lassette, *J. Chem. Phys.*, **44**, 2219 (1966).
 66. K. J. Miller and M. Krauss, *J. Chem. Phys.*, **48**, 2611 (1968).
 67. D. C. Cartwright, Ph.D. Thesis, California Institute of Technology, 1967.
 68. D. G. Truhlar, J. K. Rice, A. Kuppermann, S. Trajmar, and D. C. Cartwright, *Phys. Rev.*, **190**, (1970).
 69. J. D. Jobe and R. M. St. John, *Phys. Rev.*, **164**, 117 (1967).
 70. J. K. Rice, D. G. Truhlar, D. C. Cartwright, and S. Trajmar, to be published.
 71. J. K. Rice, A. Kuppermann, and S. Trajmar, *J. Chem. Phys.*, **48**, 945 (1968).
 72. C. E. Moore, *Atomic Energy Levels*, Vol. 1, National Bureau of Standards Circular No. 467, U.S. Government Printing Office, 1949, p. 4.
 73. J. A. Simpson, M. G. Menendez, and S. R. Mielczarek, *Phys. Rev.*, **150**, 76 (1966).
 74. G. E. Chamberlain and H. G. M. Heideman, *Phys. Rev. Lett.*, **15**, 337 (1965).
 75. D. C. Cartwright and A. Kuppermann, *Phys. Rev.*, **163**, 861 (1967).
 76. F. R. Gilmore, *J. Quant. Spectrosc. Radiat. Transfer*, **5**, 369 (1965).
 77. W. Benesch, J. T. Vanderslice, S. G. Tilford, and P. G. Wilkinson, *Astrophys. J.*, **143**, 236 (1966).
 78. K. Dressler and B. L. Lutz, *Phys. Rev. Lett.*, **19**, 1219 (1967).
 79. V. Cermák, *J. Chem. Phys.*, **44**, 1318 (1966).

80. P. H. Krupenie, *The Band Spectrum of Carbon Monoxide*, National Bureau of Standards Reference Data Series, Vol. 5, 1966, p. 1.
81. A. Skerbele, V. D. Meyer, and E. N. Lassette, *J. Chem. Phys.*, **44**, 4069 (1966).
82. V. D. Meyer, A. Skerbele, and E. N. Lassette, *J. Chem. Phys.*, **43**, 805 (1965).
83. R. W. Nichols, *J. Quant. Spectrosc., Radiat. Transfer*, **2**, 433 (1962).
84. C. E. Kuyatt, S. R. Mielczarek, and J. A. Simpson, *Phys. Rev. Lett.*, **12**, 293 (1964).
85. J. Geiger, *Z. Phys.*, **181**, 413 (1964).
86. E. Hutchisson, *Phys. Rev.*, **37**, 45 (1931).
87. Note that the $A^3\Sigma_u^+$, $a^1\Pi_u$, and $C^3\Pi_u$ state assignments in Figure 5 of Ref. 18a are incorrect as pointed out by Brongersma and Oosterhoff (Ref. 20).
88. C. K. Ingold and G. W. King, *J. Chem. Soc.*, **1952**, 2702.
89. This point is discussed by Dowell and Sharp (Ref. 21).
90. T. Nakayama and K. Watanabe, *J. Chem. Phys.*, **40**, 558 (1964).
91. Ref. 11c, p. 516.
92. Ref. 11c, p. 26.
93. Ref. 11b, p. 337.
94. I. G. Ross, *Trans. Faraday Soc.*, **48**, 973 (1952).
95. J. Serre, *J. Chem. Phys.*, **52**, 331 (1955); *C. R. Acad. Sci., Paris* **242**, 1469 (1956).
96. M. J. S. Dewar and N. L. Hojvat, *Proc. Roy. Soc.*, **A264**, 431 (1961).
97. M. Barfield, *J. Chem. Phys.*, **47**, 3831 (1967).
98. R. J. Beunker and S. D. Peyerimhoff, *J. Chem. Phys.*, **48**, 354 (1968).
99. P. G. Wilkinson, *Can. J. Phys.*, **34**, 643 (1956).
100. T. H. Dunning and V. McKoy, *J. Chem. Phys.*, **47**, 1735 (1967).
101. A. Lubezky and R. Kopelman, *J. Chem. Phys.*, **45**, 2526 (1966).
102. C. Reid, *J. Chem. Phys.*, **18**, 1299 (1950).
103. P. G. Wilkinson and R. S. Mulliken, *J. Chem. Phys.*, **23**, 1895 (1955).
104. R. S. Mulliken, *J. Chem. Phys.*, **33**, 1596 (1960).
105. First observed in liquid ethylene by Reid (Ref. 101) and later by D. F. Evans, *J. Chem. Soc.*, **1960**, 1735, in ethylene-oxygen mixtures.
106. Ref. 11c, pp. 533 and 629.
107. W. C. Price and W. T. Tutte, *Proc. Roy. Soc.*, **174A**, 207 (1940).
108. M. Zelikoff and K. Watanabe, *J. Opt. Soc. Amer.*, **43**, 756 (1953).
109. H. H. Brongersma, Ph.D. Thesis, FOM Institute for Atomic and Molecular Physics, Amsterdam, 1968.
110. (a) R. S. Berry, *J. Chem. Phys.*, **38**, 1934 (1963); (b) M. B. Robin, R. R. Hart, and N. A. Kuebler, *J. Chem. Phys.*, **44**, 1803 (1966); (c) M. Yaris, A. Moscowitz, and R. S. Berry, *J. Chem. Phys.*, **49**, 3150, (1968).
111. A. V. Phelps, *Rev. Mod. Phys.*, **40**, 399 (1968).
112. H. Ehrhardt and F. Linder, *Phys. Rev. Lett.*, **21**, 419 (1968).
113. K. Takayanagi, and S. Geltman, *Phys. Rev.*, **138**, A1003 (1965).
114. R. W. B. Ardill and W. D. Davison, *Proc. Roy. Soc.*, **A304**, 465 (1968).
115. A. Ramien, *Z. Phys.*, **70**, 353, (1931).
116. V. A. Bailey, *Phil. Mag.*, **13**, 993 (1932).
117. F. H. Read, *J. Phys. B (Proc. Phys. Soc.)*, **1**, 893, (1968).
118. G. J. Schulz and J. T. Dowell, *Phys. Rev.*, **128**, 174 (1962).
119. S. Trajmar, D. G. Truhlar, J. K. Rice, and A. Kuppermann, *J. Chem. Phys.* (1970).
120. S. Trajmar, J. K. Rice, D. G. Truhlar, and R. T. Brinkmann, *21st Gaseous Electronics Conf., Boulder, Colorado, October 1968, Abstract A-5 and unpublished.*
121. J. Geiger and K. Wittmaack, *Z. Phys.*, **187**, 433 (1965).

122. F. E. Fajen and C. C. Lin, *21st Gaseous Electronics Conf., Boulder, Colorado, October 1968, Abstract C-5*.
123. K. Takayanagi, *J. Phys. Soc. Jap.*, **20**, 562 (1965).
124. H. S. W. Massey, *Trans. Faraday Soc.*, **31**, 556 (1935).
125. T.-Y. Wu, *Phys. Rev.*, **71**, 111 (1947).
126. P. M. Morse, *Phys. Rev.*, **90**, 51 (1953).
127. T. R. Carson, *Proc. Phys. Soc.*, **A67**, 909 (1954).
128. E. L. Breig and C. C. Lin, *J. Chem. Phys.*, **43**, 3839 (1965).
129. D. E. Golden, H. W. Bandel, and J. A. Salerno, *Phys. Rev.*, **146**, 40 (1966).
130. E. Gerjuoy and S. Stein, *Phys. Rev.*, **97**, 1671 (1955); **98**, 1848 (1955).
131. N. F. Lane and R. J. W. Henry, *Phys. Rev.*, **173**, 183 (1968).
132. In Ref. 119, we examine the effect of changing the "cutoff" parameters and the form of f , g , and g' . The results given here are obtained with the potential which is called data set 1 in Ref. 119.
133. W. Kolos and L. Wolniewicz, *J. Chem. Phys.*, **43**, 2429 (1965).
134. R. C. Sahni and B. C. Sawhney, *Int. J. Quantum Chem.*, **1**, 257 (1967).
135. This is a modification of Rudge's procedure [M. R. H. Rudge, *Proc. Phys. Soc.*, **86**, 763 (1963); D. J. T. Morrison and M. R. H. Rudge, *Proc. Phys. Soc.*, **89**, 451 (1966)], which uses Rudge's exchange amplitude and the polarized Born approximation for the direct amplitude. The BOR without polarization was first used by D. G. Truhlar, D. C. Cartwright, and A. Kuppermann, *Phys. Rev.*, **175**, 113 (1968). For details of its application to this problem, see Ref. 119.
136. R. L. Wilkins and H. S. Taylor, *J. Chem. Phys.*, **47**, 3532 (1967).
137. J. C. Tully and R. S. Berry, to be published. The authors wish to thank Dr. J. C. Tully for his computer program for calculating DCS from phase shifts. In the calculation of the DCS we neglect terms which are second order in the d wave phase shifts.
138. B. F. Rozsnyai, *J. Chem. Phys.*, **47**, 4102 (1967).
139. J. N. Bardsley and F. H. Read, *Chem. Phys. Lett.*, **2**, 333 (1968).
140. T. F. O'Malley and H. S. Taylor, *Phys. Rev.*, **176**, 207 (1968).
141. D. Rapp, T. E. Sharp, and D. P. Briglia, *Phys. Rev. Lett.*, **14**, 533 (1965).
142. The polarized Born and polarized BOR DCS's are monotonically decreasing functions of angle at 10 eV.
143. O. Klein and S. Rosseland, *Z. Phys.*, **4**, 46 (1921).
144. L. D. Landau and E. M. Lifshitz, *Quantum Mechanics: Non Relativistic Theory*, Pergamon, London, 1958, p. 432.
145. P. D. Burrow, *Phys. Rev.*, **158**, 65 (1967).
146. P. Davidovits and P. D. Burrow, unpublished.
147. P. D. Burrow and P. Davidovits, *Phys. Rev. Lett.*, **21**, 1789 (1968).
148. A. R. Edmonds, *Angular Momentum in Quantum Mechanics*, 2nd ed., Princeton Univ. Press, Princeton, N.J., 1960.
149. D. E. Groce, D. G. Costello, J. W. McGowan, and D. F. Herring, *Bull. Am. Phys. Soc.*, **13**, 1397 (1968).

MODELS, INTERPRETATIONS, AND CALCULATIONS CONCERNING RESONANT ELECTRON SCATTERING PROCESSES IN ATOMS AND MOLECULES

HOWARD S. TAYLOR*

*Department of Chemistry
University of Southern California
Los Angeles, California*

CONTENTS

| | |
|---|-----|
| I. Mechanistic Model for Resonances | 92 |
| II. The Stabilization Method | 100 |
| A. Introduction | 100 |
| B. Heuristic Approaches | 102 |
| C. A Suggestive and Related Problem | 105 |
| D. Comment on the Mathematical Description of Resonances | 110 |
| III. Application of the Models and the Stabilization Method | 115 |
| A. The Angular Dependence in the Vibrational Excitation Process in N ₂ , CO, and H ₂ | 115 |
| B. Resonant Phenomena in the Hydrogen Molecule | 124 |
| C. Use of the One-Electron Model in the Qualitative Understanding and Choices of Significant Experiments | 140 |
| D. Resonant Scattering for the Helium Atom | 144 |
| References | 145 |

In recent years many reviews have been devoted to the subjects of resonant electron scattering, autoionization, associative detachment, dissociative attachment, and similar molecular resonant reactions.¹⁻³ Consequently there is little need for another general and comprehensive review of the subject. This article will therefore intentionally limit itself to those subsections of the field that have been of particular interest to the author. Specifically, we shall seek to review our understanding of certain physical models of resonance states that seem to be useful in predicting and interpreting the results of experiments concerning the above-mentioned processes.

* Alfred P. Sloan Foundation Fellow.

ses in such small molecules as hydrogen, nitrogen, and carbon monoxide, as well as for electron scattering in atomic systems. Throughout the discussion of the models, the emphasis will be on the type of admittedly qualitative picture that allows "understanding without calculation." The models will also prove to be useful in suggesting first approximations for state functions in iterative processes of calculating the energy and widths of resonant states.

A second emphasis of the review will be to present a deeper understanding of the stabilization method of calculating resonant energies and widths. We shall also stress Miller's⁴ method which emphasizes that once the stabilization problem is completed, one need not solve a further non-resonant scattering problem to calculate the width of the resonant state.

I. MECHANISTIC MODEL FOR RESONANCES

In the third section of this review the usefulness of having simple mechanically based physical models for electron-atom and electron-molecule resonance will be demonstrated. In fact it was the necessity to interpret experiment and to guess zero-order wavefunctions that forced and guided the development of these models.

Interestingly, although similar models exist in nuclear physics, the core excited Types I and II and single particle resonance models were developed independently in a manner based completely on experimental results in atomic and molecular physics. The models will be seen to work very well in energy regions where the targets have reasonably well-separated thresholds. The situation is not too unlike atomic or especially molecular orbital theory. At lower energies where the target spectrum is not very complex, simple classifications of specific categories of resonances into simple orbital and potential curve pictures are possible. In the higher energy regions the complexity of the spectrum eludes classification by such models. However, these models can serve as zero-order building blocks from which a more complete analysis can be made.

Resonances which appear just below the various excitation thresholds of atoms and molecules (at a fixed internuclear distance) were called core excited I (C.E. I) by the author⁵ and also are variously called Feshbach, compound state, or hole-particle resonances. Mechanistically, a process is imagined in which the incoming electron virtually excites a target electron (or electrons) to an excited orbital, thereby creating a hole in the core which allows the incoming electron to see part of the nuclear (or screened nuclear) field. The electron then gets trapped in this potential well and the resonance acts as a bound state relative to the excitation threshold (or mixture of a

group of nearby thresholds). The negative ion formed, if it can be assigned to a single excited threshold, can be viewed as due to the electron affinity of the excited states. In principle, exactly as in bound states existing below ionization thresholds, there can be an entire spectrum of C.E. I resonances. The number of states will depend on the well depth and shape. Of course one expects that in simple atoms the lowest state of the sequence will be s , then p , etc. The closer the state is to the threshold the longer it will usually live relative to other states of the same series. The electrons in orbitals with smaller overlap have less of the repulsive, decay causing effective electron interaction. For Type I resonances Newton⁶ (p. 497), among others, points out that the closed channels appear in the effective Hamiltonian as an effective attractive potential which causes the resonance. With one exception, which will be noted, the Type I resonances are narrower than those above threshold called core excited II (C.E. II). The C.E. II or shape resonance, as it was termed in nuclear theory, appears above but near the threshold of a single isolated target state. If a group of target states are close in energy, like the $n = 2$ states of helium, the C.E. II may appear, on the energy scale, among the levels or above them. Without calculations or angular dependence studies it may be difficult to distinguish between Types I and II in the case of a resonance that falls among a closely spaced group of states. There are known cases where such levels are C.E. I of a higher member of the group, C.E. II of a lower member, or a mixture of both since the $N + 1$ electron configuration constructed from the N electron targets are nearly degenerate and mix strongly. It is envisioned that a C.E. II resonance is caused by trapping the electron in a centrifugal barrier set up by the combination of its angular momentum component and the potential well it induces by exciting and polarizing the target. As such, Type II s wave resonances are not expected but p , d , etc. should be observed (see Figure 1). The reader can envision qualitatively a set of electron-target potentials similar to those used to describe rotational predissociation, viz. Figure 2. The S wave potential ($l = 0$) has no barrier. As l increases, the depth of the effective potential well decreases and the area under the barrier of any state in the well becomes smaller until an l is reached at which the analogue of centrifugal dissociation occurs, i.e., when the potential is completely repulsive. This picture enables us to envision that, if we assume only one barrier trapped level per effective l wave potential, a series of p , d , f , etc. resonances will occur above threshold, each successive resonance occurring higher in energy above threshold. The series will of course become broader for higher l waves and terminate at the l corresponding to centrifugal dissociation. A similar conclusion has been drawn by Burke¹ using the effective range formula for $l > 0$ and imagining that the $\tan \delta_l$ is plotted

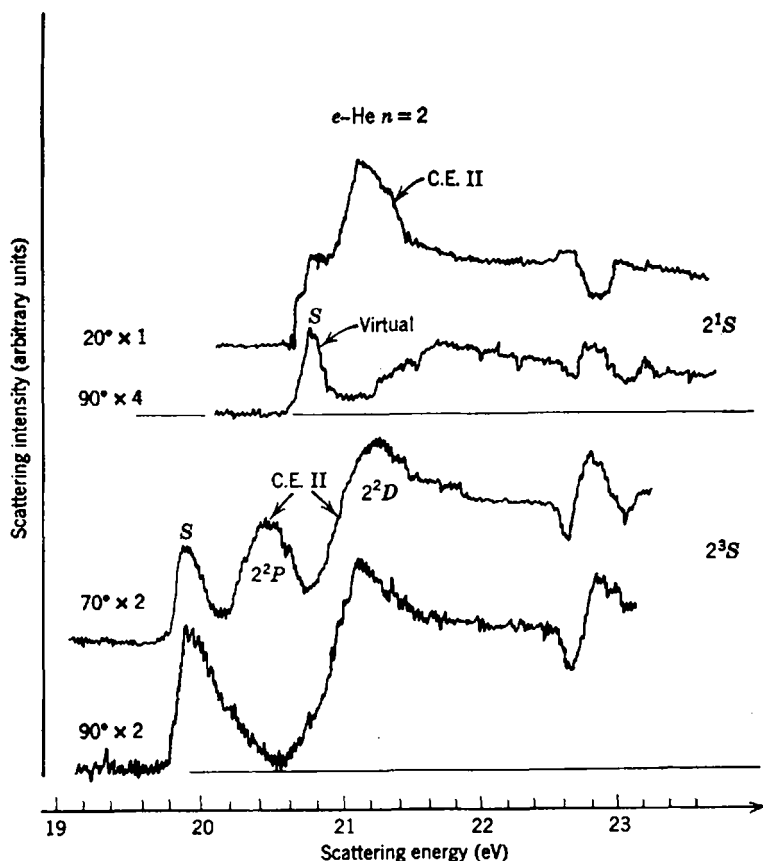


Fig. 1. Energy dependence of the differential scattering cross section for excitation to the 2^1S and 2^3S states of He. $\times 2$, $\times 3$, etc. represents the relative scale adjustments necessary for pictorial presentation. Each threshold is given at two selected angles. This figure extracted from Ref. 7.

against E (see Figure 3). These lines have smaller positive slope the higher is l , indicating that δ_l will change by π over a shorter energy range for lower l . This leads to the conclusion of lower l implying narrower resonances. Generally Type II are broader than Type I since "barriers are less effective than binding" as electron-holding mechanisms. An exception noted by Burke⁸ is when the level trapped in the barrier happens to occur at an energy just barely above threshold. At this point, since the centrifugal barrier dies off as r^{-2} , only becoming zero at the threshold energy for infinite r , the barrier can be viewed as very thick and thereby causes extremely narrow Type II resonances at this energy (viz. Figure 2). This argument loses validity rapidly as the trapped levels' energy gets above threshold. One can imagine that if one could lower the potential

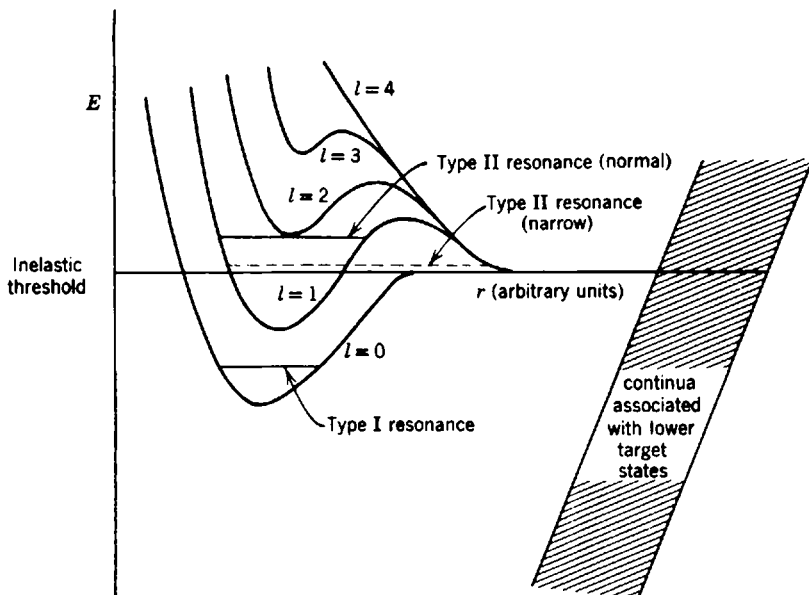


Fig. 2. Electron-atom effective potentials for various partial waves. For pedagogical purposes the electron is considered localized.

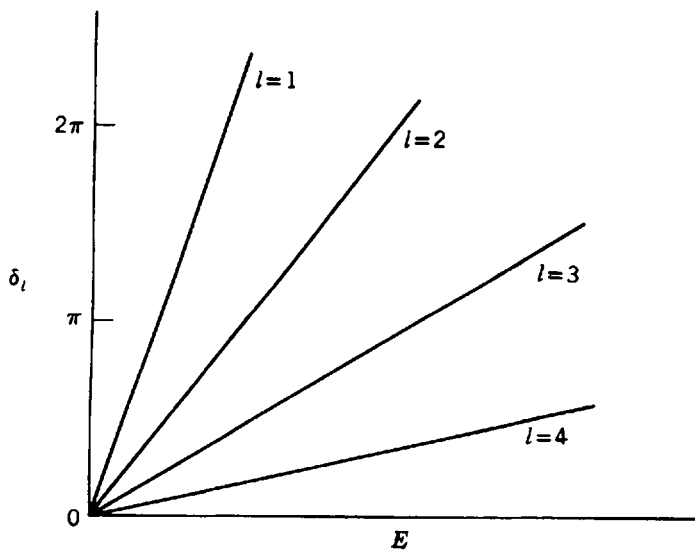


Fig. 3. Effective range phase shift as a function of energy for $l > 0$.

depth continuously, an l wave type I resonance would become unbound, pass through threshold as a narrow Type II, and then become the broader and broader Type II and eventually vanish as the repulsive centripetal potential turns the effective potential to a completely repulsive form. The ideas about Type II resonances are also discussed heuristically in Newton⁶ (Chapter 11). The narrow Type II resonance can also be inferred from effective range theory. The total picture, describing how the resonance moves relative to well depth, can also be given in terms of the position in the complex k plane of the poles of the S matrix for a single channel, $l > 0$ (Newton, Ref. 6, p. 378). Here it is pointed out that the pole moves from a (bound state) position on the positive imaginary axis down to the origin (threshold), at which point it collides with a vertical pole coming up from the negative imaginary axis. The double pole then splits and moves symmetrically with respect to the negative imaginary axis into the third and fourth quadrants, moving generally downward as the well depth decreases. When it is in the lower half-plane and near the real axis it goes from a narrow to broad resonance. Far from the real axis it is no longer a resonance since a transcription to the second sheet of the energy plane of the S matrix puts these latter poles adjacent, in the second and third quadrant, to the negative energy axis of the second sheet. This therefore is not a resonance since it does not appear along the positive energy axis where it would be observable.

A third class of resonances is the single particle type that appear just above the ground state energy but well below excited thresholds. These resonances are also of shape type and are generally caused by the trapping of the electron in the angular momentum barrier of a well set up by the induction effect of the incoming electron on the target. Again one expects no s wave single particle resonance. Since the well induced is clearly shallow, very few single particle resonances (of electronic origin) are expected, and they are clearly quite broad relative to those resonances near excited thresholds. One could, in principle, have a narrow single particle resonance exactly of the type described for C.E. II. This would be a coincidence and extremely difficult to observe experimentally since noise problems make very low energy currents difficult to measure accurately. It is also envisioned that the orbital of the resonant electron is one of the "loosely bound" type and therefore quite large in radial dimension. This type of resonance is the most difficult to calculate since it has the broadest and smallest effect. If one ignores even the subtle interplay of effects (no less the effects themselves) of core polarization, exchange, etc., the calculation will usually not show the resonance. A calculation of this type of resonance will be discussed in Section III of this review. Even such a sophisticated type of

calculation as the polarized orbital method has not been able to establish the existence of single particle resonances in places they are known to exist.

The three types of model resonances all cause structure in the observed cross sections to which they are coupled. Unfortunately for the simplicity of interpretation of experimental results, resonant-type structure is not always due to resonances. The following types of situations are worth mentioning briefly. The first type of structure occurs just above the elastic threshold in the *S*-wave *partial cross section*. This structure (viz. Figure 4) can be due,

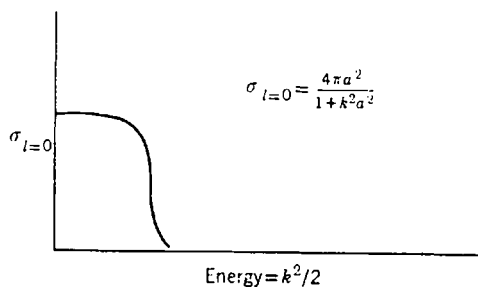


Fig. 4. Structure due to *S* wavebound state just below threshold or virtual state just above. *a* is the effective range parameter, or initial slope of the zero-energy radial continuum function.

in an experimentally indistinguishable manner, to either the existence of a bound state just below threshold or a virtual state just above it. Mathematically it is discussed in Ref. 9 (Chapters E and F) from the effective range point of view and in Newton⁶ from the point of view of poles of the *S* matrix. In the single-channel spin-free case, the virtual state is a pole on the negative imaginary axis of the *k* plane (see Burke, Ref. 1) or on the negative real axis of the second Riemann sheet in the complex energy plane. Physically, Newton⁶ shows that the virtual state can be viewed as a "bound state" that slipped out of the potential well due to an undefined mechanism that decreases its depth. Newton demonstrates how for *S* waves a pole of the *S* matrix near the origin on the positive imaginary axis in the *k* plane (a bound state) crosses the origin and moves onto the negative imaginary axis (a virtual state) as the well depth decreases. As the well depth gets even smaller this pole continues down the negative imaginary axis to collide with an upcoming virtual pole and then both poles move symmetrically downward, one pole into the third and one into the fourth quadrant of the *k* plane. The splitting does not give rise to a resonance because it occurs only at symmetrical pole positions where $\text{Im } k$ is so large that these poles, when transposed to the energy plane with the square root branch lying along the

positive real axis, will lie symmetrically placed on the second sheet near the negative real axis. Therefore they are not resonances. No resonances could be expected since the s wave has no effective barrier.

In phase shift calculations the virtual state is suggested (but not proven) when the energy derivative of the eigenphase at the threshold is positive.¹⁰ This result can also be proven using the s wave effective range formula and is demonstrated on a model problem in Newton⁶ (Chapter 11). These latter elastic effects have not yet been observed in electron-atom or electron-molecule scattering.

The second and third structural phenomena that cause visible peaks in inelastic cross sections, with s wave angular dependence, just above the threshold are quite reminiscent of the elastic effects. The first of these effects is again a virtual state (viz. Figure 1) about which statements similar to the elastic case can be made. The peak here must go to zero at threshold because of the flux factor k_f/k_i which appears in the expression for the cross section. Without an angular dependence study it would be difficult to distinguish peaks S (in 2^1S) in Figure 1 from a C.E. II resonance. Its s wave character clearly shows it is not a resonance of C.E. II type. The second effect mentioned also shows up in the inelastic cross sections. It appears just above threshold (peak S in 2^3S in Figure 1) and can have any partial wave angular dependence and still not be a Type II resonance. It is due to the overlap of the tail of an l wave C.E. I resonance. The flux factor causes the peaked nature of the l effect rather than the expected tail nature (viz. Figure 5). Such a mechanism is most likely the cause of the s wave peak in 2^3S in Figure 1. This peak caused some initial confusion when first observed since it seemed to be a C.E. II, $l = 0$, resonance which is, as we have seen, impossible. This latter type of resonance effect was discussed

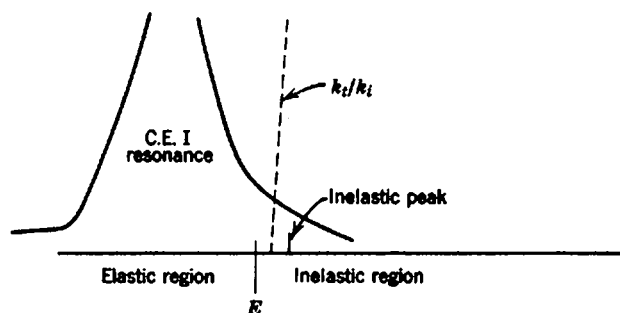


Fig. 5. Pictorial representation of the causes of the C.E. I l wave peak above threshold in Fig. 1.

finally by Newton and Fonda.¹¹ If the inelastic effects are weakly coupled to the elastic continua, this effect, except for the flux factor, is physically (but not clearly anathematically) reminiscent of the effect of a bound state just below the elastic threshold. [Clearly if one can ignore (because of small coupling) the elastic continua, the C.E. I resonance resembles a bound state.]

A model of particular interest that encompasses a special class of C.E. I and C.E. II resonances is that relevant to hydrogenlike systems. If the usual accidental degeneracy is present, Gailitis and Damburg¹² have shown that the electron near the inelastic threshold moves in an effective dipole field. This gives rise to an infinity of C.E. I resonances below threshold and in principle a second infinity above. Interestingly, these C.E. I resonances become narrow sufficiently fast so that as the energy increases they never overlap, even though they are infinitely crowded below the threshold. In the hydrogen atom they all exist between 9.6 eV, where the lowest one is observed, and the 10.2 eV $n = 2$ threshold. Their narrowness and closeness has led to the result that only two C.E. I resonances have been seen experimentally,¹³ but many others have been calculated.¹⁴ The only observed C.E. II resonance (there is possibly a second—the situation is not clear¹⁵) has been studied by A. J. Taylor and Burke¹⁶ and by Marriott and Rotenberg¹⁷ and is one of the “narrow” C.E. II types discussed previously. The “electron in the field of a dipole model” cannot be stressed enough for this problem. Early variational calculations, using hydrogenic-type one-electron orbitals to make the three-electron configurations, gave accurate results for only the lowest of the C.E. I resonances. Here one can show¹⁸ that such orbitals are not bad approximations to the dipole field orbitals. For higher numbers of the series the results were unexplainably poor until it was realized that dipole-type orbitals should be used.¹⁸

For nonhydrogenic orbitals, when the regions of energy are probed where the target states are of Rydberg nature, the near degeneracy of the s , p , d , etc. orbitals should be remembered in constructing trial wavefunctions.

Before leaving our discussion of models it is worth mentioning the single particle model which is also helpful in picking trial wavefunctions in the stabilization method (see Section II). Here it is realized that the electronic interaction between the scattered electron and the target electron cannot be great (relative to interactions in the cores of target states). (If it were, the repulsion would cause such rapid decay that the width would negate the resonance concept.) With this, one imagines that the excited target electron in C.E. I and II modes are in Rydberg-type orbitals (the core electrons are still strongly correlated). This model will be of great use when choosing the basis set in which to do calculations. A wise choice of initial orbitals will

greatly simplify the calculational problem (see Section III). It is also noteworthy that model Hamiltonians can be set up in two ways. The first and most common is to guess a H_{model} and to, in principle, diagonalize this on a complete basis set. The second way is to use the complete Hamiltonian but to use only that part of the basis that represents, in the energy region of interest, the physically expected configurations. If Q is the projection operator on this set of configurations, $QHQ \equiv H_{QQ}$ is a model Hamiltonian in the spirit of the first method which, if a complete basis is used, gives the same result as the second method. This observation, trivial as it may at first seem, is extremely useful in choosing starting points for resonant calculations. Effective potentials for electrons are hard to write down and are always quite inaccurate. This makes the first method hard to use. On the other hand, chemists have a good intuition based on atomic and molecular orbitals (especially when the single particle model is valid) and this will greatly facilitate the choice of a H_{QQ} -type model Hamiltonian. The second approach tends to stress, in a perturbation sense, expansion of matrices in small matrix elements rather than the expansion of functions in small parameters.

In molecular systems, calculations will be done for fixed internuclear distance R . The molecular state, if it is expressed as a function of R , will often fit different models (C.E. I, C.E. II etc.) as different R . This is not surprising since as we go from the separated to united atom limits, the potential an electron sees is changing. As will be seen, some molecular resonance states are actually true bound states at large R , and for progressively decreasing R can be identifiable first as C.E. I and then as C.E. II states.

II. THE STABILIZATION METHOD

A. Introduction

Let us first operationally describe the stabilization method. The first step is to make a guess at a trial *Hilbert* space wavefunction, ϕ , for the resonant state. Exactly as in the variation principle for true bound states, one tries to include in the trial function all the knowledge one has about the state of interest. The complete apparatus of atomic and molecular orbital theory is used to choose the configuration and to construct the proper symmetries (e.g., L^2 , S^2 , Σ_g , etc.). For molecules one uses the Wigner-Witmer rules as well as the fixed nuclei method of calculating electronic states. The trial function may be a single or many configuration wavefunction. Exactly as in

bound problems there is an art to choosing a good function. This art cannot be systematized but depends on the physics of the problem and is best described by specific examples which we give in the next section. Once ϕ is chosen, a secular equation is set up which represents a configuration interaction between ϕ and all Hilbert space configurations, χ_i , that could mix with ϕ . In practice one orders the χ_i , starting with those likely to mix most strongly with ϕ , and then diagonalizes successively larger sets of functions. At each step, one investigates the matrix eigenfunctions of the secular equation and chooses the eigenvalue associated with the eigenfunction that is least changed from ϕ (i.e., which has the largest component on ϕ).

A plot is then made of the eigenvalues, E_s , so chosen, against the number of configurations, n , in each step. If the curve of E_s against n has reached constancy to the desired accuracy, then E_s is taken as the resonance (complete, unshifted) energy. The associated eigenstate ψ_s is that to be used in calculating the width Γ_s (see formula below). In practice, since the computing limitations require finite dimensional matrices, one can never be any more certain that stability has been reached than one can be of reaching the "true" minimum in the Ritz variational method. Only the knowledge that the computation has included all those configurations that span the same region of position space and which have comparable energies gives the confidence of final stability. Other techniques that test for stability are (a) to vary the nonlinear parameters in those χ_i that do not seem to mix with the stabilized ψ_s so as to assure that the fixed functional forms of the basis are not the cause of the lack of mixing and that all possible parts of Hilbert space are searched, and (b) to stabilize both E_s and the width, Γ_s , calculated with the Miller formula. This latter step has never been found necessary in practice, but it is obviously desirable. An unusually large Γ_s (more than several electron volts) may also be an indication that stability is only apparent and not real. Since, as we shall see below, the method is only valid for relatively narrow resonances, large Γ_s 's are inherently suspicious. When large orthogonal basis sets are used, stabilities are readily apparent and aid in the choice of ϕ . The biggest practical problem is not in finding stabilities but in identifying those that are artifacts of the basis set.

The stabilization method will now be outlined in three stages. Initially we give the three heuristic justifications that led to its development, followed by a discussion of a related problem treated by Kato¹⁹ and Titchmarsh²⁰ of perturbing a bound spectrum in such a way that the final spectrum is a continuum. An interesting numerical example which builds confidence in the stabilization method will also be demonstrated. In the third section the ideas of this reviewer and those of Reinhardt,²¹ Miller,⁴ and Feshbach²² will be combined to mathematically formalize the method.

B. Heuristic Approaches

Two separate lines of thought, both originating in quantum chemical laboratories, led to the idea of stabilization. The idea of Holöien and Midtdal²³ as well as that of Taylor, Nazarov, and Golebiewski (T.N.G.)⁵ started with the physical but non mathematical concept of a bound state in the continuum.* Both theories realized that it could be envisioned, without changing the essential physics, that the system could be placed in a large (compared to the range of the potential) box. This would cause the bound state (formally in the continuum) to be adjacent to a now densely spaced set of bound states. In principle the energy of the bound state in the continuum could be calculated exactly as is done for true excited states. The Hylleraas-Undheim (H.U.) theory prescribes (i) that if the energy of the M th excited state is required, then the trial function should have at least M linear terms (or configurations); (ii) that the space of the vectors upon which the trial function is expanded overlap the space of lower energy bound states, and (iii) that a minimum principle then exists with respect to the M th root of the secular equation. The M th root therefore is an upper bound to the desired energy. In our case there were unfortunately too many lower energy states of unknown form to explicitly represent in a finite dimensional calculation. At this point Holöien chose the Laguerre functions (which are complete in Hilbert space) to represent both a basis for the bound state of interest, ϕ , and the space of states of lower energy. He reasoned that upon adding more and more basis terms to the diagonalization one would realize the essential overlap with the lower energy states, and consequently observe the desired "minimum" property of the H.U. theory, i.e., the root and eigenvector which is to be correlated with ϕ would never increase in energy. If, at the same time, the addition of more linear terms did not lower the energy, then, by normal minimum principle logic, the (desired) energy was achieved. Combining these ideas led to the idea of adding to ϕ more and more configurations until the root neither went up

* For the real, local potentials of atomic and molecular physics there cannot be true bound states of the total Hamiltonian adjacent to a continuum of the same symmetry. The physical concept is appealing because at the resonant energy, there can be wave packets formed from the continuum that are localized and that remain so for times of the order associated with the width of the resonance. The functional form of the localized packet is quite close to that envisioned for the bound state in the continuum. Moreover, it is possible to form such localized packets at the resonance energy, because the standing wavebox normalized continuum functions at this energy have a functional form that is characterized by a large ratio of inner to outer amplitude and by its similarity to the bound state function in the inner region. In nonresonant regions of the spectrum the continuum functions do not show these characteristics.

nor down in value, i.e., it had thereby stabilized. Holöien therefore looked for stable roots in large diagonalizations, but did not, however, stress the idea of choosing the root of interest by its associated eigenvector's weight on ϕ , the initial guess.

The logic of T.N.G. was based on the seeming inconsistency of having to include many terms in the trial function in order to span the space of lower states, thereby satisfying the H.U. theorem and the idea that the resonant function should be easily representable by very few configurations of well chosen "one electron orbital product" functions. This latter idea stems from the physical realization that the trial function must not only enhance the models of the previous section (i.e., angular momentum barriers and holes in the core) but that it must also reflect the low correlation between the $N + 1$ st incoming electron and the N -target electrons. This situation is physically evident from the following: (i) the models, (ii) the simple perturbation theory of the width which takes either the Hartree-Fock or hydrogenic model as the zero order, and (iii) the intuitive idea that a quasi-stable system would just "blow up" if the strong repulsive interactions normal to inner shell correlations were allowed. Such rapid decay would infer such large widths that effectively no resonance would appear in the cross section. The fact of mathematically needing a large number of linear terms in the wave function when the physics tells one that a small number of terms is necessary must simply mean that most configurations that are required by the H.U. theorem simply do not mix in the H matrix with the few important configurations that describe the important resonant wave packet. This suggests that diagonalization using an infinite basis set (impossible, in practice) would reveal results identical to those obtained from diagonalizing larger and larger sets of configurations, beginning with the initial guess ϕ , and continuing until no other configurations can be found that significantly affect the eigenvalue associated with the eigenfunction which has ϕ as its largest component. This method is clearly the stabilization method.

This method of choosing the eigenvalue of interest is unique. In practice, if the initial guess mixes strongly with a particular χ_i , one defines two new ϕ 's, ϕ^+ and ϕ^- such that $\phi^\pm = \phi \pm \chi_i$ and tests both for stability. In choosing ϕ it is desirable to include in it from the start all correlations of the type which quantum chemists call "near degeneracies." The stabilization process is of course more convergent the better ϕ is chosen. Many configurations may be needed simply to patch up a poorly chosen ϕ . Conversely, unless the basis is extremely poorly chosen, the process of successive diagonalization, which can be done in one step if an orthogonal basis is used (stabilization shows up in a study of the eigencoeficients),

gives rise to the stable functions one might have missed guessing in the original choice of possible ϕ 's.

Intuitively, from this development, it is felt that even with a well-chosen basis, bigger widths imply a need for greater mixing of configurations and a slower convergence. As will be seen, this generally turns out to be theoretically justified and to be the case in actual calculations. We see here also that the width is certainly larger the larger the correlation of the principle configuration ϕ . In a many-body problem the width clearly depends on both correlation and the nature of the resonant mechanism (barrier, wells, etc.). The above consideration gives an indication of the difficulties encountered in ascertaining resonance widths, as opposed to the more easily calculable resonant energies. Essentially it can be a correlation-dependent property, thereby needing a much more sophisticated trial function.

Miller, aware of the Holjöien and T.N.G. work, as well as the related work of Lipsky and Russek¹⁴ (which is a less general method in that it is restricted to a hydrogenic basis set), justified stabilization by noting the resemblance between the formula* for the resonant energy, E_s , when the Q space of the Feshbach theory is taken to be one dimensional and the following two approaches. The first observation was that the calculation of E_s and ψ_s was similar to the solution of a secular equation. This analogy to a secular determinant did not solve the problem of which root to choose as E_s when the secular determinant, set up upon the basis set including ϕ , was diagonalized. This was resolved by the second noted similarity, that of the formula for E_s , given in a form in which the Green's function of the P space $P/E - H$ is expanded [H_0 is the Hamiltonian so constructed that ϕ is a point by point as opposed to matrix eigenfunction, and $V = H - H_0$] in powers of V , via a Rayleigh-Schrödinger perturbation series where ϕ is the zero-order function. The analogy between perturbation theory and diagonalization indicated that the desired root must correspond to that root for which the eigenfunction is changed least from ϕ . Clearly it is desirable to enlarge the secular basis until a perturbation series type of convergence is achieved. This again was the stability method.

The heuristic approaches of this subsection turned out to produce impressive agreement with experiment when applied. At the same time they raised such unanswered questions as to (i) the role of the scattering boundary conditions in the stabilization method;* (ii) how a scattering problem, and therefore a continuum problem, can be treated on a Hilbert space basis;

* Physically, since the resonant energy is a property of the $N + 1$ particle system and the boundary conditions simply indicate what type of observation (experiment) is to be performed, this independence is to be expected.

and (iii) what is the meaning of the stabilized root if it has the property of first appearing to stabilize, remaining stable for several augmentations of the basis set, and then becoming unstable due to the addition to the basis of a large number of weakly mixing and weakly overlapping states. (Such behavior will be demonstrated below when perturbation theory and the stabilization method are applied to a continuum but nonscattering model problem.) It should be emphasized that this behavior has never been observed in an atomic or molecular problem.

We now turn to the answers to such questions.

C. A Suggestive and Related Problem

A related problem that has long been of interest in quantum theory²⁴ is the one in which the unperturbed system has a discrete spectrum and the perturbed system has only a continuous spectrum. This problem has been called one of "weak quantization." For the sake of definiteness, the Stark effect problem or a harmonic oscillator perturbed by a perturbation $V = -\lambda x^3$, $\lambda > 0$ (see Figure 6) can be discussed. These problems have two

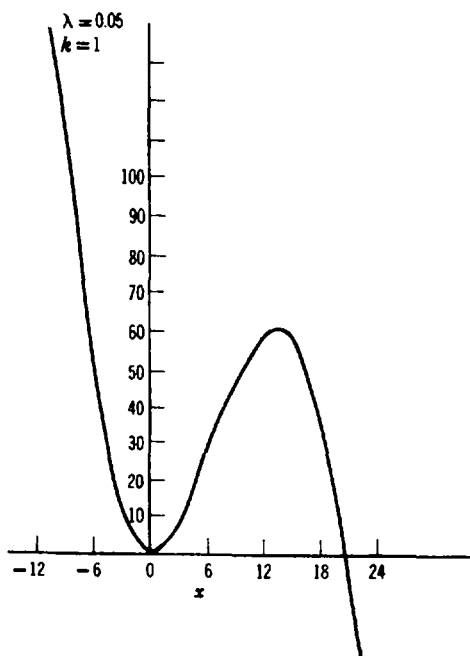


Fig. 6. The Harmonic oscillator perturbed by a $-\lambda x^3$ potential.

differences from the scattering resonance problem. First, they are not of the scattering type; the potential does not go to zero at large distances. Second, they are perturbation series problems while the stabilization method is basically a diagonalization that, as Miller pointed out, is only quite suggestive of perturbation theory. On the other hand, the continuum nature of these problems is common to those considered in this article. The difficulty here is that perturbation theory is based on the idea that as the perturbation is turned on one can uniquely follow a nondegenerate unperturbed level to a single unique perturbed level and vice versa. In the problems mentioned perturbation theory is used in cases where this basic assumption is not fulfilled. Yet it is known²⁴ that in most applications the correct answer, as determined from experiment, is obtained. Kato¹⁹ and Titchmarsh²⁰ address themselves to the questions of the meaning of the calculated results and their range of validity. We shall here only quote some of their conclusions, borrowing liberally from Palmer's review²⁵ on the subject of the perturbation theory convergence problem. After stating these conclusions the above-mentioned harmonic-oscillator perturbation problem will be treated by the stabilization method in such a way that it will be clear that perturbation theory would give a similar result. Since Kato's conclusions tell us that the numbers calculated from perturbation theory represent the real part of the resonant poles of the Green's function, and since these perturbation results will be seen to be the same (to high accuracy) as those of stabilization, it can be inferred that the results of the stabilization method gives the real part of the poles of the Green's function that are on the second sheet having relatively small widths. It is worth remarking that this example will be carried out on a Hilbert space basis (the Hermite functions, i.e., the eigenfunction of the harmonic oscillator), using discrete state methods without considering the usual non-Hilbert space aspects of continuum problems. Also to be noted will be the fact that the broader the resonances the more terms needed to stabilize. Of particular interest is the fact that the method gives *usable stabilized information even when the unperturbed level lies very near the top of the barrier* (see Figure 6), indicating that the width for localization inside the well must be quite large.

Kato's major conclusion is that "roughly speaking, (the) perturbation method gives correct results in the sense of an asymptotic expansion as long as the necessary operations are carried out in Hilbert space." Kato gives conditions on H_0 and H_1 such that a well-defined metastable state will appear in the neighborhood of the original discrete state of H_0 and such that the average energy of this state is correctly calculated by perturbation theory. Palmer summarizes Kato as follows:

Mathematically such states reveal themselves in several related ways:

(1) Let us for simplicity assume that the spectrum of $H(\lambda)$ for $\lambda > 0$ is completely continuous. Then no energy would seem distinguished. If, however, one examines the Green's function of $H(\lambda)$ as a function of the complex variable z , then one finds that in addition to having a branch line along the real axis corresponding to the continuous spectrum of $H(\lambda)$ it has poles near the real axis. These poles approach the real axis and represent the discrete states of H_0 as λ approaches zero. Perturbation theory calculates the real parts of these poles and, clearly, regions of the continuous spectrum near these poles *are* distinguished. The real part of the pole is the position of the metastable state.

(2) In spite of the continuous nature of the spectrum, the spectrum is effectively more concentrated in the regions of the real axis near the poles of the Green's function. Namely, if one expands any arbitrary function in terms of the eigenfunctions of H , one finds that contributions to the expansion will, in general, be particularly large from regions which include the metastable states, and these contributions persist as λ approaches zero.

(3) Wave packets formed by superposing eigenstates of H from a small region including the metastable states are quite well localized, this localization persisting as λ approaches zero. *This is not true if the small region does not contain a metastable state.*

The last property would seem to make contact with what one intuitively thinks of as a metastable state. Also the pole of the Green's function is reminiscent of Gamow's complex eigenvalues in the theory of α decay. To complete the connection we note that the localization referred to in (3) does not of course persist for all time. Rather one can show that it decays with a well-defined lifetime, this lifetime being determined by the imaginary part of the poles of the Green's function. With this the identification is clearly complete.

Property (3) allows Kato to apply the *theory of asymptotic perturbation series to this problem*. The operators defining the first M terms of the perturbation series are required to be defined at least on a manifold consisting essentially of the functions which are zero outside of a given bounded set which *represents the region of the physical problem*. Then the (continuum) functions belonging to a small finite interval of the continuous spectrum near the M th partial sum of a perturbed eigenvalue can be expanded in terms of the M th partial sums of the corresponding perturbed eigenfunctions, and this expansion is complete up to $O(\lambda^M)$.

Very similar statements about poles, wave packets, etc. are made in a scattering resonance context in the books by Watson and Goldberger²⁶ (Chapter VIII) and by Newton.⁶

Of particular interest is that we can stay in Hilbert space and use discrete methods at the price of, at worst, having to interpret our results in an asymptotic sense. In the example that follows the asymptotic sense is revealed in that the closer the unperturbed level is to the top of the barrier the more difficult it is to stabilize and the shorter is the region of stabilization. It is to be stressed that the destabilization has not occurred in an atomic or molecular problem *to the extent of our calculation* (of the order of fifty configurations). It may be that our method of choosing the configurations (those overlapping ϕ the most come first) is a way of resuming an asymptotic and divergent series so as to be convergent. Interestingly, Kato states that Riddell²⁷ has shown for the Stark effect that "the pseudo-eigenvalues have asymptotic expansions up to any order in λ (thus coinciding with the formed perturbation series)" Recently Alexander²⁸ solved the Stark problem for atomic hydrogen by a boundary condition method for low fields and a modified WKB resonant-type approach for high fields. Not knowing of Riddell's work, he concludes upon comparing the results of perturbation theory to his scattering type approach that the perturbation series is only an asymptotic series.

In Figure 6 we see the schematic potential of a harmonic oscillator with a $-\lambda x^3$ perturbation. In Table I we see three sections; each for a different value of λ . The smallest λ admits 20 unperturbed states inside the barrier, the next smallest λ admits ten states, and the largest λ admits two states. The area under the barrier down to the horizontal energy line of the state of interest is an estimate of the lifetime. The number of configurations used in the stabilization calculation are listed $n = 10, 20, \dots$ indicates that the first 10, 20, . . . respective Hermite functions were used. Regions of asymptotic convergence are enclosed, the $n = 1$ column of Table I giving the unperturbed root. Rather than repeat, the reader is advised to reread the introduction to this subsection to reemphasize the conclusions that can be drawn from this table.

The numbers entered in the body of the table are the stabilized energy for the given number of configurations (n). The encapsulated regions are regions of asymptotic convergence.

The near equivalence of these roots to the real part of the pole of the Green's function is obvious from the following considerations. First, Kato^{19,25} proved that if perturbation theory had been used the perturbed energy values would have asymptotically converged to the value of the pole. Second, since the Hamiltonian matrix elements have a selection rule $n \rightarrow n \pm 1, 3$, all matrix elements for many orders of perturbation theory have been used. Thus for the lowest root, $n = 50$ implies that all elements are used that are involved in the calculation of $n/3$ or 16th-order perturba-

TABLE I
Stabilization Method as Applied to
 $v = x^2/2 - \lambda x^3$

| Root number | n (No. of Configurations) | | | | | |
|-----------------|-----------------------------|------------------------|-----------------------|-----------------------|-----------------------|-----------------------|
| | 3 | 5 | 10 | 20 | 30 | 41 |
| $\lambda = .01$ | | | | | | |
| 1 | 0.4998874 | 0.4998623 ^b | 0.4998623 | 0.4998623 | 0.4998623 | 0.4998623 |
| 3 | 2.500898 | 2.497862 | 2.497604 | 2.497604 | 2.497604 | 2.497604 |
| 5 | — | 4.507259 | 4.492321 | 4.492321 | 4.492321 | 4.492321 |
| 10 | — | — | 9.580415 | 9.465725 | 9.465725 | 9.465725 |
| 15 | — | — | — | 14.42021 | 14.41972 | 14.41972 |
| 20 | — | — | — | 20.12689 | 19.35394 | 19.35394 |
| $\lambda = .05$ | | | | | | |
| 1 | 0.4971637 | 0.4964699 | 0.4964664 | 0.4964664 | 0.4964664 | 0.4964664 |
| 3 | 2.522044 | 2.446675 | 2.434969 | 2.434951 | 2.434951 | 2.434951 |
| 5 | — | 4.662525 | 4.281707 | 4.274538 | 4.274536 | 4.274536 |
| 10 | — | — | 10.77216 ^a | 9.288139 ^a | 9.381697 ^a | 9.335989 ^a |
| 15 | — | — | — | 13.85958 ^a | 14.19333 ^a | 14.56205 ^a |
| $\lambda = .1$ | | | | | | |
| 1 | 0.4883648 | 0.4846017 | 0.4843330 | 0.4843303 | 0.4843085 | 0.4843056 |
| 2 | 1.428153 | 1.399153 | 1.380175 | 1.378116 | 1.384463 | 1.381439 |
| 3 | 2.583481 ^a | 2.296817 ^a | 2.094150 ^a | 1.988783 ^a | 2.091248 ^a | 2.055161 ^a |
| 5 | — | 5.025448 ^a | 4.710078 ^a | 4.949860 ^a | 5.030527 ^a | 4.788018 ^a |
| 10 | — | — | 9.001369 ^a | 9.636047 ^a | 9.315597 ^a | 8.767132 ^a |

^a Energy is above barrier—here stability is never achieved.

^b The encapsulated figures are stable to 5 figures—much wider stability is achieved for 3 figures.

tion theory for the wavefunction and $2(n/3) + 1$ order for the energy (assuming this simple conventional relationship holds—see Titchmarsh²⁰). It is perhaps worth noting that while the unperturbed energy spacings and the smallness of λ aid convergence as n increases, the proportionality of the Hamiltonian elements to n^3 works against it.

Again, of particular interest is the fact that even the broadest of roots stabilize to several figures. In this asymptotic sense the stabilization method is useful even for broad resonances. This has been discussed by Shore²⁹ who parameterizes broad and/or overlapping resonances and finds that the formula used here for the energy is useful up to third order in the perturbation. One can *speculate* that, even though the pole position is precisely defined, one will not be able to measure it with any more precision, in the case of broad resonances, than we are able to calculate it. The experimental meaning of resonant energy seems to lose its validity in the same regions the stabilization method begins to become useless. All that this says is that *the method can satisfactorily handle all types of recognizable resonances but that it can not handle the total scattering problem*. Poles on the second sheet very far from the real axis cannot be calculated and therefore the Mittag-Leffler expansion of the S matrix and thereby the complete cross section cannot be calculated in terms of these poles.

It is of course now obvious that true bound states can be calculated with the stabilization method. This indicates a consistency of calculation if the state of interest changes from a true bound state to a resonant state as a parameter of the problem changes (e.g., a molecular problem that is bound at large internuclear separation but is resonant at small separation).

D. Comment on the Mathematical Description of Resonances

In the paper of Feshbach,²² the thesis of Reinhardt,²¹ and the book of Newton⁶ are given the general mathematical formulation of resonances from the differential equation, the determinantal method (for the S matrix), and the Green's function point of view, respectively. There is no necessity to repeat the developments. For our purpose we merely note that if the proper incoming and outgoing boundary conditions are used in the development, one obtains for the energy of the resonance, E_s , the seemingly boundary condition independent formula,

$$E_s = \langle \phi_s | H_{QO} + H_{QP} \frac{P.V.}{E_s - H_{PP}} H_{PQ} | \phi \rangle \quad (1)$$

and for the partial width for decay into the i th channel and final wave-vector k_f

$$\Gamma_i(E) = 2\pi |\langle \phi_s | H_{QP} P_i \psi_0^+(E, \hat{k}_f) \rangle|^2 \quad (2)$$

Here H_{QP} , H_{QQ} read QHP , QHQ , etc., and P.V. implies "principle value." Q is taken as the single dimensional vector projector in a Hilbert function space obtained by projecting onto ϕ_s . ϕ_s is therefore by construction an eigenvector of H_{QQ} and from our point of view it is our first guess in the stabilization method. P projects onto the orthogonal complement space of Q , and $Q + P$ represents the total space for the scattering problem. To obtain $P_i\Psi_0^+$ the potential scattering problem

$$(E - H_{PP})P_i\Psi_0^+ = 0 \quad (3)$$

must be solved.

These formulas are calculated under the following assumptions: (i) the pole of the Green's function is simple, and (ii) the width Γ and the energy shift $E_s - \langle \phi_s | H | \phi_s \rangle$ are both small relative to the energy scale on which the other quantities in the amplitude vary appreciably.

These assumptions are the assumptions that make formulas (1) to (3) valid for "narrow resonances." Interestingly our experience, as reviewed in the next section and seen in the example given in the previous subsection, shows that *Eq. (1) is useful even for broad resonances*. Shore's²⁹ development of broad overlapping resonances shows that Eq. (1) is valid to $O(V^3)$ in such cases. Unfortunately one can say no more about the exact point at which our method becomes useless than Kato¹⁹ could say about the point at which the asymptotically interpreted perturbation series would not give useful information. We reiterate our intuitive feeling, that if a resonance is "narrow enough" to be parameterized in an experimental sense, then the stabilization method will calculate it as an asymptotically stable root.

The familiar expression, Eq. (1), for the resonance energy was recognized by Miller⁴ to be nothing more than a form of the secular equation for H (in a Hilbert basis and convenient for iterative solution) that was proposed by Löwdin and Shull. The operations proving these statements are in the Ref. 4. Here we only summarize in saying that for narrow resonances the E_s of interest is one of the roots of the secular equation on a Hilbert basis and corresponds to a normalization such that $\langle \phi_s | \phi_s \rangle = 1$ (this is necessary if $Q = \phi_s \langle \phi_s |$ and $Q^2 = Q$) with the eigenvector of the secular equation corresponding to E_s given explicitly as

$$\psi_s = \left(1 + P \frac{\text{P.V.}}{E_s - H_{PP}} H_{PQ} \right) \phi_s \quad (4)$$

The formal result for E_s is $E_s = \langle \phi_s | H | \psi_s \rangle$ and $\langle \psi_s | \phi_s \rangle = 1$.

It is perhaps worth mentioning that there is a formally more conventional, but practically more difficult (in that it involves continuum-continuum

integrals and principle value integrations), way to evaluate Eq. (1). This method is that of Zumino³⁰ where first H is separated such that

$$H = H_0 + V \quad (5)$$

H_0 is defined as the Hamiltonian for which ϕ_s is an exact (as opposed to matrix) eigenvector of H_0 , i.e.,

$$H_0 \phi_s = E_s^0 \phi_s \quad (6)$$

With this one substitutes

$$\frac{\text{P.V.}}{E - H_{PP}} = \frac{1}{2} \left(\frac{1}{E - H_{PP} + i\varepsilon} + \frac{1}{E - H_{PP} - i\varepsilon} \right)$$

and by the Born expansion, expands each of the $(E - H_{PP} \pm i\varepsilon)^{-1}$ separately and regroups in powers of V . This gives a formal perturbation series (see Zumino) for E_s . It was by analogy to this formal perturbation result that led Miller to decide that the root of the secular equation that corresponds to a narrow resonance* is the one for which the unperturbed function differs the least from the ψ_s . In some sense the stabilization method is a selfconsistent method. A formula for the energy of narrow resonances is used to calculate more roots than there are existing resonances, and an added prescription is needed to pick the root consistent with the initial assumption. A poor choice of the ϕ_s will, like in all essentially iterative methods, lead to a poor convergence or even a divergence.

To calculate the width one needs to evaluate the integral in Eq. (2). Miller observed that since ψ_s is known from stabilization that an approximation to the width can be directly calculated without the need to do a "scattering problem," i.e., to solve Eq. (3). To see this the solution to Eq. (3) is written in the form

$$\begin{aligned} P_i \psi_0^+ &= \left(1 + \frac{1}{E^+ - H_{PP}} V_{PP} \right) \chi_0^i \\ &= \left(1 + \frac{\text{P.V.}}{E - H_{PP}} V_{PP} - i\pi \delta(E - H_{PP}) V_{PP} \right) \chi_0^i \quad (7) \end{aligned}$$

where χ_0^i is the solution of the problem with the proper asymptotic condition for the i th channel and the Hamiltonian PH_0P . With this, and the fact that by Eq. (6) H_0 is constructed (formally—it is never used) to

* We have indicated that for a narrow resonance E , is a root of $\det(E - H) = 0$; but all roots of $\det(E - H) = 0$ are not energies of resonances.

commute with Q (i.e., $QHP = QVP$), the integral of interest is given as

$$\begin{aligned} \langle \phi_s H_{QP} P_i \psi_0^+ \rangle &= \left\langle \phi_s \left| V + V \frac{\text{P.V.}}{E - H_{PP}} V \right| \chi_0^i \right\rangle \\ &\quad - i\pi \langle \phi_s V \delta(E - H_{PP}) V \chi_0^i \rangle \end{aligned} \quad (8)$$

The relation $P\chi_0 = \chi_0$ has been used as well as $Q\phi_s = \phi_s$. The first integral of Eq. (8) can be rearranged using Eq. (4) to give

$$\begin{aligned} \langle \phi_s H_{QP} P \psi_0^+(E) \rangle &= \langle \phi_s V P \psi_0^+ \rangle = \langle \psi_s | V | \chi_0 \rangle \\ &\quad - i\pi \sum_j \langle \phi_s V P_j \psi_0^+ \rangle \langle (P_j \psi_0^+)^+ V \chi_0^i \rangle \end{aligned} \quad (9)$$

If the second term on the r.h.s. of Eq. (9) can be ignored, one gets Miller's expression for the width when the integral is put into Eq. (2). For narrow resonances V is small because ψ_s and ϕ_s are not greatly different and therefore H_0 is not far from H . The omitted terms are of order $(V)^4$ and are probably negligible. Interestingly, Shore²⁹ in his study of broad resonances suggests exactly Miller's formula as the meaningful width parameter. This suggests that the formula is not entirely restricted to narrow resonances. The great advantage of the formula

$$\Gamma_i(E) = 2\pi |\langle \psi_s V \chi_0^i(E) \rangle|^2 \quad (10)$$

is that ψ_s is known and that, as we shall see next, χ_0^i can be chosen in a manner such that it is trivial to write down. In other words, no further scattering calculations need be done to get the width of the resonances. A knowledge of ψ_s from stability is sufficient to calculate E_s and $\Gamma_s = \sum_i \Gamma_i$.

Even more interesting is Miller's observation (private communication) that Eq. (10) no longer depends on ϕ_s and therefore on Q . This is so since ψ_s would, in the sense of the perturbation theory discussed, be the same whether it was calculated from any number of reasonable zero-order models. As such our choice of ϕ_s can be made so as to stabilize most rapidly. Once ψ_s is known we can redefine ϕ_s such that an H_0 is implied that is so simple that χ_0^i can be directly written down or trivially calculated. In fact one simply chooses a simple χ_0^i (e.g., hydrogenic, polarized orbital, etc.), infers an H_0 and V , and uses the coupled pair V and χ_0^i . The only restrictions are that the ϕ_s implied by this latter choice would have been a reasonable, even if not optimal, starting point for the calculation of ψ_s . Also, since χ_0^i and H_0 (and therefore V) are in practice simple, the associated ϕ_s will be known and the normalization of Eq. (4) obtainable. The flexibility in the choice of the coupled pair V and χ_0^i is of great practical advantage. It can be

used to further check the correctness of ψ_s . If ψ_s is "exact," then *all allowed* $V\chi_0^i$ pairs will give the same answer when put into Eq. (10). If they differ, errors must exist in ψ_s . Since ψ_s is probably best at small radial distances (because of our method of calculation), the Γ calculated with the V of shortest range is probably the best one can do with the present ψ_s .

Before leaving this section concerned with the mathematical and calculational aspects of the stabilization method, it is perhaps useful to mention a point of great application. It is highly probable that in future calculations in scattering theory, variational and other methods for doing the complete (potential and resonant) scattering over a wide range of energy will be attempted. In principle the phase shift will be solved for directly. This seems to do away with the necessity for separate calculation of resonances. On the other hand, these calculations are carried out on a grid of energies. If a narrow resonance is present, it could easily be missed if the grid points are spaced more widely than the resonance width. If a first diagonalization of the secular equation on a reasonably physical basis is carried out and if the roots are included explicitly in the energy grid, there is little danger of missing resonances. The stabilization finds most easily the narrow resonances which are exactly the points of difficulty of conventional methods. The opposite is true, of course, for very broad cross section structures. The methods are certainly complementary.

Perhaps worth a mention in this section is the Feshbach²² method of computing resonant energies. Operationally this method is exactly like that of the Ritz-Rayleigh principle except that the trial functions are restricted to a space that includes no components on target states of energy lower than the resonant energy. This method was first used for atomic and molecular calculations by O'Malley and Geltman,¹⁴ and by the present author and Williams.³¹ The former authors were familiar with Feshbach's work while the latter authors developed it independently. Interestingly, this development was heuristically inferred by attempts to calculate the energy of a wavefunction guessed using the C.E. I model.

It was observed in the calculation that while no minimum variation principle formally existed, a seeming extremum was obtained if all the off-diagonal matrix elements between the trial functions and any function which contained significant components of the lower energy target states were ignored. These elements were observed, and verified by extensive numerical calculation, to be of very small magnitude relative to the diagonal elements. This led to the convenient calculational expedient of ignoring these elements and restricting variations in the trial function to those that keep the magnitude of the partition of the H matrix containing the target states (of lower energy) basis relatively small. The method was not justified

formally but was shown to give for the C.E. I states sufficiently useful agreement to explain experiments. The method was eventually discarded for several reasons. First, the true minimum does not really correspond to the resonant energy but to the unshifted energy. The shift then needs to be calculated and to do so brings one back to stabilization. A minimum principle was gained at the price of calculating only part of an observable. More important, the method was only good for C.E. I resonances. For C.E. II (and all shape resonances) which are above threshold, projection out of the trial function of components of the threshold function would make zero exactly those trial function components corresponding to the C.E. II model.

Also worth mentioning is the simplicity of the Feshbach projection as carried out by Taylor and Williams. There have been many papers giving complicated Feshbach projection operators for many-body Fermi systems. These operators are always extremely complicated in form. In our work, the problem was trivial in that variations were carried out subject to the numerical restriction that overlap matrix elements with the target basis of lower energy was always a factor of 10^{-6} less than the diagonal element. Since the programs took exact account of antisymmetry, spin, etc., no complicated prescription was needed.

Another method tried but rejected was that used by Bardsley, Hertenberg, and Mandl.³² This formally fine method, which could be variationally presented, had the difficulty of putting in an unphysical "wall" parameter R . In the calculations different bases were chosen and the final reported results were shown to be highly independent of the choice of R . In the laboratory of this author it was found that such a happy situation was only achievable if very simple basis sets were used. These sets, in problems more complicated than H and He atoms, rarely gave quantitative answers. The results with improved basis sets seemed always to depend on R .

III.

In this section the usefulness of the models of Section I and the calculational method of Section II will be demonstrated by specific examples.

A. The Angular Dependence in the Vibrational Excitation Process in N_2 , CO, and H_2

In this example the predictive power of the single particle model can be clearly demonstrated. The processes of interest are a study of the excitation by electrons, in the 2 to 8 eV range, of the vibrational modes of the ground state N_2 , CO, and H_2 .³³ The energy resolution was insufficient to see

anything but the averaged rotational effect. The single particle model was used to predict the features of the differential cross section in the inelastic channels. For N_2 and CO total scattering (attenuation), as well as total inelastic and elastic measurements, have shown clearly in the low energy region the existence of a resonance state of N_2 and CO³⁴ (Figure 7). The interpretation that N_2^- and CO^- is formed was immediate (viz. Figure 8). Schulz³⁴ even suggested that in N_2 the scattered electron is in a π_g orbital. This means, since N_2 is $^1\Sigma_g$ that the state of N_2^- is $^2\Pi_g$. Chen³⁵ developed a generalization of the Feshbach derivation of the Breit-Wigner formalism to include the effect of the vibrational feature on a resonance in the electronic modes. He then showed that that judicious choice of parameters

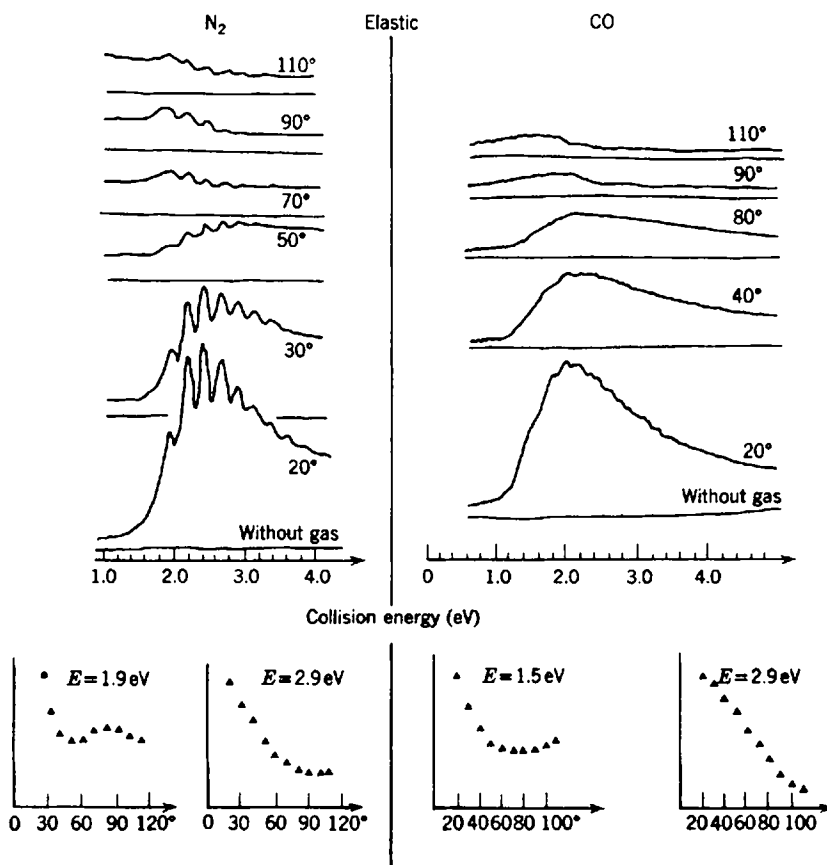


Fig. 7. Elastic scattering for N_2 and CO.

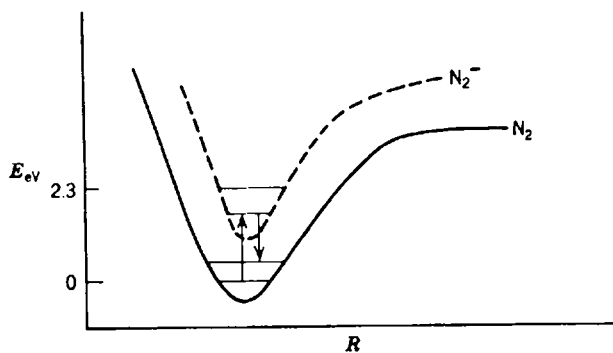


Fig. 8. Schematic of resonant vibrational excitation.

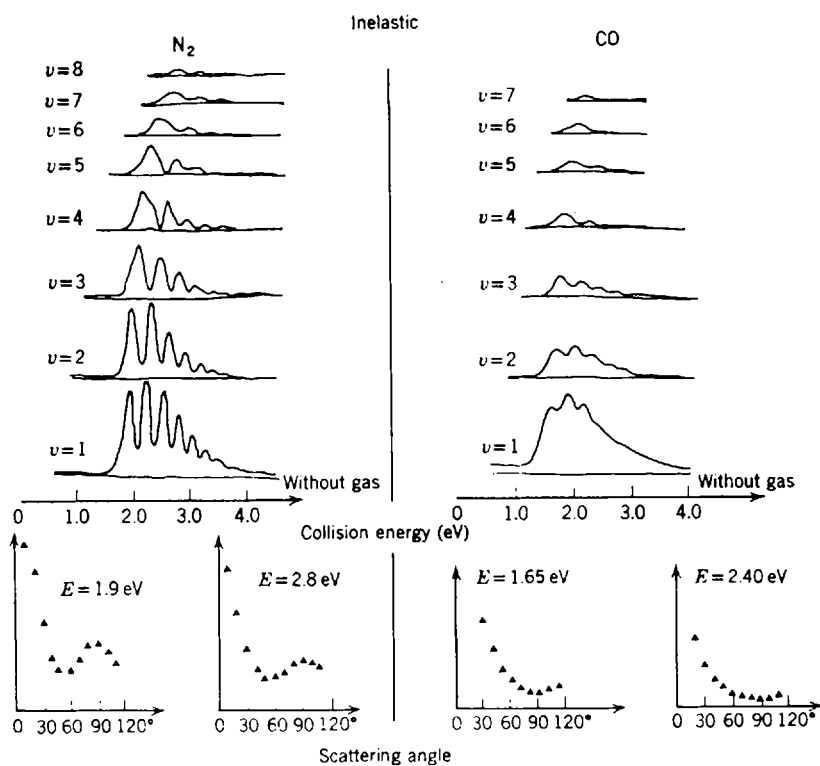


Fig. 9. Inelastic scattering for N_2 and CO .

could fit the total elastic and inelastic vibrational excitation data. The parameterization even explained the apparent shifting of peaks in the various excitation cross sections for N_2 (see Figure 9) as due simply to the behavior of the Franck-Condon factor connecting the vibrational levels of the molecule with those of the resonant state. The basic interpretation was clear from the work of Schulz and Chen: vibrational excitation was due in the elastic channel to the interference of both direct excitation

$$e(k\hat{k}) + N_2(v=0) \rightarrow e(k'\hat{k}') + N_2(v>0)$$

and resonant excitation

$$e(k\hat{k}) + N_2(v=0) \rightarrow N_2^- \rightarrow e(k'\hat{k}') + N_2(v>0)$$

In the inelastic channels, momentum transfer arguments indicate that direct excitation could be expected to be small (light electron at low energy on massive target), so that the process was resonant dominated. This observation is stressed in Ref. 33 and is easily seen by comparing the apparent upward displacement of the peaks at 20° for N_2 in Figure 7 to that in Figure 9 for $v=1$; the lifting of course being done by the direct scattering. Interestingly, a similar comparison for CO shows that at about 1 eV the direct process is not negligible in the $v=1$ channel but only from $v=2$ upward in v . This is clearly due to the enhancement of direct scattering by the dipole of CO. This effect was noted by Phelps³⁶ in Swarm experiments which are particularly suited for examination near threshold regions. He found that for N_2 , $v=0 \rightarrow v=1$, the resonance parameterization was satisfactory at threshold, while for CO a dipole-type direct parameterization was necessary. For CO, $v=0$ to $v \geq 2$, the momentum transfer is larger than for $v=1$ and the direct effects truly are very small. The Chen parameterization is basically independent of the type of resonance and really simply stresses the resonant nature of the effects. In fact it was originally thought by many that these resonances were of C.E. I type. This was rejected⁵ because of the too large electron affinity (as in +8 eV) that a C.E. I model would imply for the excited state. The single particle model was clearly implied. The fact that the vibrational spacings were near to, but slightly smaller than, that of the target implied an antibonding orbital. The antibonding orbital would weaken the bond, decrease the well depth, and cause the vibrational levels to be more closely spaced. Since π_g for N_2 and π for CO, which are the first such orbitals that are unoccupied, have antibonding nature and have orbital angular momentum, one envisions by the single particle model that the new orbital is of very large radial dimension. This allows the one center expansion of the respective orbitals. The conservation of orbital angular momentum along the internuclear axis and the gerade restriction lead for N_2 to the prediction that the π_g orbital in N_2 is

mostly D wave, with a small G component and smaller higher components. For CO, the absence of the gerade restriction leads to a largest component of P wave, then a smaller D wave, etc. If these arguments are coupled with the fact that low-energy electrons (such as are present in these experiments) emphasize the lower partial wave effects,³⁷ predictions as to the angular dependence of the outgoing electron for N_2 and CO can be made. Briefly, for N_2 and CO, since the targets are Σ , and the resonance is due to the electron configuration, one expects a D wave for N_2 and a P wave for CO for the emitted electron in resonant excitation. Since the emitted wave is relative to a molecular coordinate system, and since the experiment is done with a randomly oriented target gas (orientation and rotational effects are unresolved), an orientation average must be taken. Such a procedure, which is carried out rigorously and justified in Ref. 37, leads to an angular dependence predicted by the solid line in Figure 10. With one adjustable parameter, the normalization, one sees that the agreement is perfect for N_2 and quite satisfactory for CO in the $v = 0$ to $v = 1$ process. The model further predicts that the angular dependence prediction should be valid for all inelastic thresholds at all energies in the resonant region. This prediction is based on the purely electronic nature of the process. If anything, the momentum transfer argument predicts (i) that the fit should become better the higher the final v value and (ii) that the elastic channel should not show this constancy (since the qualitatively predictable and strongly energy-dependent angular dependence due to direct scattering interferes here with the resonant process). For CO these features are shown in Figure 11. A similar figure exists for N_2 ; viz. Figures 7 and 8. By reversing the logic one realizes that the similarity of angular dependence over the resonant region in the vibrationally inelastic channels can be a useful tool. One can detect a suspected resonant process even when the breadth of the individual peaks are such as to be overlapping and therefore not clearly resonances. Such a case exists for vibrational excitation in H_2 , viz. Figure 10. Figure 10 shows that for H_2 the expected orientation-averaged p wave angular dependence (the first antibonding orbital is σ_u and by the above logic has a p wave angular dependence) is qualitatively but not quantitatively obtained. On the other hand, Figure 12 is similar, in the nature of the points it demonstrates, to Figure 11 for CO. It shows the similarity, and lack of similarity, of the angular dependences as a function of energy for the inelastic and elastic cross sections respectively for H_2 . This feature of similarity is all that really is needed for verification of the resonance. Figure 10 adds to ones confidence in the resonant model.

It is perhaps instructive to go through the reasons for the 10% deviation in CO and the somewhat larger deviation in H_2 from the predicted formulas.³⁷ For CO, the flattening and hint of additional structure in the

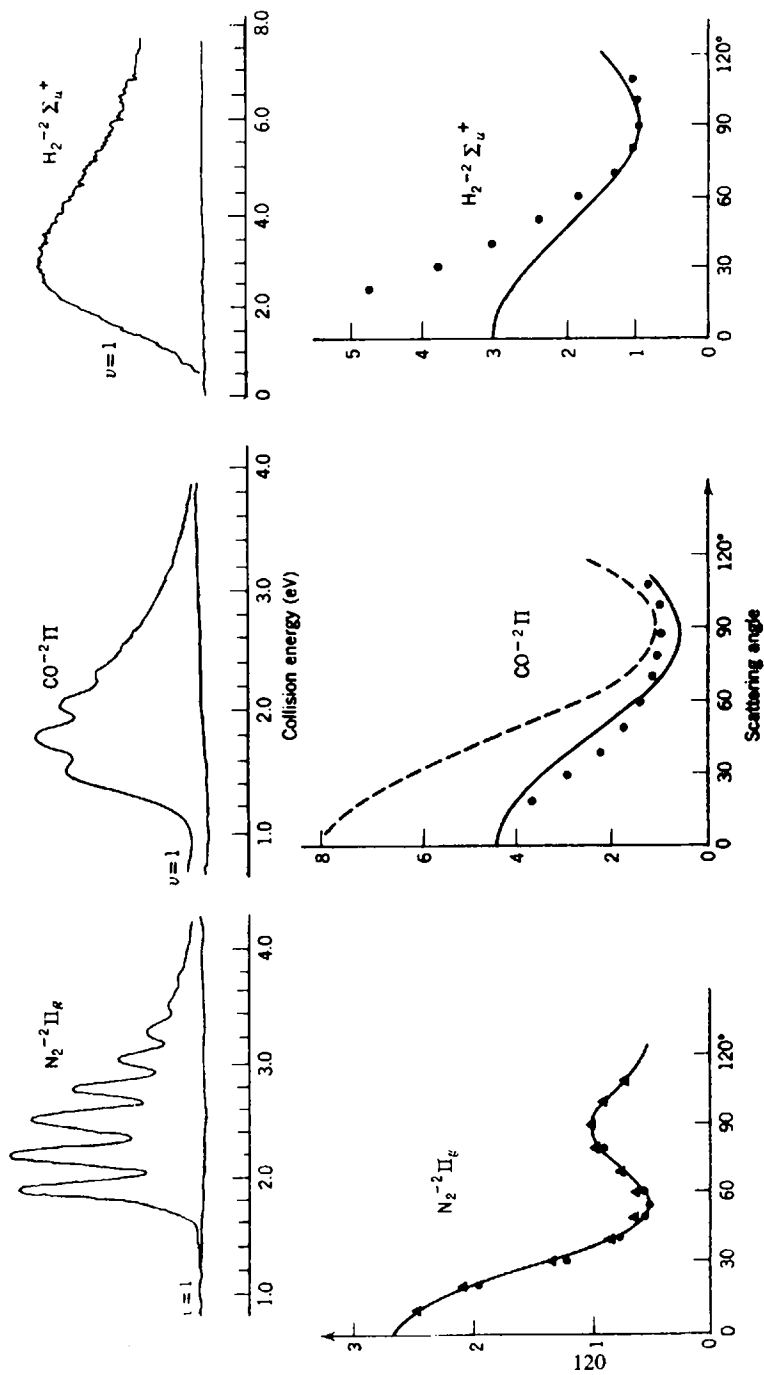


Fig. 10. Comparison of the energy dependences (upper row) and the angular dependences (below) of the resonant excitation of one vibrational quantum of N₂, CO, and H₂. For N₂ and H₂ the full lines in the graphs of the angular dependences represent the simplest theoretical expressions (Ref. 37) for the autoionization of the trapped electron. These expressions are

$$\begin{array}{ll}
 \text{H}_2 \text{ } p\sigma & \sigma(\theta) \propto 1 + 2 \cos^2 \theta \\
 \text{CO } p & \sigma(\theta) \propto 1 + 7 \cos^2 \theta \\
 \text{N}_2 \text{ } d & \sigma(\theta) \propto 1 - 3 \cos^2 \theta + \frac{14}{3} \cos^4 \theta
 \end{array}$$

For N₂ and H₂ they are normalized, together with the experimental data, to 1 at 90°. For CO: (·) experiment; (—) theory, normalized at 90°; (—) theory, normalized at 0°.

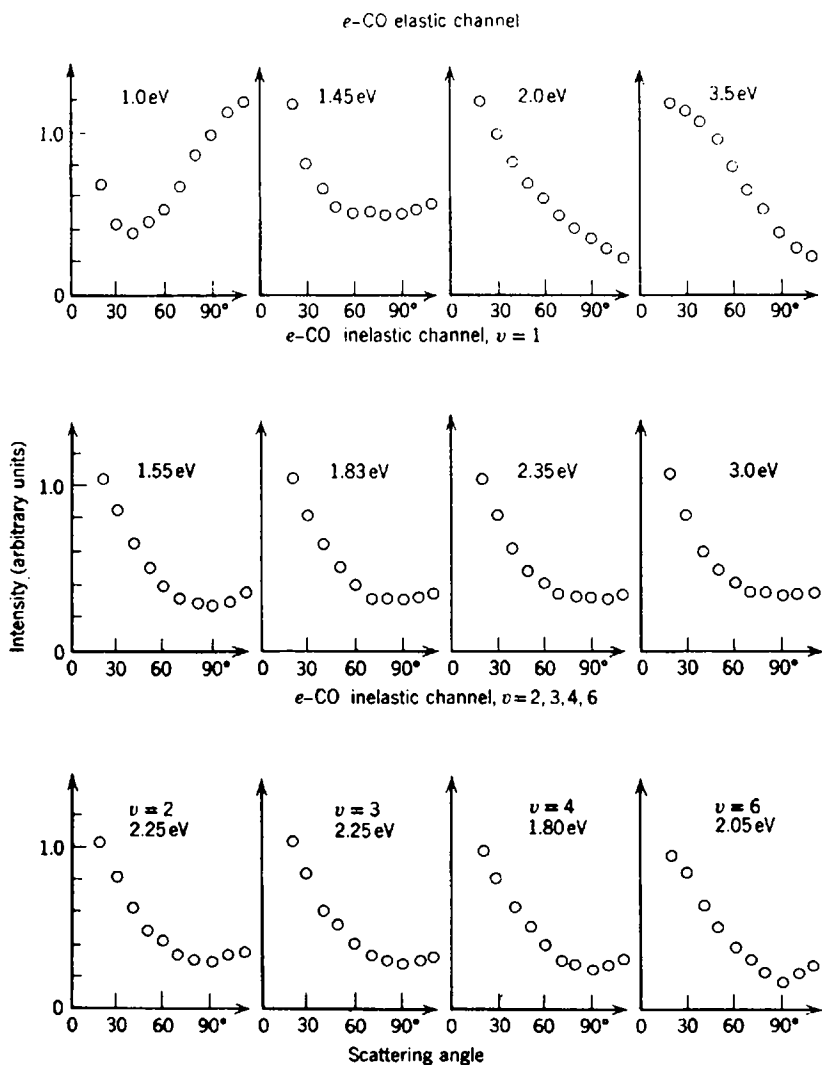


Fig. 11. Angular dependences of the elastic and inelastic scattering of electron by CO molecules at different collision energies. In the elastic channel (upper row) the angular dependence changes rapidly with energy since the scattering contains several partial waves with varying phase shifts (energy close to threshold). The constancy of the curve shapes for all inelastic channels and energies within the resonance region demonstrates that a compound state with a well-defined set of quantum numbers autoionizes and therefore only one outgoing partial wave can be detected.

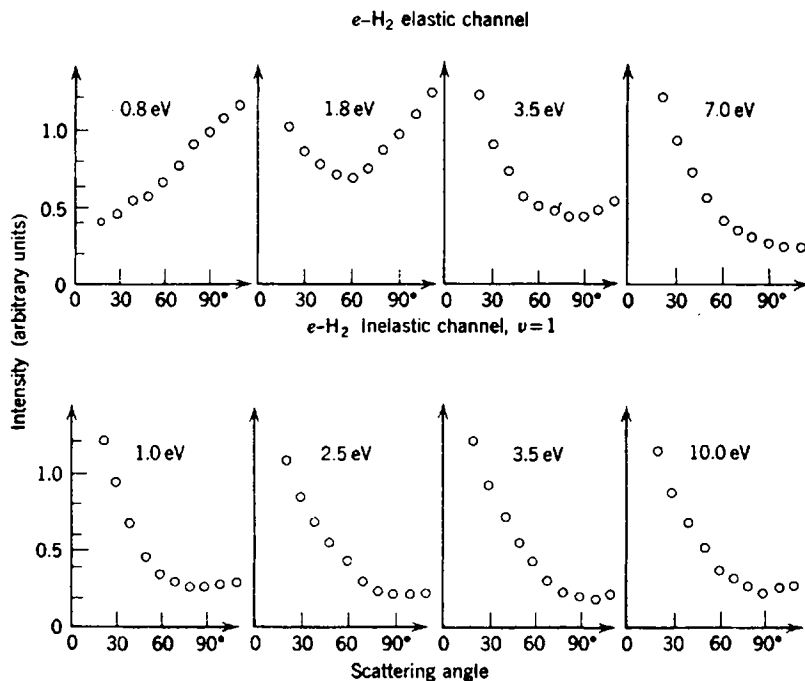


Fig. 12. Angular dependences of the elastically and inelastically (excitation of one vibrational quantum) scattered electrons from H_2 for different collision energies. The change of the angular dependence with energy in the elastic channel is due to the interference of several partial waves, whose phase shifts change with energy. This is typical for any potential scattering. In contrast, the constancy of the curve shapes for the inelastic channel shows that only one partial wave results from the autoionization of the negative ion state of H_2 . The shape of the angular dependence leads to the experimental confirmation of the configuration $^2\Sigma_u^+$ of the H_2^- .

experimental curve for the highest energy studied³³ points to $l \geq 2$ contributions, i.e., D wave, etc., as the obvious source of the results. The higher energy allows the D wave to become more evident. The deviation for the lowest energy case in CO is clearly due to the residual direct dipole scattering.

For H_2 the deviations, when traced as a function of energy and final channel, indicate that some F wave mixes into the angular dependence. Direct scattering also causes deviations from our "ideal" curve. This is to be expected in this lightest of all molecules where the momentum transfer argument must be at its worst.

Under the assumption that the differential scattering experiments are done at such a resolution that rotations cannot be resolved, O'Malley and

Taylor³⁷ have derived general formulas for differential scattering cross sections for vibrational excitation. Extremely simple formulas, of the nature given above, can be derived for N_2 , CO , and H_2 . Although it would be too space consuming to go through the rigorous mathematical derivations, it is worthwhile listing the physical assumptions under which such simple formulas can be extracted from the exact expressions. These assumptions are as follows:

(1) That the electronic matrix elements can be approximated by their first term in an expansion in spherical harmonics. This can be due to either or both of the following: (a) the electronic resonant state is rapidly convergent in a one center expansion; (b) the energy ranges of interest, the partial wave index, and the range of the force of the target are such that the lower spherical terms of the plane wave have greater amplitude.

(2) That either or both of the following slow rotation assumptions hold: (a) the rotational energy spacings are small compared to the relative nuclear kinetic energy (for R values in the Franck-Condon regions of the ground state and energetically accessible target states); (b) the rotational energy is small compared to the width, or equivalently the period of rotation is big compared to the lifetime of the resonance. Assumption (a) is the usual spectroscopic assumption which permits us to drop rotation-vibration interaction and to treat the motion in the R coordinate as occurring for fixed orientation (which is why we eventually have to average over orientation). Assumption (b) states that if the whole process takes place quickly in the time it takes to rotate, then the molecule can be considered to have fixed orientation during the process.

(3) That the Born-Oppenheimer approximation is accurate.

(4) That the process is pure resonant.

(5) That the scattering structure is due to one resonant state.

(6) That the rotation-vibration interaction is not negligible, but a slowly varying function of energy, so that the dependence of matrix elements on J , the rotational quantum number, can be replaced by an average J . This latter assumption is a quite good one.

For H_2 , since the vibrational lines are not present, the expressions (but note the predictions) of Ref. 37 could have been simplified by an averaging over vibrational states.

Recently Ehrhardt and Linder³⁸ have resolved the rotational excitation accompanying the elastic and inelastic processes discussed above. The theory of Ref. 37 can certainly be used to couple in rather than average over rotation and will give the expected rotational dependence.

The assumptions listed above are exactly those needed for deriving simple formulas for the angular dependence of products in resonant

dissociative attachment:³⁷ ($AB + e \rightarrow AB^- \rightarrow A + B^-$) Here the slow rotation approximation simply says that the resonant molecule dissociates along the line of nuclei at the moment of electron impact. This is clear since the molecular ion dissociates in a time short compared to the period of rotation. These results are, of course, also averaged properly over the random orientations of the molecules in the target gas. Unfortunately no experiments are available to compare to these results.

B. Resonant Phenomena in the Hydrogen Molecule

In this section the resonant phenomena in the hydrogen molecule below 12 eV electron impact energy will be discussed. In subsection (i) the calculated potential curves will be given and the available experimental data will be explained in terms of them. In subsection (ii) the details of the calculations of such curves will be discussed.

(i) In Figure 13 are given H_2 and H_2^- potential curves, the latter of which have been calculated in Refs. 39 and 40. Reference 39 should be consulted for the numerical presentations of the information in these figures. The first experiments to be explained are the observations of peaks in inelastic and total scattering cross sections.⁴¹⁻⁴⁵ Table II gives the experimental and calculated results for the two series of resonances. A mental transcription of the observed resonances in Table II to Figure 13 shows these resonances to be the vibrational states (rotations are unresolved and therefore effectively averaged) of two $^2\Sigma_g^+ \sigma_g 1s \pi_u^+ 2p \pi_u^- 2p'$ C.E. I states* of H_2^- . The lower (higher) state is simply an electron in the field of the $^3\pi_u \sigma_g 1s \pi_u 2p [^1\pi_u]$ state of H_2 . These H_2 states are also pictured in Figure 13.

For the lowest resonance an error of 0.21 eV exists. A glance at Figure 13 suggests that the experiment may not have observed the first level at 11.07 because of Franck-Condon overlap effects. Such a correction would improve the agreement. This latter suggestion is, of course, difficult to verify experimentally. It must also be remembered when comparing observed to calculated energies that in molecules we do not observe the electronic energies directly, and that to get vibrational energies the relatively inaccurate procedure of numerical differentiation of the calculated potential curve must be used. It is perhaps instructive to review how it was decided³¹ to try the configuration $^2\Sigma_g^+ \sigma_g 1s \pi_u^+ 2p \pi_u^- 2p'$ for the resonance. Historically it was this logic that led to the development of the C.E. I model and to the independent discovery of the Feshbach technique. The logic for the

* Since the one-electron orbitals were determined in an N -electron variation problem and not from a one-electron Hamiltonian, the symmetry σ , π , u , g , etc. has meaning but the numbering is just symbolic [i.e., viz. see Section B(ii)].

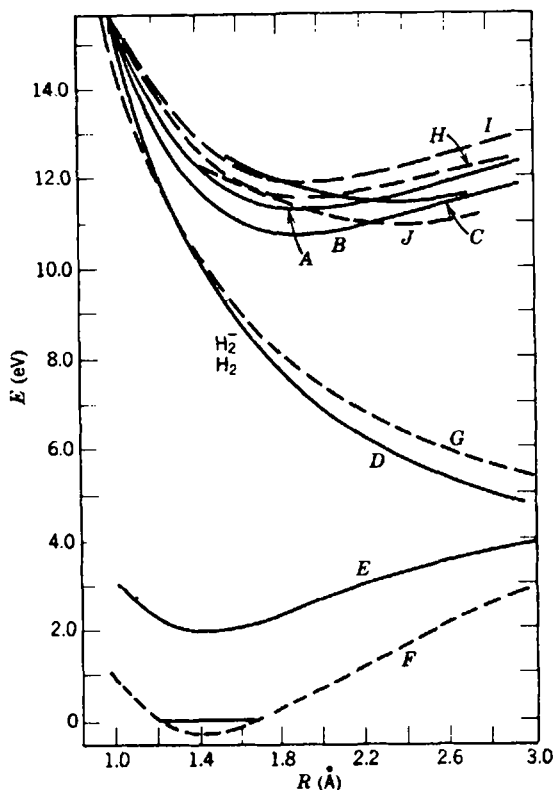


Fig. 13. Potential curves for H_2^- resonances and some associated H_2 states. (A) $\text{H}_2^- \ ^2\Sigma_g^+$ consisting of $C^1\Pi_u \cdot \pi_u 2p'$. (B) $\text{H}_2^- \ ^2\Sigma_g^+$ consisting of $C^3\Pi_u \cdot \pi_u 2p'$. (C) $\text{H}_2^- \ ^2\Sigma_g^+$ consisting of $B^1\Sigma_u^+ \cdot \sigma_u 1s'$. (D) $\text{H}_2^- \ ^2\Sigma_g^+$ consisting of $^3\Sigma_u^+ \cdot \sigma_u 1s'$. (E) $\text{H}_2^- \ ^2\Sigma_u^+$ consisting of $X^1\Sigma_g^+ \cdot \sigma_u$. (F) $\text{H}_2 \ X^1\Sigma_g^+$ (see Ref. 40). (G) One configuration result for $\text{H}_2 \ ^3\Sigma_u^+ 1\sigma_g 1\sigma_u$. This curve lies about 0.32 eV above the "exact" $^3\Sigma_u^+$ curve (Ref. 40), but is used as a comparison with the H_2^- calculation consisting of this configuration plus an extra electron. (H) Two configuration result for $\text{H}_2 \ ^3\Pi_u (1\sigma_g 1\pi_u + 1\sigma_u 1\pi_g)$. The minimum of this curve lies about 0.14 eV above the experimental minimum. The $\text{H}_2 \ u^3\Sigma_g^+$ curve lies so close to this one that they are indistinguishable on this scale. (I) Same as H for $C^1\Pi_u$ and $E^1\Sigma_g^+$. (J) $\text{H}_2 \ B^1\Sigma_u^+$.

second resonance is so similar that only the lower one will be discussed. The observation that the resonant peaks were spaced quite similarly to the vibrational levels associated with the $^3\Pi_u \sigma_g 1s \pi_u 2p$ state of H_2 implied an almost parallel potential curve for the H_2 state. Since the curvature, and not the energy, of the potential curve represents the field the nuclei feel are due to the electrons, it was concluded that in both states the field was due

TABLE II
Comparison of Experimental and Calculated Vibrational Levels
(energies in eV)

| Lower resonance | | | | Upper resonance | | | |
|-----------------------------|-----------|----------------|-----------|-----------------------------|-----------|----------------|-----------|
| Obs. level ⁴³ | Splitting | Calc. level | Splitting | Obs. level ⁴³ | Splitting | Calc. level | Splitting |
| 11.28 | | 11.07 | | 11.46 | | 11.46 | |
| | 0.28 | | 0.30 | | 0.26 | | 0.29 |
| 11.56 | | 11.37 | | 11.72 | | 11.75 | |
| | 0.28 | | 0.29 | | 0.27 | | 0.28 |
| 11.84 | | 11.66 | | 11.99 | | 12.03 | |
| | 0.27 | | 0.27 | | 0.28 | | 0.28 |
| 12.11 | | 11.93 | | 12.27 | | 12.31 | |
| | 0.26 | | 0.26 | | 0.26 | | 0.27 |
| 12.37 | | 12.19 | | 12.53 | | 12.58 | |
| | 0.25 | | 0.24 | | 0.24 | | 0.26 |
| 12.62 | | 12.43 | | 12.77 | | 12.84 | |
| | 0.24 | | 0.22 | | 0.20 | | 0.25 |
| 12.86 | | 12.65 | | 12.97 | | 13.09 | |

primarily to the same electrons, i.e., $\sigma_g 1s \pi_u^+ 2p$. Since the H_2^- was bound by 0.6 to 0.8 eV, the third electron had to see an attractive potential well. If the electron density of $\sigma_g 1s \pi_u^+ 2p$ (with the nuclear bond taken along the z axis and the π^+ taken along the y axis) is visualized, it is clear that a hole in the electronic core (relative to the ground state $^1\Sigma^+(\sigma_g 1s)^2$) exists along the x axis. The orbitals increase in energy as $\sigma_g 1s, \sigma_u 1s, \pi_u 2p \dots$. Clearly the placing of the extra electron in the first two orbitals would cause repulsion and also raise the energy relative to $H_2 \ ^3\Pi_u$. If the electron were placed in $\pi_u^+ 2p$ (along y), repulsion would again result. On the other hand, $\pi_u^- 2p$ would place the electron over the attractive potential well (i.e., total nuclear charge +2, one $\sigma_g 1s$ screening electron with the other π electron out of the way leaving a net +1 attraction) and minimize the electron repulsion which unstabilizes the system. The $\sigma_g 1s \pi_u^+ 2p \pi_u^- 2p'$ configuration implies Σ_g symmetry. The singlet nature of the target implies that the resonance must be a doublet ($^2\Sigma_g$). Since the mechanism of decay of the H_2^- is an autoionizing transition to the adjacent continuum (the mechanism of formation is inverse autoionization), the resonance and the adjacent continuum must have the same quantum numbers. The adjacent continua start at all the target states of lower energy. These states have in common the fact that they have a $\Sigma^+(\sigma)^2$ symmetry. Group theory does

not allow a single electron coupling to a $\Sigma^+(\sigma)^2$ state to form a Σ^- state. Therefore the continua and hence the resonance must be Σ^- . The picture of the electrons in spatially separate orbits led one to guess as the basic one-electron orbitals those calculated in Rydberg calculations for $^3\Pi_u \text{H}_2$.⁴⁶ The stabilization was immediate (see ii) with the results of Table II. Interestingly, the two $^2\Sigma_g$ resonances do not mix since they have spin-orthogonal cores and have such low electron interaction energy that antisymmetry plays a small role. This causes the Hamiltonian matrix elements between them to be of negligible magnitude. The low correlation argument and rapid stability indicate a narrow resonance (relative to the others we will study in H_2). Also since it takes 10^{-13} sec to vibrate, and since a vibrational spectrum is observed, a lifetime of this order can be inferred. The same lifetime can be inferred from parameterization of dissociative attachment experiments^{47,48} discussed below. Since line broadening decreases observed signal strengths if the argument is reversed and potential scattering is assumed to have small effects, a large signal (relative to other broader H_2 resonances) is implied. This perhaps explains why this resonance is historically the first one observed; in a new field with new instrumentation the larger signals are seen first.

The potential curve of the lowest $\text{H}_2^- \ ^2\Sigma_g$ resonances can be used to explain a second experiment; that being the resonant dissociative attachment* experiment whereby H^- is produced with a vertical onset at 14.0 eV, viz. Figures 14 and 15. The general mechanism of the process is that the H_2^- state is now produced, not in a bound state of its nuclear motion where it can only vibrate and decay back to H_2 (elastically or inelastically as the case may be), but in a dissociative state. The nuclei then begin to move apart as $\text{H}(2p)$ and $\text{H}^-(1s^2)$, the combined energy of which is 14.0 eV at infinite R . If the system decays electronically before the nuclei move out of the Franck-Condon regions of the lower target states, only resonant enhancement of molecular excitation cross sections are measured (with electron detectors). If, on the other hand, the system escapes without electronic decay, mass spectrometers will measure a current of H^- ions. Retarding potentials can also be used to measure the velocity of H^- formed as a function of electron impact energy. A vertical onset is qualitatively expected since dissociative attachment can begin sharply at 14.0 eV. At that value one expects the kinetic energy of the H^- ions to be zero since the total energy of the system is equal to the potential energy of infinite R . Above 14.0, nonzero kinetic energies are expected. All this has been

* Direct as opposed to resonant dissociative attachment can be eliminated by momentum transfer arguments similar to those used in the discussion of vibrational excitation.

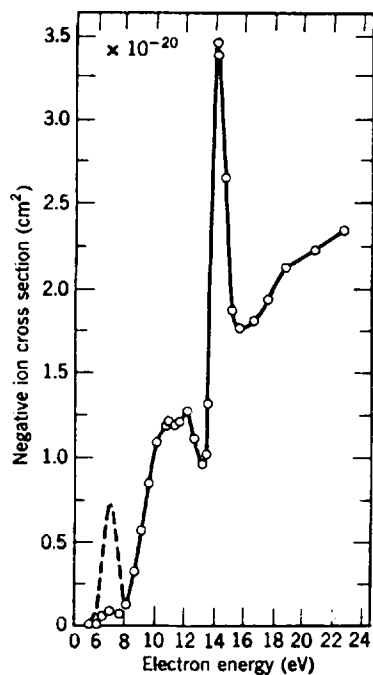


Fig. 14. The dissociative attachment cross section of Schulz.⁴⁷

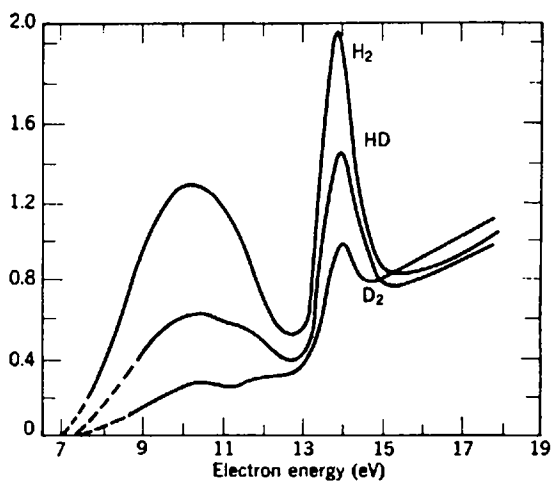


Fig. 15. The dissociative attachment cross section of Rapp, Sharp, and Briglia.⁴⁸

found, to a reasonable degree of certainty, in experiment. The lineshape is usually explained by the usual reflection principle which says that the Franck-Condon factors as a function of energy reflect the shape of the ground vibration state's Gaussian wavefunction $\chi_0(R)$. The argument says that the continuum wavefunction for nuclear motion can be approximated* by a delta function $\delta[R - R_T(E)]^{49}$, where $R_T(E)$ is the classical turning point. The Franck-Condon factor is the integral of this over R with $\chi_0(R)$ to give a χ_0 shaped function of E . A combining of the square ($\sigma = |T|^2$, T is the transition matrix) of this with the cutoff at 14.0 gives rise qualitatively to the observed shape (viz. Figures 15 and 17).

Rigorous theories of dissociative attachment^{49,50} have shown that under very wide conditions σ_{DA} is a product of a σ_{cap} , i.e., an electron capture

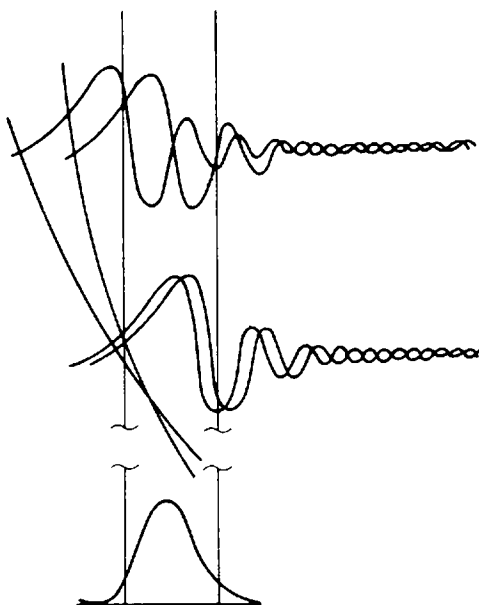


Fig. 16. Comparison of Franck-Condon factors. Note that only near the crossing point are the nuclear wavefunctions "in phase."

* In Figure 16 one sees the origin of the $\delta(R - R_T)$ or Stueckelberg approximation.⁴⁹ Simply, it is that only near $R = R_T$ does the continuum function for nuclear motion not oscillate so rapidly so as to average to zero contributions to the integral from other R . Clearly, if the upper potential curve is steep above the ground state Gaussian (viz. Figure 16) this description fits well. As the curve flattens the oscillations at R not too far from R_T are not really rapid and the argument begins to break down.

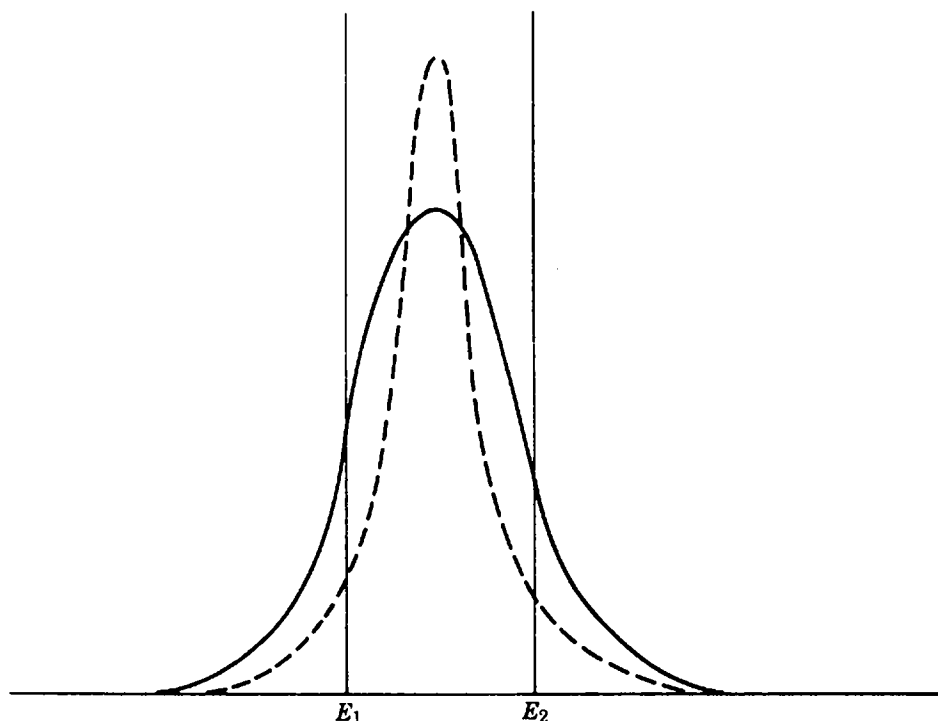


Fig. 17. E_1 and E_2 are two typically different cutoffs. Dotted line is heavier mass.

cross section and a factor $e^{-\Gamma t}$ where Γ measures the total probability for decay by electron emission,^{† 51} and t is essentially the time for the nuclei to move through the region where decay by electron emission is possible. Both of these factors have their own mass dependences and can give rise to isotope effects. The exponential factor involves the typical kinetic energy-type mass dependences. Essentially, the heavier the nuclei the longer it takes to get out of the electronic decay region and the lower the probability of dissociation. The first factor has a mass effect that can be described as follows:

(i) For vertical and non-vertical threshold the narrowing of the Franck-Condon region with increased mass makes σ_{capt} (which is proportional to $|\chi_0(E)|^2$) higher at its maximum but narrower in its breadth. The increased height can give rise to an apparent inverse isotope effect (viz. the case of

[†] Basically this says that if the two different decays occurred on widely different time scales, one of them would not be seen.

methane dissociative attachment)^{52,53} if no vertical onset occurs or if a vertical onset occurs on the low-energy side of the maximum. If, on the other hand, vertical cutoffs occur on the high-energy side, a shrinkage of the breadth of the Gaussian can cause a drastic decrease in σ_{DA} , viz. Figure 17, line E_2 and the dotted curve.

The isotope effect of the 14.0 eV peak (see Figure 15) is not clearly attributable to either cause in an exclusive way. It does tend to fit the first explanation better than the second. In fact, a recent calculation of Franck-Condon factors²¹ has thrown into doubt the *perfectly* vertical onset idea. The curves for H_2^- may be too far to the left to use the $\delta(R - R_T)$ approximation and instead may require a rigorous calculation. Certainly Figure 15 cannot be taken to definitively show a truly vertical onset although the onset behavior is not far from what the instrument with its natural line spread would record for a truly vertical onset. The 14.0 eV peak is 2.1×10^{-20} cm² at maximum intensity. Above 17.4 eV, H^- ions are produced by the process $e + H_2 \rightarrow H^+ + H^- + 2e$. This is not a resonant process so we shall not discuss it here.

Returning to Figure 13, at large R in the low-energy region, $H(1s)^2 {}^2S_g$ and $H(1s)^2 {}^1S_g$ exist at energies below that of two H atoms. The ionization energy of H is 0.75 eV. As smaller R is approached the Wigner-Witmer⁵⁴ rules tell us to expect ${}^2\Sigma_g^+$ and ${}^2\Sigma_u^+$ configurations to be formed. United atom and molecular orbital considerations tell us to expect the latter to be at lower energy. The latter configuration is clearly $(\sigma_g 1s)^2 \sigma_u 1s$ while the former is $\sigma_g 1s (\sigma_u 1s)^2$. The Σ_u state goes as $R \rightarrow 0$ to $He^- {}^2P_u(1s)^2 2p$, while the Σ_g state goes as $R \rightarrow 0$ to $He^- {}^2D_g 1s (2p)^2 [\sigma_u^2 \rightarrow (2p_z)^2 \text{ which has } m = 2 \text{ and must be } D]$. First consider the lower curve. It has been⁵⁵ shown that H_2^- cannot exist at small R with an energy lower than H_2 . From those R to the large R side of the crossing of the H_2^- and H_2 curves, the calculations of the energy were done using the Ritz-Rayleigh principle with a very flexible trial function. The results definitively show a slightly attractive force at large R and suggest a bound curve. The Pauling bond order of $1/2$ [$1/2(\text{number of bonding orbitals} - \text{number of antibonding orbitals})$] also suggests a bound state. The calculations in Figure 13 clearly bear out these expectations. The effect of this state on elastic and vibrational excitation cross sections has already been discussed in Section III.A. The curves given here are of sufficient quality to only estimate the lowest two vibrational states which come at 2.3 and 2.8 eV. If one envisions the interference of two broad overlapping peaks at these energies, their envelope could qualitatively reconstruct the part of the vibrational excitation cross section below 3.75 eV. The dropoff of the cross section above 3.75 eV is due to the vibrational excitation via transactions to and from the

continuum nuclear states. The configuration is clearly single particle. Its expected breadth is evident from the lack of distinct peaks and from the slow stabilization which will be discussed in Section B(ii) (recall Section II.B and the implications of slow stabilization.) In Section B(ii) it shall also be seen that, as expected by the model, core polarization, exchange, and their interplay are all essential in the calculation of this potential curve.

The very existence of the bound $H_2^- \ ^2\Sigma_g^+$ curve which dissociates at 3.75 eV led to the search by Schulz and Asundi^{56,57} for a vertical onset for dissociative attachment peak at 3.75 eV. This peak was found to be, as expected, of the shape associated with the " E_2 " vertical onset in Figure 17. Since Γ was so large compared to the C.E. I and II resonances, the cross section was very small (σ_{DA} at peak is here 1.6×10^{-21} cm³) compared to the higher peaks. The " E_2 "-type cutoff would be expected to result in a large isotope effect. This was observed by Schulz and Asundi⁵⁷ who measured the peak intensity as $\sigma_{DA}(\text{peak}) = 1.0 \times 10^{-22}$ cm² for HD, and 8.0×10^{-24} cm² for D₂. For this peak Γ was parameterized, indicating a lifetime of 10^{-15} sec for the low resonance. This is quite short, as expected.

The $^2\Sigma_g^+ \sigma_g \ 1s (\sigma_u \ 1s)^2$ state also approaches 3.75 eV at large R . The $-1/2$ bond order and the repulsive nature of the $^3\Sigma_u^+ \sigma_g \ 1s \sigma_u \ 1s$ anticipate the calculated result that the curve is of a repulsive nature. At large R the curve can be calculated variationally since it is bound relative to two distinct H atoms. At shorter distances the curve crosses the $^1\Sigma_g^+$ state of H_2 and becomes C.E. I in the field of its parent $^3\Sigma_u^+ \sigma_g \ 1s \sigma_u \ 1s$. At even smaller R , about the center of the Franck-Condon region (viz. Figure 13), it crosses its parent state and becomes a C.E. II state. This could be anticipated by noting that the united atom of the H_2 state is He $1s \ 2p_z \ ^3P_u$ while that of the H_2^- state is He⁻ $1s (2p_z)^2 \ ^2D_g$ which because of electron repulsion between the two $2p_z$ electrons could be expected to have a higher energy than the helium states. The calculation of this state revealed a slower stabilization of energy as R decreased. According to the discussion of section II, this indicates that the decay width generally increases with decreasing R . This result is also expected from the successive change from a bound state to C.E. I to C.E. II resonance state. Perhaps it is worth pointing out that bound states can be calculated by the stabilization method as poles of very narrow (zero) width. Therefore a consistent method exists at all R . The discrete exact eigenstate at large R is certainly stable to all variations.

For the same reason that repulsive states do not show up in spectroscopy (no discrete lines), the effect of this state is not immediately evident in scattered electron channels. The angular distribution method attempted³³ has so far failed to detect at or above 8 eV signs of the expected S and D

wave nature of this state ($^2\Sigma_g^+ = ^1\Sigma_g \times \sigma_g$ and σ_g is $S + D + \dots$). The curve passes into the Franck-Condon region at 8 eV. Again as in spectroscopy, such states are seen from their dissociation products. The arguments leading to the general Gaussian shape of σ_{DA} for repulsive potentials generally explain the bell shape of σ_{DA} in the 8 to 12 eV region (viz. Figure 15). The $\sigma_{DA}(\text{peak}) = 1.3 \times 10^{-20} \text{ cm}^2$. The isotope effect (viz. Figure 15) is perfectly explained by the kinetic energy-type argument. The failure of the σ_{DA} curve to go to zero anywhere in the 12 to 14 eV region is as yet unexplained and probably will require a rigorous calculation of an effect. The real test for the calculated curves comes in explaining the latest results of Sharp and Dowell⁵⁸ which show that there are oscillations in the cross section in the 10 to 12 eV region starting at 10 eV and hinted at in Figure 14 and in the HD and H₂ curves in Figure 15. Demkov,⁵¹ noting the dip at 10 eV in Figure 14, assumed that two unresolved peaks exist. Molecular orbital theory forbids this, and the new oscillations demand another explanation. Most striking is the reported fact that the oscillations have a period that, to experimental accuracy, is the same as the vibrational spacing of the lowest $^2\Sigma_g \sigma_g 1s \pi_u^+ 2p \pi_u^- 2p$ resonance. To explain this the following mechanism is proposed. It is noted that the $^2\Sigma_g^+ \sigma_g 1s \pi_u^+ 2p \pi_u^- 2p$ and the $^2\Sigma_g^+ \sigma_g 1s (\sigma_u 1s)^2$ come very close together at R less than 1.4 a.u. (Figure 13). Since they have the same symmetry one can have interference effects similar to predissociation and its inverse (viz. Figure 18). This interference between excitation to either state and between the states themselves would account for the oscillations in a way well known to spectroscopists. Inverting our logic, the experimental observation of the oscillations and the empirical fitting of the resonant electron scattering peaks of the $\sigma\pi\pi$

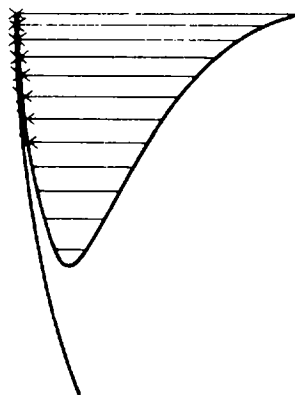


Fig. 18. Schematic diagram for inverse predissociation of resonances.

state to a potential curve (in the traditional method of vibrational spectroscopy) gives, as seen in Figure 18, a set of points through which the repulsive curve must pass. Another point is given at about 8 eV where the repulsive curve is seen from Figure 14 (the onset of σ_{DA}), to pass into the Franck-Condon region of the ground state of H_2 (which occurs at a well-determined R). These points and the known energy of 3.75 which must be asymptotically approached allow a sketch of the curve to be drawn *without any calculation*. This curve, of course, agrees well with the calculated one.

It might well be asked in reference to Figure 13, how it is known that the curves come close enough so that the Franck-Condon factors between them allow for the interference. This can be inferred spectroscopically from the work of Herzberg⁵⁹ who found a spin-orbit type predissociation between the H_2 $^3\Pi_u$ and $^3\Sigma_u^-$. Since the H_2^- states are bounded on the small R and large R sides, respectively, by the H_2 states, and since their vibrational wavefunctions of the H_2 states overlap sufficiently, we can assume that those of H_2^- do also.

Lastly, it is interesting to speculate on the decay of the $^2\Sigma_g^+ H_2^-$ into the $^3\Sigma_u^+ H_2$ at those R smaller than the crossing point. First, one notices from Figures 13 and 16 that the Franck-Condon overlap tends to make the transition improbable except at internuclear distances other than at the crossing point. On the other hand, at this point one has, from a fixed R point of view, a narrow C.E. II resonance and from our calculations no mixing of the H_2^- wavefunction with a continuum containing the H_2 $^3\Sigma_u^+$. This latter effect makes the transition at the crossing R unlikely. Perhaps a compromise R , where the C.E. II resonance would not be too narrow and where the vibrational wavefunctions would still be in phase (viz. Figure 16), would be at energies corresponding to those with R slightly less than the R of the crossing point. This means that at this energy, which is about 11 eV, a new channel for decay of H_2^- $^2\Sigma_g^+$ is added, over a small energy range, to the already existing H_2 $^1\Sigma_g^+$. This *might* cause an inelastic cusp-type effect* and cause this 11 eV region, which is very near in energy to the 11.07 eV level for $^2\Sigma_g^+ H_2^- \rightarrow \sigma\pi\pi$, to change more sharply and noticeably than could be caused alone by the simple interference oscillations discussed above. This in turn might explain the more noticeable 11 eV depression in σ_{DA} (see Figures 14 and 15). The other oscillations needed much larger statistics to be noted. A similar effect in σ_{DA} for CO is noted by

* The cusp effect is due to the fact that at a new threshold the energy of the new cross section (because of the flux factor) becomes infinite, thereby drawing all the incoming flux into the new channel. The old channel, just at threshold, responds to the change in incident flux and therefore the cross section takes a sudden dip.

Chantry⁶⁰ and is also used in an attempt to explain away what might appear as two overlapping peaks in an energy region where two states do not exist. This latter-type effect has never been proven to exist but is worth keeping in mind.

A point of confusion that has led consistently to fruitless argument is the meaning of such potential curves as the lowest one for H_2^- . It is argued that since it lives less than a period of vibration it has no reality. This author rejects and cannot see the sequence of logic to support such ideas. It is reiterated that the curve at each R is an asymptotic series approximation, in the adiabatic regions, to the real value of the pole of the Green's function in the second sheet. Hopefully, the usefulness of this curve has been demonstrated.

(ii) The curves for H_2^- in Figure 13 were calculated by the stabilization method. The programs used to do the calculation were the same ones used successfully in numerous calculations on small diatomic molecules like H_2 , HeH , He_2 , Li_2 , LiH , etc.^{55,61} and on several atoms. These programs need not be described here in detail (see Ref. 39 for details). It suffices to say that they calculate energies and wavefunctions for N electron diatomic or atomic systems when the trial function is a linear combination of products of N one-electron orbitals. Upon input specification, the programs automatically construct from the primitive function a function with the proper spin and space symmetry, i.e., ψ_{trial} is made an eigenfunction of δ^2 , Σ , Π , \dots , g , u , $+$, $-$, etc. This construction is done in the most general way using a complete spin basis. There are no restrictions to open or closed shells or to orbital pairings. All internuclear distances are treated and total antisymmetry is handled in an exact manner. The integrals are calculated, the secular equation set up and diagonalized, and parameters of the trial function varied to obtain, if desired, a minimum energy for the functional form of ψ_{trial} . All steps are internal to the program. No restrictions as to an orthonormal basis are present, and the program can work in a Hylleraas-Undheim mode so as to treat ground or excited states. The real power of the program is in the built-in flexibility of the one-electron orbital. To start, sets of orbitals were specified by specifying the value of their parameters. The orbital set so specified is called the one-electron basis. The program is then given the products of these orbitals to be used; this is the N -electron basis. In these calculations all configurations (member of the N -electron basis) were included in ψ_{trial} that had components on a specific symmetry of interest and which could conceivably mix with systems containing $\sigma_g 1s$, $\sigma_u 1s$, $\sigma_g 2s$, $\sigma_u 2s$, $\pi_u 2p$, $\pi_g 2p$, and similar orbitals for $n = 3$. A scanning of the H matrix as well as the eigenvectors and eigenfunctions revealed immediately any inherent stabilities. The increased flexibility

gained by not using an orthonormal basis in representing charge distributions had the disadvantage of not giving the simple component meaning to the coefficients of the eigenvectors. This necessitated the study of the H matrix numerical partitioning as a check on observed stability plots of E versus the number of configurations. With an orthonormal basis, stability could be noted by the near zero coefficients of all new N -electron basis functions tried. The orbital assumed by the program is described in Ref. 61. It has five parameters which specify: z component of angular momentum, i.e., σ, π ; nodes along constant ξ and η coordinates; and left-right as well as in-out distortions of the charge cloud. The orbital is a two-center orbital in elliptical coordinates. By proper choice of parameters a smeared-out or tightly-bound molecular orbital as well as any atomic orbital needed could be constructed. The only disadvantage of the orbital is that for the representation of atomic orbitals of high principle quantum number linear combinations of the two-center orbitals are needed. In nonresonant problems where the variation principle is used to get self-consistency (by parameter variation in repeated calculations) of the linear and nonlinear parameters, the orbitals have been shown to be very good approximations to the natural orbitals (the first N of which are like the Hartree-Fock orbitals). The natural orbitals are the best one-electron basis possible from the point of view of the convergence of the N electron configuration interaction wavefunction. It should be emphasized that once the non-linear or screening parameter of the one-electron basis is chosen for a stabilization calculation as contrasted to a variational one, they are not re-varied. Only after stability is achieved are the parameters of the nonmixing configurations varied so as to sweep and test any, as of yet, unreached region of Hilbert space.

The calculational procedure was easy for all but the single particle resonances of Figure 13. Regular variational calculations were carried out at those large R where the states were bound. For each R in the resonance region the following procedure was carried out. First, in order to determine a Rydberg type basis picture, a one-electron $H_2^+ \sigma_g 1s$ orbital was determined by the variation method. Then, holding this orbital fixed, for each total symmetry in a two-electron problem (e.g., $1,3\Sigma_{u,g} 1,3\Pi_{u,g} \dots$), a series of 2-electron Rydberg, or electron in the field of H_2^+ type, orbitals were determined. This was done by varying in a Hyleraas-Undheim manner a one-configuration wavefunction made up of the fixed $\sigma_g 1s$ orbital and the orbital to be determined, ϕ_1 . Then a two-configuration problem was done in which the first 2-electron configuration, $\sigma_g 1s \phi_1$, was the one determined above and the second was again $\sigma_g 1s (H_2^+)$ times an orbital to be determined, ϕ_2 . The second root of the secular equation was minimized with

respect to the nonlinear parameters. Extending the procedure using 3 configuration and the third root with respect to ϕ_3 , etc. led to the determination of all the needed basis functions. From this basis set for any given total symmetry, H_2^- functions were set up which symbolically had such forms as $\sigma_g 1s (\sigma_g 1s)' \sigma_g 2s$, $\sigma_g 1s (\sigma_g 1s)' \sigma_g 3s$, \dots ; $\sigma_g 1s \pi_u^+ np \pi_u^- np$, $n = 2, 3, \dots$; $\sigma_g 1s \sigma_u ns (\sigma_u ns)'$, $n = 1, 2, \dots$, etc. A forty to fifty configuration, three-electron secular equation was then diagonalized. Stable roots were selected and their main configurations noted. On a plot of E versus R the stable roots with the most similar first configuration (a trivial thing to recognize since the R grid was closely spaced) were connected and the potential curves for both these core excited states were the results. For details of the orbitals and the wavefunction the reader is referred to Ref. 39. Generally it was noted as expected that C.E. I resonances stabilized in one configuration while C.E. II regions took several configurations to stabilize. The two $\sigma\pi\pi$ resonances were not only stable but did not mix at all. Indications of at least one other stable root at higher energy was present but was not pursued since larger basis sets would be needed.

The calculation of the single particle state was more difficult than the core excited states. The reason for this is clear. First the new orbit is not of the Rydberg type and sees no inner charged core. The effect of this orbit on the core induces the very polarization which determines the orbit. An iterative method is needed to determine the one-electron orbitals and the primary three-electron configuration. In the calculation of the core excited resonances little trace of the single particle resonance existed. A trial function which was a good many configuration unpolarized H_2 molecule function times an elaborate σ_u orbital did not stabilize. The procedure used to find the orbitals was based on the following idea. If the σ_u orbit was reasonably guessed at each R (e.g., with the parameters of the σ_u in the $H_2 B^1\Sigma_u^+ \sigma_g 1s \sigma_u 1s$), and if it was fixed during a calculation in which the core parameters were varied *slightly* (in order to represent the core polarization), a minimum energy would be reached. The word "slightly" is emphasized since a large change of core parameters would simply ionize the system to a poor H_2 representation and an extra electron. It is intuitively clear that the H_2 molecule is in the electronic shell-like box of the σ_u orbit and that a pseudominimum for the energy exists in this box. The electronic cloud's distortion at this minimum is a type of adiabatic polarization. The newly polarized core obtained in this way was then used in a three-electron function with a linear combination of several σ_u -type orbitals. Stabilization was then achieved for this configuration. To check the process the core was reiterated in the field of the new σ_u orbital and then the σ_u again determined until the total process converged. The

new configuration showed stability and did not mix with the 40 other configurations which had reasonable electron density in the region. It was truly stable, but as we noted and might expect from the width of the single particle-type resonances, it took about five configurations to stabilize and to properly represent σ_u . The low H_2^- single particle curve of Figure 13 resulted and connected at large R to the variationally determined curve. The necessity to account for the interplay of exchange, core polarization, etc. is evident in this example.

The fact that the potential curves of H_2^- given in Figure 13 are calculated in the clamped nuclei approximation, but are drawn by connecting stable roots corresponding to electronic configurations of similar one electronic type (as opposed to connecting at all R the energy of the n th root of the secular equation), indicates that the curves are what is known as diabatic as opposed to adiabatic. A complete separated atom and united atom analysis would show that many curves would cross. An example is the $\sigma_g(\sigma_u)^2$ state of H_2^- . If the adiabatic prescription were taken, unstable roots would have to be chosen and absurd looking potential curves which do not explain experiments would result. Mandl⁶² noted this and justified the choice of the diabatic states by proving that for the diabatic states whose real energies cross as a function of R , the complex energies plotted in the complex plane do not. Because our tastes run to more physical arguments, we prefer to note that the justification really lies in the fact that the states have little electron interaction. First, it is noted that the one-electron orbitals have meaning in such a case and that the connecting of the curves in the diabatic way was only possible, since the many-electron symmetry is the same for all roots of a calculation, by being able to distinguish the fact that the most important configuration had similar one-electron orbitals. The physical reality of choosing the diabatic curve to compare to experiment becomes clear when it is noted that adiabatically calculated curves would be tangential at the crossing point. This would result in the atoms jumping, with unit probability, the adiabatic curves and following the diabatic envelopes. The reason for the tangential nature is that, by definition, the diabatic resonant processes pick the natural wavefunction (i.e., the ones that give physically evident potential curves).

We shall outline the important ideas put forward by O'Malley⁶³ which stress the need to obtain diabatic curves. Consider a two-state system denoted by $\psi_\alpha(F, R)$ and $\psi_\beta(F, R)$. F is the electron coordinates. The potential curves are given in Figure 19. If ψ_α and ψ_β are calculated adiabatically, the full lines result. If ψ_α and ψ_β are diabatically defined, the dotted lines result. Consider now the inelastic scattering $A_\alpha + B_\alpha \rightarrow A_\beta + B_\beta$. If an

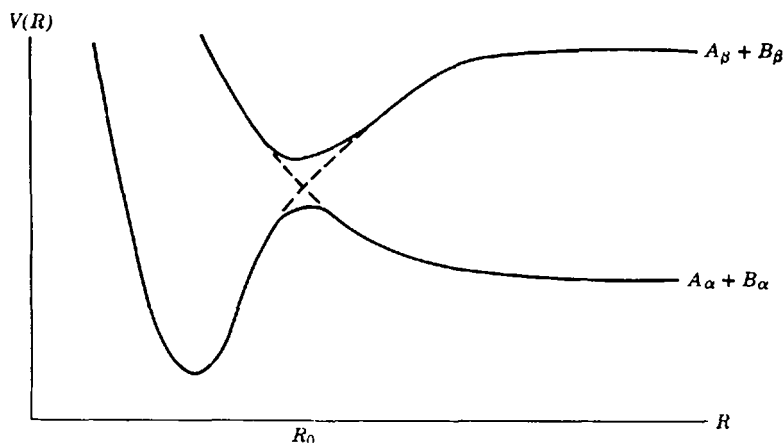


Fig. 19. Diabatic (---) and adiabatic (—) potential curves.

adiabatic basis is chosen, the potential curves are obtainable from the well-defined procedure of connecting at each R the corresponding (in order of increasing energy) roots of the secular equation. On such a basis the change of products can only be accomplished by a transition or jump near R_0 from state α to β . Since H (electronic) is diagonal on the ψ_α , ψ_β basis, the transition operator must be H (nuclear). It is then claimed that inelastic scattering is caused by the nuclear motion operators. The description is not really fortunate because the concept of transitions is usually only meaningful when the off-diagonal elements of the perturbation are small compared to the diagonal elements. Without such a situation the original basis is not observable as stationary states and in turn the coupled equations of the process cannot be solved by a convergent iteration or perturbation method (all practical methods fall in this class). In the adiabatic case the transition elements are large because they involve terms representing the curvature of ψ_α and ψ_β as functions of R . The avoided crossing due to the adiabatic potentials cause this curvature to be large near R_0 . The adiabatic picture then fails, and it is not surprising that experimentalists discussing inelastic collisions tend to draw schematic diabatic curves, i.e., the dashed lines in Figure 19. If the problem could be treated in the diabatic basis, then the smoothness of the dashed lines indicates small off-diagonal nuclear perturbations. The inelastic mechanism is now a switching as opposed to a jumping of curves. The problem is that the processes of choosing the diabatic ψ_α and ψ_β are ill-defined and are only simple in the

low electron interaction case (recall our previous discussion on diabatic resonance states). Only in low electron interaction cases can one simply connect, as a function of R , roots that have functionally similar eigenvectors. In strong interaction cases the electronic distortions as a function of R are so large that no recognizable connectable similarities exist. If one simply connects eigenvalues by using functionally inflexible (as a function of R) wavefunctions so as to preserve recognizability, the dashed curves will not merge at $R \gg R_0$ and $R \ll R_0$ with the adiabatic curves. This is unphysical. It seems to this author that only in low electron interaction situations can diabatic curves be chosen. Assuming a choice of diabatic states can be made, the transition causing perturbation can now be either or both of nuclear (now a small effect) and electronic origin. This latter is true since the H (electronic) is not now diagonal in the basis in the R_0 region. The whole understanding of the process changes. One cannot without calculation be sure that the off-diagonal elements are small in a diabatic basis and the resulting calculations simpler. The fact that the experimentalists dealing with these processes seem to find that qualitatively drawn diabatic curves explain their results is a strong indication that the calculational advantages of having small off-diagonal elements will be obtained with a diabatic basis. O'Malley's present efforts are devoted to finding new ways of computing diabatic curves. Interestingly, several spectroscopic Rydberg problems are easier to explain if nuclear motion states are chosen corresponding to diabatic curves. Considering the small electron interaction nature of Rydberg states, this becomes understandable.

C. Use of the One-Electron Model in the Qualitative Understanding and Choices of Significant Experiments

For all its faults, the one-electron model of quantum chemistry, in which the wavefunction for a state is envisioned as simply a single determinant of one-electron orbitals, is qualitatively useful. It suggests to theoreticians, without calculation, which basis functions are important, and it suggests to experimentalists simple interpretations of their results. It can also be used as a tool for the experimentalist to choose which cross sections are most useful in studying various resonances. In Section III.A we have already seen how the measurement of *inelastic* vibrational excitation cross sections is a more significant experiment for the study of resonant process than elastic or total cross-section measurements. Since the non-interacting picture is being stressed, we shall drop total orbital angular momentum from consideration and use the one-electron quantum numbers as almost good quantum numbers. The test of this way of thinking is, of course, in its

usefulness which we believe we can demonstrate below. Our only claim is that the model is perhaps the only usable one without calculation which, if used with care, can give rapid and simple insights.

In what follows we shall essentially make the Mulliken approximation in its simplest form for Hamiltonian matrix integrals, i.e., they shall be taken proportional to the overlaps of the orbitals in the initial and final state.

Recently the total inelastic cross section for excitation to each of the four $n = 2$ thresholds of helium, $2^{1,3}S$, $2^{1,3}P$, has been measured.⁶⁴ This measurement has been repeated in a more elaborate series of measurements on the inelastic differential cross sections.⁶⁵ Both laboratories revealed two C.E. I resonances just below the 3^3S threshold in helium at 22.42 and 22.60 eV, respectively. Both works find that the lower resonances gave a large signal only in the excitation of He to the 2^1S and 2^3S , while the higher resonance was evident in all four channels. The latter workers found by angular measurements these resonances to be 3^2S and 3^2P , respectively. One point is that one-electron logic had already anticipated this result⁶⁶ using the total inelastic data of Chamberlain.⁶⁴ To see this, one need only realize that the lowest C.E. I resonance is $1s(3s)^2 3^2S$ by the C.E. I model and by analogy to the well-studied state of $\text{He}^- 1s(2s^2)$, which is the lowest C.E. I below the 2^3S of He. Now for $1s(1)3s(2)3s(3)$ to be seen in the exit channels $2^{1,3}S$ of helium, one of the integrals of the form,

$$\langle 1s(1)3s(2)3s(3) | V | 1s(1)2s(2)kl(3) \rangle$$

(when kl represents a continuum function) is a transition integral from the negative ion state to the final $1s2s$ exit channel. Assuming that for any reasonable potential an overlap of a one-electron orbital (be it bound or continuum) with another orbital of different angular form is very small, one infers that $1s3s^2$ can be large because of the transition to $1s(1)2s(2)ks(3)$. Now $1s3s^2$ cannot be large in the P channels because the integral

$$\langle 1s(1)3s(2)3s(3) | V | 1s(1)2p(2)kl(3) \rangle$$

always involves an s - p one-electron overlap integral no matter which l is chosen. This agreement of the model with the experiment assured one of the predominant role of the configuration $3^2S 1s(3s)^2$ in the first resonance and anticipated that looking for it in the $2^{1,3}S$ channels would be measuring the $ks(3)$ electron and therefore the S angular dependence. The second resonance is given by the model $1s3s3p$. Chamberlain indicated it could also be given by $1s3p^2$. We can now show that only $1s3s3p$ fits the observation of large signal on both the $2^{1,3}S$ and $2^{1,3}P$ channels and that this, of course, anticipates a P wave behavior of the differential cross section to the $2^{1,3}S$

and S wave to the $2^{1,3}P$. $1s(1)3s(2)3p(3)$ can make a transition with reasonable intensity to $1s(1)2s(2)kl(3)$ for $l = 1$ and to $1s(1)2p(3)kl(2)$ for $l = 0$ (we always pick out the largest integral of the several allowed by antisymmetry). This assures that a $1s(1)3s(2)3p(3)$ has the observed strong intensity in both channels. Now $1s(1)3p(2)3p(3)$ can only go strongly to $1s(1)2p(2)kl(3)$, $l = 1$. To go to $1s(1)2s(2)kl(3)$ would require an s - p overlap. Therefore we can eliminate the $1s(3p)^2$ from consideration and guess for the second resonance $1s3s3p$.

As a second example of the one-electron method the logic is explained that tells the experimentalist to look for C.E. II resonances in their parent channels and not to expect to see them with significant intensity in channels below the parent state. The logic was the basis in helium of predicting that the C.E. II resonances above and among $2^{1,3}S$ and $2^{1,3}P$ should most easily be seen in inelastic scattering to 2^3S and 2^1S . This, of course, turned out to be the case. Elastic and total measurements only revealed near inelastic thresholds C.E. I resonances. Again the argument is based on one-electron overlap. Here we ignore potential scattering and direct excitation. Only the maximum resonant signal strength is treated using the obvious idea that if the maximum, which occurs at $E = E_{\text{resonance}}$, is too small to see, nothing else will be noted. With this the elastic cross section is given by (proportionality factors that cancel upon ratio comparisons are suppressed)

$$\sigma_i^{\text{res}}(E) \propto \frac{\Gamma_{\text{or}} \Gamma_{\text{ro}}}{\Gamma_{\text{tot}}^2} = 0(1), \quad \Gamma_{\text{tot}} \propto |\Gamma_{\text{or}}|^2$$

o = elastic continuum

r = resonance

and where $\Gamma_{\text{or}} (= \Gamma_{\text{ro}})$ is the square of the resonance-elastic continuum matrix element. Now to compare the signal for a C.E. II resonance in the C.E. II parent and the elastic channel, one needs roughly to parameterize the C.E. I to elastic and inelastic continua. Now for an inelastic case, since (a) the elastic continuum has two $1s$ orbitals times a kl orbital; (b) the inelastic continuum has one $1s$, and one $n = 2$ orbital times a $k'l$ orbital; and (c) the resonance function has one $1s$ orbital and two $n = 2$ orbitals, the overlap between the resonance and the inelastic continuum is much greater than that of the resonance and the elastic continuum. Therefore the square of these overlaps Γ_{or} and Γ_{ri} (i = inelastic) is in the ratio $\Gamma_{\text{or}}/\Gamma_{\text{ri}} = \lambda \ll 1$. It is to be noted that here the argument is based on spatial overlap since angular considerations will not differentiate between the types of information we seek. With this, Γ_{ror} for the C.E. II is given

as $\Gamma_{\text{tot}} \propto \Gamma_{\text{or}} + \Gamma_{\text{ri}} \approx \Gamma_{\text{ri}}$ and the signal in the elastic channel is proportional to

$$\frac{\Gamma_{\text{or}} \Gamma_{\text{or}}}{\Gamma_{\text{tot}}^2} = \left(\frac{\Gamma_{\text{or}}}{\Gamma_{\text{ri}}} \right)^2 = 0(\lambda^2)$$

while in the inelastic channel

$$\frac{\Gamma_{\text{or}} \Gamma_{\text{oi}}}{\Gamma_{\text{tot}}^2} = \frac{\Gamma_{\text{or}}}{\Gamma_{\text{ri}}} = 0(\lambda)$$

Hence we see that a search near the $n=2$ states in helium in the elastic channel will result in enormous C.E. I resonances ($0(1)$) relative to C.E. II resonances (viz. Ref. 67) and largely hide and swamp the C.E. II resonances. The C.E. II should be looked for in the inelastic (see Figure 1) where they have been clearly seen. Here the elastic resonance, except for a small part of its tail, is forbidden by energy consideration. Even in this case the story is not so simple since small signals of the order λ compared to 1 are to be detected. Add this to the fact that C.E. II resonances are generally broad and overlap, and one begins to appreciate the magnitude of the accomplishment of the experimental work of the Ehrhardt group. In attenuation experiments, which measure the unscattered as opposed to scattered electrons, the C.E. I and the large noise [$0(N^2)$] hides the C.E. II resonances.

This argument that says resonances just above the n th target state should be sought in the n th exit scattering channel is based strictly on spatial overlap. Similar arguments can be given for a C.E. I resonance in the field of the n th target state to appear most strongly in the $n-1$ exit channel of the target state. Clearly as n gets larger the orbits become spatially of the same dimensions, and the argument now simply says that C.E. II in the field of state n will appear largest in n , smaller in $n-1$, etc. This is clearly the case in Andrich et al. where the C.E. II states of the $n=3$ channel of helium are seen in the $2^{1,3}S$ and $2^{1,3}P$ of helium.

The idea of weak coupling to a given channel has been used by Burke et al. in the study of the C.E. II resonances above the $n=2$ channel and the C.E. I below the $n=3$ channel in helium. Since the elastic coupling was of order λ^2 , the ground state was dropped from the close coupling expansion with the expectation, which proved true on comparison to experiment, that it would not significantly effect the results.

For want of a better place, it is perhaps worth making a comment on the close coupling method.^{1,2} This powerful method becomes arduous when large numbers of strongly coupled channels exist and when the system is not spherical. The greatest trouble with the errors, though, are man made.

Since only a few channels can be included while at the same time subtle target distortions are needed, the choice of target states must be judicious.

Obviously the strongly coupled open channels (at the given energy) must clearly be included in the expansion. Not so obvious, and often forgotten, is that reliable results can be obtained only when all those channels or states are included that contribute to the polarization of the open channels. If this is not done, the distortions will be improperly represented. Besides the open channels, which must look functionally like the atomic states at large separation, the expansion should use either other target channels or target correlation functions that have proved useful in variation perturbation calculations of frequency dependent polarizability. The use of natural orbitals⁶⁸ or Hylleraas functions is called for.¹⁶

D. Resonant Scattering for the Helium Atom

In this section the resonant scattering of electrons from the helium atom will be briefly discussed. Actually this work is elastic^{33,65} in that the application of our models effects an explanation to nearly all aspects of this problem. For those resonances above the $n = 2$ channel, Burke and co-workers¹⁰ have carried out various close coupling calculations with and without the decoupling of the ground state. Added to this is the yet unpublished work of this group⁶⁹ which uses the stabilization method and arrives at results consistent with Ehrhardt's experiments and Burke's calculations. Briefly, as seen in Figure 1, in the 2^3S channel the first three peaks are $2S$, 2P , 2D with energies (widths) of 19.9 ± 0.05 (0.25), 20.45 ± 0.05 (0.5), and $21.00 \pm .05$ (0.3) eV, respectively. The theoretical results are all in quite reasonable agreement. The S wave peak is of the type explained in Figure 2c, i.e., it is due to the overlap of the C.E. I type 2S $1s(2s)^2$, which occurs at 19.3 eV with a width of 0.01 eV. All theories agree on these two type II resonances, the Type I and the S peak at the 2^3S threshold. In the 2^1S channel of Figure 1 the first peak has been assigned by Burke¹⁰ as a virtual state. It did not show up as a stable root in the work of this group. The stabilization method could not have explained this peak since a virtual state is a potential scattering phenomenon. Similarly the stabilization method could not explain the S peak at 2^3S , except in the negative way of pointing out that both peaks were not really resonances and that other explanations need be sought. No theory has been carried out below the $n = 3$ channel where, as discussed in the previous subsection, a 3^2S $1s(3s)^2$ and 3^2P $1s3s3p$ C.E. I resonance have been seen. Also unexplained as of yet are the three overlapping resonances of type C.E. II above the lowest $n = 3$ threshold. They have peculiar angular dependences in that at 120° in the 2^3P channel no trace of structure exists. Andrick et

al.⁶⁵ suggest that this may be a characteristic of degenerate resonances (i.e., nonsimple poles). Between the $n = 4$ and $n = 5$ channels Heddle and Keesing⁷⁰ have also seen unexplained structure. Almost with intent in the helium calculations, which used stabilization, two high energy stable roots, corresponding to He^- with three electrons excited, appeared at 57.2 and 58.4 eV. At 57.1 ± 0.01 and 58.2 ± 0.1 eV two resonances have been observed experimentally.^{67,71,72}

An unsettled point is the possible resonance of 19.45 eV in the P wave channel and of type $1s2s2p$. The stabilization method has calculated this energy but not the width. It appears quite narrow which may be the reason, if no error exists in the stability calculation, why Ehrhardt has not seen it and Burke's group has not calculated it. Physically one might imagine that a $1s2s2p$ combination is less correlated than the $1s(2s)^2$. This would cause the width of the former to be smaller than the latter, which is already only 0.01 eV. A similar width relationship occurs in C.E. I resonances in H atoms where the $(2s)^2$ resonances is ten times broader than the $2s2p$ resonance. An extremely narrow resonance could be missed in the close coupling method if it fell between two energies at which the close coupling calculations were done. The experiment, on the other hand, could miss it because the slit widths of the beam which are wider than the resonance could cause the resonant signal to be averaged and decreased so as to be unobservable. Interestingly, structure has been seen in total cross-section measurements⁷² at 19.45 eV.

Acknowledgment

The author would like to acknowledge in the development of these ideas the collaboration of J. K. Williams, G. Nazerooff, A. Golebiewski, I. Eliezer, Y. K. Pann, A. Hazi, and C. Rankin, all of whom worked with the author at U.S.C. Especially valuable to this work has been the scientific association of the author with H. Ehrhardt and his collaborators and with T. O'Malley. Very useful discussions have also occurred with P. G. Burke, F. Mandl, A. Herzenberg, R. Bardlsey, T. Sharp, J. Dowell, G. Schulz, W. Reinhardt, W. Miller, M. Saffren, and M. H. L. Pryce. The support for this work has come from a combination of N.S.F., Sloan Foundation, and Research Corporation grants. Drs. A. Yates, B. Schneider, C. Claydon, and Mr. Gy. Csanak are thanked for reading and correcting the manuscript.

References

1. P. G. Burke, *Advan. Phys.*, **14**, 521 (1965).
2. K. Smith, *Rep. Progr. Phys.*, **29**, 373 (1966); see also A. Temkin, ed., *Autoionization*, Mono Book Corp., Baltimore, 1966.
3. J. C. Y. Chen, *Advan. Radiat. Chem.*, Vol. 1 Wiley, New York, 1969.
4. W. H. Miller, *Phys. Rev.*, **152**, 70 (1966).
5. H. S. Taylor, G. V. Nazerooff, and A. Golebiewski, *J. Chem. Phys.*, **45**, 2872 (1966)

6. R. G. Newton, *Scattering Theory of Waves and Particles*, McGraw-Hill, New York, 1966.
7. H. Ehrhardt, L. Langhans, and F. Linder, *Z. Phys.*, **214**, 179 (1968).
8. J. Macek and P. G. Burke, *Proc. Phys. Soc.*, **92**, 351, (1967).
9. T. Wu and T. Ohmura, *Quantum Theory of Scattering*, Prentice-Hall, Englewood Cliffs, N.J., 1962.
10. P. G. Burke, A. Joanna Taylor, J. W. Cooper, and S. Ormande, *Proc. V. Int. Conf. Electronic and Atomic Collisions*, Leningrad, U.S.S.R., 1967, p. 376.
11. R. Newton and L. Fonda, *Ann. Phys.*, (N.Y.), **29**, 501 (1964).
12. M. K. Gailitis and R. Damburg, *Soviet Phys. JETP*, **17**, 1107 (1963); see also A. Temkin and J. F. Walker, *Phys. Rev.*, **140**, A1520 (1965) and M. H. Mittleman, *Phys. Rev.*, **147**, 73 (1966).
13. J. W. McGowan, *Phys. Rev.*, **156**, 164 (1967).
14. P. G. Burke, S. Ormande, W. Whitaker, *Phys. Rev. Lett.*, **17**, 800 (1966). T. F. O'Malley and S. Geltman, *Phys. Rev.*, **137**, A1344 (1965). A. K. Bhatia, A. Temkin, and J. F. Perkins, *Phys. Rev.*, **153**, 177 (1967). L. Lipsky and A. Russek, *Phys. Rev.*, **142**, 59 (1966).
15. J. F. Williams and J. W. McGowan, *Phys. Rev. Lett.*, **21**, 719 (1967).
16. A. J. Taylor and P. G. Burke, *Proc. Phys. Soc.*, **92**, 336 (1967).
17. R. Marriott and M. Rotenberg, *Phys. Rev. Lett.*, **21**, 722 (1967).
18. J. C. Y. Chen and M. Rotenberg, *Proc. V. Int. Conf. Electronic and Atomic Collisions*, Leningrad, U.S.S.R., 1967, p. 271.
19. T. Kato, *Perturbation Theory for Linear Operators*, (Springer, Berlin, 1966).
20. E. C. Titchmarsh, *Eigenfunction Expansions Associated with Second Order Differential Equations*, Oxford Univ. Press, London, 1958.
21. W. Reinhardt, Thesis, Harvard University, 1966, and private communications.
22. H. Feshbach, *Ann. Phys.*, (N.Y.), **19**, 287 (1962).
23. E. Holöien, *Proc. Phys. Soc.*, **71**, 357 (1958). E. Holöien, *Phys. Norweg.*, **1**, 53 (1961). E. Holöien, J. Midtdal, et al., *Proc. Phys. Soc.*, **A68**, 815 (1955).
24. E. C. Kemble, *The Fund. Principles of Quantum Mechanics*, Dover Publications, New York, 1937, p. 403.
25. T. W. Palmer, in Chapter XII of *Recent Developments in Perturbation Theory*, by J. O. Hirschfelder, W. Dyers Brown, and S. T. Epstein, *Advan. Quantum Chem.*, **1**, 265 (1964).
26. M. L. Goldberger, and K. M. Watson, *Collision Theory*, Wiley, New York, 1964.
27. R. C. Riddell, "Spectral Concentration of Self Adjoint Operators," Thesis, University of California, 1965.
28. M. H. Alexander, *Exact Treatment of Stark Effect in Atomic Hydrogen*, *Phys. Rev.*, **178**, 34 (1969).
29. B. W. Shore, *Phys. Rev.*, **171**, 43 (1968).
30. B. Zumino, Research Report CX-23, New York University, 1956 (unpublished).
31. H. S. Taylor and J. K. Williams, *J. Chem. Phys.*, **42**, 4063 (1965).
32. J. N. Bardsley, A. Herzenberg, and F. Mandl, *Proc. Phys. Soc.*, **89**, 305 (1966).
33. H. Ehrhardt, D. L. Langhans, F. Linder, and H. S. Taylor, *Phys. Rev.*, **173**, 222 (1968).
34. G. J. Schulz, *Phys. Rev.*, **125**, 229 (1962); **135**, A988 (1964).
35. J. C. Y. Chen, *J. Chem. Phys.*, **45**, 2710 (1966).
36. A. V. Phelps, *Rev. Mod. Phys.*, **40**, 399 (1968).
37. T. F. O'Malley and H. S. Taylor, *Phys. Rev.*, **176**, 207 (1968).

38. H. Ehrhardt, and P. Linder, *Phys. Rev. Lett.*, **21**, 419 (1968).
39. I. Eliezer, H. S. Taylor, and J. K. Williams, *J. Chem. Phys.*, **47**, 2165 (1967).
40. W. Kolos and L. Wolniewicz, *J. Chem. Phys.*, **43**, 2429 (1965).
41. C. E. Kuyatt, S. R. Mielczarek, and J. A. Simpson, *Phys. Rev. Lett.*, **12**, 293 (1964).
42. C. E. Kuyatt, S. R. Mielczarek, and J. A. Simpson in *Abstracts of Papers of the 14th International Conference of Physics of Electronic and Atomic Collisions*, Science Bookcrafters, New York, 1965, p. 113.
43. C. E. Kuyatt, S. R. Mielczarek, and J. A. Simpson, *J. Chem. Phys.*, **44**, 437 (1966).
44. D. E. Golden and H. W. Bandel, *Phys. Rev. Lett.*, **14**, 1010 (1965).
45. H. G. M. Heidemann, C. E. Kuyatt, and G. E. Chamberlain, *J. Chem. Phys.*, **44**, 440 (1966).
46. H. S. Taylor and J. K. Williams, unpublished calculations.
47. G. J. Schulz, *Phys. Rev.*, **113**, 816 (1959).
48. D. Rapp, T. E. Sharp, and D. D. Briglia, *Phys. Rev. Lett.*, **14**, 533 (1965).
49. T. O'Malley, *Phys. Rev.*, **150**, 14 (1966).
50. J. N. Bardsley, A. Herzenberg, and F. Mandl, *Proc. Phys. Soc.*, **89**, 305, 321 (1966).
51. Yu. N. Demkov, *Phys. Lett.*, **15**, 235 (1965).
52. T. E. Sharp and J. T. Dowell, *J. Chem. Phys.*, **46**, 1530 (1967).
53. T. F. O'Malley, *J. Chem. Phys.*, **47**, 5457 (1967).
54. G. Herzberg, *Spectra of Diatomic Molecules*, Van Nostrand, New York, 1950.
55. H. S. Taylor and F. E. Harris, *J. Chem. Phys.*, **39**, 1012 (1963).
56. G. J. Schulz and R. K. Asundi, *Phys. Rev. Lett.*, **15**, 946 (1965).
57. G. J. Schulz and R. K. Asundi, *Phys. Rev.*, **158**, 25 (1967).
58. J. T. Dowell and T. E. Sharp, *Phys. Rev.*, **167**, 124 (1968).
59. G. Herzberg, *Sci Light*, **16**, 14 (1967).
60. P. J. Chantry, *Phys. Rev.*, **172**, 125 (1968).
61. H. S. Taylor and F. E. Harris, *Mol Phys.*, **6**, 183 (1963); *J. Chem. Phys.*, **38**, 2591 (1963).
62. F. Mandl, *Proc. Phys. Soc.*, **87**, 871 (1966).
63. T. F. O'Malley, *Phys. Rev.*, **162**, 98 (1967).
64. C. E. Chamberlain and H. G. H. Heideman, *Phys. Rev.*, **155**, 46 (1967).
65. D. Andrick, H. Ehrhardt, and M. Fyb, *Z. Phys.*, **214**, 388 (1968).
66. H. S. Taylor to H. Ehrhardt, private communication.
67. J. A. Simpson, H. G. Mendez, and S. R. Mielczarek, *Phys. Rev.*, **150**, 76 (1966).
68. C. F. Bender and E. R. Davidson, *J. Phys. Chem.*, **70**, 2675 (1966).
69. A. Hazi, I. Eliezer, Y. K. Pann, and H. S. Taylor unpublished.
70. D. W. D. Heddle and R. G. W. Keesing, *Proc. Phys. Soc.*, **91**, 510 (1967).
71. U. Fano and J. W. Cooper, *Phys. Rev. Lett.*, **11**, 158 (1963).
72. C. E. Kuyatt, J. A. Simpson, and S. R. Mielczarek, *Phys. Rev.*, **138**, A385 (1965).

ELECTRON RESONANCE OF GASEOUS DIATOMIC MOLECULES

ALAN CARRINGTON

*Department of Chemistry, University of Southampton,
Southampton, England*

DONALD H. LEVY*

*Department of Chemistry and the James Franck Institute,
University of Chicago, Chicago, Illinois*

and

TERRY A. MILLER

Bell Telephone Laboratories, Inc., Murray Hill, New Jersey

CONTENTS

| | |
|--|-----|
| I. Introduction | 150 |
| II. Derivation of the Hamiltonian. | 151 |
| A. Foundations of the Derivation | 151 |
| B. Separation of Nuclear and Electronic Motion | 156 |
| C. Derivation of the Clamped Nuclei Hamiltonian | 167 |
| III. Calculation of the Matrix Elements | 183 |
| A. Important Results from the Theory of Angular Momentum | 183 |
| B. Matrix Elements in Hund's Case (a) | 187 |
| 1. Purely Rotational Hamiltonian | 187 |
| 2. Spin-Rotation Interaction | 190 |
| 3. Fine-Structure Hamiltonian | 193 |
| 4. Nuclear Magnetic and Electric Hyperfine Structure | 195 |
| 5. Interaction with the External Magnetic Field | 200 |
| C. Matrix Elements in Hund's Case (b) | 202 |
| 1. Fine-Structure Hamiltonian. | 202 |
| 2. Rotationally-Dependent Interactions | 203 |
| 3. External Magnetic Field Interactions | 205 |
| 4. Nuclear Magnetic and Electric Hyperfine Structure | 207 |

* Alfred P. Sloan Fellow.

| | |
|--|-----|
| IV. Interpretation of Electron Resonance Spectra. | 209 |
| A. Rotational Energy Levels | 209 |
| B. Λ -Doubling | 223 |
| C. Nuclear Magnetic and Electric Hyperfine Couplings | 227 |
| D. Intensities and Lineshape | 233 |
| E. Stark Effect | 237 |
| V. Experimental | 242 |
| References | 246 |

I. INTRODUCTION

This review is concerned with the rotational levels of diatomic molecules in open-shell electronic states. The presence of electronic angular momentum, due to spin or orbital motion, makes it possible to carry out magnetic resonance experiments using a fixed microwave frequency and a variable magnetic field. Our review deals solely with experiments of this type, which we choose to call "electron resonance," but it is important to realize that we are dealing with a specific approach to a much more general problem.

Detailed information about the rotational levels of open-shell diatomics is scarce because of experimental difficulties. There is, of course, no difficulty in using conventional microwave spectroscopy to study the stable gases $O_2(^3\Sigma)^1$ and $NO(^2\Pi)^2$, but the detection of short-lived species poses practical problems which have only been overcome in the cases of $SO(^3\Sigma)^3$ and $OH(^2\Pi)^4$. Molecular beam techniques have been used successfully in the study of H_2^5 and CO^6 in their $^3\Pi$ excited states, but the detection of free radicals in their ground states has not yet been achieved. Electron resonance techniques offer advantages in instrumentation, which we shall discuss later, and a considerable number of diatomic free radicals have now been studied. There remains a clear need for conventional microwave studies, however, and the existence of electron resonance results may simplify the problems in microwave spectroscopy.

We should make it clear that in discussing rotational levels our interest extends far beyond the determination of the rotational constant B_0 . Rotational band structure in the visible and ultraviolet spectra of free radicals has, of course, been analyzed in many cases; unfortunately, the detailed hyperfine structure arising from nuclear effects is usually beyond the resolution of optical spectrographs, and electric dipole moment determinations are possible in only a few cases and with inherently low accuracy. Measurement of nuclear magnetic and electric hyperfine splittings is important in determining electron distributions, as is the dipole moment, and the current accuracy of calculated molecular wavefunctions should be matched by correspondingly accurate and detailed experimental information.

Much of this review is devoted to the theory of the rotational levels of diatomic molecules. In Section II we lay the theoretical basis for the quantum-mechanical treatment of diatomic molecules. This treatment leads to an effective Hamiltonian which is later used to describe the electron resonance spectra of these molecules. Section III describes the calculation of the matrix elements of the effective Hamiltonian in different representations. Sections II and III together are intended to provide a rigorous and quantitative basis for the calculation of electron resonance spectra and for the interpretation of data obtained from these spectra.

In Section IV we consider the different terms of the effective Hamiltonian and discuss their qualitative effect on the spectrum. The discussion in Section IV is intended to be descriptive rather than quantitative, and therefore it is largely independent of the fine details derived in Sections II and III.

Finally, Section V describes the experimental methods used in obtaining electron resonance spectra.

II. DERIVATION OF THE HAMILTONIAN

A. Foundations of the Derivation

In this section we propose to derive the Hamiltonian appropriate to a rotating, vibrating diatomic molecule in the presence of external electromagnetic fields. As a single Hamiltonian incorporating all interactions must be rather complicated, it is desirable, as far as possible to separate the different effects and treat them individually. We shall inevitably find that there exist terms in the Hamiltonian which interrelate the various effects. However, these terms may always be treated by perturbation theory, and if the original separation is appropriately chosen, the perturbation treatment may be expected to converge rapidly.

As in the original work of Born and Oppenheimer,⁷ our separation of different terms in the Hamiltonian is based on the difference between electronic and nuclear masses. Since the forces acting on the two kinds of particle are of the same order, the electronic motion must be very rapid compared with the nuclear motion. This suggests that, to a first approximation, the electronic energy levels will be the same as if the nuclei were stationary. Likewise, to obtain the nuclear energy levels, we may examine their motion in a previously determined electronic potential.

The mathematical formulation of this physical model proceeds along the following lines.⁸ Consider an approximate Hamiltonian, \mathcal{H}_a , in terms of Schrodinger representatives including both the electronic and nuclear motions,

$$\begin{aligned}\mathcal{H}_a &= \sum_{\alpha} \frac{\mathbf{p}_{\alpha}^2}{2M_{\alpha}} + \sum_i \frac{\mathbf{p}_i^2}{2m} + V(X_i, X_{\alpha}) \\ &= -\sum_{\alpha} \frac{\hbar^2}{2M_{\alpha}} \nabla_{\alpha}^2 - \sum_i \frac{\hbar^2}{2m} \nabla_i^2 + V(X_i, X_{\alpha})\end{aligned}\quad (2.1)$$

The indexes α and i run over the nuclei and electrons of masses M_{α} and m , respectively. The potential energy $V(X_i, X_{\alpha})$ depends only on the positions (X_{α}) of the nuclei and the positions of the electrons (X_i). By restricting V in this manner, we omit all magnetic effects, specifically excluding the electronic and nuclear spin-dependent terms. These magnetic interactions are, except for very heavy atoms, much smaller than the electrostatic interactions which characterize V , and for the present purpose may be neglected. Interactions with external electromagnetic fields are also excluded from V , since they too are small compared with the intra-electrostatic interactions. \mathcal{H}_a also omits all other relativistic effects.

Consider now a molecule with infinitely massive nuclei, which may be regarded as stationary. The essentially electronic Hamiltonian, \mathcal{H}^e , is then

$$\mathcal{H}^e = -\frac{\hbar^2}{2m} \sum_i \nabla_i^2 + V(X_i, X_{\alpha}) \quad (2.2)$$

V is still a function of X_{α} because of the nuclear electrostatic repulsion. Also it should be noted that the observables corresponding to the electronic kinetic energy in (2.1) and (2.2) need not be identical. Let it now be assumed that \mathcal{H}^e satisfies an eigenvalue equation,

$$\mathcal{H}^e \psi_{\eta}^e(X_i, R) = E_{\eta}^e(R) \psi_{\eta}^e(X_i, R) \quad (2.3)$$

where R , the internuclear distance, is the only nuclear coordinate involved in \mathcal{H}^e .

It follows that the approximate Hamiltonian, \mathcal{H}_a , must also yield an eigenvalue equation of the form

$$\mathcal{H}_a \Psi = E \Psi \quad (2.4)$$

Ψ can be expanded in a complete set of functions.

$$\Psi = \sum_{\eta} \psi_{\eta}^N(X_{\alpha}) \psi_{\eta}^e(X_i, R) \quad (2.5)$$

where $\psi_{\eta}^N(X_{\alpha})$ is an as yet arbitrary function of X_{α} . Substituting Eq. (2.5) into Eq. (2.4), multiplying by $\psi_{\eta}^{e*}(X_i, R)$, and integrating over X_i gives,

$$\left[-\sum_{\alpha} \frac{\hbar^2}{2M_{\alpha}} \nabla_{\alpha}^2 + E_{\eta}^e(R) - E \right] \psi_{\eta}^N(X_{\alpha}) + \sum_{\eta'} C_{\eta\eta'} \psi_{\eta'}^N(X_{\alpha}) = 0 \quad (2.6)$$

where

$$C_{\eta\eta'} = -\sum_{\alpha} \left[\frac{\hbar^2}{M_{\alpha}} (A_{\eta\eta'}^{\alpha} \nabla_{\alpha} + B_{\eta\eta'}^{\alpha}) \right] \quad (2.7)$$

with

$$A_{\eta\eta'}^{\alpha} = \int \psi_{\eta}^{e*}(X_i, R) \nabla_{\alpha} \psi_{\eta'}^e(X_i, R) dX_i \quad (2.8)$$

$$B_{\eta\eta'}^{\alpha} = \frac{1}{2} \int \psi_{\eta}^{e*}(X_i, R) \nabla_{\alpha}^2 \psi_{\eta'}^e(X_i, R) dX_i \quad (2.9)$$

The $\eta = \eta'$ term of $A_{\eta\eta'}^{\alpha}$ is given by

$$A_{\eta\eta}^{\alpha} = \frac{1}{2} \nabla_{\alpha} \int \psi_{\eta}^{e*}(X_i, R) \psi_{\eta}^e(X_i, R) dX_i = 0 \quad (2.10)$$

because of the assumed unit normalization of $\psi_{\eta}^e(X_i, R)$ and because $\psi_{\eta}^e(X_i, R)$ is real except for a possible multiplicative factor commuting with ∇_{α} . With the aid of Eq. (2.10), Eq. (2.6) may be rewritten,

$$\sum_{\alpha} \left[-\frac{\hbar^2}{2M_{\alpha}} \nabla_{\alpha}^2 + U_{\eta}(R) - E \right] \psi_{\eta}^N(X_{\alpha}) = -\sum_{\eta' \neq \eta} C_{\eta\eta'} \psi_{\eta'}^N(X_{\alpha}) \quad (2.11)$$

where the potential function $U_{\eta}(R)$ is defined by

$$U_{\eta}(R) = E_{\eta}^e(R) - \sum_{\alpha} \frac{\hbar^2}{M_{\alpha}} B_{\eta\eta}^{\alpha} \quad (2.12)$$

If the terms $C_{\eta\eta'}$, $\eta' \neq \eta$ are neglected, a separate eigenvalue equation for the nuclear motion in terms of the function $\psi_{\eta}^N(X_{\alpha})$ is obtained.

$$\sum_{\alpha} \left[-\frac{\hbar^2}{2M_{\alpha}} \nabla_{\alpha}^2 + U_{\eta}(R) \right] \psi_{\eta}^N(X_{\alpha}) = E \psi_{\eta}^N(X_{\alpha}) \quad (2.13)$$

If the radial momentum \mathbf{p}_{zR} (defined in Eq. 2.22) is now introduced and $\psi_{\eta}^N(X_{\alpha})$ expressed as a product $\psi_{\eta}^N(R) \psi_{\eta}^N(X'_{\alpha})$, Eq. (2.13) may be rewritten in terms of two separate eigenvalue equations,

$$\sum_{\alpha} \left[\frac{1}{2M_{\alpha}} \mathbf{p}_{zR}^2 + U_{\eta}(R) + W_{\eta}(R) \right] \psi_{\eta}^N(R) = E \psi_{\eta}^N(R) \quad (2.14)$$

and

$$\sum_{\alpha} \left[\frac{1}{2M_{\alpha}} \mathbf{p}_{zX'}^2 \right] \psi_{\eta}^N(X'_{\alpha}) = W_{\eta}(R) \psi_{\eta}^N(X'_{\alpha}) \quad (2.15)$$

Equation (2.14) governs the vibrational motion of the nuclei and Eq. (2.15) their rotational motion.

In the next subsection, we shall find that even a Hamiltonian considerably more detailed than \mathcal{H}_0 leads to eigenvalue equations of the form (2.3), (2.4), and (2.5) if certain off-diagonal terms of the order of $C_{\eta\eta'}$ are

neglected. In order to determine whether a basis set consisting of the products $\psi_\eta^e(X_i, R)\psi_\eta^N(R)\psi_\eta^N(X'_\alpha)$ forms a reasonable approximation to the true eigenfunctions of the Hamiltonian, it is necessary only to estimate the size of the terms $C_{\eta\eta'}$.

In view of this we compare the size of $C_{\eta\eta'}$ with the smallest terms included in \mathcal{H}_a , $-(\hbar^2/2M_\alpha)\nabla_\alpha^2$. Since in our approximation, $C_{\eta\eta'}$ is independent of the variable X'_α , it must commute with the operator of Eq. (2.15); therefore the condition for neglect of $C_{\eta\eta'}$ reduces to

$$\frac{\int \psi_\eta^{N*}(R)\psi_\eta^{e*}(X_i, R)[\nabla_\alpha\psi_\eta^e(X_i, R)]\nabla_\alpha\psi_\eta^N(R) dX_i dR}{\int \psi_\eta^{N*}(R)\nabla_\alpha^2\psi_\eta^N(R) dR},$$

$$\frac{\int \psi_\eta^{e*}(X_i, R)\psi_\eta^{N*}(R)\psi_\eta^N(R)\nabla_\alpha^2\psi_\eta^e(X_i, R) dX_i dR}{\int \psi_\eta^{N*}(R)\nabla_\alpha^2\psi_\eta^N(R) dR} \ll 1 \quad (2.16)$$

Because of the unit normalization of ψ_η^e and ψ_η^N , inequality (2.16) will be satisfied if the rate of change of ψ_η^e with respect to internuclear distance is much less than that of ψ_η^N .

For small displacements the nuclei and electrons are subject to essentially the same restoring force. Adopting a harmonic oscillator approximation to describe the restoring force, a wavefunction $F(u)$ is obtained, where⁹

$$u = (Mk)^{1/4}\hbar^{-1/2}X \quad (2.17)$$

with M = the mass of the particle, k = the force constant, and X = the displacement coordinate. Thus the derivative of u with respect to X is of the order $M^{1/4}$, or the relative rate of change of ψ_η^e and ψ_η^N is of the order of $(m/M_\alpha)^{1/4}$. As $(m/M_\alpha)^{1/4}$ is less than 0.1 for most molecules, basis functions consisting of the products $\psi_\eta^e(X_i, R)\psi_\eta^N(R)\psi_\eta^N(X'_\alpha)$ provide a good starting point for a perturbation calculation.

Up to this point, we have considered the effects of a Hamiltonian devoid of magnetic interactions. Since it is just the effects of electronic and nuclear spin and orbital motion which are probed most deeply by electron resonance experiments, it is of the utmost importance that these terms be treated accurately in the final Hamiltonian. In the following subsections the correct Hamiltonian, including all important magnetic interactions, will be constructed. As an introduction to this derivation, it is perhaps useful to review qualitatively the effects of the various magnetic interactions in the molecule. The best means of doing this is probably in terms of Hund's coupling cases. In the description of Hund's coupling cases we encounter the quantum numbers which will be used freely throughout the remainder of this review. Moreover, Hund's coupling cases provide a physical picture (the vector model) of the different angular momenta coupling schemes which we shall use extensively.

In Hund's case (a) both the electron spin (S) and orbital (L) angular momentum are taken to be quantized along the internuclear axis, with projections Σ and Λ , respectively; the sum of these projections is denoted by Ω . The angular momentum of nuclear rotation (N) is then combined with the electronic angular momentum to form the angular momentum J . J constitutes the total angular momentum of the molecule exclusive of nuclear spin I . The eigenfunctions of J and I may then be combined in a direct product set, or a linear combination of such sets, to form either a decoupled or coupled representation. In the decoupled representation the expectation values of the space-fixed z' projections are represented by M_J and M_I . However, if I and J form a coupled representation, the resultant angular momentum F has eigenvalues for its space-fixed projections denoted by M_F .

Hund's case (b) differs from case (a) in that the spin S is not quantized along the internuclear axis (weak spin-coupling effect). The electronic orbital angular momentum combines with the nuclear rotational momentum to form an angular momentum denoted K . A linear combination of the direct products of the eigenfunctions of K and S is taken to diagonalize the resultant angular momentum, again denoted by J . I and J can be combined in case (b) in the same manner as outlined for case (a). Vector diagrams for cases (a) and (b) are shown in Figure 1.

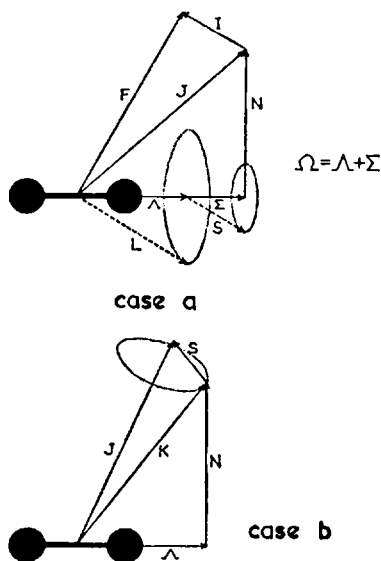


Fig. 1. Vector coupling diagrams for Hund's cases (a) and (b). In case (b), I may be added to J to form F as is shown for case (a).

Hund also described coupling cases (c), (d), and (e) which we shall find of comparatively little interest. Hund's case (c) is similar to case (a) except that the interaction between \mathbf{L} and \mathbf{S} is assumed to be very strong; thus \mathbf{L} and \mathbf{S} cannot be separately quantized, but their total projection (still denoted by Ω) along the internuclear axis is conserved. In case (d), even \mathbf{L} is not assumed to be quantized along the internuclear axis; it is added vectorially to the rotational angular momentum of the nuclei to form a resultant \mathbf{K} , which can then be combined with \mathbf{S} as in case (b). Case (e) describes a situation in which although \mathbf{L} and \mathbf{S} are strongly coupled, as in case (c), neither is quantized along the internuclear axis. The resultant of \mathbf{L} and \mathbf{S} is therefore combined with the nuclear rotational momentum to form a total resultant (exclusive of nuclear spin) which is again denoted by \mathbf{J} .

B. Separation of Nuclear and Electronic Motions

Following the procedure outlined in Section II.A, we now attempt to separate the exact Hamiltonian into a part characterizing a stationary molecule and parts characterizing the vibration and rotation of the nuclei. Let \mathcal{H}_m be the correct Hamiltonian for a molecule, neglecting the nuclear kinetic energy. In the absence of external fields,

$$\mathcal{H}_m = \mathcal{H}_m(x'_i, y'_i, z'_i, \alpha, \beta, z_\alpha, S_i, M_s, I_\alpha, M_I) \quad (2.18)$$

This expression should be interpreted to mean that \mathcal{H}_m is an operator function of the i electronic spatial and spin variables ($x'_i, y'_i, z'_i, S_i, M_s$) expressed in a cartesian coordinate system (x', y', z') with origin at the center of mass. \mathcal{H}_m is also a function of the spatial and spin variables ($\alpha, \beta, z_\alpha, I_\alpha, M_I$) of the α nuclei in the same coordinate system. For the nuclear spatial coordinates, it is rather easier for subsequent work to avoid using the cartesian form. Thus a second coordinate system (x, y, z), with the origin coinciding with that of the space-fixed system, and with the z axis along the internuclear axis, is defined. The position of a nucleus in this system is given by z_α . The location of the nuclei in the original space-fixed coordinate system is then specified by giving the orientation of the x, y, z system with respect to the space-fixed system.

This orientation may be specified by three Euler angles (α, β, γ), defined such that rotation of the space-fixed system through the angles (α, β, γ) brings it into coincidence with the molecule-fixed system. The rotation itself is to be carried out in three steps, (i), rotation through α about the z' axis; (ii), rotation through β about the new y' axis; (iii), rotation through γ about the new z axis. Rotations are assumed positive by the right-hand

screw rule. For two particles, the final rotation is redundant and we therefore choose it to be zero. (Rotation of the electrons through γ , however, is not meaningless, as will be shown.) Our conventions for the Euler angles correspond to those of Rose,¹⁰ Messiah,¹¹ and Brink and Satchler.¹²

In order to obtain the total Hamiltonian, a term describing the nuclear motion must be added to \mathcal{H}_m . Replacing the mechanical momentum operator in Eq. (2.1) by the canonical momentum to take account of a nonvanishing magnetic vector potential, we obtain

$$\mathcal{H}^N = \sum_{\alpha} \frac{1}{2M_{\alpha}} [\mathbf{p}_{\alpha} - (Z_{\alpha}e/c)\mathbf{A}_{\alpha}]^2 \quad (2.19)$$

\mathbf{A}_{α} , the magnetic vector potential at the α th nucleus, is to be interpreted as the total potential including that created by other particles as well as external fields. The exact nature of \mathbf{A}_{α} will be discussed subsequently; for the present it suffices to specify that \mathbf{A}_{α} is in a Coulomb gauge.

\mathcal{H}^N can now be simplified somewhat. If the motion of the center of mass is neglected, as is usually the case,* the orthogonal vibrational and rotational nuclear motions can be separated,

$$\mathbf{p}_{\alpha} = \mathbf{p}_{\alpha R} + \mathbf{p}_{\alpha \mathcal{R}} \quad (2.20)$$

where the rotational ($\mathbf{p}_{\alpha \mathcal{R}}$) and the Hermitian vibrational ($\mathbf{p}_{\alpha R}$) momenta are defined by

$$\mathbf{p}_{\alpha \mathcal{R}} = \frac{M_{\alpha} \hbar}{\mathcal{J}} (\mathcal{R} \times \mathbf{r}_{\alpha}) \quad (2.21)$$

$$\mathbf{p}_{\alpha R} = \frac{1}{2} \left[\left(\frac{\mathbf{r}_{\alpha}}{r_{\alpha}} \right) \cdot \mathbf{p}_{\alpha} + \mathbf{p}_{\alpha} \cdot \frac{\mathbf{r}_{\alpha}}{r_{\alpha}} \right] \boldsymbol{\mu}_R \quad (2.22)$$

In these equations,

\mathbf{r}_{α} = radius vector from the center of mass to the α th nucleus

\mathcal{R} = rotational angular momentum of the nuclei

$\mathcal{J} = (M_{\alpha} M_{\alpha}' / M_{\alpha} + M_{\alpha}') R^2$ = nuclear moment of inertia

$\boldsymbol{\mu}_R$ = unit vector along the internuclear axis ($[\boldsymbol{\mu}_R, \mathbf{p}] \equiv 0$)

Equation (2.19) may now be rewritten,

$$\begin{aligned} \mathcal{H}^N = \sum_{\alpha} \left\{ \frac{1}{2M_{\alpha}} \left[\left(\frac{M_{\alpha} \hbar}{\mathcal{J}} \right) (\mathcal{R} \times \mathbf{r}_{\alpha}) - \left(\frac{Z_{\alpha} e}{c} \right) \mathbf{A}_{\alpha} \right]^2 \right. \\ \left. + \frac{1}{2M_{\alpha}} \left[p_{\alpha R} \boldsymbol{\mu}_R - \left(\frac{Z_{\alpha} e}{c} \right) \mathbf{A}_{\alpha} \right]^2 - \frac{Z_{\alpha}^2 e^2}{2M_{\alpha} c^2} A_{\alpha}^2 \right\} \quad (2.23) \end{aligned}$$

* The motion of the center of mass cannot strictly be neglected and this point is treated in more detail in the derivation of \mathcal{H}_m .

The first and second terms of Eq. (2.23) are taken to be the rotational and vibrational parts, respectively, of the nuclear Hamiltonian. \mathcal{H}^N may be further simplified by partially performing the sum over α and introducing the internuclear distance,

$$\begin{aligned}\mathcal{H}^N = \mathcal{H}_{\mathcal{R}}^N + \mathcal{H}_v^N = B\mathcal{R}^2 - \sum_{\alpha} \left(Z_{\alpha} \frac{\hbar e}{\mathcal{J}c} \right) [(\mathbf{r}_{\alpha} \times \mathbf{A}_{\alpha}) \cdot \mathcal{R}] \\ + (e^2 Z_{\alpha}^2 / 2M_{\alpha} c^2) \mathbf{A}_{\alpha}^2 - B \left[\left(\frac{\partial}{\partial R} \right) \left(R^2 \frac{\partial}{\partial R} \right) \right] - \sum_{\alpha} \left[\left(Z_{\alpha} \frac{e}{c} \right) (\mathbf{A}_{\alpha} \cdot \boldsymbol{\mu}_R) p_{\alpha R} \right]\end{aligned}\quad (2.24)$$

where the rotational constant B is defined by

$$B \equiv \frac{\hbar^2}{2\mathcal{J}} = \frac{\hbar^2(M_{\alpha} + M_{\alpha'})}{2M_{\alpha}M_{\alpha'}R^2} \quad (2.25)$$

\mathcal{H}^N cannot be further simplified without an explicit form for \mathbf{A}_{α} . As the form of \mathbf{A}_{α} will be more obvious after the electronic Hamiltonian has been derived, we postpone the further simplification of \mathcal{H}^N and return to the problem of separating the Hamiltonian into a clamped nuclei part and a part describing the nuclear motion.

It might at first appear that this problem has already been solved, as the total Hamiltonian is given by

$$\mathcal{H}_T = \mathcal{H}_m + \mathcal{H}_{\mathcal{R}}^N + \mathcal{H}_v^N \quad (2.26)$$

However, the molecular Hamiltonian \mathcal{H}_m is still a function of the nuclear position coordinates (α, β) and so cannot commute, even approximately, with \mathcal{H}^N which involves partial differential operators with respect to these coordinates. The task is then to separate out the effects of nuclear motion from \mathcal{H}_m . After this separation, the remaining part of \mathcal{H}_m should be the electronic Hamiltonian \mathcal{H}^e of Section II.A, plus certain smaller terms which were neglected earlier.

The obvious method of eliminating the dependence of \mathcal{H}_m upon the nuclear motion is to transform the electronic variables from the space-fixed coordinate system to the (x, y, z) system gyrating with the nuclei. The change of coordinate system is equivalent to a canonical transformation of the Hamiltonian; thus, we seek a transformed Hamiltonian \mathcal{H}_T' where

$$\mathcal{H}_T' = S\mathcal{H}_T S^{-1} \quad (2.27)$$

S being the required transformation. It is clear that such a transformation on the electronic spatial variables will eliminate the α, β dependence of

terms in \mathcal{H}_m involving those variables. However, the effect of the transformation on the nuclear kinetic energy operator presents a more subtle problem. Also the effect on the electronic and nuclear spin dependent interactions must be considered.

Since we have assumed that the original basis set for \mathcal{H}_m consists of products of electronic and nuclear space and spin functions, a total transformation of \mathcal{H}_m to the gyrating system may be treated as a product of transformations for electronic spatial variables, electronic spin variables and, if appropriate, nuclear spin variables. Any of these transformations can clearly be applied independently. Thus, it is possible to distinguish several possible combinations of transformations which are, in fact, closely related to Hund's coupling cases.¹³ Case (a) excludes the nuclear spin transformation but includes transformations for both the electronic spatial and spin variables. Case (b) involves transformation of only the electronic spatial variables. Case (c) corresponds to the same set of transformations as case (a), but is distinguished from it by a different choice of electronic basis functions. In cases (d) and (e) no transformation at all is performed, the cases again differing in their choice of electronic basis functions. As was noted in Section II.A, only cases (a) and (b) are of direct interest to us; hence only the set of transformations characterizing these two cases will be considered in greater detail.

The transformation of a given set of variables to the gyrating coordinate system means that the transformed Hamiltonian \mathcal{H}'_m will be of the same form as \mathcal{H}_m with molecule-fixed variables in place of space-fixed ones. The form of \mathcal{H}_m is then summarized by

$$\mathcal{H}'_m = \mathcal{H}_m(x'_i \rightarrow x_i, y'_i \rightarrow y_i, z'_i \rightarrow z_i, S_i, M_s \rightarrow \Sigma, I_z, M_I) \quad (2.28)$$

(case a)

$$\mathcal{H}'_m = \mathcal{H}_m(x'_i \rightarrow x_i, y'_i \rightarrow y_i, z'_i \rightarrow z_i, S_i, M_s, I_\alpha, M_I) \quad (2.29)$$

(case b)

In order to work out the form of the transformed nuclear Hamiltonian \mathcal{H}^N , we note that for a rotation of axes through α and β , the coordinates, treated as functions in the two systems, are related by

$$\begin{pmatrix} x \\ y \\ z \end{pmatrix} = \mathcal{U} \begin{pmatrix} x' \\ y' \\ z' \end{pmatrix} \quad (2.30)$$

where

$$\mathcal{U} = \begin{pmatrix} \cos \alpha \cos \beta & \sin \alpha \cos \beta & -\sin \beta \\ -\sin \alpha & \cos \alpha & 0 \\ \cos \alpha \sin \beta & \sin \alpha \sin \beta & \cos \beta \end{pmatrix} \quad (2.31)$$

To determine the effect of the transformation on the operators in \mathcal{R} , it should be noted that they will now operate on a basis function of x_i, y_i, z_i , rather than one of x'_i, y'_i, z'_i . Thus by the rule for the differentiation of an implicit function,

$$\left(\frac{\partial}{\partial \alpha}\right)_s = \left(\frac{\partial}{\partial \alpha}\right)_m + \sum_i \left[\left(\frac{\partial x_i}{\partial \alpha}\right)_s \frac{\partial}{\partial x_i} + \left(\frac{\partial y_i}{\partial \alpha}\right)_s \frac{\partial}{\partial y_i} + \left(\frac{\partial z_i}{\partial \alpha}\right)_s \frac{\partial}{\partial z_i} \right] \quad (2.32)$$

and

$$\left(\frac{\partial}{\partial \beta}\right)_s = \left(\frac{\partial}{\partial \beta}\right)_m + \sum_i \left[\left(\frac{\partial x_i}{\partial \beta}\right)_s \frac{\partial}{\partial x_i} + \left(\frac{\partial y_i}{\partial \beta}\right)_s \frac{\partial}{\partial y_i} + \left(\frac{\partial z_i}{\partial \beta}\right)_s \frac{\partial}{\partial z_i} \right] \quad (2.33)$$

where s and m denote that space- or molecule- fixed variables are to be held constant in the differentiation. Insertion of Eqs. (2.30) and (2.31) into (2.32) and (2.33) yields,

$$\begin{aligned} \left(\frac{\partial}{\partial \beta}\right)_s &= \left(\frac{\partial}{\partial \beta}\right)_m + \sum_i \left\{ (-x'_i \cos \alpha \sin \beta - y'_i \sin \alpha \sin \beta - z'_i \cos \beta) \frac{\partial}{\partial x_i} \right. \\ &\quad \left. + (x'_i \cos \alpha \cos \beta + y'_i \sin \alpha \cos \beta - z'_i \sin \beta) \frac{\partial}{\partial z_i} \right\} \\ &= \left(\frac{\partial}{\partial \beta}\right)_m + \sum_i \left[-z_i \frac{\partial}{\partial x_i} + x_i \frac{\partial}{\partial z_i} \right] \\ &= \left(\frac{\partial}{\partial \beta}\right)_m - iL_y \end{aligned} \quad (2.34)$$

and

$$\begin{aligned} \left(\frac{\partial}{\partial \alpha}\right)_s &= \left(\frac{\partial}{\partial \alpha}\right)_m + \sum_i \left\{ (-x'_i \cos \beta \sin \alpha + y'_i \cos \alpha \cos \beta) \frac{\partial}{\partial x_i} \right. \\ &\quad \left. + (-x'_i \cos \alpha - y'_i \sin \alpha) \frac{\partial}{\partial y_i} \right. \\ &\quad \left. + (-x'_i \sin \alpha \sin \beta + y'_i \cos \alpha \sin \beta) \frac{\partial}{\partial z_i} \right\} \\ &= \left(\frac{\partial}{\partial \alpha}\right)_m + i(\sin \beta L_x - \cos \beta L_z) \end{aligned} \quad (2.35)$$

where \mathbf{L} denotes the total electronic orbital angular momentum about the center of mass and $i = \sqrt{j} - 1$.

For case (a) the effects of transforming the electronic spin into the molecule-fixed system are also required. The components of the spinors $\psi_{\pm 1/2}(\Sigma^i)$ for the i th electron in the molecule-fixed system are related to those $\psi_{\pm 1/2}(M_s^i)$ in the space-fixed system via a rotational matrix $D_{m, \pm 1/2}^{1/2}(\alpha, \beta, 0)$,

$$\psi_{\pm 1/2}(\Sigma^i) = \sum_m \psi_m(M_s^i) D_{m, \pm 1/2}^{1/2}(\alpha, \beta, 0) \quad (2.36)$$

where

$$D^{1/2}(\alpha, \beta, 0) = \begin{pmatrix} e^{-i\alpha/2} \cos(\beta/2) & -e^{-i\alpha/2} \sin(\beta/2) \\ e^{i\alpha/2} \sin(\beta/2) & e^{i\alpha/2} \cos(\beta/2) \end{pmatrix} \quad (2.37)$$

Expressing the total spinor $\Psi(\Sigma)$ in terms of the individual spins,

$$\begin{aligned} \frac{\partial}{\partial \beta} \Psi(\Sigma) &= \frac{\partial}{\partial \beta} \prod_i \psi_{\pm 1/2}(\Sigma^i) \\ &= \frac{\partial}{\partial \beta} \prod_i \sum_m \psi_m(M_s^i) D_{m, \pm 1/2}^{1/2}(\alpha, \beta, 0)_i \\ &= \sum_m \sum_j \prod_{i \neq j} \psi_m(M_s^i) D_{m, \pm 1/2}^{1/2}(\alpha, \beta, 0)_i \left[\frac{\partial}{\partial \beta} D_{m, \pm 1/2}^{1/2}(\alpha, \beta, 0)_j \psi_m(M_s^j) \right] \\ &= \sum_m \sum_j \frac{1}{2} \prod_{i \neq j} \psi_m(M_s^i) D_{m, \pm 1/2}^{1/2}(\alpha, \beta, 0)_i \\ &\quad \times [(-1)^{(1/2 \mp 1/2)} D_{m, \mp 1/2}^{1/2}(\alpha, \beta, 0)_j \psi_m(M_s^j)] \\ &= \sum_j \prod_{i \neq j} \frac{1}{2} [(-1)^{(1/2 \mp 1/2)} \psi_{\mp 1/2}(\Sigma^j)] \psi_{\pm 1/2}(\Sigma^i) \\ &= \sum_j \prod_{i \neq j} \psi_{\pm 1/2}(\Sigma^i) [-i S_y^j \psi_{\pm 1/2}(\Sigma^j)] \\ &= \sum_i -i S_y^i \prod_i \psi_{\pm 1/2}(\Sigma^i) \\ &= -i S_y \Psi(\Sigma) \end{aligned} \quad (2.38)$$

Similarly, we have

$$\begin{aligned}
 \frac{\partial}{\partial \alpha} \Psi(\Sigma) &= \frac{\partial}{\partial \alpha} \prod_i \psi_{\pm 1/2}(\Sigma^i) \\
 &= \frac{\partial}{\partial \alpha} \prod_i \sum_m \psi_m(M_s^i) D_{m, \pm 1/2}^{1/2}(\alpha, \beta, 0)_i \\
 &= \sum_m \sum_j \prod_{i \neq j} \psi_m(M_s^i) D_{m, \pm 1/2}^{1/2}(\alpha, \beta, 0)_i \left[\frac{\partial}{\partial \alpha} D_{m, \mp 1/2}^{1/2}(\alpha, \beta, 0)_j \psi(M_s^j) \right] \\
 &= \sum_m \sum_j \prod_{i \neq j} \psi_m(M_s^i) D_{m, \pm 1/2}^{1/2}(\alpha, \beta, 0)_i \left\{ \frac{i}{2} [\sin \beta D_{m, \mp 1/2}^{1/2}(\alpha, \beta, 0)_j \right. \\
 &\quad \left. \mp \cos \beta D_{m, \pm 1/2}^{1/2}(\alpha, \beta, 0)_j] \psi_m(M_s^j) \right\} \\
 &= \sum_j \prod_{i \neq j} \psi_{\pm 1/2}(\Sigma^i) \left\{ \frac{i}{2} [\sin \beta \psi_{\mp 1/2}(\Sigma^j) \mp \cos \beta \psi_{\pm 1/2}(\Sigma^j)] \right\} \\
 &= \sum_j \prod_{i \neq j} \psi_{\pm 1/2}(\Sigma^i) i [(\sin \beta S_x^j - \cos \beta S_z^j) \psi_{\pm 1/2}(\Sigma^j)] \\
 &= \sum_i i (\sin \beta S_x^i - \cos \beta S_z^i) \prod_i \psi_{\pm 1/2}(\Sigma^i) \\
 &= i (\sin \beta S_x - \cos \beta S_z) \Psi(\Sigma)
 \end{aligned} \tag{2.39}$$

Thus we have obtained the quite general result* that the effect of the transformation on the partial differential operators in \mathcal{R} may be expressed as

$$\left(\frac{\partial}{\partial \beta} \right)_s = \left(\frac{\partial}{\partial \beta} \right)_m - iP_y \tag{2.40}$$

$$\left(\frac{\partial}{\partial \alpha} \right)_s = \left(\frac{\partial}{\partial \alpha} \right)_m + i (\sin \beta P_x - \cos \beta P_z) \tag{2.41}$$

where the partial electronic angular momentum is defined by

$$\mathbf{P} = \mathbf{L} + \mathbf{S} \quad (\text{case } a) \tag{2.42}$$

$$\mathbf{P} = \mathbf{L} \quad (\text{case } b) \tag{2.43}$$

To determine the final form of $\mathcal{H}^{N'}$ we note that \mathbf{r}_α , R and $\partial/\partial R$ are unaffected by the transformation; thus it is only necessary to consider the transformed rotational angular momentum \mathcal{R} . The general expression¹² for \mathcal{R} in terms of the Euler angles and space-fixed axes is,

* The proof also holds for an antisymmetrized wavefunction as \mathcal{R} and the antisymmetrizing operator commute.

$$\begin{aligned}\mathcal{R} = & i\{[\cot \beta \cos \alpha(\partial/\partial \alpha)_s + \sin \alpha(\partial/\partial \beta)_s - (\cos \alpha/\sin \beta)(\partial/\partial \gamma)_s]\mu'_x \\ & + [\cot \beta \sin \alpha(\partial/\partial \alpha)_s - \cos \alpha(\partial/\partial \beta)_s - (\sin \alpha/\sin \beta)(\partial/\partial \gamma)_s]\mu'_y \\ & - (\partial/\partial \alpha)_s \mu'_z\}\end{aligned}\quad (2.44)$$

Since γ was chosen equal to zero, the last terms of the x' and y' components of \mathcal{R} vanish. Using Eqs. (2.40) and (2.41), the transformed angular momentum \mathcal{R}' is given by

$$\begin{aligned}\mathcal{R}' = & i\{[\cot \beta \cos \alpha(\partial/\partial \alpha)_m + \sin \alpha(\partial/\partial \beta)_m + i \cos \beta \cos \alpha P_x \\ & - i \sin \alpha P_y - i(\cos^2 \beta \cos \alpha/\sin \beta)P_z]\mu'_x \\ & + [\cot \beta \sin \alpha(\partial/\partial \alpha)_m - \cos \alpha(\partial/\partial \beta)_m + i \cos \beta \sin \alpha P_x \\ & + i \cos \alpha P_y - i(\cos^2 \beta \sin \alpha/\sin \beta)P_z]\mu'_y \\ & + [-(\partial/\partial \alpha)_m - i \sin \beta P_x + i \cos \beta P_z]\mu'_z\}\end{aligned}\quad (2.45)$$

In order to simplify this expression we define a total angular momentum \mathbf{J} , taken with respect to fixed molecular coordinates, and including the effect of electronic rotation about the internuclear axis. Thus,

$$\begin{aligned}\mathbf{J} \equiv & i\{[\cot \beta \cos \alpha(\partial/\partial \alpha)_m + \sin \alpha(\partial/\partial \beta)_m - (\cos \alpha/\sin \beta)(\partial/\partial \gamma)_m]\mu_x \\ & + [\cot \beta \sin \alpha(\partial/\partial \alpha)_m - \cos \alpha(\partial/\partial \beta)_m - (\sin \alpha/\sin \beta)(\partial/\partial \gamma)_m]\mu_y \\ & - (\partial/\partial \alpha)_m \mu_z\}\end{aligned}\quad (2.46)$$

The equation for \mathbf{J} differs from that for \mathcal{R} (Eq. 2.44) only in that the partial differentials are to be taken with molecule-fixed rather than space-fixed coordinates held constant. The additional stipulation is also made that $\langle P_z \rangle = \langle -i(\partial/\partial \gamma) \rangle$.

Let us now also construct the space-fixed components of \mathbf{P} . Using Eq. (2.30)

$$\begin{pmatrix} P_{x'} \\ P_{y'} \\ P_{z'} \end{pmatrix} = \mathcal{M}^+ \begin{pmatrix} P_x \\ P_y \\ P_z \end{pmatrix}\quad (2.47)$$

where \mathcal{M}^+ denotes the transpose of the real, unitary matrix \mathcal{M} . Using Eqs. (2.46) and (2.47) the vector operator $(\mathbf{J} - \mathbf{P})$ is constructed,

$$\begin{aligned}\mathbf{J} - \mathbf{P} = & i\{[\cot \beta \cos \alpha(\partial/\partial \alpha)_m + \sin \alpha(\partial/\partial \beta)_m + i \cos \beta \cos \alpha P_x \\ & - i \sin \alpha P_y - i \cos^2 \beta (\cos \alpha/\sin \beta)P_z]\mu_{x'} \\ & + [\cot \beta \sin \alpha(\partial/\partial \alpha)_m - \cos \alpha(\partial/\partial \beta)_m + i \cos \beta \sin \alpha P_x \\ & + i \cos \alpha P_y - i(\cos^2 \beta \sin \alpha/\sin \beta)P_z]\mu_{y'} \\ & + [-(\partial/\partial \alpha)_m - i \sin \beta P_x + i \cos \beta P_z]\mu_{z'}\}\end{aligned}\quad (2.48)$$

where in writing Eq. (2.48), the relation $\langle P_z \rangle = \langle -i(\partial/\partial\gamma) \rangle$ has been used.

Comparing Eqs. (2.45) and (2.48) we obtain the very important result,

$$\mathcal{H}' = \mathbf{J} - \mathbf{P} \quad (\text{for case } a) \quad (2.49)$$

$$\mathcal{H}' = \mathbf{K} - \mathbf{L} \quad (\text{for case } b) \quad (2.50)$$

In order to obtain the transformed Hamiltonian \mathcal{H}^N from \mathcal{H}^N it is necessary only to replace \mathcal{H} by $\mathbf{J} - \mathbf{P}$. This result lends itself to a clear physical interpretation. \mathcal{H} is just the nuclear rotational angular momentum expressed in terms of constant molecular coordinates. $\mathbf{J} - \mathbf{P}$ is naturally equivalent to this, since \mathbf{J} is the total angular momentum likewise expressed, while \mathbf{P} is the electronic angular momentum. Thus the difference, $\mathbf{J} - \mathbf{P}$, must be the nuclear angular momentum for constant molecular coordinates.

The total transformed Hamiltonian thus becomes, in case (a),

$$\begin{aligned} \mathcal{H}'_T = & B(\mathbf{J} - \mathbf{P})^2 + \sum_{\alpha} \left\{ \frac{-\hbar e Z_{\alpha}}{\mathcal{J}c} [(\mathbf{r}_{\alpha} \times \mathbf{A}_{\alpha}) \cdot (\mathbf{J} - \mathbf{P})] + \frac{Z_{\alpha}^2 e^2}{2M_{\alpha} c^2} \mathbf{A}_{\alpha}^2 \right\} \\ & - B \left[\frac{\partial}{\partial R} \left(R^2 \frac{\partial}{\partial R} \right) \right] - \sum_{\alpha} \left[\frac{Z_{\alpha} e}{M_{\alpha} c} (\mathbf{A}_{\alpha} \cdot \boldsymbol{\mu}_R) p_{\alpha R} \right] \\ & + \mathcal{H}'_m(x_i, y_i, z_i, z_{\alpha}, S_i, \Sigma, I_{\alpha}, M_I) \end{aligned} \quad (2.51)$$

and in case (b)

$$\begin{aligned} \mathcal{H}'_T = & B(\mathbf{K} - \mathbf{L})^2 + \sum_{\alpha} \left\{ \frac{-\hbar e Z_{\alpha}}{\mathcal{J}c} [(\mathbf{r}_{\alpha} \times \mathbf{A}_{\alpha}) \cdot (\mathbf{K} - \mathbf{L})] + \frac{Z_{\alpha}^2 e^2}{2M_{\alpha} c^2} \mathbf{A}_{\alpha}^2 \right\} \\ & - B \left[\frac{\partial}{\partial R} \left(R^2 \frac{\partial}{\partial R} \right) \right] - \sum_{\alpha} \left[\frac{Z_{\alpha} e}{M_{\alpha} c} (\mathbf{A}_{\alpha} \cdot \boldsymbol{\mu}_R) p_{\alpha R} \right] \\ & + \mathcal{H}'_m(x_i, y_i, z_i, Z_{\alpha}, S_i, M_s, I_{\alpha}, M_I) \end{aligned} \quad (2.52)$$

Equations (2.51) and (2.52) closely resemble Eq. (2.1) except that they are more complicated. In order to obtain the best possible basis set for \mathcal{H}'_T it will be well to modify slightly the basis functions $\psi_{\eta}^e(x_i, R) \psi_{\eta}^N(R) \psi_{\eta}^N(x'_{\alpha})$ of Section II.A. Consider first the Hamiltonian \mathcal{H}'_m appropriate to the clamped nuclei. As \mathcal{H}'_m is clearly not equivalent to the simpler \mathcal{H}^e it is desirable to separate \mathcal{H}'_m into two additive parts, the first part \mathcal{H}''_m omitting reference to spin or external field effects. We then define a new basis function $\psi_{\eta}^e(x_i, R)$ by the eigenvalue equation,*

$$\mathcal{H}''_m \psi_{\eta}^e(x_i, R) = E_{\eta}^e(R) \psi_{\eta}^e(x_i, R) \quad (2.53)$$

* This definition of $\psi_{\eta}^e(x_i, R)$ is appropriate for cases (a) and (b), but not for other cases.

It is also convenient to write slightly different equations for $\psi_{\eta}^N(R)$, henceforth denoted by ψ_v^N (the η dependence being understood) and $\psi_{\eta}^N(X'_\alpha)$, henceforth denoted by $\psi_{\mathcal{A}}^N$. The eigenvalue equation governing the vibrational motion need only be modified by the inclusion of the canonical momentum rather than the mechanical momentum.

$$\left\{ -B \left[\frac{\partial}{\partial R} \left(R^2 \frac{\partial}{\partial R} \right) \right] - \sum_{\alpha} \left[\frac{Z_{\alpha} e}{M_{\alpha} c} (\mathbf{A}_{\alpha} \cdot \mathbf{p}_R) \right] p_{\mathbf{A}R} + U(R) + W(R) \right\} \psi_v^N = E \psi_v^N \quad (2.54)$$

The rotational basis function is rather more difficult to define, especially since an analytical form is desirable in the interpretation of electron resonance measurements. It is not possible to derive an equation analogous to (2.53) and (2.54) which can be solved analytically, and we must therefore be content to work in a basis which incompletely diagonalizes the rotational Hamiltonian.

The terms involving the mechanical momentum should be more important than those describing magnetic effects. Thus it is desirable to find basis functions which diagonalize $(\mathbf{J} - \mathbf{P})^2$. Even this is not possible since \mathbf{P} operates on the electronic basis functions which have already been determined. However, if $(\mathbf{J} - \mathbf{P})^2$ is expanded in the molecular coordinate system,

$$\begin{aligned} (\mathbf{J} - \mathbf{P})^2 &= \mathbf{J}^2 - 2\mathbf{J} \cdot \mathbf{P} + \mathbf{P}^2 \\ &= \mathbf{J}^2 - J_z^2 - 2(J_x P_x + J_y P_y) + (P_x^2 + P_y^2) \end{aligned} \quad (2.55)$$

that part of $(\mathbf{J} - \mathbf{P})^2$ independent of \mathbf{P} is just $\mathbf{J}^2 - J_z^2$, which we can hope to diagonalize.

It would be possible to use Eq. (2.46) for the components of \mathbf{J} and derive a differential equation for $\psi_{\mathcal{A}}^N$. It is, however, easier to deduce the form of $\psi_{\mathcal{A}}^N$ simply using its rotational invariance in free space.^{14,12}

Let $\phi_m^J(X_{\alpha})$ be the eigenfunction whose square modulus gives the positions of the nuclei in the space-fixed axis system. Let us now apply a rotation \mathcal{P} to $\phi_m^J(X_{\alpha})$,

$$\begin{aligned} \mathcal{P} \phi_m^J(X_{\alpha}) &= \phi_{\Omega}^J(X'_{\alpha}) \\ &= \sum_m \phi_m^J(X_{\alpha}) D_{m\Omega}^J(\omega) \end{aligned} \quad (2.56)$$

Let the angles ω through which the rotation is performed be equal to the Euler angles[†] α, β, γ which locate the molecule-fixed coordinate system with

[†] By Eq. (2.46), γ is not to be taken equal to zero when dealing with the total angular momentum \mathbf{J} .

respect to the space-fixed one. For this choice of angles, $\phi_{\Omega}^J(X'_a)$ must be a constant, independent of α, β, γ depending only upon the geometric configuration of the nuclei, as the coordinate X'_a is essentially in a molecule-fixed coordinate system. Thus using the unitary properties of $D_{m\Omega}^J$,

$$\begin{aligned}\phi_m^J(X_a) &= \sum_{\Omega} \phi_{\Omega}^J(X'_a) D_{m\Omega}^{J*}(\alpha, \beta, \gamma) \\ &= \sum_{\Omega} K_{\Omega} D_{m\Omega}^{J*}(\alpha, \beta, \gamma)\end{aligned}\quad (2.57)$$

where K_{Ω} denotes a constant depending only upon Ω . It is further required that $\phi_m^J(X_a)$ be an eigenfunction of J_z , which implies that the eigenfunction be invariant to a rotation through γ . This is consistent with $K_{\Omega} \neq 0$ for only one value of Ω . Thus

$$\phi_m^J(X_a) = K D_{m\Omega}^{J*}(\alpha, \beta, \gamma) \quad (2.58)$$

The constant K is determined by the requirement that $\phi_m^J(X_a)$ be normalized to unity. Using the fact¹² that the square modulus of the j th order irreducible representation of the full rotation group taken over all group operations is $(8\pi^2/2J+1)$, the rotation wavefunction is

$$\psi_{\mathcal{R}}^N = \phi_m^J(X_a) = [(2J+1)/8\pi^2]^{1/2} D_{mJ\Omega}^{J*}(\alpha, \beta, \gamma) \quad (2.59)$$

for case (a), or

$$\psi_{\mathcal{R}}^N = \phi_m^K(X_a) = [(2K+1)/8\pi^2]^{1/2} D_{mK\Lambda}^{K*}(\alpha, \beta, \gamma) \quad (2.60)$$

for case (b).

To derive the complete set of basis functions, it remains to multiply the products $\psi_{\eta}^e(x_i, R) \psi_{\nu}^N \psi_{\mathcal{R}}^N$ by electronic and nuclear spin basis functions and take the appropriate linear combinations. The basis function for the electronic spin is taken to be an eigenfunction of the total electronic spin and, in case (a), its component along the internuclear axis, or in case (b), its component along the space-fixed z' axis. The nuclear spin basis functions are taken to be direct products of the eigenfunctions of the individual nuclear spins and their respective z' projections. The direct product function is usually used in electron resonance rather than a coupled total nuclear spin eigenfunction, since the forces coupling the nuclear spins are almost always much weaker than the decoupling effect of the external magnetic field used in electron resonance experiments.

Finally, it is worthwhile to consider what is nondiagonal in the new basis set. There will be the terms symbolized by $C_{\eta\eta'}$, connecting different electronic and vibrational states (see Section II.A). $C_{\eta\eta'}$ will remain as defined in Eqs. (2.7) to (2.9), except that one should use the operator of

Eq. (2.54), rather than simply the kinetic energy operator of nuclear vibration. These terms, although not necessarily negligible, are of little importance to us, since the electron resonance investigations center on the rotational energy levels. If necessary, it would always be possible to define a vibronic function that diagonalized these terms and which would provide expectation values of the molecular parameters entering into the rotational energy levels. We thus subsequently neglect these terms, assuming that where necessary, the molecular expectation values are taken over a correct vibronic function.

The other nondiagonal terms arise from the rotational Hamiltonian, plus the spin and external field dependent interactions in the clamped nuclei Hamiltonian. These terms are important in determining the rotational energy levels and must be treated in detail. As the simplification of the remaining portion of $\mathcal{H}^{N'}$ involves much the same procedure as for many of the terms in \mathcal{H}'_m , we postpone further discussion of $\mathcal{H}^{N'}$ until the clamped-nuclei Hamiltonian has been treated in the next section.

C. Derivation of the Clamped-Nuclei Hamiltonian

In order to derive \mathcal{H}'_m it is desirable to use relativistic quantum mechanics, although no mention of relativistic considerations for the nuclear kinetic energy terms has been made. \mathcal{H}'_m , nevertheless, needs to be relativistically correct since the electronic velocities are, in general, much greater than the nuclear velocities, and also since \mathcal{H}'_m concerns itself with electronic spin, an essentially relativistic phenomenon.

In what follows, the nuclei will be treated as infinitely massive force centers. The neglect of the relative electronic-nuclear motion (as distinct from the vibrational and rotational nuclear motion) is not rigorously justifiable, as we shall wish to include terms in the Hamiltonian smaller than the correction due to nuclear motion. In the center of mass system the principal effects of nuclear motion can be taken into account by introducing the reduced electronic mass in the kinetic energy terms and noting that there occur certain cross terms among the electronic momenta of order $(M_\alpha)^{-1}$.¹⁵ Both of these effects can be included in \mathcal{H}''_m and hence are of little importance to the electron resonance experiment, except for the term describing the interaction of an external magnetic field with the electronic orbital motion. Phillips¹⁶ and Abragam and Van Vleck¹⁷ have investigated the effect of this term on the g factor for the orbital angular momentum. They find it makes a contribution of the order of 1 ppm for the oxygen atom; its importance in diatomic molecules should be of the same order. As the expected accuracy of the Hamiltonian (a few ppm) we shall produce is

somewhat less than 1 ppm, we neglect entirely the relative electronic-nuclear motion. Along the same lines, Van Vleck¹⁵ has shown that, strictly speaking, not even the motion of the center of mass of the system may be neglected. However, these terms only affect the vibrational and electronic Hamiltonians (and the neglected cross terms between them) and we may therefore omit them.

There is, of course, no rigorous relativistic Hamiltonian for a many-electron system; however, the Dirac equation¹⁸ for a single electron in the presence of electromagnetic fields is Lorentz invariant.* We shall generalize the Dirac equation to the N -electron case by assuming that the interelectronic and nuclear-electronic interactions may be correctly obtained by calculating classically the fields produced at the N th electron by the other $(N - 1)$ electrons and the two nuclei, and determining the effect of such fields on the N th electron by means of the Dirac equation. The total electronic Hamiltonian is then obtained by summing over the N electrons.

The general form¹⁸ of the Dirac Hamiltonian, \mathcal{H}_D , for an electron in the presence of electromagnetic fields is

$$\mathcal{H}_D = \beta m + \alpha \cdot \pi - e\phi \quad (2.61)$$

α and β have as representatives 4 by 4 matrices determined by

$$\begin{aligned} \sum_k (\alpha^k)^2 &= 1 & \alpha^k \alpha^1 + \alpha^1 \alpha^k &= 0 \\ \beta^2 &= 1 & \alpha^k \beta + \beta \alpha^k &= 0 \end{aligned} \quad (2.62)$$

ϕ is the electrostatic potential and π is defined by

$$\pi = \mathbf{p} + (e/c)\mathbf{A} \quad (2.63)$$

The eigenfunctions of \mathcal{H}_D are, of course, four-component spinors which may be said to correspond to positive and negative energy states. Since the interaction energies in a diatomic molecule are much less than that necessary for a transition between positive and negative energy states (separated by approximately $2mc^2$), we may legitimately concern ourselves with only the positive energy solutions. We thus seek to write \mathcal{H}_D in such a way that positive and negative energy eigenfunctions are, to within a desired order of approximation, completely decoupled.

* There exists also the so called Breit^{19,20} equation for two-electron systems which is approximately Lorentz invariant. Our subsequent derivations could equally well be based upon it; the results we obtain for a two-electron system are equivalent to those deduced from the Breit equation, provided we approximate our formulas in a manner consistent with that used in deriving the Breit equation. We wish, however, to avoid some of the usual approximations, and the derivation of results from the Dirac equation seems more transparent.

To this end \mathcal{H}_D is written as a sum of even (ε) and odd (\mathcal{O}) operators,

$$\mathcal{H}_D = \beta mc^2 + \varepsilon + \mathcal{O} \quad (2.64)$$

By an even or odd operator, the following is meant. Let the four-component spinor be written

$$\begin{pmatrix} \Phi \\ \Phi' \end{pmatrix}$$

with

$$\Phi = \begin{pmatrix} \psi_1 \\ \psi_2 \end{pmatrix} \quad \text{and} \quad \Phi' = \begin{pmatrix} \psi_3 \\ \psi_4 \end{pmatrix} \quad (2.65)$$

Φ and Φ' are referred to as the large and small components of the wavefunction. An odd operator is then represented by a matrix connecting Φ and Φ' ; an even operator is represented by a matrix with no such non-vanishing elements.

If the odd operators in \mathcal{H}_D can be made to vanish, then Φ and Φ' will be uncoupled. Foldy and Wouthuysen²¹ found that by choosing properly the representation for \mathcal{H}_D , odd operators can be made to vanish to any desired order of approximation. Their method may be illustrated by removing the odd operators of lowest order in \mathcal{H}_D . Let a unitary transformation be performed on \mathcal{H}_D ,

$$\mathcal{H}'_D = U \mathcal{H}_D U^{-1} \quad (2.66)$$

where

$$U = \exp(\beta \mathcal{O} / 2mc^2) \quad (2.67)$$

Thus

$$\begin{aligned} \mathcal{H}'_D &= \mathcal{H}_D + \frac{1}{2}[\beta \mathcal{O}, \beta] + (\text{terms of higher order in } m \text{ or } c) \\ &= \beta mc^2 + \varepsilon + \mathcal{O} - \mathcal{O} + (\text{terms of higher order}) \\ &= \beta mc^2 + \varepsilon + (\text{terms of higher order}) \end{aligned} \quad (2.68)$$

where the fact that any odd operator anticommutes with β has been used.

It should be clear that this method may be repeated any number of times to obtain an even Hamiltonian (β is diagonal) to the desired order in m^{-1} or c^{-1} . If the expansion is carried out to include terms up to order m^{-3} , or $[(v/c)^4]$, the transformed Hamiltonian projected on to the space of the large components is

$$\mathcal{H}'_D = -e\phi + \frac{1}{2m}(\boldsymbol{\sigma} \cdot \boldsymbol{\pi})^2 + \frac{e}{8m^2c^2}[(\boldsymbol{\sigma} \cdot \boldsymbol{\pi})(\boldsymbol{\sigma} \cdot \boldsymbol{\pi}, \phi)] - \frac{1}{8m^3c^2}(\boldsymbol{\sigma} \cdot \boldsymbol{\pi})^4 \quad (2.69)$$

The Pauli spin matrices σ have been introduced into Eq. (2.69) by using the fact that $\alpha = \rho\sigma$ where ρ has a matrix representative which commutes with σ and whose square is unity. Use of the well-known identity,¹⁸

$$(\sigma \cdot \mathbf{a})(\sigma \cdot \mathbf{b}) = \mathbf{a} \cdot \mathbf{b} + i\sigma \cdot (\mathbf{a} \times \mathbf{b}) \quad (2.70)$$

for any two vectors \mathbf{a} and \mathbf{b} commuting with σ allows the expansion of (2.69). As we wish to treat the electromagnetic fields classically, rather than quantum mechanically, we thereafter introduce the definition $\sigma = gS$ (rather than $\sigma = 2S$) where g is the free electron g factor including its anomalous moment due to quantum electrodynamical effects.* We thus find that

$$\begin{aligned} \mathcal{H}'_D = & -e\phi + \frac{\mathbf{p}^2}{2m} - \frac{\mathbf{p}^4}{8m^3c^2} + \frac{e}{mc} \mathbf{A} \cdot \mathbf{p} + \frac{e^2}{2mc^2} \mathbf{A}^2 \\ & + \frac{\hbar ge}{2mc} (\mathbf{S} \cdot \mathbf{B}) + \frac{e\hbar}{8m^2c^2} [2g\mathbf{S} \cdot (\mathbf{E} \times \boldsymbol{\pi}) + \hbar(\nabla \cdot \mathbf{E})] \\ & - \frac{e}{2mc} (2\mathbf{A} \cdot \mathbf{p} + \hbar g\mathbf{S} \cdot \mathbf{B}) \left(\frac{\mathbf{p}^2}{2m^2c^2} \right) \end{aligned} \quad (2.71)$$

where

$$\mathbf{E} = -\nabla\phi \quad (2.72)$$

$$\mathbf{B} = \nabla \times \mathbf{A} \quad (2.73)$$

Terms quadratic or higher in \mathbf{A} or \mathbf{B} have been omitted in the reduction of the last term of Eq. (2.69), and a Coulomb gauge for \mathbf{A} has been assumed.

\mathcal{H}'_D is the Hamiltonian for a single electron in the presence of electromagnetic fields, with a corresponding two-component spinor eigenfunction. To obtain the Hamiltonian for the electron in a diatomic molecule, the potentials felt by that electron due to the presence of the other electrons, nuclei, and any external fields must be determined. The electrostatic potential may readily be seen to be

$$\phi_i = \sum_{\alpha, p} \frac{e}{|\mathbf{r}_{\alpha i} - \mathbf{r}_p|} - \sum_{j \neq i} \frac{e}{r_{ji}} - \mathbf{E} \cdot \mathbf{r}_i \quad (2.74)$$

The terms in ϕ_i correspond to the potentials generated by the nuclear protons (p), the other electrons, and any constant external electric field \mathbf{E} .

Since the first term of Eq. (2.74) involves explicit reference to nuclear

* The Lamb shift term is clearly not included by this ansatz. However, it could be incorporated in \mathcal{H}''_m and so has no real effect on the rotation energy levels.

structure, it is desirable to rearrange it somewhat. Therefore, let the first term in ϕ_i be expanded under the assumption that $\mathbf{r}_p < \mathbf{r}_{ai}$,

$$e \sum_{\alpha, p} |\mathbf{r}_{ai} - \mathbf{r}_p|^{-1} = \sum_{\alpha, p} e \mathbf{r}_{ai}^{-1} \sum_{K, M} (r_p/r_{ai})^K C_M^K(\omega_p) C_{-M}^K(\omega_{ia}) (-1)^M \\ \approx \sum_{\alpha} \left\{ \frac{Z_{\alpha} e}{r_{ai}} + \sum_{p, M} \frac{r_p}{r_{ai}^3} C_M^2(\omega_p) C_{-M}^2(\omega_{ia}) (-1)^M \right\} \quad (2.75)$$

C^K is defined as $(2K + 1/4\pi)^{-1/2}$ times the K th order spherical harmonic, with ω specifying the orientation of the vector \mathbf{r}_p or \mathbf{r}_{ai} in a spherical coordinate system. The approximation is terminated after the $K = 2$ (quadrupole) term, as higher order terms are, as yet, experimentally unimportant. The term with $K = 1$ vanishes since the nuclear energy levels may be taken to have a definite parity. Finally it should be noted that because of the spherical symmetry of internuclear electronic penetration, inclusion of terms for $r_p > r_{ai}$ could only affect the Coulomb interaction term of Eq. (2.75) and may therefore be neglected.

We now turn to the magnetic vector potential. By the application of simple magnetostatics,

$$\mathbf{A}_i = -\frac{ge\hbar}{2mc} \sum_{j \neq i} (\mathbf{S}_j \times \mathbf{r}_{ji}) r_{ji}^{-3} + \sum_{\alpha} \frac{g_{\alpha} e \hbar}{2M_{\alpha} c} (\mathbf{I}_{\alpha} \times \mathbf{r}_{\alpha j}) r_{\alpha j}^{-3} \\ - \sum_{j \neq i} \frac{e}{mc} r_{ji}^{-1} \boldsymbol{\pi}_j + \left(\frac{1}{2}\right)(\mathbf{H} \times \mathbf{r}_i) \quad (2.76)$$

The first two terms correspond to the vector potential generated by the spins of the other electrons and nuclei. The third term describes the potential generated by the motion (other than spin) of the other electrons. The last term arises from the presence of any external magnetic field \mathbf{H} . It should be noted that, strictly speaking, the penultimate term of Eq. (2.76) is incorrect. Firstly, since r_{ji}^{-1} and $\boldsymbol{\pi}_j$ do not commute, one should take a Hermitian average $(\frac{1}{2})[\boldsymbol{\pi}_j r_{ji}^{-1} + r_{ji}^{-1} \boldsymbol{\pi}_j]$. Secondly, even in this form, the divergence of the contribution to \mathbf{A} is not zero. This point, being but a matter of gauge, may be remedied by adding to \mathbf{A} the divergence of a suitable scalar function.

These points, it is clear, are irrelevant as far as the magnetic field derived from \mathbf{A} is concerned, as the curl of the additional terms is, in each case, equal to zero. However, the effect of these additions is to create a rather complicated result for the interaction of the momentum \mathbf{p}_j with this part of the vector potential. In fact, it has been found that the correct form of the momentum interaction is found only if the retardation of the electromagnetic potentials is included. To our approximation in inverse powers of c ,

\mathbf{A} is correctly given, but ϕ is not. Since the result is unimportant to us, we do not go into details but merely quote the results of Darwin²³ and Breit¹⁹ that the correct form of the momentum interaction $\mathcal{H}_{\mathcal{P}F}$ is

$$\mathcal{H}_{\mathcal{P}F} = \frac{-e^2}{2m^2c^2} \left\{ \sum_{i < j} r_{ji}^{-1} (\pi'_i \cdot \pi'_j) + r_{ij}^{-3} [\mathbf{r}_{ij} \cdot (\mathbf{r}_{ij} \cdot \pi'_i) \pi'_j] \right\} \quad (2.77)$$

where

$$\pi'_{i,j} = \mathbf{p}_{i,j} + \frac{e}{2c} (\mathbf{H} \times \mathbf{r}_{ij}) \quad (2.78)$$

We note that the first term in Eq. (2.77) is derivable from the form of \mathbf{A} given by Eq. (2.74), but the second term is not.

In order to obtain the final electronic Hamiltonian, it remains only to substitute the expressions for ϕ_i and \mathbf{A}_i (subject to the restriction of the preceding paragraph) and sum over the i electrons.* If we carry out the calculation to order[†] c^{-3} (c^{-2} for terms involving M_α or M_p in the denominator), the following Hamiltonian is obtained:

$$\mathcal{H}'_D = \mathcal{H}'_m + \mathcal{H}'_{fs} + \mathcal{H}'_{hf} + \mathcal{H}'_{Z1} + \mathcal{H}'_{Z2} + \mathcal{H}'_E \quad (2.79)$$

We now proceed to deal with each of these terms in turn.

\mathcal{H}'_m is the appropriate Hamiltonian for the electrons with clamped nuclei if spin and external field effects are disregarded. Explicitly,

$$\begin{aligned} \mathcal{H}'_m = & \sum_i \left\{ \frac{\mathbf{p}_i^2}{2m} - \frac{\mathbf{p}_i^4}{8m^3c^2} - \left(1 + \frac{e\hbar^2}{8m^2c^2} \nabla_i^2 \right) \left(\sum_\alpha \frac{Z_\alpha e^2}{r_{\alpha i}} - \sum_{j \neq i} \frac{e^2}{r_{ji}} \right) \right\} \\ & - \sum_{j \neq i} \frac{1}{4} \left(\frac{e}{mc} \right)^2 [r_{ij}^{-1} (\mathbf{p}_i \cdot \mathbf{p}_j) + r_{ij}^{-3} (\mathbf{r}_{ij} \cdot (\mathbf{r}_{ij} \cdot \mathbf{p}_i) \mathbf{p}_j)] \end{aligned} \quad (2.80)$$

The physical significance of the terms in \mathcal{H}'_m is as follows. The first term represents the kinetic energy of the electrons, and the second term is the relativistic correction to the kinetic energy. The first part of the third term represents the normal Coulomb interaction between the electrons and between the electrons and the nuclei. The second half of this term represents the so-called¹¹ Darwin correction to the Coulomb potential and is

* In this respect, it is very important not to count the interelectronic interactions twice. Formally this difficulty may be avoided by insertion of a factor of 1/2 in the potentials.²⁴

† To order c^{-3} is not a rigorous approximation since, for instance, the vector potential from the spins of other electrons may be larger than that of the external field even though it is of higher order in c . However, it can be shown that such an approximation neglects only the diamagnetic interactions between the particles, which are of little interest in determining the rotational levels.

nonvanishing only at a potential source. The final term is the orbit-orbit interaction (interaction of the orbit of one electron with the orbital motion of another electron) which has just been discussed.

The second term in Eq. (2.79), \mathcal{H}_{fs} , which may be called the fine structure Hamiltonian, gives the effect of interaction between the electronic spins and orbital currents. Explicitly, it has the form

$$\mathcal{H}_{fs}^e = \sum_i \left\{ \frac{g\beta S_i}{2mc} \cdot \left[\sum_{\alpha} \frac{Z_{\alpha} e}{r_{\alpha i}^3} (\mathbf{r}_{\alpha i} \times \mathbf{p}_i) - \sum_{j \neq i} e r_{ji}^{-3} [(\mathbf{r}_{ji} \times \mathbf{p}_i) + 2(\mathbf{r}_{ij} \times \mathbf{p}_j)] \right] \right. \\ \left. - \sum_{j > i} g^2 \beta^2 [\nabla_i \times (\mathbf{S}_j \times \mathbf{r}_{ji}) r_{ji}^{-3}] \cdot \mathbf{S}_i \right\} \quad (2.81)$$

The first two terms of \mathcal{H}_{fs} represent the usual spin-orbit coupling terms, involving the nuclear potential and the potential of the other electrons. The third term describes the spin-other-orbit interaction. Each of these terms contains an antisymmetric tensor of first rank formed from electronic position and momentum variables. The angular momentum of each electron ($\mathbf{l}_i = \hbar^{-1}(\mathbf{r}_i \times \mathbf{p}_i)$) about the center of mass is also a first rank antisymmetric tensor formed from the same variables. As there can only be one unique tensor, the matrix elements of the former terms are proportional to those of \mathbf{l}_i . Using this fact

$$\sum_i \left\{ \frac{g\beta S_i}{2mc} \cdot \left[\sum_{\alpha} \frac{Z_{\alpha} e}{r_{\alpha i}^3} (\mathbf{r}_{\alpha i} \times \mathbf{p}_i) - \sum_{j \neq i} e r_{ji}^{-3} [(\mathbf{r}_{ji} \times \mathbf{p}_i) + 2(\mathbf{r}_{ij} \times \mathbf{p}_j)] \right] \right\} \\ = \sum_i A_i \mathbf{l}_i \cdot \mathbf{S}_i \quad (2.82)$$

where

$$\langle \eta | A_i \mathbf{l}_i | \eta' \rangle = \frac{g\beta}{2mc} \langle \eta | \sum_{\alpha} \frac{Z_{\alpha} e}{r_{\alpha i}^3} (\mathbf{r}_{\alpha i} \times \mathbf{p}_i) \\ - \sum_{j \neq i} e r_{ji}^{-3} [(\mathbf{r}_{ji} \times \mathbf{p}_i) + 2(\mathbf{r}_{ij} \times \mathbf{p}_j)] | \eta' \rangle \quad (2.83)$$

where η denotes an electronic or vibronic state.

The final term in Eq. (2.81) represents the interaction between the electronic spins. For the i, j th term it can be rewritten as the Hamiltonian \mathcal{H}_{ss} ,

$$\mathcal{H}_{ss} = -g^2 \beta^2 \left(\nabla \times \frac{\mathbf{S}_i \times \mathbf{r}_{ji}}{r_{ij}} \right) \cdot \mathbf{S}_i = -g^2 \beta^2 \left(\nabla \times \nabla \times \frac{\mathbf{S}_j}{r_{ji}} \right) \cdot \mathbf{S}_i \\ = g^2 \beta^2 [\mathbf{S}_i \cdot \mathbf{S}_j \nabla^2 - (\mathbf{S}_i \cdot \nabla)(\mathbf{S}_j \cdot \nabla)] r_{ji}^{-1} \quad (2.84)$$

It is now useful to introduce a general recoupling theorem¹² for composite

tensorial operators $T^K(\mathbf{k}_1, \mathbf{k}_2)$ of rank K formed from operators of rank k_1 and k_2 . Provided the tensorial operators k_2 and k_3 commute,

$$T^K(\mathbf{k}_1, \mathbf{k}_2) \cdot T^K(\mathbf{k}_3, \mathbf{k}_4) = (2K+1)(-1)^{K_1+K_4} \sum_{K'} W(k_1 k_2 k_3 k_4; KK') \\ \times T^{K'}(\mathbf{k}_1, \mathbf{k}_3) \cdot T^{K'}(\mathbf{k}_2, \mathbf{k}_4) \quad (2.85)$$

where $W(k_1 k_2 k_3 k_4; KK')$ denotes a Racah coefficient. It is interesting to note that the well-known vector identity for the Pauli spin matrices (Eq. 2.70) is simply a special case of Eq. (2.85). Using Eq. (2.85), the last term of Eq. (2.84) may be written,

$$(\mathbf{S}_i \cdot \nabla)(\mathbf{S}_j \cdot \nabla) = \frac{1}{2}(\mathbf{S}_i \cdot \mathbf{S}_j) \nabla^2 + \frac{1}{2}(\mathbf{S}_i \times \mathbf{S}_j)(\nabla \times \nabla) + T^2(\mathbf{S}_i, \mathbf{S}_j) \cdot T^2(\nabla, \nabla) \quad (2.86)$$

The second term on the right-hand side of Eq. (2.86) vanishes since it involves an anti-symmetric product of two identical commutable factors. Thus,

$$\mathcal{H}_{ss} = g^2 \beta^2 [(2/3)(\mathbf{S}_i \cdot \mathbf{S}_j) \nabla^2 - T^2(\mathbf{S}_i, \mathbf{S}_j) \cdot T^2(\nabla, \nabla)] r_{ji}^{-1} \quad (2.87)$$

Using a nonrelativistic approximation* the first term of Eq. (2.87) is clearly equal to

$$-g^2 \beta^2 \frac{8\pi}{3} \delta(\mathbf{r}_{ji})(\mathbf{S}_i \cdot \mathbf{S}_j)$$

By expanding any possible wavefunction into spherical harmonics and computing the matrix elements of the second half of \mathcal{H}_{ss} , it can be shown to vanish at $r_{ij} = 0$. Thus expressing $T^2(\nabla_i, \nabla_j) r_{ji}^{-1}$ in terms of spherical harmonics specifying the relative positions of the electrons,

$$\mathcal{H}_{ss}^e = \sum_i \left\{ A_i \mathbf{l}_i \cdot \mathbf{S}_i - g^2 \beta^2 \sum_{j>i} \right. \\ \left. \times \left[\frac{8\pi}{3} \delta(\mathbf{r}_{ji})(\mathbf{S}_i \cdot \mathbf{S}_j) + \sqrt{6} T^2(\mathbf{S}_i, \mathbf{S}_j) C^2(\omega_{ji}) r_{ij}^{-3} \right] \right\} \quad (2.88)$$

where C^2 is defined as after Eq. (2.75).

* The whole question of the convergence of the various terms of \mathcal{H}_{ss}' at potential sources is a rather delicate one. The problems arise because the transformation is a non-local one over a domain of linear dimensions $\sim \hbar/mc$. Moreover, it is just at a source that the potentials \mathbf{A} and ϕ cease to be small enough to be treated nonrelativistically. Rigorously then, it is necessary to effect a cut-off of the singular potential at a distance roughly \hbar/mc from the source. In order for the nonrelativistic approximation to be applicable, it suffices that the energy of the potential interaction be much less than mc^2 at the cut-off point, which is true for the cases treated.¹¹

The next term in \mathcal{H}'_D is the hyperfine structure Hamiltonian \mathcal{H}_{hf}^e . Explicitly,

$$\mathcal{H}_{hf}^e = \sum_{i,\alpha} \left\{ 2\beta\beta_N g_\alpha r_{\alpha i}^{-3} [\mathbf{I}_\alpha \cdot (\mathbf{r}_{\alpha i} \times \mathbf{p}_i) \hbar^{-1}] + g\beta\beta_N g_\alpha \mathbf{S}_i \cdot [\nabla \times (\mathbf{I}_\alpha \times \mathbf{r}_{\alpha i}/r_{\alpha i}^3)] - \sum_p [e^2 r_{\alpha i}^{-3} C^2(\omega_{\alpha i}) \cdot r_p^2 C^2(\omega_{\alpha p})] \right\} \quad (2.89)$$

The first two terms of \mathcal{H}_{hf}^e consist of the coupling of the electron spin and orbital motion to the nuclear magnetic moment. The first term can be put into the more usual form,

$$\sum_{i,\alpha} [(a_{i\alpha} + a'_{i\alpha})(\mathbf{I}_i \cdot \mathbf{I}_\alpha)]$$

where

$$\langle \eta | a_{i\alpha} \mathbf{I}_i | \eta' \rangle = \langle \eta | 2g_\alpha \beta \beta_N r_{\alpha i}^{-3} \mathbf{I}_i | \eta' \rangle \quad (2.90)$$

$$\langle \eta | a'_{i\alpha} \mathbf{I}_i | \eta' \rangle = -2g_\alpha \beta \beta_N \langle \eta | r_{\alpha i}^{-3} (\mathbf{r}_\alpha \times \mathbf{p}_i) | \eta' \rangle \hbar^{-1} \quad (2.91)$$

The advantage of writing the interaction in this manner is that $\langle \eta | a'_{i\alpha} \mathbf{I}_i | \eta' \rangle = 0$ for $\eta = \eta'$ because $(\mathbf{r}_\alpha \times \mathbf{p}_i)$, being perpendicular to the internuclear axis, vanishes in a state of axial symmetry.

The second term in \mathcal{H}_{hf}^e can be treated by exactly the method of Eqs. (2.84) to (2.88). The result is

$$\mathbf{S}_i \cdot \left[\nabla \times \left(\frac{\mathbf{I}_\alpha \times \mathbf{r}_{\alpha i}}{r_{\alpha i}^3} \right) \right] = \sqrt{6} T^2(\mathbf{S}_i, \mathbf{I}_\alpha) \cdot C^2(\omega_{\alpha i}) r_{\alpha i}^{-3} + \frac{8\pi}{3} \delta(\mathbf{r}_{\alpha i}) (\mathbf{S}_i \cdot \mathbf{I}_\alpha) \quad (2.92)$$

This form was quite useful for the fine-structure interaction; however, for hyperfine structure another coupling arrangement for the dipole-dipole part is advantageous. Using again the uniqueness of a tensor product,

$$\sqrt{6} T^2(\mathbf{S}_i, \mathbf{I}_\alpha) \cdot C^2(\omega_{\alpha i}) r_{\alpha i}^{-3} = r_{\alpha i}^{-3} \sqrt{10} T^1(\mathbf{I}_\alpha) \cdot T^1(\mathbf{S}_i, C^2) \quad (2.93)$$

where the first rank tensor $T^1(\mathbf{S}_i, C^2)$ is defined by

$$T_q^1(\mathbf{S}_i, C^2) = - \sum_{q_1, q_2} T_{q_1}^1(\mathbf{S}_i) C_{q_2}^2(\omega_{\alpha i}) \langle 12q_1 q_2 | 1q \rangle \quad (2.94)$$

where $\langle 12q_1 q_2 | 1q \rangle$ is a Clebsch-Gordan coefficient. The constant $\sqrt{10}$ on the right-hand side of Eq. (2.93) is obtained by comparing a single term on the two sides of the equation.

The last term of Eq. (2.89), which arises from the second nonvanishing term in the expansion of the electrostatic potential, is usually referred to as the quadrupole interaction \mathcal{H}_Q . It can be put into an alternative form by

using the Wigner-Eckart theorem to write (neglecting matrix elements off-diagonal in nuclear states)

$$\langle IM_I | \sum_p r_p^2 e C^2(\omega_{ap}) | IM_I \rangle = k \langle IM_I | T^2(\mathbf{I}_\alpha) | IM_I \rangle \quad (2.95)$$

The traditional definition²⁴ of a quadrupole moment of a nucleus is,

$$eQ_\alpha = 2e \langle II | \sum_p r_p^2 C^2(\omega_{ap}) | II \rangle \quad (2.96)$$

Taking the $m_I = I$ matrix element of both sides of Eq. (2.95) and using Eq. (2.96) yields

$$k = \frac{\sqrt{3} e Q_\alpha}{\sqrt{2} I_\alpha (2I_\alpha - 1)} \quad (2.97)$$

Thus we have the result,

$$\mathcal{H}_Q = - \sum_{i,\alpha} \frac{e^2 Q_\alpha \sqrt{3}}{I_\alpha (2I_\alpha - 1) \sqrt{2} r_{ai}^3} C^2(\omega_{ai}) \cdot T^2(\mathbf{I}_\alpha) \quad (2.98)$$

Combining all the terms of \mathcal{H}_{hf}^e gives

$$\begin{aligned} \mathcal{H}_{hf}^e = \sum_{i,\alpha} \left\{ (a_{i\alpha} + a'_{i\alpha}) (\mathbf{l}_i \cdot \mathbf{I}_\alpha) + \left[\frac{8\pi}{3} \delta(\mathbf{r}_{ai}) (\mathbf{S}_i \cdot \mathbf{I}_\alpha) \right. \right. \\ \left. \left. + \sqrt{10} r_{ai}^{-3} T^1(\mathbf{I}_\alpha) \cdot T^1(\mathbf{S}_i, C^2) \right] g\beta\beta_N g_\alpha \right. \\ \left. - \frac{e^2 Q_\alpha \sqrt{3}}{I_\alpha (2I_\alpha - 1) \sqrt{2} r_{ai}^3} C^2(\omega_{ai}) \cdot T^2(\mathbf{I}_\alpha) \right\} \quad (2.99) \end{aligned}$$

The next terms in \mathcal{H}_D , \mathcal{H}_{z1}^e and \mathcal{H}_{z2}^e , refer to the interaction of the electrons with external magnetic fields. The division of the Zeeman effect into two parts is based primarily on their relative magnitudes. \mathcal{H}_{z1}^e contains the usual interaction of the electron paramagnetic orbital and spin motion with the external field, while \mathcal{H}_{z2}^e contains a series of correction terms to \mathcal{H}_{z1}^e that are linear in the applied field, plus the usual diamagnetic term. \mathcal{H}_{z1}^e is given by the familiar expression,

$$\mathcal{H}_{z1}^e = \sum_i \{ \beta \mathbf{H} \cdot [g \mathbf{S}_i + \hbar^{-1} (\mathbf{r}_i \times \mathbf{p}_i)] \} = \sum_i \{ \beta \mathbf{H} \cdot [g \mathbf{S}_i + \mathbf{l}_i] \} \quad (2.100)$$

\mathcal{H}_{z2}^e represents the higher order relativistic and diamagnetic effects, which enter in two ways: (i) through a velocity dependence of the electron mass and hence its magnetic moment; and (ii), through changes in the velocity dependent interactions (e.g., spin-orbit coupling) because of the external field. Explicitly \mathcal{H}_{z2}^e is given by

$$\begin{aligned}
\mathcal{H}_{Z2}^e = \sum_i \left\{ \beta \mathbf{H} \cdot [\mathbf{g} \mathbf{S}_i + \mathbf{I}_i] \left(-\frac{\mathbf{p}_i^2}{2m^2 c^2} \right) + \left(\frac{ge^2 \hbar}{8m^2 c^3} \right) \mathbf{S}_i \right. \\
\cdot \left\{ \sum_{\alpha} \frac{Z_{\alpha} e}{r_{\alpha i}^3} (\mathbf{r}_{\alpha i} \times \mathbf{H} \times \mathbf{r}_i) - \sum_{j \neq i} e [r_{ji}^{-3} (\mathbf{r}_{ji} \times \mathbf{H} \times \mathbf{r}_i) \right. \\
+ 2(\mathbf{r}_{ij} \times \mathbf{H} \times \mathbf{r}_j)] \left. \right\} - \sum_{j \neq i} \frac{e^3}{4m^2 c^3} \\
\times \{ r_{ij}^{-1} (\mathbf{H} \times \mathbf{r}_i) \cdot \mathbf{p}_j + r_{ij}^{-3} [\mathbf{r}_{ij} \cdot (\mathbf{H} \times \mathbf{r}_i) (\mathbf{r}_{ij} \cdot \mathbf{p}_j)] \} \\
+ \frac{e^2}{8mc^2} (\mathbf{H} \times \mathbf{r}_i)^2 \left. \right\} \quad (2.101)
\end{aligned}$$

The terms linear in \mathbf{H} will be dealt with initially. The first term of \mathcal{H}_{Z2}^e is due to the relativistic increase in the electron mass and corresponding decrease in its magnetic moment; it arises from the last term in Eq. (2.69). The next set of terms represents the effect of the external field on the spin-orbit and spin-other-orbit interactions. The last term of \mathcal{H}_{Z2}^e , linear in \mathbf{H} , describes the effect of the field on the orbit-orbit interaction. By manipulation of the triple vector products in Eq. (2.101), the electronically diagonal terms linear in \mathbf{H} may be written

$$\begin{aligned}
\mathcal{H}_{Z2}^e = \sum_i \{ \beta \mathbf{H} \cdot [(\mathbf{g} \delta g_{\parallel}^i + \delta g_{\perp}^i) \mathbf{S}_i \\
+ (\delta g_{\parallel}^i + \delta g_{\perp}^i) \mathbf{I}_i] + \beta (\delta g_{\parallel}^i - \delta g_{\perp}^i) H_z S_{zi} \} \quad (2.102)
\end{aligned}$$

where

$$\langle \eta | \delta g_{\parallel}^i | \eta \rangle = \langle \eta | \mathbf{p}_i^2 | \eta \rangle (-1/2m^2 c^2) \quad (2.103)$$

$$\begin{aligned}
\langle \eta | \delta g_{\perp}^i | \eta \rangle = \frac{ge}{4mc^2} \langle \eta | \sum_{\alpha} \frac{Z_{\alpha} e}{r_{\alpha i}^3} [x_i x_{\alpha i} + z_i z_{\alpha i}] - \sum_{j \neq i} e r_{ji}^{-3} \\
\times \{ [x_i x_{ji} + z_i z_{ji}] + 2[x_{ij} x_j + z_{ij} z_j] \} | \eta \rangle \quad (2.104)
\end{aligned}$$

$$\begin{aligned}
\langle \eta | \delta g_{\parallel}^i | \eta \rangle = \frac{ge}{4mc^2} \langle \eta | \sum_{\alpha} \frac{Z_{\alpha} e}{r_{\alpha i}^3} [x_i x_{\alpha i} + y_i y_{\alpha i}] - \sum_{j \neq i} e r_{ji}^{-3} \\
\times \{ [x_i x_{ji} + y_i y_{ji}] + 2[x_{ij} x_j + y_{ij} y_j] \} | \eta \rangle \quad (2.105)
\end{aligned}$$

and

$$\begin{aligned}
\langle \eta | \delta g_{\perp}^i \mathbf{I}_i | \eta \rangle = -\frac{e}{2mc} \langle \eta | \sum_{j \neq i} [(\mathbf{r}_i \times \mathbf{p}_j) r_{ij}^{-1}] \\
+ [r_{ij}^{-3} (\mathbf{r}_i \times \mathbf{r}_{ij})(\mathbf{r}_{ij} \cdot \mathbf{p}_j)] | \eta \rangle \quad (2.106)
\end{aligned}$$

In other words, the linear magnetic field effects can be accounted for by defining tensorial g factors for the interaction of the electron spin and orbital moment with the field. In the molecular reference frame the cylindrical symmetry of the molecule ensures that the g tensors have, at most, two unique components, g_{\parallel} , the component along the internuclear axis, and g_{\perp} , the component in the molecular xy plane.

Finally, the term quadratic in \mathbf{H} in \mathcal{H}_{Z2}^e may be simplified using Eq. (2.85),

$$\sum_i \frac{e^2}{8mc^2} (\mathbf{H} \times \mathbf{r}_i)^2 = \sum_i \frac{-e^2}{8mc^2} [T^2(\mathbf{H}, \mathbf{H}) \cdot T^2(\mathbf{r}_i, \mathbf{r}_i) - \frac{1}{2} \mathbf{H}^2 \mathbf{r}_i^2] \quad (2.107)$$

The second term on the right-hand side of Eq. (2.107) varies only with the electronic energy level, but the first term varies with the rotational level. Thus care must be exercised in separating its effects, quadratic in \mathbf{H} , from those of the smaller terms in the linear Zeeman operator. The diamagnetic term, it should be noted, has more than passing interest as the expectation value of $T^2(\mathbf{r}_i, \mathbf{r}_i)$ gives the electronic quadrupole moment of the molecule. However, one must again take care in attributing spectral shifts, quadratic in \mathbf{H} , to the terms of Eq. (2.107) without taking into account the terms, quadratic in \mathbf{H} , neglected in the reduction of the last term of Eq. (2.69). As neither of these effects has yet been observed in paramagnetic molecules, we henceforth neglect them.

\mathcal{H}_{Z1}^e and \mathcal{H}_{Z2}^e can now be combined to give the following simple expression for the total electronic Zeeman effect,

$$\begin{aligned} \mathcal{H}_Z^e &= \mathcal{H}_{Z1}^e + \mathcal{H}_{Z2}^e \\ &= \sum_i \{ \beta \mathbf{H} \cdot [g_s^i \mathbf{S}_i + g_l^i \mathbf{l}_i] + \Delta g^i H_z S_{zi} \} \end{aligned} \quad (2.108)$$

where

$$g_s^i = (g + g \delta g_1^i + \delta g_{\perp}^i) \quad (2.109)$$

$$g_l^i = (1 + \delta g_1^i + \delta g_{\perp}^i) \quad (2.110)$$

$$\Delta g^i = (\delta g_{\parallel}^i - \delta g_{\perp}^i) \quad (2.111)$$

The last term of \mathcal{H}_D' may be treated very simply. It describes the interaction of the electronic charge cloud with an external electric field,

$$\mathcal{H}_E^e = \sum_i e \mathbf{E} \cdot \mathbf{r}_i \quad (2.112)$$

The electronic Hamiltonian has now been derived. To obtain the Hamiltonian for the complete molecule, the interaction between the nuclei and

the external (not electronic) fields must be added to \mathcal{H}'_D . By analogy with the electronic Hamiltonian, the clamped-nuclear Hamiltonian is (to the order of accuracy required*),

$$\mathcal{H}_{CN} = \frac{Z_\alpha Z_{\alpha'} e^2}{r_{\alpha\alpha'}} - \sum_\alpha g_\alpha \beta_N \mathbf{H} \cdot \mathbf{I}_\alpha - \sum_\alpha Z_\alpha e \mathbf{r}_\alpha \cdot \mathbf{E} \quad (2.113)$$

The first term in \mathcal{H}_{CN} represents the Coulomb repulsion of the nuclei. The second and third terms of \mathcal{H}_{CN} represent the interaction of the nuclei with external magnetic and electric fields respectively.

Each of the terms in \mathcal{H}_{CN} may be combined with similar terms in \mathcal{H}'_D and the superscript e then dropped. Thus the Coulomb term may be added to $\mathcal{H}_m^{e'}$ to give \mathcal{H}_m'' , the Hamiltonian of Eq. (2.54) for a nonrotating, nonvibrating molecule without external field or spin effects. Likewise the second term may be added to \mathcal{H}_Z^e and the third to \mathcal{H}_E^e . In fact, \mathcal{H}_E now assumes a particularly simple form,

$$\begin{aligned} \mathcal{H}_E &= \mathcal{H}_E^e - \sum_\alpha Z_\alpha e \mathbf{r}_\alpha \cdot \mathbf{E} \\ &= -\mathbf{E} \cdot \sum_{\alpha, i} (-e \mathbf{r}_i + Z_\alpha e \mathbf{r}_\alpha) = -\mathbf{E} \cdot \boldsymbol{\mu} \end{aligned} \quad (2.114)$$

where $\boldsymbol{\mu}$ is the electric dipole moment of the molecule.

We may now return to that part of the Hamiltonian describing nuclear motion. As usual we work explicitly with case (a) notation but remember that the Hamiltonian for case (b) may be derived from it by making the replacements: \mathbf{J} by \mathbf{K} , \mathbf{P} by \mathbf{L} , and \mathbf{S} , Σ by \mathbf{S} , M_S . From Eq. (2.51) the rotational part of the Hamiltonian is

$$\mathcal{H}_R^{N'} = B(\mathbf{J} - \mathbf{P})^2 - \sum_\alpha \left\{ \frac{Z_\alpha \hbar e}{\mathcal{J} c} \left[(\mathbf{J} - \mathbf{P}) \cdot (\mathbf{r}_\alpha \times \mathbf{A}_\alpha) \right] - \frac{Z_\alpha^2 e^2}{2M_\alpha c^2} \mathbf{A}_\alpha^2 \right\} \quad (2.115)$$

* Nuclear chemical shift and dipole-dipole interaction terms are, for example, formally smaller than the required accuracy. However, we should note that to obtain the α' nucleus' contribution to the field gradient at the α nucleus, the nuclear electrostatic interaction should reveal that the protons of the nuclei occupy a finite spatial domain. Thus by an expansion entirely equivalent to the electron-nuclear interaction of (2.75), the nuclear contribution to the field gradient is obtained. We recognize this contribution to \mathcal{H}_Q hereafter by writing \mathcal{H}_Q as

$$\mathcal{H}_Q = \sum_{i, \alpha} \frac{e^2 Q_\alpha \sqrt{3} c}{I_\alpha (2I_\alpha + 1) \sqrt{2} r_{\alpha c}^3} C^2(\omega_{ac}) T^2(\mathbf{I}_\alpha)$$

where c denotes a charged particle, positive or negative (the sum over i and α is assumed to sum all particles c). Thus each particle makes a *signed* contribution to \mathcal{H}_Q , for electrons $c = -1$ and for nuclei $c = +Z$.

By analogy with our previous work on the electronic Hamiltonian, the vector potential at the nucleus is,*

$$\mathbf{A}_\alpha = -\sum_i \left\{ \frac{ge\hbar}{2mc} [(\mathbf{S}_i \times \mathbf{r}_{i\alpha}) r_{i\alpha}^{-3}] + \frac{e}{mc} r_{i\alpha}^{-1} \boldsymbol{\pi}_i \right\} + (\frac{1}{2})(\mathbf{H} \times \mathbf{r}_\alpha) \quad (2.116)$$

The physical significance of the terms in \mathbf{A}_α is as follows. The first two terms represent the vector potential caused by electron spin and motion. The motion term here suffers from the same deficiencies as in Eq. (2.77); we correct for them in the same way. The last term arises from the effects of any external field.

With an explicit formula for \mathbf{A}_α it is possible to simplify the cross term between \mathbf{A}_α and $(\mathbf{J} - \mathbf{P})$ in Eq. (2.115) in exactly the same manner as for the electronic Hamiltonian. Thus,

$$-\sum_\alpha \frac{Z_\alpha \hbar e}{\mathcal{J} c} [(\mathbf{J} - \mathbf{P}) \cdot (\mathbf{r}_\alpha \times \mathbf{A}_\alpha)] = \sum_i \{ (\mathbf{J} - \mathbf{P}) \cdot [\gamma_i \mathbf{S}_i + \bar{\gamma}_i S_{zi} \mathbf{l}_i + \xi_i \mathbf{l}_i] \} \\ - g_r \beta \mathbf{H} \cdot (\mathbf{J} - \mathbf{P}) \quad (2.117)$$

where

$$\langle \eta | \gamma_i | \eta' \rangle = \sum_\alpha \frac{Z_\alpha e g \beta \hbar}{c} \langle \eta | \frac{(\mathbf{r}_\alpha \cdot \mathbf{r}_{i\alpha}) r_{i\alpha}^{-3}}{\mathcal{J}} | \eta' \rangle \quad (2.118)$$

$$\langle \eta | \bar{\gamma}_i \mathbf{l}_i | \eta' \rangle = -\sum_\alpha \frac{Z_\alpha e g \beta \hbar}{c} \langle \eta | z_\alpha r_{i\alpha}^{-3} \mathbf{r}_{i\alpha} \mathcal{J}^{-1} | \eta' \rangle \quad (2.119)$$

$$\langle \eta | \xi_i \mathbf{l}_i | \eta' \rangle = \sum_\alpha \frac{Z_\alpha e \beta}{c} \langle \eta | [(r_\alpha \times \mathbf{p}_i) r_{i\alpha}^{-1} \\ + r_{i\alpha}^{-3} (\mathbf{r}_\alpha \times \mathbf{r}_{i\alpha}) (\mathbf{r}_{i\alpha} \cdot \mathbf{p}_i)] \mathcal{J}^{-1} | \eta' \rangle \quad (2.120)$$

and

$$\langle \eta | g_r | \eta' \rangle = m \sum_\alpha \langle \eta | \mathcal{J}^{-1} Z_\alpha \mathbf{r}_\alpha^2 | \eta' \rangle \quad (2.121)$$

The first three terms of Eq. (2.117) describe the coupling of the spin and orbital moments of the electron with the magnetic field created by nuclear

* As contributions to the energy from the vector potential of other nuclei are of order $(M_p)^{-2} c^{-2}$, these are neglected in \mathbf{A}_α . This causes omission of terms such as the nuclear spin-rotation coupling.

rotation.* The last term describes the interaction of the rotating nuclei with an external field. This term gives the nuclear contribution to the rotational magnetic moment of the molecule.

According to our usual approximation, the only nonvanishing contribution from the last term of (2.115) is derived from the external field. This term is then just the diamagnetic energy of the nuclei. It differs from the electronic diamagnetic energy principally by the replacement of m by M_α in the denominator. As the electronic diamagnetic term is on the limit of experimental accuracy, we neglect this term completely.

If the terms \mathcal{H}_m^e and \mathcal{H}_v^N are omitted from Eq. (2.51), the Hamiltonian, \mathcal{H} , of interest to the electron resonance experiment is obtained. Employing the simplifications outlined in the previous pages, and using case (a) notation, we have,

$$\begin{aligned}
 \mathcal{H} &= \mathcal{H}_{fs} + \mathcal{H}_{hf} + \mathcal{H}_\alpha^N + \mathcal{H}_Z + \mathcal{H}_E \\
 &= \sum_i \left[A_i \mathbf{l}_i \cdot \mathbf{S}_i - g^2 \beta^2 \sum_{j>i} \left[\frac{8\pi}{3} \delta(\mathbf{r}_{ji}) (\mathbf{S}_i \cdot \mathbf{S}_j) + T^2(\mathbf{S}_i, \mathbf{S}_j) \cdot C^2(\omega_{ij}) \right. \right. \\
 &\quad \times r_{ij}^{-3} \sqrt{6} \left. \right] + \sum_\alpha \left\{ (a_{i\alpha} + a'_{i\alpha}) \mathbf{l}_i \cdot \mathbf{I}_\alpha + \left[\frac{8\pi}{3} \delta(\mathbf{r}_{\alpha i}) \mathbf{S}_i \cdot \mathbf{I}_\alpha \right. \right. \\
 &\quad \left. \left. + \sqrt{10} r_{\alpha i}^{-3} T^1(\mathbf{I}_\alpha) \cdot T^1(\mathbf{S}_i, C^2) \right] g \beta \beta_N g_\alpha - \frac{e^2 Q_\alpha \sqrt{3} c}{I_\alpha (2I_\alpha - 1) \sqrt{2} r_{\alpha c}^3} \right. \\
 &\quad \left. \times C^2(\omega_{\alpha c}) \cdot T^2(\mathbf{I}_\alpha) \right\} + B(\mathbf{J} - \mathbf{P})^2 + (\mathbf{J} - \mathbf{P}) \cdot [\gamma_i \mathbf{S}_i + \bar{\gamma}_i S_{zi} \mathbf{l}_i + \xi_i \mathbf{l}_i] \\
 &\quad - g_r \beta \mathbf{H} \cdot (\mathbf{J} - \mathbf{P}) - \beta_N \mathbf{H} \cdot \sum_\alpha g_\alpha \mathbf{I}_\alpha + \beta \mathbf{H} \cdot [g_s^i \mathbf{S}_i + g_l^i \mathbf{l}_i] \\
 &\quad \left. + \beta \Delta g^i H_z S_{zi} - \mathbf{E} \cdot \boldsymbol{\mu} \right] \quad (2.122)
 \end{aligned}$$

This equation is directly applicable to case (a) where \mathbf{S}_i is taken to have a projection along the internuclear axis. To obtain the Hamiltonian for case (b), \mathbf{S}_i is taken to have a z' projection M_S^i , \mathbf{J} is replaced by \mathbf{K} , and \mathbf{P} is set equal to \mathbf{L} . Explicitly,

* As these terms were derived classically and $\gamma_i, \bar{\gamma}_i$ and ξ_i are operators, Hermitian averages of Eqs. (2.118–2.120) should be used in calculations.

$$\begin{aligned}
\mathcal{H} &= \mathcal{H}_{fs} + \mathcal{H}_{hf} + \mathcal{H}_a^N + \mathcal{H}_Z + \mathcal{H}_E \\
&= \sum_i \left[A_i \mathbf{l}_i \cdot \mathbf{S}_i - g^2 \beta^2 \sum_{j>i} \left[\frac{8\pi}{3} \delta(\mathbf{r}_{ji}) (\mathbf{S}_i \cdot \mathbf{S}_j) + T^2(\mathbf{S}_i, \mathbf{S}_j) \cdot C^2(\omega_{ij}) \right. \right. \\
&\quad \times r_{ij}^{-3} \sqrt{6} \left. \right] + \sum_{\alpha} \left\{ (a_{ia} + a'_{ia}) \mathbf{l}_i \cdot \mathbf{I}_{\alpha} + \left[\frac{8\pi}{3} \delta(\mathbf{r}_{ai}) \mathbf{S}_i \cdot \mathbf{I}_{\alpha} \right. \right. \\
&\quad \left. \left. + \sqrt{10} r_{ai}^{-3} T^1(\mathbf{I}_{\alpha}) \cdot T^1(\mathbf{S}_i, C^2) \right] g \beta \beta_N g_{\alpha} - \frac{e^2 Q_{\alpha} \sqrt{3} c}{I_{\alpha} (2I_{\alpha} - 1) \sqrt{2} r_{ac}^3} \right. \\
&\quad \times C^2(\omega_{ac}) \cdot T^2(\mathbf{I}_{\alpha}) \left. \right\} + B(\mathbf{K} - \mathbf{L})^2 + (\mathbf{K} - \mathbf{L}) \cdot [\gamma_i \mathbf{S}_i + \bar{\gamma}_i S_{zi} \mathbf{l}_i + \xi_i \mathbf{l}_i] \\
&\quad - g_r \beta \mathbf{H} \cdot (\mathbf{K} - \mathbf{L}) - \beta_N \mathbf{H} \cdot \sum_{\alpha} g_{\alpha} \mathbf{I}_{\alpha} + \beta \mathbf{H} [g_s' \mathbf{S}_i + g_i' \mathbf{l}_i] \\
&\quad \left. + \beta \Delta g^i H_z S_{zi} - \mathbf{E} \cdot \boldsymbol{\mu} \right] \quad (2.123)
\end{aligned}$$

Equations (2.122) and (2.123) represent Hamiltonians for cases (a) and (b) whose relative accuracy for the rotational energy levels should be quite sufficient for the calculation of these eigenvalues beyond the limits of experimental error. In general, methods are expounded for the calculation of all the nonvanishing matrix elements of these Hamiltonians in Hund's case (a) and case (b) representations. Naturally, the diagonalization of the matrices formed from these operators provides a completely general means of obtaining the eigenenergies.

A practical difficulty often arises in this approach because of the size of the matrices involved, in that the Hamiltonian operates in the infinite space of the products of vibronic and rotational states. Since the experiments usually focus on the lower rotational levels, the states arising from the higher rotational levels usually have little effect on the energies of interest, and the truncation of the matrix at a reasonably low rotational level is nearly always possible.

The infinity of electronic states, however, represents other problems. It is difficult to choose an approximate point for truncation due to the nearness of the continuum. Moreover, even if such a point could be chosen, the energy differences among the electronic states are not known, even parametrically such as those of the rotational levels. Several approximate treatments^{22,25,26} of these terms based on perturbation theory have been developed. A thorough discussion of these treatments would require a review nearly as lengthy as this one. However, several important conclusions of these efforts should be stated. The problem can usually be most

concisely treated by replacing Eqs. (2.122) and (2.123) by an "effective" Hamiltonian operating only within the rotational subspace of a given vibronic state. The "effective" Hamiltonian is determined by a perturbation treatment of the terms connecting different electronic states. Given the form of the Hamiltonians of Eqs. (2.122) and (2.123), the form of the "effective" Hamiltonian for any order of perturbation treatment may be determined. For the (usually sufficient) lowest orders of the perturbation expansion, the form of the effective Hamiltonian "mimics" exactly the form of the portion of the "real" Hamiltonian that is diagonal in electronic quantum numbers. The interpretation of the molecular constants multiplying the operators, however, must change as in the "effective" Hamiltonian they contain contributions from both the "first-order" or "real" parameters plus "higher-order" contributions arising from the terms between different electronic states treated by the perturbation theory.

The complete interpretation of the molecular parameters obtained from electron resonance experiments is not the principal purpose of this work, and we refer to the references above for a detailed account of these higher-order terms. We, however, caution that the interpretation of the interactions in terms of the "first-order" parameters alone may be misleading, and we discuss some of the most important higher-order contributions to the spectra in Section IV. In Section III, we have simply worked out the matrix elements of Eqs. (2.122) and (2.123), since the operator form of the effective Hamiltonian has in all cases of interest mimicked exactly those equations. However, as the formalism used in the matrix element calculation is so general, we quote matrix elements diagonal and off-diagonal in electronic quantum numbers with equal ease. Generally, the diagonal matrix elements will be the most important; however, the off-diagonal ones clearly show what electronic states are connected by the rotational Hamiltonian.

III. CALCULATION OF THE MATRIX ELEMENTS

A. Important Results from the Theory of Angular Momentum

Angular momentum operators normally obey commutation relations of the form,

$$\begin{aligned}[J_x, J_y] &= iJ_z \\ [J_y, J_z] &= iJ_x \\ [J_z, J_x] &= iJ_y\end{aligned}\tag{3.1}$$

This is true, for example, of the spatial components of the total angular momentum \mathbf{J} , and of the components of spin angular momentum in either space or molecule-fixed axes. If we define shift operators by the relations,

$$\begin{aligned} J_+ &= J_x + iJ_y \\ J_- &= J_x - iJ_y \end{aligned} \quad (3.2)$$

the commutation relations may be rewritten in the form

$$\begin{aligned} [J_z, J_{\pm}] &= \pm J_{\pm} \\ [J_+, J_-] &= 2J_z \end{aligned} \quad (3.3)$$

It is often convenient to transform from a Cartesian to a spherical basis and define new components,

$$\begin{aligned} J_1 &= -(1/\sqrt{2})(J_x + iJ_y) = -(1/\sqrt{2})J_+ \\ J_0 &= J_z \\ J_{-1} &= (1/\sqrt{2})(J_x - iJ_y) = (1/\sqrt{2})J_- \end{aligned} \quad (3.4)$$

We may then rewrite the commutation relations as follows:

$$\begin{aligned} [J_+, J_1] &= 0 & [J_+, J_{-1}] &= \sqrt{2}J_0 \\ [J_+, J_0] &= \sqrt{2}J_1 & [J_z, J_{\pm 1}] &= \pm J_{\pm 1} \\ [J_-, J_1] &= \sqrt{2}J_0 & [J_-, J_{-1}] &= 0 \\ [J_-, J_0] &= \sqrt{2}J_{-1} & [J_z, J_0] &= 0 \end{aligned} \quad (3.5)$$

An irreducible tensor operator $T_q^k(\mathbf{J})$ of rank k and components $q = +k, k-1, \dots, -k$, may be defined by the commutation relations,¹⁰

$$\begin{aligned} [J_{\pm}, T_q^k(\mathbf{J})] &= \{(k \mp q)(k \pm q + 1)\}^{1/2} T_{q \pm 1}^k(\mathbf{J}) \\ [J_{\pm 1}, T_q^k(\mathbf{J})] &= \mp \{\tfrac{1}{2}(k \mp q)(k \pm q + 1)\}^{1/2} T_{q \pm 1}^k(\mathbf{J}) \\ [J_z, T_q^k(\mathbf{J})] &= q T_q^k(\mathbf{J}) \\ [J_0, T_q^k(\mathbf{J})] &= q T_q^k(\mathbf{J}) \end{aligned} \quad (3.6)$$

We note that the spherical components of the vector \mathbf{J} are, in fact, the $q = +1, 0, -1$ components of the first rank ($k = 1$) irreducible tensor $T_q^k(\mathbf{J})$. In other words, the commutation relations (3.5) are special cases of (3.6).

A new problem arises when we have to deal with the components of total angular momentum \mathbf{J} in the *molecular* axis system because the commutation relations are then anomalous:²²

$$\begin{aligned} [J_x, J_y] &= -iJ_z \\ [J_y, J_z] &= -iJ_x \\ [J_z, J_x] &= -iJ_y \end{aligned} \quad (3.7)$$

We shall frequently encounter scalar products of operators, for example $\mathbf{J} \cdot \mathbf{S}$, in the molecular axis system, in which one operator obeys normal commutation relations while the other commutes anomalously. Van Vleck²² has shown how one may handle these products using the technique of reversed angular momentum, and Freed²⁶ has extended Van Vleck's method to deal with irreducible tensor operators. We will adopt a different approach, however. For an operator which obeys the commutation relations (3.7) we redefine the shift operators by the equations

$$J'_+ = J_x - iJ_y \quad J'_- = J_x + iJ_y \quad (3.8)$$

The commutation relations

$$[J'_z, J'_\pm] = \pm J'_\pm \quad [J'_+, J'_-] = 2J'_z \quad (3.9)$$

which are analogous to (3.3) then still hold. Similarly we may redefine the spherical components of \mathbf{J} by the relations,

$$\begin{aligned} J'_1 &= -(1/\sqrt{2})(J_x - iJ_y) = -(1/\sqrt{2})J'_+ \\ J'_0 &= J_z \\ J'_{-1} &= (1/\sqrt{2})(J_x + iJ_y) = (1/\sqrt{2})J'_- \end{aligned} \quad (3.10)$$

so that the commutation relations (3.5) are still appropriate. If the irreducible tensor components $T_q^k(\mathbf{J}')$ are redefined in the same manner as $J'_0, J'_{\pm 1}$, they too obey commutation relations of the form (3.6). We note the important fact that these new components $T_q^k(\mathbf{J}')$ correspond to the components of the adjoint tensor of $T_q^k(\mathbf{J})$.¹²

The scalar product of two irreducible tensor operators is defined by¹⁰

$$T^1(\mathbf{J}) \cdot T^1(\mathbf{S}) = \sum_q (-1)^q T_q^1(\mathbf{J}) T_q^1(\mathbf{S}) \quad (3.11)$$

Alternatively we may introduce the adjoint tensor, $\tilde{T}_q^k(\mathbf{J})$, and expand the scalar product in the form,

$$\begin{aligned} \mathcal{P} &\equiv T^1(\mathbf{J}) \cdot T^1(\mathbf{S}) = \tilde{\mathcal{P}} = \tilde{T}^1(\mathbf{S}) \cdot \tilde{T}^1(\mathbf{J}) \\ &= \sum_q (-1)^q \tilde{T}_q^1(\mathbf{S}) \tilde{T}_{-q}^1(\mathbf{J}) \\ &= \sum_q (-1)^q (-1)^q T_{-q}^1(\mathbf{S}) \tilde{T}_{-q}^1(\mathbf{J}) \\ &= \sum_q T_q^1(\mathbf{S}) \tilde{T}_q^1(\mathbf{J}) \end{aligned} \quad (3.12)$$

The Wigner-Eckart theorem is of fundamental importance in that it enables one to determine the projectional-dependence of the matrix

elements of an irreducible tensor operator. Thus if the spatial z' projection of \mathbf{J} is denoted by M_J and the molecular z component by Ω , the Wigner-Eckart theorem may be written,¹⁰⁻¹²

$$\langle \gamma J M_J | T_q^1(\mathbf{J}) | \gamma' J' M_J' \rangle = \langle J' 1 M_J' q | J M_J \rangle \langle \gamma J || T^1(\mathbf{J}) || \gamma' J' \rangle \quad (3.13a)$$

Since the commutation relation (3.6) determines (3.13) and the molecule-fixed components of $\hat{T}^1(\mathbf{J})$ obey these same relations

$$\langle J \Omega \gamma | \hat{T}_q^1(\mathbf{J}) | J' \Omega' \gamma' \rangle = \langle J' 1 \Omega' q | J \Omega \rangle \langle J \gamma || \hat{T}^1(\mathbf{J}) || J' \gamma' \rangle \quad (3.13b)$$

where

$$\begin{aligned} \langle \gamma J || T^1(\mathbf{J}) || \gamma' J' \rangle &= \delta_{JJ'} \delta_{\Omega\Omega'} [J(J+1)]^{1/2} \\ \langle J \gamma || \hat{T}^1(\mathbf{J}) || J' \gamma' \rangle &= \delta_{JJ'} \delta_{M_J M_J'} [J(J+1)]^{1/2} \end{aligned} \quad (3.14)$$

Here q' denotes space-fixed components and q denotes molecule-fixed components. Thus we obtain the important result that the Wigner-Eckart theorem for $\hat{T}_q^1(\mathbf{J})$ takes the same form when \mathbf{J} commutes anomalously (3.13b) as does that for $T_q^1(\mathbf{J})$ when \mathbf{J} commutes normally.

In conclusion we quote a number of important results which we shall use frequently for the matrix elements of products of tensor operators.¹⁰⁻¹²

(a) **Tensor Product of Two Tensor Operators.** If $T^k(\mathbf{k}_1, \mathbf{k}_2)$ denotes the tensor product of two noncommuting tensor operators $T^{k_1}(\mathbf{1})$ and $T^{k_2}(\mathbf{2})$, then

$$\begin{aligned} &\langle \eta J || T^k(\mathbf{k}_1, \mathbf{k}_2) || \eta' J' \rangle \\ &= \sum_{J'' \eta''} (-1)^{k-k_1-k_2} \{ (2J''+1)(2k+1) \}^{1/2} W(JJ'k_1k_2; kJ'') \\ &\quad \times \langle \eta J || T^{k_1}(\mathbf{1}) || \eta'' J'' \rangle \langle \eta'' J'' || T^{k_2}(\mathbf{2}) || \eta' J' \rangle \end{aligned} \quad (3.15)$$

If, however, $T^{k_1}(\mathbf{1})$ operates only on part 1 of a system and $T^{k_2}(\mathbf{2})$ on part 2 (i.e., they commute), the matrix elements of the tensor product are given by

$$\begin{aligned} &\langle \eta J_1 J_2 J || T^k(\mathbf{k}_1, \mathbf{k}_2) || \eta' J'_1 J'_2 J' \rangle \\ &= \sum_{\eta''} \langle \eta J_1 || T^{k_1}(\mathbf{1}) || \eta'' J'_1 \rangle \langle \eta'' J_2 || T^{k_2}(\mathbf{2}) || \eta' J'_2 \rangle \\ &\quad \times [(2J_1+1)(2J'+1)(2k+1)(2J_2+1)]^{1/2} \begin{Bmatrix} J & J' & k \\ J_1 & J'_1 & k_1 \\ J_2 & J'_2 & k_2 \end{Bmatrix} \end{aligned} \quad (3.16)$$

where the bracketed expression with nine arguments is the $9-j$ symbol of Wigner.¹²

(b) **Scalar Product of Commuting Tensor Operators.** For the scalar product of $T^{k_1}(\mathbf{1})$ and $T^{k_2}(\mathbf{2})$, the argument k in the 9- j symbol is equal to zero and (3.16) reduces to

$$\begin{aligned} & \langle \eta J_1 J_2 J M_J | T^k(\mathbf{1}) \cdot T^k(\mathbf{2}) | \eta' J'_1 J'_2 J' M'_J \rangle \\ &= (-1)^{J-J_1-J_2'} [(2J_1+1)(2J_2+1)]^{1/2} \delta_{JJ'} \delta_{M_J M_{J'}} \\ & \times W(J_1 J'_1 J_2 J'_2; kJ) \times \langle J_1 \| T^k(\mathbf{1}) \| J'_1 \rangle \langle J_2 \| T^k(\mathbf{2}) \| J'_2 \rangle \quad (3.17) \end{aligned}$$

(c) **Single Operator in a Coupled Scheme.** If $k_2 = 0$ it follows from (3.16) that $k_1 = k$ and we have the result,

$$\begin{aligned} & \langle \eta J_1 J_2 J \| T^k(\mathbf{1}) \| \eta' J'_1 J'_2 J' \rangle \\ &= (-1)^{J_1'-J_2+J-k} [(2J'+1)(2J_1+1)]^{1/2} W(J_1 J'_1 J J'; kJ_2) \\ & \times \langle \eta J_1 \| T^k(\mathbf{1}) \| \eta' J'_1 \rangle \delta_{J_2 J_2'} \quad (3.18) \end{aligned}$$

Alternatively if $k_1 = 0$,

$$\begin{aligned} & \langle \eta J_1 J_2 J \| T^k(\mathbf{2}) \| \eta' J'_1 J'_2 J' \rangle \\ &= (-1)^{J_2'-J_1'+J-k} [(2J'+1)(2J_2+1)]^{1/2} W(J_2 J'_2 J J'; kJ_1) \\ & \times \langle \eta J_2 \| T^k(\mathbf{2}) \| \eta' J'_2 \rangle \delta_{J_1 J_1'} \quad (3.19) \end{aligned}$$

B. Matrix Elements in Hund's Case (a)

In a Hund's case (a) basis we specify the dependence of the matrix elements on the quantum numbers J , S , Ω , Λ , and Σ , and η denotes all other quantum numbers specifying the vibronic state. Using the algebra of irreducible tensor operators, we express all matrix elements between case (a) functions in terms of reduced matrix elements which depend only on the vibronic wavefunctions and explicit formulas depending on rotational quantum numbers. These reduced matrix elements may be regarded as the molecular parameters whose values are determined by analysis of the electron resonance spectrum. They may, of course, be calculated theoretically for any given vibronic wavefunction.

1. Purely Rotational Hamiltonian

We deal first with the purely rotational Hamiltonian.

$$\mathcal{H}'_{\mathcal{R}} = B(\mathbf{J} - \mathbf{P})^2 \quad (3.20)$$

which we expand in the form

$$\begin{aligned}
 \mathcal{H}'_{\mathbf{J}} &= B(\mathbf{J} - \mathbf{L} - \mathbf{S})^2 \\
 &= B\{\mathbf{J}^2 + \mathbf{L}^2 + \mathbf{S}^2 - 2\mathbf{J} \cdot \mathbf{L} - 2\mathbf{J} \cdot \mathbf{S} + 2\mathbf{L} \cdot \mathbf{S}\} \\
 &= B\{J(J+1) + S(S+1) + \Lambda^2\} + B(L_x^2 + L_y^2) \\
 &\quad - 2B(\mathbf{J} \cdot \mathbf{L} + \mathbf{J} \cdot \mathbf{S} - \mathbf{L} \cdot \mathbf{S}) \quad (3.21)
 \end{aligned}$$

where in the last line we have replaced the operators \mathbf{J}^2 , \mathbf{S}^2 , and L_z^2 by their eigenvalues. We neglect the term $B(L_x^2 + L_y^2)$, which affects all levels equally, and deal with the three scalar products in turn. We note in passing that the operators in (3.21) do not operate in nuclear spin space, and it is therefore not necessary to consider the coupling between \mathbf{J} and any nuclear spin or spins which may be present. We return to this point later.

We seek the matrix elements in the $|\eta J S \Omega \Lambda \Sigma M_J\rangle$ representation and because of the rotational invariance of a scalar product, the matrix elements are necessarily independent of the space projection quantum number M_J . Furthermore the conservation of total angular momentum requires that the matrix elements of a scalar product be diagonal in J . Both of these results are implicit in the Wigner-Eckart theorem.

Considering first the matrix elements of $\mathbf{J} \cdot \mathbf{L}$ we remember that \mathbf{J} obeys anomalous commutation relations in the molecular coordinate system, and therefore by Eq. (3.12),

$$\begin{aligned}
 \langle \eta J \Omega \Lambda | 2BT^1(\mathbf{J}) \cdot T^1(\mathbf{L}) | \eta' J \Omega' \Lambda' \rangle \\
 = \sum_q \langle J \Omega | \hat{T}_q^1(\mathbf{J}) | J \Omega' \rangle \langle \eta \Lambda | 2BT_q^1(\mathbf{L}) | \eta' \Lambda' \rangle \quad (3.22)
 \end{aligned}$$

By the Wigner-Eckart theorem (3.13b), Eq. (3.22) becomes

$$\begin{aligned}
 \langle \eta J \Omega \Lambda | 2BT^1(\mathbf{J}) \cdot T^1(\mathbf{L}) | \eta' J \Omega' \Lambda' \rangle \\
 = \sum_q \langle J 1 \Omega' q | J \Omega \rangle [J(J+1)]^{1/2} \langle \eta \Lambda | 2BT_q^1(\mathbf{L}) | \eta' \Lambda' \rangle \quad (3.23)
 \end{aligned}$$

The terms in which $q = \pm 1$ give rise to Λ -doubling and are particularly important in light molecules like OH, as we shall see.

The matrix elements of $\mathbf{J} \cdot \mathbf{S}$ are handled in much the same way, as follows,

$$\begin{aligned}
 \langle \eta J \Omega \Sigma | 2BT^1(\mathbf{J}) \cdot T^1(\mathbf{S}) | \eta' J \Omega' \Sigma' \rangle \\
 = \sum_q 2B_0 \langle J \Omega | \hat{T}_q^1(\mathbf{J}) | J \Omega' \rangle \langle \Sigma \Sigma' | T_q^1(\mathbf{S}) | \Sigma \rangle \\
 = 2B_0 \sum_q \langle J 1 \Omega' q | J \Omega \rangle \langle \Sigma 1 \Sigma' q | \Sigma \Sigma \rangle [J(J+1)S(S+1)]^{1/2} \quad (3.24)
 \end{aligned}$$

The appearance of $\langle \eta \Lambda | 2BT_q^{-1}(\mathbf{L}) | \eta' \Lambda' \rangle$ and B_0 in Eqs. (3.23) and (3.24), respectively, may be explained as follows. Formally we might note that the molecular constants in the Hamiltonian of Eqs. (2.122) and (2.123) should be pre- and postmultiplied by unity where unity may be written as

$$\sum_{\epsilon} |\epsilon\rangle \langle \epsilon|$$

with ϵ denoting all the electronic quantum numbers.

In other words, B symbolizes

$$\sum_{\epsilon \epsilon'} |\epsilon\rangle \langle \epsilon| \hbar^2 (M_{\alpha} + M_{\alpha'}) / (2M_{\alpha} M_{\alpha'} R^2) |\epsilon'\rangle \langle \epsilon'| \quad (3.25)$$

and B_0 symbolizes

$$\begin{aligned} \sum_{\epsilon, \epsilon'} \langle \epsilon_0 | \epsilon \rangle \langle \epsilon | \hbar^2 (M_{\alpha} + M_{\alpha'}) / (2M_{\alpha} M_{\alpha'} R^2) | \epsilon' \rangle \langle \epsilon' | \epsilon_0' \rangle \\ = \langle \epsilon_0 | \hbar^2 (M_{\alpha} + M_{\alpha'}) / (2M_{\alpha} M_{\alpha'} R^2) | \epsilon_0' \rangle \equiv B_0 \end{aligned} \quad (3.26)$$

where the last equality is valid for $\epsilon_0 = \epsilon_0'$. The precise significance of the symbol should be clear from the context.

Similarly for the $\mathbf{L} \cdot \mathbf{S}$ term we obtain the result,

$$\begin{aligned} \langle \eta J \Omega S \Lambda \Sigma | 2BT^{-1}(\mathbf{L}) \cdot T^1(\mathbf{S}) | \eta' J \Omega S \Lambda' \Sigma' \rangle \\ = \sum_q 2(-1)^q \langle \eta \Lambda | BT_q^{-1}(\mathbf{L}) | \eta' \Lambda' \rangle \langle S \Sigma | T_{-q}^{-1}(\mathbf{S}) | S \Sigma' \rangle \\ = 2 \sum_q (-1)^q \langle \eta \Lambda | BT_q^{-1}(\mathbf{L}) | \eta' \Lambda' \rangle \langle S 1 \Sigma' - q | S \Sigma \rangle [S(S+1)]^{1/2} \end{aligned} \quad (3.27)$$

We may now collect the results given in Eqs. (3.21), (3.23), (3.24), and (3.27), and obtain a general expression for the matrix elements of the rotational Hamiltonian in Hund's case (a) as follows:

$$\begin{aligned} \langle \eta J \Omega S \Lambda \Sigma M_J | \mathcal{H}'_{\mathcal{R}} | \eta' J \Omega' S \Lambda' \Sigma' M_J \rangle \\ = \delta_{\eta \eta'} \delta_{\Omega \Omega'} \delta_{\Lambda \Lambda'} \delta_{\Sigma \Sigma'} B_0 \{ J(J+1) + S(S+1) + \Lambda^2 \} \\ - 2 \delta_{\Sigma \Sigma'} \sum_q \langle J 1 \Omega' q | J \Omega \rangle [J(J+1)]^{1/2} \langle \eta \Lambda | BT_q^{-1}(\mathbf{L}) | \eta' \Lambda' \rangle \\ - 2 \delta_{\eta \eta'} \delta_{\Lambda \Lambda'} B_0 \sum_q \langle J 1 \Omega' q | J \Omega \rangle \\ \times \langle S 1 \Sigma' q | S \Sigma \rangle [J(J+1)S(S+1)]^{1/2} \\ + 2 \delta_{\Omega \Omega'} \sum_q (-1)^q \langle \eta \Lambda | BT_q^{-1}(\mathbf{L}) | \eta' \Lambda' \rangle \\ \times \langle S 1 \Sigma' - q | S \Sigma \rangle [S(S+1)]^{1/2} \end{aligned} \quad (3.28)$$

where, in each term separately, $q = 0, \pm 1$.

2. Spin-Rotation Interaction

The term in the Hamiltonian (2.122) which represents the spin-rotation interaction is

$$\sum_i (\mathbf{J} - \mathbf{P}) \cdot [\gamma_i \mathbf{S}_i + \bar{\gamma}_i \mathbf{S}_{zi} \mathbf{l}_i + \xi_i \mathbf{l}_i] \quad (3.29)$$

This term contains sums of one-electron operators and therefore the evaluation of matrix elements may be simplified by calculating the matrix element for one electron and then summing over the N electrons. Using this procedure (3.29) may be replaced by

$$\mathcal{H}'_{NS}{}^{(1)} = \gamma_1 \mathbf{S}_1 \cdot (\mathbf{J} - \mathbf{P}) + \bar{\gamma}_1 S_{z1} [\mathbf{l}_1 \cdot (\mathbf{J} - \mathbf{P})] + \xi_1 [\mathbf{l}_1 \cdot (\mathbf{J} - \mathbf{P})] \quad (3.30)$$

or

$$\begin{aligned} \mathcal{H}'_{NS}{}^{(1)} = & \gamma(\mathbf{J} \cdot \mathbf{S}_1 - \mathbf{L} \cdot \mathbf{S}_1 - \mathbf{S} \cdot \mathbf{S}_1) + \bar{\gamma} S_{z1} (\mathbf{l}_1 \cdot \mathbf{J} - \mathbf{l}_1 \cdot \mathbf{L} - \mathbf{l}_1 \cdot \mathbf{S}) \\ & + \xi (\mathbf{l}_1 \cdot \mathbf{J} - \mathbf{l}_1 \cdot \mathbf{L} - \mathbf{l}_1 \cdot \mathbf{S}) \end{aligned} \quad (3.31)$$

where the subscript on the parameters is understood. The term in $\mathbf{J} \cdot \mathbf{S}_1$ gives

$$\begin{aligned} & \langle \eta J \Omega S \Lambda \Sigma | \gamma \mathbf{J} \cdot \mathbf{S}_1 | \eta' J \Omega' S' \Lambda \Sigma' \rangle \\ &= \sum_q \langle J \Omega | \hat{T}_q^{-1}(\mathbf{J}) | J \Omega' \rangle \langle \eta S \Lambda \Sigma | \gamma T_q^{-1}(\mathbf{S}_1) | \eta' S' \Lambda \Sigma' \rangle \\ &= \sum_q \langle J 1 \Omega' q | J \Omega \rangle [J(J+1)]^{1/2} \langle S' 1 \Sigma' q | S \Sigma \rangle \\ & \quad \times \langle \eta S \Lambda \| \gamma T^1(\mathbf{S}_1) \| \eta' S' \Lambda \rangle \end{aligned} \quad (3.32)$$

Before evaluating the next term we note that from (2.118)

$$\begin{aligned} \gamma &= \sum_a \frac{Z_a e g \beta \hbar}{\mathcal{J} c r_{a1}^3} (\mathbf{r}_a \cdot \mathbf{r}_{a1}) \\ &= \sum_a \frac{Z_a e g \beta \hbar}{\mathcal{J} c r_{a1}^3} \mathbf{r}_a (\mathbf{r}_a - \mathbf{r}_{1z}) \end{aligned} \quad (3.33)$$

Therefore although γ commutes with L_z it does not commute with L_x or L_y and in terms containing L_x or L_y we must use Hermitian averages.

Thus for the term $\Delta \Lambda = 0$

$$\begin{aligned} \langle \eta J \Omega S \Lambda \Sigma | -\gamma \mathbf{L} \cdot \mathbf{S}_1 | \eta' J \Omega S' \Lambda \Sigma \rangle &= \langle \eta J \Omega S \Lambda \Sigma | -\gamma L_z S_{1z} | \eta' J \Omega S' \Lambda \Sigma \rangle \\ &= -\Lambda \langle S' 1 \Sigma 0 | S \Sigma \rangle \langle \eta S \Lambda \| \gamma T^1(\mathbf{S}_1) \| \eta' S' \Lambda \rangle \end{aligned} \quad (3.34)$$

and for the term $\Delta\Lambda = \pm 1$, $q = \pm 1$

$$\begin{aligned} & \langle \eta J \Omega S \Lambda \Sigma | \frac{1}{2} \gamma T_q^{-1}(\mathbf{L}) T_{-q}^{-1}(\mathbf{S}_1) + \frac{1}{2} T_q^{-1}(\mathbf{L}) T_{-q}^{-1}(\mathbf{S}_1) \gamma | \eta' J \Omega S' \Lambda' \Sigma' \rangle \\ &= \langle S' 1 \Sigma' - q | S \Sigma \rangle \langle \eta S \Lambda | \frac{1}{2} \gamma T_q^{-1}(\mathbf{L}) T^1(\mathbf{S}_1) + \frac{1}{2} T_q^{-1}(\mathbf{L}) T^1(\mathbf{S}_1) \gamma | \eta' S' \Lambda' \rangle \end{aligned} \quad (3.35)$$

The term $-\gamma \mathbf{S} \cdot \mathbf{S}_1$ gives the matrix elements

$$\begin{aligned} & \langle \eta J \Omega S \Lambda \Sigma | -\gamma \mathbf{S} \cdot \mathbf{S}_1 | \eta' J \Omega S' \Lambda \Sigma \rangle \\ &= \sum_q (-1)^q \langle S \Sigma | T_q^{-1}(\mathbf{S}) | S \Sigma - q \rangle \langle S \Sigma - q | \gamma T_{-q}^{-1}(\mathbf{S}_1) | S' \Sigma \rangle \\ &= \sum_q (-1)^q \langle S 1 \Sigma - q q | S \Sigma \rangle [S(S+1)]^{1/2} \\ &\quad \times \langle S' 1 \Sigma - q | S \Sigma - q \rangle \langle \eta S \Lambda | \gamma T^1(\mathbf{S}_1) | \eta' S' \Lambda \rangle \end{aligned} \quad (3.36)$$

Adding the $q = 0$ components of (3.32) and (3.36) to (3.34) and remembering $\Omega = \Lambda + \Sigma$, we see that the $q = 0$ matrix element of the first term in (3.31) vanishes.

The second term in (3.31) must be written:

$$\frac{1}{2} T_0^{-1}(\mathbf{S}_1) \{ \bar{\gamma} \mathbf{l}_1 \cdot \mathbf{J} + \mathbf{l}_1 \cdot \mathbf{J} \bar{\gamma} - \bar{\gamma} \mathbf{l}_1 \cdot \mathbf{L} - \mathbf{l}_1 \cdot \mathbf{L} \bar{\gamma} - \bar{\gamma} \mathbf{l}_1 \cdot \mathbf{S} - \mathbf{l}_1 \cdot \mathbf{S} \bar{\gamma} \} \equiv \mathcal{H}_{NS}^{(2)} \quad (3.37)$$

Using the same procedures as before this yields matrix elements for the term $\Delta\Lambda = 0$

$$\begin{aligned} & \langle \eta J \Omega S \Lambda \Sigma | \mathcal{H}_{NS}^{(2)} | \eta' J \Omega S' \Lambda \Sigma \rangle = -\frac{1}{2} \langle S' 1 \Sigma 0 | S \Sigma \rangle \\ & \langle \eta S \Lambda | \left\{ \sum_{i=x,y} \bar{\gamma} l_{1i} L_i + l_{1i} L_i \bar{\gamma} \right\} T^1(\mathbf{S}_1) | \eta' S' \Lambda \rangle \end{aligned} \quad (3.38)$$

and for the term $\Delta\Lambda = \pm 1$, $q = \pm 1$

$$\begin{aligned} & \langle \eta J \Omega S \Lambda \Sigma | \mathcal{H}_{NS}^{(2)} | \eta' J \Omega S' \Lambda' \Sigma' \rangle \\ &= \frac{1}{2} \langle S' 1 \Sigma 0 | S \Sigma \rangle \langle J 1 \Omega' q | J \Omega \rangle [J(J+1)]^{1/2} \\ &\quad \times \langle \eta S \Lambda | \{ \bar{\gamma} l_{1q} + l_{1q} \bar{\gamma} \} T^1(\mathbf{S}_1) | \eta' S' \Lambda' \rangle \end{aligned} \quad (3.39)$$

and

$$\begin{aligned} & \langle \eta J \Omega S \Lambda \Sigma | \mathcal{H}_{NS}^{(2)} | \eta' J \Omega S' \Lambda' \Sigma' \rangle \\ &= -\frac{1}{2} \langle S' 1 \Sigma 0 | S \Sigma \rangle \langle S' 1 \Sigma' q | S' \Sigma \rangle [S(S+1)]^{1/2} \\ &\quad \times \langle \eta S \Lambda | \{ \bar{\gamma} l_{1q} + l_{1q} \bar{\gamma} \} T^1(\mathbf{S}_1) | \eta' S' \Lambda' \rangle \end{aligned} \quad (3.40)$$

The last term in (3.31), $\mathcal{H}_{NS}^{(3)}$, may be handled in exactly the same way.

Since this term does not contain S_{z1} there is no Σ dependence and the $\Delta\Lambda = 0$ matrix element is a constant within a given electronic state and cannot be further reduced on symmetry grounds alone. The $\Delta\Lambda = \pm 1$ $q = \pm 1$ terms are

$$\begin{aligned} \langle \eta J \Omega S \Lambda \Sigma | \mathcal{H}_{NS}^{(3)} | \eta' J \Omega' S' \Lambda' \Sigma' \rangle \\ = \frac{1}{2} \langle J 1 \Omega' q | J \Omega \rangle [J(J+1)]^{1/2} \langle \eta S \Lambda \| \xi l_{1q} + l_{1q} \xi \| \eta' S' \Lambda' \rangle \end{aligned} \quad (3.41)$$

$$\begin{aligned} \langle \eta J \Omega S \Lambda \Sigma | \mathcal{H}_{NS}^{(3)} | \eta' J \Omega S' \Lambda' \Sigma' \rangle \\ = -\frac{1}{2} \langle S 1 \Sigma' q | S \Sigma \rangle [S(S+1)]^{1/2} \langle \eta S \Lambda \| \xi l_{1q} + l_{1q} \xi \| \eta' S' \Lambda' \rangle \end{aligned} \quad (3.42)$$

In summary the matrix elements arising from the spin-rotation interaction are ($q = 0, \pm 1$ except where otherwise noted)

$$\begin{aligned} \langle \eta J \Omega S \Lambda \Sigma M_J | \mathcal{H}_{NS} | \eta' J \Omega S' \Lambda \Sigma M_J \rangle \\ = -\gamma_1 \sum_{q=\pm 1} \langle S 1 \Sigma - q q | S \Sigma \rangle \langle S' 1 \Sigma - q | S \Sigma - q \rangle \\ \times [S(S+1)]^{1/2} - \hbar \gamma_3 \langle S' 1 \Sigma 0 | S \Sigma \rangle + \gamma_5 \delta_{SS'} \end{aligned} \quad (3.43)$$

$$\begin{aligned} \langle \eta J \Omega S \Lambda \Sigma M_J | \mathcal{H}_{NS} | \eta' J \Omega' S' \Lambda \Sigma' M_J \rangle \\ = \gamma_1 \langle J 1 \Omega' q | J \Omega \rangle [J(J+1)]^{1/2} \langle S' 1 \Sigma' q | S \Sigma \rangle \end{aligned} \quad (3.44)$$

$$\begin{aligned} \langle \eta J \Omega S \Lambda \Sigma M_J | \mathcal{H}_{NS} | \eta' J \Omega S' \Lambda' \Sigma' M_J \rangle \\ = \gamma_2 \langle S' 1 \Sigma' - q | S \Sigma \rangle - \frac{1}{2} \gamma_4 \langle S' 1 \Sigma 0 | S \Sigma \rangle \langle S' 1 \Sigma' q | S \Sigma \rangle [S(S+1)]^{1/2} \\ - \frac{1}{2} \gamma_6 \langle S 1 \Sigma' q | S \Sigma \rangle [S(S+1)]^{1/2} \delta_{SS'} \end{aligned} \quad (3.45)$$

$$\begin{aligned} \langle \eta J \Omega S \Lambda \Sigma M_J | \mathcal{H}_{NS} | \eta' J \Omega' S' \Lambda' \Sigma' M_J \rangle \\ = \frac{1}{2} \gamma_4 \langle S' 1 \Sigma 0 | S \Sigma \rangle \langle J 1 \Omega' q | J \Omega \rangle [J(J+1)]^{1/2} \\ + \frac{1}{2} \gamma_6 \langle J 1 \Omega' q | J \Omega \rangle [J(J+1)]^{1/2} \delta_{SS'} \end{aligned} \quad (3.46)$$

where

$$\gamma_1 = \sum_i \langle \eta S \Lambda \| \gamma_i T^1 S_i \| \eta' S' \Lambda \rangle \quad (3.47)$$

$$\gamma_2 = \sum_i \langle \eta S \Lambda \| \{ \gamma_i T_q^{-1}(\mathbf{L}) + T_q^1(\mathbf{L}) \gamma_i \} T^1(S_i) \| \eta' S' \Lambda' \rangle \quad (3.48)$$

$$\gamma_3 = \sum_i \langle \eta S \Lambda \| \left\{ \sum_{j=x,y} \bar{\gamma}_i l_{ij} L_j + l_{ij} L_j \bar{\gamma}_i \right\} T^1(S_i) \| \eta' S' \Lambda \rangle \quad (3.49)$$

$$\gamma_4 = \sum_i \langle \eta S \Lambda \| \{ \bar{\gamma}_i l_{iq} + l_{iq} \bar{\gamma}_i \} T^1(S_i) \| \eta' S' \Lambda' \rangle \quad (3.50)$$

$$\gamma_5 = \sum_i \langle \eta J \Omega S \Lambda \Sigma M_J | \xi_i (l_{xi} L_x + l_{yi} L_y) + (l_{xi} L_x + l_{yi} L_y) \xi_i | \eta' J \Omega S \Lambda \Sigma M_J \rangle \quad (3.51)$$

$$\gamma_6 = \sum_i \langle \eta S \Lambda \| \xi_i l_{qi} + l_{qi} \xi_i \| \eta' S \Lambda' \rangle \quad (3.52)$$

In Eqs. (3.47)–(3.52) we have summed over the i electrons. It should be noted that the summation requires the observance of a particular convention for the reduced matrix elements $T^k(S_i)$. This convention requires that the reduced matrix element of $T^k(S_i)$ vanish unless S_i makes a nonvanishing contribution to S . Without this convention these reduced matrix elements are not well defined.

3. Fine-Structure Hamiltonian

The required matrix elements are of the form

$$\begin{aligned} & \langle \eta J \Omega S \Lambda \Sigma | \sum_i A_i T^1(S_i) \cdot T^1(l_i) | \eta' J \Omega S' \Lambda' \Sigma' \rangle \\ &= \sum_i \sum_q (-1)^q \langle S' 1 \Sigma' q | S \Sigma \rangle \langle \eta S \Lambda \| A_i T_{-q}^{-1}(l_i) T^1(S_i) \| \eta' S' \Lambda' \rangle \\ & \quad \times \delta_{\Lambda', \Lambda - \Sigma' + \Sigma} \end{aligned} \quad (3.53)$$

It is difficult to develop this equation further but one can examine certain particular cases which arise frequently in our electron resonance studies.

We will assume that S_i is independent of the quantum number η which, for instance, will be true if η is a configuration label. In this case we may factor the reduced matrix element and obtain the product

$$\langle S \| T^1(S_i) \| S' \rangle \langle \eta \Lambda | A_i T_{-q}^{-1}(l_i) \| \eta' \Lambda' \rangle$$

It is then possible to express the first factor of the product in terms of the total spin. For large numbers of electrons this expression can be very complicated and will not be treated here. However, if only one or two electrons must be considered, then the expression may take a simple form. As noted previously, in the reduced matrix elements only the unpaired electrons contribute to the sum over i as only those electrons contribute to the total spin. Thus if $S = 1/2$ it (in this single configuration approximation) is equivalent to S_i so we may write,

$$\begin{aligned} \langle S = \frac{1}{2} \| T^1(S_i) \| S = \frac{1}{2} \rangle &= \langle S = \frac{1}{2} \| T^1(S) \| S = \frac{1}{2} \rangle \\ &= [S(S+1)]^{1/2} = (3/4)^{1/2} \end{aligned} \quad (3.54)$$

If $S = 1$, then we may couple the relevant electrons S_1 and S_2 together to obtain S , then the reduced matrix elements of S_1 and S_2 are the same and given by

$$\langle S = 1, S_1, S_2 \| T^1(S_1) \| S = 1, S_1, S_2 \rangle = (-1)^{S-1} [2(2S+1)]^{1/2} \\ \times W(\frac{1}{2}\frac{1}{2}SS; 1\frac{1}{2}) \langle S_1 \| T^1(S_1) \| S_1 \rangle = 1/\sqrt{2} \quad (3.55)$$

A particularly simple case occurs for $S = 1/2$ where, under these assumptions, the reduced matrix element of the orbital operator becomes $A\Lambda$ and the total matrix element reduces to $A\Lambda\Sigma$. The same result is also obtained for the diagonal elements when $S = 1$. However, one should take care not to neglect the matrix elements off-diagonal in S for these can also be quite important, especially in $^3\Sigma$ molecules.

It there is more than one unpaired electronic spin then the second term of \mathcal{H}_{fs} involving the interaction of these spins must be taken into account. We then write

$$\mathcal{H}_{ss} = -g^2\beta^2 \sum_{i,j>i} \left[\frac{8\pi}{3} \delta(r_{ji})(\mathbf{S}_i \cdot \mathbf{S}_j) + T^2(\mathbf{S}_i, \mathbf{S}_j) \cdot C^2(\omega_{ij}) r_{ij}^{-3} \sqrt{6} \right] \quad (3.55a)$$

The first term of H_{ss} is a tensor of rank zero involving only spin variables. It may thus only shift the energy of the entire electronic state and may be neglected.

The matrix elements of the second term may be written generally as

$$\langle \eta J \Omega S \Lambda \Sigma | \sum_{i,j>i} \sqrt{6} T^2(\mathbf{S}_i, \mathbf{S}_j) \cdot C^2(\omega_{ij}) r_{ij}^{-3} | \eta' J \Omega S' \Lambda' \Sigma' \rangle \\ = \sum_{i,j>i,q} (-1)^q \langle S' 2 \Sigma' q | S \Sigma \rangle \langle \eta S \Lambda \| \sqrt{6} r_{ij}^{-3} \\ \times T^2(\mathbf{S}_i, \mathbf{S}_j) C_q^2(\omega_{ij}) \| \eta' S' \Lambda \rangle \delta_{\Lambda', \omega - \Sigma' + \Sigma} \quad (3.55b)$$

As with the spin-orbit interaction, no further general reduction is possible. However if the assumption of η independence is again made, the reduced matrix element of $T^2(\mathbf{S}_i, \mathbf{S}_j)$ may be simplified for special cases. The most important special case is for $S = S' = 1$. Then²⁴

$$\langle S S_1 S_2 \| T^2(\mathbf{S}_1, \mathbf{S}_2) \| S S_1 S_2 \rangle = (5/12)^{1/2} \quad (3.56)$$

Thus yielding

$$\langle \eta J \Omega S = 1 \Lambda \Sigma | \sum_{i,j>i} \sqrt{6} T^2(\mathbf{S}_i, \mathbf{S}_j) \cdot C^2(\omega_{ij}) \\ \times r_{ij}^{-3} | \eta' J \Omega S = 1 \Lambda' \Sigma' \rangle \\ = \sum_{q,i,j>i} (-1)^q \sqrt{5/2} \langle S 2 \Sigma' q | S \Sigma \rangle \\ \times \langle \eta \Lambda \| r_{ij}^{-3} C_q^2(\omega_{ij}) \| \eta' \Lambda' \rangle \delta_{\Lambda', \Lambda - \Sigma' + \Sigma} \quad (3.57)$$

4. Nuclear Magnetic and Electric Hyperfine Structure

We now turn to consider effects arising from the presence of nuclei with spin. We will confine ourselves to diatomic molecules with one magnetic nucleus only, since nearly all electron resonance studies so far reported deal with molecules of this type. At the end of this section we outline procedures for the extension of the theory to more than one nucleus. Using a Hund's case (a) representation, there are at least two important ways of including nuclear spin variables in the basis functions. The first vector coupling possibility is illustrated in Figure 1; \mathbf{I} is coupled to the total angular momentum \mathbf{J} to form a grand total angular momentum \mathbf{F} . The case (a) basis functions are then written $|\eta I J F \Omega S \Lambda \Sigma M_F\rangle$, where M_F is the space-projection of \mathbf{F} . We refer to this as the Hund's case (a) coupled representation. The second possibility is to use a decoupled representation $|\eta I M_I J M_J\rangle$ in which the space projections of \mathbf{I} and \mathbf{J} are separated. Both coupled and decoupled representations have been used in electron resonance studies, and we will therefore calculate the matrix elements in both representations.

The magnetic hyperfine interaction is represented by three terms in the Hamiltonian (2.122) which are (omitting the sum over the α nuclei),

$$\mathcal{H}_{mhf} = \sum_i \left\{ (a_i + a'_i) T^1(\mathbf{I}) \cdot T^1(\mathbf{l}_i) + \left[\frac{8\pi}{3} \delta(\mathbf{r}_{ai}) T^1(\mathbf{S}_i) \cdot T^1(\mathbf{I}) + \sqrt{10} r_{ai}^{-3} T^1(\mathbf{I}) \cdot T^1(\mathbf{S}_i, C^2) \right] \right\} g \beta \beta_N g_\alpha \quad (3.58)$$

which we rewrite simply as

$$\mathcal{H}_{mhf} = \sum_i \{ \bar{a}_i T^1(\mathbf{I}) \cdot T^1(\mathbf{l}_i) + b_i T^1(\mathbf{S}_i) \cdot T^1(\mathbf{I}) + c_i T^1(\mathbf{I}) \cdot T^1(\mathbf{S}_i, C^2) \} \quad (3.59)$$

where we note that $\bar{a}_i = a_i$ if $\Lambda = \Lambda'$. The first term in (3.58) describes the interaction of the nuclear spin with the orbital moment of the electrons, the second term is the Fermi contact term, and the third is the electron-nuclear dipolar interaction.

In both the coupled and decoupled representations we are assuming space-quantization of the nuclear spin and it is therefore most convenient to expand the scalar products in (3.59) in terms of space-fixed coordinates q' . On the other hand, the reduced matrix elements of $T^1(\mathbf{l}_i)$, $T^1(\mathbf{S}_i)$, and $T^1(\mathbf{S}_i, C^2)$ will usually be evaluated in the molecular coordinate system. We therefore expand the scalar products by transforming these three first-rank tensors from molecular to space-fixed axes using a first-rank rotation matrix.

We use first the coupled representation and illustrate the procedure followed with the $I \cdot I_i$ term in (3.59). We then give a procedure for obtaining the decoupled matrix elements from the coupled ones. In the section on case (b) matrix elements we reverse this procedure. Transforming $T^1(I_i)$ into space-fixed axes we expand the scalar product,

$$T^1(I) \cdot T^1(I_i) = \sum_{qq'} (-1)^{q'} T_q^{1*}(I) D_{-q'q}^{1*} T_q^1(I_i) \quad (3.60)$$

and use (3.17) to determine the F dependence. One finds:

$$\begin{aligned} & \langle \eta I J F \Omega S \Lambda \Sigma M_F | \sum_i \bar{a}_i T^1(I) \cdot T^1(I_i) | \eta' I' J' F' \Omega' S' \Lambda' \Sigma' M_F' \rangle \\ &= (-1)^{F-I-J'} [(2I+1)(2J+1)]^{1/2} \delta_{FF'} \delta_{M_F M_F'} W(I I J J'; 1 F) \\ & \quad \times \langle I || T^1(I) || I \rangle \sum_q \langle J \Omega || D_{-q}^{1*} || J' \Omega' \rangle \langle \eta \Lambda || \sum_i \bar{a}_i T_q^1(I_i) | \eta' \Lambda' \rangle \end{aligned} \quad (3.61)$$

where we have neglected excited nuclear states. The reduced matrix element of $T^1(I)$ is readily found to be

$$\langle I || T^1(I) || I \rangle = [I(I+1)]^{1/2} \quad (3.62)$$

The reduced matrix element of D_{-q}^{k*} is defined by the Wigner-Eckart theorem:

$$\begin{aligned} \langle J \Omega M_J | D_{-q}^{k*} | J' \Omega' M_J' \rangle &= \langle J' k M_J' - q' | J M_J \rangle \\ & \quad \times \langle J \Omega || D_{-q}^{k*} || J' \Omega' \rangle \end{aligned} \quad (3.63)$$

We express the rotational wavefunctions in terms of rotational matrices, so that,

$$\begin{aligned} & \langle J \Omega M_J | D_{-q}^{k*} | J' \Omega' M_J' \rangle \\ &= [(2J+1)(2J'+1)]^{1/2} / 8\pi^2 \int D_{M_J \Omega}^J D_{-q'q}^{k*} D_{M_J' \Omega'}^{J'*} \\ &= \left(\frac{2J'+1}{2J+1} \right)^{1/2} \langle J' k \Omega' q | J \Omega \rangle \langle J' k M_J' - q' | J M_J \rangle \end{aligned} \quad (3.64)$$

Equation (3.64) is derived by making use of the standard result^{10,12} for reducing the integral of a product of three rotational matrices to a product of two Clebsch-Gordon coefficients. Comparison of (3.64) and (3.63) yields the result

$$\langle J \Omega || D_{-q}^{k*} || J' \Omega' \rangle = \left(\frac{2J'+1}{2J+1} \right)^{1/2} \langle J' k \Omega' q | J \Omega \rangle \quad (3.65)$$

and substitution of (3.65) into (3.61) with $k = 1$ gives a general expression for the matrix elements of $T^1(\mathbf{I}) \cdot T^1(\mathbf{I}_i)$,

$$\begin{aligned} & \langle \eta I J F \Omega S \Lambda \Sigma M_F | \sum_i \bar{a}_i T^1(\mathbf{I}) \cdot T^1(\mathbf{I}_i) | \eta' I' J' F \Omega' S \Lambda' \Sigma' M_F \rangle \\ &= (-1)^{F-I-J'} [I(I+1)(2I+1)(2J'+1)]^{1/2} W(I I J J'; 1 F) \\ & \times \sum_q \langle J' 1 \Omega' q | J \Omega \rangle \langle \eta \Lambda \| \sum_i \bar{a}_i T_q^1(\mathbf{I}_i) \| \eta' \Lambda' \rangle \end{aligned} \quad (3.66)$$

In all cases studied so far, we can confine ourselves to a given electronic state and putting $q = 0$ in (3.66) we obtain the simplified result

$$\begin{aligned} & \langle \eta I J F \Omega S \Lambda \Sigma M_F | \sum_i \bar{a}_i T^1(\mathbf{I}) \cdot T^1(\mathbf{I}_i) | \eta' I' J' F \Omega S \Lambda \Sigma M_F \rangle \\ &= (-1)^{F-I-J'} [I(I+1)(2I+1)(2J'+1)]^{1/2} W(I I J J'; 1 F) \\ & \quad \langle J' 1 \Omega 0 | J \Omega \rangle \Lambda a \end{aligned} \quad (3.67)$$

where a denotes an average value of the parameter a_i for the electrons making a nonvanishing contribution to \mathbf{L} .

The second term in (3.59), the Fermi contact term, is handled in exactly the same way. We transform $T^1(\mathbf{S}_i)$ from molecular to spatial axes and obtain the expression

$$\begin{aligned} & \langle \eta I J F \Omega S \Lambda \Sigma M_F | \sum_i b_i T^1(\mathbf{S}_i) \cdot T^1(\mathbf{I}) | \eta' I' J' F \Omega' S' \Lambda' \Sigma' M_F \rangle \\ & \times (-1)^{F-I-J'} [I(I+1)(2I+1)(2J'+1)]^{1/2} W(I I J J'; 1 F) \\ & \times \sum_q \langle J' 1 \Omega' q | J \Omega \rangle \langle S' 1 \Sigma' q | S \Sigma \rangle \langle \eta S \| \sum_i b_i T^1(\mathbf{S}_i) \| \eta' S' \rangle \end{aligned} \quad (3.68)$$

The reduced matrix element of $T^1(\mathbf{S}_i)$ in (3.36) is readily evaluated in any given case. If, for example, $S = 1/2$ and we confine attention to a single configuration electronic state we obtain

$$\begin{aligned} \langle \eta S \| \sum_i b_i T^1(\mathbf{S}_i) \| \eta' S' \rangle &= \langle \eta S \| b T^1(\mathbf{S}) \| \eta S \rangle \\ &= b_\eta [S(S+1)]^{1/2} \end{aligned} \quad (3.69)$$

where

$$b_\eta = \frac{8\pi}{3} \eta^2(0) g \beta \beta_N g_N \quad (3.70)$$

$\eta^2(0)$ is, of course, the amplitude of the wavefunction at the nucleus.

The third term in the magnetic hyperfine Hamiltonian (3.59) is the electron-nuclear dipolar interaction. Following the procedure already outlined we first obtain

$$\begin{aligned}
& \langle \eta I J F \Omega S \Lambda \Sigma M_F | \sum_i c_i T^1(\mathbf{I}) \cdot T^1(\mathbf{S}_i, C^2) | \eta' I' J' F \Omega' S' \Lambda' \Sigma' M_F \rangle \\
& = (-1)^{F-I-J'} [I(I+1)(2I+1)(2J'+1)]^{1/2} W(IIJJ'; 1F) \\
& \quad \times \sum_q \langle J' 1 \Omega' q | J \Omega \rangle \langle \eta S \Lambda \Sigma \| \sum_i c_i T_q^1(\mathbf{S}_i, C^2) \| \eta' S' \Lambda' \Sigma' \rangle \quad (3.71)
\end{aligned}$$

We are therefore left to evaluate the reduced matrix elements of $T_q^1(\mathbf{S}_i, C^2)$ in the molecular coordinate system. We recall that the tensor is constructed according to the equation

$$T_q^1(\mathbf{S}_i, C^2) = - \sum_{q_1, q_2} T_{q_1}^1(\mathbf{S}_i) C_{q_2}^2(\omega_{ai}) \langle 12q_1 q_2 | 1q \rangle \quad (3.72)$$

and by the Wigner-Eckart theorem.

$$\begin{aligned}
& \langle \eta S \Lambda \Sigma \| \sum_i c_i T_q^1(\mathbf{S}_i, C^2) \| \eta' S' \Lambda' \Sigma' \rangle \\
& = - \sum_{q_1, q_2} \langle 12q_1 q_2 | 1q \rangle \langle S' 1 \Sigma' q_1 | S \Sigma \rangle \\
& \quad \times \langle \eta S \Lambda \| \sum_i c_i T^1(\mathbf{S}_i) C_{q_2}^2(\omega_{ai}) \| \eta' S' \Lambda' \rangle \quad (3.73)
\end{aligned}$$

Combining Eqs. (3.73) and (3.71) we obtain the general result,

$$\begin{aligned}
& \langle \eta I J F \Omega S \Lambda \Sigma M_F | \sum_i c_i T^1(\mathbf{I}) \cdot T^1(\mathbf{S}_i, C^2) | \eta' I' J' F \Omega' S' \Lambda' \Sigma' M_F \rangle \\
& = (-1)^{F-I-J'+1} [I(I+1)(2I+1)(2J'+1)]^{1/2} W(IIJJ'; 1F) \\
& \quad \times \sum_{q_1, q_2} \langle J' 1 \Omega' q | J \Omega \rangle \langle 12q_1 q_2 | 1q \rangle \langle S' 1 \Sigma' q_1 | S \Sigma \rangle \\
& \quad \times \langle \eta S \Lambda \| \sum_i c_i T^1(\mathbf{S}_i) C_{q_2}^2(\omega_{ai}) \| \eta' S' \Lambda' \rangle \quad (3.74)
\end{aligned}$$

We are usually interested only in the terms diagonal in η , S , and Λ . By the usual approximations it is then possible to factor out the spin-dependent part of the reduced matrix elements in (3.74), i.e.,

$$\begin{aligned}
& \langle \eta S \Lambda \| \sum_i c_i T^1(\mathbf{S}_i) C_{q_2}^2(\omega_{ai}) \| \eta S \Lambda \rangle \\
& = \sum_i \langle S \| T^1(\mathbf{S}_i) \| S \rangle \langle \eta \Lambda \| c_i C_{q_2}^2(\omega_{ai}) \| \eta \Lambda \rangle \quad (3.75)
\end{aligned}$$

In the particular case of $S = 1/2$, we use (3.54) to evaluate the reduced matrix element of $T^1(\mathbf{S}_i)$ and we also note that

$$\langle \eta \Lambda \| c_i C_0^2(\omega_{ai}) \| \eta \Lambda \rangle = \frac{1}{2} \langle (3 \cos^2 \theta_{ai} - 1) r_{ai}^{-3} \rangle_{\eta} g \beta_N I_N g_a \sqrt{10} \quad (3.76)$$

where θ is the angle \mathbf{r}_{ai} makes with the z axis. Thus, confining attention to a given electronic state, we obtain the general result for $S = 1/2$

$$\begin{aligned}
& \langle \eta I J F \Omega \Lambda \Sigma M_F | \sum_i c_i T^1(\mathbf{I}) \cdot T^1(\mathbf{S}_i, C^2) | \eta I J' F' \Omega' \Lambda' \Sigma' M_F' \rangle \\
&= [(10)^{1/2}/4] (-1)^{F-I-J'+1} [I(I+1)(2I+1)(2J'+1)]^{1/2} \\
&\quad \times W(IIJJ'; 1F) \sum_q \langle J' 1 \Omega' q | J \Omega \rangle \langle 1 q 2 0 | 1 q \rangle \\
&\quad \times \langle S' 1 \Sigma' q | S \Sigma \rangle \langle (3 \cos^2 \theta_{ai} - 1) r_{ai}^{-3} \rangle_{\eta} g \beta_N g_{\alpha} \quad (3.77)
\end{aligned}$$

The term in the Hamiltonian (2.122) which represents the nuclear electric quadrupole interaction for a single nucleus is

$$\mathcal{H}_Q = \sum_c \frac{e^2 Q \sqrt{3c}}{I(2I-1) \sqrt{2} r_{ac}^3} T^2(\mathbf{I}) \cdot C^2(\omega_{ac}) \quad (3.78)$$

where Q is the nuclear quadrupole moment, defined in equation (2.96). We expand the scalar product in space-fixed axes and the matrix elements in the coupled representation are given by

$$\begin{aligned}
& \langle \eta I J F \Omega \Lambda \Sigma M_F | \mathcal{H}_Q | \eta' I' J' F' \Omega' \Lambda' \Sigma' M_F' \rangle \\
&= \sum_{c,q} \frac{e^2 Q \sqrt{3c}}{I(2I-1) \sqrt{2}} (-1)^{F-I-J'} \delta_{FF'} \delta_{M_F M_F'} [(2I+1)(2J'+1)]^{1/2} \\
&\quad \times W(IIJJ'; 2F) \langle I \| T^2(\mathbf{I}) \| I \rangle \\
&\quad \times \langle \eta \Lambda \| r_{ac}^{-3} C_q^2(\omega_{ac}) \| \eta' \Lambda' \rangle \langle J \Omega \| D_q^{2*} \| J' \Omega' \rangle \quad (3.79)
\end{aligned}$$

We evaluate the reduced matrix element of $T^2(\mathbf{I})$ by decomposing the second-rank tensor into its constituent first-rank tensors, using the result

$$T_q^2(\mathbf{I}) = \sum_{q_1 q_2} \langle 11 q_1 q_2 | 2q \rangle T_{q_1}^1(\mathbf{I}) T_{q_2}^1(\mathbf{I}) \quad (3.80)$$

One then finds that

$$\langle I \| T^2(\mathbf{I}) \| I \rangle = (1/6)^{1/2} I(2I-1) \langle I 2 I 0 | I I \rangle^{-1} \quad (3.81)$$

Using the result of (3.65) for a second-rank rotation matrix, we obtain the required general result,

$$\begin{aligned}
& \langle \eta I J F \Omega \Lambda \Sigma M_F | \mathcal{H}_Q | \eta' I' J' F' \Omega' \Lambda' \Sigma' M_F' \rangle \\
&= \frac{e^2 Q}{2} \sum_{c,q} (-1)^{F-I-J'} \delta_{FF'} \delta_{M_F M_F'} [(2I+1)(2J'+1)]^{1/2} \\
&\quad \times W(IIJJ'; 2F) \langle I 2 I 0 | I I \rangle^{-1} \langle J' 2 \Omega' q | J \Omega \rangle \\
&\quad \times \langle \eta \Lambda \| r_{ac}^{-3} C_q^2(\omega_{ac}) \| \eta' \Lambda' \rangle \quad (3.82)
\end{aligned}$$

If we confine attention to matrix elements diagonal in Λ , putting $q = 0$, we may conventionally replace the reduced matrix element in (3.82) (summed over c) by $\frac{1}{2}q_0$, the axial component of the electric field gradient.

If we wish the matrix elements of the hyperfine operators in a decoupled representation it is possible to obtain these from the matrix elements in the coupled representation. To obtain matrix elements in a decoupled $|JM_JIM_I\rangle$ representation from those of the coupled $|JIFM_F\rangle$ representation one must simply multiply the latter by the appropriate factor to remove the F dependence and restore the M_I and M_J dependence. From Eq. (3.17) and the Wigner-Eckart theorem it is easily seen that the appropriate factor \mathcal{F} , is

$$\mathcal{F} = [(2J+1)(2I+1)]^{-1/2} (-1)^{J'+I-F} [W(JJ'II; kF)]^{-1} \\ \times \sum_q \langle J'kM_J'q | JM_J \rangle \langle IkM_I' - q | IM_I \rangle (-1)^q \quad (3.83)$$

where the summation over q runs over all positive and negative integers such that $q \leq k$, with k being the rank of the tensorial operators involved the matrix element.

5. Interaction with the External Magnetic Field

The magnetic field terms in (2.122) are

$$\mathcal{H}_H = \sum_i \{ \beta T^1(\mathbf{H}) [g_s^i T^1(\mathbf{S}_i) + g_l^i T^1(\mathbf{I}_i)] + \beta \Delta g^i T_0^1(\mathbf{H}) \\ \times T_0^1(\mathbf{S}_i) - g_r \beta T^1(\mathbf{H}) \cdot T^1(\mathbf{J} - \mathbf{I}_i - \mathbf{S}_i) \} - \beta_N g_N T^1(\mathbf{H}) \cdot T^1(\mathbf{I}) \quad (3.84)$$

Since the $q' = 0$ direction is defined by the direction of the external magnetic field, we expand in spatial axes,

$$\mathcal{H}_H = \sum_i \left\{ \beta H \sum_q D_{0q}^{-1*} [(g_s^i + g_r + \Delta g^i \delta_{q0}) T_q^1(\mathbf{S}_i) \right. \\ \left. + (g_l^i + g_r) T_q^1(\mathbf{I}_i) - g_r T_q^1(\mathbf{J})] \right\} - \beta_N g_N T^1(\mathbf{H}) \cdot T^1(\mathbf{I}) \quad (3.85)$$

The evaluation of the matrix elements is now straightforward. In the coupled representation one finds*

* Though Eq. (3.86) gives the matrix elements of \mathcal{H}_H for all states, it is important to remember that the corrections to the free electron g values were only defined for electronically diagonal matrix elements. For the off-diagonal elements, it should suffice to replace g_s^i and g_l^i by their free electron values.

$$\begin{aligned}
& \langle \eta I J F \Omega S \Lambda \Sigma M_F | \mathcal{H}_H | \eta' I' J' F' \Omega' S' \Lambda' \Sigma' M_F' \rangle \\
&= \beta H \sum_{i,q} (-1)^{J'-I+F'-1} \langle F' 1 M_F' 0 | F M_F \rangle [(2F' + 1)(2J' + 1)]^{1/2} \\
&\quad \times W(JJ'FF'; 1I) \langle J' 1 \Omega' q | J \Omega \rangle \{ (g_s^i + g_r + \Delta g^i \delta_{q0}) \\
&\quad \times \langle S' 1 \Sigma' q | S \Sigma \rangle \langle S || T^1(S_i) || S' \rangle + (g_l^i + g_r) \\
&\quad \times \langle \eta \Lambda || T_q^1(I_i) || \eta' \Lambda' \rangle \delta_{SS'} \delta_{\Sigma\Sigma'} - g_r \langle J' 1 \Omega' q | J \Omega \rangle \\
&\quad \times [J(J+1)]^{1/2} \delta_{JJ'} \delta_{SS'} \delta_{\Lambda\Lambda'} \delta_{\Omega\Omega'} \} - g_N \beta_N H (-1)^{I-J+F-1} \\
&\quad \times [(2F' + 1)(2I + 1)I(I+1)]^{1/2} W(IIF F'; 1J) \\
&\quad \times \langle F' 1 M_F' 0 | F M_F \rangle \delta_{JJ'} \delta_{\Omega\Omega'} \delta_{\Lambda\Lambda'} \quad (3.86)
\end{aligned}$$

To obtain the matrix elements in a decoupled representation we multiply all save the last term of (3.86) by

$$\langle J' 1 M_J' 0 | J M_J \rangle / \{ (-1)^{F'+J-1-I} W(JJ' F' F; 1I) [(2F' + 1)(2J + 1)]^{1/2} \}$$

and the last term by

$$\begin{aligned}
& \langle I 1 M_I' 0 | I M_I \rangle / \{ \langle F' 1 M_F' 0 | F M_F \rangle (-1)^{F-I-1-J} [(2F' + 1)(2I + 1)]^{1/2} \\
&\quad \times W(IIF F'; 1J) \}
\end{aligned}$$

Finally, we should indicate the methods for obtaining the matrix elements of the nuclear spin dependent terms of the Hamiltonian when more than one nuclear spin is present. If a decoupled representation is chosen the problem is very simple for then one simply multiplies each of the basis kets by a further basis ket $|I_2 M_{I_2}\rangle$ and continues to derive the total matrix element exactly as the matrix element for one nuclear spin is derived. (See Section III.C.)

If, however, one chooses a coupled representation, things are somewhat complicated by the existence of more than one nuclear spin as several coupling arrangements are then possible. Probably the most useful arrangement is the coupling of the two nuclear spins together to form a total nuclear spin I_T . The matrix elements may then be worked out using the technique illustrated previously. In this case it must be remembered that I_T is not necessarily a good quantum number and matrix elements off-diagonal in I_T must be included. If, however, the nuclei are equivalent it can easily be shown that no nuclear spin interaction tensor of order less than two can have matrix elements connecting states of different I_T .

C. Matrix Elements in Hund's Case (*b*)

The matrix elements of the case (*b*) Hamiltonian can be obtained by much the same procedures as employed for the case (*a*) matrix elements. We shall therefore treat their derivation in less detail. We also treat the terms of \mathcal{H} in a different order than in Section III.B making use of the results for one operator in the derivation of the matrix elements of another. In obtaining these results we remember that in case (*b*), the electronic spin is quantized in the space-fixed coordinate system and \mathbf{K} is added vectorally to it to form a resultant \mathbf{J} .

1. Fine-Structure Hamiltonian

To obtain the matrix elements of the first term of \mathcal{H}_f , we must relate the space-fixed and molecule-fixed components of $A_i I_i$ via a first-rank rotational matrix. Thus we find in irreducible tensor notation,

$$\begin{aligned}
 & \langle \eta \Lambda K S J | \sum_i T^1(A_i I_i) \cdot T^1(S_i) | \eta' \Lambda' K' S' J' \rangle \\
 &= \langle \eta \Lambda K S J | \sum_{i, q, q'} (-1)^q D_{qq'}^{1*} T_q^{-1}(A_i I_i) T_{-q}^{-1}(S_i) | \eta' \Lambda' K' S' J' \rangle \\
 &= \sum_i \langle \eta \Lambda \| T_q^{-1}(A_i I_i) T^1(S_i) \| \eta' S' \rangle \\
 &\quad \times [(2K' + 1)(2S + 1)]^{1/2} (-1)^{J-S-K'} W(SS'KK'; 1J) \\
 &\quad \times \delta_{JJ'} \langle K' 1 \Lambda' q' | K \Lambda \rangle
 \end{aligned} \tag{3.87}$$

As in case (*a*) no more rigorous simplification of the matrix element is possible; however, the development outlined between Eqs. (3.54) and (3.55) is equally applicable to case (*b*) and may often constitute an excellent further simplification of Eq. (3.87). To apply these simplifications it suffices that the reduced matrix element of $T^1(S_i)$ be independent of η .

We now turn to the second term of \mathcal{H}_f , which gives the interaction of the electronic spins with one another. The first part of this interaction, the electronic analogue of the Fermi contact term of \mathcal{H}_{hf} , being proportional to $(S_i \cdot S_j)$ and $\delta(\mathbf{r}_{ij})$ is again independent of rotational quantum numbers to a very high degree of approximation so we omit its matrix elements. The matrix elements of the remaining operator, corresponding to the classical dipolar part of the interaction, may be ascertained in a manner similar to that employed in obtaining the matrix elements of the previously treated interaction,

$$\begin{aligned}
& \langle \eta \Lambda K S J | \sum_{i,j>i} \sqrt{6} r_{ij}^{-3} T^2(\mathbf{S}_i, \mathbf{S}_j) \cdot C^2(\omega_{ij}) | \eta' \Lambda' K' S' J' \rangle \\
&= \langle \eta \Lambda K S J | \sum_{q,q',i,j>i} \sqrt{6} r_{ij}^{-3} (-1)^q T_q^2(\mathbf{S}_i, \mathbf{S}_j) C_q^2(\omega_{ij}) \\
&\quad \times D_{-qq'}^{2*} | \eta' \Lambda' K' S' J' \rangle = \sum_{q',i,j>i} (-1)^{J-K'-S} W(KK'SS'; 2J) \\
&\quad \times [(2S+1)(2K+1)]^{1/2} \\
&\quad \times \langle \eta \Lambda K S | \sqrt{6} r_{ij}^{-3} D_{\cdot q'}^{2*} C_q^2(\omega_{ij}) T^2(\mathbf{S}_i, \mathbf{S}_j) | \eta' \Lambda' K' S' \rangle \\
&= \sum_{q'} (-1)^{J-K'-S} W(KK'SS'; 2J) [(2K'+1)(2S+1)]^{1/2} \\
&\quad \times \langle K' 2 \Lambda' q' | K \Lambda \rangle \sum_{i,j>i} \langle \eta \Lambda S | \sqrt{6} r_{ij}^{-3} C_q^2(\omega_{ij}) T^2(\mathbf{S}_i, \mathbf{S}_j) | \eta' \Lambda' S' \rangle
\end{aligned} \tag{3.88}$$

Equation (3.88) can only be simplified further if the previous assumption about the η independence of $T^2(\mathbf{S}_i, \mathbf{S}_j)$ is made. Then if $S(S') = 1/2$ and $S'(S) \leq 1$, $T^2(\mathbf{S}_i, \mathbf{S}_j)$ has only vanishing matrix elements because of the triangle rule $\Delta(S'S2)$. The remaining special case is if $S = S' = 1$ then again

$$\langle S = 1 | T^2(\mathbf{S}_i, \mathbf{S}_j) | S = 1 \rangle = (5/12)^{1/2} \tag{3.89}$$

2. Rotationally-Dependent Interactions

We now turn to the part of the Hamiltonian generated by the rotational motion of the nuclei. We again note that the parameters γ_i , $\bar{\gamma}_i$, and ξ_i do not necessarily commute with the operator \mathbf{L} (or \mathbf{I}_i); thus we rewrite $\mathcal{H}_{\mathcal{R}}$ as

$$\begin{aligned}
\mathcal{H}_{\mathcal{R}} &= B T^1(\mathbf{K}) \cdot T^1(\mathbf{K}) + [\tfrac{1}{2} T^1(\mathbf{K}), \sum_i 2 B T^1(\mathbf{I}_i) + \tfrac{1}{2} T^1[\xi_i, \mathbf{I}_i]_+ \\
&\quad + \gamma_i T^1(\mathbf{S}_i) + \tfrac{1}{2} T_0^1(\mathbf{S}_i) T^1[\bar{\gamma}_i, \mathbf{I}_i]_+] + -\tfrac{1}{2} [T^1(\mathbf{L}), \sum_i \gamma_i T^1(\mathbf{S}_i) \\
&\quad + \tfrac{1}{2} T_0^1(\mathbf{S}_i) T^1[\bar{\gamma}_i, \mathbf{I}_i]_+ + \tfrac{1}{2} T^1[\xi_i, \mathbf{I}_i]_+] + B T^1(\mathbf{L}) \cdot T^1(\mathbf{L})
\end{aligned} \tag{3.90}$$

where the anticommutator of a scalar product is defined by $[\mathbf{A}, \mathbf{B}]_+ = \mathbf{A} \cdot \mathbf{B} + \mathbf{B} \cdot \mathbf{A}$ and $[A, B]_+ = AB + BA$. The anticommutator has been introduced to avoid writing again the lengthy formulas of Section III.B.2.

We may work out the matrix elements of the terms of Eq. (3.90) by the standard techniques. In performing this task we must, however, remember that in case (b) the angular momentum \mathbf{K} can be quantized in the molecular reference frame and in such cases obeys anomalous commutation relations as does \mathbf{J} when it is so quantized in case (a).

With this in mind we see

$$\begin{aligned} \langle \eta \Lambda K S J | B T^1(\mathbf{K}) \cdot T^1(\mathbf{K}) | \eta' \Lambda' K' S' J' \rangle \\ = \delta_{JJ'} \delta_{SS'} \delta_{KK'} \delta_{\Lambda\Lambda'} B_0 K(K+1) [3(2K+1)]^{1/2} W(KK11; 0K) \\ = B_0 K(K+1) \end{aligned} \quad (3.91)$$

where the vibronic matrix element involving B has, as explained before, been replaced by its value in the state of interest. The next term may be treated in a similar manner.

$$\begin{aligned} \langle \eta \Lambda K S J | T^1(\mathbf{K}) \cdot \frac{1}{2} \sum_i T^1[(2B + \xi_i) \cdot \mathbf{I}_i]_+ = \sum_{q,i} \frac{1}{2} \tilde{T}_q^1(\mathbf{K}) \\ \times T_q^1[(2B + \xi_i) \cdot \mathbf{I}_i]_+ | \eta' \Lambda' K' S' J' \rangle = \sum_q \delta_{KK'} \langle K' 1 \Lambda' q | K \Lambda \rangle \\ \times [K(K+1)]^{1/2} \delta_{SS'} \delta_{JJ'} \langle \eta \Lambda | \sum_i \frac{1}{2} T_q^1[(2B + \xi_i) \cdot \mathbf{I}_i]_+ | \eta' \Lambda' \rangle \end{aligned} \quad (3.92)$$

The term in γ_i may also be treated very simply although here the terms commute and the anticommutator notation may be dropped

$$\begin{aligned} \langle \eta \Lambda K S J | \sum_i T^1(\mathbf{K}) \cdot T^1(\gamma_i \mathbf{S}_i) | \eta' \Lambda' K' S' J' \rangle \\ = [K(K+1)(2K+1)(2S+1)]^{1/2} (-1)^{J-S-K} \delta_{KK'} \delta_{JJ'} W(SS'KK'; 1J) \\ \times \sum_i \langle \eta \Lambda S || T^1(\gamma_i \mathbf{S}_i) || \eta' \Lambda' S' \rangle \end{aligned} \quad (3.93)$$

The following term involves the product of $T_0(\mathbf{S}_i)$ and $\mathbf{K} \cdot \mathbf{I}_i \bar{\gamma}_i$. The latter factor's matrix elements have been calculated; those of the former are given by

$$\begin{aligned} \langle \eta \Lambda K S J | \sum_i S_{zi} = \sum_{q,i} (-1)^q T_q^1(\mathbf{S}_i) D_{-q}^{1,0} | \eta' \Lambda' K' S' J' \rangle \\ = [(2K'+1)(2S+1)]^{1/2} (-1)^{J-S-K'} \delta_{JJ'} W(SS'KK'; 1J) \\ \langle K' 1 \Lambda 0 | K \Lambda \rangle \langle \eta S || \sum_i T^1(\mathbf{S}_i) || \eta' S' \rangle \end{aligned} \quad (3.94)$$

by combining Eqs. (3.92) and (3.94) we can obtain the matrix elements of the fourth term of \mathcal{H}_A ,

$$\begin{aligned} \langle \eta \Lambda K S J | \frac{1}{4} \sum_i [T^1(\mathbf{K}) \cdot T^1[\gamma_i \cdot \mathbf{I}_i]_+, T_0(\mathbf{S}_i)]_+ | \eta' \Lambda' K' S' J' \rangle \\ = \frac{1}{4} \sum_{q,i} (-1)^q [K(K+1)(2K'+1)(2S+1)]^{1/2} (-1)^{J-S-K'} W(SS'KK'; 1J) \\ \times \{ \langle K 1 \Lambda' q | K \Lambda \rangle \langle K' 1 \Lambda' 0 | K \Lambda' \rangle \langle \eta \Lambda S || T_q^1[\gamma_i \cdot \mathbf{I}_i]_+ T^1(\mathbf{S}_i) || \eta' \Lambda' S' \rangle \\ + \langle K' 1 \Lambda 0 | K \Lambda \rangle \langle K' 1 \Lambda' q | K' \Lambda \rangle \langle \eta \Lambda S || T^1(\mathbf{S}_i) T_q^1[\mathbf{I}_i \cdot \bar{\gamma}_i]_+ || \eta' \Lambda' S' \rangle \} \end{aligned} \quad (3.95)$$

where the q subscript denotes a molecule fixed tensor component. It is also worth noting that the electronically diagonal matrix elements of $T^1_q(\mathbf{l}_i)$ are, by the Wigner-Eckhart theorem, proportional to Λ .

Of the remaining terms of \mathcal{H}_A we note that the first is of the same form as the spin-orbit operator and thus its matrix elements are of the form of those of Eq. (3.87). The rotational dependence of the remaining $\bar{\gamma}$ term is just that of $T_0^1(S_i)$ and so can be obtained from Eq. (3.94). The last two terms essentially add only constants for a given electronic state. Parameters equivalent to those of Eqs. (3.47) and (3.52) can be defined to include the sum of the variables γ_i , $\bar{\gamma}_i$, and ξ_i over i , but we do not repeat these formulas here.

3. External Magnetic Field Interactions

The next remaining term in \mathcal{H} is \mathcal{H}_Z , the Zeeman Hamiltonian. Omitting the nuclear spin interaction which we shall deal with later, we may write \mathcal{H}'_Z in irreducible tensor form

$$\mathcal{H}'_Z = \sum_i \beta T^1(\mathbf{H}) \cdot [T^1(g_s^i \mathbf{S}_i) + T^1(g_l^i \mathbf{l}_i)] - g_r \beta T^1(\mathbf{H}) \cdot T^1(\mathbf{K} - \mathbf{L}) + \sum_i \beta \Delta g^i T_0^1(\mathbf{H}) T_0^1(\mathbf{S}_i) \quad (3.96)$$

where the subscripts on the last term refer to a molecule-fixed tensor component.

To obtain the matrix elements of \mathcal{H}'_Z we assume M_J is a good quantum number. This will, of course, be true if the molecule is devoid of nuclear spin. If it is not, as in case (a), there exists a choice between coupled and decoupled representations. We shall here assume the decoupled representation; as in the case (a) section the results of a coupled representation were produced explicitly. If one chooses a coupled representation, then the following transformation should be performed. To obtain the \mathcal{H}'_Z matrix elements between states $\langle JIFM_F |$ and $|J'IF'M'_F\rangle$ from those between states $\langle JM_JIM_I |$ and $|J'M'_JIM'_I\rangle$, the latter should be multiplied by

$$(-1)^{F'+J-1-I} W(JJ'FF'; 1I) [(2F'+1)(2J+1)]^{1/2} [\langle J'1M'_J 0 | JM_J \rangle]^{-1} \langle F'1M'_F 0 | FM_F \rangle$$

Thus we find for the matrix of the isotropic spin dependent term of \mathcal{H}'_Z ,

$$\begin{aligned} \langle \eta \Lambda K S J M_J | \sum_i \beta T^1(\mathbf{H}) \cdot T^1(g_s^i \mathbf{S}_i) | \eta' \Lambda' K' S' J' M_{J'} \rangle \\ = \beta H \langle J'1M'_J 0 | JM_J \rangle \delta_{\Lambda\Lambda'} (-1)^{J+S'-1-K} [(2J'+1)(2S+1)]^{1/2} \\ W(SS'JJ'; 1K) \sum_i \langle \eta S || T^1(g_s^i \mathbf{S}_i) || \eta' S' \rangle \end{aligned} \quad (3.97)$$

where as usual the sum over i in the reduced matrix element extends only over those electrons contributing to S . Since each unpaired electron must interact with the external field, if we deal with matrix elements diagonal in S , g_s^i can be replaced by an average value (g_s') for the quantities g_s^i and the sum over S_i performed to give S . Thus the diagonal reduced matrix element may be simplified to give $g_s'[S(S+1)]^{1/2}$.

The term of \mathcal{H}'_Z proportional to $T^1(\mathbf{K})$ has matrix elements given by

$$\begin{aligned} \langle \eta \Lambda K S J M_J | -g_r \beta T^1(\mathbf{H}) \cdot T^1(\mathbf{K}) | \eta' \Lambda' K' S' J' M_J' \rangle \\ = (-1)^{J'+K-S} H \beta g_r [(2J'+1)(2K+1)K(K+1)]^{1/2} \langle J' 1 M_J' 0 | J M_J \rangle \\ \times W(KK' J J'; 1S) \delta_{KK'} \delta_{SS'} \end{aligned} \quad (3.98)$$

Combining the two terms of \mathcal{H}'_Z proportional to the electronic orbital angular momentum, we obtain the operator \mathcal{A} where

$$\mathcal{A} = \sum_{q, q'} \beta T_q^1(\mathbf{H}) (-1)^q \sum_i D_{-qq'}^{1*} [T_q^1(g_i^i \mathbf{l}_i) - g_r T_q^1(\mathbf{l}_i)] \quad (3.99)$$

The matrix elements of \mathcal{A} are*

$$\begin{aligned} \langle \eta \Lambda K S J M_J | \mathcal{A} | \eta' \Lambda' K' S' J' M_J' \rangle \\ = \sum_q \langle J' 1 M_J' 0 | J M_J \rangle [(2J'+1)(2K'+1)]^{1/2} \\ (-1)^{J'+K'-1-S} \langle K' 1 \Lambda' q' | K \Lambda \rangle W(KK' J J'; 1S) \\ \sum_i \langle \eta \Lambda | T_q^1(g_i^i \mathbf{l}_i) - g_r T_q^1(\mathbf{l}_i) | \eta' \Lambda' \rangle \delta_{SS'} \end{aligned} \quad (3.100)$$

Employing the same sort of approximations as were made on the spin dependent term of \mathcal{H}'_Z the diagonal reduced matrix element in Eq. (3.100) is given by $(g_i - g_r)\Lambda$ where g_i is an analogously defined average of g_i^i .

The remaining term of \mathcal{H}'_Z is proportional to $T_0^1(\mathbf{H})T_0^1(\mathbf{S}_i)$. To obtain the matrix elements of this term it may be noted that

$$\begin{aligned} T_0^1(\mathbf{H})T_0^1(\mathbf{S}_i) = H D_{00}^1 \sum_q D_{q0}^1 T_q^1(\mathbf{S}_i) = -H \sum_{q,k} D_{-q0}^{1*} T_q^1(\mathbf{S}_i) \langle 1100 | k0 \rangle \\ \langle k1 - qq | 10 \rangle [(2k+1)/3]^{1/2} = H/3 \{ (2/3)^{1/2} T_{q=0}^1(\mathbf{S}_i) \\ - (10)^{1/2} T_{q=0}^1 [T^1(\mathbf{S}_i), D_{00}^2] \} \end{aligned} \quad (3.101)$$

where in the last line the q 's refer to space-fixed tensor components. For a magnetic field along the z' axis the matrix elements of the first term of the right member of Eq. (3.101) are equivalent to those of $T^1(\mathbf{S}_i) \cdot T^1(\mathbf{H})$ whose

* These matrix elements are subject to the same restrictions as those of Eq. (3.86).

elements are given by Eq. (3.97). The matrix elements of the second term are from Eq. (3.16),

$$\begin{aligned} \langle \eta \Lambda K S J M_J | \sum_i T_q^{-1} [\Delta g^i T^1(S_i), D \cdot \delta^*] | \eta' \Lambda' K' S' J' M_J' \rangle \\ = \langle J' 1 M_J' 0 | J M_J \rangle \langle K' 200 | K 0 \rangle [3(2J' + 1)(2S + 1)(2K' + 1)]^{1/2} \\ \left(\begin{matrix} J & J' & 1 \\ S & S' & 1 \\ K & K' & 2 \end{matrix} \right) \sum_i \langle \eta S || T^1(S_i) \Delta g^i || \eta' S' \rangle \end{aligned} \quad (3.102)$$

Analogously to our previous discussion for diagonal elements the reduced matrix element diagonal in S may be given by $[S(S + 1)]^{1/2} \Delta g$. In general the 9- j symbols are not well tabulated. However, all relevant coefficients for $S = S' = 1/2$ or 1 have been given and hence the appearance of the 9- j symbol here should pose no obstacle to the obtainment of an analytic formula for the matrix elements.

4. Nuclear Magnetic and Electric Hyperfine Structure

We now turn to the hyperfine part of the Hamiltonian. As previously we work in a decoupled ($|J M_J I M_I\rangle$) representation. If, however, we desire the matrix elements of \mathcal{H}_{hf} in a coupled representation we may simply multiply the appropriate matrix elements in the decoupled representation by the factor, \mathcal{F} ,

$$\begin{aligned} \mathcal{F} = [\langle J' k M_J' q | J M_J \rangle \langle I k M_I' - q | I M_I \rangle]^{-1} (-1)^{F - J - I + q} \\ [(2J + 1)(2I + 1)]^{1/2} W(JJ'II; kF) \end{aligned} \quad (3.103)$$

where k is the rank of the operators involved in the matrix element, and remove the sum over q .

Following the treatment in the section on case (a) matrix elements we write the magnetic hyperfine part of the Hamiltonian as

$$\mathcal{H}_{mhf} = \sum_i T^1(\mathbf{I}) \cdot \{ \bar{a}_i T^1(\mathbf{I}_i) + b_i T^1(\mathbf{S}_i) + c_i T^1(\mathbf{S}_i, C_i^2) \} \quad (3.104)$$

These matrix elements may be worked out by the same procedures as employed previously. We transform the molecule-fixed operators of the bracketed part of Eq. (3.104) into the space-fixed coordinate system via rotational matrices and carry out the scalar products. The matrix elements of the first term may be written as

$$\begin{aligned} \langle \eta \Lambda K S J M_J I M_I | \sum_{i,q,q'} \bar{a}_i T_q^{-1}(\mathbf{I}) (-1)^q D_{-qq'}^{1*} T_{q'}^1(\mathbf{I}_i) | \eta' \Lambda' K' S' J' M_J' I M_I' \rangle \\ = \sum_{q,q',i} (-1)^q \langle I 1 M_I' q | I M_I \rangle \langle J' 1 M_J' - q | J M_J \rangle \delta_{SS'} (-1)^{J' + K - 1 - S} \\ \times [(2J' + 1)(2K' + 1)I(I + 1)]^{1/2} W(KK'JJ'; 1S) \langle K' 1 \Lambda' q | K \Lambda \rangle \\ \times \langle \eta \Lambda || \bar{a}_i T_{q'}^{-1}(\mathbf{I}_i) || \eta' \Lambda' \rangle \end{aligned} \quad (3.105)$$

The diagonal reduced matrix element with $q' = 0$ may be equated to Λa where a is an average of the a_i .

The Fermi contact part of the interaction may be treated in a similar manner yielding

$$\begin{aligned}
 & \langle \eta \Lambda K S J M_J I M_I | \sum_{i,q} b_i (-1)^q T_q^{-1}(\mathbf{I}) T_{-q}^{-1}(\mathbf{S}_i) | \eta' \Lambda' K' S' J' M_J' I M_I' \rangle \\
 &= \sum_q \delta_{KK'} \langle I M_I' q | I M_I \rangle \langle J' 1 M_J' - q | J M_J \rangle [I(I+1)(2J'+1) \\
 &\quad \times (2S+1)]^{1/2} (-1)^{J+S'-1-K+q} W(SS'JJ'; 1K) \\
 &\quad \times \langle \eta \Lambda S || \sum_i b_i T^1(\mathbf{S}_i) || \eta' \Lambda' S' \rangle \quad (3.106)
 \end{aligned}$$

If we confine our attention to matrix elements diagonal in S , it is possible to simplify the reduced matrix element appearing in Eq. (3.106). For one or two unpaired electrons it can be rewritten as

$$\{[S(S+1)]^{1/2}/N\} \langle \eta \Lambda || \sum_i b_i || \eta' \Lambda' \rangle$$

where N denotes the number of unpaired electrons and the sum over i extends over those unpaired electrons.

We now turn to the dipolar interaction between the electrons and nuclei. Its matrix elements may be obtained by procedures similar to those employed in Section III.B.4.

$$\begin{aligned}
 & \langle \eta \Lambda K S J M_J I M_I | c_i T^1(\mathbf{I}) \cdot T^1(\mathbf{S}_i, C^2) | \eta' \Lambda' K' S' J' M_J' I M_I' \rangle \\
 &= - \sum_{q,q'} \langle I 1 M_I' q | I M_I \rangle \langle J' 1 M_J' - q | J M_J \rangle [3I(I+1)(2J'+1)(2K'+1) \\
 &\quad \times (2S+1)]^{1/2} \begin{pmatrix} J & J' & 1 \\ S & S' & 1 \\ K & K' & 2 \end{pmatrix} \langle K' 2 \Lambda' q' | K \Lambda \rangle (-1)^q \\
 &\quad \times \langle \eta \Lambda S || \sum_{i,q} c_i T^1(\mathbf{S}_i) C_q^2(\omega_{ac}) || \eta' \Lambda' S' \rangle \quad (3.107)
 \end{aligned}$$

The reduced matrix element of Eq. (3.107) diagonal in S may be treated in the same manner as that in Eq. (3.106).

We now turn to the matrix elements of the quadrupole operator,

$$\mathcal{H}_Q = \sum_c \frac{e^2 Q \sqrt{3} c}{I(2I-1) \sqrt{2} r_{ac}^{-3}} C^2(\omega_{ac}) \cdot T^2(\mathbf{I}) \quad (3.108)$$

These matrix elements may be easily obtained by referring the field gradient tensor to the space fixed coordinate system; we find

$$\begin{aligned}
& \langle \eta \Lambda K S J M_J I M_I | \mathcal{H}_Q | \eta' \Lambda' K' S' J' M_J' I M_I' \rangle \\
&= \sum_{q, q', c} \langle J' 2 M_J' q | J M_J \rangle \langle I 2 M_I' - q | I M_I \rangle (-1)^{J' + K - 2 - S + q} \\
&\quad \times [(2J' + 1)(2K' + 1)]^{1/2} W(KK'JJ'; 2S) \delta_{SS'} \langle K' 2 \Lambda' q' | K \Lambda \rangle \\
&\quad \times \langle \eta \Lambda | r_{xc}^{-3} c C_q^{-2}(\omega_{xc}) | \eta' \Lambda' \rangle [\langle I 2 I 0 | I I \rangle]^{-1} e^2 Q / 2 \quad (3.109)
\end{aligned}$$

The summed reduced matrix element involving $C_q^{-2}(\omega_{xc})$ may again conveniently be taken to be one-half the electric field gradient parameter.

Finally we note that the previously omitted nuclear spin Zeeman interaction may be simply calculated. Taking the interaction as

$$\mathcal{H}_{IZ} = -g_I \beta_N T^1(H) \cdot T^1(I) \quad (3.110)$$

we find in the decoupled representation with the field in the z' -direction,

$$\begin{aligned}
& \langle \eta \Lambda K S J M_J I M_I | \mathcal{H}_{IZ} | \eta' \Lambda' K' S' J' M_J' I M_I' \rangle \\
&= -\delta_{\eta\eta'} \delta_{\Lambda\Lambda'} \delta_{KK'} \delta_{SS'} \delta_{JJ'} \delta_{M_J M_J'} g_I \beta_N H \langle I 1 M_I' 0 | I M_I \rangle \\
&\quad \times [I(I+1)]^{1/2} \quad (3.111)
\end{aligned}$$

The matrix elements of \mathcal{H}_{Z1} in a coupled representation may be obtained by multiplying the right-hand side of Eq. (3.111) by the factor,

$$\begin{aligned}
& [\langle I 1 M_I' 0 | I M_I \rangle]^{-1} \langle F' 1 M_F' 0 | F M_F \rangle (-1)^{F+I-1-J} \\
& [(2F' + 1)(2I + 1)]^{1/2} W(I I F F'; 1J)
\end{aligned}$$

For more than one nuclear spin, the discussion following the case (a) matrix elements is completely applicable to the case (b) elements.

IV. INTERPRETATION OF ELECTRON RESONANCE SPECTRA

In this section we analyze the effect upon electron resonance spectra of the various terms of the Hamiltonian. We divide these terms into four general categories: terms affecting the position of the rotational energy levels, terms affecting the hyperfine structure of these levels, terms causing Λ -doubling, and terms responsible for electric field effects. Before the treatment of electric field effects, we include a discussion on lineshapes and intensities as the electric field effects are often manifested through a variation in these parameters.

A. Rotational Energy Levels

The first of these categories, rotational energy level terms, we take to include the effects of \mathcal{H}_{fs} , $\mathcal{H}_{\mathcal{A}}^N$, and \mathcal{H}_{Z1} . We begin our discussion with $^1\Delta$

molecules where the effects of \mathcal{H}_{fs} vanish entirely because \mathcal{H}_{fs} arises, physically, from unpaired electronic spin. $\mathcal{H}_{\mathcal{A}}^N$ is relatively simple with only the term $B(\mathbf{J} - \mathbf{L})^2$ giving nonzero, nonconstant matrix elements. (The rotational moment also has a nonvanishing effect which we discuss subsequently.) \mathcal{H}_{Z1} reduces to the interaction of the magnetic field with the electronic orbital angular momentum. In zero magnetic field the eigenvalues of the Hamiltonian are well determined by the expectation values of $\mathcal{H}_{\mathcal{A}}^N$ which are, apart from an additive constant $BJ(J+1)$. The application of the magnetic field has the important effect of removing the $(2J+1)$ -fold degeneracy of the rotational states. The splitting of the magnetic sublevels, denoted by M_J , is given approximately by the expectation value of \mathcal{H}_{Z1} , which is, from Eqs. (2.100), (3.86), and the transformation following

$$g_L \beta H \Lambda^2 / J(J+1)$$

where g_L is taken to be the free electron orbital g factor of 1. As electric dipole transitions are allowed between Λ -doublet components of adjacent M_J levels (see Sections IV.B and IV.D), the position of the electron resonance spectrum can be predicted *via* the g values given by the above expression, which yields $g = 2/3$ for $J = 2$, $g = 1/3$ for $J = 3$, etc.

The nonvanishing matrix elements of \mathcal{H}_{Z1} are not confined to those diagonal in J . As Eq. (3.86) shows, there are also nonvanishing elements between adjacent J states. The most important effect of the mixing of J levels by the magnetic field is the production of an inequality in the spacings between M_J states in a given J level. This inequality is, in second order, inversely proportional to the splitting between J states and gives rise to the characteristic four line spectrum (see Figure 2, the ${}^1\Delta$ SO spectrum) arising from ${}^1\Delta$ molecules in their lowest rotational level with $J = 2$. As the energy difference between rotational levels is determined by the rotational constant of the molecule, the molecule's B value and hence bond length may be determined from the electron resonance spectrum. Rotational constants have been determined from electron resonance experiments for both ${}^1\Delta$ SO²⁷ and ${}^1\Delta$ SeO²⁸. The B_0 values (the subscript denotes the value of B in the ground vibronic state) for ${}^1\Delta$ SO and ${}^1\Delta$ SeO are, respectively, 0.709 and 0.461 cm^{-1} . From these constants the bond lengths, r_0 , may be determined respectively to be 1.493 and 1.657 Å.

We have thus seen how the combined effects of rotational motion and magnetic interaction with the electronic orbital angular momentum produce the basic pattern of the spectra of ${}^1\Delta$ molecules. We shall, of course, find these effects present in other states as well, plus other interactions. For instance, if there is unpaired electronic spin in the molecule, it interacts

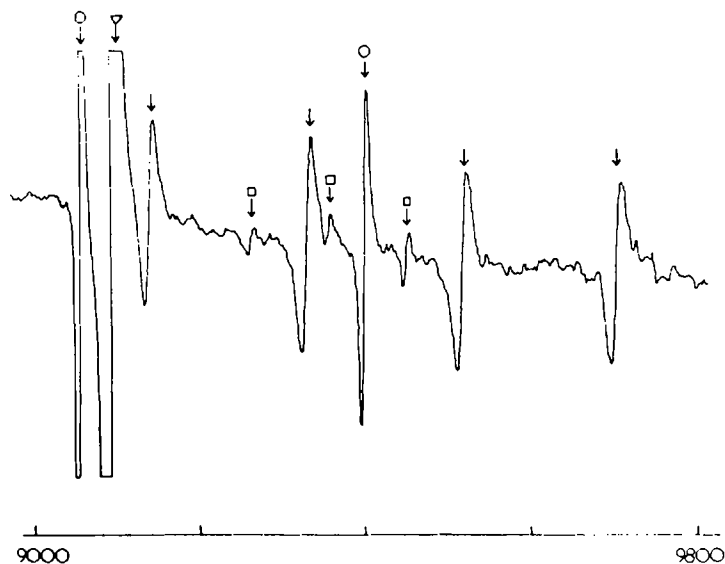


Fig. 2. Spectrum of ${}^1\Delta\text{SO}$ arising from transitions between adjacent Zeeman levels of the $J = 2$ state. The lines marked with open circles arise from ${}^3\Sigma\text{O}_2$; those marked with squares arise from ${}^1\Delta\text{O}_2$; that marked with a triangle arises from ${}^3\Sigma\text{SO}$; the lines marked with vertical arrows constitute the ${}^1\Delta\text{SO}$ spectrum.

with the external magnetic field in much the same way as the orbital angular momentum, sharing the task of tuning the energy levels to resonance.

In nonsinglet molecules the terms of the fine-structure part of the Hamiltonian, \mathcal{H}_{fs} , also have important direct and indirect effects. In what follows we shall examine these effects as well as the smaller magnetic field effects contained in \mathcal{H}_{Z2} and contributed by the rotational moment term of \mathcal{H}_R . Before proceeding to more complicated cases it is perhaps advisable to return to the ${}^1\Lambda$ state to ascertain the effects of the small magnetic interactions.

As the resultant electronic spin is zero, to ascertain the effects of \mathcal{H}_{Z2} we need only concern ourselves with the orbital angular momentum g factor,

$$g_l^i = (1 + \delta g_1^i + \delta g_l^i) \quad (4.1)$$

From Eq. (2.103) it is obvious that δg_1^i is negative and given by the ratio of the electron's kinetic energy to its rest mass energy. One can easily calculate the order of magnitude of this term. For a hydrogen atom, using the virial theorem and remembering the ionization potential of the atom is

13.6 eV, $\delta g_1^i = -0.27 \times 10^{-4}$. For heavier nuclei δg_1^i might be expected to increase somewhat, but for most cases of practical interest a value of the order of -1×10^{-4} seems reasonable.

The second correction term of g_l^i , δg_l^i , is more difficult to estimate; however, a calculation¹⁷ of it for the oxygen atom gave a value of -0.3×10^{-4} . Thus we see that we might well expect g_l^i to be decreased from its free electron value of one by something of the order of 100 ppm. This we note would correspond to a shift, at *X*-band frequency, of the resonance field for a $^1\Delta$ spectrum of the order of 1 gauss.

However, in obtaining the final position of the spectrum, one must also take into account the combined effect of the nuclear and electronic rotational moments. The nuclear part of the moment is given by Eq. (2.121) and the electronic part arises, in second-order perturbation theory, from cross terms between the magnetic field-electronic orbital angular momentum interaction and the L-uncoupling interaction to states with $|\Lambda| = 2 \pm 1$. In $^1\Delta$ states both of these terms take the form $(\mathbf{J} - \mathbf{L}) \cdot \mathbf{H}$. From the section on matrix elements we see that a term of this form has two effects upon the energy levels, one proportional to M_J alone and a second expressible by further modification of the orbital angular momentum g factor. For a given rotational level both of these effects clearly just shift the center of gravity of the spectrum; because of the term proportional to M_J alone, the rotational moment may be determined separately from g_l^i by measurements in more than one rotational level. However, electron resonance experiments on $^1\Delta$ molecules²⁷⁻²⁹ have thus far been confined to the first rotational level where experimentally the relativistic and diamagnetic and the rotational moment effects appear roughly to cancel.

The effect of the terms of the fine-structure Hamiltonian, \mathcal{H}_{fs} , upon the electron resonance spectrum depends greatly upon the electronic state and the molecule in which the effects are observed. Since, physically, \mathcal{H}_{fs} describes the interaction of unpaired electronic spin with its environment, \mathcal{H}_{fs} has no effect upon the spectra of molecules in singlet states, such as $^1\Delta$ states. In Σ states the effects of the first term of \mathcal{H}_{fs} also vanish in first order as the expectation value of the electronic orbital angular momentum is zero. However, the second term of \mathcal{H}_{fs} , the spin-spin interaction term, may still give a nonvanishing contribution if the multiplicity of the state is greater than or equal to 3. It is also possible to obtain second- and higher-order contributions in such states from the first term of \mathcal{H}_{fs} , which may be quite important. If the electron resonance spectrum of a molecule is observed in a non- Σ , nonsinglet state, then it is possible to obtain first-order effects from the first term of \mathcal{H}_{fs} and, if the multiplicity is greater than two, first-order effects from the second term also.

To explain more specifically the importance of the fine-structure Hamiltonian and its interaction with other terms in the Hamiltonian, it is well to deal individually with the remaining two electronic states in which electron resonance spectra have been observed, $^2\Pi$ and $^3\Sigma$. In $^2\Pi$ states we expect the spin-orbit operator to have a first-order effect and since the spin-orbit coupling constant A (equivalent for a doublet state to A_l for the unpaired electron) is typically of the order of hundreds of cm^{-1} , this first-order effect should be the dominate factor in the determination of the energy levels of the state. Physically we should also expect that unless the molecule is very light, the effect of this term will be to tie the electronic spin to the internuclear axis and so achieve case (a) quantization. From Section III.B.3 we see that the diagonal matrix elements of this term are given by $A\Sigma\Lambda$. Thus the fine-structure Hamiltonian will cause the $^2\Pi$ state to be split into two fine-structure components, respectively, with $\Sigma = \pm 1/2$ and separated by approximately A .

In point of fact the separation between the fine-structure states is not exactly A because of the magnetic field independent term of \mathcal{H}_A^N given by Eq. (2.117) and the last term of (3.21). By considering the matrix elements of Eqs. (3.34)–(3.36) and (3.38), it is possible to see that only the terms involving $\tilde{\gamma}$ and B have nonvanishing, nonconstant matrix elements diagonal in both Σ and Λ , and that these are, in fact, proportional to Σ ; thus these terms give a small contribution to the fine-structure splitting (see Eqs. 3.28, 3.43, 3.44, 3.47, and 3.49). [It can be similarly seen that only the terms involving γ and B have nonvanishing, nonconstant matrix elements diagonal in Λ , but connecting different fine-structure states (see Eqs. 3.24, and 3.37–3.40 and the discussion following).] These elements, as will be seen subsequently, may affect the determination of the value of the fine-structure splitting from the electron resonance spectrum.

The state with $\Omega = 1/2$, the $^2\Pi_{1/2}$ state, is essentially nonmagnetic since the orbital and spin moments are oppositely aligned and hence cancel. This point may be verified by the matrix elements of \mathcal{H}_{Z1} given by Eq. (3.86). In the $^2\Pi_{3/2}$ state with $\Omega = 3/2$, the spin and orbital moments are aligned parallel and hence re-enforce. Thus electron resonance observations in $^2\Pi$ states are usually confined to the $\Omega = 3/2$ component of the fine structure doublet.

The dominant magnetic field interactions within the $^2\Pi_{3/2}$ rotational energy levels are in many respects similar to those in $^1\Delta$ states, only now we have additional paramagnetism from unpaired electronic spin. Its principal effects upon the spectrum are determined by the expectation value of \mathcal{H}_{Z1} . From Eqs. (2.100), (3.86) and the transformation following we see that the diagonal matrix elements are

$$M_J \Omega H \beta (\Lambda + g \Sigma) / J(J+1)$$

which gives an overall g value of 0.8 for the level in which $J = \Omega = 3/2$ and smaller g factors for higher rotational levels.

As is the case of $^1\Delta$ molecules, there are also Zeeman matrix elements between adjacent J states and this insures that through higher-order interactions the transitions between different M_J states do not occur at the same frequency or experimentally at the same field. This effect accounts for the basic three-line spectrum of $^2\Pi_{3/2}$ molecules in their lowest rotational level wherein there are allowed three separate transitions between adjacent M_J levels. Advantage has been taken of the higher order Zeeman effects to determine the rotational moments of several $^2\Pi$ diatomic molecules. These molecules, together with their rotational constants, are given in Table I.

TABLE I
Rotational Constants of $^2\Pi$ Molecules

| Molecule | B_0 (cm $^{-1}$) |
|---------------------------------|---------------------|
| SeH ^a | 7.98 |
| TeH ^a | 5.56 |
| $^{35}\text{Cl}^{36}\text{O}^b$ | 0.622 |
| SF ^c | 0.5527 |
| SeF ^c | 0.3625 |
| $^{79}\text{Br}^{16}\text{O}^d$ | 0.4282 |
| IO ^d | 0.3389 |

^a Ref. 51.

^b Ref. 32.

^c Ref. 31.

^d Ref. 46.

It should, perhaps, at this juncture, be pointed out that electron resonance in the $^2\Pi_{1/2}$ state of OH has been reported.³⁰ This fact in no way invalidates the preceding conclusions about the nonmagnetic nature of the $^2\Pi_{1/2}$ state, as in very light molecules such as OH, terms of the rotational part of the Hamiltonian, \mathcal{H}_r^N , may strongly mix the fine-structure components of a given J state. Thus what is nominally a $^2\Pi_{1/2}$ state may be endowed with considerable $^2\Pi_{3/2}$ character and hence considerable paramagnetism. This rotationally induced paramagnetism, combined with a large zero-field splitting of the Λ -doublets in OH, accounts for the observation of the $^2\Pi_{1/2}$ state by electron resonance techniques.

Although in reasonably heavy molecules the ${}^2\Pi_{1/2}$ state is nonmagnetic, it should not be inferred that the magnetic field cannot connect the ${}^2\Pi_{1/2}$ and ${}^2\Pi_{3/2}$ states. As the matrix elements of \mathcal{H}_{Z1} connecting the two states are commonly smaller than those of $\mathcal{H}_{\mathcal{A}}^N$, the primary field-dependent second-order effect of such terms is to give an energy correction to the ${}^2\Pi_{3/2}$ levels which is proportional to the perturbing term of $\mathcal{H}_{\mathcal{A}}^N$, the magnetic field interaction, and the reciprocal of the energy difference between the fine-structure states.

From the case (a) matrix elements (Eqs. 3.24 and 3.37–3.40), one sees that the perturbing matrix elements of $\mathcal{H}_{\mathcal{A}}^N$ are proportional to γ and B . It has been shown³¹ that by using a second-order treatment for the electronic states, one also obtains an additive contribution to that of γ and B from the coupling of the electronic spin to the field created by the rotating electrons. In a similar manner the electronic spin part of the Zeeman interaction also has a contribution which describes the interaction of the external field with the electronic orbital angular momentum mixed in by spin-orbit coupling. This has the effect of making the g tensor in \mathcal{H}_{Z1} much more anisotropic and making its \perp component, which is of importance in this context, *a priori* uncalculatable. The effect of neglecting these higher order corrections and taking the perturbing matrix elements of $\mathcal{H}_{\mathcal{A}}^N$ and \mathcal{H}_{Z1} respectively proportional to B and g has been analyzed³¹ for the ${}^2\Pi$ molecules SF and SeF. By such neglect, a shift of the center of gravity of the spectrum is expected which is, in second order, proportional to g , B , and the reciprocal fine-structure separation. For SF and SeF, it was found³¹ that the determination of the fine-structure separation from this shift and the above assumption leads to a value which is probably accurate to 5–10%. As the shift in the spectrum is relatively small for large values of the fine-structure separation, the experimental error may lead to a larger uncertainty in A than that derived from the invalidity of the previous assumptions.

It might also be pointed out that observations of a limited number of transitions may also make it difficult to untangle to the fullest extent possible all the small magnetic interactions affecting the center of gravity of the spectrum and thereby to increase further the uncertainty in the fine-structure separation. The rotational g factor has an unknown value and in a given rotational level the first-order effects just shift the center of gravity of the spectrum.^{31,32} As in the case of ${}^1\Delta$ molecules, the parallel component of the orbital angular momentum g factor is not exactly known. From Eq. (2.102) it is easy to see that the g factor for the electronic spin interaction is subject to similar uncertainties. Although the parallel components of the g factors are expected to be much closer to their isotropic free electron values than the \perp components, their effect upon the spectrum occurs in

first order and so may cause a considerable shift in the center of gravity of the spectrum. It is usually possible to estimate^{31,33} these effects and so obtain a value of the fine-structure splitting from the electron resonance spectrum, which is more nearly correct than it would otherwise be, but it is impossible to completely eliminate these uncertainties. However, one important advantage of the electron resonance method is that it always provides an unambiguous determination of the sign of the fine-structure perturbation and hence whether the molecule has normal or inverted fine-structure. The fine-structure separations have been determined for quite a number of $^2\Pi$ molecules by the electron resonance method. The various molecules and the fine-structure intervals are given in Table II.

TABLE II
Fine-Structure Constants for $^2\Pi$ Molecules

| Molecule | A^a (cm^{-1}) |
|------------------|----------------------------|
| SeH ^b | -1600 |
| TeH ^b | -2250 |
| ClO ^c | -282 |
| SF ^d | -387 |
| SeF ^d | -560 |
| BrO ^e | -815 |
| IO ^e | -446 |

^a A is defined as the coefficient of the operator of the Hamiltonian whose expectation value is $\Lambda\Sigma$.

^b Ref. 51.

^c Ref. 32.

^d Ref. 31.

^e Ref. 46.

As the fine-structure operator is large in magnitude, not only its first-order but its higher-order effects should be considered. It has been shown²⁵ that most of its higher-order effects vanish in states with multiplicities less than three, so we now turn our attention to $^3\Sigma$ states. The detailed appearance of the energy levels will be seen to depend greatly upon the particular molecule considered; however, several general observations may be made. As was noted previously, the first-order effects of the spin-orbit operator of \mathcal{H}_{fs} vanish in any Σ state; since in molecules this usually implies a lack of strong coupling of the electronic spin to the molecular frame, case (b) quantization is often appropriate.

The operator for nuclear rotation is then $B(\mathbf{K} - \mathbf{L})^2$. The \mathbf{K}^2 part of this term gives a first-order contribution $[BK(K+1)]$ to the rotational energy level splitting; the cross term gives a perturbation between electronic states; the final term yields essentially a constant for the rotational levels. We may now turn to the remainder of \mathcal{H}_R^N , the magnetic interaction resulting from nuclear rotation. It can be seen from the matrix elements of Section III.C.2 that only the term involving γ^* has electronically diagonal nonvanishing, nonconstant matrix elements in a case (b) rotation basis and that these are diagonal in K . This term thus slightly alters the eigenvalues of the $B\mathbf{K}^2$ operator.

Whereas in $^1\Delta$ molecules the external magnetic field interaction was entirely with the resultant electronic orbital angular momentum, in $^3\Sigma$ molecules the dominant magnetic field interaction is with the unpaired electronic spin. Except in the heavier $^3\Sigma$ molecules, like SeO, it is impossible to predict simply even the approximate resonance fields, because of the competitiveness of the intramolecular and external magnetic field interactions. However, diagonalization of the Hamiltonian matrices formed from the elements in Section III.C does, of course, supply field positions which can be made exact by the inclusion of all the effects to be discussed subsequently.

* Traditionally $^3\Sigma$ spectra have been described in terms of three parameters B , γ , and λ where B is the familiar rotational constant. The only electronically diagonal, nonvanishing, nonconstant contribution to the spin-rotation interaction is

$$\sum_i T^1(\mathbf{K}) \cdot T^1(\gamma_i \mathbf{S}_i)$$

which is often replaced by

$$\gamma T^1(\mathbf{K}) \cdot T^1(\mathbf{S})$$

Thus for a $^3\Sigma$ state of a given configuration,

$$\gamma = \frac{1}{2} \sum_i' \gamma_i \quad (4.2)$$

Likewise, the electronically diagonal spin-spin interaction may be written

$$-g^2\beta^2 \sum_{i,j>i} \sqrt{6} r_{ij}^{-3} T_0^2(\mathbf{S}_i, \mathbf{S}_j) C_0^2(\omega_{ij}) = \frac{2}{3} \lambda \sqrt{6} T_0^2(\mathbf{S}, \mathbf{S}) \quad (4.3)$$

Then, by using Eq. (3.89) and the reduced matrix elements of $T_0^2(\mathbf{S}, \mathbf{S})$, the reduced matrix in Eq. (3.88) may be expressed as follows:

$$\frac{2}{3} \lambda = -g^2\beta^2 \sum_{i,j>i}' \langle \eta, \Omega, S = 1 || r_{ij}^{-3} C_0^2(\omega_{ij}) || \eta, \Omega, S = 1 \rangle \quad (4.4)$$

Since the spin-orbit effects vanish in first order, the only remaining matrix elements of \mathcal{H}_{fs} are those of the spin-spin interaction, which are both diagonal in K and connect states $K' = K \pm 2$. Physically this interaction ties the electronic spin to the figure axis as does spin-orbit coupling; however, since the former is usually much smaller in magnitude it commonly splits a given K state into closely spaced components (less than the rotational energy level splittings) rather than into the widely separated fine-structure components that were typical of ${}^2\Pi$ molecules.

The effects of spin-orbit coupling, and possibly spin-spin coupling, are also very important in higher orders in ${}^3\Sigma$ states. It has been shown²⁵ that the entire higher-order effect of \mathcal{H}_{fs} for a particular electronic state may be expressed in terms of a series, with suitable coefficients, of irreducible tensors formed from the total electronic spin. If the molecule is in a triplet state only tensors with $k \leq 2$ may have nonvanishing matrix elements for angular momentum to be conserved. The tensor with $k = 0$ constitutes simply an additive constant to the energy and the tensor with $k = 1$ may be shown to vanish. Thus all higher-order effects of the spin-orbit coupling interaction and the spin-spin interaction must be of the form of the electronic expectation value of the spin-spin interaction.

This result has experimental verification in the ${}^3\Sigma$ spectra of O_2 , SO , and SeO . In all cases a second-rank spin tensor accounts sufficiently for the observed spin effects; however, as the molecules become heavier, the value of its coefficient, λ , increases markedly. This means that the spectra of O_2 , SO , and SeO , the ${}^3\Sigma$ molecules observed by electron resonance techniques, are quite different. O_2 , of course, is a stable gas and has only magnetic dipole allowed transitions, which must occur between levels of the same parity. SO and SeO are transient species whose only observable transitions are the much stronger electric dipole allowed transitions between levels of opposite parity. (See Section IV.D for the selection rules, etc., governing transitions.)

For O_2 the energy of the second-rank spin interaction and the external field are both rather smaller than the energy of rigid body rotation. Since the transitions are magnetic dipole they may occur within a given K state between different M_J levels (see Section IV.D). At low magnetic fields each K state is split into a triplet, each component of the triplet being resolved into Zeeman components. If one simplifies Eq. (3.88) and uses (4.4), it is possible to see that the $J = K \pm 1$ levels are separated from the $J = K$ level by approximately λ and separated from each other by a much smaller interval. As the magnetic field is increased strongly the Zeeman splittings become larger than the zero-field intervals and all adjacent J states with the same value of K are strongly mixed. At very high magnetic fields, the

Paschen-Back decoupling of the electronic spin from the molecular frame occurs and again each rotational level is split into a triplet, now characterized by the space-fixed projections of the electronic spin. These triplet levels are again resolved into further components characterized now by the possible values of the space-fixed projection of \mathbf{K} .

The magnetic resonance spectrum of O_2 at X-band frequency then arises in the following general way. Most of the low-field transitions are between different Zeeman components of the states designated nominally by $J = K \pm 1$. These states are separated by both the Zeeman energy and the small zero-field splitting. At higher fields, resonances are observed between the Zeeman components of a given J state as these are now separated by an X-band quantum. The calculation of the positions of these resonances, however, is a rather complicated matter³⁴ because of the mixing of adjacent J levels by the magnetic field and hence incipient Paschen-Back effects. Failure to take into account the possibility of resonance between states with $J = K \pm 1$ has in the past led to much confusion and misinterpretation of the molecular O_2 spectrum.^{35,36} Conservation of angular momentum would, of course, forbid these transitions were it not for the external magnetic field mixing different J states, rendering J not a good quantum number and allowing the transitions.

As we progress down the periodic table to SO, we find many differences compared to O_2 . The observed transitions are electric dipole allowed and thus, because of parity considerations, between adjacent K states (see Section IV.D). In SO λ has increased from under 2 to over 5 cm^{-1} , so at first appearance it would seem that the energy levels of SO would resemble those of O_2 with the spacing between the $K = J \pm 1$ and $K = J$ levels increased. However, as was shown by Eq. (3.88), the second-rank spin tensor connects states with $K' = K \pm 2$. As the rotational constant in SO is considerably less than λ , this mixing of different K states is very important in SO, especially in the lowest rotational levels where electron resonance is observed. The effect of these off-diagonal terms can best be calculated by numerical diagonalization of the Hamiltonian matrix.

It fortunately results that in SO the eigenvalues of the Hamiltonian which may still be nominally labeled by $J = K = 1$ and $K = 2, J = 1$, are separated by approximately an X-band microwave quantum. These energy levels are shown in Figure 3. For higher rotational levels, the \mathcal{H}_{\star}^N interaction dominates the \mathcal{H}_{fs} interaction and adjacent K states are more widely separated. Thus at X-band, the electron resonance spectrum is limited to the above-mentioned transitions.

The analyses of the O_2 and SO spectra yield much the same sort of information. As has been implied, the zero-field constants λ , B , and γ are

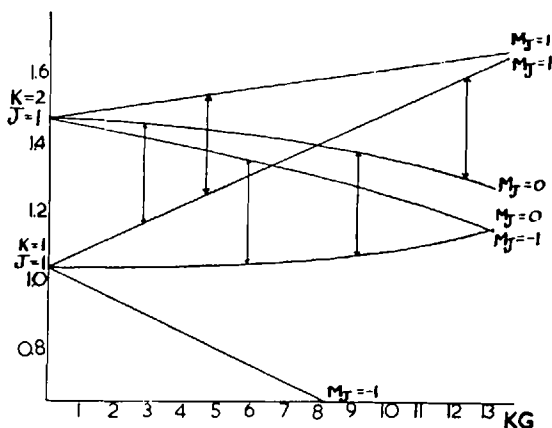


Fig. 3. Energy level diagram for two rotational states in SO. The arrows represent the observable transitions at X-band frequency. The energy units are cm^{-1} and the field units are kilogauss.

actually sums of first-order contributions given by the Hamiltonian of Eq. (2.123) and second-order contributions from the terms of that Hamiltonian which connect the different electronic states. B contains an electronic contribution to the moment of inertia as well as the nuclear contribution. γ contains the coupling of the electronic spin's moment to the field produced by the rotating nuclei and electrons. The electronic contributions to these parameters arise in second-order perturbation theory respectively from L-uncoupling interactions and from cross L-uncoupling, spin-orbit interactions to $^3\Pi$ states. The reader is referred to the original papers for details of the derivation of these terms.^{34,37,38} It was originally thought^{34,37} that λ represented the sum of the electronic dipole-dipole interaction plus the second-order spin-orbit coupling energy to $^3\Pi$ states. Kayama and Baird³⁹ were apparently the first to show that there is also a contribution to λ from spin-orbit coupling to $^1\Sigma$ states. It was later shown²⁵ that, in fact, λ represents the total higher order effects of spin-spin and spin-orbit coupling to all excited states.

If one obtains a high-resolution spectrum of a $^3\Sigma$ molecule such as SO or O_2 in zero magnetic field, then the overall values of B , λ , and γ may be determined. Accurate values for these parameters had, in fact, been obtained for both O_2 and SO prior to their investigation by electron resonance techniques. The dominant feature characterizing the addition of a strong external magnetic field is, of course, the interaction with the unpaired electronic spin which allows the energy levels to be tuned to resonance at a fixed microwave frequency. There are, however, much smaller

magnetic interactions which are in many ways more interesting. These are the magnetic interactions caused by the partial unquenching of the electronic orbital angular momentum in the $^3\Sigma$ ground state by the spin-orbit and L-uncoupling perturbations to $^3\Pi$ states. It has been shown^{34,37,38} that the former perturbation results in an alteration of the two components of the electronic spin's g factor and that the latter produces a perturbing term of the same form as the nuclear rotational g factor. Physically this latter term may be ascribed to the coupling with an external field of the magnetic moment created by the rotation of the electrons. If the zero-field constants for a molecule are known, then it is possible to fit the electron resonance spectrum by varying slightly the values of the rotational g factor and the components of the g tensor from its isotropic free electron value. Such analyses have been attempted with O_2 ^{34,40} and SO ^{37,38} and have met with good success. However, the interpretation of these parameters and their relationship with the zero-field parameters have not been unambiguous.

Kayama and Baird⁴¹ have published the latest and seemingly most authoritative interpretation to date. Their work, which gave particular attention to O_2 , essentially extended the treatment of the spin-orbit interaction to higher than second order by modifying the coefficient of the dominant $^3\Sigma$ state in the wavefunction. They retained the second order treatment of other perturbations, which is, of course, formally justified if the spin-orbit perturbation is much larger than the other terms. They also neglected other possible third-order corrections due to spin-orbit coupling, but since it has been noted that such contributions can only affect the parameter preceding the second-rank spin tensors, this is not vitally important.

Under these assumptions they showed that the third-order correction considered further modifies the spin-rotation coupling constant and the components of the spin g value. The assumption was made that most of this third-order correction arises from a low-lying $^1\Sigma$ state, and a relation between the modified g value components and the spin-rotation coupling constant established. By calculation of the nuclear part of the spin-rotation coupling constant *via* molecular wavefunctions for O_2 , the value of the g factor components excluding the third-order, relativistic, and diamagnetic effects may be determined from the experimental results. Kayama and Baird attributed the remaining anisotropy of the g factor components to the third-order effects alone and thereby obtained the squared coefficient of the $^1\Sigma$ state in the true ground state wavefunction to be of the order of 10^{-4} . They, however, offered no justification of the neglect of the relativistic and diamagnetic correction terms given by \mathcal{H}_{Z2} , and judgment con-

cerning the quantitative significance of their determination of the $^1\Sigma$ character of the ground state would seem to have to await the clarification of this point.

We have postponed discussion of the SeO spectrum until now, since even though it has a $^3\Sigma$ ground state, the spectrum⁴² obtained therefrom is quite different than those discussed previously. From O_2 to SeO the coefficient λ of the second-rank spin tensor has increased some fortyfold. The origin of this increase almost certainly lies in stronger higher-order effects of spin-orbit coupling (especially to the low-lying $^1\Sigma$ state of the same configuration) present in the heavier molecule. Where in O_2 and SO the term in λ was respectively subordinate to and competitive with the nuclear rotational term, it is dominant in SeO where the ratio B/λ is less than 10^{-2} .

It thus is convenient to change the representation for SeO from case (b) to case (a). In this representation $\Sigma = \Omega$ has three possible values, ± 1 and 0. However, for $\Omega \neq 0$, basis functions with a definite value of Ω are not most appropriate. We thus take the symmetric and antisymmetric linear combinations of these basis vectors to form functions $f^{S/A}$. (For a detailed discussion of the motivation and mechanics of this step, see Section IV.B.) The function with $\Omega = 0$ is already of definite symmetry which, incidentally, alternates with J . Using these basis functions and the matrix elements of the previous section, it is easily shown that the three Ω components of a given J state are singularly located. The levels $f^{S/A}$ are separated from the level with $\Omega = 0$ by approximately 2λ or in SeO by about 170 cm^{-1} , and the different J states are as usual separated by approximately $2BJ$ from the term BJ^2 of \mathcal{H}_R^N . The rotational expectation values of the states $f^{S/A}$ for a given J are degenerate, but they are unmixable by any parity conserving Hamiltonian. The degeneracy is broken by the $\mathbf{J} \cdot \mathbf{S}$ term of \mathcal{H}_R^N which may be seen to connect the $\Omega = 0$ state with the $f^{S/A}$ state of the same symmetry and the value of J . As Eq. (2.34) shows, the matrix elements of this perturbation increase in magnitude as J increases, which means that the zero-field splitting between the states $f^{S/A}$ increases with increasing J . This *spin doubling* of the $f^{S/A}$ states in heavier $^3\Sigma$ molecules is in every respect similar to the Λ -doubling effect in light molecules, which is discussed in Section IV.B.

The effects of a magnetic field upon this energy level structure can be ascertained from \mathcal{H}_{Z1} in Eq. (3.86). We see that its expectation value in all Ω states is given by

$$\frac{g\beta H\Omega^2}{J(J+1)}$$

which implies that the $\Omega = 0$ state is nonmagnetic and the $f^{S/A}$ states have overall g values of 1 for $J = 1$; $1/3$ for $J = 2$, etc. Electric dipole transitions are allowed between the $f^{S/A}$ states and herein arises the electron resonance spectrum, the approximate spacings between the M_J levels being given *via* the above g factors and the zero-field splittings.

B. Λ -Doubling

For all electronic states other than $^{2S+1}\Sigma_0$, each state, in fact, consists of two components $|\eta, J, S, \Omega, \Lambda, \Sigma, M_J\rangle$ and $|\eta, J, S, -\Omega, -\Lambda, -\Sigma, M_J\rangle$. These two components differ only in that they have opposite signs for the projections of all angular momenta in the molecule-fixed coordinate system, and in a hypothetical cylindrically symmetric nonrotating molecule they are degenerate. In an actual rotating molecule the rotation of the nuclei destroys the cylindrical symmetry and splits the two degenerate states. This splitting, known as the Λ -doubling in states where $|\Lambda| \geq 1$, can have a significant effect on the electron resonance spectrum, and we now consider this effect.

As has been mentioned, the Λ -doubling arises principally from the $q = \pm 1$ matrix elements such as given in Eqs. (3.28), (3.61), (3.87), (3.92), etc. which connect electronic states of $\Delta\Lambda = \pm 1$. Of course, a quantitative calculation of the Λ -doubling involves the details of these matrix elements and the inclusion (in principle) of all excited electronic states. However, some important qualitative features of the Λ -doubling can be revealed by considering only the interaction of two pairs of states $|\Lambda\rangle$, $|\Lambda + 1\rangle$, $|\Lambda - 1\rangle$ where all quantum numbers other than Λ have been suppressed. In this basis the matrix for that part of the Hamiltonian responsible for the Λ -doubling is given symbolically by

$$\mathcal{H}_\Lambda = \begin{matrix} & \begin{matrix} |\Lambda\rangle & |\Lambda + 1\rangle & |-\Lambda\rangle & |-\Lambda - 1\rangle \end{matrix} \\ \begin{pmatrix} a + E & l & f & g \\ l^* & b & h & 0 \\ f^* & h^* & c + E & j \\ g^* & 0 & j^* & d \end{pmatrix} \end{matrix} \quad (4.5)$$

where E is the presumably large energy difference between the 2 electronic states. The matrix element $\langle \Lambda + 1 | \mathcal{H}_\Lambda | -\Lambda - 1 \rangle$ is between states with $\Delta\Lambda \geq 2$ and is presumed to be zero.

This 4 by 4 matrix may be simplified by consideration of the inversion operator, I , and by transformation to a new set of basis functions which are eigenfunctions of I . We use case (a) basis functions for this example; the arguments for case (b) follow analogously. As was shown in Eq. (2.59), the

basis function $|\eta, J, S, \Omega, \Lambda, \Sigma, M_J\rangle$ is proportional to ${}^S f_\Omega D_{M_J, \Omega}^{J*}(\alpha, \beta, \gamma)$ where ${}^S f_\Omega$ is a function depending only on spin and relative spatial coordinates. We now examine separately the effect of I on ${}^S f_\Omega$ and $D_{M_J, \Omega}^{J*}$.

An inversion is equivalent to the following transformation of the Euler angles:¹⁴ $\alpha \rightarrow \alpha + \pi$, $\beta \rightarrow \pi - \beta$, $\gamma \rightarrow \pi - \gamma$. Insertion of this transformation into the formula for the rotation matrix¹⁰

$$D_{M_J, \Omega}^{J*}(\alpha, \beta, \gamma) = e^{iM_J\alpha} [(J + \Omega)!(J - \Omega)!(J + M_J)!(J - M_J)!]^{1/2} \sum_x \frac{(-1)^x}{(J + M_J - x)!(J - \Omega - x)!(x - M_J + \Omega)!x!} \left(\cos \frac{\beta}{2}\right)^{2J - \Omega + M_J - 2x} \left(\sin \frac{\beta}{2}\right)^{-M_J + \Omega + 2x} e^{i\Omega\gamma} \quad (4.6)$$

leads to the result that $ID_{M_J, \Omega}^{J*}(\alpha, \beta, \gamma) = (-1)^{J - \Omega} D_{M_J, -\Omega}^{J*}(\alpha, \beta, \gamma)$. Since ${}^S f_\Omega$ depends only on spin and relative spatial coordinates, the effect of I on ${}^S f_\Omega$ is the same as the effect of σ_{xz}^V on ${}^S f_\Omega$ where σ_{xz}^V is the reflection in the plane containing the molecule fixed x and z axes. Chiu⁴³ has shown that $\sigma_{xz}^V {}^S f_\Omega = (-1)^{\Omega - S} {}^S f_{-\Omega}$ and combining these two results leads to

$$I|\eta, J, S, \Omega, \Lambda, \Sigma, M_J\rangle = (-1)^{J - S} |\eta, J, S, -\Omega, -\Lambda, -\Sigma, M_J\rangle \quad (4.7)$$

Thus, although $|\eta, J, S, \Omega, \Lambda, \Sigma, M_J\rangle$ is not itself an eigenfunction of I , it may be seen that the linear combinations

$$(1/\sqrt{2})\{|\eta, J, S, \Omega, \Lambda, \Sigma, M_J\rangle \pm (-1)^{J - S} |\eta, J, S, -\Omega, -\Lambda, -\Sigma, M_J\rangle\}$$

are eigenfunctions with eigenvalues ± 1 .

Thus, the new basis functions have a definite parity, and no parity conserving operator such as \mathcal{H}_Λ can have matrix elements between functions of different parity. Using this fact and for simplicity writing the new basis set as

$$\begin{aligned} \sqrt{2}|\Lambda^\pm\rangle &= |\Lambda\rangle \pm |-\Lambda\rangle \\ \sqrt{2}|\Lambda + 1^\pm\rangle &= |\Lambda + 1\rangle \pm |-\Lambda - 1\rangle \end{aligned} \quad (4.8)$$

we find that \mathcal{H}_Λ is factored into 2 two by two matrices and is given by

$$\mathcal{H}_\Lambda = \begin{matrix} & \begin{matrix} |\Lambda^+\rangle & |\Lambda + 1^+\rangle & |\Lambda^-\rangle & |\Lambda + 1^-\rangle \end{matrix} \\ \begin{pmatrix} \alpha + E & \epsilon & 0 & 0 \\ \epsilon^* & \beta & 0 & 0 \\ 0 & 0 & \gamma + E & \phi \\ 0 & 0 & \phi^* & \beta \end{pmatrix} & \end{matrix} \quad (4.9)$$

where

$$\begin{aligned}
 2\alpha &= a + c + f + f^* \\
 2\beta &= b + d \\
 2\varepsilon &= e + g + h^* + j \\
 2\gamma &= a + c - f - f^* \\
 2\phi &= e - g - h^* + j
 \end{aligned} \tag{4.10}$$

Diagonalization of \mathcal{H}_Λ gives the eigenvalues W_Λ^\pm and $W_{\Lambda+1}^\pm$ which, in turn, give the Λ -doubling frequencies (suppressing h) in the 2 electronic states, v_Λ and $v_{\Lambda+1}$, as

$$\begin{aligned}
 v_\Lambda = W_\Lambda^+ - W_\Lambda^- &= \frac{1}{2}\{(\alpha - \gamma) + \sqrt{(\alpha' - \beta)^2 - 4(\alpha'\beta - \varepsilon\varepsilon^*)} \\
 &\quad - \sqrt{(\gamma' + \beta)^2 - 4(\gamma'\beta - \phi\phi^*)}\}
 \end{aligned}$$

$$v_{\Lambda+1} = W_{\Lambda+1}^+ - W_{\Lambda+1}^- = (\alpha - \gamma) - v_\Lambda \tag{4.11}$$

where $\alpha' = \alpha + E$, $\gamma' = \gamma + E$. We see that unless $\Lambda = 0$ the $\Delta\Lambda = 1$ selection rule requires that $f = g = h = 0$ and therefore $\alpha = \gamma$, $\varepsilon = \phi$, and $v_\Lambda = v_{\Lambda+1} = 0$. Thus within the approximation of only two interacting states, Λ -doubling occurs only in states due to their interaction with Σ states. The general validity of the approximation may be seen by the fact that Λ -doubling has only been observed in the electron resonance spectra of Π states, though the physically distinct spin-doubling has been observed in $^3\Sigma$ states.

For the case of a Π state interacting with a Σ state the Λ -doubling is given by

$$\begin{aligned}
 v_\pi = v_{\Lambda+1} &= \frac{1}{2}\{(f + f^*) - (\alpha' - \beta)\sqrt{1 + 4\varepsilon\varepsilon^*/(\alpha' - \beta)^2} \\
 &\quad + (\gamma' - \beta)\sqrt{1 + 4\phi\phi^*/(\gamma' - \beta)^2}\} \\
 &\cong \frac{1}{2}(f + f^*) - \frac{\alpha' - \beta}{2} - \frac{\varepsilon\varepsilon^*}{(\alpha' - \beta)} + \frac{\gamma' - \beta}{2} + \frac{\phi\phi^*}{(\gamma' - \beta)} \\
 &= \frac{\phi\phi^*}{\gamma' - \beta} - \frac{\varepsilon\varepsilon^*}{\alpha' - \beta}
 \end{aligned} \tag{4.12}$$

where the quantities under the square root have been expanded assuming $(\alpha' - \beta)^2 \gg 4\varepsilon\varepsilon^*$ and $(\gamma' - \beta)^2 \gg 4\phi\phi^*$. Further expanding the denominator and assuming $2E \gg \gamma - \beta$, $\alpha - \beta$ gives

$$v_\pi = \frac{\phi\phi^* - \varepsilon\varepsilon^*}{E} - \frac{\phi\phi^*(\gamma - \beta) - \varepsilon\varepsilon^*(\alpha - \beta)}{E^2} \tag{4.13}$$

The second term is, in general, always nonzero. However, since it is second order in the expansion parameter E^{-1} it makes only a minor contribution to the Λ -doubling and we therefore ignore it in this discussion.

Substitution of Eq. (4.10) into Eq. (4.13) produces for the first term

$$v_{\pi} = \frac{1}{E} \operatorname{Re} \{ (e + j)(g^* + h) \} \quad (4.14)$$

In general e and j are nonvanishing, but there are further restrictions on the states involved to assure that g and h are nonzero. These latter quantities are matrix elements of the type $\langle \Lambda + 1, \Omega_{\pi} | \mathcal{H}_{\Lambda} | -\Lambda, -\Omega_{\pi} \rangle$ where the previously suppressed quantum number has been restored. The selection rule $\Delta\Omega = 0, \pm 1$ requires that $\Omega_{\pi} \leq 1$ for g and h be nonzero, i.e., to first order, Λ -doubling can only occur in Π_0 , $\Pi_{1/2}$, and Π_1 states. All the Π states thus far observed by electron resonance spectroscopy have been $^2\Pi$ states,

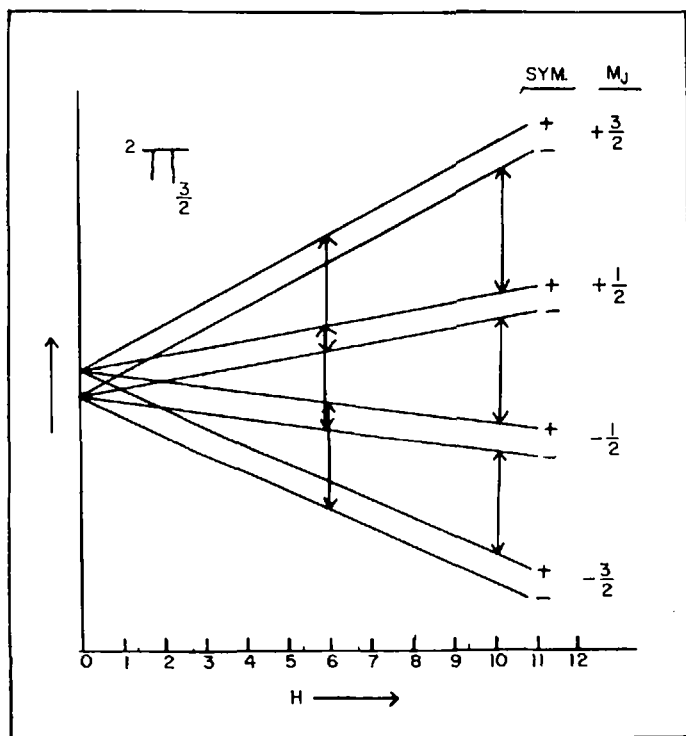


Fig. 4. Effect of Λ -doubling on the electron resonance spectrum of a hypothetical molecule. Hyperfine and nonlinear Zeeman effects have been ignored.

and the ${}^2\Pi_{1/2}$ is essentially nonmagnetic. However, as has been mentioned, the rotational motion of the molecule mixes the fine structure states giving the magnetic state some ${}^2\Pi_{1/2}$ character, and Λ -doubling has therefore been observed by electron resonance spectroscopy.

The principal effect of the Λ -doubling on the electron resonance spectrum is to super-impose a zero-field splitting on the level structure discussed previously. Since the Λ -doublets are of opposite parity the effect is to split the normal electron resonance spectra into two spectra as shown in Figure 4. Since the Λ -doubling adds to the Zeeman splitting in one spectrum and subtracts in the other, the separation of the two spectra is roughly $\Delta H = 2\nu_{\Lambda}/g_{\text{eff}}\beta$.

The matrix elements e and j which appear in Eq. (4.14) each contain a term linear in B , the rotational "constant" operator, and a term linear in A_i , the spin-orbit coupling operator. The matrix elements g and h are linear in B and therefore the magnitude of the doubling depends largely on the product $A_i B$. Although for larger molecules B decreases, in general A_i increases and even quite heavy molecules have large Λ -doublings in their ${}^2\Pi_{1/2}$ state. However, since the observation of Λ -doubling in electron resonance spectroscopy depends on the mixing of the fine structure states, and since this mixing decreases as the ratio B/A_i decreases, the observation of Λ -doubling is confined to hydrides and other light molecules. Since the phenomenon of Λ -doubling is caused by rotational uncoupling of Λ from the internuclear axis, it is larger in the higher rotational states (increases with increasing J). As electron resonance usually observes only the lower rotational states, this further restricts the observation of Λ -doubling. However, the Λ -doubling in several light molecules has been measured by electron resonance and the values are given in Table III.

C. Nuclear Magnetic and Electric Hyperfine Couplings

We first recall that the nuclear magnetic hyperfine interaction consists of three physically distinct contributions, summarized in the hyperfine Hamiltonian,

$$\mathcal{H}_{mhf} = \sum_{a,i} \left\{ (a_i + a_i') T^1(\mathbf{I}) \cdot T^1(\mathbf{I}_i) + \left[\frac{8\pi}{3} \delta(\mathbf{r}_{ai}) T^1(\mathbf{S}_i) \cdot T^1(\mathbf{I}) \right. \right. \\ \left. \left. + \sqrt{10} r_{ai}^{-3} T^1(\mathbf{I}) \cdot T^1(\mathbf{S}_i, C^2) \right] g g_a \beta \beta_N \right\} \quad (4.15)$$

The matrix elements in case (a) and case (b) representations were given in Section III; it remains for us to describe the observable effects in the electron resonance spectra. The main point of interest is the extent to which the

TABLE III
 Λ -Doubling in $^2\Pi_{3/2}$ Molecules.

| Molecule | J | $\nu_A(\text{Mc})$ |
|-------------------------------|-----------|--------------------|
| O^{16}H^a | $J = 3/2$ | 1666.34 |
| O^{16}H^a | $J = 5/2$ | 6033.5 |
| O^{16}H^a | $J = 1/2$ | 13437.8 |
| O^{16}D^a | $J = 3/2$ | 310.12 |
| SeH^b | $J = 3/2$ | 14.4 |
| TeH^b | $J = 3/2$ | 6.6 |
| SH^c | $J = 3/2$ | 111.42 |
| SD^d | $J = 3/2$ | 16 |
| $\text{N}^{14}\text{O}^{16e}$ | $J = 3/2$ | 0.906 |
| $\text{N}^{14}\text{O}^{16e}$ | $J = 5/2$ | 3.601 |
| $\text{N}^{15}\text{O}^{16e}$ | $J = 3/2$ | 0.814 |
| $\text{N}^{15}\text{O}^{16e}$ | $J = 5/2$ | 3.224 |

^a Ref. 49.

^b Ref. 51.

^c Ref. 50.

^d C. C. McDonald, *J. Chem. Phys.*, **39**, 2587 (1963). ν_A calculated from measured splittings assuming $g_{SD} = 0.8205$.

^e Ref. 33.

three contributions can be separated and their relative magnitudes assessed.

The case of molecules in $^1\Delta$ states is readily dealt with, since the three-electron resonance spectra described so far have not shown hyperfine structure. Myers⁴⁴ and co-workers have observed ^{17}O hyperfine structure in the $^1\Delta$ state of $^{17}\text{O}^{16}\text{O}$ but the details have not yet been published. The interpretation should be relatively simple, since the electron spin-dependent terms in (4.15) vanish.

Most of the electron resonance spectra studied so far refer to radicals in the $J = 3/2$ rotational level of the $^2\Pi_{3/2}$ state. The simplest cases are those in which the Λ -doubling is not resolved, for example, ClO ,⁴⁵ BrO ,⁴⁶ IO ,⁴⁶ NS ,⁴⁷ SF ,³¹ SeF ,³¹ CF ,⁴⁸ etc. The observable effect of hyperfine interaction with a nucleus of spin I is a splitting of each $\Delta M_J = \pm 1$ transition into $2I + 1$ components. The hyperfine splitting may be readily identified, as in the cases of SF and SeF (Figure 5) which show doublet splitting from ^{19}F ($I = 1/2$) and ClO (Figure 6) where we have a quartet splitting from the chlorine nuclei ($I = 3/2$). In BrO and IO , however, the hyperfine splitting

is comparable with the second-order Zeeman splitting of the $\Delta M_J = \pm 1$ groups, and the assignment of the spectrum is somewhat more difficult. This point is illustrated in Figure 7 which shows the two spectra. In BrO hyperfine interaction with ^{79}Br and ^{81}Br results in two spectra of twelve lines each ($I = 3/2$) which are of equal intensity because of the almost

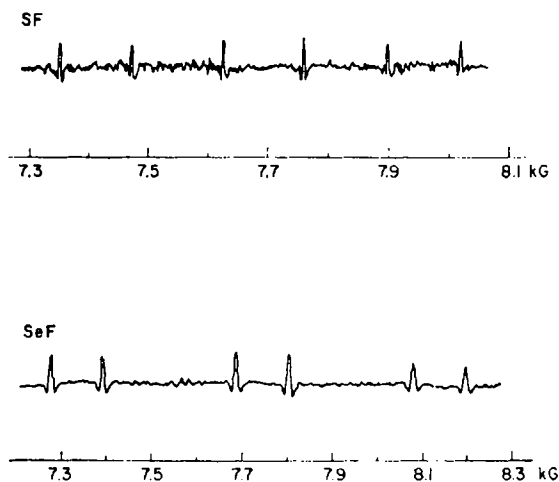


Fig. 5. The electron resonance spectra of SF and SeF in the $^2\Pi_{3/2}$, $J = 3/2$ state observed with Stark modulation.

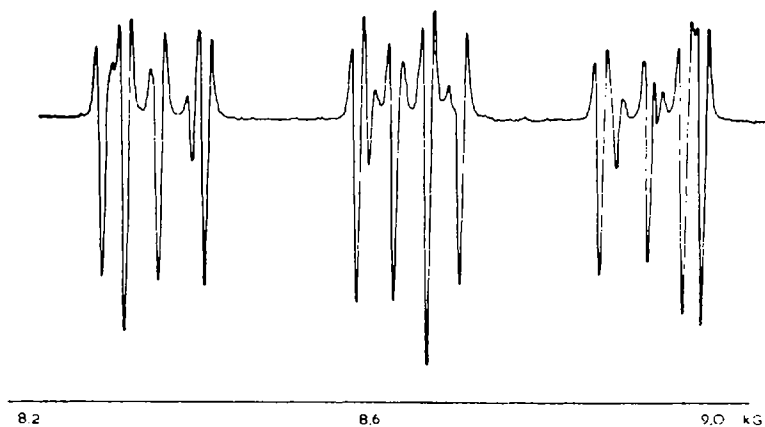


Fig. 6. The electron resonance spectrum of ClO in the $^2\Pi_{3/2}$, $J = 3/2$ state observed with Stark modulation.

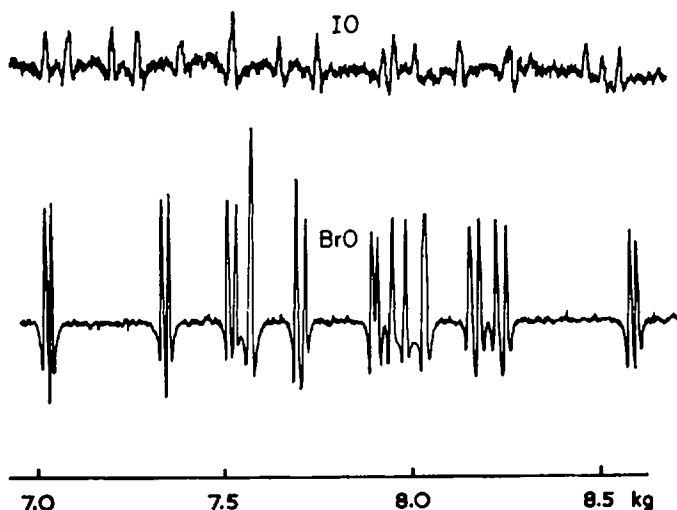


Fig. 7. The electron resonance spectrum of BrO and IO in the $^2\Pi_{3/2}$, $J = 3/2$ state observed with Stark modulation.

equal natural abundance of the two isotopes. The spectrum of IO is somewhat easier to interpret since only ^{127}I gives hyperfine splitting, the nuclear spin $I = 5/2$ resulting in a sixfold splitting of each $\Delta M_J = \pm 1$ group.

As we have shown earlier, the observed hyperfine splitting arises from three different interactions and, ideally, one would wish to separate the three contributions. However, this is not usually possible on the basis of the electron resonance spectrum alone, particularly if the radical conforms closely to Hund's case (a) coupling. Resonance experiments are then restricted to $^2\Pi_{3/2}$ states and they yield the total hyperfine component along the internuclear axis. Employing Eqs. (3.67), (3.69), (3.70), and (3.77), we see that this component, which we call h , is given by

$$h = a + (1/2)\alpha' + \beta' \quad (4.16)$$

where

$$\begin{aligned} a &= 2\beta g_N \beta_N \langle r_{\alpha i}^{-3} \rangle_\eta \\ \alpha' &= \left(\frac{8\pi}{3} \right) \psi_\eta^2(0) g \beta g_N \beta_N \\ \beta' &= g \beta g_N \beta_N \langle r_{\alpha i}^{-3} C_0^2(\omega_{\alpha i}) \rangle_\eta \end{aligned} \quad (4.17)$$

and the expectation values are the average values for the unpaired electrons. Measurements in the $^2\Pi_{1/2}$ state would enable one to separate a from α' and β' but since this state is essentially nonmagnetic in a good case (a) molecule, electron resonance measurements are not possible. In this situation it is particularly desirable to have pure microwave data available.

One further point concerns the signs of the hyperfine parameters. If the hyperfine interaction is large enough for matrix elements off-diagonal in M_J and M_I to have a significant effect, it is possible to determine both the sign and magnitude of the hyperfine component along the internuclear axis. This has been accomplished in BrO and IO, but not in ClO where the hyperfine interaction is much smaller.

We turn now to radicals in which Λ -doubling effects are important, particularly the diatomic hydrides OH,⁴⁹ SH,⁵⁰ and SeH.⁵¹ The hyperfine Hamiltonian contains terms which are not invariant upon reflection σ_{xz}^V of electron coordinates in a plane through the figure axis, and hence may be expected to lift the Λ -degeneracy. In $^2\Pi_{3/2}$ states, however, these effects are much smaller than those arising from rotational distortion, and what one observes experimentally is a difference in the hyperfine interaction for each Λ -doublet. Inspection of Eq. (4.15) reveals that the only terms in the Fermi contact and $\mathbf{I} \cdot \mathbf{L}$ interactions which are not unchanged under the operation σ_{xz}^V are also off-diagonal in Σ or Λ and by Eqs. (3.66) and (3.68) only connect states with $|\Delta\Omega| = 1$. They will only be responsible for hyperfine doubling *via* interactions with excited electronic states, and such doubling is too small to have been observed up to the present time. The remaining terms in (4.15), representing the electron-nuclear dipolar coupling must, however, be examined more closely. The term in $C_0^2(\omega_{ai})$ is unchanged by reflection in the xy plane of the molecule and so contributes equally to each Λ -doublet. On the other hand, the subsequent terms are not invariant to σ_{xz}^V ; $C_{\pm 1}^2$ terms, like the contact and $\mathbf{I} \cdot \mathbf{L}$ interactions only connect with excited electronic states, lifting the Λ -degeneracy, but producing effects which are too small to be measured so far. The $C_{\pm 2}^2$ terms by Eq. (3.74) interconnect the component states $|- \Lambda, -\Sigma\rangle$ and $|\Lambda, \Sigma\rangle$ of a Λ -doublet eigenfunction giving equal and opposite contributions to each Λ -doublet. These terms have matrix elements only within the $\Pi_{1/2}$ Λ -doublets, but exhibit observable effects in the $\Pi_{3/2}$ states because of rotational mixing. Measurements of these effects yield values for a fourth hyperfine constant, d , which we define by

$$d = \sum_{q=\pm 2} g\beta g_N \beta_N \langle r_{ai}^{-3} C_q^2(\omega_{ai}) \rangle_\eta \quad (4.18)$$

Hyperfine interactions in OH have been discussed extensively by Radford^{50,1} for the ^1H coupling, and by Carrington and Lucas⁵² for the ^{17}O coupling.

Because of the very large rotational constant, mixing of ${}^2\Pi_{1/2}$ and ${}^2\Pi_{3/2}$ states is sufficient for both states to be measurable by electron resonance techniques. Combination of the electron resonance and pure microwave studies yields complete separation of the hyperfine terms.

Finally, we deal with molecules in ${}^3\Sigma$ states, the most important examples being O_2 and SO . Hyperfine interactions with ${}^{17}\text{O}$ in O_2 ($I = 5/2$) and with ${}^{33}\text{S}$ in SO ($I = 3/2$) have been studied. The most important difference between these systems and the ${}^2\Pi_{3/2}$ molecules discussed earlier is that effects due to orbital angular momentum are much less important. The fact that the electronic spin is not strongly coupled to the internuclear axis means that, in general, electron resonance studies yield more information on the hyperfine coupling than in good case (a) ${}^2\Pi_{3/2}$ states. The ${}^{33}\text{S}$ hyperfine interaction in SO has been studied by Carrington, Levy, and Miller,⁵³ using electron resonance and by Amano et al.,⁵⁴ using pure microwave techniques. Accurate values of the hyperfine parameters b and c were obtained.

We now deal with the observable effects of the nuclear electric quadrupole interaction, which are particularly well illustrated by the spectrum of ClO shown in Figure 6. The four hyperfine lines in the central group of the ${}^{35}\text{Cl}{}^{16}\text{O}$ spectrum are essentially equally-spaced, but the quartet spacings in the low and high field groups are clearly unequal. This is due to the electric quadrupole interaction, which we recall for a single nucleus can be expressed in the form

$$\mathcal{H}'_Q = \sum_c \frac{c e^2 Q \sqrt{3}}{I(2I-1) \sqrt{2} r_{ac}^3} T^2(I) \cdot C^2(\omega_{ac}) \quad (4.19)$$

The matrix elements of \mathcal{H}'_Q in a decoupled case (a) representation can be obtained from the slightly more general Eqs. (3.82) and (3.83). The most important terms are those for which $q = q' = 0$ and the summed reduced matrix elements $\langle \eta \Lambda \| r_{ac}^{-3} C_0^2(\omega_{ac}) \| \eta \Lambda \rangle$ is then conventionally expressed as q_0 , the axial component of the electric field gradient. (The quantity $e^2 q_0 Q$ is usually called the quadrupole coupling constant.) Expansion of the Clebsch-Gordon symbols in (3.82) when $q = q' = 0$ reveals that the first-order quadrupole coupling energy is proportional to $M_J^2 M_I^2$. Since the center group in the ClO spectrum arises from the $M_J = 1/2$ to $-1/2$ transition, with $\Delta M_I = 0$ the first-order quadrupole term does not affect the positions of the lines, which are therefore almost equally spaced (the second-order interaction introduces slight inequalities in spacing). The outer groups, however, arise from transitions between levels of different M_J^2 , and the first-order quadrupole energy therefore affects the line positions. Determination of both the magnitude and the sign of the quadrupole

coupling constant is straightforward, and has been carried out for ^{14}N in NO^{55} and NS^{47} , ^{35}Cl and ^{37}Cl in ClO , ^{79}Br and ^{81}Br in BrO , ^{127}I in IO and ^{17}O in OH^{52} .

We note finally that quadrupole terms for which $q \neq 0$ are only likely to be of interest in molecules with measureable Λ -doubling effects, and they have been discussed in detail by Lin and Mizushima,⁵⁶ and by Brown and Radford,³³ for ^{14}N in $^{14}\text{N}^{16}\text{O}$. Table IV contains the measured hyperfine constants for molecules observed by electron resonance.

TABLE IV
Hyperfine Constants of $^2\Pi$ Molecules

| Molecule | eqQ (Mc) | Magnetic hyperfine constant (Mc) |
|---------------------------------|----------------------------------|--|
| SeH^a | — | $A_1 = 1.9$ |
| TeH^a | — | $A_1 = 1.8$ |
| $^{35}\text{Cl}^{16}\text{O}^b$ | -88 | $h = 111$ |
| SF^c | — | $h = 428.4$ |
| SeF^c | — | $h = 325.6$ |
| $^{79}\text{Br}^{16}\text{O}^d$ | 649.8 | $h = 504.5$ |
| IO^d | -1907.0 | $h = 582.1$ |
| NS^e | 3.1 | $h = 56.8$ |
| SH^f | — | $A_1 = 5.61$ |
| $^{14}\text{N}^{16}\text{O}^g$ | $eqq_1 = 1.81$ $eqq_2 = 15.4$ | $a = 84.28$ $\alpha' = 22.2$ $\beta' = -19.6$ $d = 95$ |
| OH^h | — | $a = 86.0$ $\alpha' = -74.6$ $\beta' = 44.4$ $d = 46.1$ |

^a Ref. 51. A_1 is defined in Ref. 49 and equals $.4h$ for a pure $^2\Pi_{3/2}$, $J = 3/2$ state.

^b Ref. 32.

^c Ref. 31.

^d Ref. 46.

^e Ref. 47.

^f Ref. 50.

^g Ref. 33.

^h Ref. 49.

D. Intensities and Lineshape

For a pressure-broadened nonsaturated microwave transition the imaginary part of the magnetic susceptibility, $\chi''(\omega)$, can adequately be represented near resonance by⁵⁷

$$\chi''(\omega) = \frac{\omega}{kT} |\mu_{ij}|^2 f(\omega - \omega_0) (N/Z) \exp(-E_i/kT) \quad (4.20)$$

where μ_{ij} is the transition dipole matrix element between the transition states, $f(\omega - \omega_0)$ is the normalized lineshape as a function of transition frequency, N is the total number of molecules, and Z is the partition function. In an electron resonance experiment the microwave frequency is kept constant and the system is tuned to resonance by sweeping the applied magnetic field. Therefore, in order to calculate the observed signal shape and intensity the lineshape must be expressed as a function of field. Kronig and Strandberg⁵⁸ have shown that this may be done using the formula

$$f(\omega - \omega_0) = \frac{\hbar}{g_{\text{eff}} \beta} f(H - H_0) \quad (4.21)$$

where β is the Bohr magneton and $g_{\text{eff}} = (\hbar/\beta)(d\omega/dH)$.

It is customary to apply a modulating magnetic field in addition to the dc field, and therefore the lineshape of $f(H - H_0)$ may be a quite complicated function. The signal detected by the spectrometer, $\chi''(H)$, is passed through a narrow-band, phase-sensitive detector tuned to the modulation frequency, and therefore the recorded signal is not proportional to $\chi''(H)$ but to the amplitude of the Fourier component of $\chi''(H)$ at the modulation frequency.

Wahlquist⁵⁹ has calculated the Fourier amplitudes of $f(H - H_0)$ assuming a Lorentzian lineshape. Using his calculations together with the Van Vleck-Weiskopf formula⁵⁷ and the $f(\omega) \rightarrow f(H)$ transformation of Kronig and Strandberg,⁵⁸ the recorded electron resonance signal for the transition $i \rightarrow j$ is given by

$$S(H) = \frac{C\omega N_i \hbar}{KT g_{\text{eff}} \beta} |\mu_{ij}|^2 \frac{\delta H}{2\pi} \mathcal{A}_1(H) \quad (4.22)$$

Here ω is the transition frequency, δH is the full linewidth, and C is a constant which depends only on instrumental parameters. N_i , the number of molecules in the i th state has been substituted for $(N/Z) \exp(-E_i/kT)$ to allow for nonequilibrium distribution. The Fourier amplitude $\mathcal{A}_1(H)$ (given explicitly by Wahlquist⁵⁹) is the recorded signal shape and reduces to the familiar derivative of a Lorentzian in the limit $H_\omega \ll \delta H$ where H_ω is the peak-to-peak modulation amplitude. The maximum peak-to-peak recorded signal height is given by

$$S_p = \frac{2\sqrt{3}C\omega N_i \hbar}{\pi K T g_{\text{eff}} \beta H_\omega} |\mu_{ij}|^2 [\phi(\phi - 2)]^{-1/2} \quad (4.23)$$

where $\phi = 2 + 4/3 \theta^2 + 4/3 \theta(\theta^2 + 3/4)^{1/2}$ and $\theta = \delta H/2H_\omega$.

The transition dipole matrix elements may refer to either magnetic or electric dipole transitions. For magnetic dipole transitions the transition operator describes the interaction with an external microwave magnetic field, which, from Eqs. (2.100) and (2.113) has the approximate form

$$\mu^M = \beta \mathbf{H}_{\text{osc}} \cdot (g_L \mathbf{L} + g_S \mathbf{S} + g_N \mathbf{N} - \sum_{\alpha} g_I^{\alpha} \mathbf{I}) \quad (4.24)$$

where H_{osc} is the microwave magnetic field and the sum is over all magnetic nuclei. We deal with paramagnetic systems and $g_N/g \approx g_I/g \approx \beta_N/\beta$ where β_N is the nuclear magneton; therefore only the first two terms will contribute to the transition moment to any observable extent. The transition operator may be written in spherical tensor form as

$$\mu^M \approx \beta \sum_q (-1)^q T_{-q}^{-1}(\mathbf{H}) T_q^{-1}(g_L \mathbf{L} + g_S \mathbf{S}) \quad (4.25)$$

Using the Wigner-Eckhart theorem the matrix elements $\mu_{ij}^M = \langle JM_J \gamma | \mu^M | J' M_J' \gamma' \rangle$ may be easily derived as

$$\begin{aligned} \mu_{ij}^M = & -\beta \sum_q (-1)^q T_{-q}^{-1}(\mathbf{H}) \frac{\langle J' 1 M_J' q | JM_J \rangle}{\langle J' 1 M_J 0 | JM_J \rangle} \\ & \langle JM_J \gamma | g_L T_0^{-1}(\mathbf{L}) + g_S T_0^{-1}(\mathbf{S}) | J' M_J' \gamma' \rangle \end{aligned} \quad (4.26)$$

where the matrix element appearing in Eq. (4.26) has already been derived in Section III in connection with the dc Zeeman effect. For a coupled representation J must be replaced by F and M_J by M_F .

For electric dipole transitions the transition operator may be taken from Eq. (2.114) to be

$$\mu^E = \mathbf{E}_{\text{osc}} \cdot \boldsymbol{\mu} = \sum_q (-1)^q T_q^{-1}(\mathbf{E}) T_{-q}^{-1}(\boldsymbol{\mu}) \quad (4.27)$$

where E_{osc} is the microwave electric field and $\boldsymbol{\mu}$ is the molecular electric dipole moment. Since E_{osc} is defined in the space-fixed coordinate system and $\boldsymbol{\mu}$ is defined in the molecule-fixed system, we must rotate the components of the dipole moment using the rotation matrix $D_{0q}^{-1*}(\alpha\beta\gamma)$. Because only the $T_0^{-1}(\boldsymbol{\mu})$ component of the dipole moment has a nonvanishing expectation value in the molecule-fixed system, the transition operator is

$$\mu^E = \mu_0 \sum_q (-1)^q T_q^{-1}(\mathbf{E}) D_{q0}^{-1*} \quad (4.28)$$

Using the relationship between the Hund's case (*a*) basis functions and the rotational matrices given in Eq. (2.59), and expressing the integral of three rotational matrices as a product of Clebsch-Gordon coefficients (see

Eq. 3.64), the matrix elements of μ^E in a decoupled case (*a*) basis are given by

$$\begin{aligned}\mu_{ij}^E &= \langle J\Omega M_J | \mu^E | J'\Omega' M_J' \rangle \\ &= \mu_0 \sum_q (-1)^q T_q^1(\mathbf{E}) \langle J'1M_J'q | JM_J \rangle \langle J'1\Omega'0 | J\Omega \rangle \left(\frac{2J'+1}{2J+1} \right)^{1/2} \quad (4.29)\end{aligned}$$

In a coupled case (*a*) representation the electric dipole transition operator operates only on the part of the wavefunction not associated with the nuclear spin, and in this case the method of Section III.A for deriving the matrix elements may be used. Explicitly these matrix elements are

$$\begin{aligned}\mu_{ij}^E &= \langle FJI\Omega M_F | \mu^E | F'J'I\Omega' M_F' \rangle = \mu_0 \sum_q T_q^1(\mathbf{E}) (-1)^{q+I+1-J'-F} \\ &\quad \langle F'1M_F'q | FM_F \rangle [(2J+1)(2F'+1)]^{1/2} W(JFJ'F'; 11) \\ &\quad (J\Omega || D_0^{1*} || J'\Omega') \quad (4.30)\end{aligned}$$

where the reduced matrix element is the same as that in Eq. (4.29); that is

$$(J\Omega || D_0^{1*} || J'\Omega') = \left(\frac{2J'+1}{2J+1} \right)^{1/2} \langle J'1\Omega'0 | J\Omega \rangle \quad (4.31)$$

To obtain the matrix of μ^E in a Hund's case (*b*) representation we first consider a representation which separates the electron spin from the other variables. This may be regarded as the electron spin decoupled representation related to the case (*b*) functions via the Clebsch-Gordon coefficients, the good quantum numbers being $|K\Lambda M_K S M_S\rangle$. These basis functions are therefore formed from the direct product of the symmetric top eigenfunction $|K\Lambda M_K\rangle$ and a spin function $|S M_S\rangle$. Since μ^E does not operate on $|S M_S\rangle$ the necessary matrix may be derived in the same way as was Eq. (4.29) and this gives:

$$\begin{aligned}\mu_{ij}^E &= \langle JK S \Lambda M_J | \mu^E | J'K' S \Lambda' M_J' \rangle = \mu_0 \sum_q T_q^1(\mathbf{E}) (-1)^{q+S+1-K'-J} \\ &\quad \langle J'1M_J'q | JM_J \rangle [(2K+1)(2J'+1)]^{1/2} W(KJK'J'; S1) \\ &\quad (K\Lambda || D_0^{1*} || K'\Lambda') \quad (4.32)\end{aligned}$$

where

$$(K\Lambda || D_0^{1*} || K'\Lambda') = \left(\frac{2K'+1}{2K+1} \right)^{1/2} \langle K'1\Lambda'0 | K\Lambda \rangle \quad (4.33)$$

An exactly similar transformation as that which led to Eq. (4.30) yields μ_{ij}^E in a coupled case (*b*) representation.

For many molecules, simple symmetric and antisymmetric combinations of the basis functions used to calculate the transition dipole moment matrix elements are to a very good approximation eigenfunctions of the molecular Hamiltonian \mathcal{H} . In these cases the matrix elements derived above (in conjunction with the parity selection rules discussed below) can be used directly in Eq. (4.23) to calculate the signal height. If the basis set chosen is not an approximate eigenfunction of \mathcal{H} , then the matrix μ_{ij} must first be transformed by the transformation which diagonalizes \mathcal{H} .

Equations (4.23), (4.26), (4.29), (4.30), and (4.32) provide a general way of calculating the observed heights of electron resonance spectral lines. However, without any further calculations on specific molecules, certain general conclusions may be drawn from these equations. In the first place, the ratio of electric to magnetic transition moments, R , is given by $R \equiv \mu_{ij}^E/\mu_{ij}^M = (\mu E/\beta H)Q$ where Q is a ratio of quantum numbers which is of the order of unity. For an electromagnetic wave in free space $E = H$ using cgs units, and the ratio $R \approx [\mu_0 \text{ (Debye)} \times 10^{-18}/\beta \text{ (ergs/gauss)}] \approx 10^2$ for a molecule with a dipole moment of 1 D. Since the ratio of signal heights goes as R^2 , it may be seen that in the limit of nonsaturation, electric dipole transitions are of the order of 10^4 times as strong as magnetic dipole transitions.

Moreover, the usual polarization and angular momentum selection rules may be easily obtained from the formulas for the transition dipole matrix elements. The requirements for the nonvanishing of the Clebsch-Gordon coefficient $\langle JIM_j q | J'M_j' \rangle$ that appears in Eqs. (4.26), (4.29), (4.30), and (4.32) leads to the selection rules $\Delta J = 0, \pm 1$ (or $\Delta F = 0, \pm 1$) and $\Delta M = q$ for both magnetic and electric dipole transitions. The latter selection rule implies that x' and y' components of E and H give rise to $\Delta M = \pm 1$ transitions and the z' component gives rise to $\Delta M = 0$ transitions, a significant factor in the design of experiments.

E. Stark Effect⁶⁰

If, in addition to the strong dc magnetic field, one applies a static electric field, there is an effect on the electron resonance spectrum. This effect is caused by the interaction of the electric field with the permanent electric dipole moment of the molecule and therefore may be used to measure electric dipole moments in diatomic radicals. The Hamiltonian for this interaction, which we will call \mathcal{H}_s , is just that given in Eqs. (2.114), (4.27), and (4.28) where now $T_q^1(\mathbf{E})$ refers to the components of the static electric field. In order to observe the largest effect the static electric field is always experimentally arranged parallel to the dc magnetic field, and therefore

only $T_0^1(\mathbf{E})$ is nonvanishing.* This Hamiltonian is a perturbation on the zero electric field Hamiltonian, \mathcal{H}_0 , and we wish to examine the effects of this perturbation on molecules in which the electronic (spin and orbital) angular momentum is quantized along the internuclear axis. It is only in this type of molecule where an experimentally obtainable electric field produces an observable effect on the electron resonance spectrum.

Since the electronic angular momentum is quantized along the internuclear axis, it is reasonable to set up the problem in a Hund's case (a) basis. However, the Hund's case (a) basis functions themselves are not eigenfunctions of \mathcal{H}_0 . The reason for this involves the symmetry operator I , the inversion of all particles through the center of mass. \mathcal{H}_0 commutes with I and therefore any eigenfunction of \mathcal{H}_0 must also be an eigenfunction I , i.e., it must have a definite parity. However, as was shown in Section IV.C, the application of I to the case (a) basis function $|\Omega\rangle$ gives plus or minus $|- \Omega\rangle$, and thus the case (a) functions themselves are not eigenfunctions of I . The correct eigenfunctions of both \mathcal{H}_0 and I were shown to be of the form†

$$\psi_{JM_J|\Omega}^{S/A} = \frac{1}{\sqrt{2}} \{ f_{\Omega} U_{M_J\Omega}^J \pm (-1)^J f_{-\Omega} U_{M_J-\Omega}^J \} \quad (4.34)$$

where the $U_{M_J|\Omega}^J$ are the case (a) basis functions. Although $\psi_{JM_J|\Omega}^{S/A}$ may be an eigenfunction of \mathcal{H}_0 , it does not have to be as J , M_J , and $|\Omega|$ need not be good quantum numbers of \mathcal{H}_0 . In the following discussion it is assumed that $\psi_{JM_J|\Omega}^{S/A}$ is, in fact, an eigenfunction of \mathcal{H}_0 . In all molecules in which the Stark effect has been observed (with the possible exception of $^3\Sigma$ SeO) departures from case (a) coupling have been small and have led to barely observable effects. The extension to cases in which case (a) coupling breaks down involves matrix diagonalization but presents no new problems.

Since the electric field interaction operator changes sign under inversion, and since the $\psi^{S/A}$ are of a definite parity, there will be no diagonal matrix elements of \mathcal{H}_S in the $\psi^{S/A}$ basis. With the electric fields used the Stark energy is small (of the order of 100 Mc), and there must therefore be nearly degenerate energy levels in order to observe a Stark effect. The levels ψ^S

* As may be seen from Eq. (4.29) a perpendicular electric field (here the z' direction is defined by the magnetic field) would mix states of different M_J . Since these states are separated by the Zeeman energy and since the Stark energy is much smaller than the Zeeman energy, a perpendicular field would produce only a small Stark effect.

† It is clear that $\psi_{JM_J|\Omega}^{S/A}$ might need to be multiplied by a nuclear spin function. Reference 60 shows that all complications resulting from such a possibility can be easily disposed with using perturbation theory for all molecules examined thus far.

and ψ^A are separated by an energy δ by the Λ -doubling discussed above, and if δ is not too large this near-degeneracy leads to an observable Stark effect.

Using the matrix elements of Eq. (4.29) one can set up and diagonalize the matrix of $\mathcal{H}_0 + \mathcal{H}_S$ in the $\psi^{S/A}$ basis. The eigenvalues and eigenfunctions which this leads to are

$$\begin{aligned} W_1 &= W_0 + \frac{\delta + R}{2} \\ W_2 &= W_0 + \frac{\delta - R}{2} \\ \psi_1(M_J) &= \frac{1}{\sqrt{2R}} \{ \xi(R + \delta)^{1/2} \psi^S + (R - \delta)^{1/2} \psi^A \} \\ \psi_2(M_J) &= \frac{1}{\sqrt{2R}} \{ (R - \delta)^{1/2} \psi^S - \xi(R + \delta)^{1/2} \psi^A \} \end{aligned} \quad (4.35)$$

where $R = [\delta^2 + 4\epsilon^2]^{1/2}$, $\epsilon = -E_0\mu_0\Omega M_J/J(J+1)$, $\xi = -M_J/|M_J|$, and W_0 is an eigenvalue of \mathcal{H}_0 .

The Stark effect consists not only of changes in line positions caused by the dependence of W_1 and W_2 on E_0 , but also of changes in intensity caused by the dependence of ψ_1 and ψ_2 on E_0 . We may calculate the changes in intensity by calculating $T_{\alpha\beta}$, the probability of a transition $\psi_\alpha \rightarrow \psi_\beta$. The observed transitions are all $\Delta J = 0$, $M_J \rightarrow M_J + 1$ and using Eqs. (4.29) and (4.35) these transition probabilities are

$$\begin{aligned} T_{11} = T_{22} &= \left| \frac{\xi_a[(R_a + \delta)(R_b - \delta)]^{1/2} + \xi_b[(R_a - \delta)(R_b + \delta)]^{1/2}}{2(R_a R_b)^{1/2}} \right|^2 |\mu_{ij}^E|^2 \\ T_{12} = T_{21} &= \left| \frac{[(R_a - \delta)(R_b - \delta)]^{1/2} - \xi_a \xi_b [(R_a + \delta)(R_b + \delta)]^{1/2}}{2(R_a R_b)^{1/2}} \right|^2 |\mu_{ij}^E|^2 \end{aligned} \quad (4.36)$$

$$(4.37)$$

where a and b distinguish quantities evaluated for M_J and $M_J + 1$ states, respectively.

Two limiting cases of considerable interest arise when the Stark energy is respectively much greater than or much less than the Λ -doubling. For these cases the energies, eigenfunctions, and transition probabilities are

$$\begin{aligned}
 E_0 \mu_0 &\gg \delta \\
 W_1 &= W_0 + \xi \varepsilon & W_2 &= W_0 - \xi \varepsilon \\
 \psi_1(M_J) &= f_{\xi \Omega} U_{M_J, \xi \Omega}^J & \psi_2(M_J) &= -f_{-\xi \Omega} U_{M_J, -\xi \Omega}^J \\
 T_{12} &= T_{21} = 0 & T_{11} &= T_{22} = |\mu_{ij}^E|^2
 \end{aligned} \quad (4.38)$$

$$\begin{aligned}
 E_0 \mu_0 &\ll \delta \\
 W_1 &= W_0 + \delta + \varepsilon^2/\delta & W_2 &= E_0 - \varepsilon^2/\delta \\
 \psi_1(M_J) &= \xi \psi^S & \psi_2(M_J) &= -\xi \psi^A \\
 T_{12} &= T_{21} = |\mu_{ij}^E|^2 & T_{11} &= T_{22} = 0
 \end{aligned} \quad (4.39)$$

These two extremes are called first-order and second-order Stark effects, respectively, because of the electric field dependence of the energy.

Figure 8 shows the energy levels of the $J = 3/2$ state of a ${}^2\Pi_{3/2}$ molecule as a function of electric field, and the allowed transitions in the two extreme

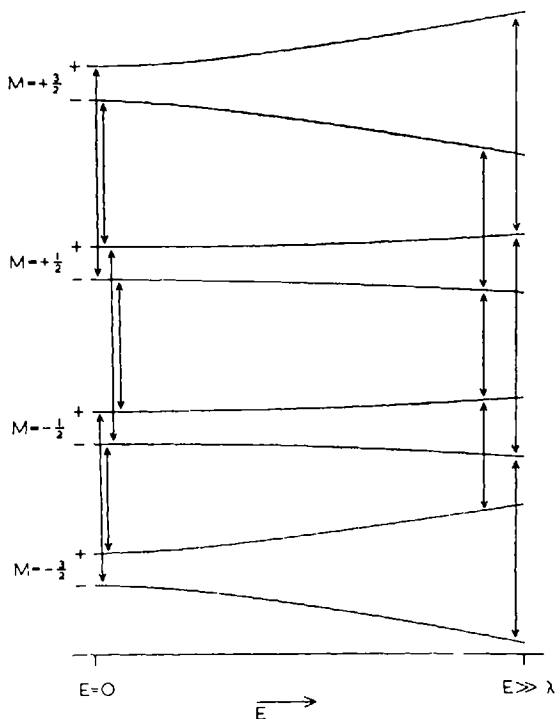


Fig. 8. Energy levels and allowed electric dipole transitions of the $J = 3/2$ state of a molecule as a function of electric field. Magnetic field is held constant.

cases. Of course, in the intermediate cases all the indicated transitions are allowed to some extent. It should be noted that in the weak field limit the two outside transitions are affected more strongly by the electric field than is the center transition. It should also be noted that for an $M_J \rightarrow M_J + 1$ where $|M_J| = |M_J + 1|$, the transition probabilities are independent of electric field and the same two transitions are allowed in the strong and weak field case. Figure 9 shows the stick diagram of the spectrum of this

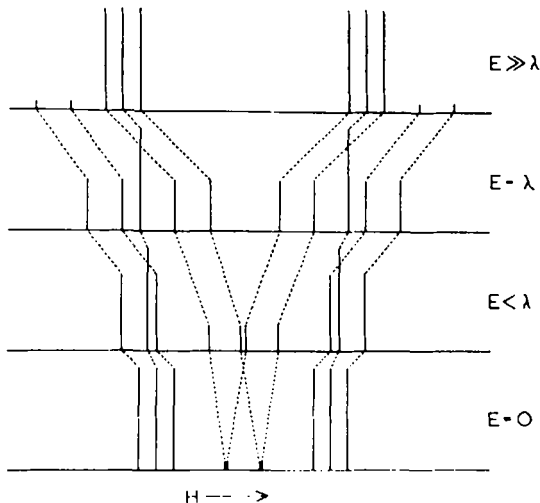


Fig. 9. Stick diagram of electron resonance spectrum (absorption vs. magnetic field) of $J = 3/2$ state of a $^2\Pi_{3/2}$ molecule at various values of electric field. Dotted lines indicate correlation of spectral lines as electric field changes.

hypothetical molecule for several values of electric field.

As shown above, the Stark effect allows one to measure dipole moments by application of a static electric field. It also provides a means of modulating the spectrum by application of an alternating field, and this Stark modulation has several advantages over the usual Zeeman modulation. The difficulties of introducing a high audio frequency magnetic field through the metal walls of the sample cavity are not encountered if one uses the walls themselves as Stark electrodes. Moreover, interference from other paramagnetic species such as O_2 , OH , or atoms is avoided if these species have a small or vanishing Stark effect due to large Λ -doubling or zero dipole moment.

The shape of the recorded signal when using Stark modulation differs from that given in Eq. (4.21). The effect of the electric field is to change the energy levels according to Eq. (4.35) and this, in turn, is equivalent to a

change in magnetic field. One can define a function $H'(|E_0 + E_\omega \cos \omega t|, \gamma)$ which is the pseudomagnetic field which would produce the same effect as the electric field. Here E_0 is the static electric field, E_ω is the peak-to-peak amplitude of the modulating electric field, and γ represents all the quantum numbers and other quantities necessary to define the Stark effect for a given transition. In general, γ is different for each transition, but because the Stark energy appears with plus and minus signs in Eq. (4.33), the transitions always occur in pairs such that the pseudomagnetic field for the two transitions in a pair is $\pm H'(|E_0 + E_\omega \cos \omega t|, \gamma)$. The fact that H' is a function of the absolute value of the total field arises from the fact that R occurring in Eq. (4.33) depends on E_0^2 . The field H' may be inserted into the lineshape function $f(H - H_0 \pm H')$ and this may be Fourier analyzed to yield a recorded lineshape. Because of the pairing property mentioned above, the complete spectrum will consist of pairs of lines where each line in the pair has the same shape and height but the two lines are 180° out of phase. The fact that H' depends on the absolute value of the field means that if $E_0 = 0$, $f(H - H_0 + H')$ will only have Fourier components at harmonics of the modulating frequency but not at the fundamental. Thus, a static electric bias field is necessary for Stark modulation just as the strong dc magnetic field is necessary for Zeeman modulation.

It may be shown⁶⁰ that for a first-order Stark effect the recorded lineshape for Stark modulation is the same as that for Zeeman modulation with the exception of the 180° phase shift which occurs in half the lines. The two lines in each pair are separated by the static Stark splitting and, if this is approximately the same size as the linewidth, the partial superposition of the two out-of-phase lines (which are approximate first derivatives of Lorentzians) produces a lineshape which resembles a second derivative Lorentzian line.

One further effect occurs for second-order or intermediate Stark effects where some of the observed transitions are forbidden in zero electric field. If the modulating electric field is a large part of the total electric field, these transitions are intensity modulated as well as position modulated. To calculate the resulting observed lineshape the Fourier analysis would have to be carried out using a lineshape function

$$IT(|E_0 + E_\omega \cos \omega t|)f(H - H_0 + H')$$

where the function IT describes the intensity modulation.

V. EXPERIMENTAL

Electron resonance spectroscopy differs from ordinary microwave spectroscopy in that the spectrometer operates at a single fixed frequency

and the energy levels are tuned into resonance by a magnetic field. For a transition to be both electric dipole allowed and magnetic field tuneable there must be a coupling between the electric and magnetic dipole moments of the molecule. In a linear molecule in a nonsigma state this coupling may be provided by the spin-orbit interaction, and in a triplet multiplet state the coupling may be provided by either the second-order spin-orbit coupling or the spin-spin interaction. Although this places a restriction on the molecules that can be studied by electron resonance spectroscopy, for these molecules this method is considerably more sensitive than ordinary swept frequency microwave spectroscopy.

Because only a single microwave frequency is used, the spectrometer may employ a resonant cavity as an absorption cell. The relative sensitivity of resonant cavity versus nonresonant waveguide cells has been discussed by Townes and Schawlow,⁶¹ who have shown that the sensitivity (expressed as a minimum detectable absorption coefficient, α_{\min}) of a nonresonant absorption cell of length L is

$$\alpha_{\min}^{NR} = \frac{4}{L} \left(\frac{2KT\Delta\nu N}{P_0 e^{-\alpha_0 L}} \right)^{1/2} \quad (5.1)$$

where $\Delta\nu$ and N are, respectively, the bandwidth and noise figure of the detector, P_0 is the power incident on the cell, and α_0 is the attenuation coefficient of the empty cell. For a resonant cavity absorption cell they have shown that the sensitivity is given by

$$\alpha_{\min}^R = \frac{2\pi}{Q\lambda} \left(\frac{4KT\Delta\nu N}{P_0} \right)^{1/2} \quad (5.2)$$

where Q is the cavity "Q factor." Equations (5.1) and (5.2) would imply that in both cases the spectrometer sensitivity could be increased indefinitely by increasing the power which the sample sees, but this, of course, neglects the fact that eventually power saturation will occur. In fact, there is an optimum power level, P , which occurs when the sample is just beginning to saturate and which produces maximum sensitivity. In the resonant system the power that the sample sees is Q times the incident power, and for maximum sensitivity $P_0 = (P/Q)k$ where $k \approx 1$. Assuming optimum power in both cases and $k = 1$, the ratio of resonant to nonresonant sensitivity is given by

$$\frac{\alpha_{\min}^{NR}}{\alpha_{\min}^R} = \frac{\sqrt{2Q^{1/2}\lambda e^{\alpha_0 L/2}}}{\pi L} \quad (5.3)$$

For unlimited sample volume the nonresonant path length, L , can usually be increased to offset the advantage of a resonant system. However, for short-lived species generated in a flow system the sample length is given by the species lifetime times the mean velocity in the direction of flow. In most of the systems studied the sample path length is of the same order of magnitude as λ (a few centimeters or less), and since α_0 is around 10^{-3}cm^{-1} the use of a resonant cavity leads to an improvement in sensitivity of the order of $Q^{1/2} \approx 100$.

There is a further advantage in the use of a resonant cavity when studying systems at fairly high pressure ($\sim 1\text{--}10$ Torr) or when observing weak transitions such as magnetic dipole transitions. As mentioned above, optimum sensitivity requires sufficient microwave power to almost saturate the transition. For a nonresonant system this amount of power might require an impractically powerful microwave source. However, since in a resonant system the effective power is Q times the incident power, almost all gas-phase transitions can be saturated with a convenient microwave source.

The most difficult problem in electron resonance spectroscopy is generating a sufficient steady-state concentration of radicals in the spectrometer cavity to allow observation of a spectrum. The earliest experiments on unstable species generated the radical in a discharge located some distance upstream of the spectrometer cavity.^{50,37} The time required to pump the radicals from the discharge to the cavity limits this type of experiment to species with reasonably long effective lifetimes. In later work it was possible to generate observable concentrations of shorter lived species by the heterogeneous reaction of atoms with solid materials deposited on the walls of the spectrometer cavity.⁵¹ All of the experiments of these authors have been carried out in the flow system, shown in Figure 10, and in most experiments the radicals are produced by reacting unstable atoms with a stable gas inside the spectrometer cavity.

In a typical experiment the small pumps are closed off from the system, the large pump is opened, and a primary gas, such as O_2 or N_2 , is bled through the needle valve into the primary manifold to a steady state pressure of a few torr. The primary gas is pumped through the microwave discharge cavity, where it is partially dissociated into atoms and through the spectrometer cavity. Sufficient secondary gas is then admitted through the secondary manifold to titrate the atoms, the atomic electron resonance signal being used to monitor atom concentration. In some experiments the radical of interest is formed in the discharge and then pumped into the spectrometer cavity. With the mixing technique the radical of interest is formed at the point of observation, and very short-lived species have been observed.

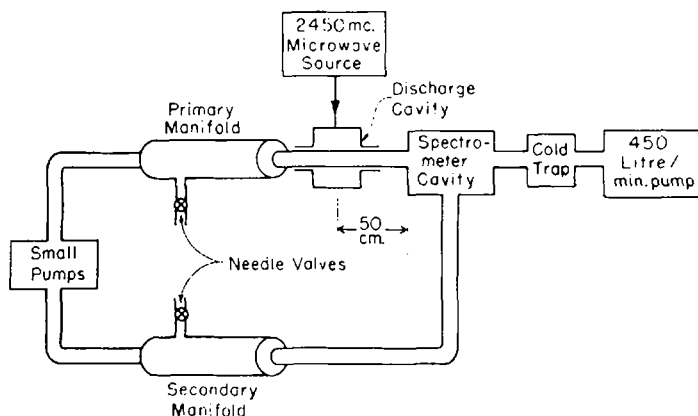


Fig. 10. Diagram of flow system used in mixing experiments.

The spectrometer used in these experiments is a standard EPR spectrometer and magnet, however, two specialized cylindrical sample cavities have been developed. The first cavity, shown in Figure 11, operates in the TE_{011} mode and is oriented with the cylinder axis parallel to the dc magnetic field. The body of the cavity is machined from brass and is gold-plated. A Teflon liner provides electrical insulation between the cavity body and end plates and also provides a groove for the O-ring vacuum seal. The end plates are gold-plated titanium disks with thin-walled pockets machined in them. Modulation coils placed behind the thin walls allow a 100-kc modulating magnetic field to be applied to the sample. The metal end plates of the cavity may be used to apply both static and modulating electric fields. The disks and coils are potted in epoxy resin for mechanical strength. As this cavity is vacuum tight it may be directly connected to the inlet and exhaust vacuum systems and no glass sample cell insert is necessary. Because of the orientation of the cavity, the filling factor is optimized for $\Delta M_J = \pm 1$ electric dipole transitions and $\Delta M_J = 0$ magnetic dipole transitions, but is very poor for $\Delta M_J = \pm 1$ magnetic dipole transitions and zero for $\Delta M_J = 0$ electric dipole transitions. An early model of this cavity has been described in detail elsewhere.^{6,2}

The second cavity also operates in the TE_{011} mode but is oriented with the cylinder axis perpendicular to the magnetic field. This cavity was constructed of epoxy resin with silver wire coils forming the inner cylinder wall and solid metal end plates. This cavity has no provision for Stark modulation but produces a very effective Zeeman modulation field. The sample is contained in a cylindrical quartz pillbox which fits inside the

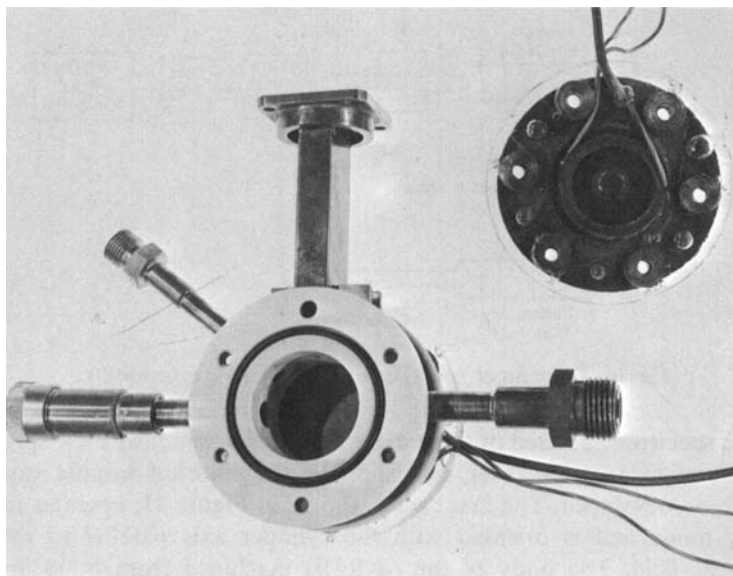


Fig. 11. Stark and Zeeman modulated electron resonance microwave cavity.

cavity, and the inlet and outlet tubes pass through one-inch holes in the cavity end plates. The orientation of the cavity provides the optimum filling factor for $\Delta M_J = \pm 1$ magnetic dipole transitions and good, but less than optimum, filling factor for all electric dipole transitions.

Acknowledgments

D.H.L. wishes to thank the National Science Foundation and the Advanced Research Projects Agency for support of this research.

References

1. M. Mizushima and R. M. Hill, *Phys. Rev.*, **93**, 745 (1954).
2. C. A. Burrus and J. D. Graybeal, *Phys. Rev.*, **109**, 1553 (1958).
3. F. K. Powell and D. R. Lide, *J. Chem. Phys.*, **41**, 1443 (1964).
4. G. C. Dousmanis, T. M. Sanders, and C. H. Townes, *Phys. Rev.*, **100**, 1735 (1955).
5. W. Lichten, *Phys. Rev.*, **119**, 848 (1960); **126**, 1020 (1962).
6. R. S. Freund and W. Klemperer, *J. Chem. Phys.*, **43**, 2422 (1965).

7. M. Born and J. R. Oppenheimer, *Ann. Phys.*, **84**, 457 (1927).
8. M. Born and K. Huang *Dynamical Theory of Crystal Lattices*, Oxford Univ. Press, London, 1954.
9. H. Eyring, J. Walter, and G. E. Kimball, *Quantum Chemistry*, Wiley, New York, 1944.
10. M. E. Rose, *Elementary Theory of Angular Momentum*, Oxford Univ. Press, London, 1962.
11. A. Messiah, *Quantum Mechanics*, Vol. 2, North Holland, Amsterdam, 1961.
12. D. M. Brink and G. R. Satchler, *Angular Momentum*, Oxford Univ. Press, London, 1962.
13. See, for instance, R. de L. Kronig, *Band Spectra and Molecular Structure*, Cambridge University Press, London, 1932.
14. E. P. Wigner, *Group Theory*, Academic Press, New York, 1959.
15. J. H. Van Vleck, *J. Chem. Phys.*, **4**, 327 (1936).
16. M. Phillips, *Phys. Rev.*, **76**, 1803 (1949).
17. A. Abragam and J. H. Van Vleck, *Phys. Rev.*, **92**, 1448 (1953).
18. P. A. M. Dirac, *The Principles of Quantum Mechanics*, Oxford Univ. Press, London, 1947.
19. G. Breit, *Phys. Rev.*, **34**, 553 (1929).
20. H. A. Bethe and E. E. Salpeter, *Handbuch der Physik*, Vol. 35.
21. L. R. Foldy and S. A. Wouthuysen, *Phys. Rev.*, **78**, 29 (1950).
22. J. H. Van Vleck, *Rev. Mod. Phys.*, **23**, 213 (1951).
23. C. G. Darwin, *Phil. Mag.*, **39**, 537 (1920).
24. L.-Y. Chiu, *J. Chem. Phys.*, **40**, 2276 (1964).
25. T. A. Miller, *Mol. Phys.*, **16**, 105 (1969).
26. K. F. Freed, *J. Chem. Phys.*, **45**, 4214 (1966).
27. A. Carrington, D. H. Levy, and T. A. Miller, *Proc. Roy. Soc.*, **A293**, 108 (1966).
28. A. Carrington, G. N. Currie, D. H. Levy, and T. A. Miller, to be published.
29. A. M. Falick, B. H. Mahan, and R. J. Myers, *J. Chem. Phys.*, **42**, 1827 (1965).
30. H. E. Radford, *Phys. Rev.*, **126**, 1035 (1962).
31. A. Carrington, G. N. Currie, D. H. Levy, and T. A. Miller, *J. Chem. Phys.*, **50**, 2726 (1969).
32. A. Carrington, P. N. Dyer, and D. H. Levy, *J. Chem. Phys.*, **47**, 1756 (1967).
33. R. L. Brown and H. E. Radford, *Phys. Rev.*, **147**, 6 (1966).
34. M. Tinkham and M. W. P. Strandberg, *Phys. Rev.*, **97**, 937, 951 (1955).
35. A. F. Henry, *Phys. Rev.*, **80**, 396 (1950).
36. L. K. Keys, *J. Phys. Chem.*, **70**, 3760 (1966).
37. J. M. Daniels and P. B. Dorain, *J. Chem. Phys.*, **45**, 26 (1966).
38. A. Carrington, D. H. Levy, and T. A. Miller, *Proc. Roy. Soc.*, **A298**, 340 (1967).
39. K. Kayama and J. C. Baird, *J. Chem. Phys.*, **43**, 1082 (1965).
40. K. D. Bowers, R. A. Kamper, and C. D. Lustig, *Proc. Roy. Soc.*, **A251**, 565 (1959).
41. K. Kayama and J. C. Baird, *J. Chem. Phys.*, **46**, 2604 (1967).
42. A. Carrington, G. N. Currie, D. H. Levy, and T. A. Miller, to be published.
43. Y. N. Chiu, *J. Chem. Phys.*, **45**, 2969 (1966), **42**, 2671 (1965). It is shown in these references that the inversion operation is also represented by the transformation $\alpha, \beta, \gamma \rightarrow \pi + \alpha, \pi - \beta, 2\pi - \gamma$ and the reflection σ_{yz}^V . This leads to mathematically distinct but physically identical results.
44. R. J. Myers, private communication.
45. A. Carrington, P. N. Dyer, and D. H. Levy, *J. Chem. Phys.*, **47**, 1756 (1967).

46. A. Carrington, P. N. Dyer, and D. H. Levy, *J. Chem. Phys.*, in press.
47. A. Carrington, B. J. Howard, D. H. Levy, and J. C. Robertson, *Mol. Phys.*, **15**, 187 (1968).
48. Unpublished work.
49. H. E. Radford, *Phys. Rev.*, **122**, 114 (1960).
50. H. E. Radford, and M. Linzer, *Phys. Rev. Lett.*, **10**, 443 (1963).
51. H. E. Radford, *J. Chem. Phys.*, **40**, 2732 (1964).
52. A. Carrington and N. Lucas, to be published.
53. A. Carrington, D. H. Levy, and T. A. Miller, *Mol. Phys.*, **13**, 401 (1967).
54. T. Amano, E. Hirota, and Y. Morino, *J. Phys. Soc. Jap.*, **22**, 399 (1967).
55. M. Mizushima, J. T. Cox, and W. Gordy, *Phys. Rev.*, **98**, 1034 (1955).
56. C. C. Lin and M. Mizushima, *Phys. Rev.*, **100**, 1726 (1955).
57. J. H. Van Vleck and V. W. Weisskopf, *Rev. Mod. Phys.*, **17**, 227 (1945).
58. S. Krongelb and M. W. P. Strandberg, *J. Chem. Phys.*, **31**, 1196 (1959).
59. H. Wahlquist, *J. Chem. Phys.*, **35**, 1708 (1961).
60. A. Carrington, D. H. Levy, and T. A. Miller, *J. Chem. Phys.*, **45**, 3450 (1966); **47**, 3801 (1967).
61. C. H. Townes and A. L. Schawlow, *Microwave Spectroscopy*, McGraw-Hill, New York, 1955.
62. A. Carrington, D. H. Levy, and T. A. Miller, *Rev. Sci. Instr.*, **38**, 1183 (1967).

APPROXIMATE MOLECULAR ORBITAL THEORIES

B. J. NICHOLSON

*Trinity College,
Cambridge,
England*

CONTENTS

| | |
|--|-----|
| I. Introduction | 249 |
| II. Theoretical Background | 251 |
| III. Possible Approximations | 253 |
| A. The Mulliken Approximation | 253 |
| 1. General Discussion | 253 |
| 2. Preliminary Investigation | 256 |
| 3. Errors in the Diagonal F-Matrix Elements | 258 |
| 4. Errors in the Two-Center Off-Diagonal Elements | 260 |
| 5. Final Remarks | 265 |
| B. The Ruedenberg Approximation | 266 |
| C. The Zero Differential Overlap Approximation | 269 |
| 1. Preliminary Discussion | 269 |
| 2. Numerical Investigation. | 271 |
| D. Neglect of Inner Shells | 277 |
| E. Averaging for Rotational Invariance | 281 |
| F. Semiempirical Approximations | 285 |
| IV. Current Theories. | 289 |
| A. Using the Mulliken Approximation | 289 |
| B. Using the Mulliken and Ruedenberg Approximations | 290 |
| C. Using the Zero Differential Overlap Approximation | 291 |
| V. Present Proposals | 295 |
| A. Formulation | 295 |
| B. Calibration | 298 |
| C. Reproduction of Reference Calculations | 300 |
| D. Agreement with Experiment | 302 |
| VI. Conclusions | 305 |
| References | 305 |

I. INTRODUCTION

Recently there have been many attempts to find a simple molecular orbital theory capable of giving useful results for both saturated and unsaturated molecules. One popular approach has been to elaborate the

successful Hückel theory of unsaturated compounds, using only overlap integrals and ionization potentials. Other work has been based on the self-consistent-field (SCF) equations, with the molecular orbitals (MOs) approximated as linear combinations of atomic orbitals (LCAOs).^{1,2}

In this article I shall consider the latter approach, making extensive use of accurate calculations on polyatomic molecules to test the approximate methods. First I shall discuss critically the key approximations [the Mulliken, Ruedenberg, and zero differential overlap (ZDO) approximations, together with common subsidiary approximations such as the neglect of inner shells, the use of semiempirical integrals, and averaging for rotational invariance] which, combined in various ways, make up most simple theories. Second, I shall show how the often serious inadequacies of these approximations are reflected in currently available methods; it is unusual that the right answers are obtained for the right reasons.

The main purpose of this survey is to find a new combination of the familiar approximations which is less vulnerable to criticism. The minimum target I set was the ability to reproduce both the eigenvalues and charge distributions of accurate (minimum basis set) SCF calculations. Though this is an humble aim, the following pages show that there is as yet no simple method which satisfactorily achieves it (I have covered the literature thoroughly up to the end of 1967, and with decreasing enthusiasm through the autumn of 1968). All the critical portion of this work is therefore written up as a search for a new method. This approach is particularly evident in my discussion of the Mulliken approximation, where I consider the various corrections necessary to make this famous approximation a reliable basis for a general approach.

In the final section of this article I shall specify my method in detail and demonstrate its ability to reproduce accurate SCF calculations. Having established this, I shall go on to consider briefly the possibility of modifying my approach to improve the agreement with experiment. Finally I shall comment on the success (or lack thereof) of my method in predicting ionization potentials, dipole moments, bond lengths and angles, and force constants.

Throughout this work I shall be judging approximate theories against reference calculations (that is, accurate SCF LCAO calculations with minimum basis sets and without configuration interaction). Since the approximate theories make explicit use of the SCF LCAO equations and often employ accurate minimum basis set calculations for calibration, this is fair enough. However, the inadequacies of such reference calculations are well known,^{3*} and there is always the possibility of transcending the minimum-basis-set single-determinantal framework^{4,5} by the judicious use

of spectroscopic information, "correlated" electron repulsion integrals, and variable parameters. It is obviously dangerous to criticize a semi-empirical theory for departures from the "accurate" calculations occasioned by the deliberate use of semiempirical integral values (though it is a risk I shall take on occasion).

On the other hand empirical arguments can be misused: if a theory is based on a numerical approximation demonstrably inadequate even within the minimum basis set framework, but yet by a semiempirical approach achieves results as good as, or better than, the more accurate calculations, this should be regarded neither as justification for the original approximation, nor as an indication that electron correlation has been painlessly introduced, but rather as a fortunate cancellation of errors. The present work lends weight to the supposition that the approximate calculations are most successful when they depart least from the formal SCF LCAO equations. The one possible, and familiar, exception is the correlation of uv spectra in unsaturated hydrocarbons, and even here I think that though semiempirical integrals seem to give better agreement with experiment, this is probably for reasons quite unrelated to traditional semi-empirical ideas of electron correlation.

II. THEORETICAL BACKGROUND

In this section I give the SCF LCAO equations,^{1,2,6} and describe my notation.

I seek MOs ψ_i in the LCAO form

$$\psi_i = \sum_p c_{ip} \phi_p, \quad (1)$$

where ϕ_p are atomic orbitals (AOs). The indices $i-l$ will be reserved for MOs, $p-s$ for AOs, and A-D for atoms. I shall also use $i-l$ and $p-s$ as a shorthand for $\psi_i-\psi_l$ and $\phi_p-\phi_s$, respectively, where this cannot cause confusion. Thus p_A will refer to ϕ_p on atom A. Numerical prefixes will always be used to distinguish particular valence AOs, e.g., $1s$, $2s$, $2p$.

Variational treatment of the AO coefficients c_{ip} leads, for molecules with a closed-shell configuration, to the equations

* There are many footnotes to this work, some quite long and of very limited interest. To minimize distraction from the main argument, all the footnotes have been put in the Reference Section at the end of the paper. The appearance of an asterisk against a reference number in the text, as here, indicates a footnote rather than a reference to another paper.

$$\sum_q F_{pq} c_{iq} = E_i \sum_q S_{pq} c_{iq}, \quad (2)$$

where (using atomic units),

$$F_{pq} = H_{pq} + G_{pq}, \quad (3)$$

$$H_{pq} = T_{pq} + V_{pq} = T_{pq} + \sum_A V_{pq}^A, \quad (4)$$

$$G_{pq} = J_{pq} - K_{pq}/2, \quad (5)$$

$$T_{pq} = \langle \phi_p | -\nabla^2/2 | \phi_q \rangle, \quad (6)$$

$$V_{pq}^A = \langle \phi_p | V^A | \phi_q \rangle, \quad (7)$$

$$J_{pq} = \sum_i^{\text{occ}} 2(pq | ii) = \sum_{r,s} P_{rs} (pq | rs), \quad (8)$$

$$-K_{pq}/2 = -\sum_i^{\text{occ}} (pi | qi) = -\sum_{r,s} P_{rs} (ps | qr)/2, \quad (9)$$

$$(pq | ii) = \iint \bar{\phi}_p(1) \phi_q(1) (r_{12})^{-1} \bar{\psi}_i(2) \psi_i(2) d\tau_1 d\tau_2, \quad (10)$$

$$(pq | rs) = \iint \bar{\phi}_p(1) \phi_q(1) (r_{12})^{-1} \bar{\phi}_r(2) \phi_s(2) d\tau_1 d\tau_2, \quad (11)$$

$$S_{pq} = \langle \phi_p | \phi_q \rangle, \quad (12)$$

and

$$P_{rs} = 2 \sum_i^{\text{occ}} \bar{c}_{ir} c_{is}. \quad (13)$$

In these equations the E_i are the orbital energies, or eigenvalues, of the MOs ψ_i ; they are the roots of the secular equations

$$|F_{pq} - ES_{pq}| = 0. \quad (14)$$

F_{pq} are the matrix elements of the Fock operator, or overall Hamiltonian. H_{pq} are the matrix elements of the core Hamiltonian, and can be partitioned into kinetic energy (T_{pq}) and potential energy in the electrostatic field of all the atom cores ($\sum_A V_{pq}^A$); each core consists of the bare nucleus and those electrons, if any, which are not being explicitly considered in the calculation (the net core charge will be denoted by Z'_A). G_{pq} is the matrix element of the potential due to other electrons, and can be split into a

Coulomb (J_{pq}) and an exchange (K_{pq}) contribution. The summations \sum_i^{occ} in Eqs. (8, 9, 13) are over occupied MOs (and not over electrons; the factor of 2 allows for this). Because J_{pq} and K_{pq} , and hence F_{pq} , depend on the MO coefficients, which in turn can only be obtained from F_{pq} , iteration to self-consistency is required.

The total electronic energy is given by

$$E_{\text{electronic}} = \sum_{p,q} P_{pq}(F_{pq} + H_{pq})/2 = \sum_i^{\text{occ}} E_i + \sum_{p,q} P_{pq} H_{pq}/2. \quad (15)$$

For the total molecular energy relative to the separated valence electrons and isolated cores, the core-core repulsion (represented by a point-charge model) must be added; this gives

$$E_{\text{total}} = E_{\text{electronic}} + \sum_{A>B} Z'_A Z'_B R_{AB},$$

where R_{AB} is the A-B internuclear distance.

In matrix form I can write Eq. (2) as

$$\mathbf{F}\mathbf{c}_i = (\mathbf{H} + \mathbf{G})\mathbf{c}_i = (\mathbf{T} + \sum_A \mathbf{V}^A + \mathbf{J} - \mathbf{K}/2)\mathbf{c}_i = \mathbf{E}_i \mathbf{S} \mathbf{c}_i, \quad (17)$$

where \mathbf{F} , \mathbf{H} , \mathbf{G} , \mathbf{T} , \mathbf{V}^A , \mathbf{J} , \mathbf{K} , \mathbf{S} , are matrices the elements of which appeared in Eqs. (2-12), and \mathbf{c}_i is the column matrix c_{ip} .

These equations, approximate though they be, present formidable computational problems in large molecules because of the number and difficulty of the three- and four-center integrals. I shall therefore discuss various approximations which simplify the problem.

III. POSSIBLE APPROXIMATIONS

A. The Mulliken Approximation

1. General Discussion

The Mulliken approximation⁸ simplifies integrals by assuming that

$$\phi_p(1)\phi_q(1) = S_{pq}[\phi_p(1)\phi_p(1) + \phi_q(1)\phi_q(1)]/2. \quad (18)$$

In this formula the charge distribution $\phi_p\phi_q$ is properly recognized as to magnitude by the use of S_{pq} , but its spatial distribution has been changed so that it is now partly described by $\phi_p\phi_p$ and partly by $\phi_q\phi_q$. Thus, as pointed out by Mulliken,⁸ the approximation will be most successful when used on the integrals of functions which are fairly constant over the whole region between ϕ_p and ϕ_q . An example would be the potential from a distant point charge. Equally, for the charge distribution itself^{9a} and for dipole

moment integrals, the approximation is not so good, and for kinetic energy integrals, which do not involve charge distributions,¹⁰ it is quite unsuitable.^{9a}

Assuming that Eq. (18) is only to be used for potential energy integrals, there are two main sources of error. First, when $S_{pq} \neq 0$ there will be many important integrals for which the displacement of the charge distribution introduced by the Mulliken approximation is serious; obvious examples are the integrals $\langle p_A | V^A | q_B \rangle$ and $(p^A q_B | r_A r_A)$, and, if atom C is between atoms A and B, $\langle p_A | V^C | q_B \rangle$ and $(p_A q_B | r_C r_C)$. The sign and magnitude of the errors can be predicted approximately in most cases, by inspection^{11*}; for example $\langle p_A | V^C | q_B \rangle$ will usually be underestimated by Eq. (18) when C is between A and B, since an electron occupying the region $\phi_p \phi_q$ will on average be closer to C than will an electron in either $\phi_p \phi_p$ or $\phi_q \phi_q$.

Secondly, there is an important class of nonzero integrals which are put equal to zero by the Mulliken approximation because the relevant overlap integral is zero; examples ($p \neq q$) are the one-center exchange integrals $(p_A q_A | p_A q_A)$ and the integrals $\langle p_A | V^B | q_A \rangle$, $(p_A q_A | r_B r_B)$. The neglect of one-center exchange integrals would render calculated charge distributions unreliable, since it would introduce errors into F_{pp} ranging from zero (if ϕ_p is a hydrogen 1s AO) to over 10 eV (for a fluorine 2s AO); in most approximate theories the use of spectroscopic data automatically corrects this omission. The neglect of the other integrals noted above has been discussed elsewhere⁹; it is equivalent to the omission of the often important zero-overlap F -matrix elements between orbitals on the same center. For similar reasons F -matrix elements between orthogonal orbitals on different centers (which, though less important,^{9c} may not always be negligible¹³) are neglected by the Mulliken approximation.

If the Mulliken approximation, with no corrections, is systematically introduced into Eqs. (4, 8, 9) this gives the familiar equations^{14a}

$$H_{pq} = T_{pq} + S_{pq} \sum_A (V_{pp}^A + V_{qq}^A)/2, \quad (19)$$

$$\begin{aligned} J_{pq} &= S_{pq} \sum_r N(r) [(pp|rr) + (qq|rr)]/2 \\ &= S_{pq} \sum_A (J_{pp}^A + J_{qq}^A)/2, \end{aligned} \quad (20)$$

and

$$-K_{pq}/2 = -\sum_{r,s} P_{rs} S_{ps} S_{qr} [(pp|qq) + (pp|rr) + (qq|ss) + (rr|ss)]/8, \quad (21)$$

where $N(r)$ is the Mulliken orbital population defined by¹⁵

$$N(r) = \sum_s P_{rs} S_{rs}, \quad (22)$$

and J_{pp}^A is defined by

$$J_{pp} = \langle p | J^A | p \rangle = \sum_q^A N(q_A) (pp | q_A q_A). \quad (23)$$

J^A describes the Coulomb potential arising from atom A containing its Mulliken population of electrons (here and elsewhere the superscript A following the summation sign indicates that the sum is restricted to orbitals on atom A). Even for diffuse orbitals, such as 4p in transition-metal complexes, where the $N(r)$ do not give useful pictures of the charge distribution,¹⁶ they are still appropriate as the controlling quantities in Eq. (20).¹⁶

Several points about these equations will be important later. First, with this approximation I can write

$$V_{pq} = S_{pq}(V_{pp} + V_{qq})/2, \quad (24)$$

$$J_{pq} = S_{pq}(J_{pp} + J_{qq})/2, \quad (25)$$

but

$$K_{pq} \neq S_{pq}(K_{pp} + K_{qq})/2; \quad (26)$$

because of the permutation operator in the exchange interaction the use of the Mulliken approximation on each integral individually does not imply an overall Mulliken-type relationship between K_{pp} , K_{qq} , and K_{pq} .

It is also worth noting that even if S_{pq} is zero, F_{pq} need not be in this approximation (unless so required by symmetry); there will in general be a nonzero contribution from the exchange interaction, K_{pq} . Unfortunately this does nothing to solve the problem of nonzero one-center F_{2s2p} matrix elements; the exchange contribution from Eq. (21) is usually small and of opposite sign to the true F_{2s2p} matrix element, at least for the molecules discussed below.

Equations (19–21) are not invariant to orthogonal transformations among the basis functions.^{7a,14a} The results obtained from the use of the Mulliken approximation depend on whether or not the basis set is hybridized, and on the choice of local axes for the orientation of nonspherically symmetric AOs. This problem can be surmounted,^{7a,14a} as I shall discuss later, either by introducing considerable complexity into the calculation, or by adopting average values for the integrals causing the difficulty. However, it can also be overcome by giving an unambiguous prescription for the choice of basis set before applying the Mulliken approximation. A judicious choice may improve the results; thus the approximation is more successful for hybrids of 2s and 2p Slater AOs than for the AOs themselves.¹⁷ An important example concerns 1s inner shell and 2s valence AOs on the same atom. One may work in terms of a 2s Slater orbital, which is not

orthogonal to the $1s$ orbital, or one may use a $2s$ orbital orthogonalized to the $1s$ (by Schmidt orthogonalization, or by transformation to "spectroscopic" orbitals^{18*}). The success of the Mulliken approximation on such integrals as $\langle 2s_A | V^A | 2s_B \rangle$ will be sharply affected by this choice; for example, in ethylene, since transformation from Slater to spectroscopic $2s$ orbitals decreases this integral by nearly 10%, the corresponding overlap integral by less than 1%, and increases the integral $\langle 2s_A | V^A | 2s_A \rangle$ by more than 10% ($\langle 2s_A | V^B | 2s_A \rangle$ is naturally not much altered), and since the Mulliken approximation is good for $\langle 2s_A | V^A | 2s_B \rangle$ in terms of Slater orbitals, it can be seen that the integral over spectroscopic orbitals will be seriously overestimated by the Mulliken approximation. The result for hybrids,¹⁷ noted above, may also depend on which $2s$ orbitals are used. (As the above remarks imply, my detailed numerical investigations will be confined to molecules with atoms no heavier than fluorine, and to minimum basis sets.)

2. Preliminary Investigation

Before attempting to correct the various inadequacies in the Mulliken approximation discussed above, it seemed sensible to investigate the potential usefulness of the uncorrected approach. I therefore performed a range of calculations for several molecules^{19a*} for which minimum basis set SCF LCAO results,^{19b*} F -matrices,^{19c*} and complete tabulations of integrals^{19d*} were obtainable. The standard calculation (I) made use of Eqs. (3, 5, 19–21) without any alteration. For ease of comparison the other calculations differed from the first in only one particular. In Calculation II the one-center exchange integrals omitted by use of Eq. (21) were reintroduced by adding a correction term to F_{pp} of

$$-\sum_q^A N(q_A)(p_A q_A | p_A q_A) \quad (q \neq p) \quad (27)$$

(this form has been arbitrarily chosen for the present purposes only, and will be briefly discussed later). In Calculation III the correct values of non-zero one-center F_{2s2p} matrix elements were introduced into Calculation I. In all these calculations the (minimum) basis sets and geometries of the reference calculations were employed, inner shells were explicitly included, and the calculated values used for all integrals needed in Eqs. (19–21). The calculations were iterated to self-consistency. Rather than work in terms of nodeless Slater $2s$ orbitals all integrals were transformed to spectroscopic orbitals before Eqs. (19–21) were employed.^{24*}

Some typical results from these calculations, for NH_3 , C_2H_2 , and C_2H_4 , are reported in Table I (Calculations IV–V will be referred to later). Comparison of Calculations I and II shows the importance of one-center

TABLE I
Effects of Approximations on SCF LCAO Calculations

| Calculation ^a | Accurate | I | II | III | IV | V | This work |
|---------------------------------|----------|--------|--------|--------|--------|----------------------------|-----------|
| Orbital Populations | | | | | | | |
| For hydrogen in NH ₃ | | | | | | | |
| C ₂ H ₂ | 0.84 | 1.06 | 0.91 | 1.05 | 1.08 | 1.07 | 0.86 |
| C ₂ H ₄ | 0.81 | 0.89 | 0.75 | 1.02 | 0.90 | 1.01 | 0.81 |
| | 0.86 | 1.03 | 0.90 | 1.06 | 1.06 | 1.04 | 0.87 |
| For 2s AO(s) in NH ₃ | | | | | | | |
| C ₂ H ₂ | 1.59 | 1.10 | 1.28 | 1.09 | 0.99 | 1.12 | 1.44 |
| C ₂ H ₄ | 1.10 | 1.12 | 1.22 | 1.06 | 0.94 | 1.16 | 1.09 |
| | 1.19 | 1.06 | 1.19 | 1.04 | 0.89 | 1.09 | 1.21 |
| Eigenvalues (au) ^b | | | | | | | |
| NH ₃ | | | | | | | |
| 2a ₁ | -1.101 | -1.156 | -1.232 | -1.157 | -1.217 | -1.174 | -1.078 |
| 1e | -0.582 | -0.596 | -0.596 | -0.593 | -0.606 | -0.571 | -0.616 |
| 3a ₁ | -0.366 | -0.300 | -0.358 | -0.254 | -0.318 | -0.376 | -0.346 |
| 4a ₁ | 0.584 | (2e) | (2e) | (2e) | (2e) | (2e) | 0.745 |
| C ₂ H ₂ | | | | | | | |
| 2σ _u | -0.751 | -0.819 | -0.884 | -0.771 | -0.874 | -0.751 | -0.769 |
| 3σ _g | -0.656 | -0.541 | -0.567 | -0.585 | -0.556 | (1π _u) -0.496 | -0.651 |
| 1π _u | -0.406 | -0.337 | -0.338 | -0.378 | -0.330 | (3σ _g) -0.403 | -0.413 |
| 1π _g | 0.306 | 0.647 | 0.498 | 0.606 | 0.653 | 0.515 | 0.249 |
| C ₂ H ₄ | | | | | | | |
| 1b _u | -0.644 | -0.660 | -0.664 | -0.673 | -0.665 | -0.655 | -0.651 |
| 3a _g | -0.562 | -0.469 | -0.478 | -0.501 | -0.489 | (1b _{2u}) -0.468 | -0.601 |
| 1b _{2g} | -0.506 | -0.421 | -0.419 | -0.431 | -0.424 | (1b _{2g}) -0.412 | -0.479 |
| 1b _{2u} | -0.371 | -0.342 | -0.375 | -0.362 | -0.354 | (3a _g) -0.384 | -0.394 |
| 1b _{3g} | 0.243 | 0.519 | 0.414 | 0.498 | 0.507 | 0.419 | 0.250 |

^a These calculations are defined in detail in the text. The accurate results are taken from Ref. 20; Calculation I is based on the Mulliken approximation without corrections; Calculations II-V are as I except that one-center exchange integrals have been introduced in II, correct one-center zero-overlap *F*-matrix elements have been used in III, inner shells have been neglected in IV, and rotational averaging used in V; the last column gives results obtained from the method finally adopted.

^b Selected Mulliken orbital populations and eigenvalues of the three or four highest occupied MOs, and of the lowest vacant MO, are given for ammonia, acetylene, and ethylene. The ordering of the eigenvalues in the approximate calculations agrees with that of the accurate calculation, except where otherwise noted by orbital designations in brackets.

exchange integrals in controlling the overall charge distribution even in closed-shell molecules (quite apart from all the open-shell problems such as singlet-triplet separations where the need for one-center exchange integrals is immediately obvious); they often reverse the polarity of the X—H bonds.^{25*} Comparison of Calculation III and I leads to the conclusion reached elsewhere^{9a,c} that one-center F_{2s2p} matrix elements push charge out towards the hydrogens. The particular point I wish to make is that it is impossible to describe the trends in the polarity of the X—H bond in NH_3 , C_2H_2 , C_2H_4 (and C_2H_6) without proper consideration of these F_{2s2p} matrix elements, as the Mulliken population analysis shows (Table I); Calculation III is in good agreement with the reference calculation (in the first column of Table I) in giving an increase in Mulliken population on hydrogen of 0.04 in going from C_2H_2 to C_2H_4 ; Calculations I and II both sharply overestimate this change at about 0.15. This is the sort of trend which a worthwhile approximation should be able to reproduce reliably. (Even though the physical interpretation of Mulliken orbital populations is unclear, they are useful quantities for measuring the effects of various approximations.)

Obviously the Mulliken approximation should not be used on the one-center exchange integrals, nor on the two-center integrals $\langle 2s_A | V^B | 2p_A \rangle$ and $\langle 2s_A 2p_A | r_B r_B \rangle$ which are crucial to the proper evaluation of the one-center F_{2s2p} matrix elements. Fortunately these integrals are as easy to calculate as the Coulomb integrals already required by Eqs. (19–21). The results of calculations combining the corrections of both Calculations II and III are not given in Table I, but can be reliably estimated from the results for each correction separately (by adding the results of Calculations II and III and subtracting those of I). Comparison with the reference calculation shows that the Mulliken populations on the hydrogens are more reasonable as regards trends, but are still about 0.07 too large. Eigenvalues of occupied orbitals are usually in error by from 0.05 to 0.10 au.^{27*} In short, though these results are reasonable enough to provide a starting point, they are by no means acceptable as they stand. To proceed further I shall compare the F -matrix elements of the accurate calculation with those obtained by the above approximations.^{28*}

3. Errors in the Diagonal F -Matrix Elements

For the diagonal F -matrix elements, the use of the Mulliken approximation (Eqs. 19–21), with the reintroduction of one-center exchange integrals (Expression 27) as in Calculation II, gives values up to 0.25 au less negative than the accurate calculations. The error is sensitive to the neighboring environment, but for typical polyatomic molecules is largest for $2p$ orbitals

pointing directly at neighboring atoms (e.g., $2p\sigma$ in C_2H_2) and smallest (typically 0.1 au) for hydrogen $1s$ orbitals (thus explaining the errors in the hydrogen net charge noted above); for diatomic hydrides, however, it may be greatest for the hydrogen $1s$ orbital. In general the error depends on the number and proximity of electrons on neighboring atoms; it also increases with the atomic number of the parent atom. The origin of this error, which has an important influence on the charge distribution, and which has not been noted in previous applications of the Mulliken approximation, must lie in the electron repulsion contributions J_{pp} and K_{pp} (since H_{pp} is calculated accurately in Eq. 19). Overestimation of J_{pp} , or underestimation of K_{pp} , would make F_{pp} too positive.

In fact both the basic weaknesses of the Mulliken approximation noted above lead to the underestimation of the exchange contribution K_{pp} . The key two-center integrals in K_{pp} are $(p_A q_B | p_A q_B)$, where A and B are neighboring atoms (these are the most important since they are weighted by diagonal rather than the usually smaller off-diagonal elements of the density matrix). The Mulliken approximation entirely neglects these integrals if $S_{pq} = 0$ (in acetylene they have values up to 0.03 au); and as a general rule seriously underestimates those exchange integrals for which $S_{pq} \neq 0$ because it partly replaces the interaction of a charge distribution with itself in $(p_A q_B | p_A q_B)$ by the smaller interactions between neighboring charge distributions as in $(p_A p_A | q_B q_B)$.^{29*} Examination of a range of exchange integrals shows that they are larger than the Mulliken estimate by typically 10–50%, or by up to 0.05 au. An extreme example is the two-center exchange integral between neighboring $2p\sigma$ orbitals in acetylene which is nearly 3 times, or 0.08 au, larger than the Mulliken prediction; this agrees with the fact that our error in the diagonal F -matrix elements is worst for $2p\sigma$ orbitals.

Most of the earlier observations can now be understood. For a given orbital p_A , the error in F_{pp} will indeed depend on the number of electrons on neighboring atoms (since this controls the weighting of the exchange integrals via the density matrix), and on the distance between atom A and other atoms. For a given neighboring atom B the dependence of the error on distance should be related to the square of some average overlap integral between orbitals on A and B, S_{AB} , since this controls the order of magnitude of the exchange integrals; the use of an average overlap integral (S_{AB} is conveniently defined as the overlap integral between the spherically symmetric valence orbitals of A and B) covers also those exchange integrals involving zero-overlap charge distributions. Examination of the series C_2H_2 , C_2H_4 , C_2H_6 , shows that this estimate of the behavior of the error with distance is accurate.

The situation is too complicated to allow such a clear explanation of the dependence of the error on the atomic number of the parent atom A. Among possible reasons I mention the treatment of the integrals $(p_A q_A | p_A r_B)$ ($p \neq q$) in Eq. (9) (these integrals may exceed 0.04 au. but are zero by the Mulliken approximation^{30*}) and the approximations on the integrals $(p_A p_A | q_A r_B)$ needed to obtain Eq. (20) for J_{pp} . These errors will increase with the atomic number of atom A partly because of the increase in magnitude of the integrals involved and partly because the more valence electrons there are on A the more chance there will be of error. The overall error may thus depend on $Z'_A{}^2$ rather than Z'_A (this does in fact seem to be the case for the molecules I have investigated, but the sample^{19a*} is too small to draw general conclusions on this rather complicated matter).

In short, a correction is needed to the diagonal F -matrix elements of orbitals on atom A which depends both on Z'_A (or $Z'_A{}^2$) and $\sum_B Z'_B S_{AB}{}^2$ (Z'_B has been used as an indication of the number of valence electrons on atom B; this is adequate for the purposes of a correction, though it does not allow for detailed changes in the molecular charge distribution). The correction should reduce to zero for an isolated atom. Detailed formulas must wait until the rest of the calculation, including the treatment of inner shells, has been specified, since it may be necessary to absorb other errors into this correction. I accordingly turn to a discussion of the off-diagonal elements.

4. Errors in the Two-Center Off-Diagonal Elements

The approximate values of the two-center off-diagonal matrix elements F_{pq} do not differ much between Calculations I, II, and III, but comparison with the reference calculations is at first sight depressing. Errors of up to 0.3 au, or 50 % of matrix elements, are common; errors of less than 0.1 au are rare except in small matrix elements. Newton et al.⁹ observed (in a slightly different context) that such errors could be related to the type of interaction involved (I shall consider the valence orbital interactions H-H, H-2s, 2s-2s, H-2p, 2s-2p, 2p-2p σ , and 2p-2p π where H represents a hydrogen 1s orbital). A similar trend is found in my calculations. Where the orbitals ϕ_p and ϕ_q are on neighbouring atoms, approximate values of $|F_{pq}|$ are much too large for H-2s and 2s-2s interactions (as anticipated above, for spectroscopic 2s orbitals^{31*}), and for interactions involving 1s inner-shell electrons,^{32*} large for 2p-2p π interactions, and much too small for 2p-2p σ interactions; where the orbitals are on atoms some distance apart, with a third atom between them, $|F_{pq}|$ is generally underestimated (again as expected). More detailed comparison of the approximate and accurate calculations shows that the Mulliken approximation introduces

large errors into both V_{pq} and G_{pq} ; these errors are worse for V_{pq} , and so do not cancel too well in F_{pq} (which, being the difference between two large terms, is sensitive to error in either).

To investigate this situation further I have tested the Mulliken approximation on the integrals $\langle p_A | V^A | q_B \rangle$ and $\langle p_A | V^B | q_B \rangle$ at a range of inter-nuclear distances for all valence-shell interactions between all possible pairs of atoms up to fluorine. Slater exponents were used; for hydrogen both exponents of 1.0 and 1.2 were tested. Since in my final calculations I shall not include inner shells explicitly, the present results are based on spectroscopic 2s orbitals.^{33*} I give some results in Table II, expressed in terms of the correction factor k^V needed to make the following expression hold:

$$\langle p_A | V^A + V^B | q_B \rangle = k^V S_{pq} [\langle p_A | V^A + V^B | p_A \rangle + \langle q_B | V^A + V^B | q_B \rangle] / 2. \quad (28)$$

Thus a correction factor of less than unity implies that the Mulliken approximation has overestimated the integral.

TABLE II

Tests of the Mulliken Approximation on Nuclear Attraction Integrals:
Correction Factors k^V to satisfy Eq. (28)

| Interaction Atom ^b | 1s-1s | | 1s-2s ^a | | | | 1s-2p | | | | |
|----------------------------------|------------------|------|--------------------|--------------------|------|------|-------|----------------|------|------|------------------|
| | H-H ^c | H-H | H-Li | H-B | H-N | H-F | H-Li | H-B | H-N | H-F | H-F ^c |
| Distance | | | | | | | | | | | |
| 1.0 au | 0.99 | 0.98 | — | — | — | — | — | — | — | — | — |
| 1.5 | 0.97 | 0.95 | 0.74 | 0.85 | 0.86 | 0.86 | 1.13 | 1.05 | 0.99 | 0.95 | 0.97 |
| 2.0 | 0.94 | 0.91 | 0.85 | 0.88 | 0.86 | 0.85 | 1.10 | 1.02 | 0.95 | 0.90 | 0.91 |
| 2.5 | 0.90 | 0.86 | 0.90 | 0.88 | 0.84 | 0.84 | 1.07 | 0.97 | 0.90 | 0.86 | 0.88 |
| 3.0 | 0.86 | 0.81 | 0.92 | 0.86 | 0.82 | 0.82 | 1.03 | 0.93 | 0.85 | 0.82 | 0.85 |
| 4.0 | 0.77 | 0.71 | 0.92 | 0.79 | 0.76 | 0.79 | 0.97 | 0.84 | 0.77 | 0.77 | 0.81 |
| | | | | | | | | | | | |
| 2s-2s ^a | | | | 2s-2p ^a | | | | 2p-2p σ | | | |
| B-B | C-C | O-O | N-N | F-F | B-B | C-C | O-O | N-N | F-F | B-B | C-C |
| — | — | — | — | — | — | — | — | — | — | — | — |
| — | — | — | — | — | — | — | — | — | — | — | — |
| 0.83 | 0.86 | 0.85 | 0.83 | 0.91 | 0.93 | 0.93 | 0.89 | ^c | 1.22 | 1.22 | 1.02 |
| 0.86 | 0.86 | 0.85 | 0.79 | 0.94 | 0.91 | 0.91 | 0.84 | 1.51 | 1.06 | 1.06 | 0.90 |
| 0.87 | 0.84 | 0.82 | 0.73 | 0.94 | 0.88 | 0.88 | 0.77 | 1.22 | 0.96 | 0.96 | 0.81 |
| 0.85 | 0.77 | 0.74 | 0.64 | 0.91 | 0.80 | 0.77 | 0.65 | 1.02 | 0.83 | 0.81 | 0.68 |
| | | | | | | | | 2p-2p π | | | |
| B-B | C-C | O-O | N-N | F-F | B-B | C-C | O-O | N-N | F-F | B-B | C-C |
| — | — | — | — | — | — | — | — | — | — | — | — |
| — | — | — | — | — | — | — | — | — | — | — | — |
| 0.83 | 0.86 | 0.85 | 0.83 | 0.91 | 0.93 | 0.93 | 0.89 | ^c | 1.22 | 1.22 | 1.02 |
| 0.86 | 0.86 | 0.85 | 0.79 | 0.94 | 0.91 | 0.91 | 0.84 | 1.51 | 1.06 | 1.06 | 0.90 |
| 0.87 | 0.84 | 0.82 | 0.73 | 0.94 | 0.88 | 0.88 | 0.77 | 1.22 | 0.96 | 0.96 | 0.81 |
| 0.85 | 0.77 | 0.74 | 0.64 | 0.91 | 0.80 | 0.77 | 0.65 | 1.02 | 0.83 | 0.81 | 0.68 |

* Spectroscopic 2s orbitals (see Ref. 18) were used.

^b Slater orbital exponents were used for AOs on lithium to fluorine; for hydrogen an exponent of 1.2 was used except where indicated by Footnote c.

^c In these two columns a hydrogen exponent of 1.0 was employed.

^d It makes less than 0.01 difference which atom has the 2s AO and which the 2p.

* This value is meaninglessly large, since the corresponding overlap integral is nearly zero.

Inspection of Table II shows that H-H, H-2s, 2s-2s, 2p-2p π , and 2s-2p interactions (for which the corresponding k^V will be denoted by k_{HH}^V , k_{H2s}^V , etc.) will in general be overestimated by the uncorrected Mulliken approximation; 2p-2p σ interactions will often be underestimated for important bonding situations.^{34*} $k_{2p2p\sigma}^V$ is 1.27 for the carbon-carbon interaction in acetylene; neglect of this correction would introduce an error of 0.4 au. All this agrees with the trends in the errors in the approximate *F*-matrix elements. Values of k^V usually drop as the orbital exponents involved become larger, and as internuclear distances increase (contraction of orbitals is, of course, similar to increasing the internuclear distance as far as two-center integrals are concerned); the only exceptions involve spectroscopic 2s orbitals on atoms of low atomic number. Comparison of the results for C-O and N-N interactions shows that k^V depends more on the sum of the orbital exponents involved than on the individual exponents. The largest changes in k^V are not surprisingly found in 2p-2p σ interactions, where the overlap charge distribution contains important contributions of either sign from overlap between the various 2p orbital lobes. Almost all these trends can easily be interpreted in terms of the displacement of the charge distribution implied by the Mulliken approximation; thus k^V is only greater than unity for short-range interactions involving 2p σ orbitals, which are the only ones where the overlap charge distribution may be closer to the attracting cores than is provided for by the Mulliken approximation.

I have so far concentrated on what may be termed the local part of the nuclear attraction arising from the cores of atoms A and B; my conclusions are that a correction factor k^V is required to make the Mulliken approximation acceptable here, and that this correction factor should depend primarily on the type of interaction involved, and also to a significant extent on the internuclear distance and the particular orbital exponents. I shall now consider briefly the nonlocal part of the nuclear attraction, $\langle p_A | \sum_{C \neq A, B} V^C | q_B \rangle$. When A and B are neighboring atoms, then the Mulliken approximation will be quite successful since the total potential from all other atom cores will be fairly constant over the region between A and B; the most usual error will be a slight overestimation of the nonlocal nuclear attraction, because in most structures the atom C nearest a pair of bonded atoms, A,B, is usually closer to either A or B than to the bonding region between A and B (the implications of this in terms of the Mulliken approximation require a little thought^{12,35*}). When A and B are some distance apart the situation is similar except that, as noted earlier, nuclear attraction from cores in the region between A and B will be underestimated by the Mulliken approximation^{35*}; this leads to the observed underestima-

tion of the corresponding F -matrix elements, despite the fact that the (small) local part of the nuclear attraction is overestimated at large internuclear distances (Table II).

One useful conclusion from the above discussion is that in evaluating the integrals $\langle p_A | V^C | q_B \rangle$ ($C \neq A, B$) by the Mulliken approximation it will not matter much which one-center charge distributions on A and B I use to replace $\phi_p \phi_q$ when applying Eq. (18). For example, the integral $\langle 2p\sigma_A | V^C | 2p\sigma_B \rangle$ would be reduced by the Mulliken approximation to the integrals $\langle 2p\sigma_A | V^C | 2p\sigma_A \rangle$ and $\langle 2p\sigma_B | V^C | 2p\sigma_B \rangle$; it will however be simpler and just as reasonable to replace these latter integrals by $\langle 2s_A | V^C | 2s_A \rangle$ and $\langle 2s_B | V^C | 2s_B \rangle$. The directional information contained in the first pair of integrals is of no use, and may indeed be misleading; the real errors were introduced right at the beginning when transferring the charge distribution from the bonding region to the atoms. It is easy to imagine situations where this simplification improves the Mulliken approximation, and others where it makes things worse; in general it is just as good an approximation. This will be a considerable help when I come to consider rotational invariance problems.

Note that the above argument cannot safely be applied to the local part of the nuclear attraction; here the directional information retained by the proper use of the Mulliken approximation (after transformation of the orbitals to be σ and π with respect to local axes) is usually relevant. If the simpler approach were adopted almost all the errors discussed earlier would be exaggerated; for example $k_{2p2p\sigma}^V$ would take even larger values at small internuclear distances and would vary more rapidly with distance.

I will now consider the electron repulsion contribution G_{pq} . As far as the Coulomb repulsion contribution J_{pq} is concerned, the above discussion can be taken over word for word except for numerical alteration, the replacement of k^V by k^J and of V^A by J^A .^{36*} k^J is defined analogously to k^V in Eq. (28). I have however not performed a comparatively detailed analysis, partly because it would be rather more difficult, and partly because I shall ultimately be absorbing into k^J errors introduced by the use of Eq. (21) for the exchange interaction. Such comparison as I have performed with the correctly calculated matrix elements J_{pq} (for HF, N_2 , H_2CO), and with individual integrals, shows that the values of k^J are usually nearer unity than for k^V .^{37*} Consequently, in the absence of correction factors, the error in V_{pq} is the dominating error in F_{pq} .

The expression for the exchange contribution (Eq. 21) does not lend itself to analysis along the above lines. However, numerical work (on HF, N_2 , H_2CO) shows that it is a bad approximation. Except for $2p-2p\pi$ interactions the true exchange contribution is greater in absolute magnitude

than the estimate of Eq. (21) by typically a factor of 1.5 (or nearly 2 in N_2); this represents an error of generally more than 0.1 au. Despite the fact that J_{pq} is usually several times larger than $-K_{pq}/2$, the absolute error from the Mulliken approximation is sometimes smaller in J_{pq} . The exchange contribution is more sensitive to the exact description of the overlap charge distributions.

I shall not attempt to suggest specific corrections for this error, partly because it is easily allowed for when choosing values for k^J (arbitrary as this may be it is doubtful that any other simple correction would be more effective), and partly because I shall evaluate the exchange contribution in another way in view of the fact that there are severe computational drawbacks to the use of Eq. (21).^{38*} These drawbacks might be acceptable if Eq. (21) produced accurate results; since, however, the Mulliken approximation is not at all good for the exchange contribution, to use it would merely waste machine time and limit the size of the molecules I could investigate. I shall suggest an alternative procedure which completely avoids the computational difficulty, and is, if anything, more accurate.

To sum up the discussion on off-diagonal two-center matrix elements between orbitals p_A and q_B , I have found that the use of the Mulliken approximation introduces serious errors of several electron volts into V_{pq} , J_{pq} , K_{pq} , and F_{pq} . These errors can be separated into local and nonlocal contributions by considering first atoms A and B, and then all the other atoms. The local contribution to the error is the most serious, but can be partly dealt with by the use of correction factors.

This distinction between local and nonlocal effects is very important if one hopes to produce a method of calculation reliable for large molecules by calibration against reference calculations on small molecules. For example, correction factors obtained for the nuclear attraction in small molecules obviously refer mainly to local effects; if used also for the very large nonlocal contributions possible in large molecules (mainly arising from distant cores where the Mulliken approximation is accurate), serious error would accumulate. Even in small molecules this distinction is needed to deal equally effectively with interactions of a given type both when the orbitals involved are on neighboring atoms, and when they are on non-neighboring atoms; an averaging procedure^{9a,c} will blur important detail. It is also important to use different correction factors for nuclear attraction and electron repulsion; the use of one overall correction factor to give the correct F -matrix elements can lead to serious error in the nuclear attraction contribution, which is needed to obtain the total molecular energy.

I have not discussed at all the problem of two-center matrix elements between orthogonal orbitals since this is unimportant for the molecules discussed here (except once or twice in considering H-2p interactions).

5. Final Remarks

In the preceding sections I have analyzed the main errors introduced by the use of the Mulliken approximation, and have indicated the general form of the corrections I shall use. The numerical details of the calibration against the reference calculations must be left until other problems have been discussed. The aim has been to introduce corrections with as little complication as possible. It would have been easy enough to suggest the calculation of more integrals^{41*} (or the use of a more sophisticated approximation^{42*}) each time the Mulliken approximation was found inadequate, but corrections would still be needed, and the process would rapidly get out of hand.

The most worthwhile elaboration of this kind would be to calculate all the two-center nuclear attraction integrals $\langle p_A | V^A | q_B \rangle$; this would be easy enough to do, and would eliminate the need for the correction factors k^V . It would be much more difficult to dispense with the electron repulsion correction factors k^J , which absorb several different errors. Indeed, if nuclear attraction integrals were accurately calculated, considerable care would be needed with the k^J to ensure that, for example, their dependence on distance was properly allowed for; otherwise, because of cancellation of errors between V_{pq} and G_{pq} in F_{pq} , the approximate approach to nuclear attraction integrals might be better.^{43*}

It may be felt that the errors I have been discussing are unimportant in view of the inadequacies of a minimum basis set of Slater orbitals, particularly as far as the diagonal elements are concerned. But since these errors will remain whatever basis set is used, they make attempts at improvement difficult. For example, Hartree-Fock AOs are known to be a better starting point than Slater AOs,⁴⁴ but their introduction (either explicitly, or implicitly by the use of spectroscopic data) into a theory based on the uncorrected use of the Mulliken approximation might well give worse results. The errors are important physical defects of the Mulliken approximation, not numerical artifacts, even if "chemical intuition" may not recognize them as such.

Since I shall be using reference calculations on small molecules for purposes of calibration, it must remain uncertain how far the problem of the many important three- and four-center integrals⁴⁵ in larger molecules has been solved. The Mulliken approximation will be adequate for many, but not all, of these integrals; cancellation of errors will depend largely on the behavior of the density matrix elements between distant orbitals, and is hard to analyze. Comparison with accurate calculations on large molecules will be necessary; some slight cause for optimism can be found in my results for methyl acetylene, discussed later, where the agreement with the

reference calculation (not used for calibration) is as good as for smaller molecules. I have already noted^{38*} that the computational problem of the number of the three- and four-center integrals is not entirely solved by the Mulliken approximation; I shall now discuss another approximation which might be used to simplify the evaluation of the exchange interaction.

B. The Ruedenberg Approximation

Ruedenberg suggested that in some circumstances the following approximation might be preferable to the Mulliken approximation in evaluating electron repulsion integrals:^{46*}

$$\phi_p(1)\phi_q(2) = S_{pq}[\phi_p(1)\phi_p(2) + \phi_q(1)\phi_q(2)]/2. \quad (29)$$

This approximation is quite inappropriate for use on J_{pq} , but is very attractive for K_{pq} , since Eq. (9) reduces to⁴⁷

$$\begin{aligned} K_{pq} &= S_{pq} \sum_r N(r) [(pr|pr) + (qr|qr)]/2 \\ &= S_{pq} \sum_A (K_{pp}^A + K_{qq}^A)/2, \end{aligned} \quad (30)$$

where K_{pp}^A is defined analogously to J_{pp}^A (Eq. 23) as

$$K_{pp}^A = \sum_q N(q_A) (pq_A|pq_A). \quad (31)$$

The origin of Expression (27) for the one-center exchange correction is now apparent.

In contrast to the inequality of Eq. (26), this approximation allows me to write

$$K_{pq} = S_{pq}(K_{pp} + K_{qq})/2. \quad (32)$$

If the Mulliken approximation is used for J_{pq} , and the Ruedenberg for K_{pq} , then from Eqs. (25, 32)

$$G_{pq} = S_{pq}(G_{pp} + G_{qq})/2 \quad (33)$$

If I define the elements of the total potential energy matrix U as

$$U_{pq} = V_{pq} + G_{pq} \quad (34)$$

then from Eqs. (24, 33) (that is, using the Mulliken and Ruedenberg approximations)

$$U_{pq} = S_{pq}(U_{pp} + U_{qq})/2. \quad (35)$$

Inspection of Eqs. (30–32) shows that the calculation of the exchange interaction is much simplified by the use of the Ruedenberg approximation.

Numerical work also reveals several advantages. As for as the diagonal elements, K_{pp} , are concerned, Eq. (30) is fairly accurate, for the obvious reason that the most important integrals, $(p_A q_B | p_A q_B)$, are not approximated at all (and one-center exchange integrals are automatically included without the need for special corrections); the serious errors found earlier when the Mulliken approximation was used on these integrals are thus avoided. The main errors in the present approach occur in the integrals $(p_A q_B | p_A p_A)$. Combination of the Mulliken approximation for J_{pp} (Eq. 20) and the Ruedenberg approximation for K_{pp} (Eq. 30) gives quite accurate estimates of G_{pp} ; G_{pp} is usually overestimated, but by less than 0.1 au. The error is generally about one-half that discussed earlier when only the Mulliken approximation is used (and one-center exchange integrals reintroduced).

However, these advantages are purely formal, since they hinge upon the accurate calculation of the two-center exchange integrals (which are harder than Coulomb integrals because they involve two-center charge distributions). This is the sort of complication I wish to avoid, yet to use the Mulliken approximation for these integrals after having used the Ruedenberg approximation is an inconsistent procedure, and reintroduces all the errors discussed earlier. Equally if I were to calculate the exchange integrals, I could use them to correct the Mulliken approximation without invoking the Ruedenberg approximation at all.

For the two-center off-diagonal elements K_{pq} there is considerable numerical disagreement between the two approaches. With the crucial exception discussed below, the Ruedenberg approximation often gives better results; the estimates of K_{pq} are of larger absolute magnitude than those given by the Mulliken approximation, which as noted above is desirable. The differences are unimportant in view of the absorption of errors into k^J , and the advantage depends partly on the accurate calculation of the two-center exchange integrals.

The fundamental drawback to the Ruedenberg approximation appears most clearly when considering interactions where the density matrix element P_{pq} is large. The dominating term in the correct exchange interaction will then be $-P_{pq}(pp|qq)/2$. This would be unaltered by the Mulliken approximation, but the Ruedenberg approximation, used as in Eq. (30), includes the approximation that

$$(pp|qq) = S_{pq}^2[(pp|pp) + (qq|qq) + 2(pq|pq)]/4. \quad (36)$$

This, of course, is drastically in error; a large Coulomb integral is reduced almost to zero. The Ruedenberg approximation was never intended for use on Coulomb integrals (analogously the Mulliken approximation is worse

for two-center exchange integrals, but not so dramatically). The use of the Mulliken approximation for J_{pq} and the Ruedenberg approximation for K_{pq} would be seriously inconsistent, despite the apparent analogy between Eq. (20) and Eq. (30); large Coulomb integrals $(pp|qq)$ appearing in J_{pq} would be accurately calculated, but effectively neglected in K_{pq} . This is particularly unsatisfactory since the algebraic cancellation required between some of the electron repulsion contributions would be quite lost.^{49*}

The serious implication of this error is best illustrated by considering the two-center $2p-2p\pi$ interactions in ethylene, both in and out of the molecular plane. For the out-of-plane interaction P_{pq} is 0.79, and, for the in-plane interaction, -0.03 (from the reference calculation²⁰). The term $-P_{pq}(pp|qq)/2$ is -3.7 eV in the former case, and $+0.1$ eV in the latter. The corresponding F -matrix elements are -8.8 and -6.3 eV. The Ruedenberg approximation thus effectively neglects a major contribution to the $2p-2p\pi$ out-of-plane F -matrix element; it leads to a reversal of the relative magnitudes of the in-plane and out-of-plane interactions. Similarly it will lead to unreliable results in comparing different π -bonds in aromatic molecules, where P_{pq} may vary widely. This is obviously no basis on which to build a general molecular orbital theory; attempts could be made to correct the situation by explicit calculation of the term $-P_{pq}(pp|qq)/2$, but this is rather arbitrary (though perhaps not more so than the analogous correction for one-center exchange integrals needed when the Mulliken approximation is used).

All in all, despite an initial attractiveness, the Ruedenberg approximation has several drawbacks; I shall give examples from current theories later. I still need to find a satisfactory method of handling the exchange interaction.

For later reference, one final point should be made before leaving the Mulliken and Ruedenberg approximations. The derivation of Eq. (30) demands the double application of the Ruedenberg approximation to the accurate expression (Eq. 9), first to the orbital pair r, s , and then to the pair p, q .^{50*} If the approximation is only applied once, to the pair r, s , this gives

$$K_{pq} = \sum_r N(r)(pr|qr) = \sum_A K_{pq}^A \quad (37)$$

and if only to the pair p, q ,

$$K_{pq} = S_{pq} \sum_{r,s} P_{rs}[(pr|ps) + (qr|qs)]/2 \quad (38)$$

Only in the latter case does Eq. (32) hold good. Equations (37, 38) both

imply for individual Coulomb integrals that

$$(pp|qq) = S_{pq}[(pp|pq) + (qp|qq)]/2. \quad (39)$$

The error is only marginally less serious than when the Ruedenberg approximation is applied twice (Eq. 36).

There is a similar situation when applying the Mulliken approximation to J_{pq} . Repeated application gives Eq. (20), but application only to the orbital pair r, s , in Eq. (8) gives

$$J_{pq} = \sum_{r,s} N(r)(pq|rr) = \sum_A J_{pq}^A, \quad (40)$$

and only to the pair p, q , gives

$$J_{pq} = S_{pq} \sum_{r,s} P_{rs}[(pp|rs) + (qq|rs)]/2. \quad (41)$$

Only in the latter case does Eq. (25) hold. I shall later give examples of the use of Eqs. (37-41).

C. The Zero Differential Overlap Approximation

1. Preliminary Discussion

In the most comprehensive application of the zero differential overlap (ZDO) approximation, all integrals including overlap integrals which involve overlap charge distributions between different basis orbitals would be put equal to zero (the kinetic energy integrals would be unaffected since they do not involve overlap charge distributions¹⁰). As an approximation to individual integrals this would be, of course, disastrous. However, many theoretical and numerical investigations⁵¹ have established that if the calculation is taken to refer to an orthogonalized AO (OAO) basis set, rather than to the original AO basis set, the approximation is more acceptable. Indeed, this is intuitively obvious since it can then be regarded as nothing more than another application of the familiar Mulliken approximation.⁵⁴ It has often been pointed out that in special homonuclear situations the use of the Mulliken approximation over AOs gives results similar or identical to the ZDO approximation⁵³ (c.g., for electron repulsion integrals and the total electronic energy). In general, however, the results differ; this is yet another manifestation of the dependence of the Mulliken approximation on transformations among the basis set. Furthermore, the results will depend on which of the infinity of possible orthogonalized basis sets is used.

The differences will certainly be significant, but they will not be drastic provided one crucial reservation is noted; all the integrals which remain after the use of the Mulliken approximation on some basis set must be

evaluated, and the resulting MO coefficients interpreted, in terms of that basis set. This is obviously essential for a hybrid basis set, but is often ignored for OAOs (i.e., the ZDO approximation), where it is common to evaluate the few remaining integrals as if they referred to AOs. This approximation is an essential part of the approach, since to obtain the few integrals accurately over OAOs would require the evaluation of all three- and four-center integrals over AOs. (For the rest of this work the phrase "the ZDO approximation" will be reserved not only for the use of the Mulliken approximation over OAOs, but also for the further approximation of obtaining the remaining integrals directly from AO values without the necessary transformation to OAOs.)

To apply the ZDO approximation it is thus necessary to choose OAOs which resemble the AO basis set as closely as possible. The familiar Löwdin OAOs, to be defined shortly, satisfy this requirement in a least-squares sense.^{7b,55} But it will be of interest to introduce Löwdin OAOs by a slightly different argument. Consider the case of two overlapping AOs on neighboring atoms, p_A, q_B ; if M_{pp}, M_{pq}, M_{qq} , and $M'_{pp}, M'_{pq}, M'_{qq}$, are the accurate matrix elements of some potential energy operator over AOs and OAOs, respectively, the ZDO approximation will be sound if

$$M'_{pp} = M_{pp}, \quad (42)$$

$$M'_{qq} = M_{qq}, \quad (43)$$

and

$$M'_{pq} = 0. \quad (44)$$

The most reasonable way of making sure that the ZDO approximation is about as accurate as the Mulliken approximation over AOs is to require that the OAOs should be chosen so that when the Mulliken approximation is accurate for M_{pq} , that is

$$M_{pq} = S_{pq}(M_{pp} + M_{qq})/2, \quad (45)$$

then the accurate value of M'_{pq} obtained after transforming properly to OAOs will be zero (as would be assumed in the ZDO approximation).

In the homonuclear case ($M_{pp} = M_{qq}$), if the Mulliken approximation holds for M_{pq} then \mathbf{M} is merely a multiple of \mathbf{S} and Eqs. (42–44) must hold for all orthogonalized basis sets. The heteronuclear case is more interesting. If the Mulliken approximation holds for M_{pq} (Eq. 45), it can be easily shown that M'_{pq} will *only* be zero (and the ZDO approximation for M'_{pq} accurate) when Löwdin's symmetrically orthogonalized AOs ϕ' , defined by

$$\phi' = \phi S^{-1/2} \quad (46)$$

are used. This is easily understood since the Mulliken approximation and the Löwdin procedure are both symmetrical in the way they apportion the overlap charge distribution between the atoms.

The full expressions obtained for M'_{pp} , M'_{qq} , M'_{pq} over Löwdin OAOs are

$$M'_{pp} = [(M_{pp} + M_{qq} - 2S_{pq}M_{pq}) + (M_{pp} - M_{qq})/(1 - S_{pq}^2)^{1/2}]/2(1 - S_{pq}^2), \quad (47)$$

$$M'_{qq} = [(M_{pp} + M_{qq} - 2S_{pq}M_{pq}) + (M_{qq} - M_{pp})/(1 - S_{pq}^2)^{1/2}]/2(1 - S_{pq}^2), \quad (48)$$

$$M'_{pq} = [M_{pq} - S_{pq}(M_{pp} + M_{qq})/2]/(1 - S_{pq}^2). \quad (49)$$

The simplifications in the homonuclear case are obvious.⁵⁶ If M_{pq} is given by the Mulliken approximation, Eqs. (47–49) show that M'_{pq} is zero, but that in general M'_{pp} does not equal M_{pp} (nor M'_{qq} , M_{qq}).

Löwdin OAOs have often been used in analyzing the ZDO approximation (mainly in the special case of π -systems^{52,53}; for σ -systems with their large overlap and heteronuclearity a numerical rather than an analytical approach is needed, and, besides general cautions,^{52b} there have been only a few detailed comments²⁶). My particular concern has been to trace the intimate connection between the Mulliken approximation applied to AOs and the ZDO approximation applied to Löwdin OAOs.^{57*} I have found that if the Mulliken approximation holds for M_{pq} , then over Löwdin OAOs the original requirements for the success of the ZDO approximation (Eqs. 42–44) are fairly well satisfied even in the heteronuclear case; the discrepancy between M_{pp} and M'_{pp} (or M_{qq} and M'_{qq}) arising from Eqs. (47, 48) will be small except when M_{pp} and M_{qq} differ significantly and S_{pq} is large, and will be such as to make the difference between M'_{pp} and M'_{qq} larger than the difference between M_{pp} and M_{qq} . When the Mulliken approximation is bad for M_{pq} (as we have seen is often the case), this will be reflected in the breakdown of the ZDO approximations of Eqs. (42–44).

2. Numerical Investigation

The above discussion (despite the use of such a simple example) provides a convenient framework for analyzing the dangers in the ZDO approximation in terms of my earlier work on the Mulliken approximation. Before doing so I give the equations obtained when the ZDO approximation is ruthlessly introduced into the original Roothaan SCF LCAO equations. I retain the primes as a reminder that the quantities are defined over Löwdin OAOs, even though this is ignored in the ZDO approximation.

I have

$$\psi_i = \sum_p c'_{ip} \phi'_p, \quad (50)$$

$$\sum_q F'_{pq} c'_{iq} = E_i c'_{ip}, \quad (51)$$

$$F'_{pq} = H'_{pq} + G'_{pq}, \quad (52)$$

$$H'_{pp} = T'_{pp} + V'_{pp} = T'_{pp} + \sum_{\Lambda} V'_{pp}{}^{\Lambda}, \quad (53)$$

$$H'_{pq} = T'_{pq} \quad (p \neq q), \quad (54)$$

$$G'_{pq} = J'_{pq} - K'_{pq}/2, \quad (55)$$

$$J'_{pp} = \sum_i^{\text{occ}} 2(p'p' | ii) = \sum_r P_{rr}'(p'p' | r'r'), \quad (56)$$

$$J'_{pq} = 0 \quad (p \neq q), \quad (57)$$

$$-K'_{pq}/2 = -\sum_i^{\text{occ}} (p'i | q'i) = -P'_{pq}(p'p' | q'q')/2$$

$$(\text{including the case } p = q). \quad (58)$$

$$P'_{rs} = 2 \sum_i^{\text{occ}} \bar{c}'_{ir} \bar{c}'_{is}, \quad (59)$$

and, for the new secular equations,

$$|F'_{pq} - E\delta_{pq}| = 0. \quad (60)$$

These equations have two obvious attractions over those obtained from the Mulliken approximation over AOs; the form of the exchange interaction is much simpler and the secular equations are rather easier to handle. The ZDO approximation introduced into all the potential energy integrals as above is known as the CNDO (complete neglect of differential overlap) approximation when used on general molecules rather than π -systems only (particular methods based on this approach are referred to as CNDO/1, CNDO/2^{7b}). One obvious drawback to the above equations is the neglect of one-center exchange integrals. This is as serious, and as easy to rectify, as the corresponding situation with the Mulliken approximation. One merely adds to K'_{pp} the correction term (cf. Eq. 27)

$$-\sum_q^{\Lambda} P'_{qq}(p'_{\Lambda} q'_{\Lambda} | p'_{\Lambda} q'_{\Lambda})/2 \quad (p \neq q). \quad (61)$$

With this correction the method is known as IN(intermediate neglect)DO.^{71,59} Increasingly more complicated expressions can be obtained by further corrections, in particular the ND(neglect of diatomic)DO approach where the ZDO approximation is applied only to two-center

charge distributions^{7a,58a,60}; analogies to these methods for the Mulliken approximation over AOs could easily be developed. Since these corrections are not relevant to the real difficulties facing the ZDO approximation, I shall not need to discuss them further.

Another weakness in the above equations is the inadequate treatment of the important one-center F'_{2s2p} matrix elements. Assuming that the kinetic energy contribution (which would not be zero if properly transformed to OAOs) is being neglected, as is usually the case, then the only contribution to the one-center F'_{2s2p} matrix elements will come from the exchange interaction of Eq. (58). However, it so happens that this often gives better estimates of the F' -matrix elements (with the right sign and a magnitude sometimes small but sometimes reasonable in the cases investigated) than I found in the corresponding situation with the Mulliken approximation over AOs discussed earlier. Nevertheless, significant errors remain.

In passing I note that if the Ruedenberg approximation held, then the off-diagonal elements K'_{pq} would be zero in the 2×2 case discussed above (see Eqs. 32, 49). The sharp discrepancy between this and the important term involving a Coulomb integral correctly retained in K'_{pq} by the ZDO approximation in Eq. (58) shows the dangers of the Ruedenberg approximation very clearly.

To investigate the general usefulness of Eqs. (53–59) I have examined, for various molecules,^{19a*} the correctly calculated T, V (and the individual V^A), H, G, F matrices over AOs (using spectroscopic orbitals) and the corresponding Löwdin OAOs.^{61*} For a check on the ideas suggested by the simple example discussed earlier I have also transformed to OAOs the approximate nuclear attraction matrices obtained over AOs assuming the Mulliken approximation holds. Though the resulting two-center off-diagonal matrix elements are by no means always zero, except for the simple 2×2 case as above, they are small, certainly when compared to the true nuclear attraction matrix elements over OAOs; in heteronuclear situations with large overlap integrals the diagonal elements of the approximate matrix transformed to OAOs differ sharply both from the original values over AOs and the true values over OAOs, as expected.

Examination of the transformed matrices shows that, as expected above, the ZDO approximation is fully as serious as the Mulliken approximation over AOs. It is easiest to consider the nuclear attraction contributions. The local part of the nuclear attraction $\langle p'_A | V^A + V^B | q'_B \rangle$, neglected in the ZDO approximation, can be large over OAOs (greater than 0.3 au for several interactions in acetylene, for example), and, as expected from Eqs. (47–49) and the fact that the values of k^V are usually less than unity (Table I), is often different in sign from the corresponding AO quantity. Broadly

speaking, the departure of these integrals from zero is comparable to the severe error incurred by using the uncorrected Mulliken approximation over AOs. The nonlocal part of the nuclear attraction, where the Mulliken approximation is more successful (and the integrals smaller) is naturally nearer zero but often exceeds 0.1 au over OAOs; again, the neglect of this contribution by the ZDO approximation is comparable to the use of the Mulliken approximation over AOs (which I have noted may be acceptable in this instance).

For the diagonal elements of the nuclear attraction matrices the behavior is as suggested by Eqs. (47-49). For nuclear attraction from core A for orbitals p_A and q_B , V_{pp}^A will naturally be much larger (in absolute magnitude) than V_{qq}^A ; this difference is increased for $V_{pp}^{\prime A}$, $V_{qq}^{\prime A}$. The difference between V_{pp} and V_{qq} will be less dramatic, but the general trend remains that in a heteropolar situation V_{pp}' and V_{qq}' will differ more sharply than V_{pp} and V_{qq} (for example, by nearly 1 au more for the orbitals involved in the C—H bond in acetylene). Finally, there is superimposed on this effect a general increase in the absolute magnitude of V_{pp}' relative to V_{pp} , expected from Eqs. (47-49) and the fact that the values of k^V are usually less than unity.

I have not done a similarly exact analysis of the behavior of the J -matrix on transformation, because it would have involved much work for few results which are not obvious. A considerable amount of approximate information accumulated during the course of this work (for example, the results of transforming the approximate, but quite accurate, J -matrix obtained by the method described later, and the results of subtracting approximate K' -matrices from the G' -matrix) confirms that the situation is nearly as serious as for the nuclear attraction.

As far as two-center off-diagonal matrix elements are concerned, I noted earlier that the Mulliken approximation was less in error for J_{pq} than for V_{pq} , but that the error in J_{pq} was quite sufficient to demand correction, and that to calculate V_{pq} accurately while omitting to correct J_{pq} would be wasted effort.^{43*} As expected, corresponding remarks can be made about the ZDO approximation, which wrongly puts J_{pq}' and V_{pq}' equal to zero: there is some cancellation of errors, but not enough because V_{pq}' is usually significantly larger than the by no means negligible J_{pq}' . The accurate calculation of V_{pq}' would destroy the cancellation of errors and thus would improve the situation little, if at all. It is often tempting to justify the ZDO approximation for J_{pq}' by showing that individual electron repulsion integrals are very small over OAOs, but one must remember that J_{pq}' is the sum of many integrals and may compare in magnitude to V_{pq}' . In general, it little profits an approximate theory to calculate nuclear attraction integrals more accurately than the corresponding electron repulsion integrals.

The most important result I shall need from this discussion concerns the exchange interaction. It turns out that the simple expression in Eq. (58), interpreted in terms of the OAO density matrix and the AO Coulomb integrals, gives results extremely close to those obtained by calculating the exchange matrix by the complicated method of Eq. (21) using the Mulliken approximation, when compared over the same basis set. On back-transforming the results from Eq. (58) to AOs, the difference in the off-diagonal matrix elements (for valence-shell interactions) between the two approaches rarely exceeds 0.01 au; for the diagonal elements the difference is usually equally small, but on occasion can reach 0.04 au. These errors are obviously negligible compared with those involved in both approaches, and will be absorbed in the calibration. This, then, is the solution to the problem of the exchange interaction; by evaluating it in terms of the ZDO approximation over OAOs and back-transforming to AOs, the results are equivalent to those from Eq. (21), and the calculation becomes trivial.^{62*} I have all the formal simplicity of the Ruedenberg approximation without the major drawbacks; admittedly I will have lost the exact cancellation of terms in **J** and **K**,^{49*} but it will still hold to a good approximation (in any case it is lost by the use of the correction factors k' ; which in part absorb errors in the exchange interaction, and by the approximation I shall use to maintain rotational invariance).

The above discussion assumed that one-center exchange integrals were being omitted. When they are included, by Expression (27) for AOs and Expression (61) for OAOs, the equivalence between the two approaches breaks down. On back-transformation of the results from the ZDO approximation with one-center exchange, the diagonal elements are still closely equal to those obtained from the Mulliken approximation with one-center exchange, but the off-diagonal elements for nearest-neighbor interactions are consistently larger by around 0.05 au. The difference can easily be absorbed in the choice of values of k' ; indeed, earlier remarks show that it represents an improvement in the estimation of the exchange contribution to F_{pq} .

Useful as this correspondence between the Mulliken and ZDO approximations is, I should stress that both are inaccurate. It is because of this, and the comparative smallness of the exchange interaction, that I have not thought it worth attempting to use Coulomb integrals adjusted to OAOs²⁶ when using Eq. (58).

In view of the inaccuracy of the ZDO approximation for both **J'** and **K'** it is no surprise to find that comparison of the approximate G'_{pq} given by Eqs. (55–58) with the correctly calculated G'_{pq} reveals many discrepancies approaching 0.3 au in both off-diagonal and diagonal elements (despite the use of Expression 61 to allow for one-center exchange integrals).

It remains to consider the kinetic energy. It was assumed above that the kinetic energy was to be properly transformed to OAOs in Eqs. (53, 54). The Mulliken and (equally) the ZDO approximation are not suitable for the kinetic energy integrals. However, to allow me to discuss current approximate theories it will be necessary to examine the implications of applying a ZDO approximation (i.e., Eqs. 42–44) to the kinetic energy. Since the use of the Mulliken approximation on the kinetic energy over AOs usually overestimates the off-diagonal elements by a factor of around 3, it would be expected from Eqs. (47–49) that T'_{pp} would be much larger than T_{pp} (this is so, by up to 1 au in acetylene) and T'_{pq} of the reverse sign to T_{pq}^{52a} (this is also the case).

I can now summarize the position as far as the F -matrix is concerned. For the diagonal elements the main changes between F_{pp} and F'_{pp} come from the kinetic energy (which becomes more positive over OAOs) and somewhat less from the exchange interaction (which is less negative over OAOs as correctly indicated by comparison of Eqs. 21, 58). The changes between V_{pp} and V'_{pp} will cancel with those between J_{pp} and J'_{pp} to some extent, but where they do not will usually tend to make F'_{pp} more negative than F_{pp} . For the hydrogen $1s$ and carbon $2s$, $2p\sigma$, $2p\pi$ AOs in acetylene I find, respectively, the following changes in the diagonal elements in au: for $(T'_{pp}-T_{pp})$ 0.37, 0.82, 0.85, 0.11; and for $(F'_{pp}-F_{pp})$ 0.56, 0.69, 0.72, 0.12. (These numbers were obtained using valence orbitals which had been Schmidt-orthogonalized to inner shells on other atoms.^{61*} They show dramatically that π -systems, where ZDO theories have been so successful, are a very special case; not only are overlap integrals small, but the Mulliken approximation is also quite accurate.)

The fact that F'_{pp} is more positive than F_{pp} is a fundamental consequence of bonding. If the Mulliken approximation held for F -matrix elements as in Eq. (45), then F'_{pq} would be zero in the simple 2×2 case (Eq. 49), and there would be no bonding. F_{pq} must be greater than a Mulliken-type relationship would predict, as a result of which (Eq. 47) F'_{pp} must be more positive than F_{pp} ; the change can be seen to depend on the square of the overlap integral (from Eq. 47, taking the off-diagonal elements as proportional to the overlap integral), and is of extreme importance in σ -systems.

As far as the approximations of Eqs. (52–58) are concerned, they provide no hope of consistently coming within 0.3 au of the true diagonal F -matrix elements, even if both T'_{pp} and V'_{pp} are properly transformed to OAOs (without these transformations things are even worse).

For the two-center off-diagonal F -matrix elements, for the various reasons discussed above the formal ZDO approximation which retains only a kinetic energy and an exchange contribution will be inadequate, whether

or not the kinetic energy is properly transformed to OAOs. No simple way can be suggested of correcting the situation (recent attempts which consider, approximately⁵⁸ or accurately,²⁶ the errors in H'_{pq} more carefully than those in J'_{pq} do not solve the problem). In practice some semi-empirical procedure is usually adopted; this can be quite effective, as I shall discuss.

In short, the uncorrected use of the ZDO approximation is quite as unacceptable as the use of the uncorrected Mulliken approximation over AOs.

Finally I will compare the density matrices P_{pq} and P'_{pq} . The formal analysis^{52b} shows that the diagonal elements should only differ slightly, but the off-diagonal elements more sharply. This is the case. P_{pp} is generally rather smaller than P'_{pp} for reasons of normalization; the appropriate comparison is between $N(p)$ and P'_{pp} . These quantities agree quite well, though sometimes differ sufficiently to change the qualitative picture of the charge distribution. For example the polarity of CO is reversed depending on whether one thinks in terms of $N(p)$ or P'_{pp} ,⁶³ and in hydrocarbons $N(p)$ gives typically 0.06 fewer electrons on the hydrogen atoms than does P'_{pp} . There is little connection between P_{pq} and P'_{pq} , but if one obtains the Chirgwin-Coulson bond orders⁶⁴ over AOs they are in close agreement with P'_{pq} .

D. Neglect of Inner Shells

The whole weight of chemical intuition suggests that explicit consideration of inner shells should not be necessary to describe most chemical phenomena.^{65*} Numerical investigations^{23b,66,67} have reached the same conclusion, provided that valence orbitals are first Schmidt-orthogonalized to inner shells. A detailed theoretical analysis of the consequences on matrix elements involving only valence-shell orbitals of such orthogonalization has been given elsewhere,^{14a,c} and only the results necessary to interpret my numerical analysis will be reproduced here.

If (for this section only) the indices p, q are reserved for valence orbitals, and r, s for inner shells, Schmidt-orthogonalization of the valence orbitals ϕ_p to the inner shells gives us new "effective valence orbitals" $\bar{\phi}_p$ which are approximately given by

$$\bar{\phi}_p = (\phi_p - \sum_r S_{pr} \phi_r) N, \quad (62)$$

where N is the approximate normalizing factor $(1 - \sum_r S_{pr}^2)^{-1/2}$, and the summation runs only over the core orbitals. Transformed F -matrix ele-

ments then become

$$\bar{F}_{pq} = \left[F_{pq} - \sum_r (S_{pr} F_{rq} + F_{pr} S_{rq} - S_{pr} S_{rq} F_{rr}) \right] N^2, \quad (63)$$

where I have ignored interactions F_{rs} ($r \neq s$) between different core orbitals. With the same approximation, matrix elements between valence orbitals and inner shells are given by

$$\bar{F}_{pr} = (F_{pr} - S_{pr} F_{rr}) N. \quad (64)$$

Inspection of Eq. (63) shows that \bar{F}_{pq} will only differ significantly from F_{pq} when both p and q can interact significantly with the same inner shell orbital r , otherwise $S_{pr} F_{rq}$, $F_{pr} S_{rq}$, $S_{pr} S_{rq}$ will all be small. The two most important cases where \bar{F}_{pq} and F_{pq} will differ are, first, when both p and q are on the same atom and neighboring atoms have inner shells, and, second, when p and q are on different atoms A, B, and r is on a third atom near both A and B. In the latter case, if A and B are neighboring atoms the difference between F_{pq} and \bar{F}_{pq} should be small, since other atoms cannot easily be near both A and B (inner shells on A or B can have little effect according to Eq. 63, since one-center F_{1s2s} matrix elements are negligible, and S_{1s2s} zero, for spectroscopic orbitals). When A and B are not neighboring atoms, then the inner shell orbital r must be on an atom between A and B, and near to both, to be important. Equation (64) shows that interaction between the $\bar{\phi}_p$ and inner shells should be much smaller than for ϕ_p .

To investigate the above predictions I have transformed the F -matrix (and its components) to orthogonalized valence orbitals (defined as in Eq. 62, working always in terms of spectroscopic orbitals)¹⁰ for HCN, C_2H_2 , C_2H_4 , and NH_3 . The only inner-shell orbitals in this study are, obviously, $1s$ orbitals. The most immediate and dramatic result is that in terms of $\bar{\phi}_p$ inner-shell orbitals are almost completely excluded from the valence shell MOs; the inner-shell coefficients never exceed 0.007 and are usually much less (they may reach 0.1 in terms of ϕ_p and spectroscopic orbitals). This is definitely encouraging. Similarly, F -matrix elements for interactions between inner- and valence-shell electrons almost vanish (being less than 0.03 au, instead of as large as 1 au over ϕ_p). Examination of the F -matrix elements involving only valence orbitals bears out the earlier remarks. In acetylene diagonal F -matrix elements become more positive over $\bar{\phi}_p$ relative to ϕ_p ^{68*} by 0.06, 0.05, 0.14, and 0 au for the hydrogen $1s$, carbon $2s$, $2p\sigma$, and $2p\pi$ orbitals, respectively. One-center F_{2s2p} matrix elements are sharply reduced in magnitude (by 0.09 au in acetylene, to half the original value). Two-center F -matrix elements between orbitals on neighboring atoms are effectively unchanged, and those involving orbitals on

more distant atoms may change significantly if there are other atoms with inner shells in between (by nearly 0.1 au for F -matrix elements involving hydrogen and the distant carbon in acetylene; there is a smaller change for the H-H interaction in NH_3). A convenient rule-of-thumb is

$$\bar{F}_{pq} = F_{pq} + \sum_r S_{pr} S_{qr} Z_A^2 / 3, \quad (65)$$

where r is on atom A with atomic number Z_A (Z_A is not an effective core charge). This expression usually gives the change to within 10%; it follows from Eq. (63) and the observations that $S_{rq} F_{rr}$, $S_{rp} F_{rr}$, and $-Z_A^2/3$ are good approximations for F_{rq} , F_{pr} , and F_{rr} , respectively.

It is a fortunate coincidence that all the main changes in going from F_{pq} to \bar{F}_{pq} are similar to changes in F_{pq} already erroneously introduced by the Mulliken approximation. I shall take advantage of this in my later calculations by omitting inner shells, but neglecting to transform from ϕ_p to $\bar{\phi}_p$. For example, I noted that the use of the Mulliken approximation made the diagonal F -matrix elements, F_{pp} , considerably too positive, particularly for $2p\sigma$ as compared to $2p\pi$ AOs (in molecules where this distinction is meaningful). From the differences between F_{pp} and \bar{F}_{pp} quoted above for acetylene, it can be seen that the approximate approach to F_{pp} will give results nearer to the correct \bar{F}_{pp} than to the correct F_{pp} . Even judged against \bar{F}_{pp} , the approximate F -matrix elements are still too positive, by from 0.05 to 0.15 au in polyatomic molecules; though this is a significant error which requires correction, it is about half the error found earlier when judging against F_{pp} . Furthermore, the problem has been simplified by the fact that, judged against \bar{F}_{pp} , the error is now about the same for all the $2p$ AOs on a given atom.

I also found earlier that the Mulliken approximation led to the underestimation of F -matrix elements between orbitals on distant atoms when a third atom was situated between them. I suggested a possible correction for this,^{35*} but in view of the fact that the error is such as to give good estimates of \bar{F}_{pq} (so much so that applying the correction, and then Eq. 63, would probably not give better results), I shall not need to pursue this matter further. The method I shall adopt later for one-center F_{2s2p} matrix elements, though not readily susceptible to improvement, underestimates the matrix elements significantly (in the few examples at my disposal); however, it gives good estimates of \bar{F}_{2s2p} , and again I accept this situation gratefully.

The main drawback to this procedure is that these errors from the Mulliken approximation mainly occur in the electron repulsion and exchange terms; detailed examination of the effect of Schmidt-orthogonalization on

the various components of the F -matrix shows that the changes of Eq. (63) occur mainly in the core part, H_{pq} . Though the cancellation will be all right as far as F_{pq} is concerned, it will be slightly less reliable when calculating total molecular energies.

I have so far discussed effects arising from interactions between inner shells and valence orbitals. I must also deal with penetration effects which arise because the inner shells do not shield the nuclei perfectly from the valence electrons [I include here also the effects of exchange integrals ($pr|pr$) between inner- and valence-shell orbitals]. For diagonal F -matrix elements the shielding of neighboring atoms by their $1s$ core electrons can be assumed perfect; for the extreme case of the carbon $2p\sigma$ orbital in HCN the penetration (including exchange) of the nitrogen core amounts to 0.02 au. However, the shielding of the nucleus by inner-shell electrons on the same atom as the valence electrons under consideration is not nearly so good; this must be allowed for when inner shells are neglected. For first-row atoms the stabilization of a spectroscopic $2s$ orbital on atom A from penetration of (including exchange with) the $1s$ inner shell is given accurately by^{69*}

$$-0.063Z'_A; \quad (66)$$

for a $2p$ orbital the corresponding stabilization is

$$-0.0072Z'_A, \quad (67)$$

both in au. These formulas hold to 0.001 au for boron to fluorine. These important negative contributions to F_{pp} are included automatically when spectroscopic data are used, but for my calculations must be introduced explicitly. The final inner-shell penetration effects to be mentioned are for two-center matrix elements F_{pq} between valence orbitals, with respect to inner shells on the atoms directly involved. These are small and in any case will be absorbed in the correction factors k^V, k^J .

To obtain an idea of the errors which would result if inner shells were omitted without any attempt at Schmidt-orthogonalization with the valence AOs, I performed Calculation IV (Table I). This calculation is like Calculation I except that inner-shell $1s$ electrons have been entirely absorbed into the effective core (the one-center penetration effects described by Expressions 66, 67 were however retained).^{70*} It can be seen that the total atomic charges are not much affected, but that there is a considerable shift of electrons from the $2s$ AOs into the $2p$ AOs on the same atom if inner shells are neglected without proper precautions. The other main difference between Calculations I and IV is the significant shifts of particular eigenvalues (those which refer to MOs with σ - rather than π -character);

in NH_3 and C_2H_2 one eigenvalue becomes 0.06 au more negative. The corresponding effects on antibonding MOs are larger. The comparative smallness of these changes means that only an approximate allowance for the effects of Schmidt-orthogonalization, in the *ad hoc* way discussed above, is required to remedy the situation.

E. Averaging for Rotational Invariance

I have already observed that the use of the Mulliken approximation leads to equations which are not invariant to rotation of the local coordinates in which nonspherically symmetric AOs are defined. This is well known.^{14a} A particularly thorough discussion of the problem has been given for the simpler case when the ZDO approximation is applied.^{7a} For example, consider the nuclear attraction integrals involving $2p$ orbitals on atom A and the core of atom B. In general one has two choices: either to average all integrals $\langle 2p_{u_A} | V^B | 2p_{u_A} \rangle$ ($u = x, y, z$) and neglect all integrals $\langle 2p_{u_A} | V^B | 2p_{v_A} \rangle$ ($u, v = x, y, z, u \neq v$), or to evaluate *all* the integrals properly. The same applies to the two-center electron repulsion integrals ($2p_{x_A} 2p_{y_A} | 2p_{y_B} 2p_{z_B}$); one must either evaluate all these integrals correctly (which leads to the serious complication of the NDDO method), or retain only the Coulomb integrals, all of which must be given the same average value for a particular pair A, B.

The obvious way of averaging over $2p$ AOs is to replace $2p_{u_A} 2p_{u_A}$ ($u = x, y, z$) by $2s_A 2s_A$.^{7a} Thus the CNDO version of the ZDO approximation can be made rotationally invariant by replacing all one-center Coulomb integrals on atom A by $(2s_A 2s_A | 2s_A 2s_A)$, and all two-center Coulomb integrals by $(2s_A 2s_A | 2s_B 2s_B)$, and also by representing the attraction of an electron on atom A by core B by $\langle 2s_A | V^B | 2s_A \rangle$ irrespective of whether the electron occupies a $2s$ or a $2p$ AO. These approximations are also sufficient to make Eqs. (19-21) for the Mulliken approximation over AOs rotationally invariant.

If in a CNDO theory it is desired to introduce one-center exchange integrals by use of Expression (61), to preserve rotational invariance all one center Coulomb integrals between $2p$ orbitals must be properly differentiated [e.g., $(2p_{x_A} 2p_{x_A} | 2p_{x_A} 2p_{x_A})$ and $(2p_{y_A} 2p_{y_A} | 2p_{x_A} 2p_{x_A})$].^{7a} To introduce the corresponding correction (Expression 27) over AOs would cause much more complication because the quantities $N(p_A)$ explicitly involve electrons in orbitals on other atoms; if however the diagonal density matrix elements P_{pp} are used instead of $N(p_A)$, then one could proceed much as above.

To investigate the effects of the approximations needed to retain rotational invariance as discussed above, I have performed Calculation V

(Table I) which is like Calculation I except that the necessary spherical averaging of the Coulomb repulsion and nuclear attraction integrals involving $2p$ orbitals has been introduced.^{71*} Comparison of Calculations V and I show that these approximations do not provide a sound basis for a general molecular theory; they introduce a sharp change into the polarity of the C—H bond in C_2H_2 (but not in C_2H_4), cause changes in some eigenvalues of 0.1 au or more, and completely upset the correct ordering of the eigenvalues in C_2H_2 and C_2H_4 . The main reason for all these results is apparent on inspection of the F -matrix elements in acetylene. As remarked elsewhere,^{9a} there is a severe anisotropy in the environment of the carbon atom in acetylene, which is reflected by the fact that F_{pp} is 0.58 au more negative for the $2p\sigma$ than for the $2p\pi$ AO, in the accurate calculation. Most of this (0.47 au) is preserved in Calculation I (the decrease is a reflection of the errors in F_{pp} discussed earlier, which are larger for the $2p\sigma$ AO). However in Calculation V the anisotropy is only 0.10 au; the $2p\sigma$ diagonal F -matrix element is less negative than in Calculation I, the $2s$ about the same, and the $2p\pi$ more negative. The inevitable consequences have been noted above; there is a shift of charge in the σ -system towards hydrogen, and the eigenvalues of π -MO's become more negative relative to σ -MOs.

There are two main contributions to this anisotropy (besides a negligible one-center effect arising from different populations of the various $2p$ AOs). First, there is the contribution from K_{pp} ; the $2p\sigma$ AO is involved in larger exchange integrals with orbitals on other atoms than is the $2p\pi$ AO. The main part of this effect will be retained when the rotational averaging approximations are introduced; it is about 0.2 au in the accurate calculation and about 0.1 au when the Mulliken approximation is used for the exchange integrals. Second, there is the contribution from neutral penetration integrals, which are in total about 0.3 au larger for the $2p\sigma$ than the $2p\pi$ AO; the $2p\sigma$ AO penetrates significantly into the neighboring neutral atoms. It is this effect which is entirely lost by the use of the approximations needed to retain rotational invariance, since these ascribe the same importance to neutral penetration integrals for $2s$, $2p\sigma$, and $2p\pi$ AOs. This averaging of neutral penetration integrals may be acceptable for saturated molecules, but invalidates any attempt to discuss the σ -systems of unsaturated compounds.

On the other hand in the CNDO method the alternative to averaging is the considerable complication of the NDDO method. With the Mulliken approximation over AOs the problem becomes truly formidable if averaging is not introduced. The simplest way of applying the Mulliken approximation to the integral $(p_A q_B | r_C s_D)$ ($A \neq B$, $C \neq D$) in a rotationally-invariant manner without averaging is to transform p_A and q_B to axes σ

and π with respect to the A—B bond (and analogously for r_C and s_D) before applying the Mulliken approximation.⁷² This is impracticable [the problem does not appear in the ZDO formulation because all these integrals are zero, but is encountered in practice when choosing approximations for $\langle p'_A | H | q'_B \rangle$ ($A \neq B$), where one must average over $2p$ AOs^{7a} or transform to local coordinates].⁷² To make the Mulliken approximation over AOs rotationally invariant without overwhelming complication, I must therefore seek a compromise, by averaging where it is not important, and transforming to local axes only for the critical integrals.

The groundwork for such a compromise has been given in earlier sections. Consider first the nuclear attraction integrals which make up V_{pq} . If ϕ_p and ϕ_q are on the same atom, V_{pq} must be properly calculated for $p = q$ and $p \neq q$; only then can I make the crucial distinction between the attraction of neighboring cores for electrons in $2p\sigma$ and $2p\pi$ AOs. If ϕ_p and ϕ_q are on different atoms A and B, then for the local part of the nuclear attraction, from cores A and B, I have already noted that averaging over $2p$ AOs would not be a good idea. And the whole philosophy behind the introduction of correction factors depending on the type of interaction demands that the $2p$ AOs first be transformed to be σ and π with respect to the A—B axis. So for these integrals I shall transform to local coordinates before applying the Mulliken approximation. Finally, for the nonlocal part of the nuclear attraction I have already seen that averaging over $2p$ AOs is perfectly acceptable.

Examination of the form of J_{pq} (Eq. 20) shows that with one further assumption J_{pq} can be handled as easily as V_{pq} . J_{pq} describes the repulsion between the charge distribution $\phi_p \phi_q$ and all the electrons in the molecule; despite the fact that individual integrals appear in J_{pq} , it is their total effect that matters. Thus whether or not I introduce averaging in handling the charge distributions $\phi_r \phi_s$ in the summation over r, s in Eq. (8), the summation will ensure that the results are much the same. The point is most easily seen in the form for J_{pq} in Eq. (40) obtained after using the Mulliken approximation on the orbital pair r, s , but not p, q ; if the three $2p$ valence AOs on each atom are equally occupied, then it will be no approximation at all to simplify Eq. (40) further, as

$$J_{pq} = \sum_A N(A)(pq | AA), \quad (68)$$

where $N(A)$ is the total Mulliken atomic population in the valence orbitals on atom A (I am now assuming that inner shells are not being explicitly considered), and A in $(pq | AA)$ has been used for the spherically symmetric valence orbital on atom A. In fact the $2p$ valence orbitals on any atom are

not all equally occupied in molecules; nevertheless, they are nearly so in many cases, and even when they are not Eq. (68) will still be a good approximation, containing the main features I wish to preserve. The rest of the discussion of J_{pq} is exactly as for V_{pq} above, where instead of a core attraction potential I now have the Coulomb potential of $N(A)$ electrons in a spherically symmetric valence orbital.

The problem of making the exchange contribution K_{pq} rotationally invariant can be dealt with very simply. Any approach other than complete averaging for all $2p$ AOs would lead to formidable complication; this would be quite unjustified in view of the known inadequacies of the Mulliken approximation for the exchange interaction. Furthermore inspection of the summation involved in K_{pq} in Eq. (9) shows that even if individual integrals were separated properly the effect would be largely lost in the final matrix element. In later work I shall therefore replace $2p$ AOs by the corresponding $2s$ AOs in Eq. (21) and (similarly in Eq. 58 for the ZDO approximation) except for one-center exchange and Coulomb integrals which will be dealt with as mentioned earlier (computational details will be given later).

I do not have a comparable calculation to Calculation I in Table I giving the results of the approach outline above, because it was decided on after that part of the analysis was complete. However I have found these approximations entirely satisfactory in practice, and have detected no trace of the errors introduced in Calculation V by the more drastic averaging procedure; I am certain that any errors there may be are negligible compared with those discussed elsewhere.

There are some obvious drawbacks to this approach. First, in a formal sense I use different values for the same integral at different times; $(pq|rs)$ is given three different values depending on whether it appears in J_{pq} , J_{rs} , or K_{pq} . This is not serious in practice because the individual integrals are never specified; I am really always approximating the sum of a number of integrals. The cancellation of the repulsion of an electron with itself discussed earlier will not be perfect as a result of these approximations, but I have already accepted this for other reasons. The main drawback is that I cannot readily give values to the individual electron repulsion integrals; as a result I cannot unambiguously transform these integrals to obtain the integrals $(ii|jj)$, $(ij|ij)$, which I would need to do configuration interaction or to predict molecular spectra from the eigenvalues of empty MOs obtained in a ground-state calculation (the better procedure of recalculating for the excited state would however present little ambiguity in the present approach). But in any case I have already lost track of the values of the individual integrals by using the correction factors k^J , which absorb various errors. Furthermore I do not think that meaningful predictions of

molecular spectra are likely to be possible for other than π -systems with the sort of theory at present under consideration, and π -systems can be safely left to the well-established methods. My accuracy will certainly not justify the use of configuration interaction for purposes other than spectra.

I have not discussed hybridizational invariance. In applying the Mulliken approximation to two-center charge distributions, provided the average of the $2p$ AOs is taken as the $2s$ AO invariance to hybridization will automatically be preserved. As far as one-center non-overlapping charge distributions involving $2s$ and $2p$ AOs are concerned, one should ignore them when averaging is taking place (e.g., in the sum over r, s , in J_{pq}), but should include them when $2s$ and $2p$ AOs are being properly distinguished (e.g., for p, q , in J_{pq}). This implies retaining the charge distribution $2s_A 2p_A$ in $\langle 2s_A | V + J | 2p_A \rangle$, which I have already noted is necessary purely on numerical grounds.

F. Semiempirical Approximations

I shall not be concerned in this section with the common practice of choosing quantities to obtain agreement with some molecular property, but only with the use of atomic spectroscopic data to simplify the calculation of the Coulomb integrals and diagonal (and hence, in some approximations, the off-diagonal) F -matrix elements.

Koopmans' theorem^{2,73} shows that the eigenvalues of occupied MOs are approximations to the ionization potentials and of vacant MOs to electron affinities in an SCF calculation. There are two main errors (assuming the solution is at a Hartree-Fock level). First, the MOs should be recalculated for the species with one less or one more electron to allow for "scaling" effects. Second, the correlation energy will change with the number of electrons. As has been pointed out,^{8,74} the practical success of Koopmans theorem hinges on the cancellation of these two quite sizeable errors. Atomic Hartree-Fock calculations⁷⁴ show that this cancellation can be quite accurate.

The crucial point is that the cancellation only occurs when one uses Koopmans' theorem for ionization potentials. To calculate electron affinities of, say, a neutral species from the vacant MO eigenvalues of the neutral species leads to the combination, rather than the cancellation, of the scaling and correlation errors. While the difference between the quantities may be small, their sum is typically 4 eV for the first-period atoms. This is sufficient to invalidate the procedure. Electron affinities must be obtained by calculating the ionization potential of the negative ion.

The usual semiempirical procedures for interpreting atomic spectra to

help with MO calculations can be conveniently judged in terms of Koopmans' theorem. Success is to be expected only when one makes use of the two-center attraction terms. To emphasize one side of this cancellation only theorem in such a way as to ensure the cancellation of errors discussed above. Unfortunately this is not usually the case. For example, both the original semiempirical arguments for π systems⁷⁵ and a recent more general formulation of the same principle,⁷⁶ fail this test. They attempt to interpret both the energy difference between cation and neutral atom, and that between neutral atom and anion, in terms of neutral atom quantities; only the first part of this procedure is likely to be at all accurate. Indeed, as is well known, these semiempirical approaches give a value for the neutral carbon Coulomb integral ($2p\ 2p|2p\ 2p$) (to which I shall confine the discussion) of about 11 eV, much lower than the calculated value over Hartree-Fock AOs (which is about 16 eV depending on the valence state used⁷⁷). The discrepancy is too great to be ascribed to correlation corrections⁷⁷⁻⁸⁰; however the semiempirical value is in good agreement with the calculated value over Hartree-Fock AOs of the carbon anion, after correlation corrections.^{77,81}

I have so far only considered the atomic situation; I must now consider the various arguments employed to justify the use of semiempirical Coulomb integrals in MO calculations. The original argument⁷⁵ was that within the usual π -electron approximations only the semiempirical approach gave reasonable energies for the ionic structures (involving a carbon anion and cation) relative to the covalent structures (involving neutral atoms). This is, of course, true when the carbon atoms are well separated. But consider the ionic structure in ethylene, the key molecules in testing semiempirical theories. Here the carbon anion and cation are separated by only 1.3 Å. The carbon anion now sees a nearby positive charge, and so resembles a neutral nitrogen atom as much as it does an isolated carbon anion. (Similarly, optimization of orbital exponents in the ionic structure for the hydrogen molecule gives an orbital *contracted* relative to the free hydrogen atom^{82,83*}). The semiempirical argument breaks down; to use a value for the Coulomb integral which refers to an AO of the carbon anion is inappropriate (this criticism applies equally to claims that, since ionic structures may be more important in excited states than in the ground state, the semiempirical Coulomb integral should be used for predicting spectra^{77b}).

Another argument is that the semiempirical approach simulates the effects of configuration interaction on the molecular ground state.^{75b,85} Detailed examination of the two-orbital problem of hydrogen shows that this does provide some justification for decreasing the one-center coulomb

integrals,⁸⁵ but also that two-center Coulomb integrals should be increased from the calculated value⁸⁵ (whereas in practice they are decreased^{75b}). Also the configuration interaction argument does not apply nearly so directly to the singly excited states (singlet and triplet) of the two-orbital problem; ironically much of the experimental justification for the semiempirical approach comes from these states of the ethylene π system.

In another approach,⁷⁹ the $2p\pi$ orbital exponent was optimized in the planar methyl radical; an expanded orbital and a lower one-center Coulomb integral relative to those of the carbon atom were obtained, and were considered to be more appropriate for use in calculations on π systems. This is not a valid argument. Optimization of isolated nonbonding AOs in molecules may well give expanded orbitals relative to the orbitals of the isolated atom but for AOs involved in bonding this is not the case (see the results for the $2p\pi$ orbitals in NH , HF , C_2 , and N_2 ⁸⁶).

One other attempt to justify the semiempirical integral values should be noted.⁸⁷ For a $2p$ electron in a singly occupied orbital on a neutral carbon atom there is obviously no repulsion from other electrons in the same orbital. But in a singly occupied $2p\pi$ orbital in a closed shell π system this is not so; the orbital must now be regarded as being occupied by half an electron of each spin. If the carbon $2p$ AOs are reoptimized including this extra repulsion term, then naturally orbitals expanded relative to those of the free atom are obtained, and Coulomb integrals closer to the semiempirical values.⁸⁷ This argument is fallacious. Consider the simple two-orbital problem as in ethylene. If half an electron of each spin is put on each carbon atom, and the repulsions and attractions added up (remembering that an electron cannot repel itself) it will be seen that the extra repulsion term relative to the free atom situation is nearly cancelled by two-center attraction terms. To emphasize one side of this cancellation only is quite artificial. Confirmation, if needed, can be found in the fact that the optimized $2p\pi$ orbital in C_2 is slightly contracted relative to the free atom.⁸⁶

The real justification for the semiempirical approach lies in its well-known success in correlating uv spectra. It so happens that decreasing the value of the one-center Coulomb integral compensates for the many errors implicit in the approximate approach to uv spectra. This is particularly the case for the separation of the lowest excited singlet and triplet states of ethylene, the classic problem in this area. Optimization of the $2p\pi$ orbital exponents in both the bonding and antibonding MOs of ethylene,⁸⁸ and allowance for electron correlation and σ - π interactions,⁸⁹ produce the same sort of improvement as does the semiempirical approach.

In short, the semiempirical approach to Coulomb integrals is a successful example of adjusting a calculation to agree with an experimental pro-

perty. Theoretical justifications are unnecessary and unsound. For most MO work, however, the calculated values of the Coulomb integrals are to be preferred on grounds of simplicity, rigor, and lack of ambiguity. The semiempirical approach provides too much scope for random variations in method. Besides the uncertainties encountered in interpreting atomic spectra, there are also possibilities such as scaling first the two-center Coulomb integrals (to match the reduced values of the one-center integrals), and then, inevitably, the corresponding two-center nuclear attraction integrals, and finally, as in some recent work,^{90c,91} the core-core repulsions.

My final comments concern the effect on an SCF calculation (at the Hartree-Fock level) of replacing calculated one-center Coulomb integrals by the semiempirical values. Provided this is done in the usual way with corresponding changes in one-center nuclear attraction and kinetic energy integrals so that the calculated AO energies are equal to ionization potentials, there will be little change, since Hartree-Fock orbital energies follow ionization potentials quite closely. But this brings up an important point. Slater orbitals (that is, a minimum basis set of single exponent orbitals with exponents given by Slater's rules) fail to describe adequately the trend in AO energies along the periodic table. For example, the ionization potential,⁹² Hartree-Fock eigenvalue,⁹³ and Slater orbital energy for the $2p$ electron in the ground state of the boron atom are, respectively, -0.30 , -0.31 , and -0.29 au, but for the fluorine atom the corresponding values are -0.64 , -0.73 , and -0.48 au.^{94*} Slater orbitals fail to reproduce the sharp increase in AO stability in going from boron to fluorine (indeed they give no increase at all for $2p$ AOs in going from nitrogen to fluorine). This failure renders them unsatisfactory for discussing molecular charge distributions; one must get the relative atomic energies correct first (a double-exponent representation of the orbitals would be adequate). Semiempirical methods which use ionization potentials for AO energies in MO calculations naturally avoid this danger. But it must be stressed that attempts to compare such semiempirical work with reference calculations using a minimum basis set of Slater orbitals are meaningless. I shall return to this point.

This concludes my criticism of the basic approximations commonly used in MO work. I shall now discuss a few of the many theories based on these approximations. I shall assume knowledge of these theories and, except for the most popular method, shall confine myself to pointing out briefly their major weaknesses. I shall not consider work which has been confined to π -systems.

IV. CURRENT THEORIES

A. Using the Mulliken Approximation

Many calculations make use of the Mulliken approximation at some point but there have been only two serious attempts to develop a general MO theory principally based on the Mulliken approximation over AOs with the retention of overlap.

One method⁹⁰ uses the uncorrected Mulliken approximation for electron repulsion contributions, thus introducing the errors and computational difficulties discussed earlier. Zero overlap matrix elements are neglected. Two formulas^{90a,b} are suggested for relating the off-diagonal elements of the H -matrix to the diagonal elements (the V - and T -matrices are not treated separately); neither is likely to be more accurate than the use of the Mulliken approximation for nuclear attraction integrals, criticized earlier (and if it were would merely weaken the cancellation of errors with the electron repulsion terms). The drastic averaging approximations invoked to preserve rotational invariance and the handling of the nuclear attraction contributions ensure the neglect of neutral penetration integrals. Consequently the ordering of the eigenvalues is wrong in molecules such as ethylene. The use of ionization potentials in the method means that the published comparisons with minimum basis set calculations are of doubtful value. Conclusions from this simple approach must be suspect.

Another approach¹⁴ is more satisfactory. Here the AO basis functions are taken as the Hartree-Fock AOs of the neutral atoms and as much as possible of the local parts of the F -matrix elements dealt with accurately by using the fact that the AOs are eigenfunctions of the atomic problem. All the rest of the calculation is dealt with by the Mulliken approximation. One-center zero-overlap matrix elements are included, and rotational averaging is introduced in such a way as to allow properly for neutral penetration integrals. However, there are drawbacks. The diagonal elements of the F -matrix will be inaccurate as discussed earlier (ironically the care taken in this work to correct for the omission of inner shells will prevent cancellation of errors at this point). Also, close inspection shows that it will often be necessary to evaluate important electron repulsion terms in the off-diagonal F -matrix elements by the uncorrected Mulliken approximation. Despite algebraic manipulation, the exchange interaction is still awkward to handle. Few applications have been reported, and no comparisons with reference calculations. In short, many of the weaknesses of the Mulliken approximation survive, despite the elegant formulation.

B. Using the Mulliken and Ruedenberg Approximations

There have been several methods proposed recently using the Mulliken approximation for J_{pq} and the Ruedenberg approximation for K_{pq} .^{9,16,47,48} When it is admitted explicitly that the Ruedenberg approximation is in use (not always the case), it is usually assumed that the Ruedenberg and Mulliken approximations are in some sense equivalent. Sometimes the Ruedenberg approximation is applied once, either as in Eq. (37)^{16,47} or Eq. (38),⁹ and sometimes twice as in Eq. (30).⁴⁸ Examination of the various methods in the light of my earlier analysis will show up their strengths and weaknesses.

I only wish to comment briefly here on the one method where there has been comparison with accurate calculations, and which shows clearly the serious consequences of using the Ruedenberg approximation. In this work⁹ the off-diagonal F -matrix elements were obtained by calculating T_{pq} accurately and estimating U_{pq} from Eq. (35), with the introduction of correction factors k^U depending on the type of interaction (with values chosen by matching accurate F -matrix elements). Many of the trends in the values of k^U are like those of k^V in Table I (except for differences connected with the use of Slater $2s$ rather than spectroscopic orbitals), but there is one crucial exception. It was found impossible to reproduce both the in-plane and out-of-plane $2p-2p\pi$ interaction in ethylene with the same value of k^U ; in fact the value in the latter case needed to be 50% higher. This is a direct reflection of the use of the Ruedenberg approximation as in Eq. (35) (which leads to the neglect of the important exchange contribution to the out-of-plane interaction, as already discussed). I shall avoid this problem in my approach.

Apart from the above point, the main weakness of this method can be summed up as a failure to distinguish between local and nonlocal contributions to the F -matrix elements. This is most serious in the diagonal elements, which are chosen from accurate calculations on small molecules. This procedure gives considerable overall accuracy, but lacks sensitivity to the detailed molecular environment, and does not permit iteration to self-consistency. Consequently accurate eigenvalues are obtained, but charge distributions are unreliable. (See, for example, the work on methyl acetylene^{9,5} which constitutes the first real test of this method on a molecule not used in the original calibration procedure.) A later attempt to improve this method¹³ does not escape the above criticism. It is often more important for chemical purposes to sacrifice overall accuracy for accurate reproduction of the small differences between similar molecules.

C. Using the Zero Differential Overlap Approximation

Many methods have been proposed using the ZDO approximation for general MO calculations.⁹⁶ To see how my earlier strictures apply in practice I shall comment on two methods^{7,26} where the ability to reproduce accurate calculations has been among the stated aims. Equally serious theoretical criticism applies to the more avowedly empirical approaches, but final judgment of these is best left to the experimentalists they purport to help.

In one method,²⁶ the H' -matrix is calculated accurately while the G' -matrix is obtained by use of the NDDO approximation. I have already noted the dangers of the NDDO approximation as far as J'_{pq} is concerned, and doubt that the use of hybridized orbitals in defining the OAOs avoids the problem (moreover the choice of hybrids is not always unambiguous). In this approach the cancellation of errors between nuclear attraction and electron repulsion contributions has been lost; the accurate calculation of the H' -matrix may not be worthwhile. No eigenvalues from this approach have been published, and few comparable approximate and accurate charge distributions. However even in a molecule as small as methane this method leads to an error of 0.7 au in the molecular energy compared to the reference calculation.

The most widely used method is that of Pople and Segal⁷; there are two main variants, known as CNDO/1 and CNDO/2. The CNDO/1 approach is based on Eqs. (50-60), with averaging of Coulomb integrals and nuclear attraction integrals to preserve rotational invariance (thus averaging neutral penetration integrals). The core integrals $\langle p'_A | T + V^A | p'_A \rangle$ are obtained by subtracting the appropriate number of Coulomb integrals from the observed ionization potential.^{97*} The core integrals H'_{pq} are obtained from the formula

$$H'_{pq} = S_{pq}(\beta_A + \beta_B)/2 \quad (69)$$

where β_A, β_B are parameters depending only on the atom concerned,^{98*} with values chosen by matching the results of accurate minimum basis set calculations on diatomic molecules.

The most serious error in the CNDO/1 method is the failure to transform integrals to OAOs. For the off-diagonal F' -matrix elements the use of parameters in Eq. (69) obviates this criticism, and for the diagonal elements the errors in the nuclear attraction and electron repulsion will cancel to some extent; but there remains the fundamental problem of the kinetic energy, which has been wrongly evaluated over AOs by the use of

an ionization potential.^{99*} Comparison with earlier remarks shows that this will make the diagonal elements of the F' -matrix too negative, and introduce a distortion of principle into the description of the bonding.

This transformation error is most serious for the orbitals which overlap most with neighboring orbitals; it is thus largest for spherically symmetric valence orbitals. It is also large for $2p\sigma$ orbitals in molecules such as acetylene, but small for $2p\pi$ orbitals, thus making comparison of σ - and π -systems difficult; the averaging of neutral penetration integrals, by introducing a positive error into the diagonal F' -matrix elements for $2p\sigma$ orbitals and a negative one for $2p\pi$ orbitals, eases this situation to a limited extent. Formaldehyde provides a good example of the resulting errors; the CNDO/1 diagonal F' -matrix elements are too negative compared to those for the accurate minimum basis set elements over OAOs by from 0.13 to 0.37 au, with the largest error for the carbon $2s$ AO, and the smallest for the $2p\pi$ out-of-plane AOs.

The off-diagonal F' -matrix elements obtained from the CNDO/1 approach are in impressive agreement with the reference calculations (the comparison can be made over AOs or OAOs, but if over AOs the inaccurate diagonal elements of the CNDO/1 F' -matrix must be corrected before back-transformation). The individual elements are often in error by less than 0.04 au, and are nearly as accurate as those I shall obtain later using the Mulliken approximation over AOs with correction factors depending only on the type of interaction. The main error in both cases comes in the $2p$ - $2p\sigma$ interaction in C_2H_2 , C_2H_4 , and C_2H_6 , which decreases much more rapidly than the simple approaches allow for (see Table I).^{100*} An additional error in the CNDO/1 approach is that the $2p$ - $2p\pi$ interactions are overestimated, a consequence of the averaging procedure implied by Eq. (69).

The CNDO/1 approach is successful for F'_{pq} because the use of parameters in Eq. (69) for H'_{pq} absorbs the errors in G'_{pq} ; where the component parts of F'_{pq} are needed, as when calculating molecular energies, this procedure is less satisfactory.

Using the CNDO/1 method it was found possible to reproduce quite well the charge distributions of accurate minimum basis set calculations, not only for the diatomic molecules used in the calibration procedure, but also for polyatomic molecules such as NH_3 , H_2CO , and HCN . This seeming success comes because the error in the diagonal F' -matrix elements varies more between σ - and π -systems than between different orbitals in a σ - or a π -system, and so does not greatly alter charge distributions. But this situation must be examined more closely. So far I have been content, in common with the original work,^{7b} to compare the CNDO/1 results with

accurate calculations using a minimum basis set of Slater orbitals. But, as noted earlier, this is inappropriate for methods where use is made of ionization potentials. The comparison should be with an accurate calculation in which the AOs employed have atomic energies compatible with the "average" ionization potentials used in the CNDO/1 method; this requires Hartree-Fock rather than Slater AOs. For a heteronuclear molecule involving atoms heavier than carbon a significantly different picture of the charge distribution is obtained when Hartree-Fock AOs are used. Judged in this light the CNDO/1 approach is much less successful; it is an unsatisfactory, not a satisfactory, feature of the method that it agrees so well with calculations using Slater AOs. I shall consider the effects of replacing Slater AOs by Hartree-Fock AOs in more detail later, but one example will be given here: the charge on the hydrogen atom in HF, calculated over OAOs, is +0.36 in an accurate calculation using Hartree-Fock AOs,¹⁰¹ +0.10 using Slater AOs,^{23a} and +0.08 in the CNDO/1 approach.

Returning to my numerical example of formaldehyde, proper allowance for the use of "average" ionization potentials gives a fairer estimate of the error in the CNDO/1 approach; I now find that the diagonal F' -matrix elements are too negative by from 0.1 to 0.3 au for carbon valence orbitals, by from 0.0 to 0.1 au for those on oxygen, and (as before) by 0.3 au for the hydrogen orbital. In these terms it becomes clear that the errors are worse for carbon than for oxygen AOs, an expected consequence of the larger number of atoms bonded to carbon.

In general I expect and find that the CNDO/1 method leads to transfer of electrons from terminal atoms (except hydrogen) towards nonterminal atoms and hydrogen atoms, relative to minimum basis set calculations using Hartree-Fock AOs; hydrogen counts as a nonterminal atom here because the magnitude of the overlaps it takes part in makes the transformation error large despite the isolation of a terminal position. Inspection shows that for most of the molecules in the original work,^{7b} exactly these changes will be produced by replacing Hartree-Fock AOs by Slater AOs in an accurate calculation; it is on this fortunate coincidence that the apparent success of the CNDO/1 approach is based.^{102*}

Other difficulties with the method (eigenvalues much too negative, bond lengths too short, and dissociation energies too high^{7b}) can be understood in terms of the errors discussed above.

I have discussed the CNDO/1 approach at some length because the theoretical issues are clearer there than in the more widely used CNDO/2 method. In the CNDO/2 version there are two changes from the CNDO/1 approach.^{7c} First, by equating nuclear attraction integrals to the corresponding Coulomb integrals, neutral penetration integrals are completely

neglected. This is an improvement since it leads to a somewhat better cancellation of the transformation error than does the mere averaging of neutral penetration integrals used in the CNDO/1 approach. With this modification the approximate diagonal F' -matrix elements for formaldehyde would become more positive by about 0.17 au for hydrogen and carbon AOs and 0.10 au for oxygen AOs. This would give better eigenvalues and limited improvement in the charge distribution, and would probably be the most satisfactory version of the CNDO method.^{103*} However, the CNDO/2 approach incorporates another modification as well. Previously only ionization potentials were used in obtaining the core integrals $\langle p'_A | T + V^A | p'_A \rangle$ from atomic spectra; now, for reasons which I criticized in the discussion on semiempirical approximations, electron affinities are used equally with ionization potentials. This makes the core integrals more negative by about 0.16 au for hydrogen and oxygen AOs, and 0.10 au for carbon AOs.

In formaldehyde the net effect of these two modifications is to make H'_{pp} change by about +0.02, +0.06, and -0.07 au for hydrogen, carbon, and oxygen valence orbitals, respectively. This leads to transfer of charge from carbon to hydrogen and oxygen relative to the CNDO/1 or accurate Slater minimum basis set calculations, whereas to match an accurate calculation using Hartree-Fock AOs a transfer of charge from hydrogen to carbon and from carbon to oxygen is required. This is a typical result, in that neither the CNDO/1 nor the CNDO/2 method is obviously the better; the differences hinge on the cancellation of the effects of the two important changes in method.

Despite all its theoretical weaknesses the CNDO/2 method (with its INDO analogue) has enjoyed considerable success in practice. This I shall not attempt to evaluate, except to express the opinion that when the right answers are obtained it is not for the right reasons, a common situation which bedevils approximate MO theory and leads inevitably to endless recalculations with "improvements" (several modifications and reparameterizations of the CNDO theories described above have already appeared.¹⁰³⁻¹⁰⁵ For example, the approximate procedure used to calculate dipole moments often leads to errors of more than 0.6 D in diatomic molecules,^{7b} and to better agreement with experiment than my discussion of the wavefunctions might suggest. One must have grave reservations about a theory which bases its success on a numerical cancellation involving the neglect of two effects whose balance is in fact crucial to a proper description of the bonding. There is always the danger of an absurd result as, for example, the calculation that the C—C bond in ethane is longer but stronger than in ethylene.^{7e}

To sum up and generalize all the above discussion, current approximate theories involve assumptions which, when introduced into accurate calculations, affect the results sharply; this does not inspire confidence. Among approximate methods aimed explicitly at reproducing accurate calculations, none has yet demonstrated its reliability for both eigenvalues and charge distributions. The Mulliken approximation offers fewer concealed dangers than the ZDO approximation, but it has not yet been given a fair and thorough trial. The final section of this paper is offered as an attempt to rectify this situation.

V. PRESENT PROPOSALS

A. Formulation

The method I propose to use is implicit in the preceding material; it is based on the Mulliken approximation, with corrections. Here I shall give the precise formulation, but shall not indulge in much further discussion. All the approximations have been considered already. The method will only be defined for closed-shell molecules, with atoms up to fluorine; removal of these restrictions would present no more than the usual difficulties.

The basic equations of the present approach are: for diagonal matrix elements for p_A ,

$$H_{pp} = T_{pp} + \sum_B V_{pp}^B \quad (70)$$

$$J_{pp} = \sum_B J_{pp}^B + \sum_q^A P_{qq} [(p_A p_A | q_A q_A) - (p_A p_A | AA)] \quad (71)$$

$$K'_{pp} = - \sum_q^A P_{qq} (p_A q_A | p_A q_A) / 2; \quad (72)$$

for one-center off-diagonal (zero-overlap) elements between p_A and q_A ,

$$H_{pq} = T_{pq} + \sum_B V_{pq}^B \quad (73)$$

$$J_{pq} = \sum_B J_{pq}^B + 2P_{pq} (p_A q_A | p_A q_A) \quad (74)$$

$$K'_{pq} = -P'_{pq} [(p_A p_A | q_A q_A) + (p_A q_A | p_A q_A)] / 2; \quad (75)$$

and for two-center off-diagonal elements between p_A and q_B ,

$$H_{pq} = T_{pq} + k^V S_{pq} (V_{pp}^A + V_{qq}^A + V_{pp}^B + V_{qq}^B) / 2 \\ + S_{pq} \sum_{C \neq A, B} (V_{AA}^C + V_{BB}^C) / 2 \quad (76)$$

$$J_{pq} = k^J S_{pq} (J_{pp}^A + J_{qq}^A + J_{pp}^B + J_{qq}^B)/2 \\ + S_{pq} \sum_{C \neq A, B} (J_{AA}^C + J_{BB}^C)/2 \quad (77)$$

$$K'_{pq} = -P'_{pq} (AA|BB)/2 \quad (78)$$

The summations in Eqs. (70, 71, 73, 74) are over all atoms though in Eqs. (73, 74) there is no contribution from atom A; the second summation in Eq. (71) and the summation in Eq. (72) are confined to orbitals on atom A. All Coulomb repulsion contributions are calculated with the rotational averaging of Eq. (68); for example,

$$J_{pp}^A = N(A)(pp|AA), \quad (79)$$

where $N(A)$ is the Mulliken gross atomic population on atom A. As before, the use of A or B in Eqs. (71, 76–79) where p or q would normally be expected implies that the spherically symmetrical valence orbital is to be used (that is, $2p$ AOs are to be taken as $2s$ AOs with the same orbital exponent). Thus, in Eq. (77), J_{AA}^C stands for $N(C)(AA|CC)$.

The last term in Eq. (71) for J_{pp} is of little numerical importance, but has been introduced so that, as far as possible, one-center electron repulsion integrals are accurately handled (as in the exchange interaction of Eqs. 72, 75) rather than averaged. To preserve rotational invariance this can only be done for terms appearing in the rigorous formulation of Eqs. (8, 9), and not for terms resulting from the use of the Mulliken approximation; this accounts for the use of density matrix elements. Furthermore all terms in Eqs. (8, 9) involving one-center integrals must be retained, which explains the extra term in Eq. (74) for J_{pq} .

The exchange matrix obtained from Eqs. (72, 75, 78) is to be taken as referring to Löwdin OAOs; it must not be added to the rest of the F -matrix without the necessary transformation. (This can be done over either basis set; over OAOs one has

$$\mathbf{F}' = \mathbf{S}^{-1/2}(\mathbf{H} + \mathbf{J})\mathbf{S}^{-1/2} + \mathbf{K}', \quad (80)$$

in which case the simpler form of the secular equations, Eq. 60, is applicable.^{62*} As indicated in Eqs. (72, 75, 78) OAO density matrix elements are used, but all electron repulsion integrals are assigned their AO rather than OAO values (an unimportant approximation for this purpose). It is to be noted that Eqs. (72, 75) differ from the normal ZDO equations in that one-center exchange integrals have been retained.

In applying these equations there are three elaborations or corrections not indicated above. First, although $1s$ inner shells are not explicitly included (nor is Schmidt orthogonalization allowed for, for reasons discussed

earlier), penetration of the inner shells by valence electrons on the same atom must not be ignored. For $2s$ and $2p$ electrons on atom A the (negative) corrections of Formulas (66) and (67), respectively, are added to the value of H_{pp} obtained from Eq. (70).

Second, the correction factors k^V, k^J are allowed to depend on the type of interaction as discussed below (but not on the internuclear distance or orbital exponents). These correction factors are for interactions defined in terms of local axes (e.g., $2p-2p\sigma$, $2p-2p\pi$). Before applying the Mulliken approximation to $\langle p_A | V^A + V^B | q_B \rangle$, or $\langle p_A | J^A + J^B | q_B \rangle$ when one or both of p_A, q_B , are $2p$ valence AOs, the AOs must be expressed in terms of components σ and π with respect to the A—B bond. This has not been included explicitly in Eqs. (76, 77); for general $2p-2p$ interactions there will be a term in H_{pq} involving $k_{2p2p\sigma}^V$ and another involving $k_{2p2p\pi}^V$ (and similarly for J_{pq}).

Third, the correction to the diagonal F -matrix elements discussed earlier takes the form of an extra term which is added to J_{pp} : for $1s$ orbitals on hydrogen (atom A) this term is

$$-0.04 \sum_{B \neq A} Z'_B S_{AB}^2; \quad (81)$$

for $2s$ valence orbitals on atom A,

$$-0.011(Z'_A/2 + Z'_A) \sum_{B \neq A} Z'_B S_{AB}^2; \quad (82)$$

and for $2p$ valence orbitals on atom A,

$$-0.006(Z'_A/2 + Z'_A) \sum_{B \neq A} Z'_B S_{AB}^2. \quad (83)$$

S_{AB} is the overlap integral between the spherically symmetric valence orbitals on atoms A and B.

In my calculations all integrals appearing in Eqs. (70–83) were evaluated correctly. With exceptions to be mentioned, Slater orbitals were used to represent the valence AOs. The orbital exponents were input parameters; usually (and where not otherwise stated) the Slater values were used, with an exponent of 1.2 for hydrogen, but in some cases the effect of exponent variation was investigated. I should be using spectroscopic rather than Slater $2s$ orbitals. For all the two-center integrals left in Eqs. (70–78) the difference is negligible, but this is not so for one-center integrals. One-center kinetic energy and nuclear attraction integrals involving the $2s$ valence AOs were evaluated in terms of spectroscopic orbitals,^{18*} and one-center electron repulsion integrals calculated over Slater orbitals and corrected by multiplying by factors of 0.975, 0.985, and 0.960 for the integrals

$(2s2s|2s2s)$, $(2s2s|2p2p)$, and $(2s2p|2s2p)$, respectively (this gives results accurate to 0.002 au for atoms up to fluorine).

All calculations were iterated to self-consistency. For a few of the more difficult iterations there may be uncertainty of one in the last figure quoted in the following results (particularly for dipole moments). Severe convergence difficulties were frequently encountered in molecules with distinct σ and π systems. The Newton-Raphson procedure¹⁰⁶ usually led to convergence.

From the point of view of computing time the calculation of integrals was never a significant factor. The manipulations of Eqs. (70-78) are easy to handle, and increase less rapidly than N^3 . Almost all the time was spent on solving the secular equation.

B. Calibration

The only parts of this theory obtained by calibration against reference calculations are the values of k^V and k^J for different types of interactions, and the Corrections (81-83). The rest of the theory is predetermined.

Though many reference calculations were examined, the values of k^V and k^J were in fact assigned (see Table III) almost entirely by reference to

TABLE III
Mulliken Correction Factors for Use in Eqs. (76, 77)

| Interaction | H-H | H-2s | H-2p | 2s-2s | 2s-2p | 2p-2p σ | 2p-2p π |
|-------------|------|------|------|-------|-------|----------------|-------------|
| k^V | 0.75 | 0.84 | 0.84 | 0.85 | 0.91 | 1.15 | 0.89 |
| k^J | 0.65 | 0.94 | 0.83 | 0.98 | 1.00 | 1.10 | 0.97 |

Table II and ethylene (noted elsewhere, and confirmed here, to be an "average" molecule for calibration purposes^{9c}). It will be noticed that the values used for k^V_{H-2p} , and, particularly, k^V_{H-H} , are smaller than inspection of Table II would suggest. This is because the nonlocal contribution to the nuclear attraction is very important relative to the local contribution (on which k^V acts) for interactions involving hydrogen. Errors introduced by the use of the Mulliken approximation on the nonlocal part (these are particularly large for H-2p interactions) have been to some extent absorbed in k^V . Since the nonlocal situation may vary significantly in different molecules, this is not entirely satisfactory, as will appear.

The above values of k^V and k^J were chosen to match the accurate V - and G -matrices after these had been transformed first to spectroscopic AOs and

then to valence AOs Schmidt-orthogonalized to inner shells on other atoms. Only interactions between nearest neighbors were considered. It is clear from Table II that the values of k^V (and k^J) would need to be smaller for long-range interactions, but the interactions themselves are then small, and the errors in the nonlocal contributions dominant.

The constants at the beginning of the Corrections (81–83) to J_{pp} were also found mainly by reference to ethylene. Other molecules give similar results; a change of more than 20% in the values of these constants would markedly worsen the agreement with the accurate F -matrix elements. Even this freedom (which is only a small change in a fairly small correction term) is sufficient to affect the results, but since the values I chose initially from matching F -matrix elements were as satisfactory as any, I did not vary these quantities.

The one part of the calibration which did need a wide range of reference calculations was the choice of the expression inside the brackets of corrections (82, 83). I chose the simplest form which matched the general trends, but there is not sufficient information to be dogmatic. This part of the correction, though it does give better agreement with the reference calculations, is not as important as the term in $Z'_A{}^2$ might suggest: when Z'_A is large, as for fluorine, there are few directly-bonded atoms and $\sum_{B \neq A} Z'_B S_{AB}{}^2$ is usually small.

To see how the method as defined and calibrated above could reproduce F -matrix elements, I calculated approximate F -matrices for the reference molecules^{19a*} (with the reference geometries and exponents) using the density matrices from the accurate calculations. In general, the approximate matrix elements are within 0.03 au of the accurate values (appropriately transformed to spectroscopic AOs, with valence AOs Schmidt-orthogonalized to inner shells on other atoms), and are often correct to 0.01 au. The H - and G -matrices are in equally good agreement with the reference calculations. I shall only discuss here the main cases where the results are not so satisfactory.

First, there are errors of often 0.05 au (and up to 0.10 au) in the F -matrix elements for $2s$ - $2p$ and, particularly, $2p$ - $2p\sigma$ interactions. These latter tend to be underestimated at short bond lengths as in acetylene, and overestimated for long bond lengths as in ethane. This is the inevitable result of the failure to make k^V and k^J depend on the internuclear distance.

Second, the handling of H - $2p$ interactions in the diatomic hydrides BH to HF is not satisfactory using a fixed value of k^V , as would be expected from Table II. In addition there are significant (0.05 au) errors in the H - $2p$ interactions in molecules such as H_2O and NH_3 , where the nonlocal contribution to the interaction is small; this is because k^V_{H-2p} has been

chosen to absorb errors occasioned by the use of the Mulliken approximation on the larger nonlocal contributions in molecules like acetylene and ethylene.

Third, in heteronuclear situations with short bonds, such as CO, the errors in the diagonal F -matrix elements, though small for both atoms, combine to reduce the differences between orbitals on the two atoms (by up to 0.05 au). Thus charge transfer in such situations may be underestimated.

Probably none of these errors is acceptable in a completely general method, but I shall now show that they do not prevent the reproduction of accurate minimum basis set calculations.

C. Reproduction of Reference Calculations

The approximate method presented above has proved reliable in simulating the results of accurate minimum basis set calculations. Some typical results are given in the last column of Table I, where it will be seen that both eigenvalues and charge distributions are in satisfactory agreement with the reference calculations. A general survey of my results for the polyatomic molecules BH_3 , H_2O ,^{107*} NH_3 , CH_4 , C_2H_2 , C_2H_4 , C_2H_6 , B_2H_6 , H_2CO , HCN ,^{19b*} and CH_3CCH ⁹⁵ reveals the following discrepancies. Of the 48 distinct eigenvalues for occupied MOs, 27 are in error by less than 0.025 au (16 by less than 0.015 au), 17 by between 0.025 and 0.055 au, 3 by between 0.055 and 0.075 au, and 1 by 0.10 au. The ordering of eigenvalues is correct except for one inversion of levels in B_2H_6 (which also has the most inaccurate eigenvalue). As is to be expected, eigenvalues for empty MOs are less reliable (except for MOs with only π character). In these same molecules Mulliken atomic populations for hydrogen are accurate to within 0.03 (except for an error of 0.04 in H_2O and of 0.14 for the bridging hydrogens in B_2H_6); for other atoms the error in atomic population is on the average 0.05, only exceeding 0.10 in CH_4 and B_2H_6 . Individual orbital populations are of comparable accuracy, except that transfer of as much as 0.15 of an electron from the $2s$ AO to the $2p$ AO with most σ character on the same atom commonly occurs. For the range of diatomic molecules^{19b*,86} Li_2 , C_2 , N_2 , CO , LiH , and BH equally good results are obtained, except that the (Mulliken) charge transfer to oxygen in CO is underestimated by 0.15 of an electron. Agreement is worse for LiF , BF , and HF , and worst of all for F_2 (where one eigenvalue is in error by 0.22 au); my use of correction factors is inaccurate for these interactions.

Two points are worth noting. The results for methyl acetylene (CH_3CCH) are quite as satisfactory as those for ethane and acetylene, giving grounds for hope that the method will be reliable for large molecules. The small but

important differences between the diagonal F -matrix elements of CH_3CCH and those of C_2H_6 and C_2H_2 ⁹⁵ are sensitively reproduced, and the dipole moment is in satisfactory agreement with the reference calculation (see later).

The results for B_2H_6 are less accurate, as noted above. The main reason is an error in handling the interaction between $2p$ AOs on boron and the bridging hydrogens. If one thinks in terms of $2p$ AOs σ and π with respect to the B—H bond, it will be seen that there is an important nonlocal contribution from the other boron atom to the H— $2p\pi$ zero overlap interaction which is ignored in my use of the Mulliken approximation. In general when two-center zero-overlap matrix elements are important (that is, when the molecular environment of a given bond is sharply asymmetrical as, for example, in cyclopropane), my method will be less successful.

Dipole moments (accurately calculated) from the present method for LiF, BF, CO, H_2O , NH_3 , HCN, H_2CO , and CH_3CCH are respectively (with the value from the corresponding reference calculation^{108*} in brackets) 3.18 (2.94), 2.51 (2.16), 0.61 (0.73), 2.07 (1.59), 1.63 (1.76), 2.25 (2.11), 1.20 (1.01) and 0.96 (0.70) Ds. In each case the dipole is in the same direction as in the reference calculation. The agreement is satisfactory, except for H_2O (for diatomic hydrides there are errors of up to 1 D—I have already noted that my method will be unreliable here). I would stress particularly the reasonable result for CH_3CCH ; this shows the advantage of my self-consistent approach, since another non-iterative method⁹ which gives accurate eigenvalues and F -matrix elements leads to a dipole moment of 1.71 D.⁹⁵

Before comparing my total molecular energies with the reference calculations, allowance must be made for my omission of inner shells. For each $1s$ inner shell I must add to my molecular energy twice the kinetic energy of a $1s$ electron, twice the nuclear attraction energy of a $1s$ electron in the field of the parent nucleus, and finally the repulsion between the two $1s$ electrons. Using Slater AOs (equivalent here to spectroscopic^{18*} AOs), this comes to -21.97 , -32.35 , -44.72 , and -59.10 au for the atoms boron to oxygen, respectively. I then find that my total molecular energies for C_2H_2 , C_2H_4 , C_2H_6 , CH_4 , CH_3CCH , HCN, H_2CO , BH_3 , B_2H_6 , and NH_3 are in error^{108*} by -0.12 , -0.09 , 0.02 , 0.25 , -0.43 , 0.02 , -0.14 , 0.25 , 0.42 , and 0.17 au, respectively. These errors are significant (particularly disappointing is the error for CH_3CCH); it is worth noting that an earlier method^{9c} obtained just as good agreement using an approximation for the molecular energy based on the sum of the eigenvalues. On the other hand I should point out that another method²⁶ discussed above introduces errors of 0.7 au for CH_4 and C_2H_4 and 0.3 au for C_2H_2 despite accurate

calculation of all nuclear attraction integrals. In short, the simplest approximation is not necessarily the worst.

Reproduction of the reference calculation of the barrier in ethane (with exponents of 1.0 for hydrogen)¹⁰⁹ gives a barrier of 0.013 au as opposed to the reference value of 0.005 au.

Attempts to optimize orbital exponents by minimizing the energy in my approximate method were largely unsuccessful; to improve this situation it would be necessary (at least) to make the correction factors depend on the orbital exponents involved in the different interactions. However, my method is useful for seeing the effects of exponent changes on molecular charge distributions. For example, changing the hydrogen exponent from 1.0 to 1.2 (and slightly altering the molecular geometry) increases the dipole moment of H₂CO by 0.41 D in accurate calculations,^{21,95} and by 0.46 D in my method.

D. Agreement with Experiment

The inadequacies of accurate unoptimized minimum basis set calculations for predicting experimental properties are well known; it is not my purpose to document this further by detailed comparison of my approximate results with experiment. I shall merely indicate briefly where I can improve on the reference calculations by modifying the method, and also where my approximations render my method less useful even than the reference calculations.

There is one way in which it is easy to improve my method relative to a minimum basis set calculation. I have already noted that Slater orbital energies are increasingly too positive relative to Hartree-Fock orbital energies (and to the negatives of ionization potentials). Some, at least, of the advantages of using Hartree-Fock AOs can thus be gained merely by introducing a correction to the diagonal elements of the *F*-matrix obtained from my approximate method. Inspection of the Slater and Hartree-Fock atomic energies lead to the following *ad hoc* formulas for the correction for orbitals on boron to fluorine: for 2s AOs on atom A

$$-0.0031Z'_A{}^2 - 0.009(Z'_A - 3); \quad (84)$$

and for 2p AOs

$$-0.01(Z'_A - 2)^2. \quad (85)$$

There is not much information about the ability of minimum basis set calculations to predict molecular geometries; however, it is certain that my method will be considerably less successful. Without accurate two-center integrals (or at least variation of the correction factors with bond dis-

tance), bond lengths will be unsatisfactory. My approach underestimates the rate of increase in the magnitudes of interactions as bond lengths decrease, and so overestimates bond lengths by upwards of 10%. A few examples of bond lengths and stretching force constants are given in Table IV (calculated using the Hartree-Fock correction, which has little effect here except to lengthen the calculated value of the C—H bond in HCN by 0.2 au). There is obviously little chance of useful predictions in this area.

TABLE IV
Bond Lengths and Force Constants

| Molecule | Bond | Bond length (au) | | Force constant (mdyn/Å) | |
|-------------------------------|------|--------------------------|-------------------------|-------------------------|-------------------|
| | | r_e calc. ^a | r_e obs. ^a | Calc. | Obs. ^b |
| C ₂ H ₂ | C—H | 2.208 | 2.002 | 3.9 | 5.9 |
| HCN | C—H | 2.291 | 2.009 | 3.3 | 5.8 |
| C ₂ H ₄ | C—H | 2.413 | 2.052 | 3.4 | 5.1 |
| C ₂ H ₆ | C—H | 2.475 | 2.066 | 2.9 | 4.8 |
| H ₂ CO | C—H | 2.499 | 2.117 | 3.1 | 5.3 |
| C ₂ H ₂ | C—C | 2.556 | 2.281 | 11.8 | 15.8 |
| C ₂ H ₄ | C—C | 2.636 | 2.530 | 5.9 | 9.6 |
| C ₂ H ₆ | C—C | 3.029 | 2.899 | 3.1 | 4.3 |
| HCN | C—N | 2.674 | 2.183 | 13.8 | 17.9 |
| H ₂ CO | C—O | 2.723 | 2.287 | 13.5 | 12.1 |

^a Experimental geometries were taken from *Tables of Interatomic Distances and Configurations in Molecules and Ions* (The Chemical Society, London, 1958 and 1965); these geometries were retained during the calculations, except for the type of bond under immediate discussion.

^b G. Herzberg, *Infrared and Raman Spectra*, Van Nostrand, Princeton, New Jersey, 1945.

My method is also unreliable for bond angles because of the approximations in both the two- and three-center integrals. For example, H₂O would be linear and NH₃ planar according to my results. Little is known about angle predictions with accurate minimum basis set calculations.

The usefulness of this sort of calculation for estimating ionization potentials has been demonstrated elsewhere by a wide-ranging correlation between reliable approximate minimum basis set eigenvalues and experiment.⁹ My results are equally successful and there seems no point in documenting them in detail.

I have already seen that my method gives dipole moments in good agreement with the accurate minimum basis set calculations, which are usually not close to the experimental values. However, agreement with experiment can be substantially improved by incorporating my Hartree-Fock corrections.^{84,85} Results from my method with and without this correction are compared with experiment in Table V. This provides convincing evidence of the importance of using Hartree-Fock rather than Slater AO's in calculating dipole moments for molecules with atoms heavier than carbon; with the Hartree-Fock correction my method gives dipole moments in reasonable agreement with experiment. (For H₂O and NH₃ the introduction of the Hartree-Fock correction into my method leads to less accurate dipole moments. For H₂O this is partly an artifact of errors in the basic method, which led to the unsatisfactory reproduction of the dipole

TABLE V
Dipole Moments (in Debyes)^a

| Molecule ^b | This work ^c (uncorrected) | This work ^c (corrected) | Experiment ^d |
|-----------------------|---|---------------------------------------|-------------------------|
| H ₂ O | 2.07 | 2.57 | 1.85 |
| NH ₃ | -1.63 | -1.96 | -1.47 |
| HCN | 2.27 ^e | 2.91 | 2.99 |
| H ₂ CO | 1.32 ^e | 2.56 | 2.34 |
| CH ₃ CCH | 0.96 | f | 0.75 |
| CH ₃ F | 1.01 | 2.00 | 1.82 |
| CH ₃ CN | 2.73 | f | 3.96 |
| CH ₂ CO | -0.07 | 1.79 | 1.43 |
| H ₂ NCN | 3.83 | 3.81 | 4.00 |

^a The sign convention is such that a positive sign means the dipole is in the sense corresponding (in a point-charge model) to net positive charge at the left-hand end of the molecule as written.

^b Geometries were taken from Footnote a of Table IV. Slater exponents were used, with 1.2 for hydrogen.

^c Calculations using the present method both without and with the Hartree-Fock correction.

^d Values chosen from A. L. McClellan, *Tables of Experimental Dipole Moments*, Freeman, San Francisco, 1963; the signs are assumed.

^e These values differ slightly from those quoted earlier because of differences between the experimental geometry and the geometry used in the reference calculations.

^f Self-consistency was not achieved for these calculations; one would expect the dipole moment of CH₃CCH to change only slightly when the Hartree-Fock correction is introduced, but that of CH₃CN to change in the same way as for HCN.

moment of the reference calculation noted earlier. But it is also probable that for both molecules a more extended basis set is an essential elaboration if accurate dipole moments are required.)

VI. CONCLUSIONS

I have found that the Mulliken approximation, with certain simple but important corrections, allows the reproduction of both the eigenvalues and charge distributions of accurate minimum basis set calculations in little more time than is required to solve the secular equations; it is also possible to match experimental ionization potentials and (after allowing for the main inadequacy of Slater AOs) dipole moments, but not bond lengths and bond angles.

Perhaps the main point of this work has been to show how far astray one may be led by seemingly innocuous and commonly accepted approximations. I would reiterate that many of the errors on whose avoidance my success is based, as well as the errors which have limited my success, can be detected in most currently popular approximate methods, despite concealment under an empirical approach (though by the time this article is published, the situation may well have improved).

For the future, it seems desirable that empirical approaches should always be based on the most accurate calculation that is practicable. With the rapid advances now being made in programming and computing techniques this will soon be the accurate minimum basis set SCF calculation itself. Attempts to improve the method presented above would thus be of only short-term value.

Acknowledgments

I acknowledge gratefully help in various forms from Professors L. C. Allen, C. J. Ballhausen, R. Mason, and J. A. Pople, and especially Drs. M. D. Newton and G. A. Segal. I am particularly indebted to Dr. W. F. Palke for supplying the accurate integrals on which this work is based, to Professor W. N. Lipscomb for the kind hospitality during which the work was concluded, and to Professor H. C. Longuet-Higgins for much advice and encouragement.

References

1. G. G. Hall, *Proc. Roy. Soc.*, **A205**, 541 (1951).
2. C. C. J. Roothaan, *Rev. Mod. Phys.*, **23**, 69 (1951).
3. An extended basis set is necessary to give a reasonable description of the molecular charge distribution, and configuration interaction is needed to introduce the effects of electron correlation.
4. E. Clementi, *J. Chem. Phys.*, **46**, 3842 (1967).
5. O. Sinanoglu, *Proc. Natl. Acad. Sci. U.S.*, **47**, 1217 (1961).
6. I follow Ref. 7a closely.

7. (a) J. A. Pople, D. P. Santry, and G. A. Segal, *J. Chem. Phys.*, **43**, S129 (1965); (b) J. A. Pople and G. A. Segal, *ibid.*, **43**, S136 (1965); (c) J. A. Pople and G. A. Segal, *ibid.*, **44**, 3289 (1966); (d) D. P. Santry and G. A. Segal, *ibid.*, **47**, 158 (1967); (e) G. A. Segal, *ibid.*, **47**, 1876 (1967); (f) G. A. Segal and M. L. Klein, *ibid.*, **47**, 4236 (1967); (g) H. W. Kroto and D. P. Santry, *ibid.*, **47**, 792 (1967); (h) H. W. Kroto and D. P. Santry, *ibid.*, **47**, 2736 (1967); (i) J. A. Pople, D. L. Beveridge, and P. A. Dobosh, *ibid.*, **47**, 2026 (1967); (j) J. A. Pople and M. Gordon, *J. Am. Chem. Soc.*, **89**, 4253 (1967); (k) M. S. Gordon and H. Fischer, *ibid.*, **90**, 2471 (1968); (l) D. P. Santry, *ibid.*, **90**, 3309 (1968).
8. R. S. Mulliken, *J. Chim. Phys.*, **46**, 497, 675 (1949).
9. M. D. Newton, F. P. Boer, and W. N. Lipscomb, *J. Amer. Chem. Soc.*, (a) **88**, 2353 (1966); (b) **88**, 2361 (1966); (c) **88**, 2367 (1966).
10. K. Ruedenberg, *J. Chem. Phys.*, **34**, 1861 (1961).
11. For a detailed exposition of the physical argument, with many examples for $1s-1s$ and $2p-2p\pi$ interactions, see Ref. 12. I have found this approach valuable for a wide variety of integrals, though where $2p\sigma$ orbitals are involved accurate numerical guidance is particularly desirable.
12. S. Huzinaga, *J. Phys. Soc. Jap.*, **13**, 1189 (1958).
13. D. B. Boyd and W. N. Lipscomb, *J. Chem. Phys.*, **48**, 4955 (1968).
14. R. Manne, (a) *Theor. Chim. Acta.*, **6**, 299 (1966); (b) *ibid.*, **6**, 312 (1966); (c) *J. Chem. Phys.*, **46**, 4645 (1967).
15. R. S. Mulliken, *J. Chem. Phys.*, **23**, 1833, 1841, 2338, 2343 (1955).
16. (a) R. F. Fenske, K. G. Caulton, D. D. Radtke, and C. C. Sweeney, *Inorg. Chem.*, **5**, 951 (1966); (b) R. F. Fenske and D. D. Radtke, *ibid.*, **7**, 479 (1968).
17. R. Polák and J. Paldus, *Theor. Chim. Acta*, **5**, 422 (1966).
18. "Spectroscopic" orbitals were obtained by solving the atomic problem using a minimum basis set of Slater orbitals in the configuration $1s^2 2s^2 2p^n$, with the $2p$ electrons spin-randomized. To a very good approximation the results for all the atoms boron to fluorine are given by

$$(2s)_{\text{spectroscopic}} = 0.99991(2s)_{\text{Schmidt}} - 0.0135(1s),$$

$$(1s)_{\text{spectroscopic}} = 0.99991(1s) + 0.0135(2s)_{\text{Schmidt}},$$

where $(1s)$ is the $1s$ Slater orbital and $(2s)_{\text{Schmidt}}$ is obtained by Schmidt orthogonalization of the $2s$ and $1s$ Slater functions:

$$(2s)_{\text{Schmidt}} = [(2s) - S_{1s2s}(1s)] / (1 - S_{1s2s}^2)^{1/2}$$

Except for one-center integrals the use of $(2s)_{\text{spectroscopic}}$ and $(2s)_{\text{Schmidt}}$ gives similar results.

19. (a) Most investigations reported in this work were carried out for all the molecules BH_3 , NH_3 , CH_4 , C_2H_2 , C_2H_4 , C_2H_6 , HCN , H_2CO , N_2 , HF , BH , and NH . Only a fraction of the results can be given, but unless otherwise stated it can be assumed that similar conclusions hold for all molecules not specifically mentioned. (b) Minimum basis set results using Slater orbital exponents (except with an exponent of 1.2 for hydrogen), and including inner shells, are given in Ref. 20 for BH_3 , NH_3 , CH_4 , C_2H_2 , C_2H_4 , C_2H_6 , and HCN , Ref. 21 for H_2CO , and Ref. 22 for N_2 ; results with an exponent of 1.0 for hydrogen are given for HF in Ref. 23a, BH in Ref. 23b, and NH in Ref. 23c (and also for H_2CO in Ref. 21, though I did not make

- use of this calculation). (c) Obtainable from the published eigenvalues and eigenvectors. (d) The integrals for all the polyatomic species were kindly provided by Dr. W. E. Palke; for the diatomics, the integrals are given in the published papers.
20. W. E. Palke and W. N. Lipscomb, *J. Amer. Chem. Soc.*, **88**, 2384 (1966).
 21. M. D. Newton, and W. E. Palke, *J. Chem. Phys.*, **45**, 2329 (1966).
 22. C. W. Scherr, *J. Chem. Phys.*, **23**, 569 (1955).
 23. (a) A. M. Karo and L. C. Allen, *J. Amer. Chem. Soc.*, **80**, 4496 (1958); (b) R. C. Sahni, *J. Chem. Phys.*, **25**, 332 (1956); (c) M. E. Boyd, *J. Chem. Phys.*, **29**, 108 (1958).
 24. The fact that Eqs. (19–21) are not invariant to the choice of basis set is unimportant for present purposes. I did not wish at this stage to confuse the Mulliken approximation itself with the further approximations needed to maintain invariance. As a result, threefold symmetry is lost in NH_3 and BH_3 ; equivalent hydrogen Mulliken populations differ by up to 0.01, and degenerate eigenvalues by up to 0.03 eV. These differences were averaged.
 25. See also Ref. 26 where related conclusions have been reached about the importance of one-center exchange integrals between hybrids.
 26. D. B. Cook, P. C. Hollis, and R. McWeeny, *Mol. Phys.*, **13**, 553 (1967).
 27. I shall use atomic units of energy when engaging in detailed comparison of approximate and reference calculations. The conversion factor is 1 au = 27.21 eV. Thus 0.04 au is about 1 eV, and provides a reasonable criterion of accuracy by which to judge various approximations.
 28. To check that the difference in F -matrix elements between the approximate and accurate calculations is the cause, rather than the consequence, of the different charge distributions, I have obtained similar results inserting the density matrix from the reference calculations in Eqs. (20, 21).
 29. If A and B are far apart, the exchange integral will be overestimated because the influence of the one-center Coulomb integrals introduced by the Mulliken approximation becomes dominating; see Ref. 12.
 30. Partial, but inadequate, allowance for these integrals is made in Eq. (27) by the use of $N(q)$ instead of P_{qq} . See the later discussion of the Ruedenberg approximation.
 31. It might therefore be argued that I should have used Slater 2s orbitals, for which the Mulliken approximation is more satisfactory, in this analysis. However, in common with most theories I shall ultimately decide to omit inner shells, which leaves me no choice but to use spectroscopic 2s orbitals. All approximate theories which neglect inner shells must be judged in terms of spectroscopic rather than Slater 2s orbitals.
 32. See also Ref. 12. These matrix elements, although large, have comparatively little effect on the final wavefunction. It might be thought that a better approximation to $\phi_p\phi_q$ than that given by Eq. (18) would be $S_{pq}\phi_p\phi_q$ when ϕ_p (but not ϕ_q) is an inner-shell orbital, since the overlap region will be nearer to the tightly bound orbital. In fact this is rather worse than the Mulliken approximation, at least for $\langle p_A | V^A | q_B \rangle$.
 33. In weighting these integrals in Eq. (28) effective core charges (with inner shells absorbed into the nuclei) rather than atomic numbers, were used. Overlap integrals were calculated using Slater rather than spectroscopic 2s orbitals, again for comparison with my final method; the difference is usually less than 1 %, but is sometimes 3 %.
 34. These results give some grounds for hope that the Mulliken approximation will be better for σ -interactions involving hybrids of 2p and spectroscopic 2s AOs than for the AOs themselves.

35. A simple correction can be suggested for these errors in the nonlocal nuclear attraction (though I shall find for other reasons that I will not need to use it). The Mulliken estimate of the integrals $\langle p_A | V^C | q_B \rangle$ should be corrected by multiplying by $2(R_{C-A})^{-1}/(R_{C-A}^{-1} + R_{C-B}^{-1})$, where R_{C-A} and R_{C-B} are internuclear distances and R_{C-A} is the distance from atom C to the midpoint of the line joining atoms A and B. The physical interpretation of this correction is obvious on inspection of the Mulliken approximation. This gives a reliable average estimate of the correction required, without being able to allow for detailed directional effects, provided the value of the correction factor is less than 1. When C is between A and B this correction factor can become very large, and indeed infinite; numerical work shows that for values of the correction factor greater than 1 scaling is required so that the maximum value is 1.5.
36. There is, of course, an approximation involved in using J^A as if it were exactly analogous to V^A . In defining J^A the Coulomb potential arising from the electrons in MOs in Eq. (8) has been replaced in Eq. (23) by the potential from electrons distributed in but not between AOs as described by the Mulliken population analysis. Errors from this approximation will mainly be absorbed in k' .
37. Similarly the ideal correction factor for nonlocal contributions to the Coulomb repulsion is typically halfway between unity and the value calculated for the non-local part of the nuclear attraction (see Ref. 35). The fact that the Mulliken approximation is better for electron repulsion integrals $\langle p_A q_B | r_A r_B \rangle$ than for the nuclear attraction integrals $\langle p_A | V^A | q_B \rangle$ is to be expected from a comparison of the potentials concerned; however it is not always true when $2p\sigma$ orbitals are involved.
38. As Eq. (21) stands, a quadruple summation of some complexity is needed to obtain the matrix K at each stage of the iteration to self-consistency. The machine time this requires depends on N^4 where N is the size of the basis set; since the rest of the calculation depends on N^3 this rapidly becomes unacceptable. Algebraic manipulation (see Ref. 14a) reduces the effort required to a triple summation and several matrix multiplications, which together are equivalent to about 6 matrix multiplications. Since I shall find it possible to make the rest of the approximate calculation of F more rapid than one matrix multiplication, the calculation of K will be the most time consuming computational task if Eq. (14) is solved using Householder's method (see Refs. 39, 40), and still a significant problem if the slower (Ref. 39) Jacobi process is used for Eq. (14).
39. J. H. Wilkinson, *The Algebraic Eigenvalue Problem*, Clarendon Press, Oxford, 1965, Chapter 5.
40. A. J. Fox and F. A. Johnson, *Computer J.*, **9**, 98 (1966).
41. In some early SCF LCAO calculations all two-center integrals were calculated accurately, while three- and four-center integrals were obtained by the Mulliken approximation. See, for example, W. L. Clinton and B. Rice, *J. Chem. Phys.*, **29**, 445 (1958), and, for a comparison of this method with an accurate calculation on acetylene, see L. Burnelle, *J. Chem. Phys.*, **35**, 311 (1961) and references therein.
42. There have been various attempts to improve the Mulliken approximation [e.g., J. Cizek, *Mol. Phys.*, **10**, 83 (1965), A. Pellegatti, *Theor. Chim. Acta.*, **6**, 109 (1966), F. E. Harris and R. Rein, *ibid.*, **6**, 73 (1966)]. Though these procedures may be useful for obtaining accurate estimates of a few integrals, they rapidly become unwieldy for general molecular calculations, where the sheer number of the integrals is a serious problem.

43. To dispense with the correction factors k^J completely while calculating nuclear attraction integrals accurately would lead to errors in the F -matrix elements usually about as large as (but of opposite sign to) those produced by using the uncorrected Mulliken approximation on both nuclear attraction and electron repulsion integrals.
44. D. C. Pan and L. C. Allen, *J. Chem. Phys.*, **46**, 1797 (1967).
45. L. C. Allen in *Quantum Theory of Atoms, Molecules and Solids*, P.-O. Löwdin, Ed., Academic Press, New York, 1966, p. 39.
46. K. Ruedenberg, *J. Chem. Phys.*, **19**, 1433 (1951); various expressions from this work have at times been referred to as the Ruedenberg approximation (see Refs. 9, 14, 47, 48). I use the phrase in the sense of Ref. 47.
47. G. Berthier, P. Millie, and A. Veillard, *J. Chim. Phys.*, **62**, 8 (1965).
48. G. Ciullo, C. Furlani, and A. Sgarbellotti, *Coord. Chem. Revs.*, **2**, 15 (1967).
49. The Coulomb and exchange potentials in the Roothaan equations come from all 2N electrons in N occupied MOs. The inclusion of the repulsion of an electron with itself is avoided by cancellation with the exchange of an electron with itself. This cancellation is upset if the Mulliken approximation is used in some parts of the calculation and the Ruedenberg approximation in others.
50. There is an ambiguity here in that it would be equally possible to apply Eq. (29) to the orbital pairs p, r and q, s in Eq. (9). This would not however give useful expressions. The ambiguity does not arise for the Mulliken approximation.
51. See, for example, Refs. 26, 52, 53, and references therein.
52. I. Fischer-Hjalmers, (a) *J. Chem. Phys.*, **42**, 1962 (1965); (b) *Theor. Chim. Acta.*, **4**, 332 (1966).
53. R. G. Parr, *The Quantum Theory of Molecular Electronic Structure*, Benjamin, New York, 1964.
54. I am grateful to Dr. M. D. Newton for stimulating discussions on this topic.
55. B. C. Carlson and J. M. Keller, *Phys. Rev.*, **105**, 102 (1957).
56. L. C. Cusachs and B. B. Cusachs, *J. Phys. Chem.*, **71**, 1060 (1967).
57. It might be argued that since the Mulliken approximation is unsatisfactory over AOs, I should attempt to find OAOs where the ZDO approximation could give better results, instead of doing my best to ensure no change by using Löwdin OAOs. This would be an impracticable and arbitrary procedure. [However in the special case of inner shells there are advantages, at least formally (see Ref. 58b) if not numerically (compare Refs. 58b and 32. but note also the text justifying Eq. 65) in using OAOs obtained by Schmidt orthogonalization of valence orbitals to inner shells.] More to the point would be to transform the AO basis set by rotation or hybridization until the Mulliken approximation became acceptable (though it will rarely be possible to achieve this for both electron repulsion and nuclear attraction contributions simultaneously), and then to apply the ZDO approximation to Löwdin OAOs obtained in terms of the transformed AOs. In view of the comparative success of the Mulliken approximation for AO hybrids, work in terms of Löwdin OAOs formed from hybrid AOs (see Ref. 26) would seem worthwhile.
58. (a) J. P. Dahl, *Acta Chem. Scand.*, **21**, 1244 (1967); (b) J. P. Dahl and C. J. Ballhausen, *Advan. Quantum Chem.*, **4**, 170 (1968); (c) J. P. Dahl and H. Johansen, *Theor. Chim. Acta*, **11**, 8 (1968).
59. R. N. Dixon, *Mol. Phys.*, **12**, 83 (1967).
60. J. J. Kaufman, *J. Chem. Phys.*, **43**, S152 (1965).

61. The answers depend, sometimes significantly, on whether or not the valence orbitals are Schmidt-orthogonalized to inner shells on other atoms before forming the Löwdin OAOs (see Ref. 26); however, I have checked that my general conclusions do not depend on this choice.
62. In practice even the back-transformation can be bypassed by retaining the exchange interaction in its OAO form. When the rest of the F -matrix has been transformed to OAOs in the normal course of solving the secular equations, the exchange interaction can be added in. Furthermore, the OAO density matrix will be readily available as a by-product of the solution of the secular equations in the previous interactions.
63. I refer to the minimum basis set calculation, for which the Mulliken population analysis is given in E. Clementi and H. Clementi, *J. Chem. Phys.*, **37**, 2824 (1962), and the accurate OAO polarity in Ref. 7b.
64. B. H. Chirgwin and C. A. Coulson, *Proc. Roy. Soc.*, **A201**, 196 (1950).
65. The one obvious exception is shifts in inner-shell energy levels brought about by changes in the molecular charge distribution. If these are required, they can easily be obtained by a perturbation procedure (see Ref. 14). These shifts should not, of course, be allowed for in evaluating the total molecular energy if the inner shells have been included in the core during the calculation of valence MOs.
66. R. McWeeny and K. A. Ohno, *Proc. Roy. Soc.*, **255**, 367, (1960).
67. J. D. Stuart and R. P. Hurst, *Mol. Phys.*, **9**, 265 (1965).
68. That diagonal F -matrix elements should become more positive over $\bar{\phi}_p$ than ϕ_p is expected, since one is really forming the antibonding combination of the valence orbitals and the inner shells.
69. If Slater $2s$ AOs were being used, the penetration of the inner shell would be about half that of the spectroscopic $2s$ AOs.
70. Comparison of calculations I and IV should not be taken as a statement concerning neglect of inner shells in a rigorous calculation, but only within the framework of the Mulliken approximation, which overestimates core-valence shell interactions (and hence provides too severe a test of the consequences of their neglect). The danger of the collapse of high antibonding eigenvalues to negative values, which I have found can occur in molecules like C_2H_2 , HCN, when inner shells are omitted without Schmidt-orthogonalization, is avoided in calculation IV because of the errors introduced into F_{pp} by the Mulliken approximation.
71. For convenience, spectroscopic $2s$ orbitals were used as the average of the $2p$ AOs, whereas Slater $2s$ AOs would perhaps be more appropriate. The difference is unimportant.
72. Cf. Refs. 9a, 56.
73. T. Koopmans, *Physica*, **1**, 104 (1933).
74. R. E. Watson, *Phys. Rev.* **118**, 1036 (1960).
75. (a) R. Pariser, *J. Chem. Phys.*, **21**, 568 (1953); (b) R. Pariser and R. G. Parr, *ibid.*, **21**, 767 (1953).
76. L. Oleari, L. di Sipio, and G. de Michelis, *Mol. Phys.*, **10**, 97, 111 (1965).
77. (a) M. K. Orloff and O. Sinanoğlu, *J. Chem. Phys.*, **43**, 49 (1965); (b) O. Sinanoğlu and M. K. Orloff in *Modern Quantum Chemistry*, Vol. 1, Academic Press, New York, 1965, p. 221; these references provide access to the extensive literature on this topic.
78. V. McKoy and O. Sinanoğlu, *J. Chem. Phys.*, **41**, 2689 (1964).
79. R. B. Hermann, P. G. Lykos, J. D. Sharp-Ritter, and R. Moccia, in Ref. 45, p. 335.

80. M. H. Alexander, *J. Chem. Phys.*, **46**, 1953 (1967).
81. R. B. Hermann, *ibid.*, **42**, 1027 (1965).
82. S. L. Altmann and N. V. Cohan, *Trans. Faraday Soc.*, **50**, 1151 (1954).
83. For this reason I doubt the value of making orbital exponents depend on the charge on the atom, as is done in some calculations (e.g., Ref. 84); the total molecular environment is important.
84. R. D. Brown and B. A. W. Collier, *Theor. Chim. Acta*, **7**, 259 (1967).
85. A. E. Hansen, *ibid.*, **7**, 230 (1967).
86. B. J. Ransil, *Rev. Mod. Phys.*, **32**, 245 (1960).
87. (a) H. J. Silverstone, H. W. Joy, and M. K. Orloff, *J. Amer. Chem. Soc.*, **88**, 1325 (1966); (b) H. J. Silverstone and H. W. Joy, *J. Chem. Phys.*, **47**, 1384 (1967); (c) H. W. Joy and H. J. Silverstone, *Mol. Phys.*, **13**, 149 (1967).
88. S. Huzinaga, *J. Chem. Phys.*, **36**, 453 (1962).
89. T. H. Dunning and V. McKoy, *ibid.*, **47**, 1735 (1967).
90. T. Yonezawa, K. Yamaguchi, H. Kato, H. Konishi, H. Nakatsuji and T. Kawamura, (a) *Bull. Chem. Soc. Jap.*, **40**, 536 (1967); (b) *ibid.*, **40**, 1017 (1967); (c) *ibid.*, **40**, 1071 (1967); (d) *ibid.*, **40**, 2211 (1967).
91. (a) M. J. S. Dewar and G. Klopman, *J. Amer. Chem. Soc.*, **89**, 3089 (1967); (b) N. C. Baird and M. J. S. Dewar, *ibid.*, **89**, 3966 (1967).
92. C. F. Moore, *Atomic Energy Levels*, Vol. I, Circular 467 of the National Bureau of Standards.
93. E. Clementi, *IBM J. Res. Develop. Suppl.*, **9**, 2 (1965).
94. This is an average over the $2p$ electrons, to correspond to the Hartree-Fock value.
95. M. D. Newton and W. N. Lipscomb, *J. Amer. Chem. Soc.*, **89**, 4261 (1967).
96. See, for example, Refs. 7, 26, 58b, 76, 91, and references therein.
97. This procedure incorporates the one-center exchange integrals into the core integral, rather than neglecting them entirely (as was implied in Ref. 26). In the INDO modification (see Refs. 7i, 7k, 59) this simplification is avoided.
98. As usual in a ZDO calculation, nonlocal contributions to the off-diagonal elements are ignored. Because this is a reasonable approximation, it has been claimed (Ref. 26) that only with an OAO basis set can one hope to choose 'bond parameters' transferable from one molecule to another. However this will be equally successful in an AO approach, provided that the nonlocal contributions are dealt with by the Mulliken approximation (which is not at all difficult).
99. A similar point has been made in Ref. 26, but that discussion fails to consider the cancellations of errors on which the comparative success of the CNDO/1 method is based.
100. For a formula which avoids this error see Ref. 91a.
101. A. M. Karo and L. C. Allen, *J. Chem. Phys.*, **31**, 968 (1959).
102. Recalibration of the parameters in Eq. (69) against accurate calculations using Hartree-Fock AOs would not help the CNDO/1 approach significantly; the problem is in the diagonal F' -matrix elements.
103. See P. A. Clark and J. L. Ragle, *J. Chem. Phys.*, **46**, 4235 (1967), and D. F. Shriner and J. Posner, *J. Amer. Chem. Soc.*, **88**, 1672 (1966) for reparameterizations of the CNDO approach which are closer to this version than to either the CNDO/1 or CNDO/2 methods.
104. J. M. Sichel and M. A. Whitehead, *Theor. Chim. Acta*, **7**, 32 (1967); *ibid.*, **11**, 220, 239, 254, 263 (1968).

105. J. del Bene and H. H. Jaffe, *J. Chem. Phys.*, **48**, 1807, 4050 (1968); *ibid.*, **49**, 1221 (1968).
106. P.-O. Löwdin, *J. Mol. Spectr.*, **10**, 12 (1963).
107. The reference calculation for H₂O (with Slater exponents and 1.2 for H) was kindly provided by E. Switkes.
108. Reference calculations as in Refs. 19b, 86, 95, and 107.
109. R. M. Pitzer and W. N. Lipscomb, *J. Chem. Phys.*, **39**, 1995 (1963).

AUTHOR INDEX

Numbers in parentheses are reference numbers and show that an author's work is referred to although his name is not mentioned in the text. Numbers in *italics* indicate the pages on which the full references appear.

- Abragam, A., 167, 247
 Alexander, M. H., 108, 146, 286(80), 311
 Allen, L. C., 265(44, 45), 293(23a, 101), 307, 309, 311
 Altmann, S. L., 286(82), 311
 Amano, T., 232, 248
 Andrick, D., 21(45), 87, 141(65), 144, 147
 Ardill, R. W. B., 70(114), 89
 Asundi, R. K., 132, 147

 Bailey, V. A., 71(116), 89
 Baird, J. C., 220, 221, 247
 Baird, N. C., 288(91), 311
 Ballhausen, C. J., 277(58), 309
 Bandel, H. W., 74, 80, 90, 124(44), 147
 Bardsley, J. N., 17(6), 71(6), 81(139), 86, 90, 115, 129(50), 146, 147
 Barfield, M., 61(97), 89
 Bates, D. R., 18
 Beauchamp, J. L., 20(23), 87
 Bender, C. F., 144(68), 147
 Bene, J. del, 294(105), 312
 Benesch, W., 43, 45(77), 46, 88
 Berry, R. S., 1(1), 14, 63(110), 80, 81(137), 89, 90
 Berthier, G., 266(47), 290(47), 309
 Bethe, H. A., 1(1), 6(3), 14, 168(20), 247
 Beunker, R. J., 61(98), 89
 Beveridge, D. L., 272(7i), 291(7), 306
 Bhatia, A. K., 99(14), 104(14), 114(14), 146
 Boer, F. P., 253(9a), 254(9), 258(9a, 9c), 260(9), 264(9a, 9c), 282(9a), 290(9), 298(9c), 301(9), 303(9), 306
 Born, M., 151, 247
 Bowers, K. D., 221(40), 247
 Bowman, C. R., 19, 56, 59(19), 60(19), 63, 66(19), 86
 Boyd, D. B., 254(13), 290(13), 306
 Boyd, M. E., 307
 Breig, E. L., 72, 75, 90
 Breit, G., 168, 172, 247

 Briglia, D. P., 81(141), 90, 127(48), 128, 147
 Brink, D. M., 157, 162(12), 165(12), 166(12), 173(12), 185(12), 186(12), 196(12), 247
 Brinkmann, R. T., 26(57), 52(57), 54(57), 71(120), 72(120), 79(120), 83(120), 85(120), 88, 89
 Bromberg, J. P., 27(59), 88
 Brongersma, H. H., 20, 43, 48, 54(87), 56(87), 60, 63, 86, 89
 Brown, R. D., 304(84), 311
 Brown, R. L., 216(33), 228(33), 233, 247
 Burhop, E. H. S., 17(4, 5), 19, 20(4), 79(4), 86
 Burke, P. G., 17(8, 10), 27(10), 86, 91(1), 94, 97, 98(10), 99, 104(14), 114(14), 143-145, 145, 146
 Burnelle, L., 265(41), 308
 Burns, 48
 Burrow, P. D., 85, 90
 Burrus, C. A., 150(2), 246

 Carlson, B. C., 270(55), 309
 Carrington, A., 149, 210(27, 28), 212(27, 28), 214(31, 32, 46), 215(31, 32), 216(31, 32, 46), 220(38), 221(38), 222(42), 228(31, 45-47), 231, 232, 233(31, 32, 46, 47), 237(60), 238(60), 242(60), 245(62), 247, 248
 Carson, T. R., 72, 78(127), 90
 Cartwright, D. C., 26(57), 28(60), 31(67, 68, 70), 32(70), 33, 40(70), 41(68, 70), 42(75), 47(70), 52(57), 54(57), 80(135), 88, 90
 Caulton, K. G., 255(16), 290(16), 306
 Cermák, V., 46(79), 88
 Chamberlain, G. E., 21(40, 42, 43), 24(54), 25(54), 26, 32, 36, 40(40), 41(74), 43, 46, 52, 87, 88, 124(45), 141, 147
 Chantry, P. J., 135, 147
 Chen, J. C. Y., 91(3), 99(18), 116, 118, 145, 146

- Chirgwin, B. H., 277, 310
 Chiu, L.-Y., 172(24), 176(24), 194(24), 247
 Chiu, Y. N., 224, 247
 Christophorou, L. G., 20(22), 43(22), 87
 Ciullo, G., 290(48), 309
 Cizek, J., 265(42), 308
 Clark, P. A., 294(103), 311
 Clementi, E., 250(4), 277(63), 288(93), 305, 310, 311
 Clementi, H., 277(63), 310
 Clinton, W. L., 265(41), 308
 Cohan, N. V., 286(82), 311
 Coller, B. A. W., 304(84), 311
 Compton, D. N., 20(22), 43, 87
 Cook, D. B., 271(26), 275(26), 277(26), 291(26), 301(26), 307
 Cooper, J., 1(1), 14
 Cooper, J. W., 98(10), 144(10), 145(71), 146, 147
 Costello, D. G., 86(149), 90
 Coulson, C. A., 277, 310
 Cox, J. T., 233(55), 248
 Currie, G. N., 210(28), 212(28), 214-216(31), 222(42), 228(31), 233(31), 247
 Cusachs, B. B., 271(56), 309
 Cusachs, L. C., 271(56), 309

 Dahl, J. P., 273(58a), 277(58), 309
 Dalton, B. J., 1(1), 14
 Damburg, R., 99, 146
 Daniels, J. M., 220(37), 221(37), 244(37), 247
 Darwin, C. G., 172, 247
 Davidovits, P., 85, 90
 Davidson, E. R., 144(68), 147
 Davison, W. D., 70(114), 89
 Demkov, Yu. N., 130(51), 133, 147
 Dewar, M. J. S., 61(96), 89, 288(91), 311
 Dillon, M. A., 20, 42(35), 43, 48(35), 49, 63(29), 65(35), 71, 82(36), 87
 Dirac, P. A. M., 168, 170(18), 247
 Dixon, R. N., 272(59), 309
 Dobosh, P. A., 272(7f), 291(7), 306
 Doering, J. P., 20(33), 21, 26, 30(33), 43, 63, 64, 66(33c), 87, 88
 Dorain, P. B., 220(37), 221(37), 244(37), 247
 Dousmanis, G. C., 150(4), 246
 Dowell, J. T., 20, 51, 56(89), 71, 87, 89, 131(52), 133, 147

 Dressler, K., 46(78), 88
 Drexler, K., 21(49), 88
 Dunning, T. H., 61(100), 89, 287(89), 311
 Dyer, P. N., 214(32, 46), 215(32), 216(32, 46), 228(45, 46), 233(32, 46), 247, 248
 Dymond, E. G., 19, 86

 Edmonds, A. R., 90
 Ehrhardt, H., 21, 70(112), 71, 77(46), 81, 87, 89, 94(7), 115(33), 118(33), 122(33), 123, 141(65, 66), 144, 145, 146, 147
 Eliezer, I., 124(39), 137(39), 144(69), 147
 Evans, D. F., 61(105), 89
 Eyb, M., 141(65), 144(65), 145(65), 147
 Eyring, H., 154(9), 247

 Fajen, F. E., 72, 90
 Falick, A. M., 212(29), 247
 Fano, U., 6(4), 14, 145(71), 147
 Fenske, R. F., 255(16), 290(16), 306
 Feshbach, H., 101, 110, 114, 146
 Fischer, H., 291(7), 306
 Fischer-Hjalmers, I., 271(52), 276(52a), 277(52b), 309
 Foldy, L. R., 169, 247
 Fonda, L., 99, 146
 Fox, A. J., 308
 Francis, 63
 Franck, J., 19, 86
 Freed, K. F., 182(26), 185, 247
 Freund, R. S., 150(6), 246
 Fundaminsky, A., 18
 Furlani, C., 290(48), 309

 Gailitis, M. K., 99, 146
 Geiger, J., 21, 52-54, 63, 72, 87-89
 Geltman, S., 70(113), 78, 89, 99(14), 104(14), 114, 146
 Gerjuoy, E., 75, 90
 Gilmore, F. R., 42, 88
 Goldberger, M. L., 17(2), 86, 107, 146
 Golden, D. E., 74, 80, 90, 124(44), 147
 Golebiewski, A., 92(5), 102, 118(5), 145
 Gordon, M. S., 291(7), 306
 Gordy, W., 233(55), 248
 Gottfried, K., 25(55), 88
 Grace, D. E., 86, 90
 Graybeal, J. D., 150(2), 246

 Hall, G. G., 250(1), 251(1), 305

- Hansen, A. E., 286(85), 287(85), 304(85), 311
 Harris, F. E., 131(55), 135(55, 61), 147, 265(42), 308
 Hart, R. R., 63(110), 89
 Hazi, A., 144(69), 147
 Heddle, D. W. D., 145, 147
 Heideman, H. G. M., 21(40, 42, 43), 32(40), 36(40), 40(40), 41(74), 43, 46, 52, 87, 88, 124(45), 141(64), 147
 Henry, A. F., 219(35), 247
 Henry, R. J. W., 79(131), 90
 Hermann, R. B., 286(79, 81), 287(79), 310, 311
 Herring, D. F., 86(149), 90
 Hertz, G., 19, 86
 Herzberg, G., 17(11), 18(11a), 51(11b), 59, 61(91–93, 106), 66(11c), 86, 89, 131(54), 134, 147, 303
 Herzenberg, A., 115, 129(50), 146, 147
 Heubner, R. H., 20(22), 43(22), 87
 Hill, R. M., 150(1), 246
 Hirota, E., 232(54), 248
 Hojvat, N. L., 61(96), 89
 Hollis, P. C., 271(26), 275(26), 277(26), 291(26), 301(26), 307
 Holbien, E., 102–104, 146
 Howard, B. J., 228(47), 233(47), 248
 Huang, K., 151(8), 247
 Hurst, G. S., 20(22), 43(22), 87
 Hurst, R. P., 277(67), 310
 Hutchisson, E., 53, 54, 89
 Huzinaga, S., 262(12), 287(88), 306, 311
 Ingold, C. K., 56, 89
 Jaffe, H. H., 294(105), 312
 Jobe, J. D., 18(69), 31, 33(69), 41(69), 88
 Johansen, H., 277(58), 309
 Johnson, F. A., 308
 Joy, H. W., 287(87), 311
 Kamper, R. A., 221(40), 247
 Karo, A. M., 293(23a, 101), 307, 311
 Kato, H., 288(90c), 289(90), 311
 Kato, T., 101, 106–108, 111, 146
 Kaufman, J. J., 273(60), 309
 Kawamura, T., 288(90c), 289(90), 311
 Kayama, K., 220, 221, 247
 Keesing, R. G. W., 145, 147
 Keiffer, L. J., 30(63), 88
 Keller, J. M., 270(55), 309
 Kemble, E. C., 105(24), 106(24), 146
 Keys, L. K., 219(36), 247
 Kimball, G. E., 154(9), 247
 King, G. W., 56, 89
 Klein, M. L., 291(7), 306
 Klein, O., 84(143), 90
 Klemperer, W., 150(6), 246
 Klopman, G., 288(91), 311
 Kolos, W., 79, 90, 124(40), 125(40), 147
 Konishi, H., 288(90c), 289(90), 311
 Koopmans, T., 285, 310
 Kopelman, R., 61(101), 63(101), 89
 Krasnow, 42
 Krauss, M., 31, 33(66), 88
 Krongelb, S., 234, 248
 Kronig, R. de L., 159(13), 247
 Kroto, H. W., 291(7), 306
 Krupenie, P. H., 48, 89
 Kuebler, N. A., 63(110), 89
 Kuppermann, A., 15, 17(119), 18(71), 20(32, 34, 56), 21, 26(57), 28(60), 30(32), 31, 32(70), 33, 36, 40(70), 41(68, 70), 42(75), 43, 46, 47(70), 48, 49, 51, 52(57), 53, 54(57), 57–60(56), 63, 64, 66(32a), 71(119), 72(119), 74–78(119), 79(119, 132), 80(119, 135), 81(119), 87, 88, 90
 Kuyatt, C. E., 17(53), 20(38), 21(40–43), 22, 24, 25(54), 26(54), 27(58), 32(40), 36(40), 40(40), 43, 46, 52, 87–89, 124(41–43, 45), 145(72), 147
 Landau, L. D., 84(144), 85(144), 90
 Lane, N. F., 79(131), 90
 Langhans, L., 21(46), 71(46), 77(46), 81(46), 87, 94(7), 115(33), 118(33), 122(33), 144(33), 146
 Lassette, E. N., 17(25), 20, 21(49), 30(25), 31, 40, 42, 43, 46, 48(35, 81, 82), 49, 52, 57, 58, 63, 65, 71, 82(36), 87–89
 Leech, J. W., 18
 Levy, D. H., 149, 210(27, 28), 212(27, 28), 214(31, 32, 46), 215(31, 32), 216(31, 32, 46), 220(38), 221(38), 222(42), 228(31, 45–47), 232, 233(31, 32, 46, 47), 237(60), 238(60), 242(60), 245(62), 247, 248
 Lichten, W., 150(5), 246
 Lide, D. R., 150(3), 246
 Lifshitz, E. M., 84(144), 85(144), 90

- Lin, C. C., 72, 75, 90, 233, 248
 Linder, F., 21(46), 70(112), 71, 77(46),
 81(46), 87, 89, 94(7), 115(33), 118(33),
 122(33), 123, 143(33), 146, 147
 Linzer, M., 228(50), 231(50), 233(50),
 244(50), 248
 Lipscomb, W. N., 253(9a), 254(9, 13),
 258(9a, 9c), 260(9), 264(9a, 9c), 268(20),
 282(9a), 290(9, 13, 95), 298(9c), 301(9,
 95), 302(95, 109), 303(9), 306, 307, 311,
 312
 Lipsky, L., 99(14), 104, 114(14), 146
 Lowdin, P.-O., 111, 298(106), 312
 Lubezky, A., 61(101), 63(101), 89
 Lucas, N., 231, 248
 Lustig, C. D., 221(40), 247
 Lutz, B. L., 46(78), 88
 Lykos, P. G., 286(79), 287(79), 310

 McClellen, A. L., 304
 McConkey, 48
 McDonald, C. C., 228
 Macek, J., 94(8), 146
 McGowan, J. W., 86(149), 90, 99(13, 15),
 146
 McKoy, V., 61(100), 89, 286(78), 287(89),
 310, 311
 McWeeny, R., 271(26), 275(26), 277(26,
 66), 291(26), 301(26), 307, 310
 Mahan, B. H., 212(29), 247
 Mandl, F., 17(6), 71(6), 86, 115, 129(50),
 138, 146, 147
 Manne, R., 254(14a), 255(14a), 277(14a,
 14c), 281(14a), 289(14), 306
 Manson, S. T., 1(1), 14
 Marriott, R., 99, 146
 Massey, H. S. W., 17(3-5), 18, 19, 20(4),
 28(3a), 29(3), 41(3c), 72, 79(4), 86, 90
 Mendez, H. G., 143(67), 145(67), 147
 Menendez, M. G., 32(73), 41(73), 88
 Messiah, A., 16(1), 86, 157, 172(11),
 174(11), 186(11), 247
 Meyer, V. D., 20(26, 28), 42(28), 46,
 48(81, 82), 49(81, 82), 87, 89
 Michelis, G. de, 286(76), 310
 Midtdal, J., 102, 146
 Mielczarek, S. R., 21(39, 41, 44), 24-26(54),
 27(44), 30(39, 41), 31, 32(73), 33(44),
 41(73), 52, 63, 87-89, 124(41-42),
 143(67), 145(67, 72), 147
 Miller, K. J., 31, 33(66), 88
 Miller, T. A., 149, 182(25), 210(27, 28),
 212(27, 28), 214(31), 215(31), 216(25,
 31), 218(25), 220(25, 38), 221(38),
 222(42), 228(31), 232, 233(31), 237(60),
 238(60), 242(60), 245(62), 247,
 248
 Miller, W. D., 19, 56, 59(19), 60(19), 63,
 66(19), 86
 Miller, W. H., 92, 101, 104, 111, 113, 145
 Millie, P., 266(47), 290(47), 309
 Mittleman, M. H., 99(12), 146
 Mizushima, M., 150(1), 233, 246, 248
 Moccia, R., 286(79), 287(79), 310
 Moiseivitsch, B. L., 30(64), 88
 Moore, C. E., 31, 88, 288(92), 311
 Morino, Y., 232(54), 248
 Morrison, D. J. T., 80(135), 90
 Morse, P. M., 72, 90
 Moscowitz, A., 63(110), 89
 Mott, N. F., 17(3), 28(3a), 29(3), 41(3c), 86
 Mulliken, R. S., 21(49), 42(49), 46(49), 61,
 63, 66(103), 87, 89, 253, 254, 285(8),
 306
 Myers, R. J., 212(29), 228, 247

 Nakatsuji, H., 288(90c), 289(90), 311
 Nakayama, T., 57, 59(90), 89
 Nazaroff, G. V., 92(5), 102, 118(5), 145
 Newton, M. D., 253(9a), 254(9), 258(9a,
 9c), 260, 264(9a, 9c), 282(9a), 290(9, 95),
 298(9c), 301(9, 95), 302(21, 95), 303(9),
 306, 311
 Newton, R. G., 93, 96-99, 107, 110, 146
 Nichols, R. W., 48, 49, 89
 Nicholson, B. J., 249

 Oak Ridge National Laboratory, 19(16), 86
 Ohmura, T., 146
 Ohno, K. A., 277(65), 310
 Oleari, L., 286(76), 310
 O'Malley, T. F., 81(140), 90, 99(14), 104(14),
 114, 119(37), 120(37), 122, 123(37),
 124(37), 129(49), 131(53), 138, 140, 146,
 147
 Oosterhoff, L. J., 20, 43, 48, 54(87), 56(87),
 60(20), 86, 89
 Oppenheimer, J. R., 19, 86, 151, 247
 Orloff, M. K., 286(77), 287(87), 310, 311
 Ormande, S., 98(10), 99(14), 104(14),
 114(14), 144(10), 146

- Paldus, J., 255(17), 256(17), 306
 Palke, W. E., 268(20), 302(21), 307
 Palmer, T. W., 106, 108(25), 146
 Pan, D. C., 265(44), 308
 Pann, Y. K., 144(69), 147
 Pariser, R., 286(75), 287(75b), 310
 Parr, R. G., 269(53), 271(53), 286(75),
 286(75), 287(75b), 309, 310
 Pellegatti, A., 265(42), 308
 Percival, I. C., 28(61), 88
 Perkins, J. F., 99(14), 104(14), 114(14),
 146
 Peshkin, M., 1
 Peyerimhoff, S. D., 61(98), 89
 Phelps, A. V., 70(111), 89, 118, 146
 Phillips, M., 167, 247
 Pitzer, R. M., 302(109), 312
 Polák, R., 255(17), 256(17), 306
 Pople, J. A., 255(7a), 270(7b), 272(7b, 7i),
 273(7a), 281(7a), 283(7a), 291, 292(7b),
 293(7b, 7c), 294(7b), 306
 Posner, J., 294(103), 311
 Powell, F. K., 150(3), 246
 Price, W. C., 59, 63(107), 89

 Radford, H. E., 214(30, 51), 216(33),
 228(33, 49–51), 231, 233, 244(50, 51),
 247, 248
 Radtke, D. D., 255(16), 290(16), 306
 Raff, L., 20(32), 21, 30(32), 51, 63, 64,
 66(32a), 87
 Ragle, J. L., 294(103), 311
 Ramien, A., 71(115), 89
 Ransil, B. J., 287(86), 300(86), 311
 Rapp, D., 81(141), 90, 127(48), 128, 147
 Read, F. H., 20(24), 71(117), 81(117, 139),
 87, 89, 90
 Reid, C., 61(102, 105), 89
 Rein, R., 265(42), 308
 Reinhardt, P. W., 20(22), 43(22), 87
 Reinhardt, W., 101, 110, 131(21), 146
 Rice, B., 265(41), 308
 Rice, J. K., 15, 17(119), 18(71), 20(34, 56),
 21(51, 52), 23(52), 25(52), 26(57), 31,
 32(52, 70), 33, 36, 40(70), 41(68, 70),
 43, 46, 47(70), 48, 49, 52(57), 53,
 54(57), 57–60(56), 64(52), 65(52),
 71(119, 120), 72(119, 120), 74–78(119),
 79(119, 120, 132), 80(119), 81(119),
 83(120), 85(120), 87–90

 Riddell, R. C., 108, 146
 Ridge, D. P., 20(23), 87
 Robertson, J. C., 228(47), 233(47), 248
 Robin, M. B., 63(110), 89
 Roothaan, C. C. J., 250(2), 251(2), 285(2),
 305
 Rose, M. E., 4(2), 8(2), 14, 157, 184–186(10),
 196(10), 247
 Ross, I. G., 61(94), 89
 Ross, K. J., 20(31, 35), 42(35), 46(35),
 48(35), 49(35), 63, 65, 87
 Rosseland, S., 84(143), 90
 Rotenberg, M., 99, 146
 Rozsnyai, B. F., 75(138), 77(138), 80, 90
 Rudge, M. R. H., 80(135), 90
 Ruedenberg, K., 254(10), 266, 269(10),
 278(10), 306
 Russek, A., 99(14), 104, 114(14), 146

 Sahni, R. C., 79, 90, 277(23b), 307
 St. John, R. M., 18(69), 31, 33(69), 41(69)
 48, 88
 Salerno, J. A., 74, 80, 90
 Salpeter, E. E., 6(3), 14, 168(20), 247
 Sanders, T. M., 150(4), 246
 Santry, D. P., 255(7a), 273(7a), 281(7a),
 283(7a), 291(7), 306
 Satchler, G. R., 157, 162(12), 165(12),
 166(12), 173(12), 185(12), 186(12),
 196(12), 247
 Sawhney, B. C., 79, 90
 Schawlow, A. L., 243, 248
 Scherr, C. W., 307
 Schultz, N., 21(47), 48, 87
 Schulz, G. J., 19, 51, 56, 60, 71, 86, 89,
 116, 118, 127(47), 128, 132, 146, 147
 Seaton, M. T., 28(61), 88
 Segal, G. A., 255(7a), 270(7b), 272(7b),
 273(7a), 281(7a), 283(7a), 291, 292(7b),
 293(7b, 7c), 294(7b, 7e), 306
 Serre, J., 61(95), 89
 Sgarbellotti, A., 290(48), 309
 Sharp, T. E., 20, 51, 56(89), 81(141), 89,
 90, 127(48), 128, 131(52), 133, 147
 Sharp-Ritter, J. D., 286(79), 287(79), 310
 Shore, B. W., 111, 113, 146
 Shriner, D. F., 294(103), 311
 Shull, 111
 Sichel, J. M., 294(104), 311
 Silverman, S. M., 31, 40, 88

- Silverstone, H. J., 287(87), 311
 Simpson, J. A., 20, 21(39-41, 44), 22, 24-26(54), 27(44), 30(39, 41), 31, 32(40, 73), 33(44), 41(73), 48, 52, 63, 87-89, 124(41-43), 143(67), 145(67, 72), 147
 Sinanoğlu, O., 250(5), 286(77, 78), 305, 310
 Sipio, L. di, 286(76), 310
 Skerbele, A., 20, 42(28, 35), 43, 46, 48(35, 81, 82), 49, 63(29), 65(35), 71, 82(36), 87, 89
 Smith, K., 17(9), 27(9), 86, 91(2), 143(2), 145
 Smith, S. J., 30(64), 88
 Stanton, 48
 Stein, S., 75, 90
 Stickel, W., 21(49), 88
 Strandberg, M. W. P., 219-221(34), 234, 247, 248
 Stuart, J. D., 277(67), 310
 Sweeney, C. C., 255(16), 290(16), 306
 Switkes, E., 300(107), 312

 Takayanagi, K., 70(113), 72, 75, 78, 89, 90
 Taylor, A. J., 98(10), 99, 144(10, 16), 146
 Taylor, H. S., 17(7), 21(46), 71(7, 46), 75(136), 77(46, 136), 80, 81, 86, 87, 90, 91, 92(5), 102, 114(31), 115, 118(5, 33), 119(37), 120(37), 122(33), 123, 124(31, 37, 39), 127(46), 131(55), 135(39, 55, 61), 137(39), 141(66), 144(33, 69), 145-147
 Tekaatt, T., 21(47), 87
 Temkin, A., 80, 91(2), 99(12, 14), 104(14), 143(2), 145, 146
 Tilford, S. G., 45(77), 46(77), 88
 Tinkham, M., 219-221(34), 247
 Titchmarsh, E. C., 101, 106, 110, 146
 Townes, C. H., 150(4), 243, 247, 248
 Trajmar, S., 15, 17(119), 18(71), 20(34, 56), 21(51), 26, 31, 32(70), 33, 36, 40(70), 41(68, 70), 43, 46, 47(70), 48, 49, 52, 53, 54(57), 57, 58-60(56), 71(119, 120), 72(119, 120), 74-78(119), 79(119, 120, 132), 80(119), 81, 83(120), 85(120), 87-90
 Truhlar, D. G., 17(119), 28(60), 31, 32(70), 33(68), 40(70), 41(68, 70), 47(70), 70, 71(119, 120), 72(119, 120), 74-78(119), 79(119, 120, 132), 80(119, 135), 81(119), 83(120), 85(120), 88-90
 Tully, J. C., 1(1), 14, 80, 81(137), 90
 Tutte, W. T., 63(107), 89

 University of Colorado, 19(15), 86

 Vanderslice, J. T., 45(77), 46(77), 88
 Van Vleck, J. H., 167, 168, 182(22), 184(22), 185, 233(57), 234, 247, 248
 Veillard, A., 266(47), 290(47), 309
 Vriens, L., 21(44), 27(44), 31, 33(44), 87

 Wahlquist, H., 234, 248
 Walker, J. F., 99(12), 146
 Walter, J., 154(9), 247
 Watanabe, K., 57, 59(90), 63, 89
 Watson, K. M., 17(2), 86, 107, 146
 Watson, R. E., 285(74), 310
 Wayland, H., 30(62), 88
 Wei, P. S. P., 20(32, 56), 21, 30(32), 57-60(56), 63(32), 64(32d), 87, 88
 Weisskopf, V. W., 233(57), 234, 248
 Whitaker, W., 99(14), 104(14), 114(14), 146
 Whitehead, M. A., 294(104), 311
 Whiterod, G. L., 20(24), 87
 Wigner, E. P., 165(14), 224(14), 247
 Wilkins, R. L., 75(136), 77(136), 80, 81, 90
 Wilkinson, J. H., 308
 Wilkinson, P. G., 45(77), 46(77), 59, 61(99, 103), 63(99), 66(99, 103), 88, 89
 Williams, A. J., IV, 20(33), 21, 30(33), 43, 63(33c), 64, 66(33c), 87
 Williams, J. F., 99(15), 146
 Williams, J. K., 114, 115, 124(31, 39), 127(46), 135(39), 137(39), 146, 147
 Willman, K., 21(45, 47), 87
 Wittmaack, K., 21(50), 63, 72, 88
 Wolniewicz, L., 79, 90, 124(40), 125(40), 147
 Wouthuysen, S. A., 169, 247
 Wu, T., 146
 Wu, T.-Y., 72, 90

 Yamaguchi, K., 288(90c), 289(90), 311
 Yaris, M., 63(110), 89
 Yonezawa, T., 288(90c), 289(90), 311
 Yurev, M. S., 18

 Zare, R. N., 1(1), 14
 Zelikoff, M., 63, 89
 Zumino, B., 112, 146

SUBJECT INDEX

- Absolute cross sections, 27
Adiabatic potential curve, 138
Angular momentum, 183
Angular resolution, 23, 86
Asymptotic perturbation theory, 107
- Bardsley, et. al. method, 115
BOR calculations, 80, 81
Born Approximation, 20, 21, 31, 65, 72,
74, 75, 78, 80, 81
Born-Oppenheimer exchange approximation,
31, 33
BrO, 216, 228, 229, 231, 233
- CO, 48
CF, 228
ClO, 216, 228, 231, 232, 233
Close-coupling calculations, 72
Coupled representation, 195
Cusp-type effect, 134
- Decoupled representation, 195
Detailed balancing, 84
Diabatic potential curve, 138
"Differential scattering cross section "(DCS),
16, 30, 39, 74
Dirac Hamiltonian, 168
Discharges, 84
Dissociative attachment, 129
Distorted wave approximation, 75
Double scattering, 24, 25, 26
- Effective Hamiltonian, 183
Effective scattering length, 24, 26
Elastic scattering, 72, 74, 80, 81
Electric dipole moment, 75
Electric dipole transitions, 235
Electric field Hamiltonian, 178
Electric quadrupole moment, 65, 74, 78, 83
Electron beam method, 20
Electron exchange, 15, 17, 19, 80
Electronic excitation, 15, 17, 21, 42, 48, 49,
51, 56, 57, 60, 61, 63
Ar, 21
C₂H₂, 56, 57
C₆H₆, 21
CO, 49, 60, 71
H₂, 21, 71, 72, 81, 82, 83
He, 21
H₂O, 70, 71
N₂, 20, 21, 60, 71, 72, 82, 83
NO, 71
Electron swarms, 19, 71
Exchange scattering, 57, 60, 67, 70, 80, 86
of electrons, 15, 17, 19, 25, 26, 30, 42,
43, 46, 69
excitation via a direct mechanism, 30
singlet-triplet transitions, 20, 21, 67
Excitation or deexcitation of internal
states of the target, 15
External magnetic field Hamiltonian, 205,
206, 207
matrix elements in the coupled representa-
tion, 200
matrix elements in a decoupled representa-
tion, 201
- Feshbach theory, 104, 115, 116
Fine structure Hamiltonian, 173
of the first term, 202
matrix elements, 193, 202
Fine structure separations, 216
Flux factor, 98, 99
Franck-Condon factor, 42, 46, 48, 58, 129
Franck-Condon principle, 124
- Hund's case (a), 155, 181
(b) 155, 156, 182
(c) 156
Hylleraas-Undheim theory (H.U.), 102
Hyperfine structure, 195
Fermi contact term, 208
Hamiltonian, 175
matrix elements, 207
in a decoupled representation, 200, 201
- Inner shells, neglect of in MO calculations,
277
Intensities and lineshape, 233
Intensity ratio, 25, 30, 32, 39, 40, 49, 51,
55, 65, 68, 72, 82

- IO, 216, 228, 231, 233
 Irreducible linear operator, 185, 186
 scalar product, 185
 Inversion operator, 223

 Magnetic dipole transitions, 235
 Magnetic hyperfine Hamiltonian, 195, 197
 Electron-nuclear dipolar interaction, 197
 Fermi contact term, 197
 I, I_1 term, 196
 Miller formula, 101
 Model Hamiltonian, 100
 Mulliken approximation, 253, 289
 and SCF matrix elements, 258
 and SCF MO Calculations, 256
 in current use, 289
 Multipole expansion, 83

 Negative ion formation, 63
 NO, 228, 233
 NS, 228, 233
 Nuclear electric quadrupole interaction, 199
 matrix elements in the coupled representation, 199, 208
 Nuclear spin Zeeman interaction, 209
 matrix elements, 209

 O₂, 71, 218, 219, 220, 221, 222, 232
 Ochkur-Rudge exchange approximations,
 31, 33, 80, 81
 OH, 214, 228, 231, 233

 Plane wave approximation, 78
 Plasmas, 84
 Polarization of electronic charge cloud of
 target by electrons, 72, 74
 Positron scattering, 86
 Predissociation, 133
 Projection operator, 100, 111

 Quadrupole Hamiltonian, 175
 Quadrupole transition, 63, 65

 Resonances, 17, 63, 71, 81
 angular momentum barrier, 96
 core excited, 1, 92, 99
 mechanistic model, 92, 93
 position relative to CE II, 93
 special class, 99
 temporary formation of negative ion, 93
 core excited II, 93
 difficulty in distinguishing, 93
 mechanistic model, 93
 relation to potential well depth, 93, 96
 width relative to type I, exception to, 94
 electron affinity of the excited states, 93
 Feshbach compound state, 92
 hole-particle, 92
 inclusion of core polarization, 137
 induction effect, 96
 mathematical formulation, 110, 111
 single particle, 96, 99, 115, 137
 Resonant cavity, 244
 sample cavities, 244
 Rotational energy levels, 209
 Rotational excitation, 15, 70
 Rotational Hamiltonian, 187, 203
 matrix elements, 204
 Rotationless invariance averaging in MO calculations, 281
 Rudenberg approximation, 266, 290
 in current use, 290

 SD, 228
 SeF, 215, 216, 228, 233
 SeH, 216, 228, 231, 233
 Semiempirical approximation, effect of in MO calculations, 285
 SeO, 218, 219, 220, 221, 222
 SF, 215, 216, 228, 233
 SH, 228, 231, 233
 Singlet-singlet transitions, 54, 56, 57
 Singlet-triplet transitions, 20, 21, 43, 46, 57,
 60, 67, 69
 Small magnetic interactions, 211, 220, 221
 SO, 218, 219, 220, 221, 222, 232
 Spin-exchange inelastic processes, 25
 Spin-forbidden transitions, 19, 21
 Spin-free Hamiltonian, 172
 Spin-rotation interaction, 190, 192
 matrix elements, 192
 Spin-spin Hamiltonian, 173
 matrix elements, 194, 202
 Stabilization method, 99, 100, 101, 102, 103
 bound state in the continuum, 102
 matrix eigenfunctions, 101
 test for stability, 101
 validity, 101
 Stark effects, 105, 236, 237
 matrix elements, 236, 237
 Stark modulation, 241

- line shape, 242
- Superelastic scattering, 15, 83, 84, 85
- Symmetry-forbidden transitions, 19, 20, 39, 42, 63, 65
- TeH, 216, 228, 233
- "Threshold excitation spectra," 19, 20, 43
- "Total cross section," 16
- Transition probabilities, 17
 - in helium, 17
- Trapped electron method, 19, 43, 48, 51, 60, 63, 71
 - technique, 51
 - work, 51
- Triplet/singlet ratios, 32, 48, 53, 56, 58, 60, 66, 69
- Vibrational excitation, 15, 17, 21, 70, 71, 72, 74, 80, 81, 82, 83, 86
 - angular dependence, 119, 122
 - C₂H₄, 21, 72
 - CO₂, 70, 71, 72
- Virtual state, 98
- Weak quantization, 105
- Zeeman Hamiltonian, 176
- Zero differential overlap approximation, 269, 291
 - in current use, 291
 - and orthogonalized AOS, 269
 - and SCF matrix elements, 271